

Frontiers
in
Artificial
Intelligence
and
Applications

ARTIFICIAL INTELLIGENCE RESEARCH AND DEVELOPMENT

Edited by
Cecilio Angulo
Lluís Godó

IOS
Press

ARTIFICIAL INTELLIGENCE RESEARCH AND DEVELOPMENT

Frontiers in Artificial Intelligence and Applications

FAIA covers all aspects of theoretical and applied artificial intelligence research in the form of monographs, doctoral dissertations, textbooks, handbooks and proceedings volumes. The FAIA series contains several sub-series, including “Information Modelling and Knowledge Bases” and “Knowledge-Based Intelligent Engineering Systems”. It also includes the biennial ECAI, the European Conference on Artificial Intelligence, proceedings volumes, and other ECCAI – the European Coordinating Committee on Artificial Intelligence – sponsored publications. An editorial panel of internationally well-known scholars is appointed to provide a high quality selection.

Series Editors:

J. Breuker, R. Dieng-Kuntz, N. Guarino, J.N. Kok, J. Liu, R. López de Mántaras,
R. Mizoguchi, M. Musen, S.K. Pal and N. Zhong

Volume 163

Recently published in this series

- Vol. 162. T. Hirashima et al. (Eds.), Supporting Learning Through Integrative Technologies
- Vol. 161. H. Fujita and D. Pisanelli (Eds.), New Trends in Software Methodologies, Tools and Techniques
- Vol. 160. I. Maglogiannis et al. (Eds.), Emerging Artificial Intelligence Applications in Computer Engineering – Real World AI Systems with Applications in eHealth, HCI, Information Retrieval and Pervasive Technologies
- Vol. 159. E. Tyugu, Algorithms and Architectures of Artificial Intelligence
- Vol. 158. R. Luckin et al. (Eds.), Artificial Intelligence in Education – Building Technology Rich Learning Contexts That Work
- Vol. 157. B. Goertzel and P. Wang (Eds.), Advances in Artificial General Intelligence: Concepts, Architectures and Algorithms – Proceedings of the AGI Workshop 2006
- Vol. 156. R.M. Colomb, Ontology and the Semantic Web
- Vol. 155. O. Vasilecas et al. (Eds.), Databases and Information Systems IV – Selected Papers from the Seventh International Baltic Conference DB&IS'2006
- Vol. 154. M. Duží et al. (Eds.), Information Modelling and Knowledge Bases XVIII
- Vol. 153. Y. Vogiazou, Design for Emergence – Collaborative Social Play with Online and Location-Based Media
- Vol. 152. T.M. van Engers (Ed.), Legal Knowledge and Information Systems – JURIX 2006: The Nineteenth Annual Conference
- Vol. 151. R. Mizoguchi et al. (Eds.), Learning by Effective Utilization of Technologies: Facilitating Intercultural Understanding

Artificial Intelligence Research and Development

Edited by

Cecilio Angulo

*Knowledge Engineering Research Group, Automatic Control Department,
Technical University of Catalonia (UPC), Spain*

and

Lluís Godo

*Artificial Intelligence Research Institute (IIIA), Spanish National
Research Council (CSIC), Spain*

IOS
Press

Amsterdam • Berlin • Oxford • Tokyo • Washington, DC

© 2007 The authors and IOS Press.

All rights reserved. No part of this book may be reproduced, stored in a retrieval system,
or transmitted, in any form or by any means, without prior written permission from the publisher.

ISBN 978-1-58603-798-7

Library of Congress Control Number: 2007936310

Publisher

IOS Press

Nieuwe Hemweg 6B

1013 BG Amsterdam

Netherlands

fax: +31 20 687 0019

e-mail: order@iospress.nl

Distributor in the UK and Ireland

Gazelle Books Services Ltd.

White Cross Mills

Hightown

Lancaster LA1 4XS

United Kingdom

fax: +44 1524 63232

e-mail: sales@gazellebooks.co.uk

Distributor in the USA and Canada

IOS Press, Inc.

4502 Rachael Manor Drive

Fairfax, VA 22032

USA

fax: +1 703 323 3668

e-mail: iosbooks@iospress.com

LEGAL NOTICE

The publisher is not responsible for the use which might be made of the following information.

PRINTED IN THE NETHERLANDS

Preface

“We propose that a 2 month, 10 man study of artificial intelligence be carried out during the summer of 1956 at Dartmouth College in Hanover, New Hampshire. The study is to proceed....” Last year we celebrated the 50th anniversary of the Dartmouth AI project proposal by McCarthy, Minsky, Rochester and Shannon. Years later, and following similar traditions of a number of AI associations, a call was launched in 1997 by the Catalan Association for Artificial Intelligence (ACIA¹) to organize an annual conference to promote synergies in the research community of its influence, the seeder for the 1st Catalan Conference on Artificial Intelligence (CCIA’98) which took place in Tarragona on October 1998.

We are very glad to celebrate this year the 10th anniversary of the International Conference of the ACIA (CCIA’07) in Sant Julià de Lòria (Andorra), October 25–26th, 2007. The good health of the Catalan AI community and its influence area is witnessed by the representative selection of papers gathered in this book and which were presented at CCIA’07.

The book is organized according to the different areas in which the papers were distributed for their presentation during the conference. Namely: Constraint Satisfaction, Agents, Data Processing, Case-Based Reasoning, Computer Vision, Natural Language Processing, Uncertainty and Fuzziness, Robotics, and Applications. Papers have been selected after a double blind review process in which distinguished AI researchers from all over Europe participated. Among the 54 papers received, 23 were selected as oral presentations and 23 as posters. The quality of the papers was very high in average, and the selection between oral or poster presentation was only based on the potential degree of discussion that a paper we thought could generate. We believe that all the papers collected in this volume can be of interest to any computer scientist or engineer interested in AI.

We would like to express our sincere gratitude to all the authors and members of the scientific and organizing committees that have made this conference a success. Our special thanks go also to the plenary speakers, Gábor Lugosi and Jordi Vitrià, for their effort in preparing very interesting lectures, and to the president of the ACIA, Núria Agell, for her kind support.

Sant Julià de Lòria, October 2007

Cecilio Angulo
Technical University of Catalonia (UPC)

Lluís Godo
AI Research Institute (IIIA), CSIC

¹ ACIA, the Catalan Association for Artificial Intelligence, is member of the European Coordinating Committee for Artificial Intelligence (ECCAI). <http://www.acia.org>.

Conference Organization

CCIA 2007 was organized by the University of Andorra and the Associació Catalana d'Intel·ligència Artificial.

General Chair

Lluís Godo, Artificial Intelligence Research Institute – CSIC

Program Committee Chair

Cecilio Angulo, Technical University of Catalonia

Scientific Committee

Aïda Valls, Rovira i Virgili University

Andreu Català, Technical University of Catalonia

Angeles López, Jaume I University

Antonio Moreno, Rovira i Virgili University

Beatriz López, University of Girona

Carles Sierra, Artificial Intelligence Research Institute – CSIC

Carlos Ansotegui, University of Lleida

Carlos Iván Chesñevar, University of Lleida

David Masip, Open University of Catalonia

Elisabet Golobardes, Ramon Llull University

Enric Martí, Computer Vision Center

Enric Plaza, Artificial Intelligence Research Institute – CSIC

Enric Trillas, European Center for Soft Computing

Ester Bernardó, Ramon Llull University

Eva Onaindia, Technical University of Valencia

Felip Manyà, University of Lleida

Filiberto Pla, Jaume I University

Francesc J. Ferri, University of Valencia

Gábor Lugosi, Pompeu Fabra University

Gustavo Deco, Pompeu Fabra University

Héctor Geffner, Pompeu Fabra University

Ignasi R. Roda, University of Girona

Isabel Aguiló, University of the Balearic Islands

Jesús Cerquides, University of Barcelona

Joan Martí, University of Girona

Joaquim Meléndez, University of Girona

Jordi Recasens, Technical University of Catalonia

Jordi Sabater, Artificial Intelligence Research Institute – CSIC

Jordi Vitrià, Computer Vision Center

Josep Aguilar, Laboratoire d'Architecture et d'Analyse des Systèmes – CNRS

Josep Lluís de la Rosa, University of Girona

Josep M. Garrell, Ramon Llull University

Josep Puyol-Gruart, Artificial Intelligence Research Institute – CSIC

Juan A. Rodríguez, Artificial Intelligence Research Institute – CSIC
 Llorenç Valverde, University of the Balearic Islands
 L. Travé-Massuyès, Laboratoire d'Architecture et d'Analyse des Systèmes – CNRS
 M. Teresa Escrig, Jaume I University
 Maite López, University of Barcelona
 María Vanrell, Computer Vision Center
 Miguel Ángel Cazorla, Universitat d'Alacant
 Miquel Sánchez-Marrè, Technical University of Catalonia
 Mónica Sánchez, Technical University of Catalonia
 Monique Polit, University of Perpignan ‘Via Domitia’
 Núria Agell, Ramon Llull University
 Oriol Pujol, University of Barcelona
 Pablo Noriega, Artificial Intelligence Research Institute – CSIC
 Petia Radeva, Computer Vision Center
 Rafael García, University of Girona
 Ramon López de Mántaras, Artificial Intelligence Research Institute – CSIC
 Ricardo Toledo, Computer Vision Center
 Teresa Alsinet, University of Lleida
 Ulises Cortés, Technical University of Catalonia
 Vicenç Torra, Artificial Intelligence Research Institute – CSIC
 Vicent J. Botti, Technical University of Valencia
 Wamberto Vasconcelos, University of Aberdeen
 Xari Rovira, Ramon Llull University
 Xavier Binefa, Autonomous University of Barcelona

Additional Referees

Benjamin Auffarth, Xavier Cufí, Marc Esteva, Andrea Giovannucci, Xavier Lladó,
 Arnau Oliver, Isaac Pinyol, Norman Salazar, David Sánchez, Daniel Villatoro

Organizing Committee

Miquel Nicolau, University of Andorra
 Florenci Pla, University of Andorra

Web Manager and Secretariat

Aleix Dorca, University of Andorra
 Sergio Gil, University of Andorra

Sponsoring Institutions



UNIVERSITAT D'ANDORRA



This page intentionally left blank

Contents

Preface <i>Cecilio Angulo and Lluís Godo</i>	v
Invited Talks	
Sequential Prediction Under Incomplete Feedback <i>Gábor Lugosi</i>	3
Beyond the User: A Review of Socially Aware Computing <i>Jordi Vitrià</i>	6
Constraint Satisfaction	
An Efficient Estimation Function for the Crew Scheduling Problem <i>Javier Murillo and Beatriz Lopez</i>	11
What Is a Real-World SAT Instance? <i>Carlos Ansótegui, María Luisa Bonet, Jordi Levy and Felip Manyà</i>	19
Mendelian Error Detection in Complex Pedigrees Using Weighted Constraint Satisfaction Techniques <i>Marti Sanchez, Simon de Givry and Thomas Schiex</i>	29
Distributed Meeting Scheduling <i>Ismel Brito and Pedro Meseguer</i>	38
Agents	
The Impact of Betweenness in Small World Networks on Request for Proposal Coalition Formation Problems <i>Carlos Merida-Campos and Steven Willmott</i>	49
On the Multimodal Logic of Elementary Normative Systems <i>Pilar Dellunde</i>	57
Agents and Clinical Guidelines: Filling the Semantic Gap <i>David Isern, David Sánchez and Antonio Moreno</i>	67
A Monitor for Digital Business Ecosystems <i>Gabriel Alejandro Lopardo, Josep-Lluís de la Rosa i Esteva and Nicolás Hormazábal</i>	77
Confidence Management in FIPA Environments: Agent Unique Representation <i>Amadeu Albós and Alan Ward</i>	87
Completing the Virtual Analogy of Real Institutions via iObjects <i>Inmaculada Rodríguez, María Salamó, Maite López-Sánchez, Jesús Cerquides, Anna Puig and Carles Sierra</i>	95

Appraisal Variance Estimation in the ART Testbed Using Fuzzy Corrective Contextual Filters <i>Esteve del Acebo, Nicolás Hormazábal and Josep Lluís de la Rosa</i>	104
Punishment Policy Adaptation in a Road Junction Regulation System <i>Maite Lopez-Sánchez, Sanja Bauk, Natasa Kovac and Juan A. Rodriguez-Aguilar</i>	112
Scholar Agent: Auction Mechanisms for Efficient Publication Selection on Congresses and Journals <i>Josep Lluís de la Rosa and María de los Llanos Tena</i>	120
Data Processing	
Modeling Problem Transformations Based on Data Complexity <i>Ester Bernadó-Mansilla and Núria Macià-Antolínez</i>	133
Semantic Blocking for Record Linkage <i>Jordi Nin, Víctor Muntés-Mulero, Norbert Martínez-Bazán and Josep L. Larriba-Pey</i>	141
Case Based Reasoning	
Explanation of a Clustered Case Memory Organization <i>Albert Fornells, Eva Armengol and Elisabet Golobardes</i>	153
Assessing Confidence in Cased Based Reuse Step <i>F. Alejandro García, Javier Orozco and Jordi González</i>	161
Computer Vision	
Efficient Tracking of Objects with Arbitrary 2D Motions in Space-Variant Imagery <i>M. Luis Puig and V. Javier Traver</i>	171
Ground Plane Estimation Based on Virtual Camera Rotation <i>Adria Perez-Rovira, Brais Martínez and Xavier Binefa</i>	181
Weighted Dissociated Dipoles for Evolutive Learning <i>Xavier Baró and Jordi Vitrià</i>	189
Blood Detection in IVUS Longitudinal Cuts Using AdaBoost with a Novel Feature Stability Criterion <i>David Rotger, Petia Radeva, Eduard Fernández-Nofreiras and Josepa Mauri</i>	197
A Colour Space Based on the Image Content <i>Javier Vazquez, Maria Vanrell, Anna Salvatella and Eduard Vazquez</i>	205
An Evaluation of an Object Recognition Schema Using Multiple Region Detectors <i>Meritxell Vinyals, Arnau Ramisa and Ricardo Toledo</i>	213

An Input Panel and Recognition Engine for On-Line Handwritten Text Recognition	223
<i>Rafael Ramos-Garijo, Sergio Martín, Andrés Marzal, Federico Prat, Juan Miguel Vilar and David Llorens</i>	
Georeferencing Image Points Using Visual Pose Estimation and DEM	233
<i>Xavier Mateo and Xavier Binefa</i>	
Natural Language Processing	
Semantic Disambiguation of Taxonomies	245
<i>David Sánchez and Antonio Moreno</i>	
POP2.0: A Search Engine for Public Information Services in Local Government	255
<i>Antonio Manuel López Arjona, Miquel Montaner Rigall, Josep Lluís de la Rosa i Esteva and Maria Mercè Rovira i Regàs</i>	
Automatic Reading of Aeronautical Meteorological Messages	263
<i>Luis Delgado and Núria Castell</i>	
Uncertainty and Fuzziness	
Maximum and Minimum of Discrete Fuzzy Numbers	273
<i>Jaume Casasnovas and J. Vicente Riera</i>	
A Fuzzy Rule-Based Modeling of the Sociology of Organized Action	281
<i>Sandra Sandri and Christophe Sibertin-Blanc</i>	
Multidimensional OWA Operators in Group Decision Making	291
<i>Isabel Aguiló, Miguel A. Ballester, Tomasa Calvo, José Luis García-Lapresta, Gaspar Mayor and Jaume Suñer</i>	
Reasoning About Actions Under Uncertainty: A Possibilistic Approach	300
<i>Juan Carlos Nieves, Mauricio Osorio, Ulises Cortés, Francisco Caballero and Antonio López-Navidad</i>	
Ranking Features by Means of a Qualitative Optimisation Process	310
<i>Mónica Sánchez, Yu-Chiang Hu, Francesc Prats, Xari Rovira, Josep M. Sayeras and John Dawson</i>	
Robotics	
Tactical Modularity in Cognitive Systems	323
<i>Cecilio Angulo, Ricardo A. Téllez and Diego E. Pardo</i>	
Using the Average Landmark Vector Method for Robot Homing	331
<i>Alex Goldhoorn, Arnau Ramisa, Ramón López de Mántaras and Ricardo Toledo</i>	

Distance Sensor Data Integration and Prediction <i>Zoe Falomir, M. Teresa Escrig, Juan Carlos Peris and Vicente Castelló</i>	339
Applications	
Neural Network Modeling of a Magnetorheological Damper <i>Mauricio Zapateiro and Ningsu Luo</i>	351
Knowledge Discovery in a Wastewater Treatment Plant with Clustering Based on Rules by States <i>Karina Gibert and Gustavo Rodríguez Silva</i>	359
Forecasting New Customers' Behaviour by Means of a Fuzzy Unsupervised Method <i>Germán Sánchez, Juan Carlos Aguado and Nuria Agell</i>	368
Integrating a Feature Selection Algorithm for Classification of Voltage Sags Originated in Transmission and Distribution Networks <i>Abbas Khosravi, Toni Martínez, Joaquim Meléndez, Joan Colomer and Jorge Sanchez</i>	376
Multiobjective Evolutionary Algorithm for DS-CDMA Pseudonoise Sequence Design in a Multiresolutive Acquisition <i>Rosa Maria Alsina Pagès, Lluís Formiga Fanals, Joan Claudi Socoró Carrié and Ester Bernadó Mansilla</i>	384
Renewable Energy for Domestic Electricity Production and Prediction of Short-Time Electric Consumption <i>Stéphane Grieu, Frédéric Thiery, Adama Traoré and Monique Polit</i>	392
An Argument-Based Approach to Deal with Wastewater Discharges <i>Montse Aulinás, Pancho Tolchinsky, Clàudia Turon, Manel Poch and Ulises Cortés</i>	400
Analysis of Common Cause Failure in Redundant Control Systems Using Fault Trees <i>David Bayona i Bru, Joaquim Meléndez and Gabriel Olguin</i>	408
Kalman Filters to Generate Customer Behavior Alarms <i>Josep Lluis de la Rosa, Ricardo Mollet, Miquel Montaner, Daniel Ruiz and Víctor Muñoz</i>	416
A Knowledge Discovery Methodology for Identifying Vulnerability Factors of Mental Disorder in an Intellectually Disabled Population <i>Xavier Lluis Martorell, Raimon Massanet Vila, Karina Gibert, Miquel Sànchez-Marrè, Juan Carlos Martín and Almudena Martorell</i>	426
Author Index	437

Invited Talks

This page intentionally left blank

Sequential prediction under incomplete feedback ¹

Gábor LUGOSI

*ICREA and Department of Economics and Business
Universitat Pompeu Fabra
Ramon Trias Fargas 25–27
08005 Barcelona, Catalunya, Spain*

Abstract. We survey various variants of the randomized sequential forecasting problem when the forecaster has limited access to the past outcomes of the sequence to be predicted. This problem has various applications in on-line learning, learning in games, and information theory.

Keywords. sequential prediction, on-line learning, incomplete feedback

Introduction

In this talk we survey various variants of a sequential forecasting—or on-line learning—problem. In the most basic version of the problem, the *predictor*—or *forecaster*—observes one after another the elements of a sequence y_1, y_2, \dots of symbols. We assume that $y_t \in \mathcal{Y}$ where \mathcal{Y} is a set of outcome symbols (which may be finite or infinite). At each time $t = 1, 2, \dots$, before the t -th symbol of the sequence is revealed, the forecaster guesses its value y_t based on the previous $t - 1$ observations.

In the classical statistical theory of sequential prediction, the sequence of elements—that we call *outcomes*—is assumed to be a realization of a stationary stochastic process. Under this hypothesis, statistical properties of the process may be estimated based on the sequence of past observations, and effective prediction rules can be derived from these estimates. In such a setup, the *risk* of a prediction rule may be defined as the expected value of some *loss function* measuring the discrepancy between predicted value and true outcome, and different rules are compared based on the behavior of their risk.

Here we abandon the basic assumption that the outcomes are generated by an underlying stochastic process, and view the sequence y_1, y_2, \dots as the product of some unknown and unspecified mechanism (which could be deterministic, stochastic, or even adversarially adaptive). To contrast it with stochastic modeling, this approach has often been referred to as prediction of *individual sequences*.

Without a probabilistic model, the notion of risk cannot be defined, and it is not immediately obvious how the goals of prediction should be set up formally.

¹This research was supported in part by the Spanish Ministry of Science and Technology grant MTM2006-05650, by Fundación BBVA, by the PASCAL Network of Excellence under EC grant no. 506778

In the model discussed here, at each time instance, the forecaster chooses one of N actions $i \in \{1, \dots, N\}$ and suffers loss $\ell(i, y_t)$ if the outcome is y_t where ℓ is some fixed loss function taking values in the interval $[0, 1]$. The performance of the forecaster is compared to the best “constant” predictor, that is, the fixed action i that achieves the smallest loss over the n periods of prediction.

The difference between the forecaster’s accumulated loss and that of a fixed constant action is called *regret*, as it measures how much the forecaster regrets, in hindsight, of not having followed this particular action. Thus, the goal of the predictor is to make (almost) as few mistakes as the best constant strategy. Ideally, the forecaster’s objective is to achieve that the regret, divided by the number of time instances, converges to zero.

Since the sequence of outcomes is completely arbitrary, it is immediate to see that for any deterministic forecasting strategy there exists a sequence y_1, \dots, y_n of outcomes such that the forecaster always chooses the worst action, making it impossible to obtain any nontrivial regret bound. Surprisingly, if the forecaster is allowed to randomize (that is, to flip a biased coin before making a prediction) then the situation becomes dramatically different as this simple tool turns out to be extremely powerful.

After introducing the standard randomized prediction problem, we show simple randomized forecasters that achieve a sublinearly growing regret for all possible sequences of outcomes. We also discuss various modifications of the problem in which the forecaster has limited access to the past outcomes of the sequence to be predicted.

In a “label efficient” version of the prediction game, only a small fraction of the outcomes is made available to the forecaster. Surprisingly, a vanishing per-round regret may be achieved under the only assumption that the number of outcomes revealed after n prediction rounds grows faster than $\log(n) \log \log(n)$.

In the *multi-armed bandit* problem the forecaster observes his own loss after making a prediction, but he cannot calculate what would have happened had he chosen a different action. We show how this problem can be solved by a simple randomized predictor.

We formulate prediction problems with limited information in a general framework. In the setup of prediction under *partial monitoring*, the forecaster, instead of his own loss, only receives a feedback signal. The difficulty of the problem depends on the relationship between losses and feedbacks. We determine general conditions under which small regret can be achieved. The best achievable rates of convergence are also established.

We also describe an on-line problem of selecting a path in a network with arbitrarily varying costs on the edges of the network with the added difficulty that the forecaster only gets to see the costs of the edges over the path he has chosen but not those of the edges on other paths.

A comprehensive treatment of such prediction problems and various related issues may be found in Cesa-Bianchi and Lugosi [1].

For surveys of closely related topics, we refer to Merhav and Feder [7], Foster and Vohra [4], Vovk [8].

In the talk we mention some results obtained in Cesa-Bianchi, Lugosi, and Stoltz [2], [3], György, Linder, Lugosi, and Ottucsák [5], and Lugosi, Mannor, and Stoltz [6].

References

- [1] N. Cesa-Bianchi and G. Lugosi. *Prediction, Learning, and Games*. Cambridge University Press, New York, 2006.

- [2] N. Cesa-Bianchi, G. Lugosi, and G. Stoltz. Minimizing regret with label efficient prediction. *IEEE Transactions on Information Theory*, 51:2152–2162, 2004.
- [3] N. Cesa-Bianchi, G. Lugosi, and G. Stoltz. Regret minimization under partial monitoring. *Mathematics of Operations Research*, 31:562–580, 2006.
- [4] D. Foster and R. Vohra. Regret in the on-line decision problem. *Games and Economic Behavior*, 29:7–36, 1999.
- [5] A. György, T. Linder, G. Lugosi, and Gy. Ottucsák. The on-line shortest path problem under partial monitoring. *Journal of Machine Learning Research*, to appear, 2007.
- [6] G. Lugosi, S. Mannor, and G. Stoltz. Strategies for prediction under imperfect monitoring. Submitted, 2007.
- [7] N. Merhav and M. Feder. Universal prediction. *IEEE Transactions on Information Theory*, 44:2124–2147, 1998.
- [8] V. Vovk. Competitive on-line statistics. *International Statistical Review*, 69:213–248, 2001.

Beyond the user: A review of socially aware computing

Jordi VITRIÀ

Centre de Visió per Computador

Universitat Autònoma de Barcelona

08193 Bellaterra, Barcelona, Catalunya, Spain

Abstract. Social cognition is the main channel through which human beings access the social world, very much like vision and hearing are channels through which people access the physical world. For a long time, researchers have addressed the computational implementation of vision and hearing in domains like computer vision and speech recognition, but only early attempts have been made to do the same with social cognition. In other words: machines are beginning to be effective in handling perceptual aspects of the physical world, but up to now are devoid of social context.

Keywords. Socially aware computing, non-verbal behavior, machine learning, interaction, decision making.

Introduction

Social Cognition (SC) is the human ability of making sense of people and social interactions. Human beings make use of SC each time we are capable of extracting information, often in few seconds, from a social interaction: when we feel interpersonal conflicts among people we do not know (despite the apparent lack of explicit signs), when we feel that our interlocutors in a face-to-face conversation are not listening (despite possible attempts to conceal it), when we feel that speakers are boring or interesting few seconds after the start of a talk. The keyword here is feeling: social cognition is not reasoning, but rather performing unconscious cognitive processes based mostly on nonverbal communication cues. For most of us, SC is used unconsciously for some of the most important actions we take in life: finding a mate, negotiating economic and affective resources in the family and the workplace, making new friends and maintaining social links, and establishing credibility, leadership, and influence with strangers and peers. SC is so important that its lack is associated with serious developmental disabilities like autism.

Social interaction has commonly been addressed, from a computational point of view, within two different frameworks. One framework comes from cognitive psychology, and focuses on emotion [1]. P. Ekman [5] is the most well-known advocate of this approach, which is based roughly on the theory that people perceive others' emotions through stereotyped displays of facial expression, tone of voice, etc. The simplicity and perceptual grounding of this theory has recently given rise to considerable interest in the computational literature . However serious question about this framework remains,

including the issue of what counts as affect? Does it include cognitive constructs such as interest or curiosity, or just the base dimensions of positive-negative, active-passive attitude? Another difficulty is the complex connection between affect and behaviour.

The second framework for understanding social interaction comes from linguistics, and treats social interaction from the viewpoint of dialog understanding. Kendon [2] is among the best known pioneers in this area, and the potential to greatly increase the realism of humanoid computer agents has generated considerable interest from the computer graphics and human-computer interaction community. In this framework prosody and gesture are treated as annotations of the basic linguistic information, used (for instance) to guide attention and signal irony. At the level of dialog structure, there are linguistic strategies to indicate trust, credibility, etc., such as small talk and choice of vocabulary. While this framework has proven useful for conscious language production, it has been difficult to apply it to dialog interpretation, perception, and for unconscious behaviors generally.

Recently, a third view, that has been called *socially aware computing* has been developed that aims at the understanding of human social signalling in everyday life situations [3]. Although the capacity of inferring affective/emotional states is a basic attribute for intelligent systems, with important implications in communication and decision making processes (this is also true for dialog understanding), this view advocates for the study of an alternative/parallel inference channel focused on non-verbal behavior. This research has been conducted at MIT Media Lab under the supervision of Alex Pentland. The strategic importance of this research has been the replication by artificial means of some human predictions, like the "thin-slice" theory in social psychology [6].

The main hypothesis of this new research area is that there are some real social contexts where human decisions are mainly (but not exclusively!) based on the content conveyed by this specific communication channel between humans, that we call social signalling [4]. Social signalling can be defined as *what you perceive when observing a conversation in an unfamiliar language, and yet find that you can still "see" someone taking charge of a conversation, establishing a friendly interaction, or expressing empathy for the other party*. These situations may include job interviews or salary negotiations, (just to mention a few).

Several large psychological studies have recently taken into account this view and have considered the communication value of nonverbal human signals. They have investigated the hypothesis that there exists a subconscious communication channel between humans that conveys information about speaker attitudes, regulates speaker roles and is used to make decisions. These studies have shown that the non-linguistic messages (even considered at small time scale = 30s) are means to analyze and predict human behavior. So, mainstream literature in social psychology suggests that people subconsciously use social signals to communicate. Through this independent communication channel, a consistent attitude signal is expressed via various modalities; voice, facial expression, posture and gesture.

To quantify these social signals we can develop automatic methods to analyze different types of social signals, such as **activity level, engagement, emphasis, and mirroring**. To date audio features representing these signals have been used to successfully predict outcomes of salary negotiations, effectiveness of business pitches, as early indicators of clinical depression, and to conversational interest and dating outcomes with accuracy comparable to that of human experts in analogous situations.

Research in this area will continue along different lines: definition of new social signals, integration of different modalities (speech, face expressions, gesture, posture, body movement), development of specialized social sensors, development of new learning methods to learn from interaction data, etc.

The range of application areas for socially aware systems touches on many aspects of computing, and as computing becomes more ubiquitous, practically every aspect of interaction with objects, and the environment, as well as human-human interaction will make use of these techniques, including systems for monitoring elderly people, socially aware communication systems and non intrusive mobile phones.

Acknowledgements

Thank's to Petia Radeva (CVC, Catalunya), Alex Pentland (MIT Media Lab, USA), Nicu Sebe (University of Amsterdam, Netherlands), Daniel Gatica (IDIAP, Switzerland) and José Santos Victor (IST, Portugal) for our fruitful discussions about non autistic computing.

References

- [1] R. Picard, *Affective Computing*. MIT Press, 1997
- [2] A. Kendon, R. M. Harris, and M. R. Key. *Organization of behavior in face to face interaction*. The Hague: Mouton, 1975.
- [3] A. Pentland, Socially Aware Computation and Communication, IEEE Computer, March 2005, 63-70.
- [4] A. Pentland, (2004, October). Social Dynamics: Signals and Behavior. *International Conference on Developmental Learning, Salk Institute, San Diego, CA*.
- [5] P. Ekman and W. Friesen. *Facial Action Coding System*. Consulting Psychologists Press, 1977.
- [6] N. Ambady, R. Rosenthal. *Thin slices of expressive behavior as predictors of interpersonal consequences: A meta analysis*. Psychological Bulletin, **111**, 2, Feb. 1992, 256-274.

Constraint Satisfaction

This page intentionally left blank

An efficient estimation function for the crew scheduling problem

Javier Murillo¹, Beatriz Lopez

University of Girona

Abstract. In this paper we explain an estimation function for the crew scheduling problem in the coach transportation domain. Thanks to this function we obtain an estimation that is very close to the real cost of the solution and we can efficiently prune the search space with a branch and bound approach. Consequently we find the optimal solution in less time than with other estimations such as the Russian doll method.

Keywords. Crew scheduling, road passenger transportation, optimization, branch and bound, estimation function

1. Introduction

In a road passenger transportation scenario we are posed with the problem of optimizing the drivers' driving costs while assigning sequences of actions to them (drivers' duties). Given a set of resources drivers $D = \{d_1, \dots, d_n\}$ and a set of tasks (services) $S = \{s_1, \dots, s_n\}$ to be performed using the resources, the problem consists of finding the best assignment of drivers to services given a cost function and subject to the constraints provided by the administration. We are dealing, then, with a constraint optimization problem in which we attempt to minimize the driver's cost, both in time and distance. The solution of the problem should be a complete set of services. This includes which sequence of actions each driver should perform (planning outcomes) and when (schedule outcomes). Thus, the components of the problem are: drivers, services, constraints and the cost function.

First, each driver is characterized by a basic cost imposed by his contract, a cost per kilometer, a cost per time unit, a starting point and a final point (often the same), and the number of hours that he has driven during the previous two weeks.

Second, each service is characterized by the start location and the final location (where the service is), the start time and the final time (when). There are two kinds of services to be considered: requested and intervening. Requested services are the ones that customers have applied for, while intervening services are those required to move the driver from the end location of a service to the start location of the next service assigned to him. Analogously, if the first service that the driver performs is different to his/her current initial place, the corresponding amount of time needed to drive from the initial

¹Correspondence to: Javier Murillo, University of Girona, Campus Montilivi, edifici P4, 17071 Girona, Spain. Tel.: +34 972 418 391; Fax: +34 972 417 949; E-mail: jmurillo@eia.udg.es.

place to the first service should also be computed into the scheduling. This is similar to the ending location if the final service is different to the driver's ending place. Requested services are the problem data, and intervening services are generated while building the solution.

Third, there are several constraints regarding driving time (see [4] for a complete list). For the sake of simplicity, in our first approach to the problem we consider the four main constraints described below.

- **Overlapping.** A driver cannot be assigned to two different services with overlapping times. In addition, a driver assigned to a service that ends at time t and location l cannot be assigned to another service that starts at time $t + 1$, unless the location of the new service is the same (l). That is, the overlapping constraint also takes care of the transportation of the driver from the end location of a service to the start location of the next service to be performed.
- **Maximum driving time.** By driving time we mean that in addition to the driving time dedicated to the services requested, the driving time required for the intervening services should also be computed.
- **Maximum journey length.** Between one service and the next one, drivers can enjoy free time in which no driving activities are being performed. The sum of driving time plus free time cannot be greater than the maximum journey length allowed.
- **Maximum driving time per two-weeks.** There are some regulations regarding driving and resting time. One of them stipulates that the maximum driving time per two weeks cannot be over 90 hours.

Finally, a cost function is required to measure the quality of the solutions, that is, the cost of the allocation of services to drivers. The goal, then, is to find the allocation with the lowest cost subject to the constraints.

Our approach divides the solution process into two steps: the planning and the scheduling steps.

The planning step generates a set of feasible plans, sorted according to their estimated costs. A plan consists of a set of compatible journeys. Each journey is the sequence of services (both requested and intervening) that can be assigned to a driver. Among the possible plans, only the most promising ones are filtered out to the scheduling step, in such a way that memory space is kept to a minimum and the time of the overall process is reduced. The selection of plans is performed according to the algorithm shown in Figure 1. At the beginning, the first plan is generated. For the remaining plans, an upper cost bound is defined, in such a way that if their estimated costs are below this bound, the plans are stored and passed on to the scheduling step. Two cost functions are used: the estimating cost function (f_e) and the real cost of the first solution of a plan (f_1). The description of the former is the aim of this paper. The latter is obtained in a very short time since we are computing a solution, not the best one.

The scheduling step is applied once for each plan provided in the previous planning step. The journeys of each plan are assigned to drivers through a branch and bound method. Therefore, an upper and a lower bound are also established. The upper bound is set to the best solution found so far, while the lower bound is set to the estimated cost of the remaining assignments.

Note, then, that in both steps, an estimating cost function is defined in a plan. In the planning step it is used to both filter plans and sort the feasible ones. In the scheduling

```

Let J be the set of journeys
 $p_i = \text{firstPlan}(J);$ 
 $\text{upper\_bound} = \infty$ 
While  $p_i$  do
    if  $f_e(p_i) < \text{upper\_bound}$  then
        store( $p_i$ )
        if  $f_1(p_i) < \text{upper\_bound}$  then
             $\text{upper\_bound} = f_1(p_i)$ 
        end-if
    end-if
     $p_i = \text{nextPlan}(J);$ 
end-while

```

Figure 1. Planning algorithm.

step is it used to prune the search space. In this paper we focus on the description of the heuristics employed in this estimation function, which has several benefits:

- First, we can avoid keeping all the plans in memory, saving a great amount of memory.
- Second, we can obtain a good solution of the problem quickly.
- And third, we can prune some branches of the planning and scheduling process.

2. Heuristic description

The estimation function of a plan is based on heuristics that take into account both the minimum driving cost and the number of drivers required in the solution. First, we define a Minimum Cost Matrix M_{min} , in which rows are journeys of the plans and columns are driver's cost relationships. Each element $c_{i,j}$ represents the cost of the j journey when assigned to the i driver. For example, given a plan p_k composed of four journeys $\{j_1, j_2, j_3, j_4\}$, we have the M_{min} matrix shown in Figure 2 (left).

M min					M dif					
	CM 1	CM 2	CM 3	CM 4	CM 5	dif 1	dif 2	dif 3	dif 4	
J1	3:100	5:110	1:130	2:135	4:151	J1	10	20	5	16
J2	3:150	1:153	5:155	4:161	6:172	J2	3	2	6	11
J3	3:200	1:210	5:211	2:221	7:250	J3	10	1	10	29
J4	3:90	1:92	5:93	4:95	2:110	J4	2	1	2	15
						r _{dif}	1	2	0	2

Figure 2. Matrix examples for calculating the estimated cost. Left M_{min} . Right M_{dif}

Cells are sorted inside a row according to their cost. So $c_{1,1}$ has the value of the minimum cost corresponding to journey j_1 . In order to know which driver this cost corresponds to, we annotate the value cost with the driver number. According to that, 3 : 100 means that the minimum cost is 100 and corresponds to the 3rd driver. The cost in the

first column, correspond to the drivers with the minimum cost. In the particular case of Figure 2, left, all minimum costs belong to the same driver 3.

According to the M_{min} values, we can compute an estimating function based on the total of the minimum values from each row (that is, minimum cost for each journey of the plan). In the example in Figure 2, this sum is 540 (100+150+200+90). However, this total underestimates the real solution cost since it does not take into account that all the minimum costs correspond to the same driver and that at most one journey can be assigned to a driver. So, the number of drivers required in the solution should also be incorporated into the estimation.

For this purpose, we complement the M_{min} matrix with a second matrix, M_{dif} , in which the columns contain differential information about M_{min} . That is, the dif_i column contains the differences between the i and $i+1$ column of M_{min} representing the increasing cost when we consider the solution of M_{min} column $i+1$ instead of i . Figure 2 (right) provides the M_{dif} matrix of our example. We have also added a new last row, r_{dif} , in which we annotate the information related to differential drivers. For example, the last row of the M_{dif} matrix of Figure 2 (right) contains the following values: 1 (there is a single driver in column 1 of M_{min}), 2 (there are two new drivers in the second column of M_{min} , 5 and 1, that were not in the previous column), 0 (no new drivers appear) and 2 (the 2 and 4 driver costs are in this last column).

Then, we use the values of both, M_{min} and M_{dif} , to estimate the cost of a solution as shown in the algorithm of Figure 3. Basically, the algorithm computes the sum of the minimum cost of each journey as follows. We start by estimating the minimum cost, e_{cost} , as the addition of all costs in column 1 of M_{min} ($minValue$ function in the algorithm). This minimum is provided by as many drivers as expressed in the first element of the r_{dif} row, noted as $r_{dif}(1)$. Regarding a plan p_k , we need as many drivers as $length(p_k)$, since we can assign only one driver to a journey. Then, if $length(p_k) - r_{dif}(1)$ is positive, it means that we have over-assigned drivers.

```

Let be  $p_k$  the current plan
 $col = 1$ 
 $e_{cost} = minValue(p_k)$ 
 $neededDrivers = length(p_k)$ 
while  $neededDrivers > 0$  do
     $newDrivers = min(r_{dif}(col), neededDrivers)$ 
     $neededDrivers = neededDrivers - newDrivers$ 
     $e_{cost} = e_{cost} + minDif(col, neededDrivers)$ 
     $col = col + 1$ 
end-while

```

Figure 3. Estimation function algorithm.

We then proceeded by considering more drivers according to the successive column of r_{dif} . In $r_{dif}(2)$ we know how many new drivers appear in the next column. Then, we add to e_{cost} as many values of M_{dif} from the second column as new drivers are being considered in $r_{dif}(2)$. Only the smallest values are added ($minDif$ function). Now, we have $r_{dif}(1) + r_{dif}(2)$ drivers, while we need $length(p_k)$. If the difference is still

positive, we continue adding new differences from the dif_3 column, and so on until the required number of drivers is attained.

In our example we know that all values of the first column correspond to the same driver. So, in the first iteration, three cost from the first column of M_{dif} matrix will be added (*needed drivers* = 4, *new drivers* = 1 ($r_{dif} = 1$), so 3 new will be required). In the second iteration, two new drivers have found ($r_{dif} = 2$), so only one more driver is required (3-2=1) and consequently, only one additive cost of $M_{dif}(2)$ is added.

The fourth cost will be in the fourth column because in the 3rd column there are no new drivers and in the fourth there are 2 new drivers. So, in the example, four iterations of the algorithm are required as shown in Figure 4, getting as result an estimated cost of 558, much more accurate than the initial min value of 540.

	e_{cost}	col	needed Drivers	new Drivers	numDiff	$r_{dif}(col)$
Initial values	540	1	4	-	-	1
1st iteration	540+(2+3+10)	2	3	1	4-1=3	2
2nd iteration	550+(1)	3	1	2	3-2=1	0
3rd iteration	556 + (2)	4	1	0	1-0=1	2
4th iteration	558	5	0	1	1-1=0	-

Figure 4. Iterations of the algorithm in the case example.

3. Experimental results

In order to experimentally analyze the different techniques, up to 70 examples have been generated with different complexity. The first example has a single service and a single driver; the second example two services and two drivers; and so on until the 70th example. The data corresponding to service and drivers have been generated randomly for each example. In this sense, the complexity of the 70th example is greater than in a real case of the application we are dealing with.

In Figure 5 we compare the estimations when we consider the minimum driving costs, the outcomes of our estimation function, and the real solution cost. It is possible to

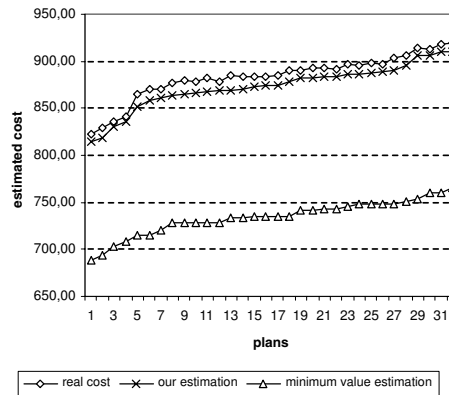


Figure 5. Cost comparison between the estimated costs and the real cost of the solution

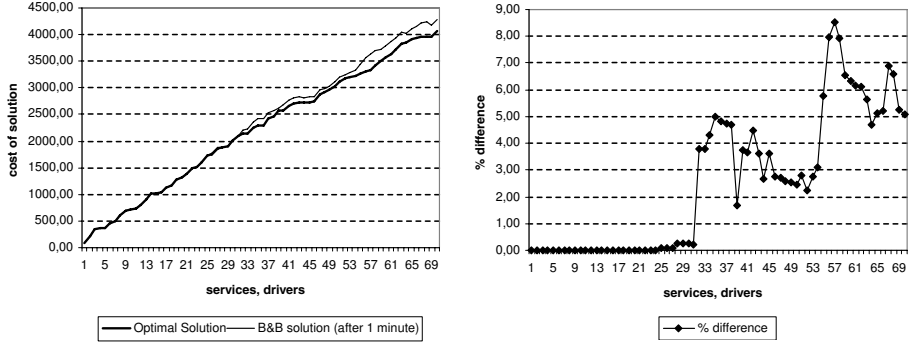


Figure 6. Difference between the solution obtained in 1 minute and the optimal solution

see how close our estimation is to the real cost, and how much it is improved regarding the minimum estimation.

In addition, our heuristics allow us to find a good solution to the problem at the beginning of the process. Later the algorithm wastes a lot of time obtaining small improvements until the optimal solution is reached. Consequently, we can stop the algorithm at any time and get a good solution. In Figure 6 we can see the difference between the optimal solution and the solution found in 1 minute of execution. The graph on the left shows the two solutions and the graph on the right shows the percentage of the real cost of the difference with respect to the optimal solution. Therefore, this heuristic can be applied for scenarios where we need a good but not necessarily the optimal solution.

We compared our approach with the Russian doll method [12]. This method consists of pre-calculating the problem with less complexity to obtain a estimation for pruning the search space. the Russian doll method is applicable when two consecutive subproblems differ in one variable only [7]. This is our case. For example, to solve the problem with 20 services and drivers, we solve the problem with 19, and we use this solution to estimate the cost of the 20th problem. Figure 7 shows the estimation given by the doll method compared to our estimation function during a scheduling process. For example, when the algorithm performs the first assignment, our algorithm estimates the rest of the journeys not yet assigned with a cost of 1472,95 while the Russian doll method estimates the journeys at 1450,55. Thus, we can see that the Russian doll estimation is lower than ours.

Finally, we have also applied our method to solve a real problem. In this experiment the number of services and drivers is 67, less than the synthetic case example. The main differences between the real and the synthetic data is that the lengths of the services in the real data are longer. Also in the real data the time window is 24 hour of execution, while in the synthetic it is only of 12 hours. This different nature of the services makes the problem a little bit more complex, but the results obtained are very similar to the synthetic case as shown in [10].

4. Related work

A review of the literature reveals several works regarding crew scheduling, a problem than can be modelled as a Set Covering Problem (SCP) [5] or a Set Partition Problem (SPP) [2]. In some cases the crew scheduling is applied to the road passenger transporta-

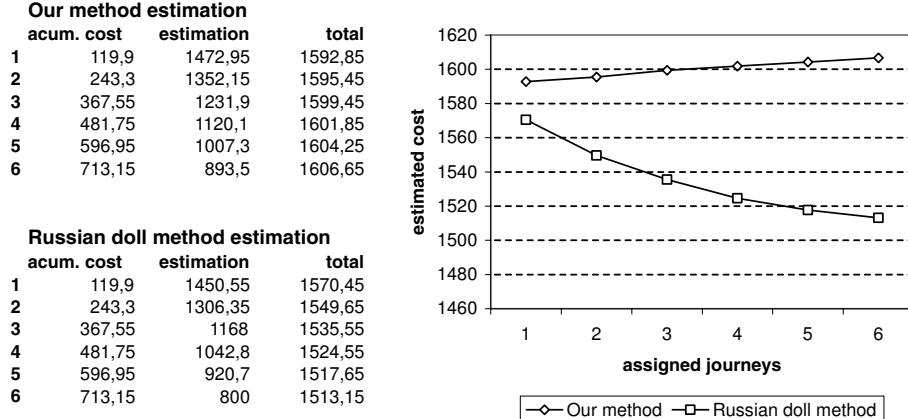


Figure 7. Estimated cost comparison between Russian dolls and our method

tion domain [13,14,5], for the railway optimization [13,9] or the airline crew scheduling [11,3,6,1].

The most used techniques are the family of the exact methods like branch and bound and linear programming. These techniques are complete and they are able to guarantee a solution or to prove that one does not exist. For example, in [14,13] these techniques are applied in the road passenger transportation domain, in [13,9] in the railway optimization, and in [11,3,6,1] in the airplane domain. In our work we have focused in the branch and bound mechanism to deal with the crew scheduling problem in the road passenger transportation domain.

Other authors have dealt with the crew scheduling using non-exact methods like local search and bio-inspired methods. These methods are usually incomplete, they are not able to guarantee that a solution can be found, and they cannot prove that a solution does not exist, but they have a solution at a reasonable computation cost. Among all of these methods, it is interesting to point out the successfullness of the tabu search method for the road passenger transportation [5,13] and the railway optimization [13]. Finally two bio-inspired non-exact methods have been used for the crew scheduling: Genetic algorithms, inspired in the biological evolution, and Ant Colony Optimization (ACO) inspired in the behaviour of ants in order to find food. In [13] we can find approaches with these two methods to the road and the railway optimization.

5. Conclusions

In this paper we have described a heuristic for a road passenger transportation problem that allows the definition of an estimating function very close to the real cost. We have compared our approach to another very well known method, the Russian doll, and we get much better results. Our approach is computationally costly, but the proposed algorithm exhibits an anytime behaviour in which solutions very close to the optimal (less than 9%) are obtained very quickly. These limitations of our approach could be overcome in a future with the combination of liner programming techniques when computing the estimation function.

We are also studying other alternative mechanisms to accelerate the problems solution, as for example, symmetries [8] or learning techniques [5].

Acknowledgements

This research has been partially funded by the Spanish MEC project TIN2004-06354-C02-02 and the DURSI Automation Engineering and Distributed Systems Group, 00296.

References

- [1] Ralf Borndörfer, Uwe Schelten, Thomas Schlechte, and Steffen Weider. A column generation approach to airline crew scheduling. *Berlin-Dahlem: Konrad-Zuse-Zentrum für Informationstechnik*, 2005.
- [2] P. Chu and J. Beasley. A genetic algorithm for the set partitioning problem. *Imperial College, London*, 1995.
- [3] Niklas Kohl and Stefan E. Karisch. Airline crew rostering: Problem types, modeling and optimizacion. *Kluwer Academic Publishers, Annals of Operations Research* 127, 223-257, 2004.
- [4] B. López. Time control in road passenger transportation. problem description and formalization. Research Report IIIA 05-04, University of Girona, 2005.
- [5] Helena Ramalhinho Lourenço, José Pinto Paixao, and Rita Portugal. Metaheuristics for the bus-driver scheduling problem. *Transportation Science*, 3(35):331–343, 2001.
- [6] Claude P. Medard and Nidhi Sawhney. Airline crew scheduling from planning to operations. *Carmen Systems AB, Sweden, Carmen Research and Technology Report CRTR-0406*, 2004.
- [7] Pedro Meseguer and Martí Sánchez. Specializing Russian doll search. *Lecture Notes in Computer Science*, 2239, 2001.
- [8] Pedro Meseguer and Carme Torras. Exploiting symmetries within constraint satisfaction search. *Artif. Intell.*, 129(1-2):133–163, 2001.
- [9] Jasper Möller. Seminar on algorithms and models for railway optimization crew scheduling. *University of Konstanz, Iler-seminar*, 2002.
- [10] J. Murillo. Road passenger transportation: study and resolution with optimization techniques. Msc, University of Girona, July 2006. In Catalan.
- [11] Ravi Sandhu and Diego Klabjan. Integrated airline planning. *Department of Mechanical and Industrial Engineering, University of Illinois at Urbana-Champaign Urbana*, 2004.
- [12] Gerard Verfaillie, Michel Lemaître, and Thomas Schiex. Russian doll search for solving constraint optimization problems. In *AAAI/IAAI, Vol. 1*, pages 181–187, 1996.
- [13] Anthony Wren. Heuristics ancient and modern : Transport scheduling through the ages.
- [14] Tallys H. Yunes, Arnaldo V. Moura, and Cid C. de Souza. A hybrid approach for solving large scale crew scheduling problems. *Lecture Notes in Computer Science*, 1753:293+, 2000.

What Is a Real-World SAT Instance?

Carlos ANSÓTEGUI^a, María Luisa BONET^b, Jordi LEVY^c and Felip MANYÀ^a

^aComputer Science Department, Universitat de Lleida (UdL), Lleida, Spain

^bLlenguatges i Sistemes Informàtics (LSI), Universitat Politècnica de Catalunya (UPC), Barcelona, Spain

^cArtificial Intelligence Research Institute (IIA, CSIC), Bellaterra, Spain

Abstract. Frequently, in the SAT and CSP communities, people talk about real-world problems, without any formal or precise definition of what “real-world” means. This notion is used as opposed to randomly generated problems and theoretical combinatorial principles, like the pigeonhole. People agree that modern SAT and CSP solvers perform well in these real-world problems with a hidden structure, and more so as more intelligent are the strategies used on them.

Here we define a formal notion, called the Strahler number, that measures the degree of structure of an unsatisfiable SAT instance. We argue why this notion corresponds to the informal idea of real-world problem. If a formula has a small Strahler number, then it has a lot of structure, and it is easy to prove it, even if it has many variables. We prove that there is a SAT solver, the Beame-Pitassi algorithm [2], that works on time $O(n^s)$, being n the number of variables, and s the Strahler of the formula. We also show that Horn and 2-SAT unsatisfiable formulas, that can be solved in polynomial time, have Strahler number 1 and 2 respectively.

We compare the Strahler number with other notions defined with the same purpose like backdoors [15], and prove that the Strahler number can be arbitrarily smaller than the size of strong backdoors. We show the same relation for the size of cycle-cutsets and the treewidth in tree decompositions. Finally, we compare with the space of resolution calculus, defined for a different purpose.

Keywords. Propositional satisfiability, Satisfiability algorithms.

Introduction

The notion of real-world problem is used in the SAT and CSP communities to describe those instances that come from “real” problems, as opposed to “artificial” instances randomly generated. It is assumed that practical SAT/CSP solvers have to perform well on these real-world instances, and random ones are believed to have a distinct nature. Most SAT solvers are based on a search process where we try to find a satisfying assignment by iterating the instantiation of some variable. They are also based in some sort of tree-like resolution proof construction, and they spend a lot of time trying to select the best next variable to instantiate, using some heuristics, in order to get a small proof (that usually means shorter computation time). If the tested formula has been randomly generated among a uniformly distributed set of formulas, then all variables look similar to the heuristics, and their instantiations produce similar effects, so the size of the resolution proof is independent of the order we instantiate the variables. Therefore, it is not worth spending time trying to select the best variable. On the other hand, real-world problems,

as a result of the encoding, may contain a significant quantity of dependent variables, and a *hidden structure* worth to be exploited.

Obviously, a better knowledge about the nature of real-world problems would help to design better practical SAT solvers. This was the main motivation of [15], when they defined backdoors. They answer two key questions: (1) What is the size of the backdoors in real-world instances? Experimentally they conclude that they are small. (2) Even taking into account the expense of searching for backdoors, can one still obtain an overall computational advantage using them? They prove that, for constant-bounded backdoor size, there exists a polynomial decision algorithm, being the size of the backdoor its degree. In CSP there are two notions that can also characterize problems with hidden structure: the size of cycle-cutsets, and the treewidth. These two notions also share the good properties of backdoors: when they are constant-bounded, they measure the degree of a polynomial decision algorithm.

In this paper we propose the use of another measure: the minimum Horton-Strahler number of tree-like resolution proofs. Like for the previous ones, we also prove that constant-bounded Strahler implies the existence of a polynomial decision algorithm, being the Strahler the degree of the polynomial (see Theorem 6). Moreover, we prove that the Strahler is smaller than the size of cycle-cutsets and backdoors. Our project can be formalized as:

Find a measure ψ , and an algorithm that given a formula Γ decides satisfiability in time $\mathcal{O}(n^{\psi(\Gamma)})$. The smaller the measure is, the better it characterizes the hardness of a formula.

Therefore, according to this project, the Strahler number characterizes problems with hidden structure, and hence real-world problems, better than strong backdoors and cycle-cutsets. We also show that there are cases where the Strahler number is arbitrarily smaller than the treewidth (one is 2 whereas the other is equal to the number of variables).

To justify the optimality of our measure we use the following argumentation. A problem is “easy” for an actual solver if there is a “small measure” such that instantiating one of the variables (smartly selected) by one truth value, the measure strictly decreases, and instantiating by the other truth value it doesn’t increase. This is the minimum requirement for ensuring polynomial solvability (in the measure) by tree search (being the degree of the polynomial the value of the measure), and this is precisely the Strahler definition. Contrarily, with strong backdoors we force the measure to decrease in *both* sub-trees, and the selected variables are the same in all the branches (the ones belonging to the backdoor). Instead, for Strahler, selected variables don’t have to be the same in all branches.

Finally, we show that the Strahler number corresponds to the *space* of tree-like resolution proofs, a measure used in proof complexity. Therefore, some theoretical results can be imported and help us understand better the nature of some SAT instances.

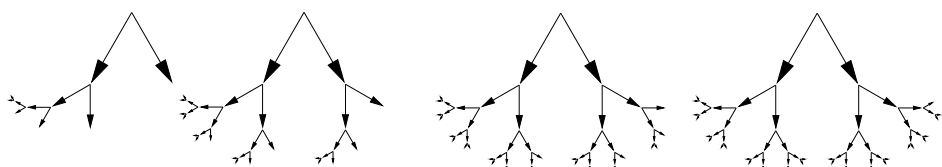


Figure 1. Examples of trees with Strahler equal to 1, 2, 3 and 4.

1. The Strahler of an Unsatisfiable Formula

The *Horton-Strahler number* [11,14] of a tree was originally defined in the area of geology to study the morphology of rivers.¹ Later, it was re-defined, in the area of computer science [6], as the minimum number of registers needed by a CPU to evaluate an arithmetic expression (built up from binary operations) and represented as a binary tree.² The notion is quite natural, and for some people quite unknown, which has propitiated that it had to be re-invented several times. These are three equivalent definitions of the Strahler number of a tree.

Definition 1 (1) *The Strahler number of a (binary) tree is defined recursively as follows.*

$$\begin{aligned} hs(\bullet) &= 0 \\ hs \left(\begin{array}{c} \bullet \\ t_1 \quad t_2 \end{array} \right) &= \begin{cases} hs(t_1) + 1 & \text{if } hs(t_1) = hs(t_2) \\ \max\{hs(t_1), hs(t_2)\} & \text{otherwise} \end{cases} \end{aligned}$$

where \bullet is a node and t_1 and t_2 are trees.

- (2) *The Strahler number of a binary tree t is the depth of the biggest complete tree (i.e. tree where all branches have the same length) that can be embedded into t .*
- (3) *The Strahler number of a binary tree is the minimum number of pointers (memory) that we need in order to traverse it, minus one.*

The Strahler of a tree is bounded by its maximal depth, and both measures are equal in perfectly balanced trees.

Definition 2 *The Strahler of a unsatisfiable CNF formula Γ , noted $hs(\Gamma)$, is defined as the minimum among all the Strahler numbers of tree-like refutations of the formula.*

Notice that the Strahler of a formula is bounded by the number of variables. However, in most of the real-world SAT instances, the Strahler is quite small, compared with the number of variables. In particular, as we will see in Lemma 13, it is smaller than the size of strong backdoors.

Lemma 3 *The Strahler number satisfies the following three properties*

- (1) $hs(\Gamma \cup \{\square\}) = 0$
- (2) *For any unsatisfiable formula Γ , and any truth assignment ϕ , we have $hs(\phi(\Gamma)) \leq hs(\Gamma)$.*
- (3) *For any unsatisfiable formula Γ , if $\square \notin \Gamma$, then there exists a variable x and an assignment $\phi : \{x\} \rightarrow \{0, 1\}$, such that $hs(\phi(\Gamma)) \leq hs(\Gamma) - 1$.*

*The Strahler of a formula is the minimum measure on formulas that satisfy (1), (2) and (3). In other words, we could define the Strahler as:*³

$$\begin{aligned} hs(\Gamma) &= \min_{\substack{x, \bar{x} \in \Gamma \\ b \in \{0, 1\}}} \{ \max\{hs(x \mapsto b(\Gamma)) + 1, hs(x \mapsto \bar{b}(\Gamma))\} \} & \text{if } \square \notin \Gamma \\ hs(\Gamma) &= 0 & \text{if } \square \in \Gamma \end{aligned}$$

¹In this paper we will call it Strahler, to abbreviate.

²In fact the minimum number of register is the Horton-Strahler number plus one.

³Notice that, since Γ is unsatisfiable, it either contains \square or it contains a variable with both signs.

PROOF: (1), (2) and (3) are easy to prove. For the last part, suppose that x and b are the values that give us the minimal. W.l.o.g. assume that $b = 1$. From the proof tree of $x \mapsto b(\Gamma) \vdash \square$, adding the literal \bar{x} in the clauses where $x \mapsto b$ has remove it, but preserving the structure of the proof tree, we get a proof of $\Gamma \vdash \bar{x}$. Since we preserve the structure, we also preserve the Strahler number. We proceed similarly for $x \mapsto \bar{b}(\Gamma) \vdash \square$. Adding a cut of x to these two tree proofs, we get a proof of $\Gamma \vdash \square$, where the Strahler is the maximum between one of the original Strahler numbers, and the other plus one. Hence, satisfies the equality. ■

In most SAT solvers, based in DPLL, we proceed by selecting a variable, instantiating it by a truth value, and later by the contrary, generating two sub-trees in our proof search tree. This process, in the worst case, generates an exponential refutation proof tree, on the number of variables. In the absence of backjumping, clause learning, and other features, the *proof-search tree* has the same size as the *proof tree* resulting from the search. Notice that in real-world instances, it would be worth searching for a smaller proof tree, even on the expense of having a proof search tree bigger than the proof tree. In fact, this is the case with the Beame-Pitassi algorithm described in Theorem 6. The size of a tree with maximal depth n and Strahler s (i.e. the size of the proof tree) is bounded by $2 \sum_{i=1}^s \binom{n}{i}$. Therefore, for formulas with small Strahler $2 \sum_{i=1}^s \binom{n}{i} = O(n^s)$, and the size of the proof tree, and the time needed by the Beame-Pitassi algorithm to find it, are both $\mathcal{O}(n^s)$ (see Theorem 6). For s close to n , the size of the proof tree is $\mathcal{O}(2^n)$, and the time needed $\mathcal{O}(n^n)$.

Lemma 3 helps us understand the goodness of this behavior: when we are forced to try two distinct assignments for a variable, if we are smart enough selecting the variable, we can get, in at least one of the sub-trees, a formula with a strictly smaller Strahler (and the same or smaller in the other). This ensures that, if the Strahler is small, we will avoid the combinatorial explosion of the worst-case.

2. Instances with Small and Big Strahler Number

The DPLL algorithm, as well as all its sequels, introduce important features that make the solvers more efficient than a simple blind check of all possible variable instantiations. In particular, they use the so-called “unit clause propagation”. The following lemma characterizes the set of clauses that can be proved unsatisfiable only using unit propagation, as the formulas with Strahler one. This set of clauses is equal to the set of *Horn renamable* clauses [10], i.e. the set of clauses that using a renaming of variables can be transformed into Horn clauses.

Lemma 4 *A formula Γ is Horn renamable if and only if $hs(\Gamma) \leq 1$.*

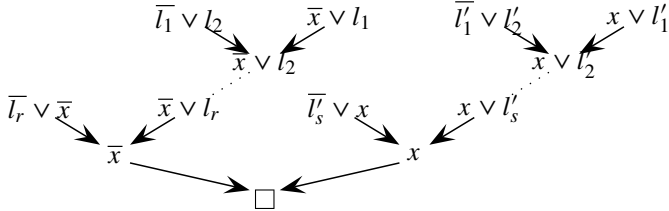
PROOF: The equivalence between Horn renamable clauses and formulas that can be proved only using unit propagation is found in [10]. And the equivalence between these ones and formulas that can be proved by linear tree-like resolution is found in [1].

Now, it is easy to see that linear tree-like resolution proofs have Strahler number equal to one. ■

Lemma 5 *Unsatisfiable 2-CNF formulas have Strahler number at most 2.*

PROOF: If a 2-CNF formula is unsatisfiable, then either it can be proved with unit clause propagation, or we have a cycle of implications $x \rightarrow l_1 \rightarrow \dots \rightarrow l_r \rightarrow \bar{x} \rightarrow l'_1 \rightarrow \dots \rightarrow l'_s \rightarrow x$, for some variable x and a list of pair-wise distinct literals (variables with sign) l_1, \dots, l_r and a similar list l'_1, \dots, l'_s .

In such case, we can construct the following proof with Strahler two:



■

Other measures of the complexity of a problem have been defined in the area of proof complexity. Some of these measures are: the *size* of a tree-like proof, the *space* needed to construct the proof, and the minimal *width* of the largest clause in all proofs of a formula. There are also some relationships between these measures. For instance, $\text{width} \leq \text{space} \leq \text{strahler} \leq \log \text{size}$. We do not use measures smaller than the Strahler because there are not known algorithms that working in time n to the measure and using a reasonable amount of space could check satisfiability.

In [7, Lemma 1.1] it is proved that the space needed in a refutation of a formula coincides with the number of pebbles needed for the pebble game played on a resolution refutation graph of the formula. For tree-like refutations, the number of pebbles coincides with the number of pointers needed to traverse the tree, hence (see Definition 1) with the Strahler number of the proof. Therefore, for tree-like resolution, the Strahler and the space of a formula coincide. This fact allows us to export some theoretical upper and lower bounds for the space, to the Strahler.

In particular, [3] prove that for random k -CNF formulas over n variables, with αn clauses (being $\alpha < 4.506$), with probability tending to 1 as n tends to ∞ , resolution requires space $\Omega(\sqrt{\frac{n}{\alpha}} \frac{\log \frac{n}{\alpha}}{2 \log n})$. Since the space for general resolution is smaller or equal than the space for tree-like resolution, this lower bound also applies to the Strahler of random formulas. This big lower bound explains why random formulas are difficult “practical” SAT instances.

3. Proving Real-World Instances

The algorithm we propose searches for the Strahler number for an unsatisfiable formula starting with Strahler number equals to one. This is done in the function `beamé_pitassi`. For each particular possible Strahler number we apply the procedure `try_strahler`. In this procedure we cycle through all $2n$ possible literals trying to recursively figure out if the formula resulting from falsifying this literal has Strahler number one less. Once we find such a literal, we recursively call `try_strahler` only once with the opposite literal and the same Strahler number. If a satisfying assignment is found with some of the instantiations, the algorithm aborts execution.

Theorem 6 *Satisfiability of a CNF formula Γ can be decided in time $\mathcal{O}(n^{s+1})$, where n is the number of variables, and $s = hs(\Gamma)$.*

```

function try_strahler( $\Gamma, s, \phi$ ) returns  $\langle \text{bool}, \text{prooftree} \rangle$ 
  if  $s = 0$  then return  $\langle \text{false}, \_ \rangle$ 
  if  $\phi$  falsifies a clause  $C \in \Gamma$  then return  $\langle \text{true}, \text{hypothesis}(C) \rangle$ 
  if  $\phi$  satisfies all clauses of  $\Gamma$  then print  $\phi$  return  $\langle \text{true}, \_ \rangle$ 
    foreach variable  $x \notin \text{domain}(\phi)$  and  $b \in \{\text{true}, \text{false}\}$  do
       $\langle \text{found}, t_1 \rangle = \text{try\_strahler}(\Gamma, s - 1, \phi \cup x \mapsto b)$ 
      if found
        then  $\langle \text{found}, t_2 \rangle = \text{try\_strahler}(\Gamma, s, \phi \cup x \mapsto \neg b)$ 
      return  $\langle \text{found}, \text{cut}(x, t_1, t_2) \rangle$ 
    endfor
  return  $\langle \text{false}, \_ \rangle$ 
endfunction

function beame_pitassi( $\Gamma$ )
   $\text{proved} = \text{false}$ 
   $i = 1$ 
  while  $i \leq \text{numvarsof}(\Gamma)$  and  $\neg \text{proved}$  do
     $\langle \text{proved}, \text{proof} \rangle = \text{try\_strahler}(\Gamma, i, \_)$ 
     $i = i + 1$ 
  endwhile
  exit  $\langle \text{unsat}, \text{proof} \rangle$ 
endfunction

```

Figure 2. The code of a variation of the Beame-Pitassi algorithm [2].

PROOF: The algorithm is the adaptation of the Beame-Pitassi algorithm [2] of Fig. 2. Let $T(s, n)$ be the worst-case time needed by the `try_strahler` function to check a formula with n variables and Strahler s . We can establish the recurrence $T(s, n) \leq 2n T(s - 1, n - 1) + T(s, n - 1)$. The solution of this recurrence is $T(s, n) = O(n^s)$. For the `beame_pitassi` function the worst-case time needed is $\sum_{i=1}^s O(n^i) = O(n^{s+1})$. ■

Notice that the size of the proof tree computed by the algorithm is dominated by the recursion $S(s, n) \leq S(s - 1, n - 1) + S(s, n - 1) + 1$, with solution $S(s, n) = 2 \sum_{i=1}^s \binom{n}{i} = O(n^s)$. Notice that for small values of s , this upper bound is tight.

4. The Strahler Number of Satisfiable Formulas

There are several natural extensions of the Strahler definition to satisfiable formulas. Here we propose two of them, resp. denoted by hs^a and hs^b . The following are some standard and preliminary definitions.

Definition 7 Let ϕ be a partial assignment, we define the clause associated to ϕ , noted C_ϕ , as $\bigvee_{\phi(x)=0} x \vee \bigvee_{\phi(y)=1} \bar{y}$.

Given a formula Γ and a partial assignment ϕ , the formula $\phi(\Gamma)$ is the set resulting from Γ after removing all clauses containing a literal x such that $\phi(x) = 1$, and removing all literals x such that $\phi(x) = 0$.

A partial assignment ϕ is said to satisfy a formula Γ if $\phi(\Gamma) = \emptyset$.

Definition 8 Let Γ be a formula, then

$$\begin{aligned} hs^a(\Gamma) &= \max\{hs(\phi(\Gamma)) \mid \phi(\Gamma) \vdash \square\} \\ hs^b(\Gamma) &= hs(\Gamma \cup \{C_\phi \mid \phi(\Gamma) = \emptyset\}) \end{aligned}$$

Notice that both definitions are extensions of the Strahler definition for unsatisfiable formulas: if Γ is unsatisfiable, then $hs(\Gamma) = hs^a(\Gamma) = hs^b(\Gamma)$. We can also prove the following results.

Lemma 9 For any formula Γ , we have $hs^a(\Gamma) \geq hs^b(\Gamma)$

Lemma 10 The adaptation of the Beame-Pitassi algorithm of Figure 2, given a satisfiable formula Γ , finds in time $O(n^{hs^b(\Gamma)})$ a complete set of satisfying assignments.

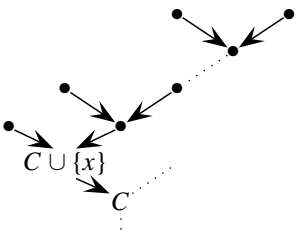
PROOF: Sketch: The algorithm does a similar work for Γ and for $\Gamma \cup \{C_\phi \mid \phi(\Gamma) = \emptyset\}$. The only difference is that, in one case uses the clauses from $\{C_\phi \mid \phi(\Gamma) = \emptyset\}$ to get a contradiction, whereas in the other case prints the satisfying assignment. ■

These results imply that the second definition is better than the first one.

An example of “easy” satisfiable formulas are sudokus encoded as SAT formulas. The complexity of this problem is studied in [13]. In particular, they give the percentage of problems (from a database of sudoku problems) that can be solved with unit propagation and other forms of restricted inference rules. One of these rules is the so-called *failed literal rule* [8]. It is applied as follows, if after assigning $x \rightarrow b$, where $b \in \{0, 1\}$, and performing unit propagation we get a conflict, then we assign $x \rightarrow \bar{b}$. This rule together with the unit clause propagation rule characterizes the set of formulas with Strahler number two.

Lemma 11 *A formula Γ can be proved unsatisfiable only using unit propagation and the failed literal rule, if, and only if, $hs(\Gamma) \leq 2$.*

PROOF:



The proof of the equivalence is similar to the proof of Lemma 4. We only need to notice that the resolution steps corresponding to this restricted form of inference have the form of the left.

In other words, the failed literal rule corresponds to a resolution step where one of the premises has Strahler one, since it is proved only using unit clause propagation. ■

Since all the sudokus analyzed in [13], using the so-called extended encoding (i.e. adding some redundant clauses that make the problem easier), can be solved only using unit clause propagation and the failed literal rule, we can conclude that all these (extended) encodings have Strahler two.

5. Comparison with Backdoors

In this section we compare our results about the Strahler of an unsatisfiable formula with the size of the minimum *strong* backdoor of the formula. In what follows, when we say backdoor we mean *strong* backdoor.

Given a sub-solver A , and a unsatisfiable formula Σ a strong backdoor [15, Definition 2.4] is a subset S of the variables such that, for every partial variable assignment $\phi: S \rightarrow \{0, 1\}$, the sub-solver concludes unsatisfiability for $\phi(\Sigma)$ in polynomial time.

The first thing that must be noticed is that this definition depends on the given sub-solver. For instance, if P turns to be equal to NP , then there would be a polynomial solver for any formula. Therefore, any formula would have the empty set as a strong backdoor! Consequently, we must fix the sub-solver algorithm. In this section, we will assume that it only performs unit clause propagation, i.e. we will assume that, if the sub-solver accepts a formula, and determines its unsatisfiability, then this formula has Strahler one. In [15, Theorem 4.1], it is proved that deciding if a formula with a backdoor of size b is satisfiable is in $\mathcal{O}(p(n) \left(\frac{2n}{b^{1/2}}\right)^b)$, where $p(n)$ is a polynomial, related with

the performance of the sub-solver. In our case, we will assume that $p(n) = n$, as it is the case for the sub-solvers we are considering.

Compared with the performance obtained with the Beame-Pitassi algorithm (Theorem 6) this complexity is better, since we have $b^{1/2}$ in the denominator. However, for constant backdoors sizes and constant Strahler, we have polynomial complexity in both cases, being the Strahler and the backdoor size the exponent of the polynomial.

The following lemma will help us compare the Strahler of a formula with the size of backdoors and cycle-cutsets.

Lemma 12 *Given a formula Γ , a set of variables S , and value $k \geq 0$, if for any assignment $\phi : S \rightarrow \{0, 1\}$ we have $hs(\phi(\Gamma)) \leq k$, then $hs(\Gamma) \leq k + |S|$.*

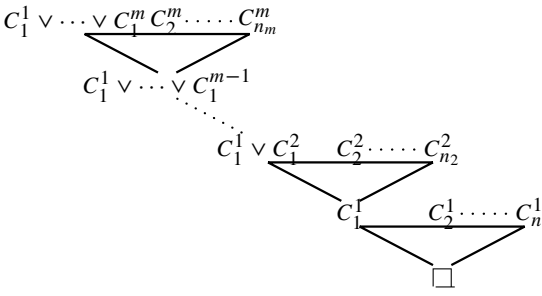
PROOF: For each ϕ , we construct a tree-like resolution proof $\phi(\Gamma) \vdash \square$, with Strahler bounded by k . Now, from ϕ , we construct the clause that falsifies the assignment $C_\phi = \bigvee_{\phi(x)=0} x \vee \bigvee_{\phi(y)=1} \bar{y}$. Adding some of the literals of C_ϕ to the clauses of $\phi(\Gamma)$ we can get Γ . Doing the same to the proof $\phi(\Gamma) \vdash \square$, we get a proof $\Gamma \vdash C'_\phi$, where $C'_\phi \subseteq C_\phi$, with the same structure, hence Strahler number, as the original proof. Therefore, for each one of the $2^{|S|}$ clauses C built up from the variables of S , we have a subclause $C' \subseteq C$, and a proof $\Gamma \vdash C'$. Now, cutting the variables of S we can construct a proof tree of maximal depth $|S|$ that derives the empty clause from the clauses C' . The composition of these trees results in a tree with Strahler bounded by $k + |S|$ that derives the empty clause from Γ . ■

From this lemma, assuming that the sub-solvers used in the backdoor technique only accept formulas satisfying $hs(\Gamma) = 1$, we can conclude:

Lemma 13 *Given a sub-solver A that only accepts formulas with Strahler one, if the subset of variables S is a strong backdoor in the formula Γ , then $hs(\Gamma) \leq |S| + 1$.*

On the other hand, the Strahler number may be arbitrarily smaller than the size of strong backdoors, as the following example shows.

Example 14 Assume that the following family of unsatisfiable formulas $\Gamma^j = \{C_1^j, \dots, C_{n_j}^j\}$ are difficult for the sub-solver, for $j = 1, \dots, m$, and assume that they have disjoint variables. Let b^j be the minimal size of backdoors of Γ^j . Let us define the unsatisfiable formula $\Gamma = \{C_1^1 \vee \dots \vee C_1^m\} \cup \bigcup_{j=1}^m \{C_2^j, \dots, C_{n_j}^j\}$.



To get an easy formula for the sub-solver we have to instantiate all variables of some backdoor of each subformula, hence the size of minimal backdoors of Γ is $\sum_{j=1}^m b^j$. However, the Strahler of Γ is bounded by $\max_{j=1}^m \{hs(\Gamma^j)\} + 1$. To prove the statement, we can construct the refutation tree on the left.

The backdoor size satisfies the following property: for any formula Γ , there exists a variable x , such that for any assignment $\phi : \{x\} \rightarrow \{0, 1\}$, we have

$\text{backdoorsize}(\phi(\Gamma)) \leq \text{backdoorsize}(\Gamma) - 1$. Therefore, the backdoor size decreases in both subtrees of the proof. Notice that this property is similar to property (3) of lemma 3, but more restrictive. This results into a bigger measure.

6. Comparison with Cycle-CutSets and Treewidth

In the area of CSP there are two prototypical solving methods: one based on cycle-cutset decompositions, and the other based on tree decompositions. Since SAT is a special case of CSP, we can export these methods to SAT.

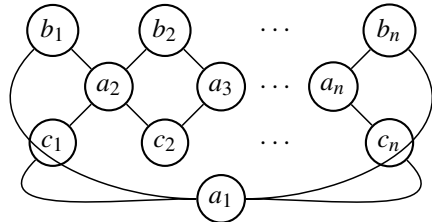
The cycle-cutset technique consists in breaking cycles in graphs of variable dependencies (here, two variables are dependent if they share the same clause) by instantiating some of the variables. A cycle-cutset is a set of variables that after instantiation transform the dependency graph into a tree. Once we have a tree of dependencies, we can apply simple methods to get the instances of the rest of variables. Therefore, the size of minimal cycle-cutsets gives an idea of how hard a problem is, in fact the method has a time complexity $O(n 2^c)$, where n is the number of variables, and c the cycle-cutset size. However, we can prove that the Strahler number is smaller than the size of the cycle-cutset:

Lemma 15 *For any formula Γ , with a cycle-cutset S we have $hs(\Gamma) \leq |S| + 1$.*

PROOF: Sketch: The proof is similar to Lemma 13. After instantiating the cycle-cutset variables, we get a formula with a dependency graph with tree shape. This formula is Horn renamable, hence its Strahler is at most one. ■

Example 16 The following unsatisfiable formula has Strahler two (since it is a 2-CNF). However, its graph of variable dependencies contains n independent cycles. Therefore, the cycle-cutset size is n .

$$\left\{ \begin{array}{l} \overline{a_i} \vee b_i \\ b_i \vee a_{i+1} \\ \overline{a_{i+1}} \vee c_i \\ \overline{c_i} \vee a_i \end{array} \right\}_{i=1,\dots,n-1} \cup \left\{ \begin{array}{l} \overline{a_n} \vee b_n \\ \overline{b_n} \vee \overline{a_1} \\ a_1 \vee c_n \\ \overline{c_n} \vee a_n \end{array} \right\}$$



The previous lemma and example show that the Strahler of a formula is always smaller than the cycle-cutset size, and can be arbitrarily smaller. Therefore the Strahler is a better measure to study how easy a SAT instance is. Obviously, the separation only applies to SAT as a particular case of CSP.

In the tree decomposition method [5], we put some variables into clusters of variables and structure those clusters as a tree satisfying (1) for every clause, all its variables are inside some of the clusters, and (2) for every variable, the set of clusters containing this variable induces a (connected) subtree. With this method we get a complexity $\mathcal{O}(n 4^w \log n)$, where n is the number of variables, and w is the treewidth of the decomposition (i.e. the size of the biggest cluster). As it is proved in [9], this method is *better* than the cycle-cutset method. However, like cycle-cutsets, it characterizes tractability due to the structure, not to the constraint relation. This makes easy to find, similarly to Exam-

ple 16, an unsatisfiable set of clauses where every variable is related with every variable by a binary clause. This formula has Strahler number 2, but the treewidth is equal to the number of variables.

7. Conclusions and Further Questions

We have proposed the use of the Strahler number of a formula as a measure of the complexity of proving the unsatisfiability of the formula by tree-like resolution. We also propose the use of the Beame-Pitassi algorithm, or variants, as a proof-search algorithm when the Strahler of the formula is small, i.e. in real-world SAT instances.

Several questions arise from this work:

Can we establish a relationship between the treewidth and the Strahler? In particular, is it possible to prove that the second is smaller than the first, like we do for the size of cycle-cutsets?

Classical DPLL can be seen as a variant of Beame-Pitassi where we first try to prove a subtree by unit-propagation (i.e. with Strahler bounded by one), and in case of failure, with any Strahler number. The Beame-Pitassi algorithm tries Strahler $s - 1$. What makes more sense is to keep trying increasing Strahler numbers starting from 1, for one of the recursive calls to `try_strahler` (as it is done in the function `beame_pitassi`). We are currently exploring this implementation.

References

- [1] P. Beame, H. A. Kautz, and A. Sabharwal. Towards understanding and harnessing the potential of clause learning. *J. of Artificial Intelligence Research*, 22:319–351, 2004.
- [2] P. Beame and T. Pitassi. Simplified and improved resolution lower bounds. In *Proc. of the 37th Annual Symposium on Foundations of Computer Science, FOCS'96*, pages 274–282, 1996.
- [3] E. Ben-Sasson and N. Galesi. Space complexity of random formulae in resolution. *Random Struct. Algorithms*, 23(1):92–109, 2003.
- [4] J. M. Crawford and L. D. Anton. Experimental results on the crossover point in satisfiability problems. In *Proc. of the 11th National Conf. on Artificial Intelligence, AAAI'93*, pages 21–27, 1993.
- [5] R. Dechter and J. Pearl. Tree clustering for constraint networks. *Artificial Intelligence*, 38(3):353–366, 1989.
- [6] A. P. Ershov. On programming of arithmetic operations. *Communications of the ACM*, 1(8):3–6, 1958.
- [7] J. L. Esteban and J. Torán. Space bounds for resolution. *Information and Computation*, 171(1):84–97, 2001.
- [8] J. W. Freeman. *Improvements to Propositional Satisfiability Search Algorithms*. PhD thesis, University of Pennsylvania, 1995.
- [9] G. Gottlob, N. Leone, and F. Scarcello. A comparison of structural CSP decomposition methods. *Artificial Intelligence*, 124(2):243–282, 2000.
- [10] L. J. Henschen and L. Wos. Unit refutations and Horn sets. *J. of the ACM*, 21(4):590–605, 1974.
- [11] R. E. Horton. Erosion development of streams and their drainage basins, hydrophysical approach to quantitative morphology. *Bull. Geol. Soc. of America*, 56:275–370, 1945.
- [12] C. M. Li and Anbulagan. Look-ahead versus look-back for satisfiability problems. In *Proc. of the 3th Int. Conf. on Principles and Practice of Constraint Programming, CP'97*, pages 341–355, 1997.
- [13] I. Lynce and J. Ouaknine. Sudoku as a SAT problem. In *Proc. of the 9th Int. Symp. on Artificial Intelligence and Mathematics, AIMATH'06*, 2006.
- [14] A. N. Strahler. Hypsometric (area-altitude) analysis of erosional topology. *Bull. Geol. Soc. of America*, 63:1117–1142, 1952.
- [15] R. Williams, C. P. Gomes, and B. Selman. Backdoors to typical case complexity. In *Proc. of the International Joint Conf. Artificial Intelligence, IJCAI'03*, 2003.

Mendelian error detection in complex pedigrees using weighted constraint satisfaction techniques

Marti SANCHEZ^a, Simon DE GIVRY^a and Thomas SCHIEUX^a

^a {msanchez,degivry,tschiex}@toulouse.inra.fr

INRA-UBIA Toulouse, France

Abstract. With the arrival of high throughput genotyping techniques, the detection of likely genotyping errors is becoming an increasingly important problem. In this paper we are interested in errors that violate Mendelian laws. The problem of deciding if Mendelian error exists in a pedigree is NP-complete [1]. Existing tools dedicated to this problem may offer different level of services: detect simple inconsistencies using local reasoning, prove inconsistency, detect the source of error, propose an optimal correction for the error. All assume that there is at most one error. In this paper we show that the problem of error detection, of determining the minimum number of error needed to explain the data (with a possible error detection) and error correction can all be modeled using soft constraint networks. Therefore, these problems provide attractive benchmarks for weighted constraint network (WCN) solvers. Because of their sheer size, these problems drove us into the development of a new WCN solver `toulbar2`¹ which solves very large pedigree problems with thousands of animals, including many loops and several errors. This paper is a summary of an extended version to appear [17].

Keywords. Constraint Satisfaction Problems, Bayesian Networks, Bioinformatics.

Biological background and motivations

A pedigree is defined by a set of individuals, their parental relationship and their associated genetic information. For each individual we consider its *genotype*, that is the pair of *alleles* (genetic information at one position in the chromosome) inherited from the parents. An individual is called a founder if its parents are not among the individuals present in the pedigree. Genotypes are not always completely observable and the indirect observation of a genotype (its expression) is termed the *phenotype*. The genetic information may be corrupted because of experimental and human errors. We only consider in this paper typing errors, also called phenotype error. A typing/phenotype error means simply that the phenotype in the pedigree is incompatible with the true (unknown) genotype. Phenotype errors are also called Mendelian errors when they make a pedigree inconsistent with Mendelian law of inheritance which states that the pair of alleles of every individual is composed of one paternal and one maternal allele. The problem of checking pedigree consistency is actually shown to be NP-complete in [1].

The detection and correction of errors is crucial before the data can be further exploited. Because of its NP-completeness, most existing tools only offer a limited polynomial time checking procedure. The different tools we are aware of that try to tackle this problem are either incomplete, restricted by strong assumptions (such as unique error), or incapable of dealing with large problems.

In this paper, we introduce soft constraint network models, the problem of determining the minimum number of errors needed to explain the data and the problem of proposing an optimal correction to an error. In Section 2, we describe the algorithms used to solve these problems. We report extensive results using the weighted constraint network solver `toulbar2` and other solvers in Section 3.

1. Modeling the problems

A Weighted Constraint Network (WCN) $(\mathcal{X}, \mathcal{D}, \mathcal{C})$ [6] is defined by a set of n variables $\mathcal{X} = \{x_1, \dots, x_n\}$, a set of matching domains $\mathcal{D} = \{D_1, \dots, D_n\}$ with maximum size equal to d and a set of e constraints \mathcal{C} . Every variable $x_i \in \mathcal{X}$ takes its value in the associated domain D_i . A constraint $c_S \in \mathcal{C}$ is a cost function that assigns an integer cost (from 0 to a maximum k) to all the possible assignments of variables in S . The minimum and maximum costs will be also denoted by \perp and \top . We redefine the sum to include an absorbing element k : $a \oplus b = \min\{k, a + b\}$. The set S is called the scope of the constraint and $|S|$ its arity. For every variable assignment A , $c_S(A[S]) \in N$ represents the cost of the constraint for the given assignment where $A[S]$ is the projection of A on the constraint scope S . In this paper we consider arities of one, two and three: a unary weighted constraint C_i is a cost function $C_i(a \in D_i) \rightarrow [0..k]$. A binary constraint C_{ij} is a cost function $C_{ij}(a \in D_i, b \in D_j) \rightarrow [0..k]$. A ternary constraint C_{ijl} is a cost function $C_{ijl}(a \in D_i, b \in D_j, c \in D_l) \rightarrow [0..k]$. We assume the existence of a unary constraint C_i for every variable and a zero-arity constraint (i.e. a constant), noted C_\emptyset .

The aim is then to find an assignment A of all variables such that the sum of all tuple costs $\bigoplus_{c_S \in \mathcal{C}} c_S(A[S])$ is minimum. This is called the Weighted Constraint Satisfaction Problem (WCSP), and is NP-hard. Several recent algorithms for tackling this problem, all based on the maintenance of local consistency properties have been recently proposed [8,4,7]. They are presented in Section 2.

Now consider a pedigree defined by a set I of individuals. For a given individual $i \in I$, we note $pa(i)$ the set of parents of i . Either $pa(i) \neq \emptyset$ (non founder) or $pa(i) = \emptyset$ (founder). At the locus considered, the set of possible alleles is denoted by $\{1, \dots, m\}$. Therefore, each individual carries a genotype defined as an unordered pair of alleles (one allele from each parent, both alleles can be identical). The set of all possible genotypes is denoted by G and has cardinality $\frac{m(m+1)}{2}$. For a given genotype $g \in G$, the two corresponding alleles are denoted by g^l and g^r and the genotype is also denoted as $g^l | g^r$. By convention, $g^l \leq g^r$ in order to break symmetries between equivalent genotypes (e.g. $1|2$ and $2|1$). The experimental data is made of phenotypes. For each individual in the set of observed individuals $I' \subset I$, its observed phenotype restricts the set of possible genotypes to those which are compatible with the observed phenotype. This set is denoted by $G(i)$ (very often $G(i)$ is a singleton, observation is complete).

A corresponding weighted constraint network encoding this information uses one variable per individual i.e. $\mathcal{X} = I$. The domain of every variable $i \in \mathcal{X}$ is simply defined

as the set of all possible genotypes G . If an individual i has an observed phenotype, a unary soft constraint that involves the variable i is added. To model the possibility of typing errors, genotypes in G which are incompatible with the observed phenotype $G(i)$ should not be completely forbidden. Instead, a soft constraint forbids them with a cost of 1 (since using such a value represents one typing error). Finally, to encode Mendelian law, and for every non founder individual $i \in X$, a single ternary constraint involving i and the two parents of i , $pa(i) = \{j, k\}$ is added. This constraint assigns cost 0 to triples (g_i, g_j, g_k) of genotypes that verify Mendelian inheritance *i.e.* such that one allele of g_i appears in g_j and the other appears in g_k . Equivalently: $(g_i^l \in g_j \wedge g_i^r \in g_k) \vee (g_i^l \in g_k \wedge g_i^r \in g_j)$. Ternary constraints assign the maximum cost k to forbidden combinations. For a pedigree with n individuals among which there are f founders, with m possible alleles, we obtain a final WCSP with n variables, a maximum domain size of $\frac{m(m+1)}{2}$, n unary constraints (the unobserved individuals have a trivially null unary constraint) and $n - f$ ternary constraints.

If we consider an assignment of all variables to indicate the real genotype of all individuals, the sum of all the costs induced by all unary constraints on this assignment precisely gives the number of errors made during typing. Finding an assignment with a minimum number of errors follows the traditional parsimony principle (or Occam's razor) and is consistent with a low probability of independent errors (quite reasonable here). This defines the Parsimony problem. One solution of the corresponding WCSP with a minimum cost therefore defines a possible diagnostic. The model shifts from satisfaction to optimization.

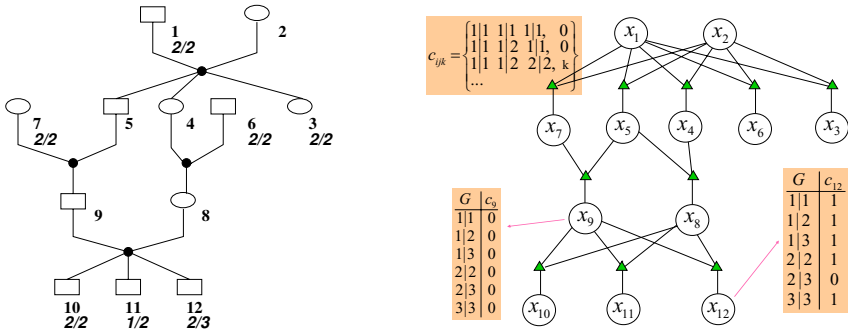


Figure 1. Left: A pedigree taken from [14]. Right: its corresponding WCSP.

Example 1 An example is given in Fig. 1. There are $n = 12$ individuals and $m = 3$ alleles. A box corresponds to a male individual and an ellipse to a female. The arcs describe parental relations (individuals 1 and 2 have three children 3,4, and 5). Individuals 1,2,6, and 7 ($f = 4$) are founders. The possible genotypes are $G = \{1|1, 1|2, 1|3, 2|1, 2|2, 2|3, 3|1, 3|2, 3|3\}$. 7 individuals (1,3,6,7,10,11, and 12) have an observed phenotype (a single genotype). The corresponding WCSP has 12 variables, 8 ternary constraints and 7 soft unary constraints. The minimum number of typing errors is one. An optimal solution is $\{(1,2|2), (2,1|2), (3,2|2), (4,1|2), (5,2|2), (6,2|2), (7,2|2), (8,1|2), (9,2|2), (10,2|2), (11,1|2), (12,2|2)\}$ such that the erroneous typing 2|3 of individual 12 has been changed to 2|2.

1.1. Error correction

When errors are detected, one would like to optimally correct them. The simple parsimony criterion is usually not sufficient to distinguish alternative values. More information needs to be taken into account. Being errors and Mendelian inheritance typically stochastic processes, a probabilistic model is attractive. A Bayesian network is a network of variables related by conditional probability tables (CPT) forming a directed acyclic graph. It allows to concisely describe a probability distribution on stochastic variables. To model errors, a usual approach is to distinguish the observation O and the truth T . A CPT $P(O|T)$ relates the two variables and models the probability of error.

Following this, we consider the following model for error correction: we first have a set of n variables T_i each representing the true (unknown) genotype of individual i . The domain is G . For every observed phenotype, an extra observed variable O_i is introduced. It is related to the corresponding true genotype by the CPT $P_i^e(O_i|T_i)$. In our case, we assume that there is a constant α probability of error: the probability of observing the true genotype is $1 - \alpha$ and the remaining probability mass is equally distributed among remaining values.

For the individual i and its parents $pa(i)$, a CPT $P_i^m(T_i|pa(i))$ representing Mendelian inheritance connects T_i and its corresponding parent variables. Finally, prior probabilities $P^f(i)$ for each genotype must be given for every founder i . These probabilities are obtained by directly estimating the frequency of every allele in the genotyped population. The probability of a complete assignment $P(O, T)$ (all true and observed values) is then defined as the product of the three collections of probabilities (P^e, P^m and P^f). Note that equivalently, its log-probability is equal to the sum of the logarithms of all these probabilities.

The evidence given by the observed phenotypes $G(i)$ is taken into account by reducing the domains of the O_i variables to $G(i)$. One should then look for an assignment of the variables $T_i, i \in I'$ which has a maximum a posteriori probability (MAP). The MAP probability of such an assignment is defined as the sum of the probabilities of all complete assignments extending it and maximizing it defines an NP^{PP} -complete problem [15], for which there exists no exact methods that can tackle large problems. The PEDCHECK solver [13,14] tries to solve this problem using the extra assumption of a unique already identified error. This is not applicable in large data-sets. Another very strong assumption (known as the Viterbi assumption) considers that the distribution is entirely concentrated in its maximum and reduces MAP to the so-called Maximum Probability Explanation problem (MPE) which simply aims at finding a complete assignment of maximum probability. Using logarithms this problem directly reduces to a WCSP problem where each CPT is transformed in an additive cost function. This allows to solve MPE using WCSP dedicated tools.

2. Soft constraint algorithms: extension to ternary constraints

In order to find an optimal solution and prove its optimality, a classical depth-first branch and bound algorithm is applied. An initial upper bound (\top) is given by the number of genotyping data plus one for the parsimony pedigree problem. For MPE, we multiply for each individual the minimum probabilities different from zero of P^e, P^m and P^f (see

Section 1.1) and take the opposite of its logarithm (to get additive positive costs). Each time a better solution is found, its cost becomes the new upper bound.

Inside branch and bound at each node of the search we enforce a local consistency. In this section, we present several local consistency properties, previously defined for binary constraints [7] and extended to the case of ternary constraints in order to deal with our pedigree problem. The technical difficulty resides in the simultaneous enforcement of two important soft local consistency properties (AC and DAC which are defined below) in polynomial time. We show how to enforce DAC in one direction of a ternary constraint without breaking AC in the two other directions. This allows to close an open question from [4] (Section 4) “whether a form of directional k-consistency can be established in polynomial time for $k > 2$ ”. The answer is yes for ternary constraints and we believe it can be generalized to any bounded constraint arity.

Two WCSPs defined over the same variables are said to be *equivalent* if they define the same cost distribution on complete assignments. Local consistency properties are widely used to transform problems into equivalent simpler ones. When enforcing a local consistency property at every node of the search, implicit costs can be deduced and so the search space can be hopefully reduced and variable values pruned earlier (a non trivial lower bound is given by C_\emptyset).

The simplest form of local consistency we used is node consistency (NC): $\forall x_i \in \mathcal{X}, (\exists a \in D_i / C_i(a) = \perp) \wedge (\forall a \in D_i / C_\emptyset \oplus C_i(a) < \top)$. Any WCSP can be easily transformed into an equivalent NC instance by projecting every unary constraint towards C_\emptyset and subsequently pruning unfeasible values. We continue by extending the notion of soft (directional) arc consistency to ternary cost functions, for this, we extend the classic notion of support. Given a binary constraint C_{ij} , $b \in D_j$ is a *simple support* for $a \in D_i$ if $C_{ij}(a, b) = \perp$. Similarly, for directional arc consistency, $b \in D_j$ is a *full support* for $a \in D_i$ if $C_{ij}(a, b) \oplus C_j(b) = \perp$.

For a ternary cost function C_{ijk} , we say that the pair of values $(b \in D_j, c \in D_k)$ is a simple support for $a \in D_i$ if $C_{ijk}(a, b, c) = \perp$. Similarly, we say that the pair of values $(b \in D_j, c \in D_k)$ is a full support for $a \in D_i$ if $C_{ijk}(a, b, c) \oplus C_{ij}(a, b) \oplus C_{ik}(a, c) \oplus C_{jk}(b, c) \oplus C_j(b) \oplus C_k(c) = \perp$.

A WCSP is arc consistent (AC) if every variable is NC and every value of its domain has a simple support in every constraint. Given a static variable ordering, a WCSP is directional arc consistent (DAC) if every value of every variable x_i has a full support in every constraint C_{ij} such that $j > i$ and in every constraint C_{ijk} such that $j > i \wedge k > i$. A WCSP is full directional arc consistent (FDAC) if it is both AC and DAC [8].

The enforcing of simple and full supports for ternary constraints has to be carefully adapted from the previous existing algorithms for binary constraints. The idea is to extend unary and binary costs involved in the scope of ternary constraint C_{ijk} in such a way that a maximum projection is achievable on variable i without losing simple supports for variables j and k . The details of how this extension is done, proofs and implementation are given in the longer version [17].

The strongest form of local consistency we use is existential directional arc consistency (EDAC) [7]. A WCSP is existential arc consistent (EAC) if every variable x_i has at least one value $a \in D_i$ such that $C_i(a) = \perp$ and a has a full support in every constraint. A WCSP is EDAC if it is both FDAC and EAC. EAC enforcement is done by finding at least one *fully supported* value per variable i.e. which is fully supported in all directions.

If there is no such value for a given variable, then projecting all the constraints towards this variable will increase the lower bound, resulting in at least one *fully supported* value.

The complexity of ternary EDAC is time $O(ed^3 \max\{nd, T\})$ and space $O(ed^2)$, where n is the number of variables, d is the maximum domain size, e is the number of constraints and T is the maximum cost. The proof can be found in [17].

We maintain EDAC during search, producing a lower bound in C_\emptyset . The DAC variable ordering corresponds to the pedigree file order, which is usually a temporal order. If $C_\emptyset \geq T$ then, the algorithm backtracks. We use dynamic variable and value ordering heuristics. We add a basic form of conflict back-jumping by always choosing the last variable in conflict (i.e. its assignment results in an empty domain or $C_\emptyset \geq T$) [10]. The value ordering heuristic chooses first the fully supported value found by EAC. We use a binary branching scheme: the chosen variable is assigned to its fully supported value or this value is removed from its domain. Finally, we apply a limited form of variable elimination during the search as proposed in [9].

3. Experimental evaluation

In the experimental section we want to compare the accuracy of error detection for the different models introduced: MAP, MPE and Parsimony. The most complex MAP problem is a mixed optimization/integration problem that can be only solved by dedicated Bayes net solvers. Among them, we have chosen Samiam (version 2.2.1) because it is one of the most efficient and robust solver available according to the last BN solving competition. The MPE problem is a pure optimization problem which requires however to be able to deal with very large costs such as those produced by logarithms of probabilities (see Section 2). These problems can be addressed again by Samiam but also by toolbar2 which has been extended to use very large integer costs. MPE can only be solved on small or mid-size instances. Finally, the simplest Parsimony problem can be directly tackled by toolbar2. We also used a version of toolbar called toolbar/BTD which integrates a specific tree-decomposition based branch and bound (version 2.2) [5] that should perform well on pedigree problems which have usually a tree-width much smaller than the number of variables. It also uses only binary EDAC and thus will show the interest of higher order consistencies. Parsimony problem can be solved on very large instances.

Because the pedigree analysis problem is not a new problem, one must also acknowledge the existence of different solvers for the real problem. However, none of these tools will be considered in the analysis because they either make very strong assumptions incompatible with the pedigree size considered (PedCheck [13] assumes that there is only one error), may be incomplete solvers (CheckFam [16] can prove inconsistency but produces only local corrections on nuclear families that may not always restore consistency while GenCheck [2] provide corrections that do not optimize parsimony of likelihood either) or have very limited efficiency compared to the solvers considered here (GMCheck [18] tackles the MPE problem but is totally dominated by SamIam).

Two types of pedigree have been used to perform the evaluation: random pedigree and real pedigree. The random pedigree have been generated using a pedigree generator designed by geneticists at INRA. We then randomly erase the genotypes of some individuals with a given probability and introduce errors in some individuals with a given

probability. The original correct genotypes are recorded in order to be able to evaluate the accuracy of error correction. We used a genotyping error probability $\alpha = 5\%$ (see Section 1.1). For random pedigree, all experiments have been performed on a 3 GHz Intel Xeon with 2 Gb of RAM.

Real instances are human genotyped pedigrees (genetic studies of eye, cancer and Parkinson diseases) as reported in [13,14] and two groups (*berrichon* and *langlade*) are pedigree instances coming from sheep animals provided by the CTIG (*Centre de Traitement de l'Information Génétique*) in France. For real pedigree, all experiments have been performed on a 3 GHz Intel Xeon 64-bit with 16 Gb of RAM.

To compare the error prediction accuracy provided by the MAP, MPE and Parsimony, we had to limit ourselves to relatively small instances that could be solved to optimality by Samiam. The MPE problem has been solved using `toulbar2` and Samiam. Finally, Parsimony was solved using `toulbar2` only.

Two features were evaluated: the prediction of the individuals (denoted *ind*) containing an error in the pedigree and the prediction of the correct genotype (denoted by *geno*). The sensitivity of the prediction is the percentage of features that should be detected which are actually correctly predicted. Similarly, specificity is percentage of predicted features which are correct. Summarizing, MAP has 10% higher genotype specificity, meaning that is more robust in predicting the corrections of genotypes, as expected. However, it is too costly in terms of CPU time and can only deal with small instances. MPE gives very similar results while Parsimony is interesting for just restoring consistency. In our experiments `toulbar2` outperforms Samiam on the MPE problem. We further compared Parsimony and MPE on larger data sets using `toulbar2`. This is reported in Fig. 2. MPE has nearly a 10% better individual sensitivity and a 15% better genotype sensitivity and specificity on larger problems. We observe that the CPU-time needed to solve the instances is highly sensible to the treewidth for both MPE and Parsimony. For tree-widths above 50, `toulbar2` encountered some hard MPE instances it could not solve in the time limit².

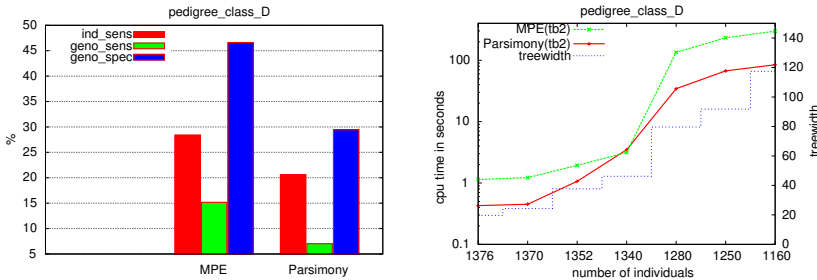


Figure 2. Left: Histograms compare the sensitivities and specificities of MPE and Parsimony. Right: `toulbar2` CPU-time for both problems.

Since our aim is to solve very large real size instances, we conclude the evaluation by comparing time efficiency of different solvers on the simplest Parsimony problem. Indeed, on the largest real instances defined by the sheep pedigree, MPE remained un-

²Notice that the treewidth is anti-monotone in the number of individuals. This is because the increase in the treewidth is achieved (parameterizing the simulator) by increasing the number of males in a population. Increasing the number of males has the side effect of decreasing the number of individuals.

solvable in less than 10 hours. Despite its lower accuracy, Parsimony still provides the essential service of consistency restoration and this with minimum loss of data, a criterion that may look attractive in practice to biologists.

We tried several solvers and observed that as the problem size increases, `toulbar2` has the best performance. In fact only `toulbar2` is able to tackle real pedigree instances. For the parsimony problem, we were able to solve real pedigrees with up to 120,000 individuals in a few seconds. These problems were modeled as soft constraint networks with up to 9,500 variables and 17,000 constraints (after `toulbar2` preprocessing and variable elimination). All real pedigrees can be solved in a maximum of one minute of CPU time and have from 2 to 106 errors found. Solving such a large network is possible thanks to the powerful lower bounds provided by soft local consistencies, in particular EDAC extended to ternary constraints. As the size of instances increase EDAC is an order of magnitude better. The combination of the conflict heuristic and variable elimination has the best performance and corresponds to the combination used in all the previous experiments.

4. Conclusion

This paper deals with detecting Mendelian errors and providing an optimal correction. Compared to existing tools dedicated to this problem [13,16,2,18], the novelty of our approach is to provide an optimal correction based on parsimony or maximum likelihood criterion for large pedigree data. This application lead us to the development of new algorithms, described in Section 2, for ternary constraints. We believe this result can be directly generalized to n -ary constraints, by considering all the intermediate arity levels. Using the parsimony model and the dedicated extension to ternary constraints we were able to solve large real pedigree instances of 9,500 variables that were unsolved up to now.

For MAP and MPE, we have shown on simulated data that MPE is a good approximation of MAP and is orders of magnitude faster to solve than MAP. However, on large real pedigrees, MPE could not be solved by `toulbar2`.

In the future, we will explore more complex probabilistic models in order to detect non Mendelian errors. It implies working on multi-locus models, where other interesting biological questions have been recently investigated by the AI community [11,12].

References

- [1] Aceto, L., Hansen, J. A., Ingólfssdóttir, A., Johnsen, J., and Knudsen, J. The complexity of checking consistency of pedigree information and related problems. *Journal of Computer Science Technology* 19, 1 (2004), 42–59.
- [2] J. Bennewitz and N. Reinsch and E. Kalm GENCHECK: A program for consistency checking and derivation of genotypes at co-dominant and dominant loci *Journal of Animal Breeding and Genetics* (2002), 119(5):350-360.
- [3] Bistarelli, S., Fargier, H., Montanari, U., Rossi, F., Schiex, T., and Verfaillie, G. Semiring-based CSPs and valued CSPs: Frameworks, properties and comparison. *Constraints* 4 (1999), 199–240.
- [4] M. Cooper. High-order Consistency in Valued Constraint Satisfaction. *Constraints*, 10(3):283–305, 2005.
- [5] S. de Givry and T. Schiex and G. Verfaillie Exploiting tree decomposition and soft local consistency in weighted CSP. In *Proc. of AAAI-06*, page 6p., Boston, MA, 2006.

- [6] Dechter, R. *Constraint Processing*. Morgan Kaufmann Publishers, 2003.
- [7] Larrosa, J., de Givry, S., Heras, F., and Zytnicki, M. Existential arc consistency: getting closer to full arc consistency in weighted CSPs. In *Proc. of the 19th IJCAI* (Aug. 2005).
- [8] Larrosa, J., and Schiex, T. In the quest of the best form of local consistency for weighted CSP. In *Proc. of the 18th IJCAI* (Aug. 2003), pp. 239–244.
- [9] J. Larrosa, E. Morancho and D. Niso On the practical applicability of Bucket Elimination: Still-life as a case study. *Journal of Artificial Intelligence Research* (2005), 23 :421-440.
- [10] C. Lecoutre and L. Sais and S. Tabary and V. Vidal Last Conflict based Reasoning. In *Proc. of ECAI-06* (2006), pp. 133–137, Trento, Italy.
- [11] I. Lynce and J.P. Marques Silva Efficient Haplotype Inference with Boolean Satisfiability. In *Proc. of AAAI-06*, page 6p., Boston, MA, 2006.
- [12] R. Marinescu and R. Dechter Memory Intensive Branch-and-Bound Search for Graphical Models. In *Proc. of AAAI-06*, page 6p., Boston, MA, 2006.
- [13] O'Connell and Weeks PedCheck: a program for identification of genotype incompatibilities in linkage analysis. *American Journal of Human Genetics* 63, 1 (1998), 259–66.
- [14] O'Connell and Weeks An optimal algorithm for automatic genotype elimination. *American Journal of Human Genetics* 65, 6 (1999), 1733–40.
- [15] Park, J. D., and Darwiche, A. Complexity results and approximation strategies for map explanations. *Journal of Artificial Intelligence Research* 21 (2004), 101–133.
- [16] Saito, M. and Saito, A. and Kamatani, N. Web-based detection of genotype errors in pedigree data. *Journal of human genetics* (2002), 47(7):377-379.
- [17] Sanchez, de Givry, Schiex Mendelian error detection in complex pedigrees using weighted constraint satisfaction techniques. *Constraints* Special issue on Bioinformatics, to appear.
- [18] Thomas, A. GMCheck: Bayesian error checking for pedigree genotypes and phenotypes *Bioinformatics* (2005), 21(14):3187–3188.

Distributed Meeting Scheduling

Ismel BRITO ^aand Pedro MESEGUER ^{a,1}

^a *IIIA, Institut d'Investigació en Intel·ligència Artificial
CSIC, Consejo Superior de Investigaciones Científicas
Campus UAB, 08193 Bellaterra, Spain*

Abstract. Meetings are an important vehicle for human communication. The Meeting Scheduling problem (*MS*) is a decision-making process affecting several people, in which it is necessary to decide *when* and *where* several meetings could be scheduled. *MS* is a naturally distributed problem which has a clear motivation to be tried using distributed techniques: people may desire to preserve the already planned meetings in their personal calendars during resolution. In this paper, we evaluate three distributed algorithms for *MS* according to efficiency and privacy loss. Two of these algorithms view *MS* as a Distributed Constraint Satisfaction problem.

Keywords. meeting scheduling, distributed constraint satisfaction

1. Introduction

The Meeting Scheduling problem (*MS*) consists of a set of people which use their personal calendars to determine *when* and *where* one or more meeting(s) could take place [4]. This problem is naturally distributed because (1) each person knows only his/her own personal calendar before resolution and (2) people may desire to preserve the already planned meetings in their personal calendars during resolution. In the centralized approach, all people must give their private information to one person, who solves the problem and returns a solution. This approach results in a high privacy loss (each person must give his/her personal calendar to the solver). In a distributed approach, people work together, revealing some information of their personal calendars, in order to agree upon the time and the place that the meetings could be planned. In such context, it is natural to view *MS* as Distributed Constraint Satisfaction problem (*DisCSP*) with privacy requirements.

Regarding privacy, two main approaches have been explored in the context of *MS*. One considers the use of cryptographic techniques [6]. Alternatively, other authors try to enforce privacy by using different search strategies [4,3]. In this paper, we follow this line. Here, we provide an empirical comparison of three distributed approaches (two synchronous and one asynchronous) for *MS* in terms of efficiency and privacy loss. Among these approaches, two are *DisCSP* algorithms: Synchronous Conflict-backjumping (*SCBJ*) [2] and Asynchronous Backtracking (*ABT*) [7].

¹Correspondence to: Pedro Meseguer, IIIA-CSIC, Campus UAB, 08193 Bellaterra, Spain. Tel.: +34 93 580 9570; Fax: +34 93 580 9661; E-mail:pedro@iiia.csic.es.

2. The Meeting Scheduling Problem

The Meeting Scheduling [4] problem (in short *MS*) is a decision-making process affecting several people, in which it is necessary to decide *when* and *where* several meetings could be scheduled. Formally, an *MS* is defined by the following parameters:

- $P = \{p_1, p_2, \dots, p_n\}$, the set of n people; each with his/her own calendar, which is divided into r slots, $S = \{s_1, s_2, \dots, s_r\}$;
- $M = \{m_1, m_2, \dots, m_k\}$, the set of k meetings;
- $At = \{at_1, at_2, \dots, at_k\}$, the set of k collection of people that define which attendees must participate in each meeting, i.e. people in at_i must participate in the meeting m_i , $1 \leq i \leq k$ and $at_i \subseteq P$;
- $c = \{pl_1, pl_2, \dots, pl_o\}$, the set of o places where meetings can be scheduled.

Initially, people may have several slots reserved for already filled planning in their calendars. A solution to this problem answers the *where* and *when* of each meeting. This solution must satisfy the next rules:

- attendees of a meeting must agree *where* and *when* the meeting is to take place,
- no two meetings m_i and m_j can be held at same time if they have at least one attendee in common,
- each attendee p_i of a meeting m_j must have enough time to travel from the place where he/she is before the meeting starts to the place where the meeting m_j will be. Similarly, people need sufficient time to travel to the place where their next meetings will take place.

2.1. Meeting Scheduling as Distributed CSP

The Meeting Scheduling problem is a truly distributed benchmark, in which each attendee may desire to keep the already planned meetings in his/her calendar private. So this problem is very suitable to be treated by distributed techniques, trying to provide more autonomy to each person, and to keep preferences private. For this purpose, we define the Distributed Meeting Scheduling problem (*DisMS*).

Every *DisMS* instance can be encoded as a Distributed Constraint Satisfaction problem (*DisCSP*). A *DisCSP* is a constraint satisfaction problem whose variables and constraints are distributed among autonomous agents [7]. In the *DisCSP* formulation for *DisMS*, there exists one agent per person. Every agent includes one variable for each meeting in which the corresponding person wishes to participate. The domains of the variables enumerate the possible alternatives of *where* and *when* meetings may occur. That is, each domain includes $k \times o$ values, where k means the number of places where meetings can be scheduling and o represents the number of slots in agents' calendars. There are two types of binary constraints between variables: equality and difference constraints. There exists a binary equality constraint between each pair of variables that belongs to different agents and corresponds to the same meeting. There exists a binary difference constraint between each pair of variable which belongs to the same agent.

3. Privacy on *DisMS* Algorithms

To solve a *DisMS* instance, agents must cooperate and communicate among them in order to determine *when* and *where* meetings will take place. During this process, agents reveal some information about their personal calendars. Privacy loss is concerned with the amount of information that agents reveal to other agents. In the *DisCSP* formulation for *DisSM*, variable domains represent the availability of people to hold a meeting at a given time and place, which actually is the information that agents desire to hide from other agents. In that sense, measuring the privacy loss of a *DisMS* modeled as *DisCSP* is actually the same as measuring the privacy loss of variable domains.

Later on this section we will analyze privacy loss on three distributed algorithms for *DisMS*. From *DisMS* perspective, agents in these algorithms make proposals to other agents about *when* and *where* meetings could take place. A proposal can be accepted or rejected by recipient agents. Depending on the answers of recipient agents, the proposing agent can infer some information about the other agents. Similarly, when an agent receives an assignment proposal, some information is leaked about the proposing agent. In following we describe which knowledge can be inferred by agents in each case [3]:

1. When a proposal is rejected, the proposing agent can infer that it may be because the rejecting agent either has a meeting in that slot already or has a meeting that could not be reached if the proposed meeting was accepted.
2. When a proposal is accepted, the proposing agent can infer that the accepting agent does not have a meeting in that slot, that possible meetings that are incompatible with the proposal do not occur in the possible another agent's calendar.
3. When an agent receives a proposal from another agent, the recipient agent can infer that the proposing agent has not a meeting in that slot, nor in any slot that would be incompatible because of the distance constraints.

The aforementioned points constitute what we call *the process of knowledge inference*. In this work, we actually consider only part of the information that agents can infer by using the first point. The inferred knowledge in this case is very vague because the agent that receives a rejection cannot deduce anything for certain regarding the personal calendar of the rejecting agent. From the other two cases (points 2 and 3), we identify three kinds of information that can be deduced from agents:

Positive Information: This is the information that denotes that can have a meeting in certain locations at certain times.

Negative Information: This is the information that denotes that an agent cannot have a meeting in certain locations at certain times.

Free Slots: This is the information related to slots in which an agent surely does not have any meeting already in any of the places.

The concepts of **Positive Information** and **Negative Information** are similar to the definitions of "present-meeting information" and "future-meeting information" given in [3]. Regarding **Free Slots**, this information can be deduced by an agent if its proposal is accepted by another agent. In this case, the accepting agent does not any meeting already in a time-and-city that is incompatible with the proposal because the distance constraints.

In the following subsections we analyze the details of the process of knowledge inference within each considered algorithm presuming that the number of meetings to be scheduled is simply one ($k = 1$).

3.1. The RR Algorithm

RR was presented and used in [4] to solve *DisMS*. This algorithm is based on a very simple communication protocol: one agent at a time proposes to the others agents the time and the location that meeting may occur. The ordering in which proposals are made follows the Round Robin strategy. When an agent receives a proposal, it responds only to the proposing agent if this proposal is possible according to its calendar.

RR agents exchange six types of messages: **pro**, **ok?**, **gd**, **ngd**, **sol**, **stp**. **pro** messages are used by agents to select the proposing agent. When an agent receives a **pro** message, this causes the agent to become the proposing agent. After the proposing agent chooses the time/place that the meeting can be scheduled, it informs about its decision to rest of agents via **ok?** messages. When an agent receives an **ok?** message, it checks if the received proposal is valid with respect to the previously scheduled appointments in its calendar. If this proposal is consistent, the agent sends a **gd** message to the proposing agent announcing it accepts the proposal. Otherwise, the agent sends a **ngd** message to the proposing agent saying that it rejects the proposal. Messages **sol** and **stp** are responsible for announcing to agents that a solution has been found or the problem is unsolvable, respectively.

Based on the previously discussed message system, it follows that the process of knowledge inference is clear-cut. The message system is simple: proposals are sent via **ok?** messages; which are accepted via **gd** messages or rejected via **ngd** messages.

3.2. SCBJ

Synchronous Conflict-backjumping algorithm (*SCBJ*) is a very simple distributed algorithm for solving *DisCSP* [7,2]. In *SCBJ* algorithm assign variables sequentially. They exchange assignments and nogoods through **ok?** and **ngd** messages, respectively. From the point of view of *DisMS*, agents propose or reject the proposals made by other agents. **ok?** messages are used for the agents to send proposals regarding the time and the place that are acceptable for a meeting. Contrary to what happens in *RR*, **ngd** messages only mean that someone has rejected the proposal, but the agent who has done such is not easily discovered. It is important to note that *SCBJ* loses some possible privacy in the sense that as the agents send **ok?** messages down the line, each subsequent agent knows that all the previous agents have accepted this proposal.

For the purpose of clarification, take for example, a problem consisting of five agents each one representing a person with its own personal calendar. Suppose that the first agent sends a proposal to the second agent about meeting Monday at 9:00 am in Barcelona. The second agent accepts the proposal and sends it to the third agent. Then, the third agent finds this proposal to unacceptable and therefore sends a **ngd** message to the second agent, effectively eliminating the possibility of meeting Monday at 9:00 in Barcelona. In this case, it is impossible for agent 1 or 2 to know where the rejection originated, because any of the agents situated ahead of them, could be responsible, as the **ngd** message came via the third agent. Furthermore, it is impossible for both the first and second agents to discover the agent that rejected the proposal, as it could have been any of the agents situated ahead of them, as was simply relayed back to them via the third agent. However, in such systems, there is one specific case in which it is possible to determine which agent has rejected a proposal. In this example, such a case would occur

if all of the agents 1-4 have already received the proposal and then the fifth agent rejects. When this happens, the fourth agent knows that it was the fifth agent that rejected the proposal as the latter is the only agent capable of sending such a message, assuming that the fourth agent knows that the system contains only five agents in total.

3.3. ABT

The Asynchronous Backtracking algorithm (*ABT*) is a reference algorithm for *DisCSP* [7]. Agents in *ABT* assign the variables asynchronously and concurrently. Mainly, agents exchange assignments and nogoods through **ok?** and **ngd** messages, respectively. Similar to *SCBJ*, **ok?** messages represent proposals, while **ngd** messages represent rejections. The previous discussion regarding **ngd** message in *SCBJ* is still valid for this algorithm, however, there is a difference with respect to **ok?** messages. This difference is that since a sending agent may send an **ok?** to all of the lower priority agents, the information contained in this message is only valid for the sending agent and is revealed only to the receiving agents.

4. Experimental Results

In this section, we evaluate two synchronous algorithms (*RR* and *SCBJ*) as well as one asynchronous algorithm (*ABT*) for solving *DisMS* instances. In order to compare the algorithms, we make use of three measures: computation effort, communication cost, and privacy loss. We measure computation effort using the number of non concurrent constraint checks (*nccc*) [5], communication cost in terms of the number of messages exchanged (*msg*) and privacy loss using the three types of information that agents may deduce regarding other agents' calendars: **Positive Information**, **Negative Information**, **Free Slots**.

Lower priority agents in *SCBJ* and *ABT* tend to work more than higher priority ones, which causes them to reveal more information than higher priority agents. In order to analyze the difference in the amount of privacy loss, we give the minimum, maximum and average amount data for each type of information that agents can find out from other agents' plans.

In our experiments, we deal with *DisMS* instances in which there has to be only one meeting scheduled and which admit at least one solution. Each problem is composed of 12 people, 5 days, with 8 time slots per day and 3 meeting places. This gives $5 \cdot 8 \cdot 3 = 120$ possible values in each agent's domain. Meetings and time slots are both one hour long. The time required for travel among the three cities is 1 hour, 1 hour and 2 hours. *DisMS* instances are generated by randomly establishing p predefined meetings in each agent's calendar. The value of p varies from 0 to 14.

In *RR*, we look at one constraint check each time that an agent checks to see if a meeting can occur at a certain time/place. In all algorithms, each time an agent has to propose, it chooses a time/place at random. Agents in *ABT* process messages by packets instead of processing one by one [2] and implement the strategy of selecting the best nogood [1].

Figure 1 gives the results in terms of *nccc* (on the left) and *msg* (on the right) for each algorithm averaged over 100 instances. For every value of p , we observe that *RR*

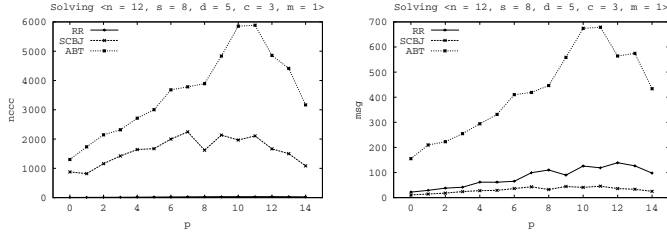


Figure 1. Constraint checks and number of messages for RR, SCBJ and ABT on Distributed Meeting Scheduling instances.

requires less *nccc* than *SCBJ*, and *ABT* has the worst results. This can be explained by looking at how agents reject invalid proposals in each algorithm. In *RR*, the proposing agent broadcasts its proposal to all the other agents. Then, the receiving agents check if this proposal is valid or not. This process can be performed concurrently by all receiving agents, and therefore, its computation effort is just one non concurrent constraint check. (Actually, the *nccc* value for *RR* is equal to number of proposals made before finding a solution.) In *SCBJ*, the active agent sends the proposal (received from prior agents) to the next agent when this is valid for him/her. It could happen that a proposal made by the proposing agent in *RR* and by the first agent in the ordering in *SCBJ* and *ABT* decide to meet at certain time and certain place which is inconsistent for an agent lower in the ordering for *SCBJ* and *ABT*. In *RR*, this inconsistency will be found as soon as this agent responds to the proposing agent. In *SCBJ*, otherwise, this will be found when this agent receives the proposal, after that all the prior agents have accepted it and have performed several non concurrent constraint checks. Regarding *ABT*, this results can be explained because (1) agents choose their proposals randomly and (2) these proposals are made possibly without knowing the proposals of higher priority agents. The combination of these two facts make *ABT* agents more likely to fail when trying to reach an agreement regarding *where* and *when* the meeting could take place. Considering *msg*, the relative ordering among agents changes only in the sense that *RR* is worse than *SCBJ*. This difference between both algorithms occurs probably because *SCBJ* omits the accept messages used by *RR*.

Figure 2 report the privacy loss with respect to each information type. Regarding **Positive Information** (plots in the upper area of Figure 2), we observe that according to minimum values of **Positive Information**, *ABT* and *SCBJ* have similar behavior, while *RR* is a little worse, especially for more difficult problems ($p > 6$). This plot indicates that the less informed agent in terms for each algorithm infers only the **Positive Information** derived from the problem solution. That is, when a solution is reached, this agent can deduce that all the other agents can meet at the time and the location given by the found solution.

In terms of maximum values it is apparent that the difference between algorithms is greater. *ABT* is always less private than *SCBJ* and *RR* is the algorithm with the best results. From these values we may conclude that the better informed agent in *RR* has less **Positive Information** than the better informed agent in the other two algorithms. In terms of average values of **Positive Information**, the plot shows that *ABT* agents discover on average approximately two time slots in which each agent is available while for agents

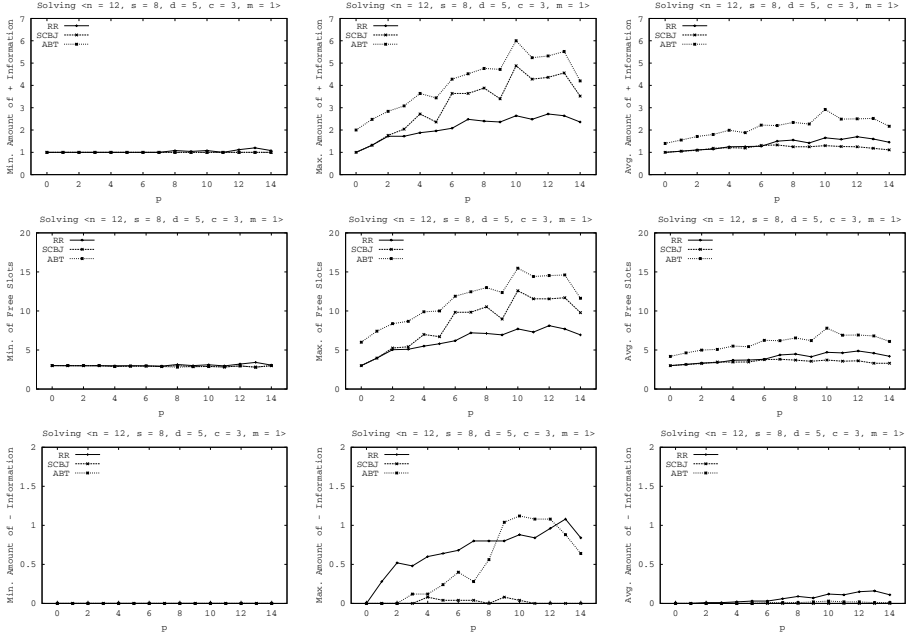


Figure 2. Privacy loss for RR, SCBJ and ABT on Distributed Meeting Scheduling instances.

in the other two algorithms this value is approximately one. *SCBJ* shows better results than *RR* on instances with larger numbers of already planned appointments.

Considering the number of **Free Slots** that agents leak from other agents, in terms of minimum values, we observe that the three algorithms have results similar to **Positive Information** ones. The less informed agent for each algorithms identifies almost 10 free slots from the other agents' calendars. In terms of maximum values, the better informed agent in *ABT* infers almost twice more **Free Slots** than the better informed agent in *RR*, while the better informed agent in *SCBJ* discovers more than this agent in *RR*. In terms of average values, *ABT* agents also find more **Free Slots** than the other two algorithms. *SCBJ* lightly outperforms *RR* on instances with $p > 6$.

The amount of **Negative Information** deduced in each algorithm is practically null. Only for instances with higher number of already planned appointments, the better informed agent in *ABT/RR* can identify at most one rejection from the other agents.

From the above results, we observe the following. Regarding computation effort and communication cost, *ABT*, the asynchronous algorithm, is less economic than the other two algorithms. This is because *ABT* agents work concurrently and select their proposals randomly, which makes more difficult *ABT* agents to reach an agreement regarding *when* and *where* they can meet together. Consistently for all tested instances, *SCBJ* requires less messages than *RR*, however, it performs more constraint checks. Regarding privacy, for the three algorithm the greater amount of information revealed identifies time slots in which agents surely does not have any meeting in any of the places. In terms of this parameter, *ABT* is always worse than the synchronous algorithms. On average, *SCBJ* agents reveal less information than *RR*. However, the better informed agent in *SCBJ* deduce more information than in *RR*.

5. Scheduling Multiple Meetings

This work is focused on *DisMS* instances in which only a meeting have to be planned. Previous works [4,3], that also use *RR* to solve *DisMS*, make the same assumption. This is motivated by the fact that agents in *RR* have to plan only one meeting at a time. Nevertheless, the extension of *RR* to deal with *DisMS* instances in which several meetings must be scheduled is direct. For these instances, *RR* agents schedule one meeting after the other. If agents reach an agreement about the time and the place where the current meeting may occur, another not yet scheduled meeting is considered as the current meeting. Otherwise, if the current meeting cannot be scheduled, backtracking occurs and the previous scheduled meeting is changed. This process continues until all the meetings have been planned or every alternative of place and time for the first meeting has been considered without reaching an agreement. With *DisCSP* formulation, agents in *SCBJ* and *ABT* may schedule several meetings simultaneously. In this case, agents may hold multiple variables.

6. Conclusions

In this work we have evaluated privacy loss of three distributed algorithms for the Meeting Scheduling problem, a naturally distributed benchmark. Our experimental results show that the two synchronous approaches outperform the asynchronous one regarding computation effort, communication cost as well as privacy loss. These results do not imply that synchronous algorithms should be considered as the choice for solving this problem. Synchronous and asynchronous algorithms have different functionalities (i.e. synchronous algorithms are less robust to network failures). Regarding privacy, neither of the distributed algorithms that we have considered is worse than the centralized approach, which needs to gather the whole problem into a single agent to solve it.

References

- [1] C. Bessière, A. Maestre, I. Brito, P. Meseguer. Asynchronous Backtracking without Adding Links: a New Member to ABT Family. *Artificial Intelligence*, **161**(1–2), pp. 7–24, 2005.
- [2] I. Brito and P. Meseguer. Synchronous, Asynchronous and Hybrid Algorithms for DisCSP. *Proc. of DCR Workshop at CP-2004*, 2004.
- [3] M. S. Franzin, F. Rossi, E. C. Freuder, R. Wallace. Multi-Agent Constraint Systems with Preferences: Efficiency, Solution Quality, and Privacy Loss. *Computational Intelligence*, **20**, pp. 264–286, 2004.
- [4] Freuder E.C., Minca M., Wallace R.J. Privacy/efficiency trade-offs in distributed meeting scheduling by constraint-based agents. *Proc. of DCR Workshop at IJCAI-01*, pp. 63–71, USA, 2001.
- [5] Meisels A., Kaplansky E., Razgon I., Zivan R. Comparing performance of distributed constraint processing algorithms. *Proc. of DCR Workshop at AAMAS-02*, pp. 86–93, Italy, 2002.
- [6] M. C. Silaghi. Meeting Scheduling Guaranteeing n/2-Privacy and Resistant to Statistical Analysis (Applicable to any DisCSP). *Proc. of the 3th Conference on Web Intelligence*, pp. 711–715, 2004.
- [7] M. Yokoo, E. H. Durfee, T. Ishida, K. Kuwabara. The Distributed Constraint Satisfaction Problem: Formalization and Algorithms. *IEEE Trans. Knowledge and Data Engineering*, **10**, pp. 673–685, 1998.

This page intentionally left blank

Agents

This page intentionally left blank

The impact of betweenness in small world networks on request for proposal coalition formation problems

Carlos MERIDA-CAMPOS, Steven WILLMOTT

Universitat Politecnica de Catalunya, Software Department, E-08034 Barcelona
{dmerida,steve}@lsi.upc.edu

Abstract. The analysis of societies demonstrates the recurrent nature of small world topology in the interactions of elements in such worlds. The small world topology proves to have beneficial properties for system's performance in many cases, however there are also scenarios where the small world topology's properties negatively affect the system's outcome; thus in depth knowledge on the small world weaknesses is needed in order to develop new generations of artificial societies and new models of economic systems. In this paper, a multi-agent system based on request for proposal protocol and coalition formation organisational paradigm is used to analyse properties of small world social networks of agents. Experiments center on nodes in the network with high betweenness and in particular the distribution of agents in the population across these nodes. Results show that small world topology scenarios lose their beneficial properties when non-competitive agents are positioned as high betweenness nodes in the network.

Keywords. Network analysis, Small World, Request for proposal, Coalition formation

1. Introduction

Interactions are the cause and effect of any society. In human societies, the number of those interactions is reduced because they are affected by geographic constraints and many other different events that bias the way people interact in an homophilic manner. A recurrent topology resultant on those constraints is the *Small World* [16], which beneficial properties have been studied for many different environments ([17,18] amongst many others), however, this topology is not exempt of weaknesses, as it has recently been revealed in [8], where small world networks are compared with other topologies proving faster convergence to near optimal outcomes but worse long term behavior. A similar result was obtained in [10] where high clustering coefficient in small world networks proved to be a handicap in some specific search problems. The present work extend those results giving an explanation on the negative effects observed in small world topologies.

The specific problem for which network analysis is performed is *Coalition Formation*. Coalitional systems are organisational mechanisms where agents have to explore a search space of agent group combinations in order to improve data flow, allocate resources efficiently, solve a problem in a coordinated manner, or to improve their out-

comes by creating alliances. Those systems have been traditionally studied from a far-sighted perspective, and focused on the problem of finding stability concepts ([15,14] amongst many others). Multi-Agent Systems research introduced the possibility of experimenting with coalitional systems with a limited number of possible interactions [1,12], and more recently myopic agents have been studied with concrete knowledge network topologies in team formation [5,6] as well as in firm formation models [2]. In this line, the work presented here defines a model that considers different small world underlying social networks on an specific type of electronic market allocation mechanism called Iterated Request For Proposal (RFP from now on). This model was first studied in [7], and further explored in [9], [11] and [10]. In this environment, an entity regularly issues a call for tender to provide specific goods or services with certain characteristics. Providers compete amongst themselves (either individually or in consortia – *coalitions*). Structures created are based on complementarity of their members. The more complementary they are, the better outcome they obtain. However structures do not grow in an uncontrolled manner, instead they optimise their size leaving out redundant members that would decrease the share of the eventual income of the coalition. There are many existent real systems that follow the RFP type procedures such as public building projects, competitive tender for government contracts or even collaborative research project grants. A main characteristic of the model is that instead of having agents that dynamically adjust their social connections [8,5] or that propagate/contaminate their neighbors through a social network [3,13], agents are constrained by a unmovable social network where no social capital is transmitted. However, agents can iteratively and incrementally form coalitions as long as there is a direct neighbor in the coalition – leading to an evolutionary process that converges to a Nash equilibrium. These dynamics gives shape to coalitions by putting together agents that can be far away from each other in the social network. Results obtained explain how the system performance is affected by the concrete capabilities of agents placed in specific positions of the social network. Concretely the positions studied are those with high betweenness [4]. Betweenness is a well known centrality measure that examines the extent to which an actor (node) is between all other actors within the network. This concept has been extensively used and adapted in network research area becoming one of the most important centrality concepts. In the present work evidence is provided to support the argument on the importance of betweenness central nodes in the network in the context of an iterated coalitional system, and specifically, experiments are addressed to provide data to explain the negative performance observed in small world networks in [10].

The rest of the paper is structured as follows: section 2 presents a formalisation of the RFP mechanism. Section 3.1 describes an specific metric that records the amount of dynamism that a certain topology generates as well as other metrics used to perform the analysis and the experimental setup. Results on the importance of positioning of agents with specific individual properties (*versatility* and *competitiveness*) in certain parts of the social network are provided and analysed in section 3.3. Finally, section 4 summarises the main conclusions.

2. Iterative RFP Coalition Formation Model

A population $I = \{1, 2, \dots, n\}$ consists of a finite number of n individuals or *agents*. Agents compete for creating the best solution proposal to a given task *task T*. A parti-

tion $\sigma = \{\sigma_1, \sigma_2, \dots, \sigma_p\}$ of the population I is a specification of p coalitions of agents $\sigma_i = \{\sigma_{i1}, \sigma_{i2}, \dots, \sigma_{im}\}$, where σ_{ij} represents an agent from population I forming part of coalition σ_i . By forming coalitions, agents are able to increase their competitiveness towards the specified task, they are encouraged to do so as coalitions would be priced according to their ranking. Moreover they are encouraged to reduce coalition size hence increasing individual benefits by splitting the potential payoff amongst less members. Agents have heterogeneous capabilities, thus having different performance levels in different skills. A finite number of k skills, indexed from 1 to k is set for which each agent σ_{ij} has a fixed value: $\sigma_{ij} = \langle \sigma_{ij}^1, \sigma_{ij}^2, \dots, \sigma_{ij}^k \rangle$. This way, it is possible to define a continuum of possibilities between agents that are *specialised* in the performance of a certain skill being unskilled for the rest of them, and agents that are *versatile*, being averagely apt for the performance of all the skills defined. A Task T is specified by a set of k skill requirements: $T = \langle T^1, T^2, \dots, T^k \rangle$. Each one of the k skills have a degree of requirement. These requirements are modeled in the form of a number. In a coalition, skills of agents are aggregated in such a way that each agent gives the best of itself in a join effort to create a group as competitive as possible under the requirements of the Task. The coalition has a value in each skill representing the aggregated effort of its members. The aggregation for every skill $l : 1 \leq l \leq k$ in the coalition is modeled as:

$$\sigma_i^l = \max(\sigma_{ij}^l) : 1 \leq j \leq m \quad (1)$$

Each skill is considered as a necessary subtask for performing task T . By using the aggregation function shown in equation 1, the agent in a coalition which is the best fit for performing a certain subtask will be the one that performs it. This specific type of aggregation is chosen because it is characteristic of many different socio-economic processes. The aggregated effort of agents in equation 1 is used to measure an score $scr(\sigma_x, T)$ that indicates how well the agents in coalition σ_x perform together for accomplishing a task specification T . The score of a coalition is computed as the scalar product between σ_i and T . Amongst many possible choices, this metric is chosen because it captures in a simple way the different importance of subtasks T^l , and the additive valuation of all the required skills:

$$scr(\sigma_i, T) = \sum_{l=0}^k (\sigma_i^l * T^l) \quad (2)$$

2.0.1. Agent Choices and Strategies

Each player's strategic variables are its coalition choice to join σ_j and a set of agents in this coalition $\phi_{jk} : \{(\phi_{jk} \subset \sigma_j) \vee (\phi_{jk} = \emptyset)\}$ to eliminate. The possibility for optimisation responds to the change of value that certain agents can experiment when in their coalition they are out-skilled by a new member and so they become redundant. Only those actions accepted by a majority (more than the half) of members in the affected coalition, are performed. An agent that is requested to take an action can submit a finite number of requests in an specific order, in such a way that if an action is not accepted, the next action is checked and so on. If none of its action proposals is accepted, the agent stays in the same coalition where it was.

All the agents in the population follow the *Competitive Strategy* [9], that consists on proposing a set of actions that contain every proposal that either improves the score of

the coalition the agent is in, or keeps the same score while reducing the size of the coalition. When they receive a proposal from an outsider, they accept if they are not in ϕ_{jk} 's proposal, and if the proposal improves the score or keeps it while reduce the coalition size.¹ Every agent j has a fixed social network α_j that is a non-empty set of agents. When considering to join a different coalition, agents are limited to just evaluating coalitions of agents in α_j .

2.0.2. RFP Iterated Model

At time 0, every agent is a coalition of just one element ($\sigma_i = \{\sigma_{ii}\}$). A task T is issued and a run of negotiation starts in which every agent, sequentially and following a random order, is asked about an action to take (see previous subsection). Agents have no knowledge on the order in which they are requested for an action, and when they are asked they can consider any action involving the coalitions in which there is some member of their social network. The run ends when all agents have been requested for an action. The process last as many runs as necessary until it converges to an stable state. Stability is reached when in a complete run, no agent is willing to leave the coalition is in or none of its actions are accepted by the hosting coalition.² When the system has reached equilibrium, coalitions' scores are captured for further analysis.

3. Experiments

3.1. Metrics used in the experiments:

In order to measure how competitive an agent is in a simple way, every agent in the population is endowed with the same total number of skill capabilities, but distributed differently across skills. A highly competitive agent has higher concentration of capabilities in a reduced set of skills while a versatile agent is averagely apt in every skill. This way we can define a simple metric of *Competitiveness*: $com(\sigma_{ij})$, by just measuring the standard deviation in its skill values weighted by the task values. Analogously, *Versatility* is defined as the inverse of *Competitiveness*: $(ver(\sigma_{ij}) = 1/com(\sigma_{ij}))$.

In order to test the dynamics that a certain underlying social network permits, a metric called *Historical Average Degree* (HAD from now on) is defined. This metric measures the distance that exists in the social network between agents in a coalition. What makes this metric different from the classical distance definition (minimal path length between two nodes), is that the distance is measured just using the links between the coalition members. The HAD value between two members does not change through the addition or abandon of partners. When an agent A joins a coalition there is at least 1 member (B) with path-length equal to 1, (otherwise this agent would not directly know any of the members of the coalition, hence it could not consider that coalition). The distance to the other members corresponds to 1 (distance from A to B) plus the minimal path length from B to the member of the coalition through a complete HAD valued network between members of the coalition. The coalition HAD value is the mean of each

¹In [11] a payoff optimisation based strategy (conservative) is compared with the *competitive* approach used in here, resulting in worse general results for conservative populations

²In [11] it was shown how the system always converge to an stable state when the population follows an score maximizing strategy.

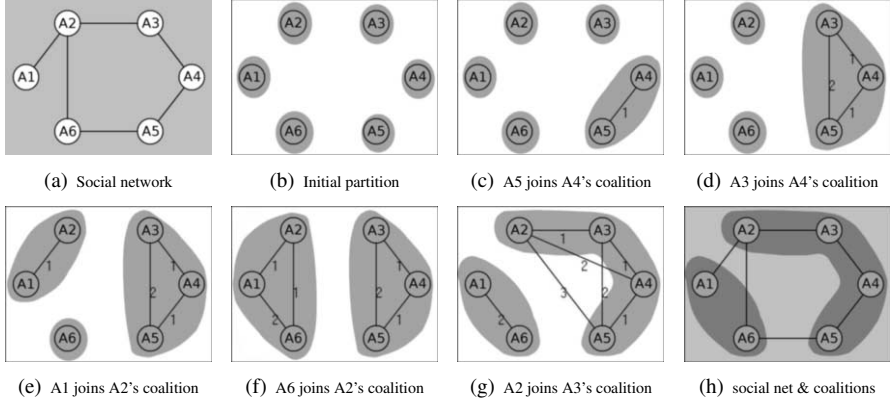


Figure 1. Example of iterated coalition formation process. Edge's values reflect the HAD between nodes. Shaded areas denote coalitions.

HAD value between each member of the coalition. This mean is computed for every coalition when the system has reached equilibrium. Figure 1 exemplifies how the metric is computed during the process of coalition formation.

The global performance of the system is computed by measuring the quality (score) of the coalitions formed. It is assumed that for the entity who issues the RFP, it is important to obtain the higher score in the top coalitions rather than obtaining many coalitions with averagely high score. The concrete function used to measure this, is defined as follows: $Sc(\sigma) = \sum_{rank=0}^p (scr(\sigma_{rank}, T) * 1/2^{rank})$. This way, a certain experiment ends up with better or worse results depending on how efficient the best agents are in getting to know each other.

3.2. experimental set-up

In order to investigate the effects of the identity of agents in high betweenness positions, a significant number of experiments have been performed. A total of 1000 networks with 500 nodes have been tested, all of them are *Small World* networks (using the Watts-Strogatz model [16] with $p = 0.07$). For each one of the networks, 3 different mappings have been created in the following way: on the one hand, for every network, nodes are ordered decreasingly by *betweenness centrality*. On the other hand, 2 different orders of agents are created by computing *com*, and *ver* metrics in every agent (see section 3.1) and ordering agents decreasingly by each metric's values. Every experiment maps every agent in one of the 2 specific orders (*ver-ord* or *com-ord*), to a node according to its *betweenness* order in the network. An additional random mapping *rdm-ord* has been used to create the third tested order. That creates a total setup of 3000 experiments: for each one of the 1000 different small world networks, 3 different sets of experiments are performed, each one with a concrete mapping between node betweenness and agent characteristics. Experiments are run until the system has converged to an equilibrium (see section 2.0.2).

For space restriction reasons, not all the experiments performed are shown. Some of the variables have been fixed. These variables are: the population composition (500 agents with 10 skills and, for every agent a total value of 100, heterogeneously distributed

amongst the skills. The stdev. in the skill distribution is homogeneously distributed from 5 to 20. The task used in all the experiments is: $T = \langle 1, 2, 3, 4, 5, 6, 7, 8, 9, 10 \rangle$ ³. The connectivity degree k is also fixed to an average of 10.3 with very few deviation, hence connectivity is homogeneously distributed and results are not affected by the degree factor showed in [10].

3.3. Experiments Results

Results obtained by each different mapping at the end of each experiment (each experiment has a different underlying network) are compared in terms of $Sc(\sigma^*)$ (see section 3.1). This way, each mapping gets a rank between 1 and 4 (as there are 4 different configurations under test). Figure 2(a) shows the sum of each ranking for each of the configurations tested through 1000 experiments. The main conclusion to drawn from those results is that *btw-com* is the mapping that gets better performance (preceded, of course by farsighted setup, that permit the agents to have perfect sight of the population). This is indicating that when competitive agents (see metric description in section 3.1) are those with higher betweenness in the social network, performance of the system increases. Inversely, if versatile agents occupy the most betweenness-central positions, the system performance is clearly worse. As expected, random mapping is placed in between those two results, occupying the third ranking. The observed advantage of competitive agents has the following explanation:

If the network would be a totally structured graph generated by Watts-Strogatz model (with parameter $p=0$), the coalition created by a competent agent could only improve its score by attracting agents longitudinally through tightly interconnected clusters. Watt-Strogatz small world model slightly break this structure and rewire some connections shortening the distance between different parts of the graph. Rewired nodes are those who have higher betweenness, as they are involved in many short paths between nodes in the graph. If agents with high attractive potential (competent agents) are situated in rewired nodes or nodes close to rewired nodes, competent coalitions will have more possibilities to grow up in more than one dimension –as it was the case of an structured network, hence increasing the opportunities of getting into touch with other competent and compatible agents.

A different perspective for analysing the advantage of positioning competitive agents in highly central positions is by monitoring the dynamism in the coalitions. Figure 2(b) shows the historical average degree (HAD) for each mapping. The three configurations have a similar shape: Starting in the first ranked coalition with a similar value, increasing until a critical point and decreasing. For explaining the reason and implications of their differences it is necessary to understand how the coalitional process is registered by the HAD metric: the best ranked coalition is usually the first one to converge. The process is top-down as during the formation process of the leading coalition, many agents are accepted and then made redundant of the coalition when they are outperformed by another joining agent. If an agent is made redundant from the leading coalition it creates dynamism in lower ranking coalitions, hence until top coalitions do not stabilise, lower ranking coalitions suffer changes. In *com-ord* configuration, as top ranking coalitions stabilise, those agents, that because of their capabilities are meant to form lower ranking

³the difference between values favors the diversity of Competitiveness and Versatility degrees (see section 3.1). None of the values is 0, so that all the skills are required (see section 2)

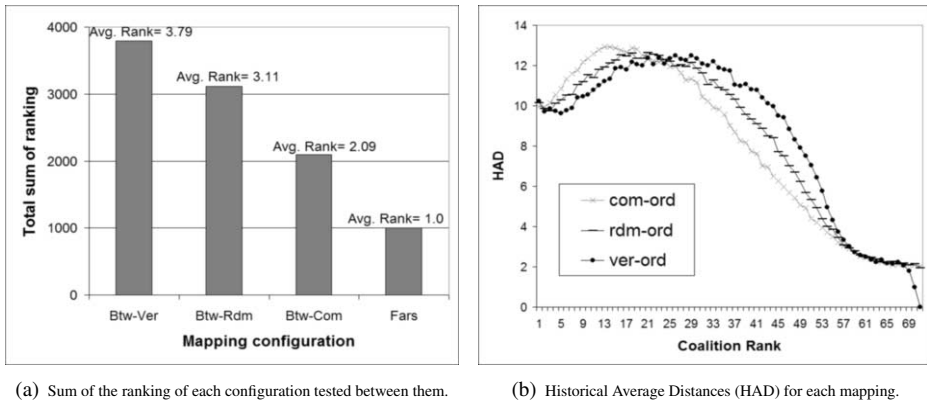


Figure 2. Performance results measured in global score terms and dynamism. Competent agents placed in high betweenness positions prove the best results compared to Versatile or Random mappings.

coalitions, have more limited possible paths to get their way to each other. This is because possible paths through nodes in top ranking coalitions are blocked. As the stability process is top-down, second order coalitions reflect a higher HAD value because agents have to jump through alternative paths as long as their members have enough attraction power. After a critical point is reached, the HAD value start decreasing reflecting that agents are not able to find their way to get in contact. The only difference from the three lines in figure 2(b) is that *com-ord* (that is competitive agents occupying high betweenness positions) reaches the maximal point in a smaller ranking coalition. This fact indicates that the most competitive agents are concentrated in the top coalitions. Remaining agents have less attractive potential, hence they register lower dynamism in the coalitions created. The average convergence time registered for *com-ord* configuration is 20% lower than for *ver-ord*, this data supports the previous argument on the low dynamism in *com-ord* configurations.

4. Conclusions

Large scale multi-agent systems need to have a reduced agent's interaction space in order to avoid combinatorial explosion of interaction possibilities. Research on efficient social network topologies can be of great help in this area, however every interaction model requires specific research. In this paper it is shown that the two main properties of small world topologies (high clustering coefficient and low average path length) fail to create good global outcome in a general interaction model based on coalition formation organisational paradigm. On the one hand, as it was shown in [10], high clustering coefficient involves redundant connections and less possibilities of explorations than in other non-structured models. On the other hand, in this paper it has been shown that short average path length property is seriously compromised when low competitive agents are placed in highly betweenness-central nodes of the social network.

Betweenness positioning effects have been measured with two different methods: a quantitative metric on the aggregation of the coalitions scores and an analysis based on the HAD metric. While the former depends upon an explicit definition of a valuation

of the results obtained, the HAD metric defined in the paper, permits a more abstract analysis just based on the social distances that separate each agent of the coalition. The HAD metric is an innovative analytical tool with interesting applications in the area of dynamic coalition formation. In this area, the research line followed in this paper takes an step further by studying in depth the combination of the use of social networks to map limited awareness of agents .

References

- [1] R. Axtell. The emergence of firms in a population of agents: Local increasing returns, unstable nash equilibria, and power law size distributions. Working Paper 3, Center on Social and Economic Dynamics, Brookings Institution, 1999.
- [2] R. Axtell. Effects of interaction topology and activation regime in several multi-agent systems. In *Proceedings of the MABS00 Intl. Workshop*, pages 33–48, London, UK, 2000. Springer-Verlag.
- [3] J. Delgado, J. M. Pujol, and R. Sangüesa. Emergence of coordination in scale-free networks. *Web Intelligence and Agent Systems*, 1(2):131–138, 2003.
- [4] L. C. Freeman. Centrality in social networks conceptual clarification. *Social Networks*, 1(3):215–239.
- [5] M. E. Gaston and M. desJardins. Agent-organized networks for dynamic team formation. In *Proceedings of AAMAS '05*, pages 230–237, New York, NY, USA, 2005. ACM Press.
- [6] M. E. Gaston, J. Simmons, and M. desJardins. Adapting network structures for efficient team formation. In *Proceedings of AAMAS-04, Workshop on Learning and Evolution in Agent-based Systems*, 2004.
- [7] S. Kraus, O. Shehory, and G.Tasse. Coalition formation with uncertain heterogeneous information. In *Proceedings of AAMAS'03*, pages 1–8, 2003. Melbourne, Australia.
- [8] D. Lazer and A. Friedman. The hare and the tortoise: the network structure of exploration and exploitation. In *dg.o2005: Proceedings of the 2005 national conference on Digital government research*, pages 253–254. Digital Government Research Center, 2005.
- [9] C. Merida-Campos and S. Willmott. Agent compatibility and coalition formation: Investigating two interacting negotiation strategies. In *Trading Agent Design and Analysis & Agent Mediated Electronic Commerce VIII (TADA/AMEC), AAMAS'06, 2006. LNAI 4452*, pages 75–90.
- [10] C. Merida-Campos and S. Willmott. Exploring social networks in request for proposal dynamic coalition formation problems. In *Proceedings of the 5th. International Central and Eastern European Conference on Multi-Agent Systems CEEMAS'07, Leipzig, Germany*.
- [11] C. Merida-Campos and S. Willmott. The effect of heterogeneity on coalition formation in iterated request for proposal scenarios. In *Proceedings of the EUMAS Workshop*, 2006. Lisbon.
- [12] I. Milchtaich and E. Winter. Stability and Segregation in Group Formation. *Games and Economic Behaviour*, 38:318–346, 2001.
- [13] J. M. Pujol, A. Flache, J. Delgado, and R. Sangüesa. How can social networks ever become complex? modelling the emergence of complex networks from local social exchanges. *Journal of Artificial Societies and Social Simulation*, 8(4):12, 2005.
- [14] O. Shehory and S. Kraus. A kernel-oriented model for coalition-formation in general environments: Implementation and results. In *AAAI/IAAI, Vol. 1*, pages 134–140, 1996.
- [15] J. von Neumann and O. Morgenstern. *Theory of Games and Economic Behaviour*. Princeton University Press, 1944.
- [16] D. J. Watts and S. H. Strogatz. Collective dynamics of 'small-world' networks. *Nature*, (393):440–442, 1998.
- [17] A. Wilhite. Bilateral trade and 'small-world' networks. *Computational Economics*, 18(1):49–64, August 2001. available at <http://ideas.repec.org/a/kap/compec/v18y2001i1p49-64.html>.
- [18] H. Zhang, A. Goel, and R. Govindan. Using the small-world model to improve freenet performance. *Comput. Networks*, 46(4):555–574, 2004.

On the Multimodal Logic of Elementary Normative Systems

Pilar DELLUNDE¹

IIIA (Artificial Intelligence Research Institute)

Abstract. We introduce Multimodal Logics of Normative Systems as a contribution to the development of a general logical framework for reasoning about normative systems over logics for Multi-Agent Systems. Given a multimodal logic L , with standard Kripke semantics, for every modality \Box_i and normative system η , we expand the language adding a new modality \Box_i^η with the intended meaning of $\Box_i^\eta\phi$ being " ϕ is obligatory in the context of the normative system η over the logic L ". In this expanded language we define the Multimodal Logic of Normative Systems over L , for any given set of normative systems N , and give a sound and complete axiomatisation for this logic, proving transfer results in the case that L and N are axiomatised by sets of Sahlqvist or shallow modal formulas.

Keywords. Multimodal Logics, Normative Systems, Multi-Agent Systems, Model Theory, Sahlqvist Formulas,

1. Introduction

Recent research on the logical foundations of Multi-Agent Systems (MAS) has centered its attention in the study of normative systems. MAS could be regarded as a type of dialogical system, in which interactions among agents are realized by means of message interchanges, all these interactions taking place within an institution. The notion of electronic institution is a natural extension of human institutions by permitting not only humans but also autonomous agents to interact with one another. Institutions are used to regulate interactions where participants establish commitments and to facilitate that these commitments are upheld, the institutional conventions are devised so that those commitments can be established and fulfilled (see [1] for a general reference of the role of electronic institutions to regulate agents interactions in MAS). Over the past decade, normative systems have been promoted for the coordination of MAS and the engineering of societies of self-interested autonomous software agents. In this context there is an increasing need to find a general logical framework for the study of normative systems over the logics for MAS.

Given a set of states S and a binary accessibility relation R on S , a normative system η on the structure (S, R) could be understood as a set of constraints $\eta \subseteq R$ on the transitions between states, the intended meaning of $(x, y) \in \eta$ being "the transition from state x to state y is not legal according to normative system η ". Several formalisms have

¹Correspondence to: Pilar Dellunde, IIIA, Campus de la Universitat Autonoma de Barcelona, 08193 Cerdanyola del Valles, Catalonia, Spain. E-mail: pilar.dellunde@uab.cat

been introduced for reasoning about normative systems over specific logics, two examples are worth noting: Normative ATL (NATL), proposed in [2] and Temporal Logic of Normative Systems (NTL) in [3]. NATL is an extension to the Alternating-Time Temporal Logic of Alur, Henzinger and Kupferman (see [4]), NATL contains cooperation modalities of the form $<< \eta : C >> \phi$ with the intended interpretation that " C has the ability to achieve ϕ within the context of the normative system η ". NTL is a conservative generalization of the Branching-Time Temporal Logic CTL (see [5]). In NTL, the path quantifiers A ("on all paths...") and E ("on some path...") are replaced by the indexed deontic operators O_η ("it is obligatory in the context of the normative system η that...") and P_η ("it is permissible in the context of the normative system η that...").

For our purpose of developing logical models for MAS, it would be worth to work in a generalization to arbitrary logics of the approaches taken in [2] and [3]. The Multimodal Logics of Normative Systems introduced in this article are a contribution to define such a general logical framework. There are some advantages of using these logics for reasoning about MAS: it is possible to compare whether a normative system is more restrictive than the other, check if a certain property holds in a model of a logic once a normative system has restricted its accessibility relation, model the dynamics of normative systems in institutional settings, define a hierarchy of normative systems (and, by extension, a classification of the institutions) or present a logical-based reasoning model for the agents to negotiate over norms.

We have restricted our attention to multimodal logics with Kripke semantics, outlining at the end of the paper how these results could be applied to other formalisms of common use in modelling MAS, such as Hybrid Logics. Our definition of normative system is intensional, but the languages introduced permit to work with extensional definitions like the one in [3]. We present completeness and canonicity results for logics with normative systems that define elementary classes of modal frames, we have called them *Elementary Normative Systems (ENS)*. On the one hand, the choice of ENS seems the more natural to start with, because elementary classes of frames include a wide range of formalisms used in describing MAS, modelling different aspects of agenthood, some Temporal Logics, Logics of Knowledge and Belief, Logics of Communication, etc. On the other hand, at the moment, we are far from obtaining a unique formalism which addresses all the features of MAS at the same time, but the emerging field of combining logics is a very active area and has proved to be successful in obtaining formalisms which combine good properties of the existing logics. In our approach, we regard the Logic of Normative Systems over a given logic L , as being the fusion of logics obtained from L and a set of normative systems over L , this model-theoretical construction will help us to understand better which properties are preserved under combinations of logics over which we have imposed some restrictions and to apply known transfer results (for a recent account on the combination of logics, we refer to [6]).

This paper is structured as follows. In Section 2 we introduce the notion of *Elementary Normative System (ENS)*, a kind of normative system that defines elementary classes of modal frames, and we study the Multimodal Logics of Elementary Normative Systems, proving completeness, canonicity and some transfer results in the case that the logic L and the normative system N are axiomatised by sets of Sahlqvist or shallow modal formulas. In section 3, we give an example to illustrate how our framework can work in Multiprocess Temporal Structures, and we show that we can axiomatise with elementary classes a wide range of formalisms used in describing MAS, modelling dif-

ferent aspects of agenthood: some Temporal Logics, Logics of Knowledge and Belief, Logics of Communication, etc. and to which we can apply also our framework. In Section 4 we present some related work and compare our results with the ones obtained by other approaches. Finally, Section 5 is devoted to future work.

2. Elementary Normative Systems on Multimodal Languages

We begin the section by introducing the notion of First-order Normative System and its corresponding counterpart in modal languages, Elementary Normative Systems. Let L be a first-order language whose similarity type is a set $\{R_i : i \in I\}$ of binary relational symbols. Given an L -structure Ω with domain A , we denote by Ω^* the following set of sequences of elements of A :

$$\Omega^* = \{(a_0, \dots, a_m) : \forall j < m, \exists i \in I \text{ such that } a_j R_i^\Omega a_{j+1}\}$$

We say that a formula $\phi(x_0, \dots, x_k) \in L$ is a *First-Order Normative System* iff for every L -structure Ω ,

$$\{(a_0, \dots, a_k) : \Omega \models \phi[a_0, \dots, a_k]\} \subseteq \Omega^*.$$

A *modal similarity type* $\tau = \langle F, \rho \rangle$ consists of a set F of modal operators and a map $\rho : F \rightarrow \omega$ assigning to each $f \in F$ a finite arity $\rho(f) \in \omega$. A propositional modal language of type τ is defined in the usual way by using propositional variables, the operators in F and the boolean connectives $\wedge, \vee, \neg, \rightarrow, \leftrightarrow, \top, \perp$.

Given a set of modal formulas Σ , the *frame class defined by* Σ is the class of all frames on which each formula in Σ is valid. A frame class is *modally definable* if there is a set of modal formulas that defines it, and it is said that the frame class is *elementary* if it is defined by a first-order sentence of the frame correspondence language (the first-order language with equality and one binary relation symbol for each modality). An *Elementary Normative System* (ENS) is a propositional modal formula that defines an elementary class of frames and such that its translation is a First-Order Normative System.

From now on, we assume that our modal languages have standard Kripke semantics and its modal similarity types have only a countable infinite set of monadic modalities $\{\Box_i : i \in I\}$ and a countable infinite set of propositional variables. We introduce a new set of symbols Θ to denote normative systems. Given a modal language of similarity type τ , for every $\eta \in \Theta$, let τ^η be the similarity type whose modalities are $\{\Box_i^\eta : i \in I\}$. For every set of formulas Γ , let us denote by Γ^η the set of formulas of type τ^η obtained from Γ by substituting every occurrence of the modality \Box_i by \Box_i^η . We define the operators \Diamond_i in the usual way, $\Diamond_i \phi \equiv \neg \Box_i \neg \phi$ and we introduce the corresponding \Diamond_i^η . For the sake of clarity from now on we will denote by η both the term which indexes the modality and the formula that expresses the normative system.

Given a logic L and a set of normative systems N over L , for every $\eta \in N$, let us denote by $L(\eta)$ the smallest normal logic of similarity type τ^η which includes $L^\eta \cup \{\eta\}$. We define the *Multimodal Logic of Normative Systems* over L and N , denoted by L^N , as being the smallest normal logic in the expanded language which contains L , N and every L^η . We now present a sound and complete axiomatisation and prove some transfer

results in the case that L is axiomatised by a set of Sahlqvist formulas and N is a set of Sahlqvist formulas.

Definition 1. (Sahlqvist formulas) A modal formula is positive (negative) if every occurrence of a proposition letter is under the scope of an even (odd) number of negation signs. A Sahlqvist antecedent is a formula built up from \top, \perp , boxed atoms of the form $\Box_{i_1} \dots \Box_{i_l} p$, for $i_j \in I$ and negative formulas, using conjunction, disjunction and diamonds. A Sahlqvist implication is a formula of the form $\phi \rightarrow \varphi$, when ϕ is a Sahlqvist antecedent and φ is positive. A Sahlqvist formula is a formula that is obtained from Sahlqvist implications by applying boxes and conjunction, and by applying disjunctions between formulas that do not share any propositional letters.

Observe that \perp and \top are both Sahlqvist and ENS formulas. Intuitively speaking, \perp is the trivial normative system, in \perp every transition is forbidden in every state and in \top every action is legal. In the sequel we assume that for every set N of ENS, $\top \in N$.

Theorem 2. Let L be a normal modal logic axiomatised by a set Γ of Sahlqvist formulas and N a set of ENS Sahlqvist formulas, then:

1. $\Gamma^N = \Gamma \cup N \cup \bigcup \{\Gamma^\eta : \eta \in N\}$ is an axiomatisation of L^N .
2. L^N is complete for the class of Kripke frames defined by Γ^N .
3. L^N is canonical.
4. If L and L^η are consistent, for every $\eta \in N$, and \mathbf{P} is one of the following properties:
 - Compactness
 - Interpolation Property
 - Halldén-completeness
 - Decidability
 - Finite Model Property²

then L^N has \mathbf{P} iff L and $L(\eta)$ have \mathbf{P} , for every $\eta \in N$.

Proof: 1 – 3 follows directly from the Sahlqvist's Theorem. The main basic idea of the proof of 4 is to apply the Sahlqvist's Theorem to show first that for every $\eta \in N$, the smallest normal logic of similarity type τ^η which includes $\Gamma^\eta \cup \{\eta\}$ is $L(\eta)$, is a complete logic for the class of Kripke frames defined by $\Gamma^\eta \cup \{\eta\}$ and is canonical (observe that this logic is axiomatised by a set of Sahlqvist formulas). Now, since for every Elementary Normative System $\eta \in N$ we have introduced a disjoint modal similarity type τ^η , we can define the fusion of the logics $\bigoplus < L(\eta) : \eta \in N >$. It is enough to check that $L^N = \bigoplus < L(\eta) : \eta \in N >$ (remark that $L^\top = L$) and using transfer results for fusions of consistent logics (see for instance [7] and [8]) we obtain that L^N is a conservative extension and that decidability, compactness, interpolation, Hálden-completeness and the Finite Model Property are preserved. \square

We study now the relationships between normative systems. It is interesting to see how the structure of the set of all the ENS over a logic L (we denote it by $N(L)$) inherits

²For the transfer of the Finite Model Property it is required that there is a number n such that each $L(\eta)$ has a model of size at most n .

its properties from the set of first-order counterparts. A natural relationship could be defined between ENS, the relationship of being one *less restrictive* than another, let us denote it by \preceq . Given η, η' , it is said that $\eta \preceq \eta'$ iff the first-order formula $\phi_{\eta'} \rightarrow \phi_\eta$ is valid (when for every $\eta \in N$, ϕ_η is the translation of η). The relation \preceq defines a partial order on $N(L)$ and the pair $(N(L), \preceq)$ forms a complete lattice with least upper bound \perp and greatest lower bound \top and the operations \wedge and \vee .

Now we present an extension of the Logic of Elementary Normative Systems over a logic L with some inclusion axioms and we prove completeness and canonicity results. Given a set N of ENS, let I^{N^+} be the following set of formulas:

$$\left\{ \square_{i_1} \dots \square_{i_l} p \rightarrow \square_{i_1}^\eta \dots \square_{i_l}^\eta p : i_j \in I, \eta \in N \right\}$$

and I^{N^*} the set:

$$\left\{ \square_{i_1}^{\eta'} \dots \square_{i_l}^{\eta'} p \rightarrow \square_{i_1}^\eta \dots \square_{i_l}^\eta p : i_j \in I, \eta \preceq \eta', \eta, \eta' \in N \right\}$$

Corollary 3. *Let L be a normal modal logic axiomatised by a set Γ of Sahlqvist formulas and N a set of ENS Sahlqvist formulas, then:*

1. $\Gamma^{N^+} = \Gamma^N \cup I^{N^+}$ is an axiomatisation of the smallest normal logic with contains L^N and the axioms I^{N^+} , is complete for the class of the Kripke frames defined by Γ^{N^+} and is canonical. We denote this logic by L^{N^+} .
2. $\Gamma^{N^*} = \Gamma^N \cup I^{N^*} \cup I^{N^+}$ is an axiomatisation of the smallest normal logic with contains L^N and the axioms $I^{N^*} \cup I^{N^+}$, is complete for the class of the Kripke frames defined by Γ^{N^*} and is canonical. We denote this logic by L^{N^*} .
3. If L^N is consistent, both L^{N^+} and L^{N^*} are consistent.

Proof: Since for every $i_j \in I$ every $\eta, \eta' \in N$, the formulas $\square_{i_1} \dots \square_{i_l} p \rightarrow \square_{i_1}^\eta \dots \square_{i_l}^\eta p$ and $\square_{i_1}^{\eta'} \dots \square_{i_l}^{\eta'} p \rightarrow \square_{i_1}^\eta \dots \square_{i_l}^\eta p$ are Sahlqvist, we can apply Theorem 2. In the case that L^N is consistent, consistency is guaranteed by the restriction to pairs $\eta \preceq \eta'$ and for the fact that η and η' are ENS. \square

It is worth to remark that Corollary 3 allows us to see that our framework could also be applied to deal with an extensional definition of normative systems (for example like the one presented in [3], where normative systems are defined to be subsets of the accessibility relation with certain properties), taking $N = L$ in the statement of Corollary 3, the logics L^{N^+} and L^{N^*} have the desired properties. Observe also that for every frame $(S, R_i, R_i^\eta)_{i \in I, \eta \in N}$ of the logic L^{N^*} ,

$$R_{i_1}^\eta \circ \dots \circ R_{i_l}^\eta \subseteq R_{i_0} \circ \dots \circ R_{i_l},$$

and for $\eta \preceq \eta'$, $R_{i_1}^\eta \circ \dots \circ R_{i_l}^\eta \subseteq R_{i_1}^{\eta'} \circ \dots \circ R_{i_l}^{\eta'}$, where \circ is the composition relation.

We end this section introducing a new class of modal formulas defining elementary classes of frames, the shallow formulas (for a recent account of the model theory of elementary classes and shallow formulas we refer the reader to [9]).

Definition 4. *A modal formula is shallow if every occurrence of a proposition letter is in the scope of at most one modal operator.*

It is easy to see that every closed formula is shallow and that the class of Sahlqvist and shallow formulas don't coincide: $\square_1(p \vee q) \rightarrow \diamond_2(p \wedge q)$ is an example of shallow formula that is not Sahlqvist. Analogous results to Theorem 2 and Corollary 3 hold for shallow formulas, and using the fact that every frame class defined by any finite set of shallow formulas admits polynomial filtration, by Theorem 2.6.8 of [9], if L is a normal modal logic axiomatised by a finite set Γ of shallow formulas and N is a finite set of ENS shallow formulas, then the frame class defined by Γ^N has the finite model property and has a satisfiability problem that can be solved in NEXPTIME.

3. Multiprocess Temporal Frames and other examples

Different formalisms have been introduced in the last twenty years in order to model particular aspects of agenthood (Temporal Logics, Logics of Knowledge and Belief, Logics of Communication, etc). Logics of ENS defined above are combinations of different logics, and consequently, they reflect different aspects of agents and the agent multiplicity. We show in this section that several logics proposed for describing Multi-Agents Systems are axiomatised by a set of Sahlqvist or shallow formulas and therefore we could apply our results to the study of their normative systems. We introduce first the basic temporal logic of transition systems, not because it is specially interesting in itself, but because is the logic upon which other temporal logics are built and because it is a clear and simple example of how the ENS framework can work.

Given a modal similarity type τ , a τ -frame $\Xi = (S, R_0, \dots, R_k)$ is a *multiprocess temporal frame* if and only if $\bigcup_{i \leq k} R_i$ is serial. Observe that a τ -frame $\Xi = (S, R_0, \dots, R_k)$ is a multiprocess temporal frame if and only if the formula

$$\diamond_0 \top \vee \dots \vee \diamond_k \top \text{ (MPT)}$$

is valid in Ξ . Let us denote by $MPTL$ the smallest normal logic containing axiom (MPT). For every nonempty tuple (i_1, \dots, i_l) such that for every $j \leq l$, $i_j \leq k$, consider the formula $\square_{i_1} \dots \square_{i_l} \perp$. Observe that every formula of this form is shallow and ENS. We state now without proof a result on the consistency of normative systems over $MPTL$ that will allow us to use the logical framework introduced in the previous section.

Proposition 5. *Let X be a finite set of formulas of the form $\square_{i_1} \dots \square_{i_l} \perp$ and let η be the conjunction of all the formulas in X . Then, if $\perp \notin X$ and the following property holds:*

If $\square_{i_1} \dots \square_{i_l} \perp \notin X$, there is $j \leq k$ such that $\square_{i_1} \dots \square_{i_l} \square_j \perp \notin X$.

the logic $MPTL^\eta$ is consistent, complete for the class of Kripke frames defined by $\{MPT, \eta\}$, canonical, has the finite model property and has a satisfiability problem that can be solved in NEXPTIME.

Now we give an example of logic to which our framework could be applied. In a multi-agent institutional environment, in order to allow agents to successfully interact with other agents, they share the dialogic framework (see [10]). The expressions of the communication language in a dialogic framework are constructed as formulas of the type $\iota(\alpha_i : \rho_i, \alpha_j : \rho_j, \phi, \tau)$, where ι is an illocutionary particle, α_i and α_j are agent terms, ρ_i

and ρ_j are role terms and τ is a time term. A scene is specified by a graph where the nodes of the graph represent the different states of the conversation and the arcs connecting the nodes are labelled with illocution schemes that make scene state change.

Several formalisms for modelling interscene exchanges between agents have been introduced using multi-modal logics. In [11] the authors provide an alternating offers protocol to specify commitments that agents make to each other when engaging in persuasive negotiations using rewards. Specifically, the protocol details, how commitments arise or get retracted as a result of agents promising rewards or making offers. The protocol also standardises what an agent is allowed to say or what it can expect to receive from its opponent which, in turn, allows it to focus on making the important negotiation decisions.

The logic introduced in [11] is a multimodal logic in which modalities \square_ϕ for expressions ϕ of the communication language are introduced. The semantics are given by means of Multiprocess Temporal Frames. Therefore, we can use our framework to analyse different protocols over this multimodal logic, regarding protocols as normative systems. Some examples of those protocols are formalised by formulas of the following form $\square_{\phi_1} \dots \square_{\phi_l} \perp$, for example with the formula $\square_{Offer(i,x)} \square_{Offer(i,y)} \perp$, for $x \neq y$ we can express that it is not allowed to agent i to do two different offers one immediately after the other.

In general, a normal multimodal logic can be characterized by axioms that are added to the system K_m , the class of *Basic Serial Multimodal Logics* is characterized by subsets of axioms of the following form, requiring that AD is full:

- $\square_i p \rightarrow \diamond_i p$ AD(i)
- $\square_i p \rightarrow p$ AT(i)
- $\square_i p \rightarrow \square_j p$ AI(i)
- $p \rightarrow \square_i \diamond_j p$ AB(i,j)
- $\square_i p \rightarrow \square_j \square_k p$ A4(i,j,k)
- $\diamond_i p \rightarrow \square_j \diamond_k p$ A5(i,j,k)

An example of Kripke frame of *MPTL* in which none of the previous axioms is valid is $\Xi = (\{0, 1, 2\}, \{(0, 1), (2, 0)\}, \{(1, 2)\})$. In particular, our example shows that the Multimodal Serial Logic axiomatised by $\{AD(i) : i \leq k\}$, is a proper extension of *MPTL*. Observe that any logic in the class BSML is axiomatised by a set of Sahlqvist formulas, therefore we could apply the framework introduced before to compare elementary normative systems on these logics.

Another type of logics axiomatised by Sahlqvist formulas are many Multimodal Epistemic Logics. Properties such as positive or negative introspection can be expressed by $\square_i p \rightarrow \square_i \square_k p$ and $\neg \square_i p \rightarrow \square_i \neg \square_i p$ respectively. And formulas like $\square_i p \rightarrow \square_j p$ allow us to reason about multi-degree belief.

The Minimal Temporal Logic K_t is axiomatised by the axioms $p \rightarrow HFp$ and $p \rightarrow GPp$ which are also Sahlqvist formulas. Some important axioms such as linearity $Ap \rightarrow GHp \wedge HGp$, or density $GGp \rightarrow Gp$, are Sahlqvist formulas, and we can express the property that the time has a beginning with an ENS. By adding the nexttime modality, X , we have an ENS which expresses that every instant has at most one immediate successor.

4. Related work

Several formalisms have been introduced for reasoning about normative systems over specific logics: Normative ATL (NATL), proposed in [2] and Temporal Logic of Normative Systems (NTL) in [3]. NATL is an extension to the Alternating-Time Temporal Logic of Alur, Henzinger and Kupferman (see [4]), NATL contains cooperation modalities of the form $\langle\langle \eta : C \rangle\rangle \phi$ with the intended interpretation that "C has the ability to achieve ϕ within the context of the normative system η ". NTL is a conservative generalization of the Branching-Time Temporal Logic CTL (see [5]). In NTL, the path quantifiers A ("on all paths...") and E ("on some path...") are replaced by the indexed deontic operators O_η ("it is obligatory in the context of the normative system η that...") and P_η ("it is permissible in the context of the normative system η that..."). In our article we have extended these approaches to deal with arbitrary multimodal logics with standard Kripke semantics. Our definition of normative system is intensional, but the languages introduced permit to work with extensional definitions like the ones in [3] and [2].

A general common framework that generalizes both, the results from [3], [2] and the results we present here can be found in [12]. There we go beyond logics with standard Kripke semantics, defining normative systems over polyadic logics that satisfy the two conditions below:

1. For every modality f in the logic similarity type F , the semantics of $f(p_0, \dots, p_{\rho(f)})$ is a monadic first-order formula build from predicates $P_0, \dots, P_{\rho(f)}$, the relational symbols $\{\overline{R_f} : f \in F\}$ and equality.
2. For every modality f in the logic similarity type F , there is a derived connective \square_f such that $\square_f p$ expresses $\forall x(t\overline{R_f}x \rightarrow Px)$ and is closed under the necessitation rule: If ϕ is a theorem of the logic, then $\square_f \phi$ is also a theorem of the logic. This second condition corresponds to the notion of *normality*.

In [13], D. M. Gabbay and G. Governatori introduced a multi-modal language where modalities were indexed. Their purpose was the logical formalization of norms of different strength and the formalization of normative reasoning dealing with several intensional notions at once. The systems were combined using Gabbay's fibring methodology. Our approach is different from their, because our main purpose is the comparison between normative systems at the same level, over a fixed logic. Our approaches also differ in the methodologies in use. It could be interesting to combine both perspectives to model the dynamics of norms in hierarchical systems.

5. Future work

In our paper we have dealt only with multimodal languages with monadic modalities, but using the results of Goranko and Vakarelov in [14], on the extension of the class of Sahlqvist formulas in arbitrary polyadic modal languages to the class of inductive formulas, it is possible to generalize our results to polyadic languages. We could apply also our results to different extended modal languages, such as reversive languages with nominals (in [14], the elementary canonical formulas in these languages are characterized) or Hybrid Logic (in [9], Hybrid Sahlqvist formulas are proved to define elementary classes of frames).

We will proceed also to the study of computational questions for the multimodal logics introduced, such as model checking. This kind of results will give us a very useful tool to compare normative systems and to answer some questions, for example, about the existence of normative systems with some given properties. It is known that, if L is a multimodal logic interpreted using Kripke semantics in a finite similarity type, given a finite model and a formula ϕ , there is an algorithm that determines in time $O(|M| \times |\phi|)$ whether or not $M \models \phi$ (see [15], p. 63), using this fact, since we build our formalisms for normative systems by means of fusions, complexity results for fusion of logics could be applied (see for instance [16]).

Most state-of-the-art SAT solvers today are based on different variations of the Davis-Putnam-Logemann-Loveland (DPLL) procedure (see [17] and [18]). Because of their success, both the DPLL procedure and its enhancements have been adapted to handle satisfiability problems in more expressive logics than propositional logic. In particular, they have been used to build efficient algorithms for the Satisfiability Modulo Theories (SMT) problem. Future work will include the study of the (SMT) problem for a Multimodal Logic of Normative Systems L : given a formula ϕ , determine whether ϕ is L -satisfiable, i.e., whether there exists a model of L that is also a model of ϕ .

Using the framework introduced in [19] it would be possible to integrate fusions of logics on a propositional framework. In [19], an Abstract DPLL, uniform, declarative framework for describing DPLL-based solvers is provided both for propositional satisfiability and for satisfiability modulo theories. It could be interesting to work with a Quantified Boolean formulas engine instead of the usual SAT engines used by several SMT solvers, in order to deal with formulas that axiomatise Logics for Multi-Agent Systems.

Given a normative system, it is important also to be able to efficiently check why it is not modelling what we originally want. We could benefit from recent advances in system diagnosis using Boolean Satisfiability and adapt it to our framework. See for instance [20], where efficient procedures are developed to extract an unsatisfiable core from an unsatisfiability proof of the formula provided by a Boolean Satisfiability (SAT) solver.

Acknowledgements

The author wishes to express her thanks to Carles Sierra, Pablo Noriega and the reviewers of this paper for their helpful comments. The author was partially supported by Project TIN2006-15662-C02-01.

References

- [1] P. NORIEGA. Fencing the Open Fields: Empirical Concerns on Electronic Institutions, in O. BOISSIER, V. Dignum, G. LINDEMANN, E. MATSON, S. OSSOWSKI, J. PADGET, J. S. SICHMAN AND J. VÁZQUEZ-SALCEDA (ed.) *Coordination, Organizations, Institutions, and Norms in Multi-Agent Systems* Chapter 15, Springer (2006) 82–98.
- [2] W. VAN DER HOEK AND M. WOOLDRIDGE. On obligations and normative ability: towards a logical analysis of the social contract, *Journal of Applied Logic*, 3 (2005) 396–420.
- [3] T. ÅGOTNES, W. VAN DER HOEK, J.A. RODRÍGUEZ-AGUILAR, C. SIERRA AND M. WOOLDRIDGE. On the Logic of Normative Systems, *Twentieth International Joint Conference on AI, IJCAI07*, AAAI Press (2007).
- [4] V. ALUR, T.A. HENZINGER AND O. KUPFERMAN. Alternating-Time Temporal Logic, *Annals of Pure and Applied Logic*, 141 (2006) 180–217.

- [5] E. A. EMERSON. Temporal and Modal Logic, in J. VAN LEEUWEN (ed.) *Handbook of Theoretical Computer Science* vol. B, Elsevier (1990) 996–1072.
- [6] A. KURUCZ. Combining Modal Logics, in P. BLACKBURN, J. VAN BENTHEM AND F. WOLTER (ed.) *Handbook of Modal Logic* Chapter 15, Elsevier (2007).
- [7] F. WOLTER. Fusions of modal logics revisited, in M. KRACHT, M. DE RIJKE, H. WANSING AND M. ZAKHARYASHEV (eds.) *Advances in Modal Logic* CSLI, Stanford, CA. (1998)
- [8] M. FINGER, M. A. WEISS. The Unrestricted Combination of Temporal Logic Systems, *Logic Journal of the IGPL*, 10 (2002) 165–189.
- [9] B. D. T. CATE. Model Theory for extended modal languages, *Ph.D Thesis, Universiteit van Amsterdam* (2005).
- [10] M. ESTEVA, J.A. RODRÍGUEZ-AGUILAR, J. LL. ARCOS, C. SIERRA AND P. GARCIA. Formalising Agent Mediated Electronic Institutions, *Proceedings of the 3er Congrés Català d'Intel.ligència Artificial*, (2000) 29–38
- [11] S. D. RAMCHURN, C. SIERRA, LL. GODO, N. R. AND JENNINGS, N. R. 2006. NEGOTIATING USING REWARDS. In Proceedings of the Fifth international Joint Conference on Autonomous Agents and Multiagent Systems (Hakodate, Japan, May 08 - 12, 2006). AAMAS '06. ACM Press, New York, NY, 400–407.
- [12] P. DELLUNDE. On the Multimodal Logic of Normative Systems *Preprint*(2007).
- [13] D. M. GABBAY AND G. GOVERNATORI. Dealing with Label Dependent Deontic Modalities, *Norms, Logics and Information Systems* CSLI, Stanford, CA. (1998).
- [14] V. GORANKO AND D. VAKARELOV. Elementary Canonical Formulae: extending Sahlqvist's Theorem, *Annals of Pure and Applied Logic*, 141 (2006) 180–217.
- [15] R. FAGIN, J. Y. HALPERN, AND M. Y. VARDI *Reasoning about Knowledge*, Cambridge, MA: MIT Press (1995) 289–321.
- [16] M. FRANCESCHET, A. MONTANARI AND M. DE RIJKE. Model Checking for Combined Logics with an Application to Mobile Systems *Automated Software Engineering*, 11 (2004) 289–321.
- [17] M. DAVIS, G. LOGEMANN AND D. LOVELAND. A machine program for theorem-proving, *Comm. of the ACM*, 5 (6) (1962) 394–397.
- [18] M. DAVIS, H. PUTNAM. A computing procedure for quantification theory, *Journal of the ACM*, 7 (1960) 201–215.
- [19] R. NIEUWENHUIS, A. OLIVERAS AND C. TINELLI. Solving SAT and SAT Modulo Theories: From an Abstract Davis-Putnam-Logemann-Loveland Procedure to DPLL(T), *Journal of the ACM*, 53 (6) (2006)937–977.
- [20] L. ZHANG AND S. MALIK. Extracting Small Unsatisfiable Cores from Unsatisfiable Boolean Formulas, Sixth International Conference on Theory and Applications of Satisfiability Testing, *SAT2003*.

Agents and Clinical Guidelines: Filling the Semantic Gap

David ISERN, David SÁNCHEZ and Antonio MORENO

iTAKA Research Group - Intelligent Tech. for Advanced Knowledge Acquisition
Universitat Rovira i Virgili. Department of Computer Science and Mathematics
Avda. Paisos Catalans, 26. 43007 Tarragona, Catalunya
{david.isern, david.sanchez, antonio.moreno}@urv.cat

Abstract. Medical ontologies are developed to solve problems such as the demand for reusing, sharing and transmitting data. The unambiguous communication of complex and detailed medical concepts is a crucial feature in current medical information systems. In these systems, several agents must interact in order to share their results and, thus, they must use a medical terminology with a clear and non-confusing meaning. The paper presents the inclusion of an especially designed medical ontology in the HECASE2 multi-agent system. HECASE2 has been developed to help doctors in applying clinical guidelines to their patients in a semi-automatic fashion. In addition, it shows how intelligent agents may take profit from the modelled medical knowledge to coordinate their activities in the enactment of clinical guidelines.

Keywords. Knowledge representation, Ontologies, Multi-agent systems, Clinical guidelines

1. Introduction

A *clinical guideline* (GL) indicates the protocol to be followed when a patient is diagnosed a certain illness (*e.g.* which medical tests have to be performed on the patient to get further data, or what steps have to be taken according to the results of the tests). They provide very detailed information concerning the resources needed in the treatment of a patient [1]. They are designed to provide a standard care both within a healthcare organisation and among different organisations, and, in consequence, they allow to improve the patient's care delivery quality [14]. A hard task to be accomplished is the inclusion of a guideline execution engine in the daily work flow of practitioners. Taking this situation into consideration, in previous papers ([6,8]) a multi-agent system called HECASE2 was introduced. It proposes an agent-based open architecture, that represents different entities of a healthcare organisation. The system helps doctors to collect and manage information about patients and coordinate some complex tasks, such as scheduling meetings or looking for a required service. HECASE2 includes the management of clinical guidelines by doctors in the diagnosis or treatment of diseases. All these tasks require an external element to be more flexible and efficient: a representation of the care flow and the terminology used among all entities. In order to address this issue, this paper

proposes the inclusion in HECASE2 of an application ontology that covers three main areas: *a)* representing all medical terminology used by all partners, *b)* modelling health-care entities with their relations, and *c)* assigning semantic categories to those medical concepts.

With that approach, care is improved at least in three ways:

- i)* Ontologies provide a common understandable semantic framework to execute clinical guidelines. Consequently, all the entities and concepts involved in that execution can be explicitly defined according to their relations and attributes.
- ii)* Agents can understand what they must perform at any moment and negotiate or coordinate their activities with the appropriate partners.
- iii)* Ontologies provide a high level abstraction model of the daily work flow. That model can be adapted to each particular organisation, without the agents having to change their internal behaviour. In that sense, any organisation can have an ontology adapted to its particular circumstances.

The rest of the paper is organised as follows. Section 2 comments the main features of the HECASE2 agent-based system. Section 3 describes the main components of the designed application ontology. After that, section 4 explains how the ontology is used by HECASE2 in a case study. Then, section 5 compares the presented approach with other works in the area, and finally, some conclusions are summarised.

2. HECASE2 : A Distributed Guideline-Based Health Care System

HECASE2 is a multi-agent system that maps different entities in a healthcare organization (*e.g.* medical centres, departments, services, doctors, patients) as agents with different roles. This system provides interesting services both to patients (*e.g.* booking a visit with a doctor, or looking up the medical record) and to doctors (*e.g.* support in the application of a GL to a patient). Guidelines are used to provide a high level supervision of the activities to be carried out to address a specific pathology. We use PROforma as the language to represent and share guidelines [16]. PROforma defines four types of tasks: *i)* *actions*, that are procedures that have to be executed outside the computer, *ii)* *decisions*, that are used to choose a candidate from a given set of options using arguments pros and cons, *iii)* *enquiries*, that are requests for information needed to execute a certain procedure, and *iv)* *plans*, that are sequences of sub-tasks taking into account logical or temporal constraints. Thus, a guideline can be defined as a set of plans that are composed by actions, decisions and enquiries. The agents in the system coordinate their activities in order to apply a guideline to a patient (always under the supervision of a doctor).

Fig. 1 depicts all agents and their relationships [6,8]. This is an open architecture and, depending on the situation, there will be more or less agents of each type, and more or less interaction between them. At the top, the patients are represented by *User Agents* (UAs). All UAs can talk with the *Broker Agent* (BA). The BA is the bridge between users and the medical centres, and it is used to discover information. The BA knows about the medical centres located in a city or in an area. A *Medical Centre Agent* (MCA) monitors all of its departments, represented by *Department Agents* (DAs), and a set of general services (represented by *Service Agents* (SAs)). Each department is formed by several doctors (represented by *Doctor Agents* (DRA)) and more specific services (also modelled

as SAs). Moreover, in each department there is a *Guideline Agent* (GA) that performs all actions related to guidelines, such as looking for a desired GL, storing and/or changing a GL made by a doctor, etc. This GA contains only GLs related to the department where it is located but, if it is necessary to use another guideline (*e.g.* when treating a patient with multiple pathologies), the GA could request it from other GAs. Each department also contains an *Ontology Agent* (OA) that provides access to the designed medical ontology and complements the information provided by the GA. At the bottom of the architecture there is the *Medical Record Agent* (MRA) which controls the access to a DB that stores all patient health records (PHR) in the medical centre. This agent provides a secure access to the data using authentication and ciphering through a Public Key Infrastructure (PKI).

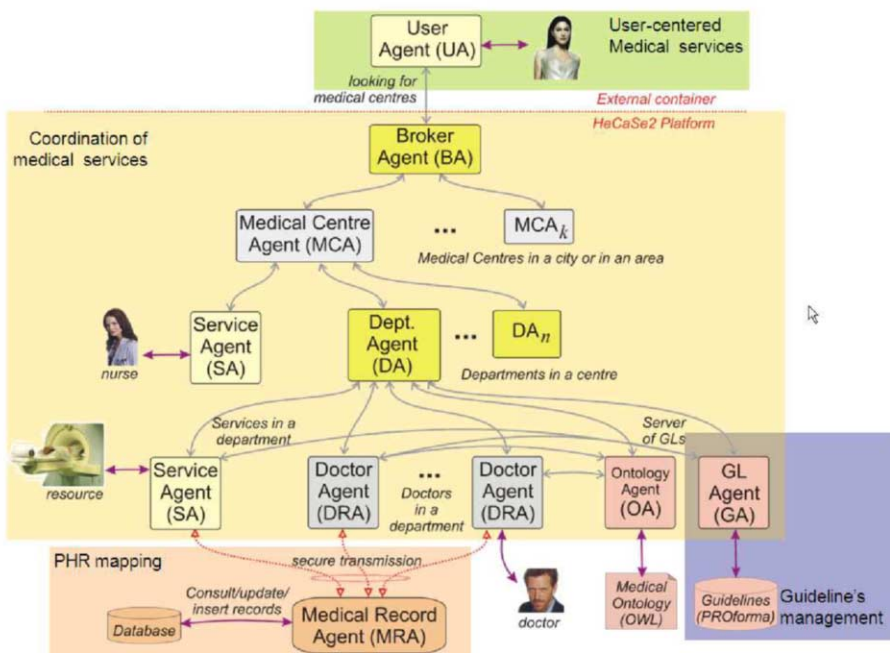


Figure 1. Agent-based architecture of HECASE2

The behaviour of the guideline-based agent system is the following:

- When the doctor diagnoses that the patient has a certain disease, its associated DRA requests from GA the associated guideline and it starts to execute it.
- The DRA has a partial knowledge of the system and it does not know all the agents or its responsibilities. The OA is intended to provide that information. Concretely, which agents perform a task or who is the responsible of a required parameter contained in an enquiry. Once the required source/agent/service has been identified, the DRA knows exactly where it can be found.
- The DRA accesses the PHR through the MRA to look for the required parameters.
- Sometimes an action has to be performed on the patient, or the guideline needs data that is not included in the PHR (*e.g.* the level of glucose in blood, which can be known with a blood analysis). In these cases, the DRA has to contact with

the appropriate SA (it is known by way of the OA) which performs the required action, from the same medical centre or another medical centre.

- The BA allows to exchange information between different medical centres and the UA.

3. Ontological representation of medical knowledge

Ontologies define terms and relations comprising the vocabulary of a topic area as well as the rules for combining terms and relations to define extensions to the vocabulary [12].

Different knowledge representation formalisms exist for the definition of ontologies. However, they share the following minimal set of components:

- a) *Classes*: represent concepts. Classes in the ontology are usually organised in taxonomies through which inheritance mechanisms can be applied.
- b) *Individuals*: are used to represent real world entities.
- c) *Properties*: they represent binary associations between ontological entities. On the one hand, *object properties* establish relationships between pairs of individuals. On the other hand, *data type properties* relate an individual to a data value (integer, string, float, etc.); they can be considered attributes.

The designed ontology was coded using one of the newest standard languages, the Web Ontology Language (OWL) [11]. There exist three different flavours of OWL with varying levels of expressiveness: OWL Full, OWL Lite and OWL DL. For our purposes we need the maximum level of expressiveness but maintaining a standard structure (classes and properties) to allow inference. For these reasons OWL DL was used.

There does not exist a unique way for modelling ontological knowledge. From the ontology engineering point of view, several methodologies and guides have been designed in the past for aiding the ontology construction process such as METHONTOLOGY or On-To-Knowledge [5]. From all of them, the *101 ontology development method* has been selected ([13]) due to both its flexibility and independence from the final language description. It divides the ontology construction process in several iterative steps, covering from the definition of the scope to the specification of each ontological entity. It also provides golden rules about how an ontology should be defined. Each step can be executed as many times as desired and in any particular order, allowing to create the final ontology in a flexible and incremental way.

The scope of our ontology covers all the relations established in the multi-agent system associated to a healthcare organisation. It has three main groups of concepts: *organisational information* of agents, all possible *semantic types* (entities and events) of the used concepts, and a set of *medical concepts* related to the clinical guidelines [7].

The *Agent* class includes all main concepts related with the internal organisation of the multi-agent system. In this class there are *Departments*, *Patients*, *Practitioners*, *Medical centres* and *Services*. All these elements have internal relations, such as *Cardiology* is-a *Department* that belongsTo *Medical-center* (see Fig. 2). More complex relations between doctors and services are also mapped, such as *Nurse* belongsTo *Department* because a nurse can be located in any department, or *Family_doctor* belongsTo (*General_medicine* \cup *Emergency* \cup *Paediatrics*) that means that an instance of family doctor could belong to any instance of three departments. Relations between *Agent* sub-

classes are inspired in usual healthcare organisations. The inverse relations are also available to know which kind of doctors compose a department or which kind of services are located in a department or medical centre.

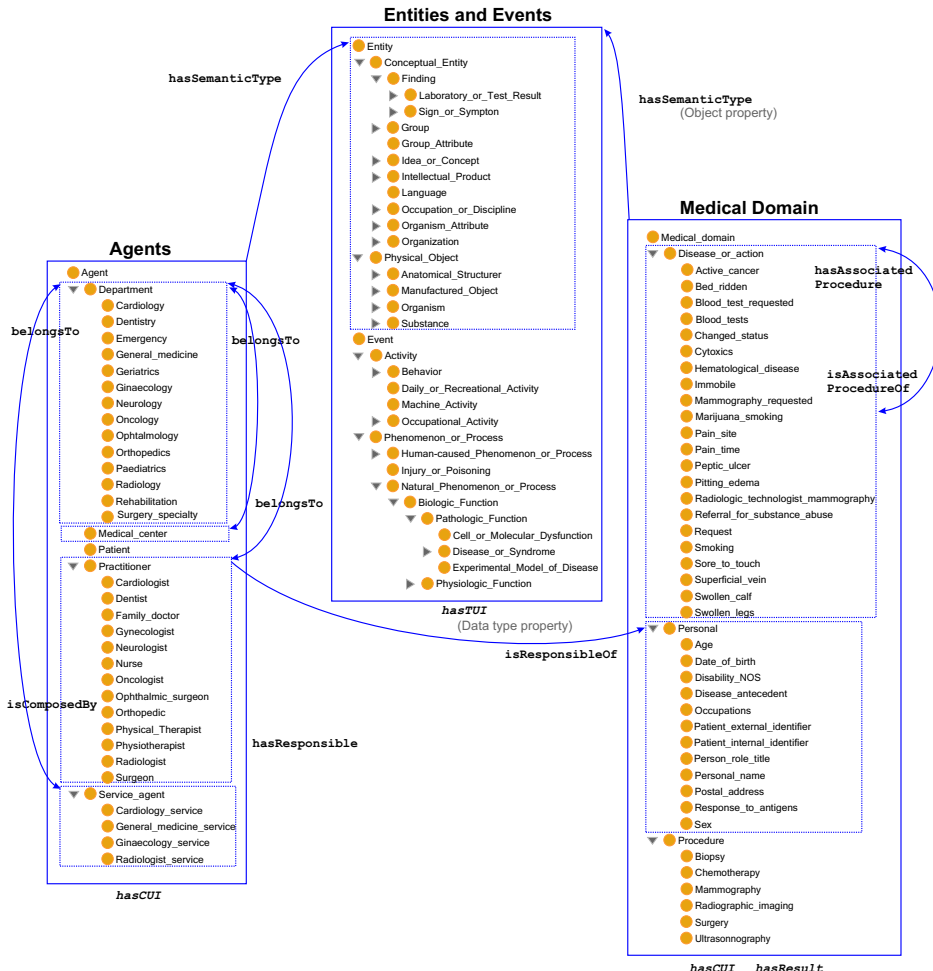


Figure 2. Subset of the designed Medical Ontology

Although most of the departments are similar in medical centres, it is possible to represent different variations. In those cases, a specialisation of the ontology could be made. For instance, the oncology department is different in a hospital or in a primary attention centre that covers a part of a city or a set of villages. In these cases, two subclasses of the oncology department will be created. The parent class will remain with all common features and the two siblings will contain the rest (and specific) features or resources for each one.

The next set of classes concerns the different semantic types of the medical concepts. There are two main hierarchies, named *Entity* and *Event*, which were picked from UMLS

Metathesaurus¹. Currently, UMLS defines 135 different semantic types divided in two groups: meanings concerned with healthcare organisations or entities, and meanings related with events or activities in a daily care flow. Both hierarchies are organised as a taxonomy with *is-a* relations between concepts, such as *Disease_or_Syndrome* *is-a* *Pathologic_function*. All this information is used by agents to know exactly which is the function of any required concept and further connections with others. For instance, if a concept is a *Finding*, and a *Finding* *isResponsibilityOf* a *Practitioner*, the agent knows that a patient's finding should be given by a practitioner.

The last part of the ontology represents the specific vocabulary used in clinical guidelines. It systematises all specific knowledge required in any guideline execution engine, divided in *Diseases*, *Procedures* and *Personal data*. It is necessary to define a set of relations between each concept and its identifier (Code Unique Identifier or CUI), its semantic type, which entity of the system is responsible of its accomplishment, and the produced result (*i.e.* if it is a number, a Boolean, an enumerate or a complex object). Relations are bidirectional because it is interesting to know that the finding *Active_cancer* *isResponsibilityOf* a *Family_Doctor*, and the family doctor's responsibilities. Each agent can access the concepts related to its own domain and be aware of the consequences of the application of an action.

Table 1. Object and data type properties defined in the *medical ontology*

<i>Object Properties</i>	<i>Description</i>
<i>belongsTo</i>	Any instance of a class that belongs to another
<i>hasAssociatedProcedure</i>	A medical concept has an associated procedure. It is used by doctors to simplify a search (from UMLS)
<i>hasResponsible</i>	Establish the responsibility of any medical concept that has to be performed by a healthcare party
<i>hasSemanticType</i>	Functional property to specify the semantic type of a concept
<i>isAssociatedProcedureOf</i>	Inverse of <i>hasAssociatedProcedure</i>
<i>isComposedBy</i>	If an instance $a \in A$ <i>belongsTo</i> $b \in B$ then, $b \in B$ <i>isComposedBy</i> $a \in A$. It is not just the inverse because the first relation is $1 - N$ and the second is $M - N$
<i>isResponsibleOf</i>	Inverse of <i>hasResponsible</i>
<i>Data type Properties</i>	<i>Description</i>
<i>hasCUI</i>	Value of the CUI (<i>Code Unique Identifier</i>) (from UMLS)
<i>hasDescription</i>	Concept definition provided from UMLS (when it is available)
<i>hasResult</i>	Type of output of an element (action or data concept)
<i>hasResultBoolean</i>	Sub class of <i>hasResult</i> that sets a Boolean as output
<i>hasResultInteger</i>	Sub class of <i>hasResult</i> that sets an Integer as output
<i>hasResultString</i>	Sub class of <i>hasResult</i> that sets a String as output
<i>hasResultEnumerate</i>	Sub class of <i>hasResult</i> that sets an array as output
<i>hasResultComplex</i>	Sub class of <i>hasResult</i> that sets a complex element formed by one or more simple results (concepts) as output
<i>hasTUI</i>	In UMLS, semantic types are labelled with a <i>Type Unique Identifier</i>

¹Unified Medical Language System (UMLS) is a repository of the US National Library of Medicine that comprises the most widely used medical terminologies and nomenclatures, as MedLine, MeSH or LOINC.

As explained above, three main groups of concepts are defined in the medical ontology: *agent-based health care concepts*, *semantic types* of entities and events, and *medical concepts* (see Fig. 2). All the defined concepts are interrelated by taxonomic and non taxonomic relations. The former are based on *is-a* relations and are established by generalisation-specialisation of concepts. Some are picked from UMLS and others are picked from healthcare organisations. The second kind of relations is more difficult to establish, due to its semantic-dependency. In fact, they are usually omitted in standard repositories [4]. By analysing the information required in the execution a clinical guideline, a set of relations were defined (see Fig. 2). They are shown in Table 1, along with their type and description. When a new GL is added, all new concepts should be added and all required relationships between concepts should be established.

4. Ontology-Driven Clinical Guideline Execution

As shown in previous sections, the combination of a knowledge base and an agent-based system that exploits that knowledge could be interesting to achieve flexibility and reusability. In order to illustrate how these elements have been integrated, in this section, we explain the procedure followed in a GL adopted from the National Guideline Clearinghouse and coded in PROforma [16] which is intended to diagnose and treat *Gastrointestinal Cancer* (GC). The GL is depicted in Fig. 3.

First, the doctor selects the GC guideline from the repository (through his DRA and the GA of the department). The DRA receives the GL which is graphically presented to the doctor. In this case, the first step of the GL is to evaluate the importance of the disease. As a result of the evaluation, it collects information about the patient and an invasive test (*Biopsy*). The DRA analyses the GL and observes that the first enquiry is composed by six parameters. For each one, the DRA asks the OA to know more details. The OA replies with the information found in the *Medical Ontology*. In this case, the parameter *Age* is included in the category of *Personal* that can be found in the medical record. The DRA demands the MRA that value. Other required parameters as *Pain site*, *Weight loss*, *Pain time* and *Smoking*, are *Findings* that the doctor can evaluate and set if the record is not found in the patient's history. The ontology also contains information about each element as the resulting format output and the allowed values by using data type properties (see Table 1). For instance, the case of *Pain time*, due to its nature, the data values allowed are *short*, *moderate*, *long*. Finally, the last value to consider is the result of the *Biopsy*.

A *Biopsy* is an invasive *Diagnostic_Procedure* that *isResponsibleOf* a *Surgery_specialty*. In that case, if the biopsy has not been performed previously, the DRA is able to look for a surgeon (*Practitioner* that *belongsTo* a *Surgery_specialty* department) and book a meeting for the patient (at first, it looks for available surgeons, and then, it begins a *contract net* negotiation with them). If agreed, the enactment is stopped after that result is received. In a future medical visit, the doctor will have the result of the biopsy and he will be able to perform a first diagnosis: if the biopsy is negative, the patient will follow a plan for gastrointestinal treatment as *Peptic_ulcer*. Otherwise, the patient suffers from cancer and should be treated for that disease.

In the case of cancer, there is a final step to be performed before referring the patient to a surgeon: to check if the patient is elderly or not. In the former case, the patient cannot

be hospitalised and should be treated with symptomatic treatments. In the latter case, there are two possible plans to follow, a chemical treatment such as *Chemotherapy*, or a *Surgery*. The decision is taken by the surgeon in a further medical visit.

As shown through the example, the GL provides the general care flow to follow (declarative and explicit knowledge) and the ontology provides semantic information about all concepts or actions to be performed. Detailed information allows to represent relations between all entities and to collect all required data by agents in order to know which decision should take. When the doctor agent considers the term *Biopsy* it does not know if that concept is a procedure or a finding or any other kind of element, and it does not know the existing relations of that concept either. The ontology allows to correlate all elements present in the GL and know exactly all the details. This information is not included in GLs because it depends on the specific scenario where the GL should run or the specific organisation.

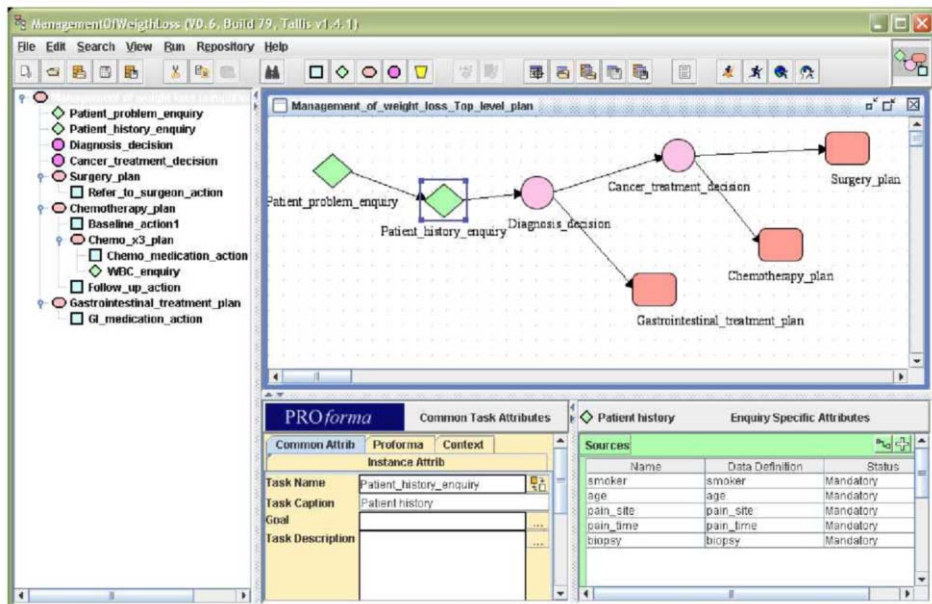


Figure 3. Case study guideline coded using PROforma composer tool (Tallis) ([16])

5. Related work

The use of ontologies in medicine has been shown to suppose an important advantage. Kumar *et. al.* [10] studied the implementation of a task ontology named Context-Task Ontology (CTO) in order to map the knowledge required in the implementation of GLs. They implemented the CTO using DAML+OIL and intended to create GLs through an independent structure that stored all relations and concepts in a unique way. They noted that this approach had some drawbacks, such as the difficulty to define and know exactly which relations are required, as well as the requirement of expert's intervention. The same authors later described the use of ontologies to define clinical guidelines by adding

a hierarchy of classes to represent medical procedures and plans [9]. However, this implied a high level of complexity as compared to flow-chart-based representations. Serban *et al.* [15] proposed the use of an ontology to guide the extraction of medical patterns contained in GLs in order to reconstruct the captured control knowledge. All these works suggest the use of UMLS as a central corpus.

Ciccarese *et al.* [2] introduced an architecture that linked a care flow management system and a guideline management system by sharing all the data and ontologies in a common layer. They proposed to represent medical and organisational information in those ontologies, but they did not use non taxonomic relations in the ontologies; all the information is stored in the flow chart-like representation used to code GLs.

Moreover, Davis and Blanco [3] suggested the use of taxonomies to model the clinical life cycle knowledge. They also described a state-based data flow model to represent all dependencies between enterprise entities.

6. Conclusions

The inclusion of a medical ontology in the multi-agent system HECASE2 has been discussed. As shown in the previous section, the use of ontologies in the medical domain is increasing and offers some advantages such as making domain assumptions explicit, separating domain knowledge from operational knowledge, and sharing a consistent understanding of what information means.

In the present work, the designed medical ontology brings the following advantages to the guideline-based execution system: *a*) to identify the required actors that are able to accomplish an action and to know the source/details of an item, *b*) to adapt the execution framework to the particular casuistry of any healthcare organisation without modifying the MAS implementation and the guideline either, and *c*) to provide an application independent context. Thus, by changing the ontology and its relations, the execution procedure also changes.

Note that the only issue that should be addressed is the manual definition of the appropriate task ontology. This question usually requires the intervention of a domain expert, but UMLS provides a large corpus of concepts and relations that can be easily reused, and the ontology creation process could be automated by collecting automatically the required information when a new GL was added to the repository.

A future research line is the use of the semantic content embedded in the relationship of classes in order to provide interoperability between several medical organizations with different ontologies. Another issue that can be addressed is the implementation of accurate coordination protocols between doctors, services and departments while a doctor follows a GL.

Acknowledgements

D. Sanchez would like to acknowledge the support of the *Departament d'Innovació, Universitats i Empresa de la Generalitat de Catalunya i del Fons Social Europeu*. The authors would like to acknowledge the feedback received from John Fox as well as his permission to use Tallis.

References

- [1] A.A. Boxwala, S. Tu, M. Peleg, Q. Zeng, O. Ogunyemi, R.A. Greenes, E.H. Shortliffe and V.L. Patel: Toward a Representation Format for Sharable Clinical Guidelines, *Journal of Biomedical Informatics* **34** (3) (2001), 157–169.
- [2] P. Ciccarese, E. Caffi, L. Boiocchi, S. Quaglini and M. Stefanelli: A Guideline Management System, in Proceedings of *11th World Congress on Medical Informatics*, M. Fieschi and E. Coiera and Y.-C.J., Li (eds.), IOS Press, Vol. 107, San Francisco, USA, 2004, pp. 28–32.
- [3] J.P. Davis and R. Blanco: Analysis and Architecture of Clinical Workflow Systems using Agent-Oriented Lifecycle Models, *Intelligent Paradigms for Healthcare Enterprises* **184** (2005), 67–119.
- [4] L. Ding, T. Finin, A. Joshi, R. Pang, R.S. Cost, Y. Peng, P. Reddivari, V. Doshi and J. Sachs: Swoogle: A Search and Metadata Engine for the Semantic Web, in Proceedings of *ACM 13th Conference on Information and Knowledge Management*, ACM Press, Washington D.C., USA, 2004, pp. 652–659.
- [5] A. Gómez-Pérez, O. Corcho and M. Fernández-López, *Ontological Engineering*, Springer Verlag, 2004.
- [6] D. Isern and A. Moreno: Distributed guideline-based health care system, in Proceedings of *4th International Conference on Intelligent Systems Design and Applications, ISDA 2004*, IEEE Press, Budapest, Hungary, 2004, pp. 145–150.
- [7] D. Isern, D. Sánchez and A. Moreno: An Ontology-Driven Agent-Based Clinical Guideline Execution Engine, in Proceedings of *Artificial Intelligence in Medicine, AIME 2007*, R. Bellazzi and A. Abu-Hanna and J. Hunter (eds.), LNAI Vol. 4594, Springer Verlag, Amsterdam, The Netherlands. 2007, pp. 49–53.
- [8] D. Isern, A. Valls and A. Moreno: Using aggregation operators to personalize agent-based medical services, in Proceedings of *Knowledge-Based Intelligent Information and Engineering Systems, KES 2006*, B. Gabrys and R. J. Howlett and L.C. Jain (eds.), LNAI Vol. 4252, Springer Verlag, Bournemouth, UK. 2006, pp. 1256–1263.
- [9] A. Kumar, P. Ciccarese, B. Smith and M. Piazza: Context-Based Task Ontologies for Clinical Guidelines, *Context-Based Task Ontologies for Clinical Guidelines* **102** (2004), 81–94.
- [10] A. Kumar, S. Quaglini, M. Stefanelli, P. Ciccarese and E. Caffi: Modular representation of the guideline text: An approach for maintaining and updating the content of medical education, *Medical Informatics and the Internet in Medicine* **28**(2) (2003), 99–115.
- [11] D.L. McGuinness and F. Harmelen: OWL Web Ontology Language. Available at: <http://www.w3.org/TR/owl-features/>. 2004.
- [12] R. Neches, F. Richard, T.W. Finin, T.R. Gruber, R. Patil, T.E. Senator and W.R. Swartout: Enabling Technology for Knowledge Sharing, *AI Magazine* **12**(3) (1991), 36–56.
- [13] N.F. Noy and D.L. McGuinness, *Ontology Development 101: A Guide to Creating Your First Ontology*, Stanford Medical Informatics, 2001.
- [14] S. Quaglini, M. Stefanelli, A. Cavallini, G. Micieli, C. Fassino and C. Mossa: Guideline-based careflow systems, *Artificial Intelligence in Medicine* **20** (2000) 5–22.
- [15] R. Serban, A. Teije, F. Harmelen, M. Marcos and C. Polo-Conde: Extraction and use of linguistic patterns for modelling medical guidelines, *Artificial Intelligence in Medicine* **39**(2) (2007) 137–149.
- [16] D.R. Sutton and J. Fox: The syntax and semantics of the PROforma guideline modeling language, *Journal of the American Medical Informatics Association* **10**(5) (2003) 433–443.

A Monitor for Digital Business Ecosystems

Gabriel Alejandro Lopardo¹, Josep-Lluís de la Rosa i Esteva¹, Nicolás Hormazábal¹

Abstract - This paper proposes to create a monitor of digital business ecosystems so that it provides agents with information to improve the behaviour of the ecosystem in terms of stability. This work proposes that, in digital ecosystems, monitor techniques can provide fundamental services and information. The final goal is to run the monitor algorithms, generate recommendation strategies and test them. A set of evaluation metrics must be defined as well. We want to provide an outline of some global indicators, such as heterogeneity and diversity, and establish relationships between agent behaviour and these global indicators of system performance.

Keywords: digital business ecosystems, agents, agent behaviour, recommendation

1. Introduction

According to the AgentLink's 2005 Roadmap, Virtual organisation formation and management is a challenge. Virtual Organisations (VOs) have been identified as the means to release the power of the Grid, but well-defined procedures for determining when to form new VOs, how to manage them, and ultimately how and when to disband them, are still missing. Working with complex data in dynamic environments, as it is the case of the automation of coalition or virtual organizations formations to create a dynamic packaging that requires of taking many decisions in very short time to take advantage of the business opportunities that appear through time, with the expectancy to be the first or the winner of every single deal at a short term, and gaining business and, at a long term, be more profitable. Taking into account that all Artificial Intelligence (AI) systems share a few characteristics: they are designed to work with data sets that are large, complex, or both; to search through them and find relevant data; and to look for patterns. AI systems are useful for dealing with any dynamic environment in which they have to make intelligent choices, depending upon the input, among a number of possible answers. They also use samples to form generalizations about an entire data set and, in some cases, make or help make intelligent decisions. Potentially, they could even execute tasks.

Numerical analytics systems find patterns and rules in big numerical data sets. They are most useful for problems (such as the detection of fraud) that require heavy number crunching to distinguish among different sets of items. Rule-based decision systems use predetermined rules or logic, with or without numerical data, to make decisions and determine outcomes. They are useful for automating work flows. Autonomous execution systems (also known as agents or bots), which run

¹ Gabriel Lopardo, and Josep Lluis de la Rosa EASY Center of the Xarxa IT CIDEM, University of Girona. Campus Montilivi (Edif. PIV) 17071. Girona, Catalonia. Tel. + 34 972418854, E-mail: {glozano, pepluis}@eia.udg.es

continuously, monitor information as it arrives—typically from several distributed sites—and execute specific tasks in response to what they find. These systems are most useful for automating tasks across organizations by using data shared over the Internet, especially when the underlying data are structured according to prevailing standards such as the Extensible Mark-up Language (XML). The development of machine-readable Internet content based on XML, which has spawned the use of agent or bot technologies, makes it possible to improve a company's information-exchange capabilities to an unprecedented extent. Among other possibilities, this development means that businesses can automate interactions with their partners up and down the value chain.

Although these applications of AI are promising, the technology isn't right for all information problems. First, it is overkill for simple questions and not sophisticated enough—yet—for some complex ones. Second, since many AI solutions improve performance through trial and error, AI isn't a good choice for mission-critical challenges. However, there are still some questions: Are the business processes and technologies of the company or the virtual organization sufficiently standardized for it to apply AI? In general, AI-based tools are most effective when business processes and decision logic are consistent and can be encoded; furthermore, the technology infrastructure must capture, in a timely and accurate way, the data the AI system requires. Nonetheless, even organizations without standardized process and technology infrastructures can apply AI-based tools to isolated problems. What parts of the business are best suited to AI? The virtual organizations identify activities that are complex, repetitive, information based—and not mission critical. In those areas, basic AI technologies can often be deployed in parallel with existing approaches and then iteratively refined and allowed to take over more and more of the total activity.

2. Ecosystems

This paper introduces a methodology to evaluate physical heterogeneity in physical Multi-Agent Systems (MAS) that interact to create dynamic packaging and virtual organizations. The need to measure heterogeneity or diversity is key to stabilize ecosystems of companies with dynamic deals. The main causes of instability that nowadays are foreseen are: imperfect data (lack of data, bad data, wrong data, delayed data, distorted data, etc), dynamic market (chaotic changing demand, and increasing competition), and finally the lack of appropriate electronic institutions and knowledge derived from immature technologies that do not help designers nor managers design automatic systems that help dynamic packaging nor virtual organizations.

The focus of our approach is on autonomous execution systems, namely intelligent agents, who inherit all the problems mentioned above. Their interactions will be grounded in an ecosystem of agents, where agents will be self-organised. One important question to analyse these Ecosystems is *the inclusion of interactions of the agents*. The interactions always exist as for example, the agents that trade in electronic commerce have to manage finally the negotiation for product delivery to the person or institution that these agents represent.

3. Self-Stabilising Mechanisms/Ecosystem Preservation

Another set of important issues relates to what kinds of self-regulating or self-stabilising mechanisms would characterize a large-scale information ecosystem with a complex, unpredictable dynamics such as the one envisioned. For example, this could possibly include the exploration of mechanisms to help the system rid itself of harmful behaviours, or mechanisms to help "recycle"" entities that have become obsolete, etc. The balance between the complexity of the behaviour of the individual entity and the complexity of the behaviour of the ecosystem is likely to have an impact on the "stability" of the system as a whole.

Over the years to come, an ever-growing segment of the world population will be connected to the global information infrastructure and many aspects of life will increasingly take place through or within it. A complex, dynamic and heterogeneous infrastructure environment will emerge, where "infohabitants" (people, organisations, as well as virtual entities acting on their behalf, smart appliances, smart buildings, etc.) will communicate, co-operate, negotiate, self-organise, create and offer new intermediation services, taking advantage of a dynamic set of information and communication resources to achieve their objectives or those of their owners.

"Universal Information Ecosystems" (UIE) is a research initiative launched in 1999 by the "Future and Emerging Technologies", European programme in "Information Society Technologies" (<http://www.cordis.lu/ist/>). It stems from the vision of an open global infrastructure environment that constantly evolves in an attempt to best meet the changing demands of its dynamic population of "infohabitants" (the given name to softbots and robots). Thus, the evaluation of heterogeneity remains still an open problem for the AI community. In this perspective a heterogeneous agent system can be understood as a community of agents that differ in their behaviours, properties and capabilities.

A metric is useful to develop a rigorous analysis of the properties of a population of agents. Having a better understanding of these systems may help to design or introduce the rules for the creation of heterogeneous agent populations. The metric presented is based on the Hierarchic Social Entropy [1] that was designed to evaluate behavioural diversity among a group of agents, and has been used as experimental setting to exemplify physical heterogeneity evaluation and team design [2].

4. Diversity Metrics

4.1. Social Entropy

Social entropy is based on information entropy [3]. This technique dates back to early days of cybernetics and was developed to quantify the uncertainty of an information source. The concepts developed by Shannon have been used by several researchers and adopted by other fields of research (biology, ecology). Information entropy presents several properties. The two most interesting properties show that H is minimised when the system is homogeneous, and it is maximised when there is an equal number of components in each different subset. This value also increases as the number of subsets with equal number of components increases. For Balch [1] there are two limitations of

this theory when using it to measure diversity: ***Loss of information***. Several (including also an infinite number) societies can match any particular value of diversity. A single value does not give any information on the classes of agents and the number in each class. And, ***Lack of sensitivity to the degree of difference between agents***. This theory does not consider how different the agents that make up the system are.

4.2. Simple Physical Heterogeneity Metric

Parker [4] defines a simple metric of heterogeneity in order to study physical heterogeneous teams of robots. This metric consists in studying how a feature changes across all the robots, the feature normally used for this purpose is the time necessary for accomplishing the mission, and it is represented by the variance. Although this metric is the first attempt to quantify physical heterogeneity, it is too simple and it does not take into account the full complexity of the problem.

4.3. Hierarchic Social Entropy

To overcome Shannon's metric drawbacks [1] defines a new metric, called hierarchic social entropy. This new metric includes the differences among the different types of members that compose the society. We think Balch's methodology is useful to quantify physical heterogeneity following the approach he follows to evaluate behavioural heterogeneity. However it presents some limitations: *Definition of physical difference between two physical agents*. For [1] one possible way of evaluating behavioural difference in a group of robots is by building an “evaluation chamber”, exposing each robot to different situations and recording its traces; *Differentiation of Homogeneous Teams*. Another limitation of this approach is that in some cases (as this work) it is interesting also to include homogenous teams as a part of the analysis of heterogeneity. However, this analysis may prove complex as different homogeneous teams may match the same level of heterogeneity (0).

5. Motivation for Ecosystems Stabilization

Hogg and Hubermann [5] proposed a mechanism to model the interaction of a large number of agents and the competition for resources among them. They showed how this model worked with simple but interesting examples. They started by modelling resource choice for a group of agents. The resource choice is modelled by the following equation:

$$\frac{df_r}{dt} = \alpha(\rho_r - f_r)$$

f_r is the fraction of agents using resource r , in this example there are two resources. α is the rate at which agents re-evaluate their resource choice and ρ is the probability that an agent will prefer resource 1 over 2. f_r is also called a population of agents.

To obtain the value of ρ , the difference of performance obtained by using resource 1 and resource 2 is computed. These performances may be obtained evaluating real

actions, as done in this work, time required to complete the task, accuracy of the solution. The authors use an algebraic function (depending on agent populations) to model performance based on the following idea. The performance of a group of agents using the same resource increases, when new agents use this resource, up to a certain value, due to co-operation among agents. From a given amount of agents on using this resource, performance diminishes because of the increasing number of conflicts (among this great number of agents) and they tend to waste efforts. Using this simple equation they do several experiments. When working with perfect information, information is up to date and available at any moment, the resource choice after a transient period stabilises (Figure 1). When this information is delayed, the agents have access to the state of the system k sample times ago, the system shows a chaotic behaviour, in which the system is continuously oscillating showing a chaotic behaviour (see the following plots).

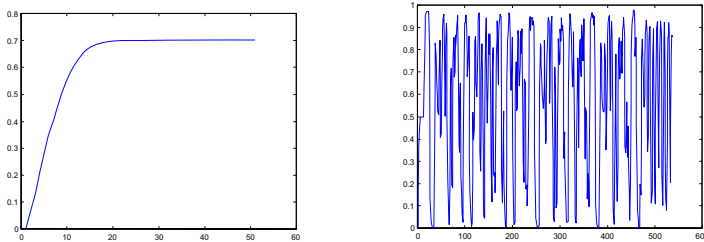


Fig. 1a. Agent with perfect info. **Fig. 1b.** Agent with delayed info.

This reward function is responsible for the stabilisation of the system together with the diversity of agents (Fig. 2). In any other case the system (resource choice) presents a chaotic behaviour, as in the example with one agent (Fig. 1b compared to Fig. 1a). With this new term the system is able to reach a stable configuration.

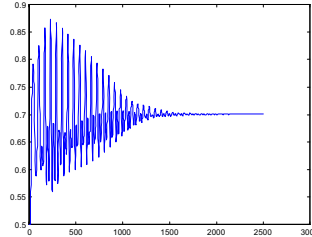


Fig. 2. Stabilisation of resource choice in a group of agents

One of the most interesting aspects of this work is how this model deals with diversity in the system, how these agents compete for bounded resources and the number of agents of each kind in the system changes depending on how well they are performing. We think that these ideas can be used for these research work, this model can be used to assign a collection of heterogeneous agents to roles in a team through competition, but at the same time co-operating, as this is one of the main features of soccer as research domain. These agents use the information about the roles in the form of rewards to decide which roles to use. The way these preferences and rewards are combined together is modelled by means of an ecosystem model. This approach also allows modeling the fitness (f) of each agents of the ecosystem, this fitness affects how agents

interact with each other, together with each agent preferences. This will have big impact in ecosystem stabilization and consequently in the efficiency of dynamic packaging and virtual organization formation.

6. Monitor for Digital Ecosystems

6.1. Measuring Ecosystem Properties

Developing a tool for studying and characterising ecosystem features, like heterogeneity, openness, stability, security and fitness of the population of the intelligent agents (one for each SME user), that impact on the distributed learning process. Monitoring of ecosystem characteristics will guarantee: equal opportunity, efficiency, effectiveness, trust and worth, and respect of private property. The monitor of the ecosystem is a tool aimed at understanding and predicting the stability properties of the ecosystem with the final aim of improving the ecosystem performance. In this task we will implement a tool (monitoring system) to measure characteristic properties such as: Openness, Dynamics, Homogeneity/Diversity, Exploitation/Exploration, Trust and worth, Security. The tool will have a user interface allowing the negotiator to assess the state of the ecosystem with respect to the mentioned characteristics. These will be monitored during the execution of the Digital Ecosystem by random samples of contracts and interactions through time, and will give hints about how to regulate the types of population (types of intelligent agents and their recommendation strategy) in the agent ecosystem. Because of required considerations of trust and privacy, it is not possible to execute this level of analysis on an ecosystem-wide basis and it is proposed that participants would be encouraged via incentive to “opt-in” to such a scheme. An incentive to participate in such an analysis mechanism could be that only those who are willing to share their information would receive the benefits of the analysis.

6.2. Philosophy

A monitor of an ecosystem as a feedback system could be inspired in a classic control loop (Fig. 3). Upon this idea we develop cellular automata as a simulator.

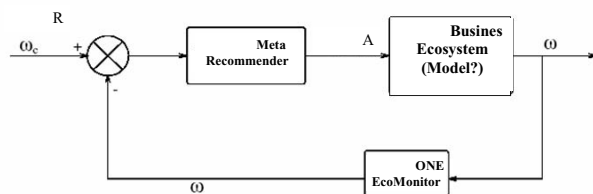


Fig. 3. An ecosystem as a feedback system

The cellular automata are a discrete model studied in computability theory, mathematics, and theoretical biology. It consists of an infinite, regular grid of cells, each in one of a finite number of states. The grid can be in any finite number of dimensions. Time is also discrete, and the state of a cell at time t is a function of the states of a finite number of cells (called its neighborhood) at time $t-1$. These neighbors are a selection of cells relative to the specified cell, and do not change. (Though the cell

itself may be in its neighborhood, it is not usually considered a neighbor.) Every cell has the same rule for updating, based on the values in this neighborhood. Each time the rules are applied to the whole grid a new generation is created [6]. Cellular automata are often simulated on a finite grid rather than an infinite one. In two dimensions, the universe would be a rectangle instead of an infinite plane. The obvious problem with finite grids is how to handle the cells on the edges. How they are handled will affect the values of all the cells in the grid. Some living things use naturally occurring cellular automata in their functioning [7].

6.3. Meta Recommender

The monitor records interactions between nodes. These interactions give information for defining the situation of the different nodes in order to determine their role in the ecosystem and its global state. Also it records negotiation types and results for future case studies. Recommender systems are a specific type of information filtering (IF) technique that attempt to present to the user information items, the user is interested in. To do this the user's profile is compared to some reference characteristics. These characteristics may be from the information item (the content-based approach) or the user's social environment (the collaborative filtering approach). The final purpose of a Recommender System is to advise the user about some product or item. Recommender Systems are based on user profiles which are a part of a user model. The Meta Recommender sets up recommendation styles for the recommender system: aggressive, passive, collaborative, competitive, etc, so that diversity in recommendation is introduced in the ecosystems, therein diversity in behaviours of the agents that work in virtual organizations driving the whole ecosystem to be stable.

6.4. Properties of Ecosystems/business

The most relevant characteristics of the digital ecosystems can be summarized as follows: Irreducible models, Interacting Factors, Feedback Mechanisms, **Resilience**, Hierarchy, Stochastic, No reductionism, Self-organisation and emergent properties (bottom-up and top-down effects), **Freedom of action**, Contingency, **Heterogeneity**, Evolution towards increasing complexity, Overall structure becomes a representation of all the information received, Complexity represents a synthesis of the information in communication. From these characteristics, six basic orientors or requirements to develop a system: *Existence*. Must not exhibit any conditions which may move the state variables out of its safe range; *Efficiency*. The exergy gained should exceed the exergy expenditure; *Freedom of Action*. Reacts to the inputs with variability; *Security*. Has to cope with the threats; **Adaptability**. If can not cope with threats, must change the system itself; *Consideration of other Systems*. Must respond to the behaviour of other systems. We will focus on the following properties: Diversity → competition, offer or demand; Stability → stability framework, predictability, security; Resilience → invisible hand, free market.

6.5. Diversity and Stability

A diverse biological system is more likely to be dynamically stable than one that is not diverse because in diverse communities interactions may often play a larger role in an agents' success. To the extent that changes in the system are driven by interactions, it is

dynamically stable, since characteristics of the system itself are determining its future state. There are some problems with this formulation of the diversity-stability hypothesis, however. It verges on circularity. The larger (more diverse) the system considered, the fewer are the things left out of it. The fewer the things left out, the smaller the possible outside influences on the system. The smaller the possible outside influences, the greater the degree of dynamic stability. Thus, dynamic stability is (almost) a necessary consequence of diversity, simply because diverse systems include many components. Although it is a key question, the relationship between diversity and stability is still being resolved. As with many topics in biodiversity, there are different ways of expressing stability. One way is to define it as *the ability of a system to return to its original state after being disturbed*, so how quickly it can return and how large a disturbance it can return from are key variables. Another definition is *how resistant to change the system is* in the first place. No matter what the definition used, however, there are definite trends that appear.

6.6. Does Diversity Lead to Stability?

If either the redundancy or rivet theories are correct, then more diversity means more stability. Current consensus is that greater diversity does lead to greater stability, for three general reasons: **Insurance Effect**: Different agents do better under different conditions. As the number of agents increases, the range of conditions that at least some agents do well in also increases. When perturbations do occur, it is more likely that some of the agents present will be able to do well, and these agents will protect the community as a whole. **Averaging Effect**: Stability is measured as variability relative to community abundance. As diversity increases, the value of the variability will naturally decrease. **Negative Covariance Effect**: Since agents are competing for resources, any gains that one agent makes will be to some extent at the expense of the other. This means that as an agent does more poorly its competitors will do better. The result is that disturbances are not as detrimental to the entire system as they could be, as the losses in one agent are offset by the gains of another.

There are at least three ways in which stability might be defined: **Constancy**: The ability of a community to resist changes in composition and abundance in response to disturbance. **Resiliency**: The ability of a community to return to its pre-disturbance characteristics after changes induced by a disturbance. Resiliency corresponds to stability the way it is studied in mathematical models. It measures a system's tendency to return to a single stable point, but many ecological systems appear to have multiple stable points. If disturbance remains below a particular threshold, it will return to its predisturbance configuration. If it exceeds that threshold, it may move to a new configuration. Furthermore, most ecological systems change not only in response to disturbance but also in response to succession change. Constancy and resiliency have this in common: both focus on agent persistence and abundance as measures of stability. **Dynamic stability**: A system is dynamically stable if its future states are determined largely by its own current state, with little or no reference to outside influences. The more complex the ecosystem, the more successfully it can resist a stress. A system that is dynamically stable is one that is relatively immune to disturbance. It reflects our hope that stable systems should be able to maintain themselves without human intervention.

6.7. Resilience

Resilience engineering provides the methods by which a system's resilience can be gauged or measured, and the means by which a system's resilience can be improved. We need to define two types of resilience: **Ecosystem resilience**. Ecosystems are communities of plants, animals, fungi and micro organisms that interact with each other and their physical environments. The ability of an environment to tolerate pressures and maintain its life-supporting capacity can be called *ecosystem resilience*. Ecosystem resilience is a complex concept, we do have a range of environmental indicators to report whether ecosystems and environments are coping with pressures or are degrading over time. **System resilience**. A common description of resilient systems is that such a system must have the following three abilities: The ability to respond, quickly and efficiently, to regular disturbances and threats; The ability continuously to monitor for irregular disturbances and threats, and to revise the basis for the monitoring when needed; The ability to anticipate future changes in the environment that may affect the system's ability to function, and the willingness to prepare against these changes even if the outcome is uncertain.

7. Structural Conditions of Interactions

Three working hypothesis are proposed to study the interaction between agents within the digital ecosystem : **H1**. The higher diversity of interactions, the higher potential for innovation; **H2**. The more versatile roles an agent assumes, the greater his potential for innovation; **H3**. The higher the structural imbalance (forbidden closed relationships), the greater potential for innovation. With the working hypotheses the following example scenarios are explored to deploy our monitor for agent ecosystems (Fig. 4).

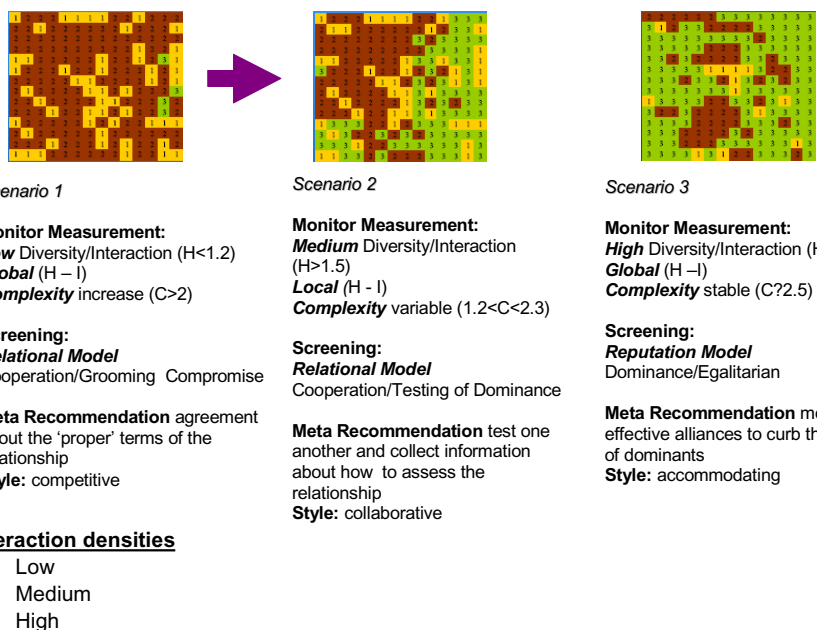


Fig. 4. Example scenarios from the monitor for agent ecosystem.

8. Final Remarks

We have proposed a Monitor for Digital Ecosystem according to the next generation of developments proposed for open environments. It will incorporate the self-organized and emergent factors to improve the meta-recommendation of the open negotiation environment. Then, we propose to make meta-recommendations (advises) within the Monitor for Digital Ecosystem and to update the Monitor for Digital Ecosystem, with the aim of improving the interaction and the relational styles in an open environment to take into account the diversity and heterogeneity of a Digital Ecosystem.

Acknowledgements

This work has been supported in part by FI-AGAUR Research Fellowship Program, Generalitat de Catalunya, Contract 2006-FI-00230, and project N° 34744 (ONE) – Open Negotiation Environment, FP6-2005-IST-5, from the European Union.

References

- [1] Balch, T. (2000) Hierarchic social entropy: an information theoretic measure of robot team diversity. *Autonomous Robots* 8(3): 209-238.
- [2] Kitano, H.; Stone, P.; Veloso, M.; Coradeschi, S.; Osawa, E.; Matsubara, H., (1997) The RoboCup Synthetic AgentChallenge 97, XV IJCAI-97 International Joint Conference on Artificial Intelligence, Vol 1, pp.24-29, Nagoya, August 1997.
- [3] Shannon, C.E. (1948) A Mathematical Theory of Computation. *Bell Syst Tech J* 27: 379-423 and 623-656.
- [4] Parker, L. (1994) Heterogeneous Multi-Robot Cooperation, Massachusetts Institute of Technology Ph.D. Dissertation, January 1994. Available as MIT Artificial Intelligence Laboratory Technical Report 1465, February 1994.
- [5] Hogg, T.; Huberman, B.A. (1991) Controlling Chaos in Distributed Systems. *IEEE Trans. on Sys. Man Cybernetics*. 21(6): 1325-1332.
- [6] von Neumann, J.; Burks, A. (eds.) (1966) *The Theory of Self-reproducing Automata*. Univ. of Illinois Press, Urbana, IL.
- [7] Peak, D.; West, J.D.; Messinger, S.M.; Mott, K.A. (2004) Evidence for complex, collective dynamics and emergent, distributed computation in plants. *Proc Natl Acad Sci USA* 101(4): 918-922

Confidence management in FIPA environments: agent unique representation

Amadeu Albós and Alan Ward¹
{aalbos, award}@uda.ad

Abstract. In this article a possible solution to the problem of confidence management in multi-agent systems based on the FIPA specification, and containing both autonomous and mobile agents, is presented. Through ensuring unique original agent representation, using a Public Key Infrastructure and validating agent actions, the validity and uniqueness of actors and interactions is demonstrated.

Keywords. Mobile and autonomous agent, FIPA specification, confidence management, uniqueness of representation, public key infrastructure.

Introduction

The evolution and globalization of multi-agent systems has recently revolutionized the services that distributed computation can offer. Some future challenges are the discovery of and adaption to new environments, cooperation and communication between agents, autonomous decision-taking and resource management and collaboration in the realization of activities with common objectives [1].

In this collaborative scenario, confidence management between actors is essential in order to offer guarantees of security to all interactions that may take place in environments that are each day more dynamic [2]. Drawing up mechanisms to guarantee confidence in terms of authentication and authorization, privacy and integrity of data is – among others – fundamental in order to obtain agents' aims.

The specification for an abstract agent architecture defined in [3] is today the base for many autonomous agent systems. Paragraph 4.7 gives the means to cypher and sign messages in order to comply with data and interaction security, authenticity and privacy between agents, and agents and human actors.

But the specification explicitly excludes aspects such as agent life-cycle management, and their identities: how to determine the identity of each agent is restricted by paragraph 11.4.4, in which the possibility “*to copy an agent or a message and clone or retransmit it*” is excluded. The authors of this paper consider that this constitutes a serious weakness of the specification, that permits implementing agent supplanting attacks easily.

In order to eliminate this weakness, we shall analyze recent works, define the problem of confidence management, present the problem of ensuring the uniqueness of

¹ Computer Security Research Group. University of Andorra, 7 Plaça de la Germandat, AD600 Sant Julià de Lòria, Principality of Andorra.

agents representing physical actors, and end up by proposing an easily implementable solution to the problem.

Related work

The importance of offering guarantees of the security of the interactions between agents and any other actor has given rise to the presentation of several initiatives towards confidence management. We shall now give a short evaluation of some of those more close to the aims of this paper.

The solution proposed in [2] is based on the construction of normative models of behavior and working – both of the agent and of the platform -, and validates agents through the presence of valid certificates. This solution can be considered a partial solution for our case, since the functional logic and internal security of an agent do not give sufficient guarantees against its being supplanted, modified or maliciously cloned.

The X-Security prototype, proposed in [4], is based on the creation of a Security Certification Authority (SCA), in the form of a local agent, that delivers certificates to agents and manages them, its main aim being the cyphering of interactions between agents. This solution solves partially the aim of this paper, but since the authorization mechanism is weak the process of migration between platforms is difficult and the authenticity of agents that make a request for a certificate is not guaranteed.

The migration mechanism proposed in [5], is based on the creation of an agent on the platform from a functional definition of its components (*blueprint*) and a current state being transferred, so as to maintain integrity during migration across heterogeneous environments. The solution proposed does not treat authentication and authorization of the mobile agent during migration, nor indiscriminate cloning despite the guarantees of integrity that the scheme does offer.

The OpenID authentication system, proposed in [6], is decentralized and aimed at web environments, where any user on the Internet and authenticated in one place may be automatically authenticated in other places through his/her URI. Requests are redirected to the OpenID server in order to obtain the pertinent credentials. The solution presented does not offer sufficient guarantees to demonstrate the authenticity of a mobile agent on platforms that may act in a fraudulent manner.

Finally, [7] proposes an XML standard known as *Security Assertion Markup Language* (SAML). The solution proposed is based on actor attribute, authentication or authorization declarations, that may be verified in execution time – between producers and consumers -. The functionalities of this solution are partial, but adequate for a possible implementation of the scheme that will be proposed, though these aspects are out of the bounds of this paper.

In all cases, the actor represented by the agent is excluded from actuation authorization, giving higher or lower levels of security against possible attacks. The uniqueness of representation of an agent is not guaranteed either by these systems.

The problem of managing confidence

As set out in [8], the computing system that represents an agent is capable of executing actions in an autonomous and flexible way, so as to attain certain objectives. A mobile

agent may also migrate between different platforms in order to relate itself with other agents [3].

This scenario makes confidence management difficult between actors, putting the authenticity of the agents in doubt. In this sense, confidence may be considered the problem of determining who is in relationship with whom, when they are in relationship and how it should take place [2].

Confidence in interactions should, as well, be based on a scheme that gives security guarantees, which is why the following questions on design following the FIPA specification should be considered and responded to [9]:

- The platform policy on internal and external communication.
- The relationship of confidence between agents.
- Agent authentication using a confidence-management authority.
- Implicit authorization through a ticket issued by a confidence-management authority.

On the other hand, the problem of managing confidence in a multi-agent system can be considered a confluence between the behavior of the agent itself (e.g. behavior restrictions), the working of the system and the validation of pertinent security certificates [2].

We consider that the fact that managing confidence for a certain agent also depends on the uniqueness of its representation on the system.

Unique representation of an agent on the system

An agent is represented in a unique way on a system when it may be determined that it maintains an unaltered relationship of integrity – aims, behavior and workings – with the original agent.

An agent is authentic when its identity and uniqueness of representation on the system may be determined.

Agent of confidence

An agent is of confidence in a certain environment (agent, platform or actor) when it is authentic and also authorized to execute actions on this environment.

Confidence management is then based on three specific aspects:

- unique determination of an agent's identity
- unique determination of the uniqueness of representation of the agent on the system
- unique determination of the authorization the agent holds to execute operations on the system

Unique determination of confidence in an autonomous and mobile agent in a multi-agent system is more complex than for its homologue in the real world for the actor that the agent represents, that already uses a Public Key Infrastructure (PKI) – for example – to certify his/her identity [10].

If an agent that represents an actor is given the actor's certificate, each and every action it executes on one or more systems may be identified as having been executed by the actor, without giving the actor him/herself the means to know which actions have been performed by the agent, nor on which systems they have been executed, nor when, nor even with which other actors the agent has been in contact.

One cannot exclude either the possibility of the agent's having been cloned with its certificate, thus compromising the certificate's private part. If the agent cannot be determined completely, it cannot represent the actor uniquely. Even a non-fraudulent clone of the agent could give rise to interaction execution on other systems without the means to distinguish between actions performed by the original or the clone. In each case, confidence is compromised in both ways.

We consider that an autonomous and mobile agent that represents a unique agent may not be granted a certificate that authorizes it to undertake actions in the name of the actor, under unknown conditions and without the actor's direct authorization.

Design of the proposed solution

In this sector we propose a possible solution to guarantee confidence in agents that represent physical actors. Before drawing up the functional scheme of the proposal, some terms must be defined. We shall then analyze the characteristics of functional entities that participate actively, and describe their protocols.

Terms

- The *blueprint* of an agent defines its functional components (e.g. signed object code) [5].
- A *policy of creation* is the rules and protocols followed to determine when, how and why an agent is created on a platform.
- A *policy of migration* is the rules and protocols followed to determine when, how and where an agent may migrate.
- A *policy of validation* is the rules and protocols followed to determine when and why a compromised interaction of an agent may be validated.
- A *compromised interaction* is an interaction of an agent that may eventually prejudice the actor that an agent represents. E.g. stock buying or selling on the stock-market.
- A *secure canal* is a point-to-point link through which data may be transmitted using cypher and signature, using security protocols and a PKI.

Functional scheme of the proposal

The proposed scheme associates two entities to confidence management:

- The Certification Authority (CA)
- The Agent's Authority (AA)

The Certification Authority (CA) acts as a depository of valid certificates that may be used to identify oneself and in order to cypher any data. The CA may – among other functionalities – determine the validity of certificates presented to it though validity requests to any actors that interact with the system.

The Agent's Authority (AA) manages the agent and represents the physical actor, so as to determine uniqueness of representation and authorization for the agent's actions based on policy emanating from the physical actor. The AA holds a certificate with which it may sign any valid operations the agent shall effectuate, and the original *blueprint* for the agent that represents the physical actor.

Figure 1 shows the functional schema of the system with the dues entities proposed. The CA manages and verifies actors' certificates in an independent way and on demand. The AA manages actuation and working policies of the physical actor, controls and authorizes the interactions undertaken by the agent, and maintains the actor's certificate that will be used to sign the agent's actions.

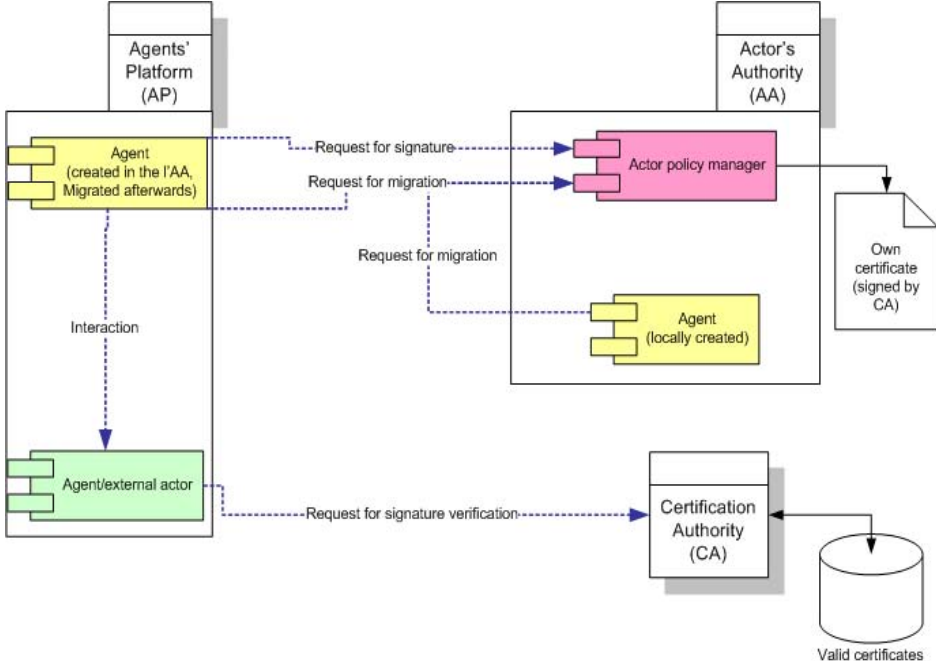


Figure 1: Functional structure of the system.

Characteristics of the Certification Authority (CA)

The Certification Authority (CA) of the PKI corresponds to the formal definition presented in [10]. It acts as a depository of valid certificates and determines actor identification as holder of the private part of the certificate.

The PKI grants and maintains valid CAs in order to control and manage certificates for all actors that take an active role in the system.

Characteristics of the Agent's Authority (AA)

The Agent's Authority (AA) represents the physical actor and centralizes the actor's policies, and manages the activity of the agent that represents him/her. It holds three main elements:

- A valid certificate to identify itself, cypher and sign any interaction with the AA or the agent that represents the physical actor.
- The actor's policy manager, that centralizes and maintains creation, migration and validation policies for the acts of the agent that represents the actor.
- The local *blueprint* for the original agent, as to offer guarantees and means of control and management for the security of the agent.

The actor's policy manager represents the knowledge base from which the AA's acts follow, its implementation is out of reach of this paper but it shall include – at least – the aim and behavior bounds of agent's acts, interactions that may be authorized and valid platforms to operate.

The AA's tasks are:

- To create and eliminate agents, based on the actor's policies.
- Authorize or initiate agent's migration to another platform.
- Guarantee unique representation of the agent in order to manage confidence, identification and security.
- Grant an individual certificate to the agent to identify it, verify its code integrity and make possible a secure canal for communications.
- Authorize possibly compromised interactions agents undertake, if they follow the policy set out by the actor.

Creating a new agent on a platform

The AA creates a new agent following the actor's creation policy. It is created within the AA using an agent factory and the *blueprint* of the original agent [5].

The new agent is granted an individual certificate to identify it, signed by the AA's private certificate. It is then autonomous and can migrate to any other platform allowed by the actor's migration policy.

Agent migration or cloning policy to another platform

When the agent must migrate to another platform, or AA's scheduling so decides, the agent emits a migration request. If the migration policy allows it, the agent initiates migration following the migration proposals set out in [5].

Accepting migration halt interaction signature, which will start again when both the old and the new platforms inform the AA through a secure canal that agent migration has successfully taken place.

Agent interaction validation policy

For each possibly compromised interaction, the agent sends the AA a copy of the action and its data through a secure canal. If in agreement with the actor's policies, the AA sends back the signed data as proof of agreement.

The AA shall register authorized interactions in a log for verification purposes.

Functional analysis of the proposal

The proposed scheme is aimed at guaranteeing confidence in autonomous agents:

- The CA guarantees independent verification of the actors involved and authenticity, privacy and non-repudiation of transmitted data.
- The AA guarantees unique representation of the agent, as it shall only authorize the interactions of the authentic agent on a valid platform agreed on following the actor's policies. It also guarantees the agent's behavior by validating its creation, migration and interactions.

As to security, two aspects may be considered:

- The security of communications in this solution is based on that offered by a PKI, considered sure for the time being.
- Security of the protocol proposed is based on the control exercised on the agent by the AA, validating its credentials, its interactions, its location and uniqueness of its representation.

With this mechanism, fraudulent attacks against integrity or privacy, whether supplanting, substituting an agent or man-in-the-middle shall be detectable wither through the PKI or the AA's exhaustive control and management policy.

Conclusions and further remarks

In this paper we present a possible solution to the problem of confidence management for multi-agent FIPA specification systems. As always, it has advantages and drawbacks. The main advantages are:

- Unique authentication of the agent as a basis for secure interactions.
- Unique representation of an authentic agent as a bases for confidence management.
- Authorizing possibly compromised interactions.
- Authorizing agent migration to other possibly restricted or unsure platforms.
- Applying the actor's policies on all interactions undertaken.
- Use of a PKI to authenticate and cypher communications.

On the other hand, several related aspects remain open. Agent cloning by error or by inducement within a same platform is out of the limits of the AA's control. So is objective control of the agent's integrity on a new platform after migration.

The relative loss of the advantages of distributed computation, autonomy and agent reactivity may also be considered, be it in exchange for better confidence management in the functional model.

The complexity of the system proposed is comparable to other multi-agent systems with guarantees of security. Prototyping is needed so as to test security and throughput.

A secure implementation of the model proposed should take into account the sensibility of data, which is why cyphering is necessary during agent migration – as studied in [11] –. The particularities of the authentication and authorization protocols between agent and AA may be considered, for example using standards such as SAML and XACML to offer security and efficiency.

Finally, the AA may end up managing a considerable number of agents, so becoming a fragile part of the system. Under these circumstances, a distributed architecture of coordinated agents such as that described in [12] could be of use to support the AA.

References

- [1] Huhns, M., Singh, M.P., Burstein, M., Decker, K., Durfee, E., Finin, T., et al. *Research Directions for Service-Oriented Multiagent Systems*. IEEE Internet Computing, november-december 2005, pp. 52-58.
- [2] Osman, N. *Formal Specification and Verification of Trust in Multi-Agent Systems* [on-line]. University of Edinburgh. <<http://homepages.inf.ed.ac.uk/s0233771/trust.pdf>> [Downloaded on: 10/05/07]
- [3] FIPA. *Abstract Architecture Specification Foundation for Intelligent Physical Agents 2002* [on-line]. FIPA. <<http://www.fipa.org/specs/fipa00001>> [Downloaded on: 11/05/07]

- [4] Novák, P., Rollo, M., Hodík, J., Vlček, T. *Communication Security in Multi-agent Systems*. CEEMAS 2003, LNAI 2691, pp. 454-463, 2003. Springer-Verlag Berlin Heidelberg 2003.
- [5] Overeinder, B., De Groot, D., Wijngaards, N., Brazier, F.. *Generative Mobile Agent Migration in Heterogeneous Environments*. Scalable Computing: Practice and Experience, Vol. 7 (2006), no. 4, pp 89-99.
- [6] OpenID. OpenID: an actually distributed identity system [on-line]. OpenID Foundation. <<http://openid.net>> [Downloaded on: 11/07/2007].
- [7] SAML. *Security Assertion Markup Language* [on-line]. OASIS Security Services Technical Committee". <http://www.oasis-open.org/committees/tc_home.php?wg_abbrev=security> [Downloaded on: 11/07/2007].
- [8] Wooldridge, M. *An Introduction to Multiagent Systems*. Chichester: John Wiley & Sons, 2002.
- [9] Vlček, T., Zach, J. *Considerations on Secure FIPA compliant Agent Architecture*. Proceedings of the IFIP TC5/WG5.3 Fifth IFIP/IEEE International Conference on Information Technology for Balanced Automation Systems in Manufacturing and Services, IFIP Conference Proceedings; Vol. 229, 2002.
- [10] IETF-PKIX Working Group. *Public-key infrastructure* (X.509) [on-line]. IETF. <<http://www.ietf.org/html.charters/pkix-charter.html>> [Downloaded on: 10/05/07]
- [11] Ward, A. *Encrypting the Java Serialized Object* [onlinel]. Journal of Object Technology, vol. 5, no. 8, Nov-Dec 2006, pp. 49-57. <http://www.jot.fm/issues/issue_2006_11/column6> [Downloaded on: 20/07/07]
- [12] Kumar, S., Cohen, P., Levesque, H. *The Adaptative Agent Architecture: Achieving Fault-Tolerance Using Persistent Broker Teams*. Proceedings of the 4th IEEE International Conference on MultiAgent Systems, 2000, pp. 159-166.

Completing the Virtual Analogy of Real Institutions via iObjects

Inmaculada RODRÍGUEZ^{a,1}, Maria SALAMÓ^a, Maite LÓPEZ-SÁNCHEZ^a,
Jesús CERQUIDES^a Anna PUIG^a and Carles SIERRA^b

^a WAI, Volume Visualization and Artificial Intelligence, MAiA Dept., Universitat de
Barcelona, email: {inma, maria, maite, cerquide, anna}@maia.ub.es

^b Artificial Intelligence Research Institute (IIIA), CSIC , email: sierra@iiia.csic.es

Abstract.

Electronic Institutions are regulated environments populated by autonomous software agents that perform tasks on behalf of users. 3D Electronic Institutions extend EI with 3D Virtual Worlds, which provide an immersive user interface so that humans can observe their agents' behaviors. In this manner, they represent a virtual analogy to real institutions. We propose to gain on realism on this analogy by adding intelligent objects to these institutions. Intelligent institutional objects (iObjects) exhibit autonomous and reactive behaviors. Furthermore, they present a limited level of proactivity such as self-configuration. Their inclusion has the advantage of improving the 3D Electronic Institutions architecture and both agent and user interactions within the institution.

1. INTRODUCTION

The implementation of successful complex multi-agent systems requires both taking care of the social issues underlying the activities the system models [11] and having a strong methodology to provide reliable interaction between the agents [3]. 3D Virtual Worlds cover the social issues by providing an immersive environment that offers a realistic experience. Electronic Institutions (EI) introduce regulatory structures establishing what agents are permitted and forbidden to do and hence provide reliable interactions.

3D Electronic Institutions (3D-EI) allow its users to interact with an Electronic Institution by means of a 3D Virtual World resembling the real world institution. However, objects and non-verbal communication are key social activities that are not present in 3D Electronic Institutions up to date. Their inclusion makes both the Electronic Institution and its 3D façade more similar to the real institution being modelled. In this paper we propose to extend Electronic Institutions by adding institutional objects (iObjects) with intelligent capabilities.

The paper is organized as follows. Section 2 reviews the related work on intelligent objects. Section 3 introduces the concept of EI, 3D-EI and details the integration of iObjects in Electronic Institutions. Next Section describes the architecture of the application

¹Correspondence to: I. Rodríguez, Dept. de Matemàtica Aplicada i Anàlisi, Universitat de Barcelona, Gran Via, 585, 08007 Barcelona, Tel.: +34 9340 39372; Fax: +34 9340 21601; E-mail: inma@maia.ub.es

that communicates EI and its counterpart in 3D, i.e., 3D-EI. Finally, in Section 5 we conclude the paper describing the benefits of this new proposal.

2. RELATED WORK

The first approximation to the concept of intelligent object was given by Levison [6]. He presented the object specific reasoning paradigm where object's inherent properties and object-avatar interactions (e.g., hand gesture to open a drawer) were stored in a database. The drawback was that each new extension of the object interaction properties would need an adjustment of the data stored in the interaction database.

A posterior research proposed a general framework of object-avatar interactions [5]. In this work, Kallmann and Thalmann introduced the *smart object* concept. An *smart object* included intrinsic features, interaction data and information relative both to avatar and object behaviors during their interaction. The goal was to encapsulate object specific data in smart objects so that different applications could incorporate them and exploit their interaction data as required. In this manner, object rendering control is transferred from the main loop in charge of the overall simulation to each specific object. Furthermore, they added these interaction features by means of a general feature modeling technique applied to CAD systems [14]. The limitation of this work was found when several avatars had to use the object simultaneously (e.g., several avatars trying to go through a "smart" door with a limited "physical" entrance points). This would imply either to modify the object or to have a specific concurrency control module.

Afterwards, based on the smart object definition, Peters [10] presented *user slots* and *usage steps* as a way of improving the control of several avatars interacting with a single *smart object*. A user slot defines the kind of avatar that can interact with the object (e.g., for a smart object 'bar', user slot 1 is a barman and user slot 2 is a customer). A user slot defines the avatar interaction with the object as a set of usage steps. A usage step contains the following information: animation that should be generated during the step, conditions to move to the following usage step, changes of state variables during the step, information that should be given to users of the object after that step, and points to focus the agent's attention.

Successive approaches to the intelligent/smart object concept have extended the type of data stored within the object. Recently, an *extended smart object* [2] has been defined to add planning information –such as preconditions, actions and effects– to the basic object features in Kallmann's initial smart object definition. The objective is to avoid working with fixed behaviors but to generate interaction plans and to relieve the avatar from interaction details. This approach is based on a standard STRIPS-like planner named Sensory Graphplan (SGP). Before the execution of the plan, avatars controlled by the SGP contingent planner try to generate a robust plan that deals with all eventualities. In fact, the resulting contingent plan may include sensing actions for gathering data that may be later used to choose among different plan branches.

Next section introduces our proposal of intelligent institutional object (*iObject*), which situates the concept of *smart object* in a deeper level (farther from the user interface than those mentioned above which locate *smart objects* at 3D rendering level). As shown below, we have an object named *iObject3D* at 3D scene level which is in charge of *iObject3D*'s aspect and behaviour and a multi-agent system at a lower level that contains its intelligent counterpart (named *iObject*).

3. ELECTRONIC INSTITUTIONS AND iOBJECTS

Our proposal based on introducing iObjects into EI aims to generate a reliable and proactive environment that gives more realism to the simulated institution. First of all, in this section, we formally define an Electronic Institution. Afterwards, we detail how to integrate iObjects into EI.

3.1. Introduction to Electronic Institutions

An Electronic Institution (EI) is a regulated virtual environment where the relevant interactions among participating entities (i.e., agents) take place [9]. An electronic institution defines (for further details refer to [8,12,4]):

- a common language that allows agents² to exchange information.
- the activities that agents may do within the institution.
- the consequences of their actions (obligations or prohibitions by means of normative rules).

Interactions between agents are articulated through agent meetings, which we call *scenes*, that follow well-defined communication protocols. Scene protocols are patterns of multi-role conversation. A distinguishing feature of scenes is that they allow agents, depending on their role, either to enter or to leave a scene at some particular moments (*states*) of an ongoing conversation. On the other hand, the protocol of each scene restricts the possible dialogical interactions between roles. For example, in an auction house, when a good is offered, the only action buyers can take is to rise their hand, indicating they take the bid; any other action is meaningless or inadmissible (and interpreted as a silent “no” to the bid). If a buyer wins a bid, the auctioneer will adjudicate the good to the buyer, charge the buyer and pay the seller for it; thus making the interactions involved relevant and meaningful to all participants.

A scene protocol is specified by a directed graph whose nodes represent the different conversation states and the arcs are labelled with illocution schemes³ or timeouts that make the conversation state evolve. Moreover, arcs can have some constraints associated which impose restrictions on the valid illocutions and on the paths that the conversation can follow. For instance, in an auction scene, following the English auction protocol, buyers’ bids must be always greater than the last submitted bid.

Figure 1 shows an EI as a “workflow” (*transitions* between scenes) of multi-agent protocols (*scenes*) along with a collection of (*norms*) rules that can be triggered by agents’ actions (*speech acts*).

We need to settle on a common illocutory language that serves to tag all pertinent interactions that can be produced inside a scene, i.e., the valid speech acts or illocutory formulas:

$$\iota(\text{speaker}, \text{hearer}, \phi, t) \quad (1)$$

²Autonomous entities capable of flexible interaction: reactive, proactive, and social.

³An illocution scheme represents a speech act [13] with some terms abstracted and represented as variables.

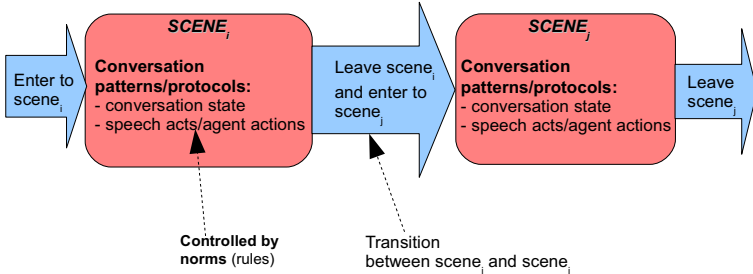


Figure 1. An Electronic Institution workflow

Speech acts start with an illocutory particle, such as *declare*, *request* or *promise*, that a *speaker* addresses to a *hearer*, at a time t , and the content ϕ of the illocution is expressed in some object language whose vocabulary is the EI's ontology.⁴

To make clear what are all the available illocutions for agent dialogues in a given institution we define a *Dialogical Framework* as a tuple:

$$DF = \langle O, L, I, R_I, R_E, R_S \rangle, \text{ where}$$

1. O stands for the EI domain ontology;
2. L stands for a content language to express the information exchanged between agents;
3. I is the set of illocutionary particles;
4. R_I is the set of internal roles (e.g., auctioneer in an auction house);
5. R_E is the set of external roles (e.g., sellers and buyers in an auction house);
6. R_S is the set of relationships over roles (e.g., roles that cannot play simultaneously, roles with authority over others).

In order to capture the relationship between scenes we use a special type of scenes: *transitions* (i.e., gateways between scenes or a change of conversation, see Figure 1). The type of transition allows to express agents synchronization: choice points where agents can decide which path to follow or parallelization points where agents are sent to more than one scene. An initial and a final scene determine the entry and exit points of the institution respectively.

Participating agents in the institution do not interact directly as done in traditional approaches. Therefore, an EI is composed by an external layer containing external agents taking part in the institution, a social layer controlling interactions between agents (e.g., AMELI [7]) and a communication layer providing a reliable and orderly transport service in a distributed architecture.

⁴We take a strong nominalistic view, the institutional ontology is made of every entity referred to in any admissible speech act or in any of the norms (conventions) that govern those acts and their consequences.

AMELI provides external agents with the information they need to successfully participate in the institution, takes care of the institutional enforcement: guaranteeing the correct evolution of each scene execution (preventing errors made by the participating agents by filtering erroneous illocutions, thus protecting the institution). AMELI also guarantees that agents' movements between scene executions comply with the specification and controls which obligations participating agents acquire and fulfil. The current implementation of AMELI is composed of four types of agents:

- *Institution Manager* (IM). It is in charge of starting an EI, authorizing agents to enter the institution, as well as managing the creation of new scene executions. It keeps information about all participants and all scene executions. There is one institution manager per institution execution.
- *Transition Manager* (TM). It is in charge of managing a transition which controls agents' movements to scenes. There is one transition manager per transition.
- *Scene manager* (SM). Responsible for governing a scene execution (one scene manager per scene execution).
- *Governor* (G). Each one is devoted to mediating the participation of an external agent within the institution. There is one governor per participating agent.

3.2. From Electronic Institutions to 3D-Electronic Institutions

Electronic Institutions (EI) allow agents to communicate and interact with each other in order to fulfill an objective. However, EIs lack of a 3D graphical user interface giving the user an intuitive feedback on what is happening inside the EI. 3D Electronic Institutions (3D-EI) are environments that enable humans to participate in a heterogeneous society of individuals visualized in a 3-dimensional virtual world. Therefore, 3D-EI broadens the agents view on Electronic Institutions, taking a human-centered perspective and concentrating on the relation between humans and agents in the amalgamation of EI and 3D virtual worlds.

Figure 2 shows an EI and its 3D counterpart, a 3D-EI. A 3D Electronic Institution is constructed doing a mapping from EI elements (i.e., scenes, transitions, agents, iObjects) to 3D-EI elements (i.e., rooms, corridor, avatars, iObjects3D). Dotted arrows in the figure show how iObjects and iObjects3D are incorporated into EI and 3D-EI respectively.

3.3. Integrating iObjects within Electronic Institutions

We propose the concept of intelligent institutional object (iObject) as a new element inside EIs. Although an iObject lacks of social behaviors, it perceives and eventually changes the state of the institution. It also presents a limited level of proactivity and can be manipulated by agents. Some examples of iObjects are:

- A door connecting two scenes. It will open or close depending on the agent that tries to pass through it.
- A remote control that submits bids to an auction when an agent presses a button, only if it fulfills the conditions established by the protocol.
- A brochure that shows advertisements adapted to the interests of surrounding agents.
- An item on sale that changes its features (e.g., a color change) to increase its attractiveness for a buyer agent.

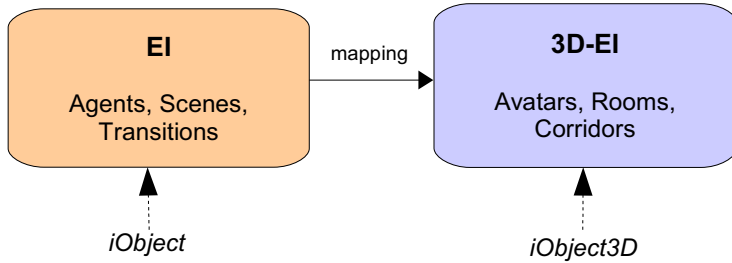


Figure 2. From EI to 3D-EI

- A playing jukebox with a button that allows the agent to skip to another song, that will be selected according to his musical preferences.

Every iObject has one or more properties which define its communication with the agent. The list of properties is:

- *State modifiers / non-state-modifiers*: Some objects, such as the door or the remote control, will change the EI state. In the first case by moving agents from one scene to another, and in the second one by modifying the current winner of an auction. On the contrary, a brochure, a jukebox or an item on sale are merely informative. We can further classify state modifiers as those that are part of the institutional infrastructure (such as a door) and those, such as remote controls, that provide an aid to incorporate non-verbal communication (actions) into specified protocols.
- *Actionable / non-actionable*: Actionable objects offer the agent the possibility to act on them. An example of an actionable object is a jukebox and a non-actionable one is a brochure.
- *Self-configurable / non-self-configurable*: A self-configurable object (e.g., a brochure or an item on sale) adapts its features according to changes in its environment. A door or a remote control are examples of non-self-configurable objects.

Any agent within an electronic institution is required to adopt some role conditioning the conversations he can be involved in and the illocution schemes (i.e., message patterns) he is allowed to use on those conversations. Similarly, an iObject is required to fulfill *interfaces*, that provide sets of action schemes that an agent can perform on it.

For example: A concrete object *door_23* fulfills the door interface which contains a single action. This action allows an agent to request to go through it.

We propose to extend the EI framework, currently containing the Communication Language (CL), with an Interaction Language (IL) that agents will use to interact with iObjects. CL let agents interact among them by following a dialog protocol (see illocutionary formula 1 in §3.1). As shown below, an IL illocution scheme is mapped onto an CL illocution scheme.

An example of illocution scheme (belonging to a CL) allowing a buyer ($?b$) in an auction to communicate the auctioneer ($?a$) that he wants to bid for a certain price ($?p$) at an instant of time ($?t$) is formalized as follows:

$$\text{request} (?b : \text{buyer}, ?a : \text{auctioneer}, \text{bid} (?p), ?t) \quad (2)$$

An example of illocution scheme (belonging to an IL) allowing a buyer ($?b$) to press a remote control button ($?r$) to submit a bid will use the following action scheme:

$$\text{press} (?b : \text{buyer}, ?r : \text{remote}, ?t) \quad (3)$$

This will isolate the buyer from knowing neither who the auctioneer is and its illocution schemes. Therefore, the remote control will be in charge of knowing how to translate the action (see Eq. 3) into the corresponding illocution (see Eq. 4) and will ensure that the protocol is satisfied. As a consequence, the Governor (see §3.1) is released from this task. In this specific case, the illocution associated with the action *press* could be:

$$\text{request} (?r : \text{remote}, ?a : \text{auctioneer}, \text{says} (?b : \text{buyer}, \text{bid} (?p)), ?t) \quad (4)$$

The remote encapsulates the functionality that the buyer's governor had until now. Therefore, it has to communicate to the auctioneer the content of the illocution given by the buyer as *says* ($?b : \text{buyer}, \text{bid} (?p)$), $?t$).

Another example of iObject application can be scene transitions. These transitions can now be directly controlled by doors through the *open* action scheme:

$$\text{open} (?b : \text{buyer}, ?d : \text{door}, ?t) \quad (5)$$

This partially relieves the Governor from intermediating with the Scene Manager (see §3.1) to perform this task. In a similar way, some other functions that are currently centralized into the Governor can be effectively split among different iObjects for a better responsibility distribution inside the EI.

4. 3D-Electronic Institutions including iObjects

Our proposal is to enhance the EI metaphor by including iObjects into EI specification (see §3.3) that are relevant to the real world institution. These iObjects will have their corresponding 3D virtual world objects, iObject3D. As a consequence, both the EI and its 3D façade become more similar to the real institution being modelled.

In a 3D-Electronic Institution [3] [1], scenes and transitions (see Figure 1) are mapped onto rooms and corridors, respectively. Doors in 3D-EI are to limit the access between rooms (i.e scenes in AMELI). In the 3D world, an avatar interaction such as *open-door* has to be translated in a query to AMELI infrastructure in order to allow/deny the avatar's action. Therefore, we need to communicate AMELI infrastructure to a module maintaining shared virtual world data.

As shown in Figure 3, a 3D-Electronic Institution is a multi-user networked 3D virtual environment based on a client-server architecture. On the client side, the user receives the current state of the institution and performs/receives changes to/from the

scene state. An user selects an avatar that will represent him in the 3D world and the user's requests are communicated to the server via http request/response mechanisms. For example, if an user moves its avatar by means of a keyboard event, this event may be propagated to the server so that it could inform the change to the rest of users.

On the server side the multi-agent infrastructure will be provided by AMELI runtime environment which will maintain communication with the Shared World Module in order to force avatars to fulfill Electronic Institutions norms and commitments.

The shared world module stores a reference to each user's browser execution context in order to update the virtual world after each avatar movement or avatar-object3D interaction. This module also has to maintain scene data such as number of user connected, correspondence between users, avatars and agents, avatars positions in the 3D scene, etc.

3D scenes, including *iObject3D*, are also stored in the server and sent to the browser when the client requests the connection to a concrete shared world, i.e., an institution. Note that yellow elliptical shapes in the figure represent iObjects in AMELI and theirs corresponding iObjects3D in the 3D virtual world. The initial EI configuration is given by a module named ISLANDER by means of an XML file. This file is read by the conversion module and converted into a 3D scene.

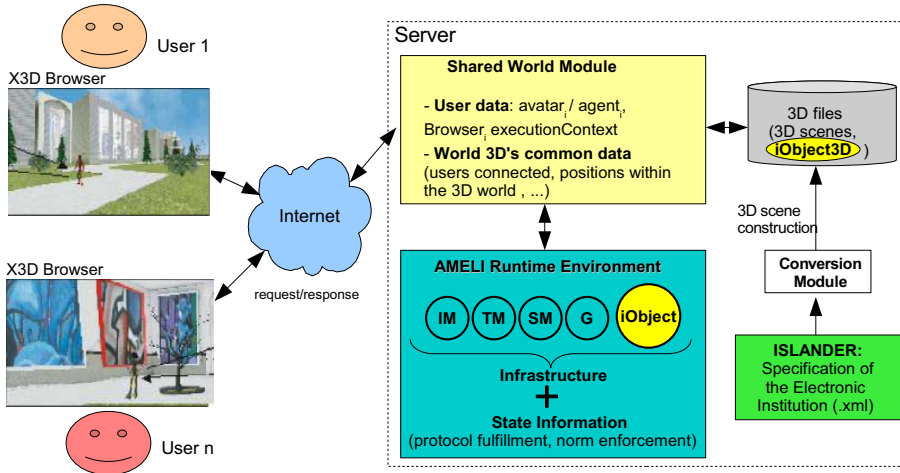


Figure 3. 3D-EI architecture including iObject and iObject3D

5. CONCLUSION

3D virtual worlds provide an immersive environment that offers a realistic experience. 3D-EI are virtual worlds which show to the user a more realistic view of an EI.

In this paper, we define an intelligent institutional object (iObject) as a new element inside EIs. An iObject perceives and changes the state of the institution. Moreover, it can be actionable and self-configurable. The key concept of iObjects addition is the extension of Communication Language (CL) to the Interaction Language (IL). We have illustrated the idea of iObjects through several examples of iObjects. An application of iObjects would be an e-commerce system where the buying/selling experience could be attractive

on the client side and effective on the seller side. For example, an iobject3D, based on user profile or on the last user activities inside the EI, changes its appearance in order to tempt the client to buy. Additionally, iObjects can be packaged smartly, depending on how the sales are running, as a marketing strategy essential for selling success.

The metaphor of iObjects: (i) provides a more realistic and operational 3D visualization of the current state of the EI; (ii) facilitates the addition of intelligent behavior to 3D objects through a three layer architecture; (iii) eases and makes more intuitive the communication between the agents and the EI; and (iv) allows for a better separation of concerns inside an EI.

Acknowledgements

This research is partially supported by the "Autonomic Electronic Institutions"(TIN2006-15662-C02-01) project and the "Openknowledge STREP" project sponsored by the European Commission under contract number FP6-027253.

References

- [1] S. Simoff C. Sierra A. Bogdanovych, M. Esteva and H. Berger. A methodology for developing mas as 3d electronic institutions. In *Proc. 8th Int. Workshop on AGENT ORIENTED SOFTWARE ENGINEERING at AAMAS 2007*, 2007.
- [2] T. Abaci, J. Cíger, and Daniel Thalmann. Planning with smart objects. In *Int. Conference in Central Europe on Computer Graphics*, 2005.
- [3] A. Bogdanovych, H. Berger, C. Sierra, and S. Simoff. Narrowing the gap between humans and agents in e-commerce: 3d electronic institutions. In *EC-Web'05*, volume 3590 of *LNCS*, pages 128–137. Springer, 2005.
- [4] M. Esteva. *Electronic Institutions: from specification to development*. PhD thesis, Universitat Politècnica de Catalunya, 2003. IIIA monography Vol. 19.
- [5] M. Kallmann and D. Thalmann. Modeling objects for interaction tasks. In *Proc. Eu-rographics Workshop on Animation and Simulation*, pages 73–86, 1998.
- [6] L. Levison. *Connecting Planning and Acting via Object-Specific Reasoning*. 1996.
- [7] M. Esteva, J.A. Rodríguez-Aguilar, B. Rosell, and J.L. Arcos. Ameli: An agent-based middleware for electronic institutions. In *Third Int. Joint Conference on Autonomous Agents and Multi-agent Systems*, pages 19–23, 2004.
- [8] Pablo Noriega. *Agent-Mediated Auctions: The Fishmarket Metaphor*. Number 8 in IIIA Monograph Series. Institut d'Investigació en Intel.ligència Artificial (IIIA), 1997. PhD Thesis.
- [9] D. North. *Institutions, Institutional Change and Economics Performance*. Cambridge, 1990.
- [10] C. Peters, S. Dobbyn, M. Namee, and C. O'Sullivan. Smart objects for attentive agents. In *Int. Conference in Central Europe on Computer Graphics*, 2003.
- [11] J. Preece and D. Maloney-Krichmar. *Online Communities: Sociability and Usability. Human Computer Interaction Handbook*, pages 596–620. Lawrence Erlbaum Associates Inc., 2003.
- [12] Juan A. Rodríguez-Aguilar. *On the Design and Construction of Agent-mediated Electronic Institutions*. PhD thesis, Universitat Autònoma de Barcelona, 2001. IIIA monography series.
- [13] J. R. Searle. *Speech acts*. Cambridge U.P., 1969.
- [14] J.J. Shah and M. Mantyla. *Parametric and Feature-Based CAD/CAM*. 1995.

Appraisal Variance Estimation in the ART Testbed using Fuzzy Corrective Contextual Filters¹

Esteve del Acebo^{a,2}, Nicolás Hormazábal^a and Josep Lluís de la Rosa^a

^aARLab. Institut d'Informàtica i Aplicacions. Universitat de Girona

Abstract. Trust modelling is widely recognized as an aspect of essential importance in the construction of agents and multi agent systems (MAS). As a consequence, several trust formalisms have been developed over the last years. All of them have, in our opinion a limitation: they can determine the trustworthiness or untrustworthiness of the assertions expressed by a given agent, but they don't supply mechanisms for correcting this information in order to extract some utility from it. In order to overcome this limitation, we introduce the concept of reliability as a generalization of trust, and present Fuzzy Contextual Corrective Filters (FCCF) as reliability modeling methods loosely based on system identification and signal processing techniques. In order to prove their usefulness, we study their applicability to the appraisal variance estimation problem in the Agent Reputation and Trust (ART) testbed.

Keywords. Trust, Multi Agent Systems, ART Testbed, Fuzzy Corrective Contextual Filters

1. Introduction

Trust is one of the main concepts upon which human and animal societies are built. It is evident, therefore, the importance of its formalization for the construction of artificial or electronic societies. Over the last years, several attempts to make such formalization have been carried out from diverse points of view (recommender systems, social networks, electronic commerce...) All of them suffer, in our opinion, from a quite serious limitation. While they can provide a number, category or even fuzzy statement measuring the trustworthiness of a given agent or, more precisely, the trustworthiness of the information provided by a given agent, they fail in the sense that they don't supply any filtering or correcting method in order to make the provided information useful, even if wrong. The main point of this paper is: In some cases, false information transmitted by an agent can be useful if conveniently filtered.

¹This work was supported in part by the Grant TIN2006-15111/Estudio sobre Arquitecturas de Cooperación from the Spanish government and by the EU project Num.34744 ONE: Open Negotiation Environment, FP6-2005-IST-5, ICT-for networked Businesses.

²Correspondence to: Esteve del Acebo, Escola Politècnica Superior, Universitat de Girona, Spain. E-mail: esteve.acebo@udg.edu.

The aim of this paper is threefold. In the first place, we want to make evident the importance of such filtering mechanisms in order for an agent to improve its performance in a multiagent environment, introducing the concept of reliability as an extension or generalization of trust. Secondly, we present fuzzy contextual corrective filters (FCCF) as a convenient and straightforward way, loosely inspired in systems identification and signal processing techniques, to implement those filtering/correcting mechanisms. Finally, we demonstrate the usefulness of FCCF by applying it to the appraisal variance estimation problem in the Agent Reputation and Trust (ART) testbed domain.

2. The Need for Trust Formalization in MAS

An essential characteristic of MAS is the existence of an information interchange between the individual agents forming the system. In the case of collaborative MAS, the aim of this communication is the improvement of the global performance of the system. Therefore agents, in general, do not lie each other consciously. In the case of competitive environments, however, individual agents are selfish, in the sense that its behavior is addressed to maximize some kind of individual utility function, even if that means a prejudice for the individual interests of the other agents or the diminution of the overall performance of the system. Communicative acts in competitive MAS are therefore addressed to obtain individual benefit and it is more suitable (because it can be profitable) the conscious communication of false information.

Both in collaborative and in competitive MAS, however, an emitter agent can communicate false information to a recipient agent because of several reasons. The main ones being:

1. The emitter agent is, simply, wrong. He is honest, in the sense that he believes he is communicating a true statement, but the transmitted information is false.
2. Emitter and recipient agents do not use the same language. The message encloses a true statement, as understood for the emitter agent, but has a different and false meaning for the recipient agent. That's why ontologies are used, just to try to assure that all the agents in a domain speak the same language
3. A transmission error occurred. The emitted and received messages are different.
4. The emitter agent consciously transmits a false information to the recipient agent. The aim of such behavior can be supposed to be the obtaining of some benefit from the prejudicing of the recipient agent. That is the typical behavior we can expect in competitive environments

Whatever could be the reason behind the transmission of false information, individual agents need some kind of mechanism that allow them to deal with it. Agents can't afford (specially in competitive environments) to believe everything the other agents tell to them. A car vendor agent who commits itself to deliver a car "soon" and who says that the car is "fast" can be honest even if the car lasts a year to arrive and it can not run faster than 100 kilometers per hour. Perhaps he really believed what he was saying, perhaps the words "soon" and "fast" have a different meaning in the car vending language or even, perhaps, he said "late" and "slow" but somehow the sounds changed in their way from their mouth to our ears. More probably, however, he is deliberately lying to take profit from us. In either case, we need to learn from our experience in order to know what

can be expected from him in further deals. Here is where trust and reputation modeling methods come in as an important field of study inside the theory of MAS.

3. Beyond Trust. Reliability

It is not inside the scope of this document to give a detailed account of the several trust and reputation formalizations that have been proposed along the last years, so we refer the interested reader to [1] for a survey of them. Nevertheless, a point seems to have been so far overseen, to our knowledge, by these trust formalisms. *It is not necessary to trust an agent (in the sense of believing it is saying the truth) in order to get some utility from the information provided by it.* This information can be useful even if it is false, provided we had some method to correct it.

The key concept in order to be able to correct messages coming from other agents is reliability³. If an agent tends to communicate similar information under similar circumstances, a moment will arrive when we will be able to extrapolate the circumstances, more or less correctly, from the received messages. On the contrary, if an agent emits just random messages it will be very difficult, if not impossible, to obtain from them any utility at all.

The corrective mechanisms, which we will call filters, can have very different structures. The filter for a watch agent that goes two hours and a half in retard could be as simple as adding 150 minutes to the time he says it is. On the other hand, we will need a much more sophisticated filter when dealing with the car vendor agent, maybe some kind of expert system. In the following section we will show how simple filters, based on fuzzy systems, can be constructed and how they can be learned and used to improve the performance of individual agents in their environment.

4. Fuzzy Contextual Corrective Filters

Think about the following problem: An agent A interacts with several other agents in a multi-agent environment requesting from them some kind of information, which they supply (this information can be false because of any of the reasons exposed in section 2). Suppose also that the correct answers to A 's requests are made available to A by the environment in a posterior time instant, in such a way that A is able to know which agents told the truth and which agents lied, and how much. Our point is: for A to be able to perform well in this kind of environment it has to maintain a set of filters (one of them for each agent it interacts with) which allows it to correct the information received from the other agents, as well as to assess the possible utility of the corrected information. These filters must be dynamic, in the sense that they must evolve and adapt to changes in the environment and in the behavior of the other agents. So, (see figure 1) filters act as a translative layer that eases the process of interpretation of the messages sent by other agents.

It is also very important for the agent that owns the filter to have some kind of measure of the correctness of the filtered information, that is, the degree to which it can be expected to reflect the reality. We will call this value *reliability* and the filter will

³ From reliable, in the sense of “giving the same result in successive trials”. [2]

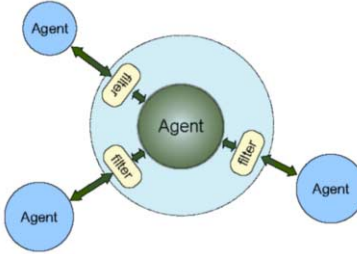


Figure 1. The set of filters of an agent act as a translative layer.

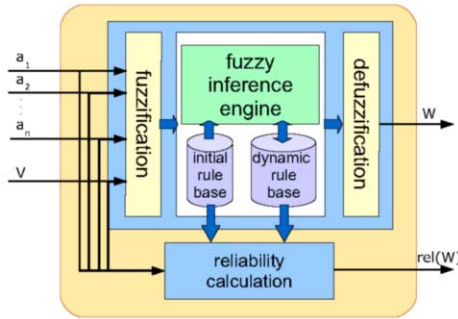


Figure 2. Structure of a fuzzy contextual corrective filter

compute it from the observed regularities in the behavior of the filtered agent in past interactions.

Figure 2 shows the suggested structure for the construction of these filters, which we call fuzzy corrective contextual filters (FCCF) [3]. A FCCF F has two parts, the corrective module and the reliability calculation module. The corrective module is a special case of a Mamdani fuzzy inference system⁴ where the fuzzy rules have the form:

$$\text{If } A_1 \text{ is } S_1 \text{ and } \dots \text{ and } A_n \text{ is } S_n \text{ and } V \text{ is } L_1 \text{ then } W \text{ is } L_2$$

where:

- $S_1, S_2 \dots S_n$ are linguistic labels, defined by fuzzy sets on universes of discourse $X_1, X_2 \dots X_n$, respectively.
- $A_1, A_2 \dots A_n$ are fuzzy variables taking values over the fuzzy power sets of $X_1, X_2 \dots X_n$, respectively.
- L_1 and L_2 are linguistic labels defined by fuzzy sets over the universes of discourse U_1 and U_2 , respectively. U_1 and U_2 can be, and usually are, the same set.
- V and W are fuzzy variables taking values over the fuzzy power sets of U_1 and U_2 , respectively.

⁴A explanation of fuzzy sets, fuzzy logic and fuzzy inference systems' theories is beyond the scope of this paper. We refer the interested reader to [4] where several excellent introductory chapters can be found.

We will call $A_1, A_2 \dots A_n$ the *context variables*, V the *main variable* and W the *filtered variable*. We can see the operation of the corrective module as a transformation of fuzzy sets over a certain universe U_1 to fuzzy sets over the universe U_2 , in a way that depends on the values of the context variables as well as on the value of the main variable. The corrective module of a FCCF, then, filter the values (fuzzy sets) of the main variable to obtain new values (fuzzy sets over the same universe or another one) which are expected to be more suitable for some purpose. As is the case with general Mamdani fuzzy systems, it is possible to use FCCF on crisp input values to produce crisp filtered values by using appropriate fuzzification and defuzzification procedures.

The rule base of the corrective module has two components, the static and dynamic rule bases. The static rule base is fixed (and possibly the same) for every agent. It expresses the *a priori* assumptions about the behavior of the other agents in the environment and serve as a departing point in the interpretation of other agents's assertions. It can be as simple as identity or can, for instance, incorporate some common sense knowledge about the behavior which can be expected from certain kinds of agents. The dynamic rule base is built upon the information extracted (in the form of fuzzy rules) from the interactions between the agent which owns the filter and the filtered agents. It is dynamic in the sense that it evolves with time and can adapt itself to changes in the environment and in the behavior of the filtered agents. The construction of the dynamic rule base can be viewed as a system identification task where the behavior of the filtered agent has to be modeled from a set of examples, the results of past interactions between the modeling and the modeled agents. As a system identification problem, several modeling methods can be used, ranging from those based on a neuro-fuzzy, backpropagation-based approach (Jang's ANFIS [4] would be a good example of this) to those based on lookup tables [5] or, even, genetic algorithms [6].

The function of the second part of the FCCF, the reliability calculation module, consists in computing the reliability of the filtered value obtained by the corrective module. Reliability will be a function of the input and context variables and will depend upon the number of prior similar interactions between filtering and filtered agents as well as upon the regularities observed during that interactions.

5. The ART Testbed

The Agent Reputation and Trust (ART) testbed [7] is a framework, based on the art appraisal domain, for experimentation and comparison of trust modeling techniques. Agents function as painting appraisers with varying levels of expertise in different artistic eras. Clients request appraisals for paintings from different eras; if an appraising agent does not have the expertise to complete the appraisal, it can request opinions from other appraiser agents. Appraisers receive more clients, and thus more profit, for producing more accurate appraisals.

Let's focus in the opinion requesting part: when an agent A does not have expertise enough to guarantee a good appraisal for a given painting, it can buy the opinion of other, more expert, agents. The process is the following: first, agent A asks all or part of the other agents to provide a value stating their confidence in the accuracy of their appraisal of the painting. Then, A decides, upon the received confidence values, which agents to trust, that is, which opinions to purchase.

This is the main point where the communication of false or misleading information can happen in the ART testbed. An agent can declare a great confidence in its appraisal just to fool the requesting agent into purchasing it, and then produce a very bad appraisal. This will result in a big error in the requesting agent's appraisal and, consequently, a big loss in its client share. On the other hand, the requesting agent has no way to know what the confidence value provided by an agent means. It is a value over an arbitrary range that has to be interpreted. It is perfectly possible for a given confidence value to mean completely different confidence levels for different agents.

6. Using FCCF for Appraisal Variance Estimation in the ART testbed

One of the main problems we faced in the construction of our ART testbed agent was the following: given two appraisals with variances α_1^2 and α_2^2 , we knew the way to combine them in order to obtain the appraisal with the minimal expected relative error. We needed, therefore, a way to guess appraisals' variances departing from the confidence values supplied.

We solved the problem providing our agent with a set of FCCF, one for each agent other than itself in the environment. The structure of the filters is very simple. They have, as input variable, the confidence value stated by the seller agent, and, as context variable, the era to which the painting belongs. The filtered variable is the square of the relative error of the appraisal. We will see how the filtering module will produce, as output, a correction of the confidence value in the form of the expected variance of the seller agent's appraisal.

Rules in the initial rule base are predefined by design and serve the purpose of providing a sensible starting point to the interpretation process. Rules in the dynamic rule base, on the other hand, are continuously obtained from interactions between our agent and the filtered agents. Each of the rules in the rule bases, however, has the same form:

$$R_i : \text{If } era = E_i \text{ and } conf = C_i \text{ then } qError = Q_i$$

where E_i ⁵ and Q_i are singleton fuzzy sets over the sets of the eras and the positive reals, respectively and C_i is a fuzzy real number. So, for instance, if we purchase an appraisal for a cubist painting for which the seller agent declares to have a confidence 0.5, and the provided appraised value is 20000 but the real price of the painting turns out to be 25000 (giving a relative error of 0.2), we will add to our dynamic rule base the following rule: If $era = cubism$ and $conf = 0.5$ then $qError = 0.04$

We will have, then, a possibly large number of fuzzy rules in this form. Now suppose that we want to consider the possibility of purchasing an appraisal for a painting of a given era e from an agent which states that it has a confidence c in its appraisal. How to estimate the variance of the appraised value?. We know that the variance is defined as the expectation of the quadratic error, so, in principle it would be enough to gather all the interactions in which the agent has stated the very same confidence in its appraisal of a painting of the same era and estimate the variance from these data as the mean of

⁵ In the ART testbed, paintings can only belong to one era, and they belong to it completely. It is possible, however, to imagine instances of the problem where paintings could belong, to a certain degree, to different eras. Our method is general enough to cope with this.

the quadratic errors made. Unfortunately, confidence values will be, in general, scattered along a big range of values, so we can hardly expect to have enough of them to make the estimation accurate. We can, nevertheless, estimate the variance computing the output of the fuzzy system in the following way:

$$\sigma_{e,c}^2 = \frac{\sum_i \pi_i(e) \cdot \mu_i(c) \cdot \text{TimeStep}_i^K \cdot Q_i}{\sum_i \pi_i(e) \mu_i(c) \cdot \text{TimeStep}_i^K} \quad (1)$$

where $\pi_i(e)$ will take the values 1 or 0 depending on whether the era of the painting corresponding to fuzzy rule R_i was e or not, Q_i is the quadratic error corresponding to fuzzy rule R_i , TimeStep_i is the iteration in which the interaction corresponding to R_i happened (we can, then, use the parameter K to vary the relative influence of the rules in the computed result, giving more or less importance to more recent interactions) and $\mu_i(c)$ is the degree to which the value c belongs to the fuzzy number C_i , which we compute as:

$$\mu_i(c) = \exp\left(-\frac{(c - C_i^*)^2}{AMP^2}\right) \quad (2)$$

where C_i^* is the central value of the fuzzy number C_i , the width of which can be controlled by the parameter AMP .

The implementation of the reliability calculation module for our problem is based in previous work by the authors [8]. It mainly takes into account the completeness of the rule bases (roughly speaking, the number of rules that fire in the calculation of the variance).

7. Results

The global behavior of agents in ART experiments is very sensitive to even small changes in the environment or in the particular behavior of single agents. In order to try to overcome this problem, two series of simulations have been carried out, using two sets of agents, a first one (Set A) with several of the best competitors in the 2006 International ART Competition (i.e. IAM, Frost, Neil, and Sabatini), and a second one (Set B) with new agents synthesized to be more trusty. Ten simulations have been done in each series. In five of them one agent called Niko uses FCCF in order to translate the certainty values provided by the other agents to variances, in the remaining five simulations Niko don't uses FCCF, that is, he assumes the other agents to talk the same language than himself.

As a consequence of ART Testbed sensitivity to initial conditions, the inherent random nature of the simulations makes the amount of money earned by the agents in every run to be very variable. Therefore one cannot simply take money as an absolute performance measure. Though other methods may apply (ranking, etc), we want a method able to keep accurately the distance between agents in the different runs, so we have decided to normalize the results by dividing the money earned by Niko by the money earned by the remaining best agent. This gives us an adimensional measure of Niko's *efficiency* that helps the comparison.

The results of the experiments can be seen in Table 1. Results are very similar in both series, although slightly better in the case of Set A, the more competitive agents.

Table 1. Results of the experiments

	With FCCF		Without FCCF			
	Mean Efficiency	Std. Dev.	Mean Efficiency	Std. Dev.	%	t
Set A	0,903	0,059	0,741	0,033	21,9	5,35
Set B	0,89	0,096	0,75	0,125	18,7	1,99

The improvement in efficiency is about 20% in both series. The t-values for the unequal variances Student's t-Test guarantees the statistical significance of the results with high probability (greater than 0.999 for Set A and greater than 0.95 for Set B).

Fuzzy Corrective Contextual Filters (along with several other tricks) allowed Niko, under the nick name of SPARTAN, to win the 4th position out of 16 participants in the last world ART competition in AAMAS 2007, May 14-18, 2007 in Hawaii.

References

- [1] Sabater, J. 2002. *Trust and Reputation for Agent Societies*. Monografies de l'Institut d'Investigació en Intel·ligència Artificial (20). Consell Superior d'Investigacions Científiques.
- [2] Merriam-Webster. 2007. Merriam-webster online dictionary. <http://www.m-w.com/>.
- [3] del Acebo, E., and de la Rosa, J. L. 2002. A fuzzy system based approach to social modeling in multi-agent systems. In *The First International Joint Conference on Autonomous Agents & Multiagent Systems, AAMAS 2002, July 15-19, Bologna, Italy*, 463–464.
- [4] Jang, J.; Sun, C.; and Mizutani, E. 1997. *Neuro-Fuzzy and Soft Computing*. MATLAB Curriculum Series. Prentice-Hall, first edition.
- [5] Wang, L.-X. 1994. *Adaptive Fuzzy Systems and Control. Design and Stability Analysis*. Prentice-Hall.
- [6] Cordon, O., and Herrera, F. 1995. A general study on genetic fuzzy systems. In *Genetic Algorithms in Engineering and Computer Science*. John Wiley & Sons.
- [7] Fullam, K.; Klos, T.; Muller, G.; Sabater, J.; Schlosser, A.; Topol, Z.; Barber, K. S.; Rosenchein, J.; Vercouter, L.; and Voss, M. 2005. A Specification of the Agent Reputation and Trust (ART) Testbed: Experimentation and Competition for Trust in Agent Societies. In *The Fourth International Joint Conference on Autonomous Agents and Multiagent Systems (AAMAS-2005)*, 512–518. ACM Press.
- [8] del Acebo, E.; Oller, A.; de la Rosa, J. L.; and Ligeza, A. 1998. Statistic criteria for fuzzy systems quality evaluation. In Pobil, A. P. D.; Mira, J.; and Ali, M., eds., *IEA/AIE (Vol. 2)*, volume 1416 of *Lecture Notes in Computer Science*, 877–887. Springer.

Punishment Policy Adaptation in a Road Junction Regulation System

Maite Lopez-Sanchez¹, Sanja Bauk², Natasa Kovac², Juan A. Rodriguez-Aguilar³

¹Universitat de Barcelona, ²University of Montenegro

³IIIA - CSIC Artificial Intelligence Research Institute (Barcelona, Spain)

Abstract. This paper studies the problem of adapting punishment policies in traffic scenarios. It focuses on a two-road junction scenario simulated by means of Simma, a Multi-Agent Based Simulation Tool. Adaptation is based on an adaptive neuro-fuzzy inference system (ANFIS) together with a hybrid learning algorithm (HLA). Basic punishment policy is provided through a knowledge base that specifies the conditions that must hold in order to assign different punishments. The aim of this paper is to show how the ANFIS system can improve this policy unsupervisedly.

Keywords. Multi-Agent System, policy adaptation, traffic regulation, ANFIS.

Introduction

Traffic regulation is a complex task, particularly in large road networks and on roads that lack of explicit regulatory elements such as traffic lights or traffic signals. In this paper we focus on a very specific scenario consisting of a junction of two roads without any regulatory elements. Figure 1 a) shows an example of this scenario in the real world. This setting can be represented as an intersection of two perpendicular roads in a discretized environment (see Figure 1 b)) and simulated with a Multi-Agent System. A Multi-agent system [1, 2] is a computational system where autonomous agents interact with each other in order to achieve common and/or individual goals. In this setting, cars are agents that drive along roads with the individual goal of reaching their target positions (Figure 1 c)).

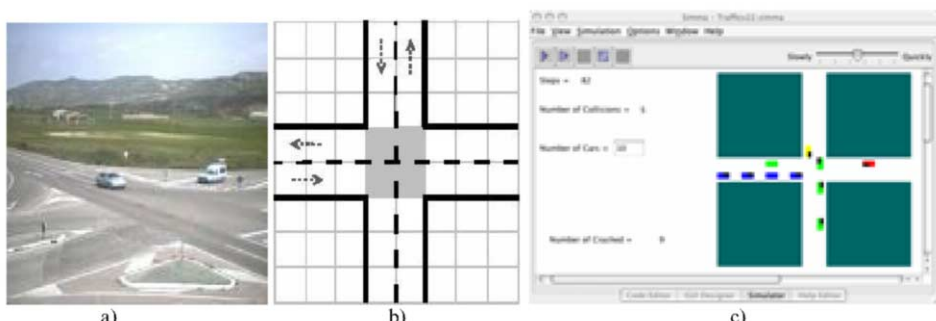


Figure 1. Two-road junction: a)real scenario, b)simplified representation, c) simulated MAS traffic system

When several cars approach a road junction simultaneously some regulations are needed in order to avoid possible collisions. These situations are usually regulated through a default priority assignment such as a “right hand” priority rule, which gives priority to the car on the right. Nevertheless, cars may not follow these rules, so that an associated punishment becomes necessary.

We have simulated this traffic scenario by developing a multi-agent system. Figure 1 c) shows a screenshot of the system, which is described in [3] and was developed with the Simma tool [4]. Briefly, in this traffic simulation agents try to reach their target positions. They are free to decide whether they follow the right-hand side priority rule or not. Additionally, agents collision whenever they get into the same position.

1. ANFIS: an Adaptive Neuro-Fuzzy Inference System

ANFIS [5,6] architecture is based on the functional equivalence between TSK (Takagi-Sugeno-Kang [7]) fuzzy inference system and RBFN (Radial Basis Function Network).

The TSK fuzzy inference system performs a fuzzy reasoning: inference operations upon fuzzy if-then rules where the output of each rule is a linear combination of input variables plus a constant term, and the final output is the weighted average of each rule’s output [7].

On the other hand, an adaptive network is a multi-layer, feed-forward network in which each node performs a particular node function based on incoming signals together with the set of parameters related to this node. Namely, each node function depends on the set of parameters which are associated to it. In the training process these parameters are being corrected in the aim of overall error minimization at the output of the network.

ANFIS is the hybrid neural-fuzzy system. It has the capability of simulating expert domain knowledge represented as if-then rules; and, after the hybrid learning procedure, it can successfully predict the adequate output for an unknown given input. The ANFIS uses back propagation to learn the premise parameters and least mean square estimation to determine the consequent parameters.

ANFIS has been successfully applied to route preference estimation in sea navigation [8] and thus, we propose here to extend its application to the road traffic case with the aim of optimizing the punishment policy.

2. Data description

When considering the road junction case, the following dynamical parameters can be considered:

- Car position: it is specified in terms of the distance to the road junction. We distinguish three different distance measures: Short Junction Distance (SJD), Medium Junction Distance (MJD), and Long Junction Distance (LJD). As Figure 2 a) shows, these linguistic qualifications are represented with Gaussian membership functions with the following numerical boundaries and

maximum values (units are assumed to be meters): SJD: (0; 0.5; 1), MJD: (0.5; 1; 1.5) and LJD: (1; 1.5; 2).

- Car speed: Similarly, we distinguish three different speed labels: Low (L), Medium (M), and High (H) and their corresponding Gaussian membership functions have the following numerical boundaries and maximum values: L (5,10,15), M: (10; 15; 20) and H: (15; 20; 25). Units are in Km/h (see Figure 2 b)).

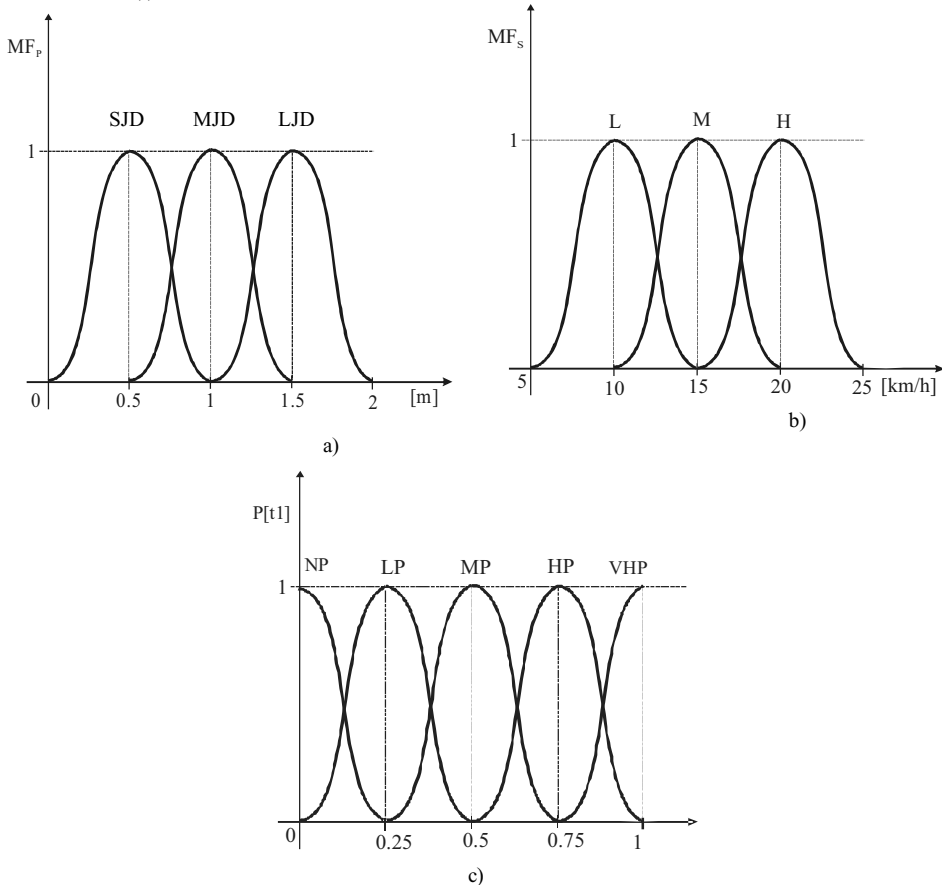


Figure 2. The Gaussian membership functions corresponding to linguistic descriptions of a) car Position b) car Speed, c) Right side priority.

- Right side priority: It describes how much priority a car has when approaching a road junction. Priority is assigned by using five different labels, which range from no priority (NP) —when there is another car on the right side of the reference car— up to complete priority (VHP: Very High Priority), when there is no car on the right side. Intermediate labels are used for describing those situations where the car on the right is approaching the junction but it is not there yet. Therefore, Low Priority (LP), Medium Priority (MP), and High Priority (HP) are assigned proportionally with the distance to the junction: the longer the distance is, the higher the priority becomes. Figure 2 c) shows their corresponding Gaussian Membership Functions, which have been described

with the following numerical values: NP: (0; 0.25)¹, LP: (0; 0.25; 0.5), MP (0.25, 0.5, 0.75), HP (0.5, 0.75, 1), and VHP (0.75, 1)¹.

- Finally, we consider the punishment applied to cars when violating the right-side rule. Punishment values correspond to the output of the overall system, and so, their five linguistic labels have been translated into numerical crisp values. These labels are: none, mid-, mid, mid+, and full. They respectively correspond to 0, 0.25, 0.5, 0.75, and 1 crisp values.

3. Our Punishment Policy Knowledge Base

In order to assign punishment values, ANFIS requires a knowledge base providing policy foundations. Usually, this policy is specified by a domain expert. We have generated this knowledge base manually. It considers the values of previous parameters—introduced in previous section—at different time steps. In this manner, our policy states the punishment for a car based on its current speed and position together with its priority² at previous time step. Therefore, we need to distinguish between time step t1 and its subsequent instant t2=t1+Δt. Next Table 1 shows the punishment policy knowledge base, which includes a semantic explanation of each set of rules.

Table 1. Punishment policy knowledge base

Priority at t1	Speed at t2	Position at t2	Punishment	Interpretation
NP	L	SJD	none	The car is not punished when its speed is low. It is independent from its junction distance (JD)and priority
NP	L	MJD	none	
NP	L	LJD	none	
NP	M	SJD	mid+	If the car doesn't have priority (P=0),and its speed =M, its punishment is inversely proportional to its JD (from mid+ to mid-)
NP	M	MJD	mid	
NP	M	LJD	mid-	
NP	H	SJD	full	If priority=0, and speed =H, its punishment is inversely proportional to its JD (from full to mid+)
NP	H	MJD	full	
NP	H	LJD	mid+	
LP	⋮	⋮	⋮	Values for priority =0.1 and 0.25 should be equivalent to the ones for priority=0.0
MP	L	SJD	none	The car is not punished when its speed is low (it is independent from its JD and priority)
MP	L	MJD	none	
MP	L	LJD	none	
MP	M	SJD	mid	If priority=0.5, and speed =M, its punishment is inversely proportional to its JD (from mid to mid-)
MP	M	MJD	mid-	
MP	M	LJD	mid-	
MP	H	SJD	mid+	If priority=0.5, and speed =H, its punishment is inversely proportional to its JD (from mid+ to mid) lower than it was for priority =0
MP	H	MJD	mid+	
MP	H	LJD	mid	
HP	L	SJD	none	The car is not punished when its speed is low (it is independent from its JD and priority)
HP	L	MJD	none	
HP	L	LJD	none	
HP	M	SJD	mid-	If priority=0.75, and speed =M, its punishment is inversely proportional to
HP	M	MJD	mid-	

¹ Both NP and VHP are half Gaussian functions.

² Priority was established in a previous work [9].

HP	M	LJD	none	its JD (from mid- to none)
HP	H	SJD	mid	If priority=0.75, and speed =H, its punishment is inversely proportional to its JD (from mid to mid-) higher than it was for speed=M
HP	H	MJD	mid	
HP	H	LJD	mid-	
VHP	L	SJD	mid-	The car is slightly punished when its speed is low and has full priority because it blocks the traffic (if JD is long then, it is worse)
VHP	L	MJD	mid-	
VHP	L	LJD	mid	
VHP	M	SJD	none	If the car has full priority, it is not punished (independently from JD)
VHP	M	MJD	none	
VHP	M	LJD	none	
VHP	H	SJD	mid-	If the car has full priority, it is not punished unless its JD is small (it is too dangerous to get at full speed in the junction)
VHP	H	MJD	none	
VHP	H	LJD	none	

4. Results: membership function adaptation

As previously mentioned, we have generated the knowledge base in previous Table 1 manually, based on the experience of simulating our traffic scenario. Each entry in the knowledge base is a fuzzy IF-THEN rule, where conditions are fuzzy labels (i.e., linguistic descriptions of speed, position and priority) and consequences are crisp values (i.e. the proposed punishment policy). We have assigned Gaussian membership functions to our fuzzy labels uniformly along the x axis. Nevertheless, there is no guarantee about this being the best possible choice. In fact, our goal is to use ANFIS³ to produce some appropriate variations on the fuzzy labels so that the overall knowledge base improves. Improvement here means to reduce discrepancies between obtained and target outputs, that is, to reduce the model output error. Adaptation is done over the membership functions by changing their center and spread values.

HLA in ANFIS combines least squares estimate (LSE) method to determine consequent parameters in forward pass (while premise parameters are fixed) and gradient descent (GD) method to determine premise parameters in backward pass (while consequent parameters are fixed). HLA is characterized by batch learning mode, while backward pass and premise parameters updates, take place after the whole training data set has been resented to the ANFIS in each epoch. On one hand, in the forward pass, a set of training data formed from input values and desired corresponding output value is presented to the system. Layer by layer, every node output is calculated. The output is a function of the input variables and the set of linear consequence parameters. These parameters are calculated by LSE. On the other hand, in the backward pass, GD method is used in updating premise non-linear parameters (Gaussian function, which represents MF, centre and spread constant) in aim to reduce overall error between obtained and target output. A detailed description of HLA can be found in [5,10].

Although the total number of fuzzy rules from Table 1 are 45, the number of training data pairs used for ANFIS training was 162 (they were randomly chosen). Additionally, the number of linear parameters was 180 whilst the number of nonlinear parameters was 22. After 70 training epochs, the average error was 0.019883.

³ ANFIS has been implemented in Pascal upon our punishment policy knowledge base.

Figures 3, 4 and 5 show the result of this membership function modification. Figure 3 a) shows initial priority membership functions, which coincide with the ones in Figure 2 c); whereas Figure 3 b) depicts their adaptation after training. As it can be observed, function shapes keep similar: centers are exactly the same and spreads are just slightly narrower, thus we can somehow discard this adaptation.

Figure 4 shows how the centers of membership functions corresponding to input fuzzy set "Speed" have been shifted. In this manner, they have been tuned properly in order to reduce errors between obtained and target outputs (i.e. the proposed punishment policy). Figure 5 shows a similar result for "Position" fuzzy sets.

Overall, we can conclude that changes in membership functions shapes for the fuzzy sets Speed and Position are significant.

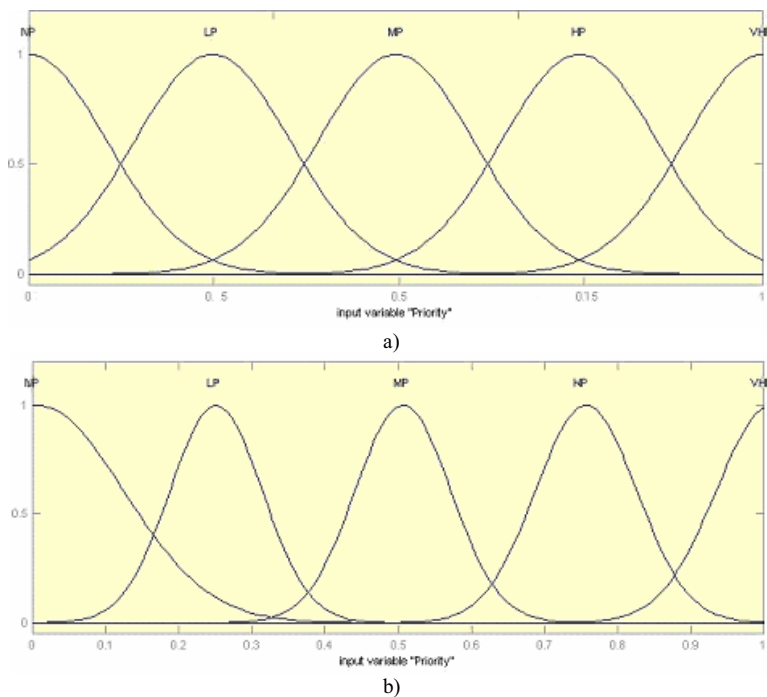


Figure 3. The input fuzzy set "Priority" membership functions: a) before, and b) after training.

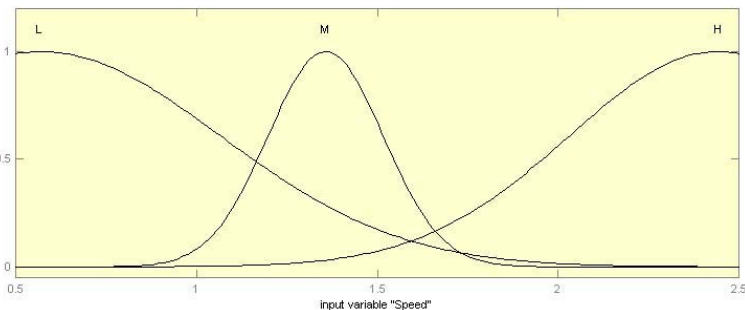


Figure 4. The input fuzzy set "Speed" membership functions after training.

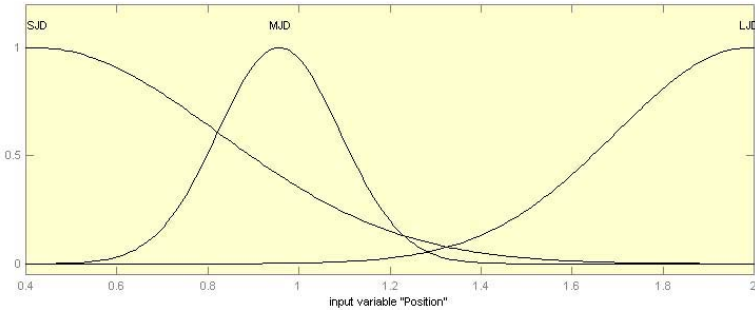


Figure 5. The input fuzzy set "Position" membership functions after training.

Figure 6 represent numerical 3D representations of mutual dependence between main parameters of the observed MAS.

By modifications of input set membership functions, ANFIS demonstrates competence in suggesting punishments in a similar way to the human reasonable punishment policy for a two road junction. Though, the ANFIS gives here clear (crisp) respond, upon the blurry (fuzzy) input data, by adapting them, what might be treated as its great advantage when clear punishment regulations are necessary for rapidly changing and unpredictable environments.

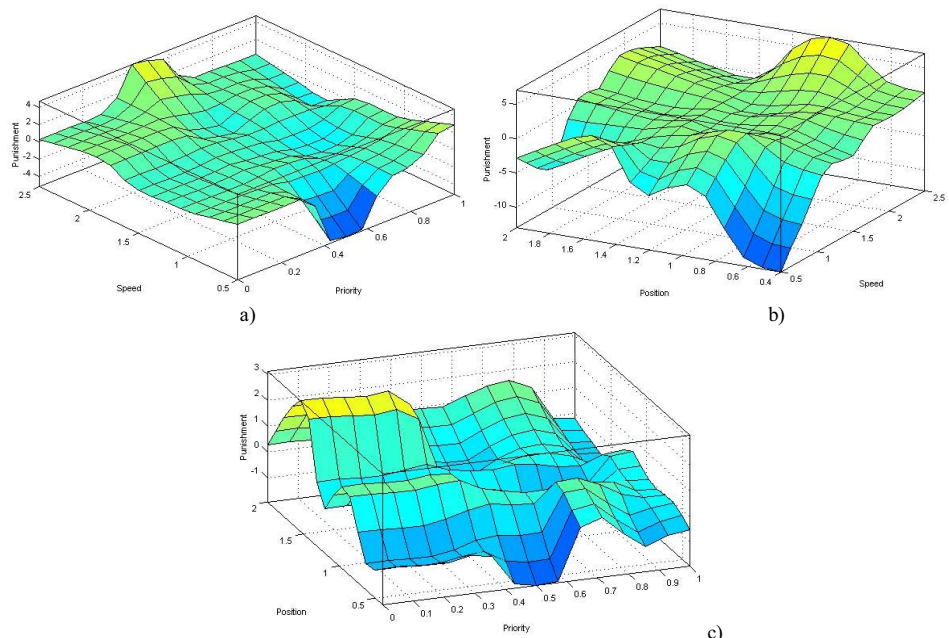


Figure 6. The 3D representations of Punishment dependence upon a) agent Speed and Priority, b) Position and Speed, and c) Position and Priority.

5. Conclusions

This paper proposes an approach to adapt a given fuzzy knowledge base that comes from empirical domain experience (a multi-agent two road junction traffic scenario, in our case). We have shown that ANFIS produces some appropriate variations on the fuzzy labels so that the overall knowledge base improves. That is, discrepancies between obtained and target outputs are reduced in an unsupervised manner. More concretely, for our specific case, the model output error has been set to 0.019883 by running ANFIS during 70 epochs. As we have seen, adaptation is done over the membership functions by changing their center and spread values.

This could provide significant help in traffic regulation, particularly when large number of criteria should to be considered for dynamic environments, or when it is not so straightforward to estimate proper punishments. Nevertheless, this is a rather theoretical approach to the computation of the optimal punishment policy, and therefore, future work should be focused on more practical experiments and real observations in traffic scenarios.

References

- [1] Nicholas R. Jennings, Katia Sycara, and Michael Wooldridge. A roadmap of agent research and development. *Autonomous Agents and Multi-agent Systems*, 1:275–306, 1998.
- [2] Agtivity: Advancing the science of Software Agent Technology. Foundations and definitions at http://www.agtivity.com/def/multi_agent_system.htm.
- [3] Eva Bou, Maite Lopez-Sánchez, Juan A. Rodríguez-Aguilar, "Adaptation of Autonomic Electronic Institutions through norms and institutional agents" in *ESAW'06, 7th International Workshop on Engineering Societies in the Agents World VII*. Dublin, Ireland. pp. 137-152. September 6-8th, 2006.
- [4] Maite Lopez-Sánchez, Francesc X. Noria, Juan A. Rodríguez-Aguilar, and N. Gilbert. Multi-agent based simulation of news digital markets. *International Journal of Computer Science and Applications*, 2(1):7–14, 2005.
- [5] Jang J.-S. R., (1993). ANFIS: Adaptive network based fuzzy inference system. *IEEE Transactions on systems man and cybernetics*, 23(3), 665-685.
- [6] Lee C.-C., (1990). Fuzzy logic in control systems: fuzzy logic controller - part 1. *IEEE Transactions on systems, man and cybernetics*, 20(2), 404-418.
- [7] Takagi T., Sugeno M., (1983). Derivation of fuzzy control rules from human operator's control actions. IFAC Symposium on fuzzy information knowledge representation and decision analysis, 55-60
- [8] Natasa Kovac, Sanja Bauk (2005), An ANFIS Navigation Decision Support Method, SYM-OP-IS, Vrnjacka Banja, pp 543-545
- [9] Sanja Bauk, Natasa Kovac, Zoran Avramovic, Maite Lopez-Sánchez Information Support to Multi-Agent Systems based on a Neuro-fuzzy Mode. In proceedings of INFO-TEH Conference- Jahorina 2007.
- [10] Natasa Kovac, Sanja Bauk, The ANFIS based route preference estimation in sea navigation, *Journal of Maritime Research*, 3(3):69-86, 2006

Scholar Agent: Auction Mechanisms for Efficient Publication Selection on Congresses and Journals

Josep Lluis de la Rosa¹ and Maria de los Llanos Tena¹

Agents Research Laboratory

EASY centre of CIDEM XIT - University of Girona

Abstract. Congresses and journals (CJ) can be like displays which can be used as a publishing medium of scholarly works when space is a scarce resource, and it is desirable to expose many papers, posters and communications (adverts of scientific work) to as wide a scientific audience as possible who will eventually cite them. Although the efficiency of such publishing systems can be improved if the CJ are aware of the identity and interests of the audience, this knowledge is difficult to acquire when users are not previously identified or inscribed in the CJ. To this end, we present Scholar Agent, an intelligent public agent, which helps CJ to select and display papers, posters and communications in response to scientists inscribed to particular sessions or tracks in the audience. Here, scientists are identified and their CJ review history tracked. Within Scholar Agent we have designed an agent system that utilises a new currency and an auction-based marketplace to efficiently select papers for the display. We show, by means of an empirical evaluation, that the performance of this auction-based mechanism when used with bidding strategy, efficiently selects the best paper in response to the audience presence (inscribed). This may have utility both presential or on-line CJ. We show how our scholarly publishing agents (Scholar Agents) will behave accordingly the private value of the paper by the scientist and how to link this initial private value with the own private value of the agents that are bench-marked with two other commonly applied selection methods for displaying papers in CJ.

Keywords. Auctions, congresses, peer-review, peer-review 2.0, currencies, agents.

1. Introduction

Classical or electronic journals and congresses (CJ) are increasing its use by an increasing offer from the scientific demand. Within these CJ, the organizing committees typically utilise a variety of delivery methods to maximise the number of different papers displayed, and thus increase their overall exposure to target audiences. This trend is similar to marketing, where agents can work in [1]. However, the existing marketing methods are typically naïve and do not take into account the current audience.

On the other hand, a number of online publications and new peer – review methods have been proposed to update the way that scholar community works. As Sergey Brin

¹ Correspondence to {pepluis, lltenal }@eia.udg.es

and Larry Page (founders of Google) suggest in [2], “the scientists must learn marketing to better target their research to their potential users”.

And talking about marketing, a number of interactive public displays have been proposed that support communication with a user through active use of handheld devices such as PDAs or phones, or to a closed set of known users with pre-defined interests and requirements [6]. Such systems assume prior knowledge about the target audience, and require either that a single user has exclusive access to the display, or that users carry specific tracking devices [3] [8] so that their presence can be identified. These approaches fail to work in public spaces, where no (or little) prior knowledge exists regarding users who may view the display, and where such displays need to react to the presence of several users simultaneously.

In contrast, we have prototyped an intelligent public peer-review and communication system that utilises a novel approach to improve the selection of papers for display. The goal of the selection is to maximise the exposure of as many papers as possible to as wide an audience as possible (i.e. to maximise the number of distinct papers seen by the population of users) and therefore maximize the number of potential citations as a payback to the authors of the paper. In doing so, the main advantage of our system design is that it achieves this goal without: (i) any exhaustive prior knowledge on the audience, (ii) the need for any specific action by the user.

As no direct feedback is *a priori* received from the audience and the only knowledge available is based on the past observations of user presence, one of the key challenges of our system is to predict which paper is likely to gain the highest exposure during the next publishing cycle. To approximate this prediction, our system utilizes history information of past users' exposure to certain sets of papers (so that we don't repeat material they have already seen), along with the information about what users are currently viewing on the CJ. In particular, we developed a multi-agent auction-based mechanism to efficiently select a paper for each CJ session or time/space slot. In this system, each agent represents a scientist that wishes to publish or communicate, and it is provided with a bidding strategy that utilises a heuristic to predict future publication exposure, based on the expected audience composition. The particular issue that makes this paper interesting is a analogy of CJ and Marketing Media (TV, Newspapers, Radio, etc), when the CJ was a media of scientific diffusion consisting in a section of first-class prestigious and appealing papers and a second section of “adverts” of scientific works trying to get its place in the scientific community². The first section may be the selection of papers by means of peer-review or other conventional mechanisms, but in the second section another selection of papers might apply, namely auctions among other approaches.

In order to evaluate our design, we conceived a very first prototype of a system consisting of advertising research papers (or projects, press releases and announcements) and developed a simulator which models users (scientists) behaviour. Here we report empirical results that show that the auction is more efficient in selecting papers to maximise exposure of this publishing material to a set of users (attendant scientists) in the shortest time possible. Specifically, the auction requires, on average, 36% fewer publishing cycles to communicate all the papers to each user, when compared to the Round-Robin approach (or 64% fewer expositions when compared to the Random selection approach).

In more detail, this paper advances the state of the art by:

² Special thanks to *Didac Busquets* for his helpful hint to this analogy of CJ and mass media

- Deploying the *Scholar Agent* prototype architecture.
- Developing a multi-agent auction-based marketplace for effectively marketing papers on the *Scholar Agent prototype*.
- Devising a heuristic-based bidding strategy that can be used by the agents in the auction mechanism to improve the private value of Scholar Agents vs. the initial private value set up by scientists.
- Benchmarking our method against two commonly used selection strategies, *Round-Robin* and *Random*, to demonstrate that auctions method can efficiently display the best set of papers given the current audience.

The remainder of this paper is organised as follows: the architecture of the system is discussed in Section 2 and the underlying auction mechanism is described in Section 3. In Section 4, we present empirical results. Section 5 concludes.

2. The Scholar Agent Architecture

This is a special type of recommender agent that will work on behalf of a scientist by taking proactive decisions in what CJ submit papers to and reach to commitments. In the state of the art of recommender systems [12] and recommender agents [13] there are mainly techniques to profile the user so that the recommender may anticipate his/her choices. We may share this basic principle but the difference is that Scholar Agent so far does not fully profile the scientist but get its Internal Private Value (IPV) in an explicit way and then executes the process of looking a CJ to display the paper in a efficient way, without taking into account more information of the scientist, though in a future the scientist profile may be included in Scholar Agent. [9] [10] introduce some definitions that are useful for Scholar Agent:

- **Agent:** in a broader sense, this is a physical person, scientist, surgeon, citizen, a juridical person or an artificial agent when they are authors of some work or potential executors of an action, such as fulfilling a contract, performing an operation, selling cars, etc.
- **Contribution:** this is some work, action or knowledge, to be executed, or already developed and authored by a scientist or an agent. It is referred as “paper” as well.
- **Citation:** when one scientist or an agent acknowledges a scholarly work, published, as useful for his work in any sense.
- **RoAC:** the Return on Auctions based Currency €. For example, a **Citations Certificate** can be the currency. Every agent can cite any other, but not himself, and an external (different from authors cited or citing) authority is allowed to verify the number of citations.
- **Wallet (W):** Also it is the number of citation that outcome the citations that have been paid in auctions to publish a scholarly paper in a CJ. In a broader sense, it is the amount of currency € units that belongs to an agent in a given moment.
- **CM (Contribution Methods):** This is any method to select contributions that use the € as currency, and auctions will be tested in this paper.
- **Arena:** this is the marketplace to perform the **CM** (in this paper will compare auctions with other methods).

Initially, each CJ (conference, congress, symposium, journal or publisher) can create its own count of citations and contracts with each participating author. Ultimately, we envision the need for a new international organization able to certificate the CW of researchers and whether they have credit or not, etc. This organization would consist of a sort of a bank, which could be named something like the World Bank of Citations (WBC), and a market place service for secure auctions linked to the submission links of the CJ. Unlike a normal Bank, the WBC will not create citations (read “money” or “currency”) but use the citations that can be counted from a normalized universal citation searcher [10]. We claim that there are correlations among the global number of citations with the scientific activity and, perhaps with a delay, with the potential wealth of the global society. Thus, the WBC bears some similarities to a conventional bank. The WBC will have the ultimate authority that could be chaired by international scientific and non-governmental organizations to keep it free from any political control and help to maintain universally free research. The WBC will include the following components (see Fig.1):

- An international escrow (BoW) to store the CW of researchers, their citation contracts and their loans, with the according interest rates, etc.
- A web-based market place (Arena) for executing auctions, rules, time, etc, linked to the escrow of the WBC to verify the credit of researchers in auctions and to implement transparent auctions. This market place will be linked to any CJ in the world requiring the services of the WBC.

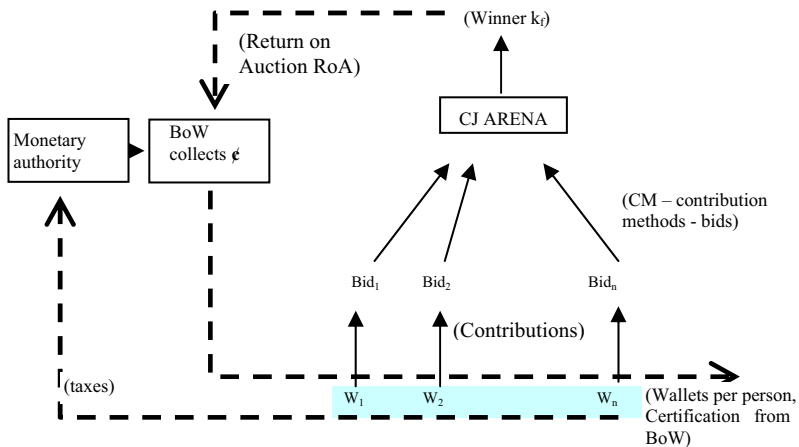


Fig. 1. The architecture for scholar Agents. K_f contains the winning agent and its contribution is published

The bids are done by the scholar agents, which are now explained. *Scholar Agent* will interact with the CJ by means of the Arena for identifying users (scientists). The CJ can record the encounters as a collocation event in terms of location and duration. The duration of this collocation event is assumed to relate to a possible level of interest in the displayed material; e.g. a user who is interested in the current publishing material will linger at the display during the session. The fact that user presence in front of the intelligent CJ can be a priori identified during the congress is feasible but it is not straightforward a priori, especially in Journals.

The basic components of the *Scholar Agent* architecture that we developed are the following, inspired from [11]:

- **Arena (or Marketplace).** The Arena facilitates the sale of publication time/space slots in a CJ. A repetitive second-price sealed-bid auction [9] is used as a selection mechanism (this choice is justified below) to determine which publishing scholar agent (if any) will display its paper on the next time slot, and its corresponding payment in citations ϵ .
- **Auction Mechanism.** *Scholar Agent* is designed to support a scaleable and a dynamic publication framework, while maximising the exposure of as many papers as possible to as wide an audience as possible, within a knowledge-poor environment. The main principle of our design is to distribute the control of the content displayed, in a way that no single entity can dictate who will advertise next. In contrast, the system, as a whole, will decide who will be the most profitable agent (i.e., expected to gain the highest exposure and future citations by displaying its paper in the next publishing cycle) and therefore will be awarded the facility of publishing in that session. Note that although the scholar agents are self interested (i.e. aim to maximise their own exposure to as large an audience as possible using their fixed budget in citations ϵ), this does not contradict our desired overall design goal, since in our context, we assume that each agent will bid a value that reflects its expected exposure from publishing on the next session/issue (namely, the next cycle). Specifically, we have implemented a repetitive, second-price sealed-bid auction that takes place before each of the publishing session/issue (cycles) as [11] proposes, that is also used for web advertising using search engines like Google and Overture [4]. The winner of each auction is the publishing agent who placed the highest bid, and it is charged for the second highest bid. As truth-revealing has been shown to be a dominant strategy in this case, the effective local decisions of each individual agent contribute towards effective overall system.

3. The Scholar Agent Architecture

In this section we start by describing the Scholar Agent model and the mechanism we developed, including the strategies of the publishing agents given their valuation for the next publishing cycle's auction. However, as our system is a knowledge-poor environment where no direct feedback is collected from the users (instead only a limited history and the current status of the detected scientists is available), in the final part of this section we provide the agent with a heuristic method to generate this value.

3.1. The Auction Model

In our model we assume that there is a single *Scholar Agent* instance available for publishing which is managed by the Arena. The publishing time is divided into discrete intervals which we term the *publishing cycle*, C^i . During each such cycle, only one agent can communicate its corresponding paper, and during this time only this agent has the ability to collect information about scientists which were detected by the *ScholarAgent* (for example, registered in the CJ Arena or by means of more sophisticated devices by means of Bluetooth as [11] shows in his experiments). However, at the end of each publishing cycle, the Arena informs all the scholarly publishing agents about any public that has registered for a session at that time.

Each scholarly publishing agent, a_i , is assumed to be self interested, and to be managed by a scientist who credit it with a fixed budget for publishing (measured in citations ϵ currency). For each publishing cycle, each publishing agent generates its

private value (discussed in detail below) and places a corresponding bid in terms of some currency (citations €). Once an agent has fully spent its budget assigned by the scientist to his paper, it is **not** deleted from the Arena of this CJ, because **bids of zero € are acceptable**. On the other hand, at any point in time, new agents may be added to the system. The goal of each scholar agent is to utilise its budget in a way that maximises its exposure.

The Arena acts as the auctioneer and runs an auction before each of the publishing cycles. As part of the auctioneer duties, it sets a reservation price that represents the minimum acceptable bid. In the case that none of the agents place bids that meet this price, a default paper is displayed (a tutorial, an awarded paper, a round table, etc). The Arena is also assumed to be trusted by the scholarly publishing agents. This feature is necessary for the proper behaviour of the system, as in a second-price sealed-bid auction no one observes the whole set of bids except the auctioneer.

3.2. Bidding Strategy for the Scholar Agents

In our model, agents participate in a *repetitive*, second-price sealed bid auction whilst facing budget constraints. For non-repetitive variants of this auction, as [11] claims, it has been shown that the bidding strategy:

$$\beta(a_j) = \min \{ \text{budget}(a_j), v \}$$

is a dominant strategy [5], where $\text{budget}(a_j)$ is the current balance of agent a_j and v is its private valuation (PV). Now, [11] claims it is easy to see that this holds for the repetitive case as well, as in each round of the second-price sealed-bid auction, a new publishing cycle is auctioned. However, there exists dependence with previous rounds in terms of the scientists that were exposed in the past, and those that are currently in front of the screen. However, this dependence is concealed in the valuation of the bidder for the next publishing cycle.

But, once the agent has generated its valuation for the next publishing cycle, its dominant strategy is truth telling.

Although the agents utilise truth telling as a dominant strategy, they still face a very challenging problem of being able to estimate their *expected exposure*, as they are provided only with information about past and current audience composition (in terms of registered scientists), and from that alone they need to estimate their future exposure, and hopefully the scientists who own these agents will do the same. In the next subsection we describe a heuristic method we developed for the bidder valuation estimation task.

3.3. Heuristics for Estimating Private Values (PV)

First of all, every scientist knows the private value (PV) of a paper. The scientists set up a scholarly publishing agent a_j with this $v_0(a_j)$ as initial PV, and a budget in € currency, that is supposed (though not necessarily is) lower than the PV so that the scientist will gain a margin of € in the long term if the paper is correctly exposed to the proper audience in the right extension, always constrained by a budget, or constrained by the wallet W of the scientist.

Now, by adapting the formulation of [11], here we provide the scholarly publishing agent, a_j , with a heuristic strategy for generating its valuation (expected utility) for the

next publishing cycle, C^{i+1} . Recall that the main target of an agent a_j is to maximise its exposure to as large an audience as possible, given its financial constraints so that it maximises the potential citations of other scientists to earn the most ϵ and gain the maximal payback of the investments in the exposure of the papers. The core principle of this heuristic is, apart from the initial private value $v_0(a_j)$, to utilise the information an agent has about past papers exposure, to predict the future expected exposure. Specifically, each time a scholarly publishing agent a_j has to make a decision about its valuation for the next cycle C^{i+1} , it has two types of information on which to base its decision:

- history observation, $H(a_j)$, of exposed scientists which were collected during the publishing cycles it won, $WonCycles(a_j)$, in the past, $H(a_j) = \{(C^t, d, x)\}$ where $C^t \in WonCycles(a_j)$, d is the scientist identification, and x is the exposure duration; and
- the current set of registered (or detected) scientists which were in the session at the end of C^t , termed $end(C^t)$.

Using this information, a scholarly publishing agent, a_j , assumes that the scientists that will be in front of the talk in C^t are $end(C^t)$. Therefore, we propose that a_j will search through its history to check if these scientists were exposed to its paper in the past, and, if so, for how long. If a scientist was exposed to the same paper during several different publishing cycles, then we propose to consider only the one in which it was exposed to the most. Formally, a_j 's valuation for C^{i+1} is:

$$v(a_j, C^{i+1}) = \sum_{d \in end(C^t)} 1 - \max \{x \mid \{C^t, d, x\} \in H(a_j)\}$$

4. Empirical Evaluations

To evaluate the bidding strategy described in the previous section within a controlled environment, a simulation was developed. This is based on the same architecture as the deployed *Scholar Agent* instance, but it additionally supports the modelling of users in the audience.

4.1. First Experimental Results

The former experiment was about the maximization of the exposure by means of guessing the public in CJ sessions. In these experiments we examine the global behaviour regarding 5 types of PV as initial value $v_0(a_j)$ of each scholar agent a_j regarding a common auction strategy for all them. They are:

- Optimistic: the PV of the scientist s_i regarding a paper p is higher than the consensus private value (CPV) that a group of peers would rate it after a peer-review process. In notation $PV(s_i, p) \geq CPV(p)$
- Pessimistic: $PV(s_i, p) \leq CPV(p)$
- Random: $PV(s_i, p)$ is assigned without any relation to $CPV(p)$
- Precise: $PV(s_i, p) = CPV(p)$
- Precise but optimist : $PV(s_i, p) \approx CPV(p) + \epsilon$, being ϵ small compared to $CPV(p)$
- Then every scholar agent on behalf of a scientist s_i is assigned the $v_0(a_j) = PV(s_i, p)$

The results (Fig. 2) after 100 auctions simulation in this environment show how the optimist agent is doing better than pessimist, rather much better than the precise agent,

but the pessimist agent performs better than the precise but optimist agent. Random agent performs only better than precise agent. This is a surprising result, but it has a sense: the PV is estimated to create a bid, but the strategy for bids need to be improved, more sophisticated.

However, there is lack of further PV estimation in terms of what CJ quality and what are the public attending the CJ sessions so that the PV of every scholar agents is different from the initial PV of the scientist, and this is solved in the following experiments.

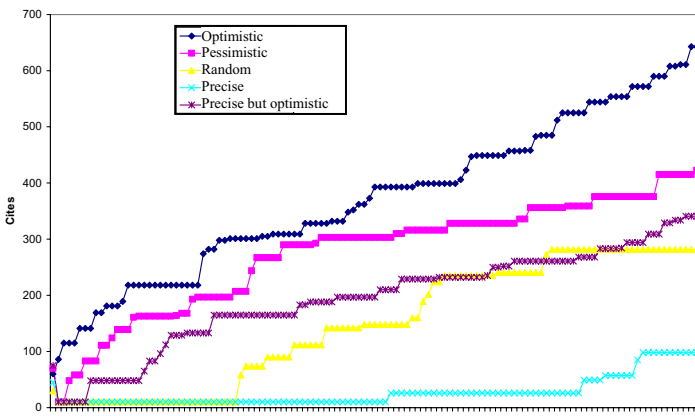


Fig 2. Evolution of 5 PV estimation behaviours for a Scholar Agent.

4.2. Second Experimental Results

The *Scholar Agent* simulation modelled CJ behaviour in terms of their likelihood of arriving at, and subsequently remaining at, a *Scholar Agent* session given the currently presented paper. The *attending scientists (public) model* was defined with the following assumptions:

- The session presence of scientist is measured in discrete sample-intervals
- The duration of the communication of a paper is assumed to be equal to a whole number of sample-intervals;
- A paper is considered as *paper fully presentation to a scientist* only when a scientist has been present for the whole duration of the paper presentation session;
- Scientists (public) can arrive at any point during an publishing cycle, whereby the probability that a researcher will arrive is P_{arrive} ;
- The probability a scientist may leave without observing the subsequent paper is P_{depart} . A scientist will automatically leave if it has *fully seen* the subsequent paper;
- Both P_{depart} and P_{arrive} assume a uniform distribution.

Two alternate selection methods were compared with the auction: *Round-Robin* selection and *Random* selection. The former is a familiar mechanism used to repeatedly cycle through a number of papers (in order). Given our scientist model, this approach represents the optimal selection mechanism when $P_{depart} = 0$ and $P_{arrive} = 1$. The latter mechanism randomly selects a new paper to display at the beginning of each new publishing cycle, independently of what has been previously selected. This method was selected as a baseline against which the other worst-case methods can be compared.

To simplify this analysis, each experiment consisted of ten papers of equal duration (i.e. six samples which is equivalent to a 15 minute communication), represented by ten scholar agents. In each experiment, papers are selected and presented until every scientist has *fully seen* all ten papers. To ensure statistical stability, the results of each experiment are averaged over 10,000 test runs, and the mean results are reported. Where necessary, a Student's t-test is used to confirm statistical significance at the 95% confidence level.

We examine the behaviour of each selection mechanism as the number of scientists present increases (Fig. 3). The number of scientists, N_d , was varied between 1 and 100, and the scientist behaviour was defined using $P_{depart} = 0.05$ and $P_{arrive} = 0.5$. The plots supports the hypothesis that paper selection using the *Scholar Agent auction* is statistically more significant than either *Round-Robin* or *Random* (assuming the modelling parameters defined above). Specifically, as N_d increases, there is a corresponding exponential rise in the number of required communications. The mean number of communications required by the *Scholar Agent auction* is lower than the *Round-Robin* selection mechanism or the *Random* selection mechanism for all numbers of scientists tested; e.g. for $N_d = 50$, the auction method required a mean of 40.24 ± 0.06 publishing cycles to communicate all 10 papers to all the scientists, compared to *Round-Robin* (64.16 ± 0.18) or *Random* (108.50 ± 0.28). This suggests that although each selection method can scale, a single scientist will be exposed to all the papers in typically 36% fewer publishing cycles than the round robin approach.

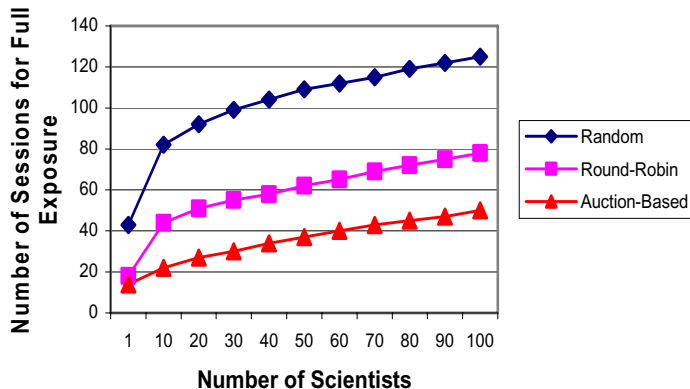


Fig. 3. The effect of varying the number of scientists in the audience; $P_{depart} = 0.05$, $P_{arrive} = 0.5$

5. Conclusions

In this paper, we addressed the problem of creating agents that creates a private value (PV) from scientists that is completed by providing audience composition data to the agents to the intelligent public display of papers. It proposes a bidding heuristic which predicted the level of expected exposure of a paper given the registered (in the future detected) audience and knowledge of previous exposure the audience members had to different papers, and accordingly a budget in terms of a new currency and a PV of scientists.

We experienced the behaviour of agents with 5 different PV estimation profiles, leading to surprising results of the behaviour of the Scholar Agent, without introducing any risk profile differentiation among agents, that will be done as future work.

Keeping on with private value (PV) adaptation of agents from the original PV guessed by scientists, we tested a simulation environment to the *Round-Robin* approach, or 64% fewer publishing cycles than the *Random* approach when using the *Scholar Agent auction* to reach the expected PV.

As future work, we plan to extend our approach to work with multiple sessions in many CJ, to increase the exposure of papers to a larger community, and to build user preferences based on the duration scientists spend viewing different papers that are categorised (thus taking into account inferred interest, as well as exposure) and create a full recommender scholar agent. Additionally, we'll compare different bidding strategies (aggressive, defensive, etc) and study further the initial private values generation. Moreover, more modelling work has to be developed to describe how the exposure of scientists to papers will conduct to citations. And finally, to test this approach in real CJ, in a future stage in RPI (Rensselaer Polytechnic Institute).

Acknowledgements

To the EU project No. 34744 **ONE**: Open Negotiation Environment, FP6-2005-IST-5, ICT-for Networked Businesses.

References

- [1] Sander M. Bohte, Enrico Gerding, and Han La Poutre, Market-based recommendation: Agents that compete for consumer attention, *ACM Trans. on Internet Tech.*, 4(4), 420–448, (2004).
- [2] David A. Vise, The Google Story, *Pan Mac Millan Ed.*, (2005)
- [3] Jeffrey Hightower and Gaetano Borriella, Location systems for ubiquitous computing, *IEEE Computer*, 34(8), 57–66, (2001).
- [4] Brendan Kitts and Benjamin Leblanc, Optimal bidding on keyword auctions, *Electronic Market*, 14(3), 186–201, (2004).
- [5] Vijay Krishna, Auction Theory, *Academic Press*, (2002).
- [6] Joseph F. McCarthy, Tony J. Costa, and Edy S. Liangosari, Unicast, outcast & groupcast: Three steps toward ubiquitous, peripheral displays, in *UbiComp '01: Proc. 3rd Int. Conf. on Ubiquitous Computing*, pp. 332–345, London, UK, (2001). Springer-Verlag.
- [7] W. Vickrey, Counterspeculation, Auctions and Competitive Sealed Tenders, *Journal of Finance*, 8–37, (1961).
- [8] Roy Want, Andy Hopper, Veronica Falcao, and Jonathan Gibbons, The active badge location system, *ACM Trans. on Information Systems*, 10(1), 91–102, (1992).
- [9] C. Carrillo, J. L. de la Rosa, A. Moreno, E. Muntaner, S. Delfin and A. Canals, Social Currencies and Knowledge Currencies, *Frontiers in Artificial Intelligence and Applications – AI Research & Development*, IOS Press, 146 (1), 266-274, (2006)
- [10] J. L. de la Rosa, Outline of Citation Auctions, *Frontiers in Artificial Intelligence and Applications – AI Research & Development*, IOS Press, 146 (1), 299-307, (2006)
- [11] Terry Payne and Ester David and Nicholas R. Jennings and Matthew Sharifi, Auction Mechanisms for Efficient Advertisement Selection on Public Displays, *The 17th European Conference on Artificial Intelligence (ECAI2006)*, pp: 54-60, Riva del Garda, Italy, (2006)
- [12] Gediminas Adomavicius, Member, IEEE, and Alexander Tuzhilin “Toward the Next Generation of Recommender Systems: A Survey of the State-of-the-Art and Possible Extensions, *IEEE Transactions on Knowledge and Data Engineering*, Vol. 17, no. 6, June 2005
- [13] Montaner M.; López B; de la Rosa J. Ll, A Taxonomy of Recommender Agents on the Internet, ISSN 0269-2821, *Artificial Intelligence Review*, Vol: 19, pp: 285-330, Kluwer Academic Publishers, Berlin, 2003

This page intentionally left blank

Data Processing

This page intentionally left blank

Modeling Problem Transformations based on Data Complexity

Ester BERNADÓ-MANSILLA and Núria MACIÀ-ANTOLÍNEZ

Grup de Recerca en Sistemes Intel.ligents
Enginyeria i Arquitectura La Salle, Universitat Ramon Llull
Quatre Camins 2, 08022 Barcelona (Spain)
{esterb,nmacia}@salle.url.edu
<http://www.salle.url.edu/GRSI>

Abstract. This paper presents a methodology to transform a problem to make it suitable for classification methods, while reducing its complexity so that the classification models extracted are more accurate. The problem is represented by a dataset, where each instance consists of a variable number of descriptors and a class label. We study dataset transformations in order to describe each instance by a single descriptor with its corresponding features and a class label. To analyze the suitability of each transformation, we rely on measures that approximate the geometrical complexity of the dataset. We search for the best transformation minimizing the geometrical complexity. By using complexity measures, we are able to estimate the intrinsic complexity of the dataset without being tied to any particular classifier.

Keywords. Data Complexity, Classification, Breast Cancer Diagnosis

1. Introduction

The data complexity analysis [1] concerns the study of to what degree patterns can be extracted from datasets. Most of the research in pattern recognition, machine learning, and other related areas have focused on designing competitive classifiers in terms of generalization ability, explanatory capabilities, and computational time. However, limitations in classification performance are often due to the difficulties of the dataset itself. The data complexity analysis is a recent area of research that tries to characterize the intrinsic complexity of a dataset and find relationships with classifier's accuracy.

This paper uses the data complexity analysis to study problem transformations for a particular case of breast cancer diagnosis. The original problem is not directly tractable by a classifier, since each patient has a variable number of descriptors. Thus, prior to the application of any classifier, the descriptors must be synthetized into a single one. Several synthetic representations are possible, each leading different classification results. Moreover, due to the nature of the problem, the domain experts are unable to specify the best one. A previous approach was to use the classifier's accuracy as a measure of quality of the different synthetic representations. A limitation of the approach was that the classifier's accuracy depended both on classifier's bias and dataset characteristics, misleading the selection of the best method and confusing the interpretation provided to

the human experts. We consider the characterization of data complexity as a method to select the best synthetic representation. The proposed methodology sets a framework that guides us in the selection of problem transformations without being tied to any particular classifier. Our results are also meaningful to the domain experts, because they provide intrinsic information of the problem at hand.

The paper is structured as follows. Section 2 reviews the data complexity analysis and its application to classification problems. Section 3 describes the problem we address in more detail. Next, we study problem transformations and their characterization by means of the complexity analysis. We present the results and finally, we summarize the conclusions and future work.

2. Analysis of Data Complexity

The complexity of a classification problem can be attributed to three main sources [2]. *Class ambiguity* is identified as the difficulty given by non-distinguishable classes. This may be due to the intrinsic ambiguity of the problem, or to the fact that the features are not sufficient to discriminate between the classes. Class ambiguity sets a lower bound on the achievable error rate, which is called Bayes error. The *sparsity of the training set* is related to the number and representativity of the available instances. The *boundary complexity*, the third source of difficulty, can be characterized by the Kolmogorov complexity, or the minimum length of a computer program needed to reproduce the class boundary. Class ambiguity and training set sparsity are properties of the specific dataset. Once the dataset is fixed, these complexities are irrecoverable. On the other hand, the geometrical complexity is more relevant to the study of classifier's behavior. The characterization of the boundary complexity may be useful to explain the different performance of several classifiers on a given dataset. That is why recent studies on data complexity have been mainly focused on the boundary complexity.

2.1. Applications of Data Complexity Analysis

One of the primary goals of the data complexity analysis was to understand the classifier's performance. The idea arose from the difficulty of traditional studies to understand the differences among several classifiers when compared on several datasets. The common table with comparison of accuracies did not reveal the reasons why a given classifier performed better or worse than others for certain problems. Thus, some studies tried to characterize the dataset complexity and relate it to the classifier's performance. By doing so, one could build a model of classifier's accuracy based on dataset complexity and use the model to set expectations of classifier's accuracy. Some studies in this direction found linear correlations between the classifier's error and some measures of complexity [3,4]. Other investigations attempted to find domains of competence of several classifiers in a space defined by complexity measures [5,6]. Thus, given a new problem characterized by its complexity, the model could be used as a guide for classifier selection. Often, a learning algorithm has different configurations available. Therefore, the same methodology could be used to extract rules for classifier's adaption to a particular problem.

The data complexity analysis can also be used at the preprocessing stages of classification, such as in prototype selection [11,10] and feature selection. There, the characterization of the dataset is employed to select a suitable problem with reduced dimension-

ability. This paper explores the application of the data complexity analysis to find proper transformations of a classification problem.

2.2. Data Complexity Measures

Ho & Basu [2] proposed a set of metrics estimating data complexity. The metrics are classified in four categories as follows.

2.2.1. Overlap of Individual Feature Values

These metrics evaluate the power of individual attributes to discriminate between classes.

Maximum Fisher's discriminant ratio (F1): For each attribute, the Fisher's discriminant ratio is calculated as: $f = (\mu_1 - \mu_2)^2 / (\sigma_1^2 + \sigma_2^2)$, where μ_1, μ_2 and σ_1^2, σ_2^2 are the means and variances of the attribute for each of the two classes, respectively. The metric uses the most discriminant feature as the one having the maximum Fisher's value.

Volume of overlap region (F2): The overlap region of a feature is computed as the overlap range divided by the total range of that feature. F2 is the product of the overlap regions of each attribute.

Feature efficiency (F3): It describes to what extent each feature contributes to the class separation. It consists in removing the ambiguous instances (i.e., those instances belonging to different classes that fall in the overlapping region) for each feature. The efficiency of each feature is the ratio of the remaining non-overlapping points to the total number of points. The largest feature efficiency of all features is taken as F3.

2.2.2. Separability of classes

This family of metrics takes into account the dispersion of classes in the feature space based on neighborhood distances.

Length of class boundary (N1): It refers to the percentage of points in the dataset that lie in the class boundary [9]. Firstly, we generate the minimum spanning tree (MST) connecting all training samples, using the Euclidian distance between each pair of points. Then, we compute the fraction of points joining opposite classes to the total number of points. This measure is sensitive to the separability of classes and the clustering tendency of points belonging to the same class.

Ratio of average intra/inter-class nearest neighbor distances (N2): For each point, we calculate its nearest neighbor point belonging to the same class and the nearest neighbor belonging to the opposite class. Then, the averaged distances connecting intra-class nearest neighbor points are divided by the averaged distances of inter-class nearest neighbors.

2.2.3. Geometry of Class Manifolds

It evaluates the overlap between classes and how the classes are distributed as hyper-spheres in the feature space. This is more related to the interior descriptions of geometry.

Nonlinearity (N4): It estimates a convex hull for each class by linear interpolation of randomly drawn pairs of points from the same class. Then, a nearest neighbor classifier is trained with the original training set and tested with the extended set of points approximating the convex hull. N4 is the error of the classifier.



Area	Number of holes
Perimeter	Convex perimeter
Compactness	Roughness
Box Min. X,Y; Max. X,Y	Length
Feret (min. bounding box) X,Y	Breadth
Feret minimum diameter	Elongation
Feret maximum diameter	Centroid X,Y
Feret mean diameter	Angle of principal axis
Feret elongation	Angle of secondary axis

Figure 1. Example of a mammographic image with several microcalcifications (left) and set of features extracted from each microcalcification (right)

2.2.4. Sparsity

The sparsity is estimated as the number of points to the number of dimensions.

3. The Problem

The problem addressed in this paper consists in the breast cancer diagnosis based on the features extracted from mammographic images. Mammographic images may contain microcalcifications, which are tiny specks of mineral deposits (calcium), that can be found scattered or clustered throughout the mammary gland. The specks may either indicate the presence of tiny benign cysts or early breast cancer. In the latter case, studies reveal that shapes and sizes of microcalcifications are relevant features to determine if they constitute high risk of malignant cancer.

The dataset we used was obtained from mammograms collected by *Dr. Josep Trueta* University Hospital, whose diagnosis was known from biopsies. Each mammogram was digitized and later processed [7]. The result was a set of 216 instances, where each instance belonged to a mammogram with variable number of microcalcifications and a class label that corresponded to the diagnosis. Each microcalcification was characterized by 23 features mostly describing shapes and sizes. Figure 1 shows an example of a mammographic image and the list of features obtained for each microcalcification. For more details, see [7].

In this application, an instance-based learner was used [12]. The reason was that the most similar images to the new case were presented to the human expert as a way of explaining the diagnosis. Due to the variable number of microcalcifications present in each instance, the problem was untractable directly by the classifier. Early works averaged the features of all microcalcifications as a synthetic case [12]. Although the classification performance reached the same accuracy as the human experts, there was uncertainty about the correct method of synthetizing the different microcalcifications. We wondered whether other methods could be used that were easier for the human experts when performing a visual inspection of the mammographic image.

A possible procedure is to test the error of the classifier with the datasets obtained from different types of transformations and then, choose the best transformation as the one with the minimum error. However, this can lead to conclusions too tied to the classifiers applied. That is, the error of the classifier is influenced both by the complexity of the dataset and the proper design of the classifier. By studying the complexity of the dataset, we can provide a more theoretical framework. Our proposal is to characterize the

Table 1. Problem transformations

Method	Synthetic case
Average	Average of all attributes
Centroid	Feature values belonging to the centroid of the cluster
Random	A random microcalcification
All	Each microcalcification constitutes a different case
Min. area	The microcalcification with the minimum area
Max. roughness	The microcalcification with the maximum roughness
Max. compactness	The microcalcification with the maximum compactness
Max. elongation	The microcalcification with the maximum elongation
Max. feret elongation	The microcalcification with the maximum feret elongation
Max. holes	The microcalcification with the maximum number of holes

complexity of each dataset resulting from the different transformations and then select the best transformation based on the minimum complexity.

4. Results

Table 1 describes the different problem transformations we analyzed to synthetize a number of microcalcifications into a single one. The average approach involves all microcalcifications present in the mammogram and computes their average feature values. These are the feature values used as the synthetic case. The centroid approach computes the centroid point of all microcalcifications, considering Euclidean distances. We included a random selection of a microcalcification to test whether the selection of a particular microcalcification was relevant. We also included the case where all microcalcifications were used as different cases, each labeled with the class corresponding to the global diagnosis given by the biopsy. The rest of methods select a particular microcalcification, based on the value of a single feature. We based our selection on an early analysis of data [8] that revealed that the most relevant set of features for cancer discrimination were: the area, compactness, feret elongation, number of holes, roughness, and elongation. Thus, the different transformations selected a single microcalcification which were: the microcalcification with the minimum area, the maximum roughness, the maximum compactness, the maximum elongation, the maximum feret elongation, and the maximum number of holes, respectively.

Table 2 shows the values of the complexity metrics computed for each problem transformation. See that each transformation is characterized by a complexity space of 6 metrics, where F1, F2, and F3 evaluate the discriminative power of features, N1 and N2 consider the separability of classes, and N4 the nonlinearity of class boundary. The rows are sorted in ascending order of metric N1.

To our understanding, the metrics that compute the discrimination of individual features are not very relevant to the complexity estimation. For example, a high value of F1 indicates that an attribute discriminates well and consequently, the problem should be easy. However, a small value for F1 does not necessarily imply a difficult problem. We should look at the rest of the metrics to complete our estimation. The values obtained in F1, F2, and F3 are very close in all transformations. The exception is the *Average* approach, which obtains simultaneously a high value in F1 and F3 (see figure 2(a)). This

Table 2. Complexity of problem transformations (columns F1 to N4) and error of nearest neighbor classifiers (columns 1-NN and 3-NN). The most complex problem according to the given metric is marked in bold, and the easiest problem is marked in italic.

Dataset	F1	F2	F3	N1	N2	N4	1-NN	3-NN
Average	<i>0.3131</i>	0.0081	<i>0.1019</i>	0.528	0.899	0.9653	0.370	0.347
Max. holes	0.0976	0.0039	0.0463	0.574	0.927	0.9730	0.398	0.394
Random	0.0356	<i>0.0015</i>	0.0509	0.588	0.961	0.9614	0.421	0.394
All	0.0150	0.0080	0.0052	0.593	0.928	<i>0.9516</i>	0.411	0.394
Max. roughness	0.0878	0.0044	0.0463	0.616	0.955	0.9730	0.421	0.458
Centroid	0.0700	0.0072	0.0463	0.620	0.972	0.9653	0.458	0.458
Max. elongation	0.0969	0.0027	0.0509	0.630	0.967	0.9691	0.472	0.449
Max. compact.	0.0969	0.0027	0.0509	0.630	0.967	0.9691	0.472	0.449
Max. feret elong.	0.2518	0.0108	0.0463	0.676	1	0.9769	0.468	0.421
Min. area	0.1379	0.0172	0.0556	0.704	0.979	0.9846	0.472	0.454

could indicate that its complexity is low. The *All* transformation gives the smallest values in F1 and F3. On the other hand, the two largest values of F2 (since F2 is the volume overlap, a large value of F2 could mean a difficult problem) correspond to *Max. feret elong.* and *Min. area*. Both transformations also give the largest values in N1 (see figure 2(b)). This couple effect may point that these are the most difficult datasets.

Metrics focused on the distribution of classes should convey more information on complexity. That is why we sorted the rows by N1. Column N1 gives the values of the length of class boundary and N2 the fraction of intra/inter-class distances. Regarding the length of class boundary, the *Average* appears as the best transformation. This also agrees with the values obtained by *Average* in F1 and F3. The worst approximations are those that select a single microcalcification based on individual feature values (except for the number of holes). Surprisingly, the approaches of using all microcalcifications and selecting a random microcalcification give boundary lengths rather small (i.e., low complexity). This means that all microcalcifications carry similar information for carcinoma detection, which justifies why the average approach appears as the best transformation. N1 and N2 are fairly correlated, as shown in plot 2(c). This is reasonable because the two metrics test the class dispersion by using nearest neighbor distances.

Finally, N4 checks for nonlinearity. Under N4, the worst transformation is *Min. area*, which agrees with the result of N1, N2, and F2.

In general, the metrics agree that the worst transformations are *Max. feret elong.* and *Min. area*, while the *Average* appears as the best transformation.

To validate whether our complexity estimation corresponded to the complexity as seen by the classifiers, we tested two k-nearest neighbors (k-NN) classifiers and computed their errors for each transformation. The classifiers' error was estimated by an stratified 10-fold cross-validation procedure. The two last columns of table 2 show the error of the nearest neighbors (k=1 and k=3 respectively) for each transformation. See that the error of the classifiers tends to rise for increasing values of N1. Also note that the worst complex problems (as predicted by the complexity metrics) correspond to the highest classifiers' error, while the easiest problems correspond to the smallest errors. Figures 2(e) and 2(f) show graphically the correlation between the classifiers' error and metric N1.

In [4] a linear correlation was observed between some classifiers' error and metrics N1 and N2. If we applied the model derived in the paper, for N1 ranging from 0.528 to

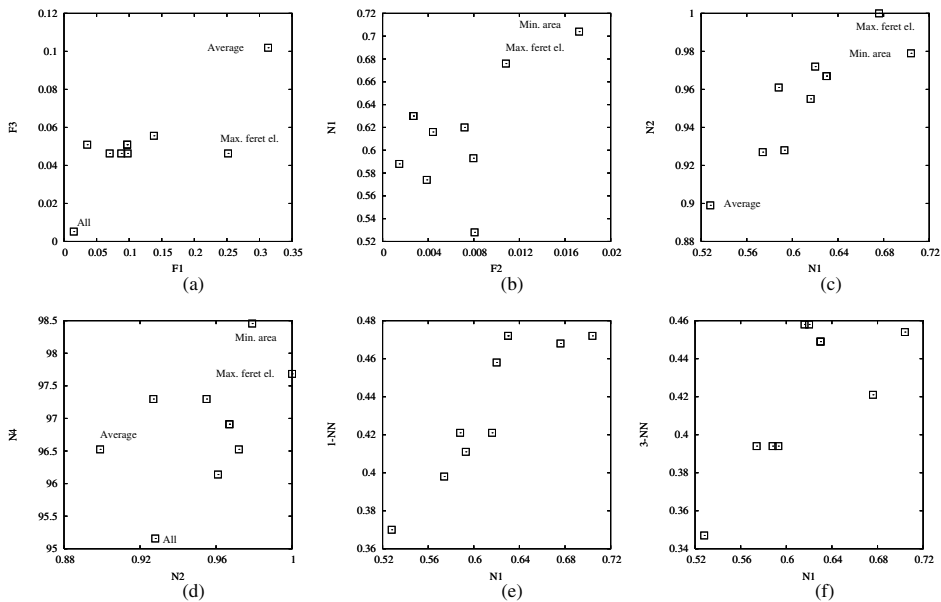


Figure 2. Complexity projections and error of classifiers. Plots (a)-(d) show each transformation plotted in several two-dimensional projections of the complexity measurement space. Plots (e)-(f) show the error of 1-NN and 3-NN vs. metric N1.

0.704, we would predict a classifier's error in the interval [0.3,0.5]. See that the results obtained by our classifiers fit correctly this model, which confirms the suitability of the complexity measurement space to set estimations of the classifier's error.

5. Conclusions

The data complexity analysis has provided a theoretical framework to select and justify the best transformation for the problem of breast cancer diagnosis based on features extracted from a variable number of microcalcifications present in a mammogram image. By selecting the transformation that minimizes data complexity, we are able to increase the generalization ability of classifiers and thus, give better support to the breast cancer diagnosis. Besides, the analysis may be meaningful to experts, since it provides guidelines on how to inspect visually the microcalcifications.

The estimation of complexity in all the studied transformations has been fairly high, which consequently has lead to a high classifier's error. The results reveal that the breast cancer diagnosis relying only on microcalcifications reach a maximum accuracy rate that seems difficult to be overcome, regardless of the efforts for transforming the dataset or using better adapted classifiers. Probably some attributes are missing, specifically those relating patient's age, antecedents, etc. (as considered by the experts). It would be interesting to see how the data complexity decreases with the addition of such new features.

Our results may be also limited due to a sparse sample. In fact, the dataset contained only 216 instances. The finite and sparse samples limit our knowledge about the geo-

metrical complexity, thus we are addressing only the apparent complexity of a problem based on a given training dataset.

The study of data complexity provides expectations on the error of classifiers. Thus, besides searching for the best classifier solving a particular problem, we may seek for problem transformations that present data in a more learnable way. A similar methodology could be adapted to processes such as feature extraction, selection, and aggregation. The data complexity analysis has also served to identify the domains of competence of classifiers in the complexity measurement space. As a further step, one could use these studies to transform a given dataset for a particular type of classifier; i.e., translating the problem to the domain of competence of the classifier of interest.

Acknowledgments

The authors thank the support of *Enginyeria i Arquitectura La Salle*, Ramon Llull University, as well as the support of *Ministerio de Ciencia y Tecnología* under project TIN2005-08386-C05-04. The authors acknowledge also J. Martí for providing the dataset, in the context of projects FIS 00/0033-02 and TIC2002-04160-C02-02.

References

- [1] Basu,M., Ho,T.K.: Data Complexity in Pattern Recognition, Springer (2006)
- [2] Ho,T.K. and Basu,M.: Complexity Measures of Supervised Classification Problems, IEEE Trans. on Pattern Analysis and Machine Intelligence, **24**:3 (2002) 289-300
- [3] Ho,T.K.: A Data Complexity Analysis of Comparative Adavantages of Decision Forest Constructors, Pattern Analysis and Applications, **5** (2002), 102-112
- [4] Bernadó-Mansilla,E., Ho,T.K.: Domain of Competence of XCS Classifier System in Complexity Measurement Space, IEEE Trans. on Evolutionary Computation, **9**:1 (2005) 82-104
- [5] Ho,T.K., Bernadó-Mansilla,E.: Classifier Domains of Competence in Data Complexity Space, In: Basu, M., Ho,T.K.(eds.): Data Complexity in Pattern Recognition, Springer (2006) 135-154
- [6] Bernadó-Mansilla,E., Ho,T.K.: On Classifier Domains of Competence, Proceedings of the 17th International Conference on Pattern Recognition, Vol.1 (2004) 136-139
- [7] Martí,J. [et al]: Shape-based feature selection for microcalcification evaluation, Proceedings of the SPIE Medical Imaging Conference on Image Processing Vol.3338 (1998) 1215-1224
- [8] Barceló,C., Thió,S.: Estudio piloto sobre el diagnóstico de benignidad o malignidad de las microcalcificaciones mamarias mediante digitalización y análisis estadístico, Technical Report, Secció d'Estadística i Anàlisi de Dades. Departament d'I.M.A. (1997)
- [9] Friedman,J.H., Rafsky L.C.: Multivariate generalizations of the Wald-Wolfowitz and Smirnov two-sample tests, The Annals of Statistics 7:4 (1979) 697-717
- [10] Mollineda, R.A. and Sánchez, J.S. and Sotoca, J.M., Data characterization for effective prototype selection, Proc. of the 2nd Iberian Conf. on Pattern Recognition and Image Analysis, (2005) 27-34
- [11] Singh, S., PRISM - A novel framework for pattern recognition, Pattern Analysis and Applications, **6** (2003) 134-149
- [12] Martí, J., Freixenet, J., Rabat,D., Bosch,A., Pont,A., Español,J., Bassaganyas,R., Golobardes,E., Canaleta,X., HRIMAC - Una Herramienta de Recuperación de Imágenes Mamográficas por Análisis de Contenido para el Asesoramiento en el Diagnóstico de Cáncer de Mama, Actas del VI Congreso Nacional de Informática de la Salud (2003)

Semantic blocking for Record Linkage

Jordi NIN^a Víctor MUNTÉS-MULERO^b Norbert MARTÍNEZ-BAZAN^b and
Josep L. LARRIBA-PEY^b

^a IIIA, *Artificial Intelligence Research Institute, CSIC, Spanish National Research Council*

^b DAMA-UPC, *Universitat Politècnica de Catalunya*

Abstract. Record Linkage (RL) is an important component of data cleaning and integration and data processing in general. For years, many efforts have focused on improving the performance of the RL process, either by reducing the number of record comparisons or reducing the number of attribute comparisons, which reduces the computational time, but increases the amount of error. However, the real bottleneck of RL is the post-process, where the results have to be reviewed by experts that decide which pairs or groups of records are real links and which are false hits.

In this paper we show that exploiting the semantic relationships (*e.g.* foreign key), established between one or more data sources, makes it possible to find a new sort of semantic blocking method that improves the number of hits and reduces the amount of review effort.

Keywords. Data processing, semantic information, blocking algorithms, record linkage, data integration, data cleansing.

1. Introduction

The amount of information stored about individuals has increased dramatically [8]. At the same time, the ubiquitous presence of computers causes this information to be distributed and represented in a large amount of heterogeneous ways. Resolving the different instances of one entity among different heterogeneous data sources is, thus, a requirement in many cases.

As a consequence, the importance of tools and techniques that contribute to the process of data cleansing [10] and data integration [9] has increased in the recent years. Among these, *Record Linkage* (RL) has gained relevance. The purpose of RL may be to either identify and link different record instances of one entity that are distributed across several data sources, or to identify records from a single data source with similar information.

In practice, since the size of the source files is usually very large, comparing all the records among them becomes unfeasible. Therefore, RL resorts to blocking methods that are meant to gather all the records that present a potential resemblance, only applying the RL process within each block. Typically, the traditional blocking methods for RL, like standard blocking [5] or sorted neighborhood [4] are based on the syntactic information of each record.

However, the quality of the results provided by these methods is very dependant on the data chosen to classify records in blocks and the quality of this data. A solution to this problem is to relax the creation of a block, by building larger blocks that allow for the comparison of a larger number of records. However, this has three clear drawbacks: (i) the number of unnecessary comparisons increases, (ii) the probability of RL to relate records belonging to different entities also increases and (iii), the review effort of the results grows and becomes the real problem.

In this paper, we propose a new blocking method that builds groups of records based on the semantic relationship among them in the data sources, instead of the syntactic information of its attributes. In order to find the relationship of a record with other records, we build a collaborative graph [6] that contains all the entities that are related to the record under analysis up to a certain degree, using, for instance, foreign key relationships. The records included in the graph are the building units of each block and we link them using regular record comparison strategies. With the preliminary results presented in this paper, we show that our blocking method can clearly improve the quality of the results by significantly reducing the number of false hits while maintaining and, in the best cases, improving the number of returned real hits.

The structure of the paper is as follows. In Section 2 we introduce the basics of RL and standard blocking methods. Then, in Section 3 we present our approach based on semantic blocking. Section 4 describes the experiments. Finally, the paper draws some conclusions and a description of future work.

2. RL: the preliminaries

The main objective of RL is to establish a link between two records provided by one or more data sources, showing that they potentially refer to the same entity. The preparation of data sources for the process of RL is divided into different steps.

First, data sources must be prepared for the RL process. This step is typically decomposed into two sub-steps: (i) filling the blanks by substituting the null attributes with values obtained by different techniques; (ii) normalizing the data, delimiting the values to intervals that simplify and allow their comparison with other data in the following steps [2].

Second, as explained in the introduction, data are split into blocks in order to avoid comparing all the records between them. In this way, unnecessary comparisons between records that differ too much and clearly do not belong to the same individual are avoided. Usually, the proposed blocking techniques [1] build the blocks using the information obtained from the values in one or more attributes (syntactic information).

Third, once the blocks have been created, RL algorithms based on attribute comparison functions are applied to all the records within a block. The whole process finishes with a post-processing step used to decide which pairs or groups produced by RL represent unique entities. This last step usually requires the human intervention by means of expert individuals. If the number of pairs produced by RL is large, the time necessary to allow human experts to review all the pairs may be really significant leading to extra unnecessary review errors.

2.1. Classic blocking methods

In this subsection, we describe the most frequently used blocking methods: *Standard Blocking* (SB) and *Sorted Neighborhood* (SN).

2.1.1. Standard Blocking.

The Standard Blocking method (SB) clusters records that share the same blocking key (BK) [5] into blocks. A BK is defined based on information extracted from one or more attributes. Usually, a BK can be either a common categorical attribute, *e.g.* *marital status* {single, married, divorced and widowed}, a common numerical attribute, *e.g.* *age*, or part of one or more string attributes, *e.g.* the first four characters of the *surname*. The cost-benefit trade-off of the BK selection is studied in [9].

2.1.2. Sorted Neighborhood.

The Sorted Neighborhood (SN) method [4] sorts the records based on a sorting key (SK) and then moves a window called Sliding Window, (SW in short) of fixed size l sequentially over the sorted records. RL is applied into the records inside the SW.

3. Semantic Blocking for RL

We propose a new family of blocking algorithms that substitute the blocking or sorting key used by classical blocking methods, by another kind of key that we define as a *semantic key* (SEMK for short). This SEMK is not based on the values of one or more attributes of the records but on the relationship established between the records in the source files. We refer to this relationship as *semantic information*.

We can use several techniques for defining a SEMK, depending on the data sources. For example, if we have a relational database as data source, we are able to obtain the semantic information from the foreign keys of the database. If we had a plain text file as a data source we can define a SEMK based on the relationships between all the records that have values with semantically the same meaning in one or more textual attributes.

This approach is very useful in databases that contain a lot of information about the relationship of an individual with the rest of the database. There are several examples of databases that have this kind of information. Bibliographic databases like Citeseer [3] or social network databases that proliferate in the web nowadays are examples of data sources that contain a large quantity of semantic information.

3.1. Semantic Graph Blocking

The Semantic Graph Blocking (SGB) proposed in this paper is based on the capabilities that collaborative graphs offer in order to extract the information about the relationships between records in the data sources. Collaborative Graphs are a common method for representing the relationships among a set of entities [6]. Nodes represent the entities, records in our case, and edges capture the relationships between entities, *i.e.* the semantic information extracted from the foreign keys in our case.

In order to build the graph we create a first node that represents the record to be examined. Following, we create a new node for every record that is directly related to the

Full name	Paper identifier
Gabriele Scheler	1
Xianshu Kong	2
Hazel Everett	2
Godfried Toussaint	2
Helge Frauenkron	3
Peter Grassberger	3

Table 1. Sample of the file downloaded from Citeseer [3].

first one. From this second level of nodes we explode their relationships again, adding all those records that did not previously exist in the graph. This process is repeated until there are no more nodes to explode. However, since all the nodes could be connected and, therefore, all the records would be included in the same block, we reinforce the stop condition either by predefining the maximum depth of the graph or by specifying a maximum number of nodes. The first case is similar to what happens with standard blocking since we cannot control the size of the block. The second case could be compared to sorted neighborhood since, limiting the number of nodes in the graph we are defining the maximum number of records per block.

Once the block is created, we use regular attribute comparison functions to detect similarities between records.

4. Experiments

In order to test our approach we have performed some experiments on the Citeseer database [3]. Citeseer is one of the most used scientific databases with more than 1,6 Million scientific papers and more than 750,000 authors. We have only downloaded a part of all the attributes stored in Citeseer: the full name of the authors and the identifier of the papers. Table 1 shows a sample of the downloaded file. As we can see, our approach only needs two attributes to exploit the semantic information stored in the Citeseer database. We are able to construct a collaborative graph using the author full name as the node and the common paper identifier as the relationship between two individuals (or records).

The Citeseer database is automatically generated using machine learning techniques. In this kind of scenarios, it is very difficult to preserve data consistency and, normally, databases contain a lot of mistakes. We can observe this in Table 2, where we present all the occurrences of the ten full professors of the department of Computer Architecture at UPC, and the different names introduced in the database for each of them.

4.1. Tests

In order to compare SGB with the two classical blocking methods, we search all the duplicated records for all the full professors of our department. We use distance based record linkage defined in [7] to obtain the matching pairs. We use two different thresholds to accept the similarity of a pair of records using their edit distance:

Strict RL: we force RL to classify as a hit only those pairs of records that differ less than 25% in their full name.

Full Professor	Duplicated Records
Eduard Ayguade	E. Ayguade, E. Ayguad, Eduard Ayguad, Eduard Ayguad E Eduard Ayguad Parra*, Eduard Ayguade Parra*, Eduardo A. Parra
Jordi Domingo-Pascual	J. Domingo-pascual*, Jordi Domingo Pascual
Jordi Garcia	J. Garcia, Jorge Garca, J. Garcia-vidal*, Jorge Garcia-vidal*
Antonio Gonzalez	Antonio Gonz Alez*, Antonio Gonzlez, A. Gonzlez*, Antonio Gonzz*
Jesus Labarta	J. Labarta, Jess Labarta, Jes Us Labarta, Jesffs Labarta*, Jes Labarta*
J. M. Llaberia	Jos Mara Llabera, Jos M. Llabera, Mara Llabera*, J. M. Llabera
Manel Medina	Manuel Medina
Juan J. Navarro	J. J. Navarro, Juanjo Navarro*, Juan J. Navarroy*
Mateo Valero	Andmateo Valero, M. Valero, Larriba-pey Mateo Valero, Advisor Mateo Valero*, Mateo Valeroy
Miguel Valero Garcia	Miguel Valero-garc, Miguel Valero-garca, M. Valero-garca*

Table 2. Duplicated records for full professors of Computer Architecture Dept. of Universitat Politècnica de Catalunya. *These authors only appear in one document.

Weak RL: we force RL to classify as a hit all the pairs of records that differ less than 50% in their full name.

The reason for using different thresholds for RL is that we want to see the influence of such parameter on the whole result and review effort for the different methods. We observed that there are several occurrences of the same individual differing in more than 25%, e.g. J.M. Llaberia is the same author than Mara Llabera¹, which allowed us to study those differences.

4.2. Parameterizations of the methods

We have tested the three approaches using three different parameterizations for each one. We show the parameterizations in Table 3. We consider small, medium and large blocks. The second column in the table shows the three different BK selected parametrization. As we can observe, the BK in the first one is expressed as $substring(Full\ name, 0, 4)$ meaning a substring containing four consecutive characters of attribute *Full name* starting at string position 0. The other two parameterizations correspond to those strings containing the first three and the first two characters, respectively. In the third column of the same table, we show parameter l that defines the window size in the SN blocking. The fourth column defines the values selected for S , that defines the maximum size in terms of nodes of the collaborative graph.

The nine parameterizations are meant to be equivalent three by three across different methods in terms of the workload per block. Thus, a *BK* defined as $substring(Full\ name, 0, 4)$ will generate small blocks of a similar size to a window size $l = 200$ and a number of nodes in a graph $S = 200$. Note, however, that block-

¹The real name is *José María Llaberia*. In the first case *José María* has been abbreviated to *J.M.* In the second case *José* has been removed possibly due to a parsing error and the fact that the vowels contain an stress sign (i), that has been omitted, generating a significantly different name (*Mara Llabera*)

Parametrization Name	Standard Blocking (SB)	Sorted Neighborhood (SN)	Semantic/Graph Blocking (SGB)
Par1	substring(Full name,0,4)	$l=200$	$S=200$
Par2	substring(Full name,0,3)	$l=500$	$S=500$
Par3	substring(Full name,0,2)	$l=1000$	$S=1000$

Table 3. Different parameterizations of blocking (SB), sorted neighborhood (SN) and blocking (SGB).

ing will generate variable sized blocks because of the skewed nature of data, which we cannot control at will. In addition, in order to build the blocks for each method, it is necessary to sort the data set for SB and SN, while it is necessary to traverse the set of relational links for SGB.

4.3. Metrics

We have used a set of metrics that measures the percentage of duplicated records found inside the blocks created. Also, we measure the RL accuracy taking into account both, the number of hits and the error rate. The metrics are defined as follows:

Completeness (C): Which measures the percentage of duplicated records that one particular blocking method is able to find:

$$C = \frac{\text{Duplicated records inside block}}{\text{Duplicated records}}$$

Hit Ratio (HR): Which measures the percentage of duplicated records found using a particular RL method. This is necessary in order to understand the accuracy of the RL algorithms in those scenarios where the duplicates of the same individual present significantly different values in the attributes used to compare them.

$$HR = \frac{\text{Correct duplicates in block}}{\text{Number of record pairs in block}}$$

False Hit (FH): Which measures the number of false hits with one particular blocking method.

$$FH = \frac{\text{Number of errors}}{\text{Duplicated records found}}$$

4.4. Results

Table 4 shows the accumulated results of the experiments run for all the full professors in the Computer Architecture Department of UPC within Citeseer. All the metrics are expressed using percentages, thus multiplying C , HR and FH by 100. We show the strict and weak RL separately in the table, although we only show one column for Completeness C . This is because this metric explains the capability of the blocking method for the method parameterizations used, which are independent of the threshold used to accept pairs of tuples as hits. On the other hand, the other two metrics HR and FH explain the

Method			Strict RL				Weak RL				
Type	P	C	HR		FH		HR		FH		
SB	Par1	16/38	42.1%	12/16	75.0%	6/18	33.3%	16/16	100.0%	419/435	96.3%
SB	Par2	23/38	60.5%	17/23	73.9 %	5/22	22.7%	17/23	73.9%	791/808	97.9%
SB	Par3	23/38	60.5%	17/23	73.9 %	5/22	22.7%	21/23	91.3%	1648/1669	98.7%
SN	Par1	15/38	39.5%	11/15	73.3%	3/14	21.4%	15/15	100.0%	226/241	93.8%
SN	Par2	17/38	44.7%	12/17	70.6%	3/15	20.0%	16/17	94.1%	377/393	95.9%
SN	Par3	22/38	57.9%	16/22	72.7%	5/21	23.8%	20/22	90.9%	460/480	95.8%
SGB	Par1	22/38	57.9%	14/22	63.6%	2/16	12.5%	20/22	90.9%	4/24	16.7%
SGB	Par2	25/38	65.9%	14/25	56.0%	2/16	12.5%	21/25	84.0%	6/27	22.2%
SGB	Par3	26/38	68.4%	14/26	53.8%	2/16	12.5%	22/26	84.6%	10/32	31.3%

Table 4. Accumulated results of the three metrics for the experiments performed. SB stands for Standard Blocking, SN stands for Sorted Neighborhood, SGB stands for Graph/Semantic blocking and P stands for Parameterization.

capability of the comparison functions used in combination with the blocking method, as we will show later.

In general, we can observe that our approach is able to build blocks containing a larger number of real hits than those created by the other blocking algorithms. Column *C* (Completeness) in Table 4 shows that our improvement is between 5% and almost 16% over the other methods. In other words, the quality of the blocks built by SGB, with its knowledge of the semantic relationships among entities, is better than those obtained by SB and SN, that only take into account the syntactic proximity of records. This metric shows that our approach pays off in terms of the potential quality.

If we observe the results for strict RL, we conclude that SGB obtains a somewhat lower hit ratio, *HR*. However, this is compensated by the fact that *C* is better and, as a consequence, the number of hits found, in absolute terms, is closer to those for SB and SN. However, our method obtains better results regarding the false hit metric, *FH*, generating only 12,5% false hits among all the returned pairs. On the other hand, the other two algorithms present *FH* ranging from 20.0% to 33.3%. However, the number of real hits found for strict RL ranges from 56.0% to 75.0% because the RL that we are using is too strict.

Therefore, we decide to relax the RL thresholds and use the weak RL, meaning that we are more permissive when comparing two records, allowing less similar records to be considered real hits. Here, we see that the absolute number of real hits *HR* found by our method is better than that for the other methods. In addition, while the *FH* ranges from 93.8% to 98.7% in the two classic methods, it only ranges from 16.7% to 31.3% with our methods. Results are clearer when we examine the absolute number of records to be reviewed, observing that this is reduced by two orders of magnitude, thus reducing the review post-processing time significantly and saving work to the human expert. It is important to note that this is achieved not only without decreasing the quality of the results, but slightly increasing it. As an example, if an expert needs 10 seconds on average to decide whether a hit is real or false and we are interested in obtaining as many real hits as possible, (i.e. we choose Par3 for the three methods using a Weak RL), the whole RL plus reviewing process would take around 4.6 hours using SB, 1.3 hours using SN and 5.33 minutes using our approach. In addition, with our approach we would obtain a slightly larger amount of real hits than with the other two approaches.

5. Conclusions and future work

In this paper, we have presented a new blocking method that we call Semantic Graph Blocking (SGB) that creates the blocks based on the semantic information of the data sources. SGB is oriented to reduce the expert review time in the RL process. We show the results of our SGB in comparison to the standard blocking and sorted neighborhood blocking methods using the Citeseer reference database.

We have shown that our approach tackles the most important problem in data integration and cleaning: the time consumed in the post-process step of RL, and at the same time, it improves the amount of hits of the classic blocking methods. Our experiments show that our technique can drastically reduce the false hit ratio and, in the best cases, reduce the number of false hits by two orders of magnitude. In addition we improve the quality of the RL process when we relax the hit acceptance threshold.

As future work we want to explore different approaches for the SGB, using strategies that allow to prune the graphs obtained without reducing the Hit Ratios. In particular, we want to explore the differences between creating blocks based on levels or number of nodes included. Also, we want to explore the possibility of using comparison weights based on the distance between the nodes compared. Finally, we want to explore the combination of syntactic and semantic blocks in order to improve the Completeness and Hit Ratio measures.

Acknowledgments

The authors from the UPC want to thank Generalitat de Catalunya for its support through grant number GRE-00352 and Ministerio de Educación y Ciencia of Spain for its support through grant TIN2006-15536-C02-02. Jordi Nin wants to thank the Spanish Council for Scientific Research (CSIC) for his I3P grant.

References

- [1] Baxter, R., Christen, P., Churches, T., (2003) A Comparison of Fast Blocking Methods for Record Linkage, Proc SIGKDD 2003, Washington.
- [2] Bilenko, M., Basu, S., Sahami, M., (2005), Adaptive Product Normalization: Using Online Learning for Record Linkage in Comparison Sopping. In proceedings of the 5th Int'l. Conference on Data Mining 2005. Pages 58–65.
- [3] Citeseer database, <http://citeseer.ist.psu.edu>
- [4] Hernandez, M., Stolfo, S., (1998), Real-world data is dirty: Data cleansing and the merge/purge problem. Data Mining and Knowledge Discovery, 1(2), 1998.
- [5] Jaro, M. A., (1989), Advances in Record Linkage Methodology as Applied to Matching the 1985 Census of Tampa, Florida. Journal of the American Statistical Society, 84(406):414-420, 1989.
- [6] Kubica, J., Moore, A., Cohn, D., Schneider, J., (2003) Finding Underlying Connections: A Fast Graph-Based Method for Link Analysis and Collaboration Queries. Proceedings of the Twentieth International Conference on Machine Learning, Washington DC, 2003.
- [7] Pagliuca, D., Seri, G., (1999), Some results of individual ranking method on the system of enterprise accounts annual survey. Technical report, Esprit SDC Project, Delivrable MI-3/D2, 1999.
- [8] Sweeney, L., (2001), Information explosion, in Confidentiality, Disclosure, and Data Access: Theory and Practical Applications for Statistical Agencies, eds. P. Doyle, J. I. Lane, J. M. Theeuwes and L. M. Zayatz, Elsevier, 43–74.

- [9] Torra, V., Domingo-Ferrer, J., (2003), Record linkage methods for multidatabase data mining, Information Fusion in Data Mining, Springer, 101-132.
- [10] Winkler, W., (2003), Data Cleaning Methods, Proc. SIGKDD 2003, Washington.

This page intentionally left blank

Case Based Reasoning

This page intentionally left blank

Explanation of a Clustered Case Memory Organization ¹

Albert Fornells ^a, Eva Armengol ^b, Elisabet Golobardes ^a

^a *Grup de Recerca en Sistemes Intel·ligents*

Enginyeria i Arquitectura La Salle, Universitat Ramon Llull

Quatre Camins 2, 08022 Barcelona (Spain)

e-mail: {afornells,elisabet}@salle.url.edu

WWW home page: <http://www.salle.url.edu/GRSI>

^b *IIIA, Artificial Intelligence Research Institute*

CSIC, Spanish Council for Scientific Research

Campus UAB, 08193 Bellaterra, Barcelona (Spain)

e-mail: eva@iiia.csic.es

Abstract. One of the key issues in Case-Based Reasoning (CBR) is the efficient retrieval of cases when the case base is huge. In this paper we propose a case memory organization in two steps: 1) the case memory is organized using an unsupervised clustering technique, and 2) explanations for each cluster are constructed using all the cases associated to each one. The role of the explanations is twofold. On one hand they index the memory and allow CBR to do a selective retrieval. On the other hand, the explanation provide to the user additional information about why the cases have been both clustered together and retrieved.

Keywords. Clustering, Case Memory Organization, CBR, Explanations.

1. Introduction

Case-based Reasoning (CBR) [10] systems predict the solution of a problem based on the similarity between this problem and already solved cases. The key point of CBR systems is the similarity measure used for assessing the similarity among cases, since of this measure depends the subset of cases that will serve as basis to solve the new problem. On the other hand, the assessment of the similarity among cases implies the exploration of all the cases stored in memory. Consequently, the organization of the case memory is a crucial issue for an efficient retrieval of appropriate cases. In previous work we introduced SOMCBR [8], a CBR system featured by organizing the case memory by

¹This work has been supported by the MCYT-FEDER Project called MID-CBR (TIN2006-15140-C03-01 and TIN2006-15140-C03-03), and the Generalitat de Catalunya for the support under grants 2005SGR-302 and 2006FIC-0043. Also, we would like to thank Enginyeria i Arquitectura La Salle of Ramon Llull University for the support to our research group.

a Self-Organization Map (SOM) [9]. SOM is an unsupervised clustering technique based on grouping cases according to their similarity without using the class label. Each group of cases is represented by a director vector, which is a numerical description of the value expected for each one of the attributes. This element is used to assess if the subset of cases is potentially similar to the new problem. Thus, it is not necessary to explore the entire case base because only those cases represented by similar director vector to the new problem will be used.

This paper introduces an additional benefit to SOMCBR, which is to characterize each cluster through explanations built using the anti-unification concept [1]. Their advantage over the director vectors is that the description of cluster is easier to understand because they use the same representation language as the one used to describe the cases.

The paper is organized as follows. Section 2 briefly reviews SOMCBR. Sections 3 and 4 present the new strategy based on explanations for setting up the case retrieval. Section 5 describes the experiments and discusses the results. Section 6 summarizes some related work about strategies for organizing the case memory and the use of explanations. Finally, Section 7 ends with the conclusions and future research.

2. Self Organization Map in a Case-Based Reasoning - SOMCBR

SOMCBR [8] is a CBR system featured by organizing the case memory to provide an efficient data access. The organization is done by an unsupervised clustering technique called Self-Organization Map (SOM) [9]. SOM projects the original N -dimensional input space into a new space with fewer dimensions where the most important data features are highlighted to identify groups of similar cases. SOM is constituted of two layers (see Fig. 1): (1) the input layer composed of N neurons, where each neuron represents one of the N -dimensional features of the input case; and, (2) the output layer composed of $M \times M$ neurons (supposing a two dimensional grid), where each one represents a set of similar cases described by a director vector. The director vector is the expected value for each one of the N features. Each input neuron is connected to all the output neurons. The optimal number of clusters is the one which minimizes the global sum of distance between the cases of each cluster and its director vector.

The case retrieval in SOMCBR is performed in two steps. First, it looks for the most similar cluster by comparing the new input case C to all the director vectors. The comparison can be done applying a metric such as for example the complement of the normalized Euclidean distance (see Eq. 1). The greater the value, the greater the similarity. Second, it looks for the K -Nearest Neighbor (K -NN) most similar cases to C using the clusters with the highest similarities [7].

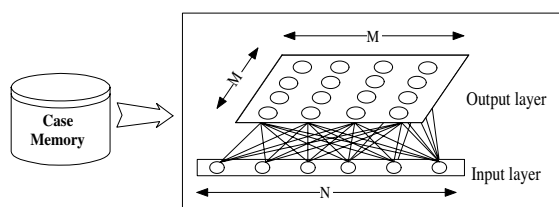


Figure 1. SOM organizes the case memory to improve the case access.

$$\text{similarity}(C, X) = \left| 1 - d(\vec{C}, \vec{X}) \right| = \left| 1 - \sqrt{\frac{\sum_{n:1..N} (C(n) - X(n))^2}{N}} \right| \quad (1)$$

The main benefits of this strategy are (1) a reduction of the computational time due to only a subset of cases are used while the accuracy rate is maintained respect to a CBR with flat organization, and (2) the user can discover hidden relation between cases.

In this last issue there are two key points from the point of view of the user: 1) why a subset of cases has been grouped together in a same cluster?, and 2) given a new problem, why the system has selected a particular subset of clusters? Notice that an important consequence of the second point is that depending on the clusters assessed as appropriate to the problem, the subset of cases to explore will be different. Therefore, it is important that the user understands why the clusters have been selected. In the next section we introduce explanations as a tool for answering the two questions above.

3. How to explain a cluster

In [2] we introduced an explanation scheme to justify the retrieval of a set of cases. Now, this scheme is used to explain why a set of cases have been clustered together. Each cluster produced by SOM has a director vector representing all the cases in that cluster. However, this director vector is not easily understood by the user. For this reason, we claim that symbolic explanations can be more useful than the director vector because they use the same representation language used to describe the cases.

Thus, we propose to explain a cluster using a symbolic description that is a generalization of all the cases contained in the cluster. This generalization is based on the anti-unification concept [1] although with some differences. The anti-unification of two objects is defined as the most specific generalization of both objects and it is a description that contains the features shared by both objects with value the most specific one. In the present paper we take only the idea of shared features among a set of objects.

Let M_i be a cluster and let c_1, \dots, c_n be the set of cases that belong to that cluster after the application of SOMCBR to the case base. Each case c_j is described by a set of attributes \mathcal{A} . The explanation D_i of why a subset of cases have been clustered in M_i is built in the following way:

- D_i contains the attributes that are common to all the cases in M_i . Attributes with *unknown* value in some case $c_j \in M_i$ are not in D_i .
- Let a_k be an attribute common to all the cases in M_i such that a_k takes symbolic values on a set \mathcal{V}_k , when the union of the values that a_k takes in M_i is exactly \mathcal{V}_k , a_k will not be in D_i .
- Numeric attributes (continuous or integer) appear in D_i with value the set of all the values that these attributes hold in the cases in M_i .

Let us illustrate with an example how to build the explanations for a cluster. Let M_i be the cluster formed by the four cases shown in the upper part of Fig. 2. The explanation D_i of the clustering of these cases is shown in Fig. 2a. Thus, attributes **steroid**, **spleen-palpable**, **spiders**, **fatigue**, **malaise**, **liver-big**, **protome**, and **ascites** are not in D_i because they are not common to all cases (f.e., **steroid** is not used in obj-137). Attributes such as **sex**, **antiviral** and **histology** are not in D_i because all take all possible values. For instance, the feature **sex** takes the value *male* in obj-136 and the value *female* in obj-137, this means that the value of this attribute is irrelevant to describe M_i .

Obj-136	Obj-137	Obj-138	Obj-139
(Age 33)	(Age 31)	(Age 78)	(Age 34)
(Sex Male)	(Sex Female)	(Sex Male)	(Sex Female)
(Steroid No)	(Antivirals Yes)	(Antivirals No)	(Antivirals No)
(Antivirals No)	(Fatigue No)	(Fatigue Yes)	(Fatigue No)
(Spleen_Palpable No)	(Malaise No)	(Liver_Big Yes)	(Malaise No)
(Spiders No)	(Liver_Big Yes)	(Spiders No)	(Anorexia No)
(Ascites Yes)	(Spleen_Palpable No)	(Ascites No)	(Liver_Big Yes)
(Varices No)	(Varices No)	(Varices No)	(Spleen_Palpable No)
(Bilirubin 0.7)	(Bilirubin 0.7)	(Bilirubin 0.7)	(Spiders No)
(Alk_Phosphate 63)	(Alk_Phosphate 46)	(Alk_Phosphate 96)	(Ascites No)
(Sgot 80)	(Sgot 52)	(Sgot 32)	(Varices No)
(Albumin 3.0)	(Albumin 4.0)	(Albumin 4.0)	(Bilirubin 0.9)
(Protim 31)	(Protim 80)	(Histology No)	(Alk_Phosphate 95)
(Histology Yes)	(Histology No)		(Sgot 28)
			(Albumin 4.0)
			(Protim 75)
			(Histology No)

D_i	d_{i1}	d_{i2}
(Age 33 31 78 34)	(Age 31 33)	(Age 34 78)
(Varices No)	(Varices No)	(Antivirals No)
(Bilirubin 0.7 0.9)	(Bilirubin 0.7)	(Liver_Big Yes)
(Alk_Phosphate 63 46 96 95)	(Alk_Phosphate 46 63)	(Spiders No)
(Sgot 80 52 32 28)	(Sgot 52 80)	(Ascites No)
(Albumin 3.0 4.0)	(Albumin 3.0 4.0)	(Varices No)
	(Protim 31 80)	(Bilirubin 0.7 0.9)
		(Alk_Phosphate 95 96)
		(Sgot 28 32)
		(Albumin 4.0)
		(Histology No)

(a)

(b)

(b)

Figure 2. Upper part shows the cases in M_i . Lower part shows the symbolic descriptions of M_i when (a) all objects belong to the same class. (b) obj-136 and obj-137 belong to the class C_1 and obj-138 and obj-139 belong to the class C_2 .

A common situation is that M_i contains cases of several classes. Let $S_1 \dots S_n$ be the solution classes of the cases in M_i . In such situation, we propose to build description d_{ij} justifying why a subset of cases belonging to the class S_j have been clustered in M_i . Each description d_{ij} is build as explained before but taking into account only the subset of cases of a class. Thus, a cluster M_i is described by a disjunction of descriptions d_{ij} . Notice that each description d_{ij} also satisfies the global description D_i of a cluster.

Let us suppose now that obj-136 and obj-137 belong to the class C_1 and that obj-138 and obj-139 belong to the class C_2 . In such situation, the cluster M_i is explained by the disjunction of the two explanations, namely d_{i1} and d_{i2} , shown in Fig. 2.

4. How to use explanations for classifying new cases

The common procedure of a CBR method (for instance, k -NN) is to compare a new problem with all the cases available in order to retrieve the k cases most similar to the new problem. The use of SOMCBR allows to reduce the number of comparisons since only a subset of cases is explored. Thus, from the clustering of the cases using the SOM method, the new problem is compared with the director vector of each cluster and the k -NN method could be applied using only the cases of the selected clusters. The justification of this procedure is that because the new problem is similar to the director vector, all cases of the cluster represented by this vector are also similar to the new problem.

The use of explanations supports the reduction of the number of cases retrieved. The idea is that the explanations d_{ij} of each subset of cases in a cluster can be used for classification. Given a problem p and the set of clusters \mathcal{M} organizing a case memory, the procedure of classification for p follows the algorithm shown in Fig. 3.

1. $CB = \emptyset$; set of retrieved cases
2. for each cluster $M_i \in \mathcal{M}$
3. for each description d_{ik} of M_i
4. if p satisfies d_{ik} then $CB := CB \cup C_{ik}$; where C_{ik} is the set of cases satisfying d_{ik}
5. apply $k\text{-NN}$ using CB as the set of precedents.

Figure 3. Algorithm followed for the classification of a new problem p

Notice that using the explanations, p is only compared with a subset of cases included in a cluster, i.e. those satisfying a particular description. Notice also, that the use of these explanations can be interpreted as a symbolic similarity among p and a particular subset of cases C_{ik} of each cluster. The justification of this similarity is that p and C_{ik} share the features contained in the description d_{ik} .

5. Experiments

This section tests the benefits of introducing explanations inside SOMCBR to: (1) maintain the solving capabilities respect to a flat $k\text{-NN}$, (2) improve the mean number of cases used to retrieve the most similar case, (3) provide to the user the explanation about why the cases are grouped in the same cluster.

The first and second issues can be discussed using Table 1. It summarizes the percentage of error over the classified cases (%Error) with its standard deviation (σ) for $k\text{-NN}$, SOMCBR featuring the clusters by means of a director vector (SOMCBR-Vectors), and SOMCBR featuring the clusters by means of explanations (SOMCBR-Explanations) over several datasets from the UCI repository [3]. Table also includes the mean percentage of the number of comparisons needed to find the most similar case (%R). The common configuration for them is: (1) the cases are normalized between 0 and 1; (2) the normalized Euclidean distance (see Eq. 1) is used as similarity function; (3) the class of the new input case is the class of the most similar case ($k\text{-NN}=1$); and, (4) the new cases are not stored in the case memory. Because explanations can select more than one cluster in SOMCBR-Explanations, we also allow the selection of more than one cluster in the SOMCBR-Vectors. For the configuration SOMCBR-Explanations, a tolerance of 0.2 (20% of similarity) when comparing numerical values is used. Finally, a 10-fold stratified cross-validation is applied to get the results.

The maintenance of the solving capabilities is test using t-test (at 95% of confidence level) between $k\text{-NN}$ and SOMCBR-Vectors, and between $k\text{-NN}$ and SOMCBR-Explanations. As we can observe, the solving capabilities are very similar and almost always there is not a significance difference in the results (the exception are Glass, Tao and Segment which has the ↓ symbol). On the other hand, there is always a high reduction of the number of operations required (↑ is an improvement less than 25%, ↑↑ is an improvement between 25 and 50%, and ↑↑↑ is an improvement greater than 50%).

Concerning the accuracy of the methods, experiments shown that there is not a method clearly outperforming the others in all the datasets. For some datasets, the best method is $k\text{-NN}$, meaning that the organization of the case memory is not actually necessary. The explanation of this fact is that both versions of SOMCBR (with and without explanations) explore only a part of the case memory, consequently it is possible that the most similar case not be found. Instead, $k\text{-NN}$ performs an exhaustive comparison

Table 1. Summary of k -NN, SOMCBR-Vector and SOMCBR-Explanations results. %Error is the mean percentage of error over the classified cases and σ is its typical deviation. The column t represents the application of t-test between k -NN and the SOMCBR configuration. %R represents the mean percentage of reduction in the number of cases needed to retrieve the most similar case between k -NN and the SOMCBR configuration. The column Impr. represents the improvement in the number of operations needed to find the most similar case: <25% (\uparrow), 25%-50% ($\uparrow\uparrow$), and >50% ($\uparrow\uparrow\uparrow$)).

Dataset	1-NN %Error (σ)	SOMCBR-Vectors				SOMCBR-Explanations			
		%Error (σ)	t	%R	Imp.	%Error (σ)	t	%R	Imp.
Bal	21.3 (3.0)	23.7 (3.9)	60.0	$\uparrow\uparrow\uparrow$		23.4 (3.2)	44.1	$\uparrow\uparrow$	
Glass	34.6 (11.3)	33.6 (14.4)	47.9	$\uparrow\uparrow$		39.3 (7.4)	\downarrow	45.3	$\uparrow\uparrow$
Heartstatlog	25.6 (6.7)	24.1 (8.8)	65.4	$\uparrow\uparrow\uparrow$		25.3 (7.9)	33.7	$\uparrow\uparrow$	
Hepatitis	21.3 (8.5)	19.4 (7.1)	67.6	$\uparrow\uparrow\uparrow$		21.5 (8.1)	61.9	$\uparrow\uparrow\uparrow$	
Ionosphere	12.8 (4.2)	12.8 (4.5)	50.8	$\uparrow\uparrow\uparrow$		14.5 (4.0)	34.3	$\uparrow\uparrow$	
Segment	2.8 (1.2)	4.7 (0.9)	\downarrow	56.5	$\uparrow\uparrow\uparrow$	2.9 (1.2)	32.7	$\uparrow\uparrow$	
Tao	4.5 (1.2)	5.9 (1.7)	\downarrow	83.3	$\uparrow\uparrow\uparrow$	\downarrow 5.5 (1.7)	\downarrow	51.4	$\uparrow\uparrow\uparrow$
Thyroids	2.8 (2.3)	2.8 (2.3)	13.1	\uparrow		3.3 (2.2)	11.4	\uparrow	
Vehicle	30.1 (4.5)	32.0 (4.6)	55.2	$\uparrow\uparrow\uparrow$		31.1 (4.3)	22.9	\uparrow	
Waveform	27.0 (1.9)	27.2 (2.2)	76.5	$\uparrow\uparrow\uparrow$		27.0 (1.9)	55.3	$\uparrow\uparrow\uparrow$	
Wbcd	4.6 (1.8)	4.9 (1.5)	52.9	$\uparrow\uparrow\uparrow$		4.6 (3.1)	45.9	$\uparrow\uparrow$	
Wdbc	4.9 (3.0)	4.0 (2.8)	44.3	$\uparrow\uparrow$		5.3 (3.4)	26.6	$\uparrow\uparrow$	
Wisconsin	3.9 (1.1)	4.0 (1.2)	55.3	$\uparrow\uparrow\uparrow$		3.9 (1.6)	22.6	\uparrow	

that can favor finding the most similar case. For this reason, both versions of SOMCBR clearly outperform k-NN concerning the number of operations. Therefore the main conclusion is that SOMCBR is more efficient than k-NN without losing accuracy. Also, both versions of SOMCBR are not significantly different from neither the accuracy nor the number of operations. Although, the version with explanations proposed in this paper sometimes clearly performs more operations than the version with director vectors. The advantage of the explanation version is that the user can easily understand the retrieval of a subset of cases. Eventually, the user can also compare the explanations satisfied by the new problem and could decide a different classification according to the attributes that he considers as the most relevant.

6. Related Work

Concerning the memory organization, there are several approaches focused on improving the retrieval of CBR. K-d trees [19] represent the features as nodes, which split the cases in function of their values. This approach has some problems with missing values and the low flexibility of the tree structure. Both problems are successfully solved in approaches such as Case Retrieval Nets [11], which organize the case memory as a graph of feature-value pair; and Decision Diagrams [15] work in a similar way to the k-d trees but using directed graphs. Other approaches as Fish-and-sink [17,21] and CRASH system [4] organize the cases according to the similarity among them. The BankXX system [16] indexes the case memory using domain knowledge rooted in a conceptualization of legal argument as heuristic search. Different approaches such as [18,5,8] use clustering algorithms to index the cases in memory.

There are also several approaches that build generalizations to characterize the clusters. Thus Zenko et al. [22] use the CN2 algorithm to induce rules that determine prototypes for each cluster. However this prototype is not symbolic but is a vector representing frequencies. Lechevalier et al. [20] also use the SOM algorithm for clustering, nevertheless they combine it with a dynamic clustering algorithm called SCLUST that allows the use of symbolic data. Malek and Amy [12] introduced a supervised approach focused on organizing the case-base of a CBR system. They propose a two-level organization of the cases and build prototypes for each group of cases. There are several differences among the symbolic descriptions introduced in the present paper and the other approaches. The main one is that commonly a prototype is a discriminant description that univocally describes a cluster. In our case, the symbolic descriptions are not discriminant.

Our work is also related with the issue of explanations in CBR. The most common form of explanation is to show the user the set of cases assessed as the most similar to the problem. Some authors agree that in some situations this may not be a good explanation. Alternative approaches propose to explain the retrieval based on similarities [14], differences[13], and both [6]. The approach introduced in [2] is based on similarities but also supports the user in detecting class differences. When that approach is applied to explain clusters as we propose, it can also explain the similarities among classes by means of the cases of the same cluster. Notice, that the explanations allow also the comparison of both similarities and differences among cases that, even belonging to the same class, they have been grouped in different clusters. In our case, the symbolic descriptions of a cluster are not discriminant since we do not take into account examples from other clusters as negative examples. A future research line could be the construction of discriminatory explanations of clusters.

7. Conclusions and Future Work

Clustering techniques can be used to organize the memory of cases of a CBR system. In our case, SOM is used for characterizing cases by means of director vectors. These director vectors can be interpreted as an average of the cases belonging to a cluster and they can be used for classification tasks as in the SOMCBR method. The present paper proposes an improvement of SOMCBR, where symbolic descriptions, that we called *explanations*, are used instead of director vectors. The advantage of explanations over director vectors is that they describe the cluster elements using the same representation language than the used to describe the cases. This produces a better understanding of both the case memory clusterization and the retrieval during the classification process. In addition, the same kind of explanations is useful to justify why cases of different classes have been grouped in the same cluster. Experiments show that the performance of SOMCBR with and without explanations is comparable in terms of both accuracy and efficiency. However, the use of explanations is a first step of several research lines. In particular we plan to compare the explanations of different classes of a same cluster and also to compare the explanations of a class obtained from cases in different clusters. Our intuition is that by defining operations on explanations (such as difference and/or merging) we could obtain more accurate descriptions of clusters than the current ones. As a consequence the accuracy of predictions could be highest.

References

- [1] E. Armengol and E. Plaza. Bottom-up induction of feature terms. *Machine Learning*, 41(1):259–294, 2000.
- [2] E. Armengol and E. Plaza. Symbolic explanation of similarities in cbr. *Computing and informatics*, 25(2-3):153–171, 2006.
- [3] C.L. Blake and C.J. Merz. UCI repository of machine learning databases, 1998.
- [4] M. Brown. *A Memory Model for Case Retrieval by Activation Passing*. PhD thesis, University of Manchester, 1994.
- [5] P. Chang and C. Lai. A hybrid system combining self-organizing maps with cbr in wholesaler's new-release book forecasting. *Expert Syst. Appl.*, 29(1):183–192, 2005.
- [6] D. Doyle, A. Tsymbal, and P. Cunningham. A review of explanation and explanation in case-based reasoning. In *Technical report TCD-CS-2003-41*. Department of computer Science. Trinity college, Dublin, "2003".
- [7] A. Fornells, E. Golobardes, J.M. Martorell, J.M. Garrell, E. Bernadó, and N. Macià. A methodology for analyzing the case retrieval from a clustered case memory. In *7th International Conference on Case-Based Reasoning*, LNAAI. Springer-Verlag, 2007. In press.
- [8] A. Fornells, E. Golobardes, D. Vernet, and G. Corral. Unsupervised case memory organization: Analysing computational time and soft computing capabilities. In *8th European Conference on CBR*, volume 4106 of *LNAAI*, pages 241–255. Springer-Verlag, 2006.
- [9] T. Kohonen. *Self-Organization and Associative Memory*, volume 8 of *Springer Series in Information Sciences*. Springer, Berlin, Heidelberg, 1984. 3rd ed. 1989.
- [10] J. Kolodner. *Case-Based Reasoning*. Morgan Kaufmann Publishers, Inc., 1993.
- [11] M. Lenz, H.D. Burkhard, and S. Brückner. Applying case retrieval nets to diagnostic tasks in technical domains. In *Proceedings of the Third European Workshop on Advances in Case-Based Reasoning*, pages 219–233. Springer-Verlag, 1996.
- [12] M. Malek and B. Amy. A pre-processing model for integrating cbr and prototype-based neural networks. In *Connectionism-symbolic Integration*. Erlbaum, 1994.
- [13] K. McCarthy, J. Reilly, L. McGinty, and B. Smyth. Thinking positively - explanatory feedback for conversational recommender systems. In *Proceedings of the ECCBR 2004 Workshops. TR 142-04*, pages 115–124, 2004.
- [14] D. McSherry. Explanation in recommender systems. *Artif. Intell. Rev.*, 24(2):179–197, 2005.
- [15] R. Nicholson, D. Bridge, and N. Wilson. Decision diagrams: Fast and flexible support for case retrieval and recommendation. In *8th European Conference on Case-Based Reasoning*, volume 4106 of *LNAAI*, pages 136–150. Springer-Verlag, 2006.
- [16] E. L. Rissland, D. B. Skalak, and M. Friedman. Case retrieval through multiple indexing and heuristic search. In *International Joint Conferences on AI*, pages 902–908, 1993.
- [17] J. W. Schaaf. Fish and Sink - an anytime-algorithm to retrieve adequate cases. In *Proceedings of the First International Conference on Case-Based Reasoning Research and Development*, volume 1010, pages 538–547. Springer-Verlag, 1995.
- [18] D. Vernet and E. Golobardes. An unsupervised learning approach for case-based classifier systems. *Expert Update. The Specialist Group on Artificial Intelligence*, 6(2):37–42, 2003.
- [19] S. Wess, K.D. Althoff, and G. Derwand. Using k-d trees to improve the retrieval step in case-based reasoning. In *Selected papers from the First European Workshop on Topics in Case-Based Reasoning*, volume 837, pages 167–181. Springer-Verlag, 1994.
- [20] R. Verde Y. Lechevallier and F. de Carvalho. Symbolic clustering of large datasets. In *Data Science and Classification*, Studies in Classification, Data Analysis, and Knowledge Organization, pages 193–201. Springer Berlin Heidelberg, 2006.
- [21] Q. Yang and J. Wu. Enhancing the effectiveness of interactive cas-based reasoning with clustering and decision forests. *Applied Intelligence*, 14(1), 2001.
- [22] B. Zenko, S. Dzeroski, and J. Struyf. Learning predictive clustering rules. citeseer.ist.psu.edu/731548.html.

Assessing Confidence in Cased Based Reuse Step

F. Alejandro García ^{a,*}, Javier Orozco ^b and Jordi González ^c

^aArtificial Intelligence Research Institute IIIA-CSIC,
Campus UAB, 08193 Bellaterra, Spain

^bComputer Vision Center CVC & Dept. de Ciències de la Computació,
Edifici O, Campus UAB, 08193 Bellaterra, Spain

^cInstitut de Robòtica i Informàtica Industrial UPC-CSIC,
C. Llorens i Artigas 4-6, 08028, Barcelona, Spain

Abstract. Case-Based Reasoning (CBR) is a learning approach that solves current situations by reusing previous solutions that are stored in a case base. In the CBR cycle the *reuse* step plays an important role into the problem solving process, since the solution for a new problem is based in the available solutions of the retrieved cases. In classification tasks a trivial reuse method is commonly used, which takes into account the most frequently solution proposed by the set of retrieved cases. We propose an alternative reuse process; we call confidence-reuse method, which make a qualitative assessment of the information retrieved. This approach is focused on measuring the solution accuracy, applying some confidence predictors based in a *k*-NN classifier with the aim of analyzing and evaluating the information offered by the retrieved cases.

Keywords. Case-Based Reasoning, Reuse, Confidence reuse, *k*-NN, Classification

1. Introduction

Case-Based Reasoning (CBR) is a learning approach that imitates human problem solving behavior by solving current situations while reusing previous solution knowledge [1]. The development of CBR systems has increased the necessity of supporting the analysis of the Case-Base (CB) structure by providing solutions with an estimated confidence. Cheetam and Price emphasized the importance for the CBR systems to be capable of attaching a solution confidence [3,2], which means that the system will produce both the solution for the target problem and a value estimating the confidence the system has with the solution proposed.

CBR systems use different classifiers within the problem solving process, where most of them produce numeric scores based on similarity measures. These systems should provide a solution beyond the quantitative value produced by a classifier, this must be a considerably and significantly quality rate to take into account in the decision

*Correspondence to: F. Alejandro García, IIIA, Institut d'Investigació en Intel.ligència Artificial, CSIC Spanish Scientific Research Council. Tel.: + 34-935809570; Fax: + 34-935809661; E-mail: fgarcia@iiia.csic.es

process. When the numeric scores become to quality scores, it could help to attach a confidence criterion solution proposed. Some approaches in CBR have been focused on keeping the stability and accuracy of traditional artificial intelligence problem-solving systems[10], and have been suggested to deal with confidence performance[7,4,9]. We highlight those works aimed to evaluate confidence in classification tasks as for example, a Spam filter case-based reasoning[5] system employed to identify Spam mail.

In this paper we propose a confidence assessment approach applied to expressive face recognition in a facial expression recognition domain. This domain presents higher complexity for the difficulty of clearly assess the different human face expressions. We have developed a CBR confidence classification system in a multi-class problem while analysing the confidence performance into each class by using confidence predictors based on k -NN classifiers in order to assess the probability of a given target problem to belong to a corresponding class.

This paper is organized as follows: in section 2 the case-based reasoning representation and the classification task into the CBR cycle. Section 3 presents some experimental results and discussions. We conclude in the section 4 summarising the main contributions and introducing some perspectives to extend the proposed approach.

2. CBR Representation

Case-Based Reasoning (CBR) is a learning approach that imitates human problem solving behavior by means of reasoning about current situations and reusing past situations. CBR solves a new problem by retrieving a previous similar situation and by reusing information and knowledge of that situation [1]. The CBR paradigm uses previous solved situations called cases, which are stored in a case-base (CB).

In CBR systems the most commonly used classification technique is the k -NN classifier, which decides the belonging class by assessing its k Nearest Neighbours.

The main tasks that describes a system CBR process is called CBR cycle[1], which contains four steps. Below, the two first are described according to facial expression analysis by assessing confidence. The last two steps of the CBR cycle are out of the scope of this paper.

1. **Case Retrieve:** The goal of this step is to retrieve the cases close to the target problem. The k -NN classifier is used in order to retrieve from the CB the k most similar cases to the target problem. This process is based on a similarity measure. We apply an Euclidean distance to compare the *problem-description* attributes of the cases.
2. **Case Reuse:** in this step, the goal to achieve is to determine a possible solution for the target problem, by using the previously collected information from the retrieved cases. We could apply a reuse solution method by applying the majority solution from the retrieved cases. This majority-reuse has some drawbacks: the first one is that the k -NN needs to employ an additional strategy for choosing the solution in case of ties (e.g. having a list of retrieve cases as A, A, B, B, C is not easy to solve). The second one is that the classification efficiency is decreasing when noise into the case-base increases. Because of this we use an alternative decision method that we call Confidence-Reuse, which is based on previous con-

fidence assessment to provide a current solution for the target problem. In other words, an evaluation of the confidence of the proposed solution.

2.1. Confidence Assessment

The confidence evaluation is based on four additional similarity measures that we call predictors. They are applied with respect to the k -NN classifier while providing additional scores. Although the predictors could be computed assuming that the target problem belongs to each one of the classes into the CB, we analyze only probable solutions acquired from the retrieved neighbours. Hence, if the retrieved solutions are A, A, B, B, C, C, the target problem is analyzed only with respect classes A, B and C.

We assess the confidence of the solution making some measures based on the k -NN classification. The measures used are similar to others existing in previous work [5], with some differences, our problem has to reason about more than the two classes used in [5] and we applied only four measures in order to keep the system *eficciency*. We assume that both the amount of neighbours and the similarity relationship between cases play an important role in the assessment of the predictors. The four confidence predictors try the sample data in a neighbourhood around to the target problem according to an additional set of similarity measures based on k -NN, Euclidean distance and solution indexing. These predictors follow the next notation:

- For a given target problem t , the neighbours are ordered by similarity distance S , which is the inverse of the Euclidean distance between two cases. The closest neighbour is the most similar.
- The set of retrieved cases is composed by relevant-neighbours (RN) (cases belonging to the same class that the target problem is *assuming*) or irrelevant-neighbours (IN) (cases belonging to different class that the target problem is *assuming*).

The confidence measures are defined as follows:

- (a) Average-index, S_1 , captures how close are the first n -IN neighbours to the target problem t . This predictor gets the average of the position or index I' for the first n -IN.

$$S_1(t, n) = \frac{1}{n} \sum_{i=1}^n I'_i(t) \quad (1)$$

- (b) Average RN-similarity, S_2 , measures the average of the similarity for the first n -RN neighbours to the target problem t .

$$S_2(t, n) = \frac{\sum_{i=1}^n S[t, RN_i(t)]}{|RN|} \quad (2)$$

- (c) Similarity ratio, S_3 , calculates the ratio of the similarity between the target problem t and its n -RN to the similarity between the target problem t and its n -IN.

$$S_3(t, n) = \frac{\sum_{i=1}^n S[t, RN_i(t)]}{\sum_{i=1}^n S[t, IN_i(t)]} \quad (3)$$

- (d) Similarity Ratio within k , S_4 , which is similar to the above measure but only considering the first k -RN and the first k -IN from the k -NN set.

$$S_4(t, k) = \frac{\sum_{i=1}^k S[t, RN_i(t)]}{\sum_{i=1}^k S[t, IN_i(t)]} \quad (4)$$

The effectiveness of each measure depends on the proportion of cases correctly predicted and the high confidence depends on the predictoros agreement. On the other hand, each predictor produces a positive score, in this way, we identify the measure that extracts the majority of accuracy by using weights. Each one of the predictor's measurements are standardised into the range [0,1] according to the theoretical maximum value. Posterior confidence value λ is computed according to a average function as follows:

$$\lambda = \frac{1}{4} \sum_{i=1}^4 S_i \quad (5)$$

The *confidence-reuse* method, is used to compute the confidence value λ , (Eq. 5). Every λ value offered by (Eq. 5) is between the range [0,1], thus we calculated the percentage of confidence values with ($\lambda * 100$). In this manner we set a confidence-threshold in 80% in order to filter cases, and regarded those cases that achieved the threshold into the CB. This filter was carried out by performing a leave-one-out process¹. Subsequently, we assume that all λ values follow a Gaussian distribution for each class, $N(\mu_c, \sigma_c)$ for $c = 1, \dots, 7$ according to the seven classes.

Once the λ is calculated in each class, we learned the mean μ_c and the standard deviation σ_c of λ values for each class c .

In order to solve a new target problem t , we firstly run a k -NN process to get a set of retrieved solutions. Then we compute the maximum probability of t to belong to each retrieved solutions as follow:

$$P(L_t = c) = P(\lambda_t | \gamma_t) = \prod_{i=1}^m N(\lambda_i; \mu_c, \sigma_c) \quad (6)$$

where L_t is the corresponding solution for the target problem, λ_t the confidence value, c is every class in the retrieved cases, and m is the length of the class c . Therefore the classification decision is made according to the minimum distance of each λ_t to the class paramters:

$$\text{Min} \left| \frac{\lambda_t(c) - \mu_c}{\sigma_c} \right| \quad (7)$$

3. Experimental Results

The experiments were aimed to analyze the behaviour of classification tasks in a multi-class case-base system. The shown results in this section were collected from the multi-class facial expression data base the FGnet², which is an image database that contains face image sequences, showing a number of subjects performing the six different basic emotions and the neutral emotion defined by Ekman and Friesen [6].

¹Leave-one-out process, leaves every case out of the case base in order to solve it as a new problem.

²<http://www-prima.inrialpes.fr/FGnet/>

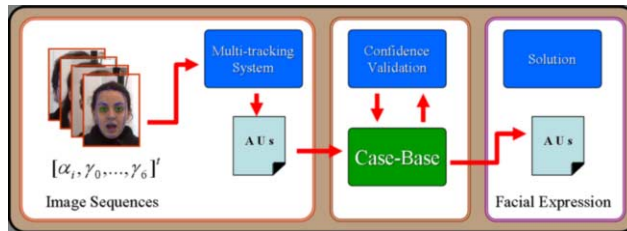


Figure 1. Problem solving system structure



Figure 2. Image sequence for happiness expression.

3.1. Case base building

By using a Multi-tracking system [8], we made use of a Facial Action Coding System (FACS)³ to describe facial movements and categorise different facial expressions, see Fig.1.

We constructed the case base with a case-structure, which employs the FACS as attributes and adopts the FGnet facial expression label as the solution or class for each element, see Fig.2. Consequently, the case-base is a categorised database which assume $\Theta = [\gamma, \mathbf{L}]$, as case structure, where γ is a seven dimensional continues valued vector for FACS, $\gamma = [Upper\ Lip, Lower\ Lip, Lip\ Stretcher, Lip\ Corners, Inner\ Brow, Outer\ Brow, Eyelid]$ and \mathbf{L} is the class label (Solution). All the cases are distributed in seven classes.

3.2. System-Training

The first training step is to build up a case-base CB with the same amount of elements per class. The information is coming from image sequences developed by different actors in each class in order to avoid redundant information. In deterministic problems the amount of elements into the case base play an important role. Even though we demonstrate that working with a small case base with learning approach it is possible to achieve high proportion of example correctly classified, see Fig.3. The case base was cautiously constructed taken into account the solving credibility associated to each element.

3.3. System-Testing

A discrete comparison towards the classification tasks was analyzed by applying confidence-reuse method explained in section 2 and comparing classification results against majority-reuse results. The tests were designed in two ways; the first one was

³Facial Action Coding System (FACS) is the most widely used and versatile method for measuring and describing facial behaviours.

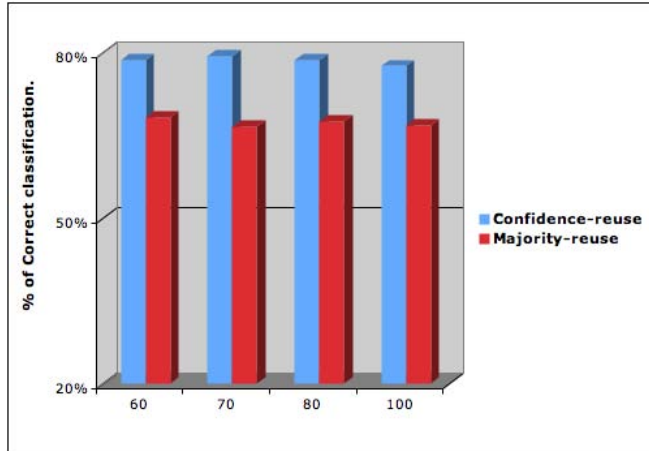


Figure 3. Average Classification using different case base sizes.

aimed to analyze robustness of the method, for that reason we compared results of k -NN classifier, with confidence evaluation and without applying it. We observed that even using different case base sizes, the confidence-reuse method did not suggest worse results than the results proposed by the majority-reuse method. Can be observed in Fig.3 in average 78% of classification correctness achieved by confidence-reuse using all classes of the case base, whilst the majority-reuse achieved in average only 67% using the same cases. It is worth to mention that each image sequence offered by FGnet-database is developed from low expressiveness until achieve the best expressiveness. Some information in the beginning and even in the middle of a sequence could appear as noise in the CB, as we can see in Fig.2, the two first images have the label *happy* but its attributes assume information similar to other classes and this information is easy to misclassify. Due to noise, enhancing the length of elements in each class does not always allow better classification results.

The rest of the tests were focused on analyzing unseen data. We consider as unseen data the image sequences of new actors in each class. We classified at least three sequences by actor, completing a total of 574 new cases. The classification per class is detailed in (Fig.4), where we can see that two important classes *sadness* and *fear* reach better performance using accuracy evaluation. In addition is possible to see the percentage of cases in those classes considered with confidence is low because of the agreement of the predictors is as low. The percentage of confidence is determined by the agreement of the solution proposed by predictors. The aim of each predictor is to evaluate the solutions (without duplicates) nearest to the target problem and re-ranking them according to its own evaluation. Finally the decision making is carried out based in all predictor's agreement.

To evaluate the confidence have an advantage to highlight, it lets know if the solution is more than good or bad, for instance we found with the results of a confusion matrix that too much cases of the class *sadness* are misclassified and confused with the class *neutral*. In this situation, even if the classification improved using confidence-reuse, the confidence evaluation shows that only 7% of cases reach high confidence, this information could be used by system manager in the final decision making, see Fig. 4.

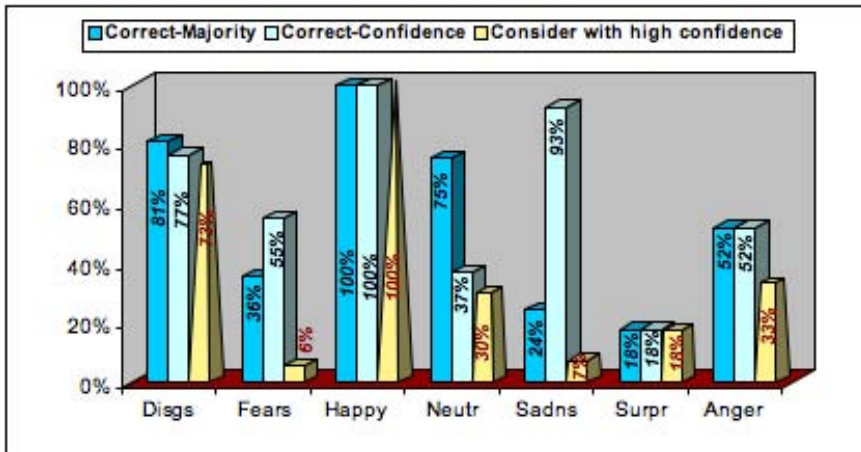


Figure 4. Classification performance by using the Confidence Reuse method.

4. Conclusions

We highlight two advantages of applying confidence evaluation in reuse step in CBR systems, the first one is that to solve some problems it is needed to know more than the solution offered by the nearest neighbours, an additionally, assessment of the information coming from the nearest neighbours lets to reach better classification result as we have demonstrated.

We have shown an efficient sampling process to compare data while enhancing the k -NN classification process. By using the confidence assessment process and the posterior comparison among classes, we could get a higher classification rate, which provide two classification descriptors; the solution and the corresponding confidence. As well, we can compare experimental results for different k -values and case-bases through the classification error and the classification confidence.

The Gaussian assumption for the confidence value in each class have allowed us to set a decision process based on previous confidence solutions and the confidence for the proposed solution, which means an alternative decision according to the quality of the solution. This parameter is worth for maintenance process, since it reveals the quality of the database for each class.

As future work, we attempt to provide an optimal k -value according to a confidence threshold in order to minimize the computational complexity related with the solving process against to the whole database. Additionally, we want to provide a strong aggregation method based on confidence assessment, which will enhance the dynamical learning capabilities of this CBR system.

Acknowledgements

This research has been supported by the Spanish project TIN2006-15140-C03-01 “MID-CBR: An Integrative Framework for Developing Case-based Systems”, for EC grants IST-027110, for the HERMES project, IST-045547, for the VIDIVideo project, by the Spanish MEC under projects TIN2006-14606 and DPI-2004-5414, for a Juan de la Cierva Postdoctoral fellowship from the Spanish MEC and a FPI fellowship.

References

- [1] A. Aamodt and E. Plaza. Case-based reasoning: Foundational issues, methodological variations, and system approaches. *Artificial Intelligence Communications*, 7(1):39–52, 1994.
- [2] W. Cheetham and J. Price. Measure of a solution accuracy in case-based reasoning systems. In Funk, P., González-Calero, P., eds.: *7th European Conference on Case-Based Reasoning (ECCBR 2004)*, 3155:106–118, 2004.
- [3] W. Cheetham. *Case-Based Reasoning with Confidence*. Book Advances in Case-Based Reasoning, 2000.
- [4] J. Chua and P. Tischer. Determining the trustworthiness of a case-based reasoning solution. In *International Conference on Computational Intelligence for Modeling, Control and Automation: 7th European Conference on Case-Based Reasoning (ECCBR 2004)*, 3155(1740881885):12–14, 2004.
- [5] S. Delany, P. Cunningham, and D. Doyle. Generating of classification confidence for a case-based spam filter. In *In 6th International Conference on Case-Based Reasoning (ICCBR 2005)*. Springer, volume 3620, pages 177–190, 2005.
- [6] P. Ekman and W. V. Friesen. Facial action coding system: A technique for the measurement of facial movement. *Consulting Psychologists Press, Palo Alto*, 1978.
- [7] M. Grachten, F.A. Garcia, and J.L. Arcos. Navigating through case base competence. In *eds.: 7th European Conference on Case-Based Reasoning (ECCBR 2004)*, Springer, volume 3155, pages 282–295, 2004.
- [8] J. Orozco and F.A. García and J.L. Arcos and J. González. patio-Temporal Reasoning for Reliable Facial Expression Interpretation. In *Proceedings of the 5th International Conference on Computer Vision Systems (ICVS'2007)*, Bielefeld, Germany, March 2007.
- [9] T. Reinartz, I. Iglezakis, and T. Roth-Berghofer. Computational intelligence. *Artificial Intelligence Communications*, 2001(17):214–234, 2001.
- [10] B. Smyth and E. McKenna. Competence models and the maintenance problem. *Computational Intelligence*, 17(2), 2001.

Computer Vision

This page intentionally left blank

Efficient tracking of objects with arbitrary 2D motions in space-variant imagery

Luis Puig M.^{a,1,2} and V. Javier Traver^{b,3}

^a DIIS-I3A, Universidad de Zaragoza, Zaragoza, Spain

^b Dep. de Llenguatges i Sistemes Informàtics, Universitat Jaume I, Castelló, Spain

Abstract. In the last few years, the biologically-motivated log-polar foveal imaging model has attracted the attention from the robot and computer vision communities. The advantages that log-polar images offer for target tracking and other active-vision tasks have been explored and exploited. However, despite the progress made, the proposed systems have some limitations, or rely on some assumptions which may be violated in practical real scenarios. Estimating complex parametric motion models in space-variant imagery is an example of one problem still deserving further investigation, and just the focus of this paper. The proposed algorithm learns to relate a set of known motions with their corresponding visual manifestations for a given reference pattern. After learning, motion estimation becomes a very efficient, search-free process. Synthetic and real experiments provide evidence on the effectiveness of this approach for motion estimation and visual tracking using log-polar images.

Keywords. Space-variant images, Motion estimation, Visual tracking, Interaction matrix

1. Introduction

In the last few years, log-polar vision [1] has experienced an increase of attention from researchers. It has been shown the interesting advantages that log-polar imagery brings to active vision tasks such as time-to-impact computation [2], vergence control [3,4], and target tracking [5,6], among others. However, in spite of all the achievements made, most of the success of the proposed systems relies on a number of assumptions which, in practice, may be violated. As a result, the performance of these systems may degrade or even fail. Regarding motion estimation and object tracking, one particular problem is that existing systems assume a limited motion model [7,6] or do not fully exploit the nature of log-polar domain [8]. Therefore, to adopt the log-polar formalism in real practical settings, and still keep its advantages, these kind of limitations should properly be addressed and overcome. The work described in this paper deals precisely with the

¹Work developed during a stay within the *Computer Vision Group, Universitat Jaume I*.

²Authors listed in alphabetical order.

³Acknowledgment to the Spanish *Ministerio de Educación y Ciencia*, through an Integrated Actions program (HP2005-0095).

problem of estimating “complex” parametric motion. By *complex* motion models, we mean those whose estimation is particularly challenging in space-variant images.

Traditionally, the log-polar mapping has facilitated scale- and rotation-related transformations, because these transformations are mapped to simple shifts in the log-polar domain [9]. However, simple translations, which are very simple in the cartesian domain, become quite complicated in the log-polar domain, due to issues such as the polar-logarithmic sampling, shape distortions, and the space-variant resolution. Because translation is a motion component of key importance for target tracking, its estimation becomes essential. However, although solutions have been proposed for this problem [10], translational motion is seldom present alone in practice. Moving one step further, similarity motion model comprises translation plus rotation and scaling, and its estimation has been addressed in [6], where translation can be kept small as a by-product of the active tracking, thus allowing an easy estimation of rotation and change of scale by exploiting the properties of log-polar sampling. Nevertheless, when it comes to more complex motion models, such as affine or higher, it becomes increasingly difficult to estimate the motion while coping with the inherent properties of discrete log-polar images. Notwithstanding these difficulties, some solutions have been proposed for these motion models. Unfortunately, they solve the problem only partially [11], or without fully resorting to log-polar coordinates during tracking [8]. Our solution builds on one efficient tracking approach [12], formulated initially for cartesian images. We study the application of that strategy to log-polar images, and analyze its implications. A key question motivating this work was: *will this approach, basically a linear method, be effective with log-polar images despite their space-variant nature and non-linear shape and motion deformations?*

The idea to make the tracking fast is preventing the use of any kind of visual search, which is typically done in feature matching or correlation-based approaches [13]. Alternatively, the motion is efficiently estimated just from the current visual pattern. To make this possible, the visual pattern to be tracked (the *reference pattern*) is initially subject to a number of *perturbations* (geometric transformations), so that a relationship between the motion parameters of each perturbation and their visual evidences in the perturbed pattern, is learnt. This relationship takes the form of an *interaction matrix*. After this off-line, learning stage, which is generally costly, on-line tracking becomes an efficient real-time process.

Beyond these interesting computational advantages, the actual benefit we get from this approach is that the process is the *same* for *any* motion model and *any* kind of sampling. In our case, the complexities of log-polar images and their interplay with the parametric motion model are completely removed, because they are dealt automatically in the learning stage. In this sense, our approach is more attractive than other similar works, which require the explicit computation of the partial derivatives of the image with respect to the motion parameters [8]. Furthermore, the discrete approximations of such derivatives are particularly tricky in space-variant images, since image differences between areas at different resolutions should be computed.

2. Interaction matrix-based parameter estimation

Before explaining the technique in its application to motion estimation, we provide a short description of a more general formulation.

2.1. General formulation

We consider a general parameter-estimation problem whose goal is to estimate a vector \mathbf{p} of p scalar parameters $\mathbf{p} = [\mu_1 \mu_2 \cdots \mu_p]^\top$ given an observation vector \mathbf{o} of n scalar samples, $\mathbf{o} = [o_1 o_2 \cdots o_n]^\top$. Let us assume that an interaction matrix \mathbf{A} exists such that the parameter vector \mathbf{p} can be found from the observation vector \mathbf{o} through: $\mathbf{p} = \mathbf{A} \cdot \mathbf{o}$. The interaction matrix \mathbf{A} can be estimated throughout a learning stage if a set of observations with their corresponding known parameters are available. The set of m observation vectors can be represented as an observation matrix \mathbf{O} : $\mathbf{O}_{m \times n} = [\mathbf{o}_1 \mathbf{o}_2 \cdots \mathbf{o}_m]^\top$, where each of its m rows \mathbf{o}_i is a single observation vector $\mathbf{o}_i = [o_{i1} o_{i2} \cdots o_{in}]^\top$.

On the other hand, the associated parameters are given with a parameter matrix \mathbf{P} : $\mathbf{P}_{m \times p} = [\mathbf{p}_1 \mathbf{p}_2 \cdots \mathbf{p}_m]^\top$, where each of its m rows \mathbf{p}_i is a single parameter vector $\mathbf{p}_i = [\mu_{i1} \mu_{i2} \cdots \mu_{ip}]^\top$, and their p columns \mathbf{q}_j correspond to the values of a parameter j along the m perturbations $\mathbf{q}_j = [p_{j1} p_{j2} \cdots p_{jm}]^\top$. Relationship expressed above for a single (\mathbf{o}, \mathbf{p}) pair should hold for all observations-parameters pairs ($\mathbf{o}_i, \mathbf{p}_i$) available for learning. Therefore, $\mathbf{P} = \mathbf{O} \cdot \mathbf{A}^\top$, with $\mathbf{A}_{p \times n} = [\mathbf{a}_1 \mathbf{a}_2 \cdots \mathbf{a}_p]^\top$. Then, each of the p rows of the interaction matrix \mathbf{A} , $\mathbf{a}_j = [a_{j1} a_{j2} \cdots a_{jn}]^\top$, corresponding to each of the p parameters, can be estimated separately as: $\mathbf{a}_j = \mathbf{O}^+ \cdot \mathbf{q}_j$, $j \in \{1, 2, \dots, p\}$, with \mathbf{O}^+ being the pseudo-inverse of the observation matrix \mathbf{O} : $\mathbf{O}^+ = (\mathbf{O}^\top \cdot \mathbf{O})^{-1} \cdot \mathbf{O}^\top$. Notice that this pseudo-inverse is the same for the p cases, so it should be computed only once.

While the main topic of this paper is motion estimation and tracking, there are several reasons why we give a generalized description rather than just focus on the motion-estimation problem. First, as explained below (Sect. 3), our approach for motion estimation in log-polar images differs in several respects from [12], while the general formulation can accommodate both of them. Second, this formulation can be applied to parameter-estimation problems other than motion estimation. Finally, as our experiments suggest, the role of the interaction matrix seems to be more than to serve as an approximation of partial derivatives.

2.2. Motion estimation

The formulation given above for a general parameter-estimation problem, is a generalization of the approach proposed in [12] for the parametric motion estimation problem. The analogy between the general formulation and its motion-estimation instantiation is summarized as follows. The parameters μ_i are *motion* parameters; the parameter matrix \mathbf{P} is built from a set of random motion parameter vectors \mathbf{p}_i ; and the observations \mathbf{o}_i are image differences. The main mathematical elements involved are collected in Table 1, for an easy and quick reference.

Now, we provide an overview of the general idea to estimate the interaction matrix for its use in visual tracking. The visual pattern to be tracked is taken as the reference (template), \mathbf{I}_0 . Then, this template is subject to m random image transformations (perturbations) \mathbf{p}_i to get both a parameter matrix \mathbf{P} and the observation matrix \mathbf{O} . In order to build \mathbf{O} , each observation vector \mathbf{o}_i can be obtained as the difference between the original template \mathbf{I}_0 and the (subsampled) perturbed image \mathbf{I}_i , $\mathbf{o}_i = \mathbf{I}_0 - \mathbf{I}_i$. For efficiency reasons, the visual pattern can be subsampled in a certain manner, to get only a

Table 1. Main mathematical elements of the learning approach

Scalar quantities		Vector and matrices elements		
Name	Symbol	Name	Symbol	Dimensions
Number of learning perturbations	m	Motion parameter vector	\mathbf{p}	$p \times 1$
Number of samples	n	Observation vector	\mathbf{o}	$n \times 1$
Number of motion parameters	p	Perturbation matrix	\mathbf{P}	$m \times p$
		Observation matrix	\mathbf{O}	$m \times n$
		Interaction matrix	\mathbf{A}	$p \times n$

reasonable amount of samples per observation. An example can be seen in Fig.1. More formally, given an image I_i , the visual pattern \mathbf{I}_i is actually built from I_i by applying a certain sampling function \mathcal{S} , i.e., $\mathbf{I}_i = \mathcal{S}(I_i)$. Given both, the perturbation and the observation matrices, the interaction matrix can be estimated. This completes the learning stage.

The usage stage (i.e., while tracking) simply consists of sampling the current (time step t) image I_t , so that the current pattern $\mathbf{I}_t = \mathcal{S}(I_t)$ is obtained. Then, the difference between the current \mathbf{I}_t and the original template \mathbf{I}_0 is performed, thus obtaining an observation vector $\mathbf{o}_t = \mathbf{I}_0 - \mathbf{I}_t$. Finally, a simple multiplication of this observation vector with the previously learnt interaction matrix \mathbf{A} provides an estimate of the motion \mathbf{p}_t the current pattern has undergone with respect to the reference pattern: $\mathbf{p}_t = \mathbf{A} \cdot \mathbf{o}_t$.

3. Visual tracking in log-polar images

This section provides details of the different aspects and design decisions of our algorithm for visual motion estimation and tracking in log-polar images, based on the formulation described above (Sect. 2).

Sampling. Visual patterns in [12] are sampled over an elliptic shape whose center and axes change as the pattern is tracked. In contrast, our patterns are built directly from the whole log-polar image. This makes sense because foveal tracking is used in active vision scenarios; as a consequence, the pattern is expected to be fixated, as it is actively tracked. Thus, the log-polar image provides an easy way to define the sampling function, as opposite to the elliptic region defined in cartesian images in [12]. Fig. 1 illustrates different samplings factors $\Delta = (\delta_u, \delta_v)$ along the radial δ_u and angular δ_v directions, which are used to subsample the log-polar image.

Parameters. The elliptic region of interest in [12] models not only the sampling function \mathcal{S} , but also the motion. Indeed, their parameter vector \mathbf{p} consists of geometric parameters defining an ellipse. This allows them to define a reduced affine transformation with 5 parameters. In contrast, we use a motion parameter vector decoupled from the sampling function, and with full 6-parameter affine motion. This decoupling makes possible and easy the use of any arbitrary motion model. However, only affine motion has been considered in this work.

Observations. We use $\mathcal{O}(\mathbf{I}_1, \mathbf{I}_2)$ to denote a general observation function depending in general on two visual patterns (although some of them might not be used). We have made

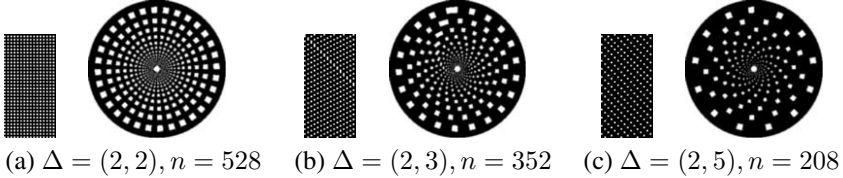


Figure 1. Examples of samplings resulting in a different number of samples n . In each of the three cases, the sampling on the left corresponds to the sampled pixels in the log-polar space; and its reconstruction to cartesian domain is shown on the right.



Figure 2. Examples of perturbed images. Up: cartesian images; down: log-polar images (shown rotated and bigger than its true size for illustration purposes). Top right: illustration of a log-polar image reconstructed into cartesian space.

experiments with two kinds of observations \mathbf{o}_i : image differences ($\mathbf{o}_i = \mathcal{O}_1(\mathbf{I}_0, \mathbf{I}_i) = \mathbf{I}_0 - \mathbf{I}_i$, as described in [12]), but also simply image gray-level values ($\mathbf{o}_i = \mathcal{O}_2(\mathbf{I}_0, \mathbf{I}_i) = \mathbf{I}_i$), with equal or better results. This suggests that the interaction matrix encodes the result of learning the relationship between observations and parameters, whatever these observations really consist of. On the other hand, note that by getting rid of the difference, the use of the original template becomes unnecessary when computing each observation.

Image transformations. The perturbations entail transforming the image according to the motion model considered. While we use log-polar images, usual parametric motion models are generally expressed more compactly in cartesian coordinates. On the other hand, by transforming log-polar coordinates forth to and back from cartesian coordinates, it is theoretically possible to warp log-polar images using any arbitrary motion model. However, due to the space-variant resolution of log-polar images, this warping would deem unnatural and result in poor-quality perturbed log-polar images. Therefore, our approach of performing the geometric transformations in cartesian images and then transforming them into log-polar images is a much more sensible choice. We denote by $\mathcal{T}(I; \mathbf{p})$ the transformation of an image I according to motion parameters \mathbf{p} . Examples of perturbed images for a traffic-scene pattern, using an affine motion model, are shown in Fig. 2.

Tracking. Even though cartesian images are used at the learning stage, we stick to log-polar images during tracking. It is worth stressing that there is no inconsistency in this perspective: cartesian images are used in learning just as a tool, but this does not prevent that hardware-based log-polar sensors [14] could be used for tracking without any support of cartesian images. All that is required for learning is a way to simulate the

transformation from cartesian to log-polar images according to the log-polar mapping template characterizing the log-polar sensor.

Off-line and on-line computational requirements. While learning is a time-consuming process, because a large number of perturbations m (maybe a few thousands) are usually required, tracking is very efficient: all that is required is a product of one matrix (the interaction matrix) and the current visual pattern. Fortunately, for a given template, learning can be performed just once, at an off-line stage. As a result, its time requirements are of little or no practical concern.

The procedures for the learning and the usage stages are given in pseudo-code in Algorithms 1 and 2, respectively. The notation introduced above regarding the different transformations and operations are used in both algorithms. Notice that the log-polar transformation \mathcal{L} is used in the learning algorithm, but *not* in the usage algorithm, since the incoming images are expected to be already in the log-polar format⁴.

Algorithm 1 Learning stage (estimating the interaction matrix)

Input: A cartesian image I_0 with the reference pattern

Output: The estimated interaction matrix \mathbf{A}

- 1: $L_0 := \mathcal{L}(I_0) // \text{log-polar transform}$
 - 2: $\mathbf{L}_0 := \mathcal{S}(L_0) // \text{sampling function}$
 - 3: **for** $i := 1, 2, \dots, m$ **do**
 - 4: $\mathbf{p}_i := \text{RandomTransformation}()$
 - 5: $I_i := \mathcal{T}(I_0; \mathbf{p}_i) // \text{geometric transformation}$
 - 6: $L_i := \mathcal{L}(I_i)$
 - 7: $\mathbf{L}_i := \mathcal{S}(L_i)$
 - 8: $\mathbf{o}_i := \mathcal{O}(\mathbf{L}_0, \mathbf{L}_i) // \text{observation function}$
 - 9: **end for**
 - 10: $\mathbf{O} := \text{BuildMatrix}(\mathbf{o}_1, \mathbf{o}_2, \dots, \mathbf{o}_m)$
 - 11: $\mathbf{P} := \text{BuildMatrix}(\mathbf{p}_1, \mathbf{p}_2, \dots, \mathbf{p}_m)$
 - 12: $\mathbf{A} := \text{EstimateInteractionMatrix}(\mathbf{O}, \mathbf{P}) // \text{see Sect. 2.1}$
-

Algorithm 2 Usage stage (estimating the motion parameters)

Input: A log-polar image L_t with the current pattern,

the estimated interaction matrix \mathbf{A} , and (optionally),

the reference pattern \mathbf{L}_0 (only if required by \mathcal{O})

Output: The estimated motion parameter vector \mathbf{p}_t

- 1: $\mathbf{L}_t := \mathcal{S}(L_t) // \text{sampling function}$
 - 2: $\mathbf{o}_t := \mathcal{O}(\mathbf{L}_0, \mathbf{L}_t) // \text{observation function}$
 - 3: $\mathbf{p}_t := \mathbf{A} \cdot \mathbf{o}_t$
-

⁴Actually, we get log-polar images by software conversion from cartesian images due both to our unavailability of a log-polar sensor and the fact of performing some experiments with synthetic image motions.

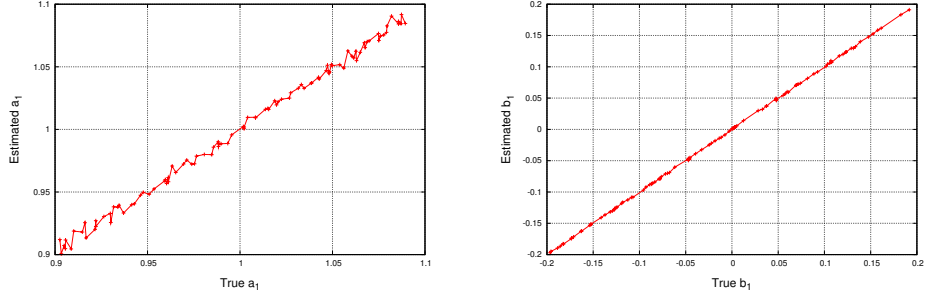


Figure 3. Estimated vs. true values for some affine parameters in the $k = 100$ test perturbations. The estimations of c_1 are similar to those of a_1 . The parameters for the y coordinate (a_2 , b_2 , and c_2) are similar to those of the x coordinate.

4. Experiments

Set up. All the experiments use the following configuration: $m = 1500$, $n = 528$, $p = 6$, $\Delta = (2, 2)$, $\mathcal{O} = \mathcal{O}_2$, the size of cartesian and log-polar images are 256×256 , and 32×64 , respectively. The sampling pattern used is shown in Fig. 1(a). The image used to test the algorithm is that shown in Fig. 2. The affine motion model is used: $(x', y') = (a_1 \cdot x + b_1 \cdot y + c_1, a_2 \cdot x + b_2 \cdot y + c_2)$. The ranges of the affine motion parameters used to both generate the learning and testing perturbations, are: $a_1, b_2 \in [0.9, 1.1]$, $a_2, b_1 \in [-0.2, 0.2]$, and $c_1, c_2 \in [-5.0, 5.0]$. For testing, a total of $k = 100$ perturbations were randomly generated.

Parameter estimation. Some of the estimated parameter are shown as a function of the true ones in Fig. 3. Each parameter of the k test perturbations is sorted and shown in ascending order. Hence, despite the nature and shape distortions introduced by the log-polar images, the algorithm exhibits a good behavior.

Number of perturbations and samples. The following two experiments show the influence of the number of perturbations and samples on the performance of the algorithm. Performance is quantified with the Euclidean distances between points transformed with the true and estimated perturbation. The final error measure e is the average of these distances over the k testing perturbations. Results in Fig. 4(a) indicate that the more the number of samples the better the results, but there is trade-off between the number of samples and the computational cost. To provide an idea of what these errors represent, we can consider that the average error in the estimates of parameters in Fig. 3 was $e \approx 0.246$. On the other hand, Fig. 4(b) shows that the global error decreases by increasing the number of perturbations, but results do not improve beyond $m = 2500$ perturbations. In these two figures, the influence of noise is studied by corrupting the original cartesian images with white Gaussian noise. It can be noticed that the method is sensitive to noise, but further work is required to clearly understand to how extent, and to devise how to increase the robustness against noise.

Target tracking. This last experiment illustrates the behavior of the algorithm while tracking a target in a real sequence. A window around the target (a face here) is extracted from the first frame in the sequence, and used as the reference pattern. To account for

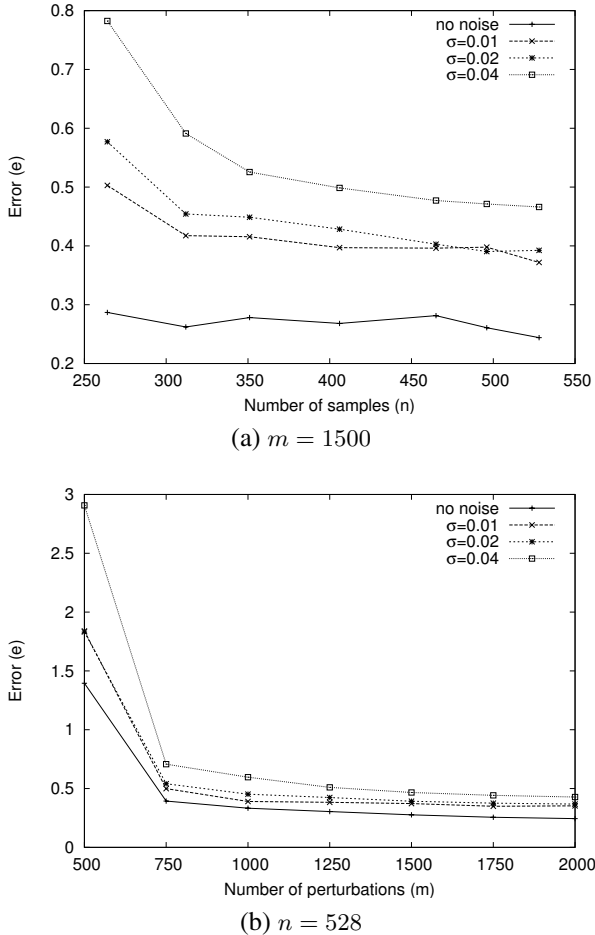


Figure 4. (a) Influence of the number of samples (n) on the performance of the algorithm (e), for a fixed number of perturbations $m = 1500$; and (b) influence of the number of perturbations (m) on the performance of the algorithm (e), for a fixed number of samples $n = 528$. In both cases, the influence of additive Gaussian noise $N(0, \sigma)$ on the original cartesian image has also been considered. Values for σ correspond to image whose gray levels are in $[0, 1]$.

the motion conditions in this sequence, the range of c_1 and c_2 was enlarged to $[-15, 15]$. After learning, motion is estimated at each frame using the incoming log-polar images. The estimated translational parameters (c_1, c_2) are used to update the position of the window within the image, from which the log-polar image is simulated⁵. The range of parameters c_1 and c_2 was changed to $[-15, 15]$, to be adapted to the motion conditions of the sequence. Fig. 5 shows some frames of the 60-frame sequence with the inverse log-polar transformation pasted on the tracked face position. It can be observed how the face,

⁵Notice that this experiment is meant to be a simulation of an active tracking. In this sense, camera motion is replaced by the window position update, and the scene is represented by the big images from which a small window, representing what the log-polar camera would actually ‘see’t, is obtained. However, alternatively, this can also be seen as an example of passive tracking using log-polar mapping as a tool.



Figure 5. Some frames corresponding to the target tracking experiment. The inverse log-polar images are placed at the tracked face position.

whose motion includes translation, as well as rotation and scaling, is successfully tracked along the sequence, even when the initial pattern includes not only the face but also some of the background, which is one of the well-known benefits of log-polar images: as the target is located on the highly resolved fovea area, the changing background at peripheral areas does not have a negative effect on the performance.

5. Conclusions

The difficult problem of estimating complex parametric motion models in space-variant image representations, has been tackled in this paper via a learning-based approach. The benefits of the proposed algorithm are two fold. On the one hand, computational advantages are obtained (since no search is required during tracking). On the other hand,

and more importantly, the formulation provides improvements over some limitations of similar previous works using log-polar images.

Both, synthetic motion estimation and real tracking experiments have been performed using (cartesian) affine motion on log-polar images. The results of these experiments suggest the suitability of this proposal of building a relationship between motion parameters and their visual consequences. Although the algorithm exhibits reasonable performance in realistic tracking situations, aspects such as occlusions or illumination changes are still not properly addressed and would deserve closer attention.

Further work could look into the required (minimum) number of samples and perturbations and their interplay, or address advanced issues such as 3D visual tracking. Other challenging directions include generalizing the approach to learn an object-invariant representation allowing the subsequent tracking of any visual pattern.

References

- [1] Marc Bolduc and Martin D. Levine. A review of biologically motivated space-variant data reduction models for robotic vision. *Computer Vision and Image Understanding (CVIU)*, 69(2):170–184, February 1998.
- [2] Massimo Tistarelli and Giulio Sandini. On the advantages of polar and log-polar mapping for direct estimation of time-to-impact from optical flow. *IEEE Trans. on Pattern Analysis and Machine Intelligence (PAMI)*, 15:401–410, 1993.
- [3] C. Capurro, F. Panerai, and G. Sandini. Dynamic vergence using log-polar images. *Intl. Journal of Computer Vision*, 24(1):79–94, 1997.
- [4] R. Manzotti, A. Gasteratos, G. Metta, and G. Sandini. Disparity estimation on log-polar images and vergence control. *Computer Vision and Image Understanding (CVIU)*, 83:97–117, 2001.
- [5] Alexandre Bernardino and José Santos-Victor. Visual behaviors for binocular tracking. *Robotics and Autonomous Systems*, 25:137–146, 1998.
- [6] V. Javier Traver and Filiberto Pla. Similarity motion estimation and active tracking through spatial-domain projections on log-polar images. *Computer Vision and Image Understanding (CVIU)*, 97(2):209–241, February 2005.
- [7] V. Javier Traver and Filiberto Pla. Motion estimation and figure-ground segmentation in log-polar images. In *Intl. Conf. on Pattern Recognition (ICPR)*, pages 166–169, Québec, Canada, August 2002.
- [8] A. Bernardino, J. Santos-Victor, and G. Sandini. Foveated active tracking with redundant 2D motion parameters. *Robotics and Autonomous Systems*, 39(3–4):205–221, June 2002.
- [9] J. C. Wilson and R. M. Hodgson. Log-polar mapping applied to pattern representation and recognition. *Computer Vision and Image Processing*, pages 245–277, 1992.
- [10] V. Javier Traver and Filiberto Pla. Dealing with 2D translation estimation in log-polar imagery. *Image and Vision Computing (IVC)*, 21(3):145–160, February 2003.
- [11] V. Javier Traver and Filiberto Pla. Radon-like transforms in log-polar images for affine motion estimation. In *Portuguese Conf. on Pattern Recognition*, Aveiro, Portugal, June 2002.
- [12] Frederic Jurie and M. Dhome. Real time tracking of 3D objects: an efficient and robust approach. *Pattern Recognition*, 35(2):317–328, 2002.
- [13] Christopher Stiller and Janusz Konrad. Estimating motion in image sequences: A tutorial on modeling and computation of 2D motion. *IEEE Signal Processing Magazine*, pages 70–91, July 1999.
- [14] G. Sandini and G. Metta. Retina-like sensors: motivations, technology and applications. In F. G. Barth, J. A. Humphrey, and T. W. Secomb, editors, *Sensors and Sensing in Biology and Engineering*. Springer-Verlag, 2003.

Ground Plane Estimation Based on Virtual Camera Rotation

Adria Perez-Rovira, Brais Martinez and Xavier Binefa

Universitat Autònoma de Barcelona,

Computer Science Department,

08193 Bellaterra, Barcelona, Spain

{adria.perez, brais.martinez, xavier.binefa}@uab.es

Abstract. In this paper we present a novel method to obtain the ground plane orientation. We assume that multiple objects are moving rigidly on a ground plane observed by a fixed camera. With an automatic tracking of some object features we do a classical "Structure from Motion" (SfM) method. This give us a static object viewed for a hypothetical camera called a "virtual camera". This camera shares the same intrinsic parameters with the real camera but moves differently due to real object motion. Assuming that the object rotates around the plane normal (equivalent to say over the ground plane), and that the virtual camera will rotate around the same vector, we use the virtual camera positions along the sequence to estimate this rotation axis, the ground plane normal.

Keywords. Ground Plane, Virtual Camera, Factorization, Camera Pose, Structure from Motion

1. Introduction

A three-dimensional scene viewed from a single static camera is a very common situation. In that case, the loss of depth perception makes quite more difficult all the possible computer vision tasks. For that reason, the different methods usually try to restrict the problems of tracking, 3D reconstruction, etc. doing some kind of assumption, implying a loss of generality in benefit of higher robustness.

One typical assumption is that the scene (or part of it) can be approximated by a plane. Known this plane, we would be able to compute the 3D position of any point lying on the plane just intersecting the projection ray of the 2D image point with the ground plane.

But the plane is not only a depth estimator tool. For instance, if this plane orientation is known, we can reformulate the problem of tracking moving objects into a more robust tracking taking into account that the movement of the vehicle has to be done over the ground plane, eliminating its freedom in the vertical direction. This technique is used in [2], where a planar-translation constraint is used to determine the object translation in a sequence viewed from a moving camera.

The information about plane orientation can also be used to achieve an accurate background subtraction. In [2], 4 co-planar points are selected manually and tracked along the sequence obtaining the homographies which describe the camera motion. In this paper (like in many others) the plane is also used to calibrate the intrinsic and extrinsic parameters of the camera, as detailed in [4] and [5].

To use the method detailed in this paper we need the trajectories of some features of the same object. For our experiments we have developed a robust tracking over Infra-Red images based on [6], [7] and [8]. Therefore, we have always worked with a kind of image more robust to luminance changes but with less information than color images, since RGB have 3 channels versus 1 in Infra-Red. Both, in Infra-Red and RGB videos, it is very useful to use the well-known Kalman filter [11] or another predictive model in order to reduce tracking noise and to work with partial occlusions.

In this paper we present a method which uses the trajectory of at least 4 points of a rigid object to obtain its shape and projections with a factorization method. After that, we extract the plane orientation using the information implicit in the computed projections. Lately, as detailed in section (3), we use the plane orientation to obtain 3D information of the objects moving over the plane. This information would be their real position, velocity, orientation and distance from the camera. Something very useful for a surveillance system able to sort all the possible targets by their danger in a higher level layer.

2. Ground Plane Estimation

As briefed in section (1), we estimate the ground plane based on a factorization algorithm [1], [5], [3] which gives us both the three-dimensional shape of the tracked object and the projections (for each frame) which transform those 3D points into the bi-dimensional points observed by the camera.

We assume to be working with a weak-perspective camera. So, if we denote 3D points as $X = (X, Y, Z)^T$, and the image 2D points as $x = (x, y)^T$, we can write the projection equation as:

$$x = R \cdot X + t \quad (1)$$

where R is a 2×3 matrix and t a 2D-vector. But, as common in such minimization problems, the translation vector t can be eliminated in advance by choosing the centroid of the points as the origin of the coordinate system. Then, equation (1) is simplified into:

$$x = R \cdot X \quad (2)$$

The goal of the factorization method is to find a reconstruction to minimize geometric error in image coordinate measurements. In other words, the factorization algorithm computes the projections $\{R_f\}$ and the 3D points $\{X_p\}$ (where f is the frame index and p the point index), such that the distance between the estimated image points

$\hat{x}_p^f = R_f \cdot X_p$ and measured image points x_p^i is minimized.

$$\min_{R_f, X_p} \sum_{fp} \| x_p^f - \hat{x}_p^f \|^2 = \min_{R_f, X_p} \sum_{fp} \| x_p^f - (R_f X_p) \|^2 \quad (3)$$

Now, the minimization problem has a very simple form when written as a matrix. Matrix W from equation (4) is built with the bi-dimensional position of the tracked points at each frame (taking into account that at least 4 points are needed) and it is used as input for the equality:

$$W = R \cdot S \quad (4)$$

The factorization algorithm computes two matrices (R and S). If P is the number of tracked points and F is the number of frames: S is a $3 \times P$ matrix which represents the object shape in a coordinate system attached to the object mass center. R is a $2F \times 3$ matrix that encodes the projections for each frame f . It transforms the static object (S) into the same 2D image points (\hat{x}^f) as observed by the camera, which is static.

Equation (4) has not a unique solution, since an arbitrary invertible 3×3 matrix M may be inserted in the decomposition as follows:

$$W = R \cdot S = R \cdot M \cdot M^{-1} \cdot S \quad (5)$$

Those transformations encoded in the M matrix, allow us to transform the shape and consequently the 2D projections in R while the equality is still true. Using this property we upgrade the structure from affine to Euclidian.

The estimated projection for each frame is denoted by R_f , and it is a 2×3 matrix composed by two 3D-vectors as rows (i_f and j_f in figure (2)) which gives us the 2D-point by means of formula (2). We can also understand those projections as a "virtual camera" moving through the scene. This virtual camera shares the same intrinsic parameters with the real one, but moves differently due to object motion. This motion is estimated by the factorization algorithm trying to minimize equation (3). Doing so, in absence of noise, there is an equality between the image points (x^f) and the ones obtained projecting the shape S through R_f .

We transform each frame projection (R_f) into a full camera pose (3-axes of orientation and a 3D position). We reuse the i_f and j_f vectors given by R_f as the right and up camera axis respectively (where f is the frame index) and we obtain the forward axis as the normalized cross product of both.

$$C_f^i = i_f \quad (6)$$

$$C_f^j = j_f \quad (7)$$

$$C_f^k = \frac{(C_f^i \times C_f^j)}{\| (C_f^i \times C_f^j) \|} \quad (8)$$

Then, we have to compute the 3D-vector T_f . This translation vector is the inverted forward axis (C_f^k) of the camera multiplied by the distance between the camera and the

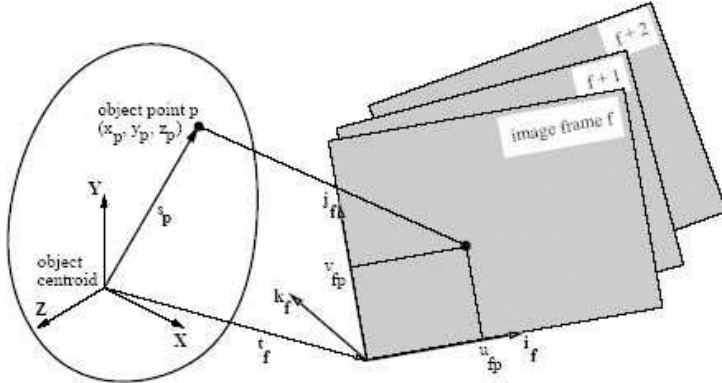


Figure 1. The system of reference in the factorization step.

world coordinate origin. This vector can be understood as the camera position in the world coordinate system.

$$T_f = -C_f^k \cdot d \quad (9)$$

Once we have both the camera axes and its position (T_f), we can build the 3×3 matrix C_f (composed by $C_f^{i^T}$, $C_f^{j^T}$ and $C_f^{k^T}$) representing the orientation of the camera. Now, with T_f and C_f we are able to transform any 3D point from world into camera coordinate system as follows:

$$X^c = C_f \cdot X^w + T_f \quad (10)$$

where the superscripts c (w) refers to camera (world) coordinate system.

After obtaining the virtual camera trajectory, we can use the properties deduced from its motion to estimate the ground plane of the scene. First of all, we know that the virtual camera moves just in the opposite way as the real object does. While the reality consists on a moving object viewed from a static camera, the factorization algorithm output is a static and rigid object viewed from a moving camera. Then, as the virtual camera projection gives us the same bi-dimensional points as the real camera does (in absence of noise), the object movement has to be implicit in the virtual camera to satisfy the equation (3).

For instance, if a real object is rotating 30 degrees over the plane in clockwise, the virtual camera does the rotation in anti-clockwise for 30 degrees while the object shape stills invariant.

Secondly, we know that the tracked vehicles rotate always over the plane (using the plane normal as a rotational axis). So, the virtual camera uses the same axis to rotate around the static object satisfying equation (4), as shown in figure (2).

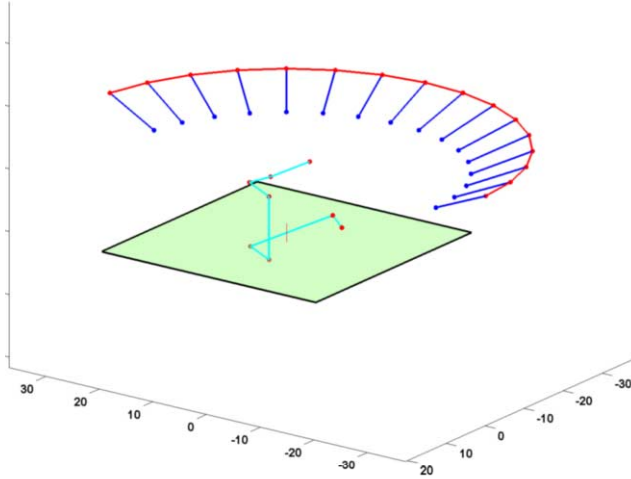


Figure 2. A fixed shape and the virtual camera rotating 180 degrees around the plane normal (different positions and the camera center path are shown), always looking at the center of the object.

Finally, if we know that the camera has no roll-rotation (it is not balanced at any side), we can conclude that the right axis of the virtual camera (C_f^i) will be perpendicular to the plane normal. In consequence, we can use all those vectors to estimate the plane with the well-known *Least Median Squares* method.

Once we have computed the plane, we do a base change for an easier manipulation of the three-dimensional data. With this purpose we build matrix M (in equation (5)) which transforms the arbitrary R^3 space obtained from the factorization into a normalized one, where the normal of the plane estimated corresponds with the *z-axis*. The *x-axis* and *y-axis* will be two arbitrary perpendicular vectors between them and with the *z-axis*, forming all three an orthonormal base. So *z-axis* is the plane normal and *x-axis* and *y-axis* are two vectors in the ground plane.

At this point we can compute the angle θ between the ground plane normal and the camera view direction. This angle is just the mean angle between all the forward vectors of the virtual camera (C_f^k) at each frame and the ground plane normal.

Using the camera pitch angle (θ) we can build the 3-vector axes of the camera. We have assumed that the real camera have no roll-rotation, therefore C_f^i will lie on the plane and then it is possible to chose an arbitrary vector for it, as $(1, 0, 0)$. In consequence, C_f^k will be perpendicular to it with a pitch angle determinated by θ , $C_f^k = (0, \cos(\theta), -\sin(\theta))$, and C_f^j will be the normalized cross product of them.

Finally, if we know the distance (d) between the camera and the central part of the image (the world center), the camera center would be:

$$c_{center} = -d \cdot C_f^k \quad (11)$$

3. 3D Object Motion Estimation

At this point we have already found the camera pose (orientation and position) in correspondence with the ground plane coordinate system. Knowing all the intrinsic parameters of the camera, we are able to transform each bi-dimension point $x(u, v)^T$ of a frame into a 3D real position over the plane $X(x, y, z)^T$.

If we don't know the height of the point (the distance to the ground), it is impossible to do this transformation due the ambiguity of its depth. But if the point is on the surface, or close to it, we can do this transformation easily. We trace a ray from the camera focal center to the scene through the image point x in our image plane. Then, we intersect this ray with the ground plane previously estimated and we obtain the 3D point of the scene.

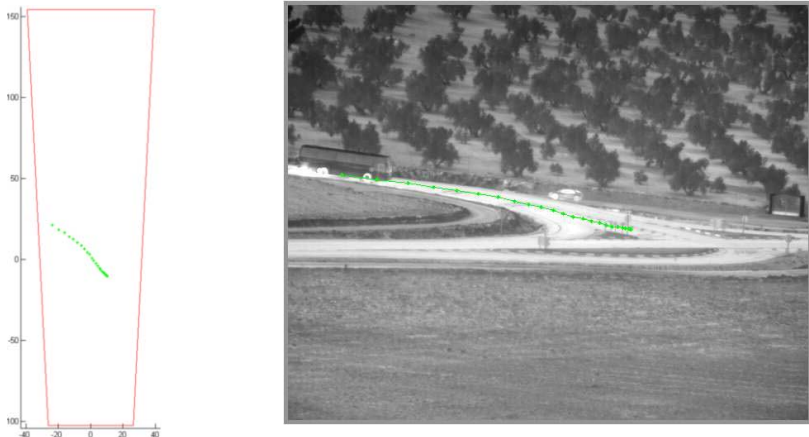


Figure 3. Left image shows the vehicle trajectory computed over the plane (with an estimated 12 degrees inclination) for an object tracked during 25 frames (in a sequence sub-sampled at 2 fps). Right image shows this trajectory projected over the first frame.

For each frame we can estimate the mass center of each object and move it down until the height of the lower tracked point. This set of points plot the object trajectory over the surface, as seen in figure (3).

With this information we are also able to obtain the object real velocity and speed at frame f with:

$$Velocity_f = (X_f - X_{f-1}) \cdot fps \quad (12)$$

$$Speed_f = \| Velocity_f \| \quad (13)$$

where fps are the frames per second of the video.

We can also obtain its orientation and the distance to the camera. As we can see in figure (4), the decreasing speed of the bus due a traffic sign is correctly estimated.

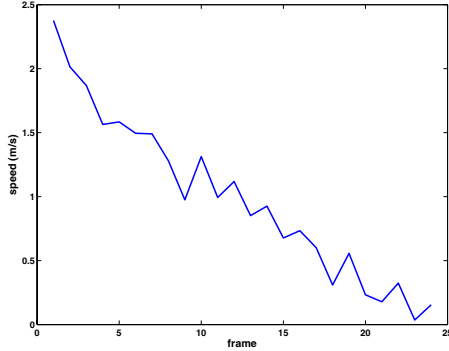


Figure 4. Real speed (in m/sec) estimated for the previous vehicle while it is stopping due a traffic sign. The sharpness is consequence of the tracking noise magnified in the factorization part

4. Conclusions and Future Work

We have presented a new approach to obtain the ground plane of a scene viewed from a static camera. From the specifications of the problem, with a fixed camera, it is important to notice that the plane have to be estimated once. After that, we can re-estimate it using as many objects as wanted, obtaining a very robust plane approximation, with the only restriction that all the objects tracked must move over the same plane. Then, the plane orientation can be used to perform adapted trackings, more accurate homographies estimation, better motion segmentation, etc. achieving more accurate results.

In the experimental tests we have seen that small tracking errors can be magnified in the factorization step giving us noise in the virtual camera movement. One possible solution to this problem is to track points over two (or more) different object faces. Unfortunately, this multi-face tracking is not always possible. In those cases we should track more points during more frames to obtain similar accuracy in the factorization algorithm step.

Although in this paper we present a static camera (with constant position and orientation), we have tested this method for a pivoting camera (with constant position but allowed to rotate). To do this we just needed to compute the homography between frames and use it to transform a 2D pixel position of any frame into the first frame coordinate system, used along the sequence as reference frame. The method used for obtaining this homography is a pyramidal optical-flow based on [9] and [10].

There are several possible directions for the future research. An iterative process using the plane approximation for a better tracking or a Structure from Motion method

done recursively with the planar-moving constraint will make our method more robust.

Another good improvement will be the avoidance of the camera right-vector usage to estimate the plane, using only the path described by the camera positions. Doing so, although we would have to work with less and more noisy information, we would be able to avoid the assumption to have a no roll-rotation camera.

References

- [1] C. Tomasi, T. Kanade: Shape and Motion from Image Streams under orthography: A Factorization approach. *International Journal of Computer Vision*, 9(2):137–154, November 1992.
- [2] C. Yuan, G. Medioni: 3D Reconstruction of Background and Objects Moving on Ground Plane Viewd from a Moving Camera. In *Computer Society Conference on Computer Vision and Pattern Recognition*. pp. 2261–2268, 2006.
- [3] Torresani L., Hertzmann A.: Automatic non-rigid 3D modeling from video. In *European Conference in Computer Vision* (2), pp. 299–312, (2004).
- [4] E. Malis, R.Cipolla: Camera self-calibration from unknown planar structures enforcing the multiview constraints between collineations. *IEEE Pattern Analysis and Machine Intelligence*, 24(9): 1268–1272, 2002.
- [5] R. Hartley, A. Zisserman: *Multiple view Geometry in computer Vision*. Cambridge University Press, 2000.
- [6] D. Comaniciu, V. Ramesh and P. Meer: Real-Time Tracking of Non-Rigid Objects Using Mean Shift. In *Computer Vision and Pattern Recognition*, pp. 142–151, 2000.
- [7] H. Zhang, Z. Huang, W. Huang and L. Li: Kernel-Based Method for Tracking Objects with Rotation and Translation. In *International Conference on Pattern Recognition*, vol. 02, pp. 728–731, 2004.
- [8] B. Martinez, A. Perez, L. Ferraz, X. Binefa: Structure Restriction for Tracking Through Multiple Views and Occlusions In *Iberian Conference on Pattern Recognition and Image Analysis*, col. 01, pp. 121–128, 2007.
- [9] E. Trucco, A. Verri: *Introductory Techniques for 3D Computer Vision*. Prentice Hall, 1998.
- [10] M. Irani, P. Anandan, S. Hsu: Mosaic based representations of video sequences and their applications. In *International Conference on Computer Vision*, pp. 605–611, 1995.
- [11] R.E. Kalman: A new Approach to Linear Filtering and Prediction Problems. *Transaction of the ASME – Journal of Basic Engineering*, pp. 35–45, March 1960.

Weighted Dissociated Dipoles for Evolutive Learning

Xavier BARÓ & Jordi VITRIÀ

Centre de Visió per Computador

Departament de Ciències de la Computació

Universitat Autònoma de Barcelona

{xbaro, jordi}@cvc.uab.cat

Abstract. The complexity of any learning task depends as in the learning method as on finding a good representation of the data. In the concrete case of object recognition in computer vision, the representation of the images is one of the most important decisions in the design step. As a starting point, in this work we use the representation based on Haar-like filters, a biological inspired feature based on local intensity differences. From this commonly used representation, we jump to the dissociated dipoles, another biological plausible representation which also includes non-local comparisons. After analyzing the benefits of both representations, we present a more general representation which brings together all the good properties of Haar-like and dissociated dipoles representations. All these feature sets are tested with an evolutionary learning algorithm over different object recognition problems. Besides, an extended statistically study of these results is performed in order to verify the relevance of these huge feature spaces applied to different object recognition problems.

Keywords. Evolutive learning, Dissociated dipoles, Haar-like features, Adaboost, Object Recognition, Friedman statistic

1. Introduction

Object recognition is one of the most challenging problems in the computer vision field. Given an image, the goal is to determine whether or not the image contains an instance of an object category or not. In the literature there are two main approaches to deal with the object recognition problem: Holistic methods and heuristical local methods.

Holistic methods use the whole image or a region of interest to perform object identification. These systems are typically based on Principal Component Analysis (PCA), Linear Discriminant Analysis (LDA) or on some form of artificial neural net. Although these methods have been used in a broad set of computer vision problems, there are still some problems that cannot be easily solved using this type of approaches. Complex backgrounds, partial object occlusions, severe lighting changes or changes in the scale and point of view represent a problem if they were to be faced under a holistic approach. An alternative are the heuristic local appearance methods or feature based methods, which provide a richer description of the image. In contrast to holistic methods that are problem independent, in this case we should select the type of features which bet-

ter adapts to the problem. We can choose from a wide variety of features, such as the fragments-based representation approach of Ullman [1], the gradient orientation based SIFT [2] or the Haar-like features used by Viola [3].

This paper is related to the feature based methods, namely, our starting point is the Haar-like feature model. Haar-like filters allow a powerful representation of an image using local contrast differences. This representation demonstrated to be a robust description to be applied over object recognition problems, specially in the case of face detection [3]. In addition, the evaluation of these filters using the integral image has a low computationally cost, being potentially useful for real-time applications.

The Haar-like filters are local descriptors, in the sense that they only compare adjacent regions. In [4], Sinha presents the dissociated dipoles, a non-local representation based on region contrast differences. The evaluation is done in the same way that in the case of the previous ones, with the only difference that now the regions do not have the adjacency constraint. In fact, some type of Haar-like features can be represented via dissociated dipoles.

Comparing Haar-like filters and dissociated dipoles, we can see that they share some desired properties as the robustness in front of the noise (they are integral based features) and severe illumination changes (they use region differences, not directly the intensity value). In contrast, the Haar-like have some filters to detect lines that the dipoles cannot simulate, and the dissociated dipoles have the non-local ability which Haar-like approach cannot perform.

In order to collect the good properties of both feature sets, a variant of dissociated dipoles is presented and evaluated. Using weights over the dissociated dipoles, we can represent most of the Haar-like features, obtaining a richer feature space that combines the benefits of both feature sets.

The evaluation of any of the above feature sets consists of the subtraction of the value of all the negative regions from the value of positive regions. Finally, the difference between the regions mean intensity is used to decide to which class a given image belongs.

At this point, two different approaches can be applied: Qualitative or quantitative. Although the most extended approach is the quantitative one used by Viola [3], which consists of finding the best threshold value to make a decision, recent works have demonstrated that qualitative approaches based only on the sign of the difference are more robust in front of noise and illumination changes [5].

All the previous feature sets have in common a high dimensionality, which difficult the application of the classical learning methods. In the case of Haar-like approaches, it is solved by scaling the samples to a small training window where the number of possible features is computationally feasible. In the case of dissociated dipoles, the original image is repeatedly filtered and subsampled to create different levels of the image pyramid. Then, a point in the deeper levels of the pyramid corresponds to the mean value of a region in the upper levels of the pyramid. Thus, we can only consider the relation between points. In this work we use an evolutionary version of Adaboost that is able to work with huge feature spaces, such as the presented before.

This paper is organized as follows: Section 2 describes the features of the three types of features and their properties. Section 3 introduces the qualitative approach to evaluate the features, and section 4 presents the learning strategy. Finally in section 5 we compare and analyze the behavior of each type of feature set using the evolutive approach.

2. Feature set

Selecting a good feature set is crucial to design a robust object recognition system. In this work we use region based features, which consist of differences between the mean values of each region. These features are robust in front of the noise and severe light conditions. In addition, using the integral image (fig. 1), the value of each region is calculated with just 4 accesses.

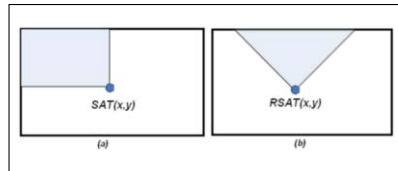


Figure 1. Integral images. Each point contains the sum value of the gray region. *a* Integral image *b* 45° rotated integral image

2.1. Haar-like features

This type of features is a discretized version of the Haar wavelets. Viola used this type of features in their real-time face detector [3] because they are easy to be computed by means of the integral image and in addition they are robust in front of noise and severe illumination changes. The original set of Haar-like features types was extended by Lienhart in [6], adding a rotated version of the original types, and demonstrating that the performance of a classifier is related to the size of the feature space. The extended set of features is shown in fig. 2. The feature set is composed by all the possible configurations of position and scale inside a training window, therefore, learning a classifier using this feature set becomes unfeasible for large window sizes.

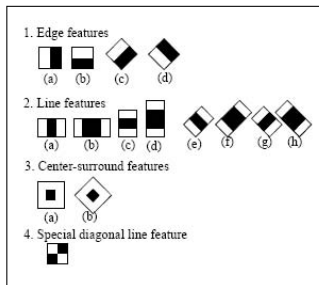


Figure 2. Extended haar-like features.

2.2. Dissociated dipoles

The sticks of dissociated dipoles where defined by Shina in [4]. In these works, the authors perform a set of physical experiments to demonstrate that as in the case of Haar-like features, the dissociated dipoles are a biological plausible type of features. This is a more general feature set, which compares the mean illuminance values of two regions,

the so called excitatory and the inhibitory dipoles (see 3). From a computational point of view, the evaluation of a dissociated dipole has the same cost as the evaluation of a Haar-like feature. They also share the robustness in front of noise and illuminance changes. In fact, the two regions Haar-like features (see edge features in fig. 2) can be represented by means of the dissociated dipoles. The feature set is composed by all the possible sizes and positions of each one of the two regions. Any exhaustive search (i.e Adaboost approach) over this feature set is unfeasible. An application based on scale-image approach can be found in [7].

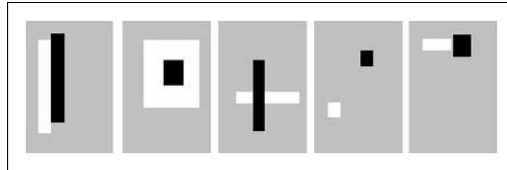


Figure 3. Dissociated dipoles.

2.3. Weighted Dissociated dipoles

Weighted dissociated dipoles are a more general definition of the dissociated dipoles, where each region has an associated weight $W \in \{1, 2\}$. With this simple modification, we can represent all the edge, line and center-surrounding types of the Haar-like feature set. As in the case of the normal dissociated dipoles, the huge dimension difficults the use of this type of features by classical approaches.

3. Ordinal Features

The term of ordinal features is related to the use of the sign instead of directly the value of the feature. In [5], a face detection approach is presented using only the sign of region intensity differences. They demonstrate that removing the magnitude of the difference, the model becomes more stable to illumination changes and image degradation.

4. Evolutive Adaboost

The huge dimensionality of all the explained feature sets is a problem for the classical learning approaches. In [8], an evolutive variation of the classical Adaboost used by Viola in [3] is presented. They propose to change the exhaustive search over the feature space performed by the weak learner by a genetic algorithm (see fig. 4). As a result, learning a classifier is formulated in terms of an optimization problem, where we want to find the parameters of the feature that minimizes the classification error.

To use that approach, we first must define the parametrization of each type of features. Let's denote $R_k = (x, y, W, H)$ the parametrization of the region R_k where the point (x, y) is the upper-left corner, and W and H the weight and height respectively. A dissociated dipole is defined by means of the excitatory and inhibitory regions, and thus we need at least 8 parameters. Analogously, the weighted dissociated dipoles, will be

Given: $(x_1, y_1), \dots, (x_m, y_m)$ where $x_i \in X, y_i \in Y = \{-1, +1\}$

Initialize $D_1(i) = 1/m$

For $t = 1, \dots, T$:

Step 1. Use a genetic algorithm to minimize:

$$\epsilon_t = \Pr_{i \sim D_t}[h_t(x_i) \neq y_i]$$

the given solution is taken as the hypothesis h_t

Step 2. Get weak hypothesis $h_t : X \mapsto \{-1, +1\}$ with error ϵ_t .

Step 3. Choose $\alpha_t = \frac{1}{2} \ln \left(\frac{1-\epsilon_t}{\epsilon_t} \right)$

Step 4. Update:

$$\begin{aligned} D_{t+1}(i) &= \frac{D_t(i)}{Z_t} \times \begin{cases} e^{-\alpha_t} & \text{if } h_t(x_i) = y_i \\ e^{\alpha_t} & \text{if } h_t(x_i) \neq y_i \end{cases} \\ &= \frac{D_t(i) \exp(-\alpha_t y_i h_t(x_i))}{Z_t} \end{aligned}$$

where Z_t is a normalization factor (chosen so that D_{t+1} will be a distribution).

Step 5. Output the final hypothesis:

$$H(x) = \operatorname{sign} \left(\sum_{t=1}^T \alpha_t h_t(x) \right)$$

Figure 4. The evolutive Discrete Adaboost

defined in the same way, but now we need to add two extra parameters $W^+ \in \{1, 2\}$ and $W^- \in \{1, 2\}$ which correspond to the weight of the excitatory and inhibitory regions. Thus, we need at least 10 parameters to describe the weighted dissociated dipoles. Finally, using the restrictions in position and size of the Haar-like features, with only one of the regions and the type of Haar-like feature we can describe all the feature set. Therefore, with just 5 parameters we can describe all that features.

It is important to notice the differences in the descriptor vector, because high dimensions difficult the task of the evolutive algorithm, which must learn a large number of parameters.

5. Results

Once all the feature sets and the evolutive learning approach are exposed, we evaluate the performance of the classifier using the three types of features. First, we describe the data and methodology used to evaluate the performance. Finally, a statistical study of the obtained results is performed in order to analyze the effect of using the different feature sets.

5.1. Performance evaluation

We evaluate the performance of the classifiers over the following tasks:

Face detection: The first task is to learn a face detector. We use the MIT-CBCL face database [9] with a random selection of 1.000 face images and 3.000 non-face images, learning a classifier to distinguish between both classes.

Traffic sign detection: A traffic sign detector must be able to distinct when a given image contains or not an instance of a traffic sign. The experiment is performed using real images acquired in the context of a mobile mapping project provided by the ICC¹. The database consists on 1.000 images containing a traffic sign and 3.000 background images.

Pedestrian detection: In this case, a detector is trained to identify instances of pedestrians. We use the INRIA Person Dataset², with 2.924 images divided into 924 pedestrian instances and 2.000 background images.

Cars detection: This problem consists of detecting instances of a car in urban scenes. We use the UIUC cars database [10], with a total of 1.050 images containing 550 instances of lateral views of different cars and 500 of background images.

Text detection: This task consist on detect text regions in a given image. We use the text location dataset from the *7th International Conference on Document Analysis and Recognition (ICDAR03)*³.

To perform the experiments we fix the maximum number of iterations in the Adaboost algorithm to 200, with a maximum of 50.000 evaluations for the genetic algorithm. The evaluation is carried out using a stratified 10-fold cross validation with a confidence interval at 95% (assuming normal distribution over the error), and the results are shown in figure 5.

The weighted dipoles outperform the other types of features in all the problems used, obtaining good performance rates in all of them. The next step is to check if the observed differences are statistically significant.

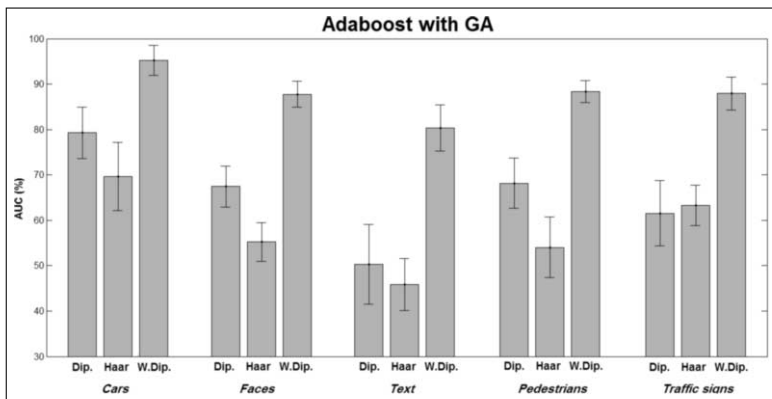


Figure 5. AUC value and confidence intervals.

¹Institut Cartogràfic de Catalunya. www.icc.es

²pascal.inrialpes.fr/data/human/

³algoval.essex.ac.uk/icdar/TextLocating.html

5.2. Statistical analysis

In [11], Demšar performs a study of the validation schemes used in the works published in the International Conferences on Machine Learning between 1999 and 2003, pointing up the main validation errors and wrong assumptions. As a result of his work, Demšar describes a methodology to compare a set of methods over different data sets. In this section, we use that methodology to find out statistical significant differences between the use of the different feature sets used in the present paper. The techniques applied and the numerical results for the statistical study are shown in table 1.

Let r_i^j be the rank of the j -th of k algorithms on the i -th of N data sets. The Friedman test compares the average ranks of algorithms, $R_j = \frac{1}{N} \sum_i r_i^j$. Under the null-hypothesis, which states that all the feature sets are equivalent, and so their average ranks R_j are equal, the Friedman statistic

$$\chi_F^2 = \frac{12N}{k(k+1)} \left[\sum_j R_j^2 - \frac{k(k+1)^2}{4} \right] = 8.4 \quad (1)$$

is distributed according to χ_F^2 with $k-1$ degrees of freedom when N and k are big enough. For a small number of algorithms and data sets, exact critical values have been computed. Iman and Davenport [12] showed that Friedman's χ_F^2 is undesirably conservative and derived a better statistic

$$F_F = \frac{(N-1)\chi_F^2}{N(k-1) - \chi_F^2} = \frac{4 \times \chi_F^2}{10 - \chi_F^2} = 21 \quad (2)$$

which is distributed according to the F -distribution with $k-1 = 2$ and $(k-1)(N-1) = 2 \times 4 = 8$ degrees of freedom. The critical value of $F(2,8)$ for $\alpha = 0.05$ is 4.4590, which is smaller than F_F , so we reject the null-hypothesis. To reject the null-hypothesis indicates that the algorithms are not statistically equivalents.

As the null-hypothesis is rejected, we can proceed with a post-hoc test. In our case, as no algorithm is singled out for comparisons, we use the Nemenyi test for pairwise comparisons. The performance of the two classifiers is significantly different if the corresponding average ranks differ by at least the critical difference

$$CD = q_\alpha \sqrt{\frac{k(k+1)}{6N}} = 1.48 \quad (3)$$

where critical values q_α are based on the Studentized range statistic divided by $\sqrt{2}$. Using averaged ranks in table 1 we calculate all the pair-wise differences. Comparing those differences with the critical value, we can conclude that the Weighted dissociated dipoles are significantly better than the Haar-like features ($2.6 - 1.0 = 1.6 > 1.48$), but we can say nothing about the Dissociated dipoles ($2.8 - 1.0 = 1.8 < 1.48$).

The conclusion of this study is that we can affirm (with $\rho = 0.05$) that the Weighted dissociated dipoles are better than the Haar-like features.

6. Conclusions and future work

Although the tests must be extended to a larger set of databases, the weighted dissociated dipoles demonstrated to perform good in combination with the evolutive strategy. As a

Table 1. Results obtained in the experiments and the obtained rank (AUC)

Data Set	Feature Set		
	Dipoles	Haar-like	Weighted dipoles
Face Det.	67.47% \pm 4.52(2.0)	55.22% \pm 4.23(3.0)	87.74% \pm 2.85(1.0)
Traffic Signs Det.	61.53% \pm 7.17(3.0)	63.30% \pm 4.41(2.0)	87.92% \pm 3.61(1.0)
Pedestrians Det.	68.16% \pm 5.57(2.0)	54.00% \pm 6.68(3.0)	88.40% \pm 2.40(1.0)
Cars Det.	79.27% \pm 5.64(2.0)	69.65% \pm 7.54(3.0)	95.21% \pm 3.28(1.0)
Text Det.	50.33% \pm 8.75(2.0)	45.84% \pm 5.75(3.0)	80.35% \pm 5.08(1.0)
Average Rank	2.20	2.80	1.00

feature work, we plan to extend the study to other evolutive strategies, as the Evolutive Algorithms based on Probabilistic Models (EAPM), which seem that can represent better the relations between the parameters that configure the features.

Acknowledgements

This work has been partially supported by MCYT grant TIC2006-15308-C01, Spain. This has been developed in a project in collaboration with the "Institut Cartogràfic de Catalunya" under the supervision of Maria Pla.

References

- [1] S. Ullman and E. Sali, "Object classification using a fragment-based representation," in *BMVC '00: Proceedings of the First IEEE International Workshop on Biologically Motivated Computer Vision*. London, UK: Springer-Verlag, 2000, pp. 73–87.
- [2] D. G. Lowe, "Object recognition from local scale-invariant features," in *Proc. of the International Conference on Computer Vision ICCV*, Corfu, 1999, pp. 1150–1157. [Online]. Available: citeseer.ist.psu.edu/lowe99object.html
- [3] P. Viola and M. Jones, "Rapid object detection using a boosted cascade of simple features," in *Proceedings of the 2001 IEEE Computer Society Conference on Computer Vision and Pattern Recognition*, vol. 1, 2001, pp. I-511–I-518.
- [4] B. Balas and P. Sinha, "Dissociated dipoles: Image representation via non-local comparisons," Annual meeting of the Vision Sciences Society, Sarasota, FL., 2003.
- [5] K. Thoresz and P. Sinha, "Qualitative representations for recognition," *Journal of Vision*, vol. 1, no. 3, pp. 298–298, 12 2001. [Online]. Available: <http://journalofvision.org/1/3/298/>
- [6] R. Lienhart and J. Maydt, "An extended set of haar-like features for rapid object detection," in *Proceedings of the International Conference on Image Processing*. Rochester, USA: IEEE, September 2002, pp. 900–903.
- [7] F. Smeraldi, "Ranklets: orientation selective non-parametric features applied to face detection," in *Proceedings. 16th International Conference on Pattern Recognition*, vol. 3, 2002, pp. 379–382.
- [8] X. Baró and J. Vitrià, "Real-time object detection using an evolutionary boosting strategy," *Frontiers in Artificial Intelligence and Applications / Artificial intelligence Research and Development, IOS Press, Amsterdam*, pp. 9–18, October 2006.
- [9] "MIT-CBCL face database." [Online]. Available: cbcl.mit.edu/projects/cbcl/software-datasets/FaceData1Readme.html
- [10] S. Agarwal, A. Awan, and D. Roth, "UIUC cars database." [Online]. Available: l2r.cs.uiuc.edu/~cog-comp/Data/Car/
- [11] J. Demšar, "Statistical comparisons of classifiers over multiple data sets," *JMLR*, vol. 7, January 2006. [Online]. Available: <http://jmlr.csail.mit.edu/papers/v7/demsar06a.html>
- [12] R. L. Iman and J. M. Davenport, "Approximations of the critical region of the friedman statistic," in *Communications in Statistics*, 1980, pp. 571–595.

Blood Detection In IVUS Longitudinal Cuts Using AdaBoost With a Novel Feature Stability Criterion¹

David ROTGER ^{a,b,2}, Petia RADEVA ^a, Eduard FERNÁNDEZ-NOFRERÍAS ^c and Josepa MAURI ^c

^a Computer Vision Center, Autonomous University of Barcelona

^b Computer Science Department, Autonomous University of Barcelona

^c University Hospital Germans Trias i Pujol, Badalona

Abstract. Lumen volume variations is of great interest by the physicians given the more it increases with a treatment the less probability of infarction. In this paper we present a fast and efficient method to detect the lumen borders in longitudinal cuts of IVUS sequences using an AdaBoost classifier trained with several local features assuring their stability. We propose a criterion for feature selection based on stability leave-one-out cross validation. Results on the segmentation of 18 IVUS pullbacks show that the proposed procedure is fast and robust leading to 90% of time reduction with the same characterization performance.

Keywords. IVUS, Blood detection, AdaBoost, Texture analysis

1. Introduction

Intravascular Ultrasound Images (IVUS) are an excellent tool for direct visualization of vascular pathologies and evaluation of the lumen and plaque in coronary arteries. However, visual evaluation and characterization of plaque require integration of complex information and suffer from substantial variability depending on the observer. This fact explains the difficulties of manual segmentation prone to high subjectivity in final results. Automatic segmentation will save time to physicians and provide objective vessel measurements [1]. Nowadays, the most common methods to separate the tissue from the lumen are based on gray levels providing non-satisfactory segmentations. This leads to use more complex measures to discriminate lumen and plaque. One of the most wide spread methods in medical imaging for such task is texture analysis. The problem of texture analysis has played a prominent role in computer vision to solve problems of object segmentation and retrieval in numerous applications [2,3]. This approach, encodes the textural features of our image, and provide a feature space in which a classification based on such primitives is easier to perform.

¹This work was supported in part by a research grant from projects TIN2006-15308-C02 and FIS-PI061290.

²Correspondence to: David Rotger Muñoz, Computer Vision Center, Edifici O, Campus UAB, 08193 Bellaterra (Cerdanyola), Spain. Tel.: +34 93 581 18 28; Fax: +34 93 581 16 70; E-mail: rotger@cvc.uab.cat.

In general, two approaches are used for texture analysis: supervised and unsupervised analysis. Our scheme will use supervised texture analysis. Texture analysis has an important problem in both approaches, the precise location of textured object boundaries. Previous works in segmentation of IVUS images have shown different ways to segment lumen and to classify tissues [4,5,6]. However, these approaches usually are semi-automatic and very sensitive to image artifacts. The classification process is a critical step in any image segmentation problem. Arcing and boosting techniques have been applied successfully to different computer vision areas. In this paper we analyze the relevance of boosting techniques, and in particular AdaBoost in Intravascular Ultrasound Image analysis for a dual task, creation of a strong classifier and feature selection. Moreover, we propose a fast, efficient and robust process to detect blood in IVUS image sequences. This process is integrated in an automatic framework for discrimination of lumen and tissue in longitudinal cuts of the IVUS sequence of images (figure 1). The method is divided in 4 steps, corresponding to feature extraction, feature selection, classification and higher level organization of data using deformable models. An objective evaluation of the different approaches is made and validated by the physicians in patients with different pathologies and images with different topologies.

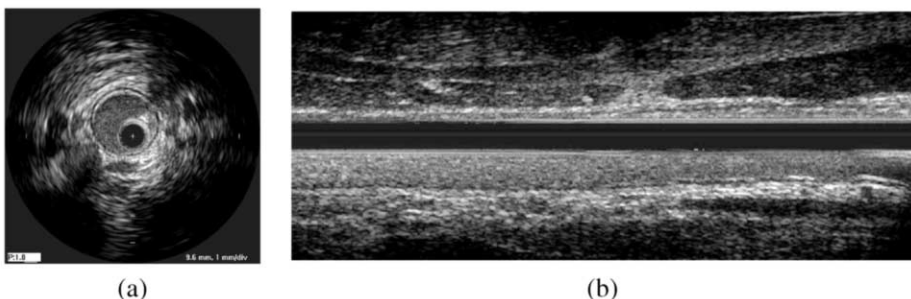


Figure 1. IVUS images: (a) original cartesian image, (b) Longitudinal cut at 45° of the IVUS sequence

2. Methods

We propose an algorithm for fast and accurate detection of the lumen borders on a longitudinal cut of IVUS sequence that consists on a pixel classification step followed by a morphological postprocessing and a final segmentation.

In order to detect the lumen borders in the IVUS sequences we use a learning approach, in particular the AdaBoost (Adaptive Boosting) classifier formulated by Freund and Schapire in [7]. This technique is a supervised learning and classification tool, created as a method for combining simple classifiers in a multiple classifier in order to obtain a very accurate precision. Roughly, it is an iterative assembling process in which each classifier is devoted to find a good division of the sub-set points formed by the samples that are more difficult classified by the "weak" classifiers estimated up to that point. It is recognized as one of the most accurate processes for high accuracy classification.

2.1. AdaBoost procedure

AdaBoost is an iterative method that allows the designer to keep adding "weak" classifiers until some desired low training error has been achieved [7,8]. At each step of the process, a weight is assigned to each of the feature points. These weights measure how accurate the feature point is being classified at that stage. If it is accurately classified, then its probability of being used in subsequent learners is reduced, or emphasized otherwise. Thus, AdaBoost focuses on difficult training points at each stage.

The classification result is a linear combination of the "weak" classifiers. The weight of each classifier is proportional to the amount of data that classifies in a correct way.

2.2. AdaBoost as feature selection process

As an additional feature, AdaBoost is capable of performing a features selection process while training. In order to perform both tasks, feature selection and classification process, a weak learning algorithm is designed to select the single features which best separate the different classes. That is, one classifier is trained for each feature, determining the optimal classification function (so that the minimum number of feature points is misclassified). And then, the most accurate classifier-feature pair is stored at that stage of the process. If feature selection is not desired, the weak classifier focuses on all the features at a time.

The original training set consisted on vectors of 263 features concerning the gray level of the image, the gradient image, a mean of the gray level of the neighbor cuts, the standard deviation, mean and a division between both of local windows of different sizes surrounding the evaluated pixel, a bank of Gabor filters (a special case of wavelets, see [9]) for several frequencies and orientations, Co-occurrence Matrices (defined as the estimation of the joint probability density function of gray level pairs in an image [10]), Local Binary Patterns [11] and Fast Fourier Transform of local windows of different sizes surrounding the evaluated pixel.

2.3. Stability criterion of the selected features

AdaBoost tries to assure the better performance given the training set and the set of features. But several authors have discussed that even the good performance of the classifier, the stability of the features selected is not warranted.

Moreover, in [12] authors assure that 'Learning from examples' is a paradigm in which systems learn a functional relationship from a training set of examples. Within this paradigm, a learning algorithm is a map from the space of training sets to the hypothesis space of possible functional solutions. A central question for the theory is to determine conditions under which a learning algorithm will generalize from its finite training set to novel examples. Therefore, we will need to characterize conditions on the hypothesis space that ensure generalization for the natural class of empirical risk minimization (ERM) learning algorithms that are based on minimizing the error on the training set.

In [13] Feature Space Mapping model is proposed. It describes an adaptive system that measures the contribution of each feature to the final classifier, useful on the reduction of multidimensional searches to a series of one-dimensional searches. It is an exhaustive method to assure that each feature added to the system, combined with the rest, does not decrease the performance of the classifier.

To assure the stability of the features selected by the AdaBoost classifier and to reduce the variance of the error of classification due to a bad election of the samples, we propose a method based on the combination of the features selected by several AdaBoost classifiers taking into account their weight at each classifier.

We left all the samples concerning to the IVUS pullbacks performed to one of the patients out at each time and trained a classifier with a randomized set of samples of the rest of the patients data.

Given that we wanted to speed up the process of blood detection in order to make it feasible in the day by day clinical practice, we did a feature study similar to Feature Space Mapping [13]. We started with a classifier trained with only the feature of maximal accumulated weight ($\epsilon = \max \omega$) up to a classifier trained with the 15 most relevant features taking into account their accumulated weights.

The feature selection algorithm for N trials following leave-one-patient-out strategy can be defined as follows:

Let C_i be the i^{th} AdaBoost classifier defined as:

$$C_i = \sum_{j=1}^{m_i} \omega_j f_j \quad (1)$$

where ω_j is the weight Adaboost has assigned to the j^{th} feature (f_j).

We define a sub-feature space S_i with the features with higher ω :

$$S_i = \{f_j, j \in 1, m_i | \omega_j > \epsilon\} \quad (2)$$

Note: $|S_i| \leq m_i$ and $\epsilon \leq \max \omega$

We then define a sub-feature space of the most stable features as:

$$S = \{f_j / f_j \in \bigcap_{i=1}^N S_i\} \quad (3)$$

We can then train a final AdaBoost classifier with all the features of S revealed as the more stable.

The results were "surprising" given that, as we can see in figure 2 only 5 features were necessary to obtain an output similar to the one obtained with the 84 features selected by the original classifier.

2.4. Postprocessing and segmentation of the lumen

Once we have the output of the classifier obtained, we filtered it to remove scattered misclassified pixels using mathematical morphology to smooth the results and adapt a snake to them.

The morphological filters used are a majority filter (sets a pixel to 1 if five or more pixels in its 3-by-3 neighborhood are 1's; otherwise, it sets the pixel to 0) to connect isolated points and an opening (erosion followed by dilation) of the obtained result with a cross as structuring element (see [14]).

The last step to detect the lumen border is to adapt a B-Snake model to the output of a distance map of the Canny edges (without loss of generality) of the previously obtained image (see [15,16,17]). Figure 3 shows the result of the filtering (a) and the adapted B-Snake model (b).

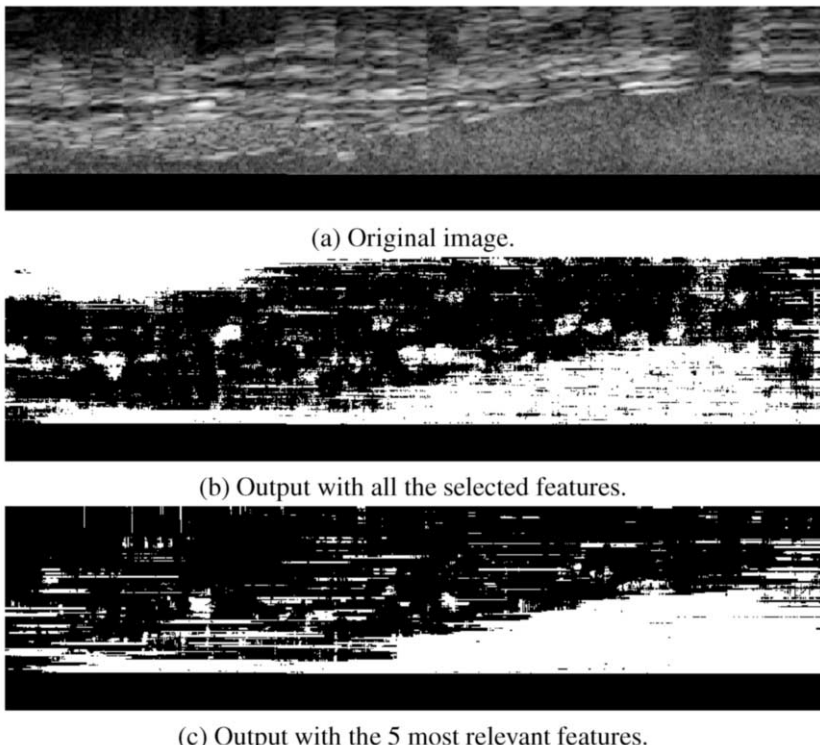


Figure 2. Output of the classifier trained with different features.

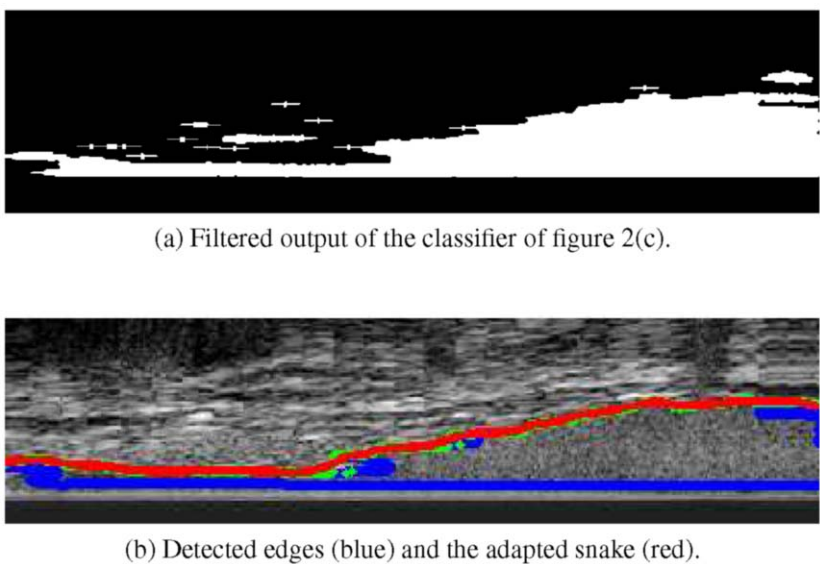


Figure 3. B-Snake model adapted to the filtered classifier output.

3. Results

A deep validation process was performed to test the stability criterion, the performance of the final classifier and the speed up of the process.

First of all, we wanted to validate our feature stability criterion. We trained 9 different classifiers. As we said before, to assure the stability of feature set, we left all the samples concerning to the IVUS pullbacks performed to one of the patients out at each time and trained a classifier with a randomized set of samples of the rest of the patients data, performing a real leave-one-out cross validation.

Each classifier reduced the dimensionality of the feature set from 263 initial features to approximately 36 by mean (see figure 4). But if we accumulate the results of all the classifiers, we can see that 84 different features were selected by at least one classifier, that is 179 features have not been selected by any classifier (see figure 5). Moreover, the selected features with higher weights are not the same in all the cases, showing the problem of stability in the feature selection using AdaBoost.

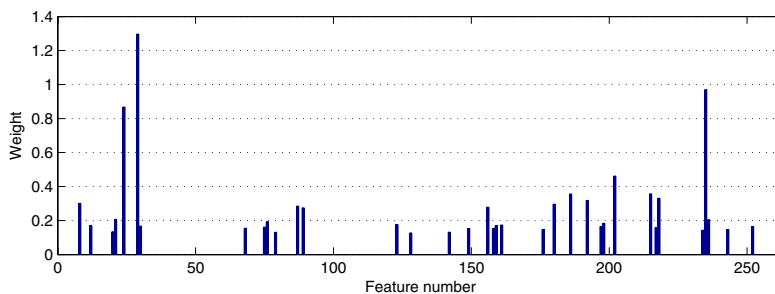


Figure 4. Selected features by one AdaBoost classifier and their weights.

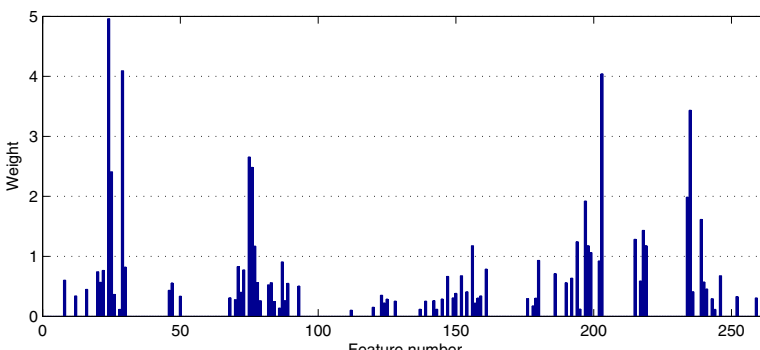


Figure 5. Addition of all the weights assigned by all the trained AdaBoost classifiers for each feature.

In terms of performance, we have trained new classifiers (always following the leave-one-out strategy for the cross validation) with a feature set increasing from 5 up to 15 features. Beginning with a classifier trained with the 5 features of higher weight of figure 5, at each step, we added a new feature, trained a new AdaBoost classifier and tested its performance. Figure 6 shows a plot of the evolution of the mean error, standard deviation and the median of the error of each multiple classifier.

In terms of speed, the most of the features with higher weight in figure 5 take almost the same time in being computed, so we can speed up the process by choosing a number

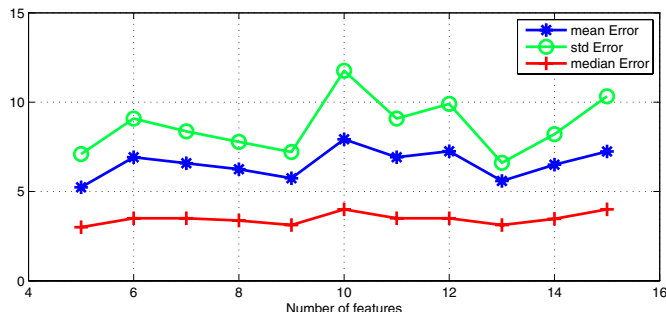


Figure 6. Evolution of the mean error (in blue, stars), standard deviation (in green, circles) and the median of the error (in red, crosses) of each multiple classifier

of features as low as possible. We can see in figure 6 that choosing a classifier trained with only 5 features we can achieve very good performance and the speed of the process has increased more than the 90% in comparison with the first approach of 84 features. We can now process a 2400 images cut in a mean time of 1.32 minutes (without code optimizations, written in MatLab) and taking into account that the most of this time is devoted to the sequence decompression and the generation of the cut. Figure 7 shows the result in the segmentation of a 2400 images longitudinal cut with only 5 features selected.

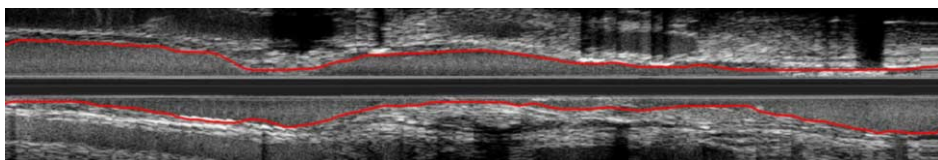


Figure 7. Result of the lumen border detection with a multiple classifier trained with 5 features.

4. Conclusions and future work

We have proposed a novel stability criterion for feature selection with AdaBoost multiple classifiers and applied it for speeding up the blood detection in an IVUS sequence with great performance.

We have seen that with a multiple classifier trained with only 5 "well chosen" features we can detect the lumen borders of any longitudinal IVUS cut with a mean error of 5.24 pixels (0.105 mm) in 1.32 minutes. We have not observed any preference in the results for any classical texton feature. Due to the nature of the data, std and mean of sliding windows of 35 to 45 pixels were selected with a higher weight (ω) in the most of the cases as the better descriptors. It is needed to say that this time can be reduced programming the feature calculation and the cut generation with a compiled language like C++ instead of our approach in MatLab.

The results are very promising to be applied in volume calculations to evaluate, for example, the effect of different drugs. In combination with three-dimensional reconstruc-

tion of the vessel shape using angiography and exact correspondence with the IVUS data as proposed in [18], we can compute the volume of any vessel in a very fast and accurate way.

References

- [1] M. Sonka, X. Zhang, M.S.e.a.: Segmentation of intravascular ultrasound images: A knowledge based approach. *IEEE Trans. on Medical Imaging* **14** (1995) 719–732
- [2] J. Malik, S. Belongie, T.L., Shi, J.: Contour and texture analysis for image segmentation. *International Journal of Computer Vision* **43** (2001) 7–27
- [3] J. Puzicha, T.H., Buhmann, J.: Unsupervised texture segmentation in a deterministic annealing framework. *IEEE Trans. on Pattern Recognition and Machine Intelligence* **20** (1998) 803–818
- [4] X. Zhang, C.M., Sonka, M.: Tissue characterization in intravascular ultrasound images. *IEEE Trans. on Medical Imaging* **17** (1998) 889–899
- [5] von Birgelen, C., van der Lugt, A., et al., A.N.: Computerized assessment of coronary lumen and atherosclerotic plaque dimensions in three-dimensional intravascular ultrasound correlated with histomorphometry. *American Journal of Cardiology* **78** (1996) 1202–1209
- [6] Klingsmith, J., Shekhar, R., Vince, D.: Evaluation of three-dimensional segmentation algorithms for identification of luminal and medial-adventitial borders in intravascular ultrasound images. *IEEE Trans. on Medical Imaging* **19** (2000) 996–1011
- [7] Freund, Y., Iyer, R.D., Schapire, R.E., Singer, Y.: An efficient boosting algorithm for combining preferences. In Shavlik, J.W., ed.: *ICML*, Morgan Kaufmann (1998) 170–178
- [8] Viola, P., Jones, M.: Rapid object detection using a boosted cascade of simple features (2001)
- [9] Daugman, J.: Uncertainty relation for resolution in space, spatial frequency and orientation optimized by two dimensional visual cortical filters. *Journal of the Optical Society of America* **2** (1985) 1160–1169
- [10] Dubes, R., Ohanian, P.: Performance evaluation for four classes of textural features. *Pattern Recognition* **25** (1992) 819–833
- [11] T. Ojala, M.P., T. Maenpaa: Multiresolution gray-scale and rotation invariant texture classification with local binary patterns. *IEEE Transactions on Pattern Analysis and Machine Intelligence* **27** (2002) 971–987
- [12] Tomaso Poggio, Ryan Rifkin, S.M., Niyogi, P.: General conditions for predictivity in learning theory. *Letters to Nature* **428** (2004) 419–422
- [13] Duch, W., Diercksen, G.H.F.: Feature Space Mapping as a universal adaptive system. *Computer Physics Communications* **87** (1995) 341–371
- [14] Haralick, R.M., Shapiro, L.G.: Computer and Robot Vision. Volume I. Addison-Wesley Longman Publishing Co., Inc., Boston, MA, USA (1992)
- [15] Michael Kass, A.W., Terzopoulos, D.: Snakes: Active contour models. *International Journal of Computer Vision* **1** (1998) 321–331
- [16] McInerney, T., Terzopoulos, D.: Deformable models in medical images analysis:a survey. *Medical Image Analysis* **1** (1996) 91–108
- [17] Canny, J.: A computational approach to edge detection. *IEEE Trans. Pattern Anal. Mach. Intell.* **8** (1986) 679–698
- [18] Rotger, D., Rosales, M., Garcia, J., Pujol, O., Mauri, J., Radeva, P.: Activevessel: A new multimedia workstation for intravascular ultrasound and angiography fusion. In: Proc. IEEE of Computers in Cardiology. Volume 30. (2003) 65–68

A colour space based on the image content

Javier Vazquez^{a,1}, Maria Vanrell^a, Anna Salvatella^a and Eduard Vazquez^a

^a *Computer Vision Center/Computer Science Department, Edifici O - Campus UAB*

Abstract. The main goal of this paper is to define a new colour space that represents the colour information of the image in such a way to give a more coherent spatio-chromatic representation. This space can allow to improve the performance of the algorithms of blob detection. To build the space we base colour representation on the ridges of the colour image distribution since it has been proved that they capture the essential colours of the image. Then we will define a colour space where each channel depends on one of the ridges. Finally, to select the essential channels we apply a Constraint Satisfaction algorithm that allows to get a reduced number of channels minimizing the correlation between them.

Keywords. colour space, blob detection

1. Introduction

In this work we propose a new colour space that adapts to the image content. The final goal for this new space is to achieve the best representation of colour information for a specific visual task. In particular, we focus on optimal representations for computational detection of colour blobs. Our proposal is a colour space that pursue the criterion of minimum inter-channel correlation. As a consequence of the procedure defined to build the space it also presents the property of similar entropy in all the channels.

In colour science a lot of different colour spaces have been defined [10]. Each one presenting different properties for different purposes. For instance, uniform spaces, such as, CIELAB or CIELUV, allow an Euclidean metric to represent perceptual similarity. Other spaces as RGB or CMY have been the basis for building acquisition, visualization or printing devices. In this paper we propose to define a new colour space that pursue a good representation to better extract the image content. As we already mentioned above, we will adapt the colour information to improve the detection of coloured image blobs.

Detection of coloured image blobs is a low-level visual task of a great importance in computer vision. In computer vision an image blob is a connected image region that presents an homogeneous colour. A successful extraction of image blobs can be the basis to overcome the subsequent steps in the image understanding process. Blob extraction is essential in the first steps of texture description [4], background subtraction [2],[3],

¹Correspondence to: Javier Vázquez Corral, Computer Vision Center/Computer Science Department, Edifici O - Campus UAB, 08193 Bellaterra (Barcelona), Spain Tel.: +34 935 811 828; Fax: +34 935 811 670; E-mail: jvazquez@cvc.uab.es.

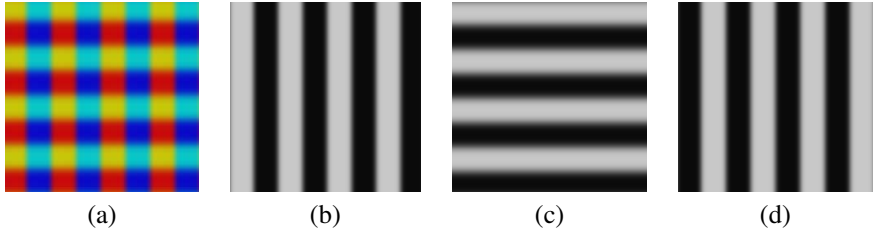


Figure 1. RGB channels of image (a), where (b) in the red channel, (c) the green channel, and (d) the blue channel

or motion analysis [5]. The computational approaches to deal with blob extraction have been essentially developed for gray-level images [6], where the laplacian filtering is the basis to extract image blobs. However, not such an effort has been done to extend this theory to colour images, and usually, the extension is done by just applying the gray-level algorithms on each colour channel separately. Hence the final detection of blobs is the combination of the blobs detected separately on each colour channel, usually red, green and blue. However, in figure 1 we can see that detecting blobs in RGB channels separately, does not assure to get the blobs we perceive in the colour image, in this case we can see small non-elongated blobs in red, yellow, light blue and dark blue, whereas in the RGB channels we have long elongated blobs in different orientations.

The results of this work are framed in the context of a project on automatic image annotation, where one of the goals is the description of textures. There are different approaches to extract and describe texture information and several works discuss how to deal with coloured texture [8]. A type of approaches are those that build the texture description based on the attribute of its blobs, following psychophysical theories [4]. These are the ones that motivates the goal of this paper, that is, to build a colour space that provide an adequate representation to detect colour image blobs as the basis for colour-texture description.

To this end, this paper has been organized as follows. In section 2 we introduce an algorithm to extract the essential colour information of an image, that is, the ridges of the colour distribution. Afterwards, in section 3 we propose a procedure to build a new colour representation based on this essential ridges. In section 4 we propose a method to reduce the number of dimensions of this new space, using a constraint satisfaction algorithm that allow to evaluate the feasibility of our proposal. Finally, we sum up the conclusions and explain different lines of research, since this is just a new research line we are just beginning to explore in this work.

2. Colour-Content Structure

In order to be able to define a colour space with the properties we have expressed above, we will need to extract the essential information of the image content. To this end we will extract this information dealing with the results of a recent work from Vazquez -et al [9] where they propose to cope the essential colour structure of an image by extracting the ridges [7] of the 3D colour distribution. In figure 2 we can see an example of the ridges of the image given in figure 1.(a). In figure 2.(a) we show a 3D coloured representation

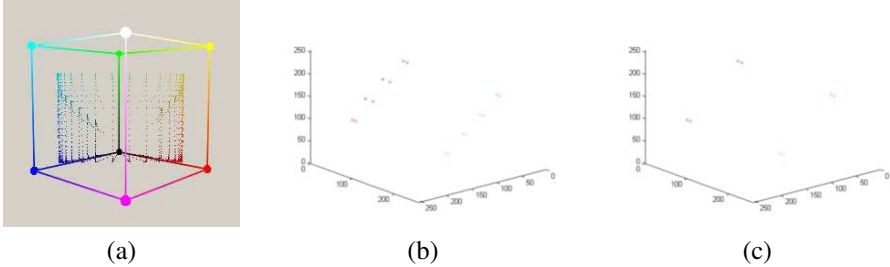


Figure 2. Explanation of the ridges of the image 1.(a). In (a) we could see a 3D coloured representation of the image, (b) are the detected ridges and (c) are the important ones

that gives an idea of its colour distribution. Figure 2.(b) gives the ridges detected by the method and in figure 2.(c) we show a simplification after removing the noisy ridges as we will explain in next section. This reduction let us to represent the four principal colours we perceive in the original image, these are red, yellow, dark blue and light blue.

It has been proved in [9] that ridges fulfill two essential properties which are those that allow them to cope the colour structure, these are:

- Connectivity of all the points in a ridge, that assure the connectivity of the influence zone.
- Peak and valley subtraction, since the ridges extract all the distribution maxima plus all their nearby important colours.

Therefore, we will use this reduced representation of the essential image colour as the basis, in some sense, of our proposal for a new space. We can do it, by considering that any image point will belong to an influent zone of a ridge, that is to an essential colour. Influent zones are computed from the Voronoi diagram of the ridges on the colour distribution. The RGB values of an image point will determine to which influence zone it belongs.

3. Content-Based Colour Space

Before to define how to compute our proposal for a content-based colour space (CBCS), we will specify which are the main requirements we pursuit with it:

1. Distances in this space should correlate with perceived colour differences
2. Important blobs must maintain its perceived geometric structure
3. Each space dimension should represent a different colour property in order to cope with most of the color information.
4. All important blobs should appear at least in one of the space dimensions.

To fulfill these requirements we propose a colour space whose dimension will coincide with the number of important ridges we extract. We decide this number applying a preprocessing step on the ridges obtained with the algorithm of section 2. It is based on an iterative process that reduces those ridges containing a minimum number of pixels in its influence zone, afterwards all these points are redistributed to the remaining ridges. This is repeated iteratively until we achieve a prefixed number of ridges that will be the number of channels of our proposed colour space. The number of ridges we select will

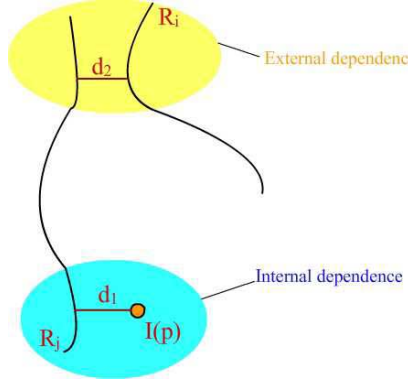


Figure 3. Scheme of ridge distances used to build the space.

determine the amount of information we are able to represent and this number will allow to fulfill the requirement 4 we have established before.

Therefore, each image channel will be related to a specific ridge. Considering that each image pixel belong to the influence zone of one specific ridge, we propose to build the components of pixel in the new space by using two distances, these are:

- The distance between the ridge of the pixel and the ridge of the channel
- The distance between the pixel and the ridge it belongs to.

This proposed distances, as it can be seen in figure 3 are representing two different dependencies, an internal dependency only depending on the pixel and its own ridge, and another external depending on the ridge of the channel. These two dependencies let the method to accomplish requirements 1 and 2.

Hence, we propose to build the i -component of a pixel p , we denote as $Ch_i(p)$ as

$$Ch_i(p) = \frac{Y_m}{\max_{q \in I} h(q)} h(p) \quad (1)$$

where p, q are pixels of the image $I : \mathbb{R}^2 \rightarrow \mathbb{R}^3$, Y_m is the maximum intensity of the channel and

$$h(p) = \max_{q \in I} (f(q)) - f(p), \quad (2)$$

where $h(p)$ takes the 0 when p is the farthest pixel to ridge i , and $h(p)$ takes its maximum when p is the nearest, where $f(p)$ is representing the distance of p to the ridge i and its defined as:

$$f(p) = k_1 d_1(I(p), R_j) + k_2 d_2(R_i, R_j) \quad (3)$$

that weights the pixels of the new channel according to the distance to the image ridges, which are denoted as R_k , and depends on the image content. In this case, R_i is the ridge related to the i channel, and R_j is the ridge whom pixel p belongs to. Distances d_1 and d_2 are defined as

$$d_1(\vec{x}, R_j) = \inf_{\vec{y} \in R_j} d(\vec{x}, \vec{y}) \quad (4)$$

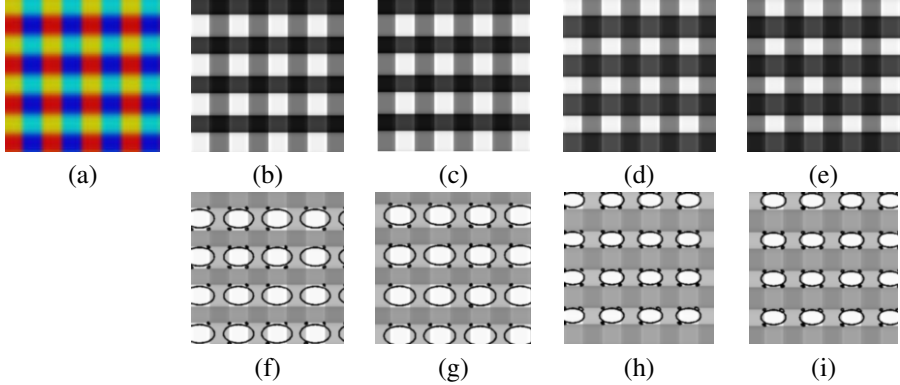


Figure 4. CBCS channels (b),(c),(d),(e) of an original image (a), and results of a blob detection (f),(g),(h),(i) in these channels where red, dark blue, yellow and light blue blobs are detected in this order

that is the infim distance between a point of the RGB space and its own ridge, and

$$d_2(R_i, R_j) = \inf_{\vec{x} \in R_i, \vec{y} \in R_j} d(\vec{x}, \vec{y}) \quad (5)$$

is the distance between two ridges, that is also computed by the infim distance between their points; $d(\vec{x}, \vec{y})$ is the euclidean distance between any two points, \vec{x}, \vec{y} of the space.

Finally, k_1 and k_2 are scalar factors that can be used to establish the entropy of the channels we have built. Depending on the distance between ridges we could serve these factors to order the ridges an increase or decrease the entropy, this would require to define k_2 as a vector of scalar factors, one for each $d_2(R_i, R_j)$.

In figure 4 we can see the results of the original image in figure 1 in our colour space at this level and the capability of our space to detect the four different types of blobs: red, yellow, light blue and dark blue.

4. Dimension reduction and evaluation

Once we have built a proposal for a content-based colour space, now we will try to see how the requirement 3 is fulfilled. That is, we propose to analyze what is the information included in each channel by the proposed space. We have proposed an algorithm based on a fixed number of channels, let say n . In this section we propose a constraint satisfaction algorithm that will allow to select a reduced version of the CBCS space based on the selection of channels that best represent all the image blobs.

The Constraint Satisfaction algorithm will allow to select a smaller number, m (where $m < n$), of channels selecting those ones that maximize the premise of better blob representation. We can see this process as searching the best m channels of the n dimensional CBCS representation fulfilling the constraint of minimum inter-channel correlation, that is to minimize:

$$F(a_1, \dots, a_m) = \sum_{i=1:m, j=1:m, i>j} |r(a_i, a_j)| \quad (6)$$

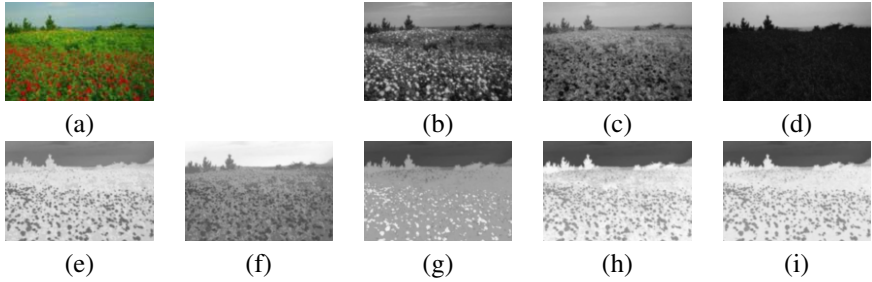


Figure 5. RGB channels and CBCS channels from an image. (b),(c),(d) are the RGB channels from image (a), and (e),(f),(g),(h),(i) are the CBCS channels where (h),(i) are the rejected ones

where $(a_1, \dots, a_m) \in A$, $A = (a_1, \dots, a_n)$ is the set of channels and r is the correlation coefficient computed as:

$$r(a_i, a_j) = \frac{\sum_{k=1:n} (x_k - \bar{x})(y_k - \bar{y})}{(n - 1)s_x s_y} \quad (7)$$

where x_k, y_k are the values of the pixels in each channel, \bar{x}, \bar{y} are the mean of these values and s_x, s_y are the standard deviation of these values.

The m-dimensional representation we can derive as a solution of this constraint satisfaction problem allow to achieve requirement 3.

To evaluate the performance of this new colour space we have posed an experiment over a set of 200 images, built from the Mayang image dataset and from the Vistex image dataset. On these images we have computed the ridges of their colour distribution and we have computed their CBCS representation for $n = 5$. Afterwards we have applied a constraint satisfaction search on these channel and we have selected those dimensions minimizing interchannel correlation, we have done it for $m = 3$.

This experiment has allowed to compare this new representation to the classical RGB representation. While the RGB representation presents a mean inter-channel correlation of 2.41, the CBCS space for $m = 3$ achieve a mean inter-channel correlation of 1.29.

In figures 5 and 6 we show some examples of the 3-dimensional CBCS we have computed by applying the minimum inter-channel correlation criterion.

In fact, in figure 5 we could see from image 5.(a), their RGB channels 5.(b),5.(c),5.(d) in RGB order, and, as in this case CBCS space has been done with $n = 5$ and $m = 3$, five CBCS channels where 5.(e),5.(f),5.(g) are the channels selected by the Constraint Satisfaction algorithm and 5.(h),5.(i) are the rejected ones. We can see that in RGB channels information could be essentially found in 5.(b). On the other hand, in CBCS channels we found some regions of the plants in 5.(e), the sky in 5.(f), and the red flowers in 5.(g). In this channel we could also try to find yellow flowers with a detection of low intensity blobs. Furthermore, we can see that refused channels 5.(h),5.(i) are quite similar to 5.(e), this means they have a great correlation coefficient between them.

Finally, in figure 6 we can see the CBCS channels of some images (images on the left of each group), and, multiplying each channel by the image (images on the right), it is easy to percept what is the detected part of the image in this channel. For example, in 6.(b) it is quite clear that we detect the two different kinds of flowers in the second and the third channel and also one part of the plants in the first. It is also clear that in 6.(c)

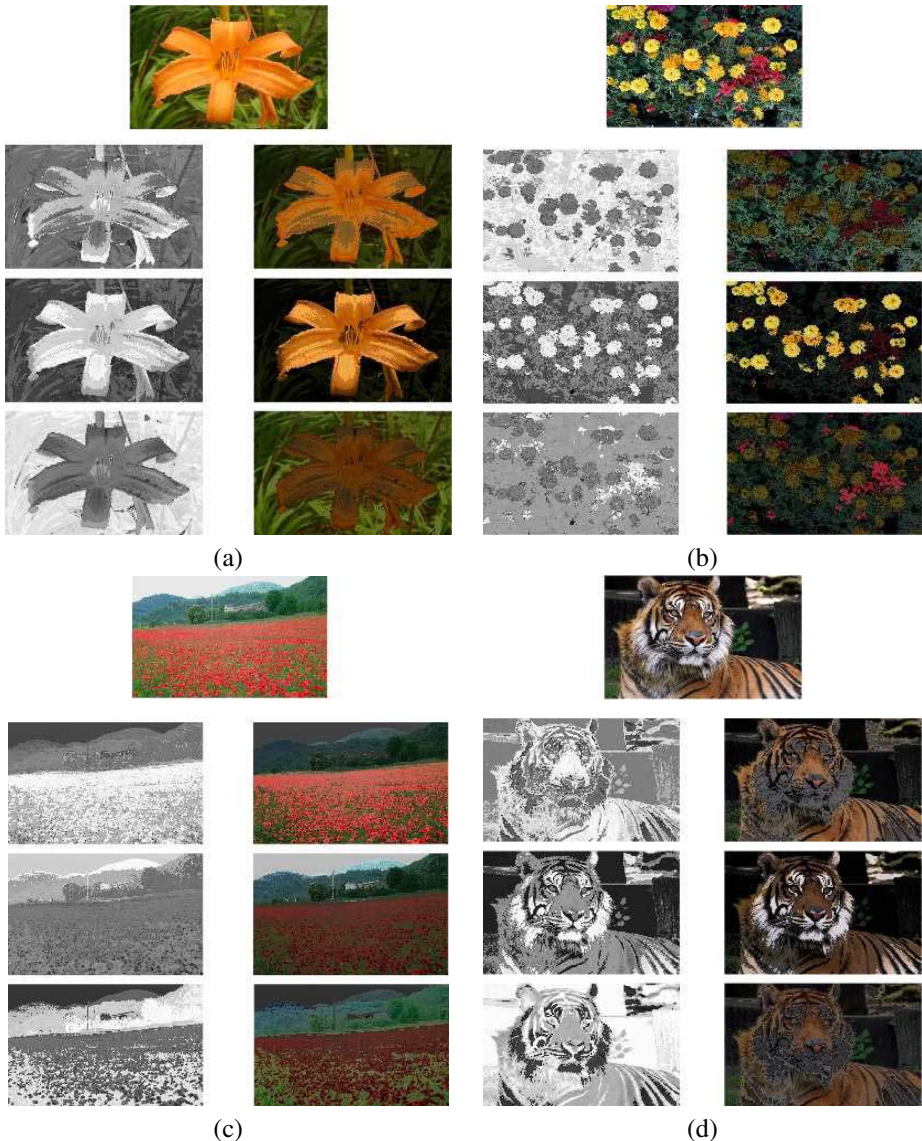


Figure 6. From each group we can see the original image (on the top), our CBCS channels (on the left) and what happens if we multiplies the original image by each CBCS channel, it means, if we stress the detected part of the image (on the right)

we are detecting red flowers in the first channel, the mountain of behind of the image in the second, and the nearest trees in the third. 6.(a) and 6.(d) show good results too.

5. Conclusions and further work

In this work, we have done a first step in our idea of adapting colour information to help texture descriptors. Results, as could be seen in section 4 are quite encouraging. But, this

is only a preliminary work that has opened some interesting ways to continue.

Firstly, considering that CBCS space is not linear some problems can appear, such as an ambiguous representation when two symmetric points in different directions of a given ridge becomes the same value in all the channels. This could be an important problem in some applications but, in the blob detecting case, as this points have different neighbours, d_1 will respect the inherent structure of the blob.

Another important research line is to make this space fully recoverable. Currently, we could do an approximation if we save the RGB values of the pixel p_{max} that has maximum intensity in the channel, and a 3D matrix, putting in its position (i, j) the values of the vector that starts in the RGB values of p_{max} and finishes in the RGB values of the pixel(i,j).

Some other further work that could be done is to change the constraints of the CSF. This would be important if we want to extend our colour space to other different applications.

Finally, the introduction of colour names [1] could improve the method with two different objectives. On the first hand, we should discard those ridges having two different names, since they can introduce confusion. On the other hand, we should join ridges sharing the same colour name. These could allow to introduce robustness in the first steps of the algorithm.

References

- [1] R. Benavente, M. Vanrell, and R. Baldrich. Estimation of fuzzy sets for computational colour categorization. *Color Research and Application*, 29(5):342–353, 2004.
- [2] R. Collins, A. Lipton, and T. Kanade. A system for video surveillance and monitoring. In *American Nuclear Society 8th Internal Topical Meeting on Robotics and Remote Systems*, 1999.
- [3] Ismail Haritaoglu, Davis Harwood, and Larry S. David. W4: Real-time surveillance of people and their activities. *IEEE Trans. Pattern Anal. Mach. Intell.*, 22(8):809–830, 2000.
- [4] B. Julesz and J.R. Bergen. Textons, the fundamental elements in preattentive vision and perception of textures. *Bell Systems Technological Journal*, 62:1619–1645, 1983.
- [5] W. Hu L. Wang and T. Tan. Recent developments in human motion analysis. *Pattern Recognition*, 36(3):585,601, 2003.
- [6] T. Lindeberg and Jan-Olof Eklundh. On the computation of a scale-space primal sketch. *Journal of Visual Communications and Image Representation*, 2(1):55–78, 1991.
- [7] Antonio M. López, David Lloret, Joan Serrat, and Juan J. Villanueva. Multilocal creaseness based on the level-set extrinsic curvature. *Computer Vision and Image Understanding: CVIU*, 77(2):111–144, February 2000.
- [8] Pietikainen Maempaa, T. Classification with color and texture: jointly or separately? *Pattern Recognition*, 37:1629–1640, 2004.
- [9] Eduard Vazquez, Ramon Baldrich, Javier Vazquez, and Maria Vanrell. Topological histogram reduction towards colour segmentation. *4477-0055 - Lecture Notes in Computer Science - Pattern Recognition and Image Analysis*, 2007.
- [10] G. Wyszecki and W.S. Stiles. *Color science: concepts and methods, quantitative data and formulae*. John Wiley & Sons, 2nd edition, 1982.

An Evaluation of an Object Recognition Schema Using Multiple Region Detectors

Meritxell Vinyals ^a Arnaud Ramisa ^{a,1}, and Ricardo Toledo ^b

^a IIIA, Artificial Intelligence Research Institute

CSIC, Spanish National Research Council

^b CVC (Computer Vision Center)

Abstract. Robust object recognition is one of the most challenging topics in computer vision. In the last years promising results have been obtained using local regions and descriptors to characterize and learn objects. One of these approaches is the one proposed by Lowe in [1]. In this work we compare different region detectors in the context of object recognition under different image transformations such as illumination, scale and rotation. Additionally, we propose two extensions to the original object recognition scheme: a Bayesian model that uses knowledge about region detector robustness to reject more unlikely hypotheses and a final verification process to check that all final hypotheses are coherent to each other.

Keywords. Object Recognition, Local Features, Affine Region Detectors, SIFT

1. Introduction

Since its beginnings, object recognition has been amongst the most important objectives of computer vision. One of the main issues to solve this challenge is finding new ways to represent objects that allow a reliable recognition under a wide range of variations in lightning, pose or noise. Lately, one of the most successful approaches to this problem has been the use of local feature regions to characterize and learn objects.

Local feature regions correspond to interesting elements of an image, which can be detected under larger changes in viewpoint, scale and illumination. Many different types of feature region detectors have been developed recently [1,2,3,4]. Mikolajczyk in [5] reviewed the state of the art of these affine covariant region detectors individually.

Lowe developed in [6,1] a object recognition scheme that uses SIFT points (Scale Invariant Feature Transform) to learn and recognize objects. Matches between the learned object models and the new image are computed and refined through various stages. This approach achieved good results detecting previously learned objects in cluttered environments with changes in pose and with partial occlusion.

In this work we use this scheme with the region detectors that give better results in the comparison done by Mikolajczyk et al. and the SIFT descriptor to test its performance in a object recognition task under changes in lightning, pose and scale. For

¹Correspondence to: Arnaud Ramisa, UAB Campus, 08193 Bellaterra, Spain. Tel.: +34 93 5809570; Fax: +34 93 5809661; E-mail: aramisa@iiia.csic.es

our experiments we use the well known object databases ALOI [7], COIL-100 [8] and GroundTruth100-for-COIL [9].

Additionally we propose two improvements to the original Lowe recognition scheme: a Bayesian model that calculates hypothesis probability using knowledge about the robustness of regions detectors to different transformations and a final verification process to asses that all final hypotheses are coherent to each other.

The rest of the paper is structured as follows: In Section 2 we explain the object recognition method developed by Lowe and our proposed enhancement. Then, in Section 3 we detail the experiments and provide an analysis of the results. Finally, in section 4 we discuss the conclusions and some lines of future research.

2. Object detection scheme

In this section we briefly describe the object detection scheme proposed by Lowe in [6,1] and our proposed modifications. An overview of this method can be seen in Fig. 1

2.1. Local region extraction

The first step in the object recognition scheme is to detect and describe the local interest regions in model and test images. Lowe proposed in [6,1] its detector and descriptor: the Difference-of-Gaussian detector (DoG's) and the Scale Invariant Feature Transform (SIFT) respectively. In our approach, in addition to the DoG's regions, we wanted to test the performance of the object recognition scheme with other local regions. Mikolajczyk et al. compared in [5] some of the latest affine-covariant region detectors. Based on this comparison we have chosen the three region detectors that obtained better results: the Harris-Affine [2], the Hessian-Affine [2] and the MSER (Maximally Stable Extremal Regions) [3]. We use all these detectors combined or separated to extract the different interest image regions.

In order to match different occurrences of an interest region it is necessary to use a local descriptor to characterize it. In this work , as in the original scheme, we have used the SIFT descriptor. This descriptor divides the local region into several sub-regions and computes histograms of the orientations of the gradient for every sub-region. The values of all bins of the histograms are then concatenated, forming a descriptor vector of 128 dimensions.

2.2. Descriptor matching

Here we explain the descriptor matching process used to identify different object instances in test images by matching image descriptors to an object descriptor database that stores the object models.

Descriptors from a test image are matched to descriptors stored in the database using Euclidean distance. Each new local descriptor is matched against its nearest neighbour in the model database. Then, the second nearest neighbour is used to decide if the match is valid or if it is a false correspondence: if the first and the second nearest neighbours are very close, the match is considered incorrect. Namely:

$$\frac{NN_2}{NN_1} > 0.8, \quad (1)$$

Where NN_1 is the distance to the first nearest neighbour, NN_2 is the distance to the second nearest neighbour, and 0.8 is a threshold value determined experimentally by Lowe [1]. Descriptors are efficiently matched using a k-d tree structure and the Best-Bin-First algorithm. As a result of this process, a set of matches between models and the test image is found. These matches are the first hypotheses about which objects appear in the new image. An example of these preliminary matches can be seen in Fig.2.

2.3. Clustering and pose estimation algorithms

In this stage the scheme combines different clustering and pose estimation algorithms to find consistent sets of descriptor matches within the initial matches set and give an estimation of the transformation occurred. We propose two modifications to the original scheme: a bayesian model combined with the RANSAC algorithm to consider hypothesis probabilities given a transformation and a process of verification of the final hypotheses.

Typically, the initial set of matches coming from the descriptor matching process is still contaminated with correspondences that come from other objects or background texture. To discard most of the false matches and distinguish between different object instances, the next step is a clustering with a generalised Hough transform. In this step, the matches belonging to the same model are clustered according to its scale, position and orientation. Each cluster with three or more matches is an hypothesis and is subject to further verification. Since each match votes for more than one bin (the selected bin and its adjacent) matches may appear in more than one hypothesis. These repeated matches

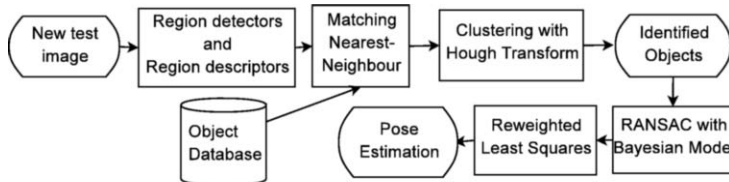


Figure 1. Diagram of the detection scheme.

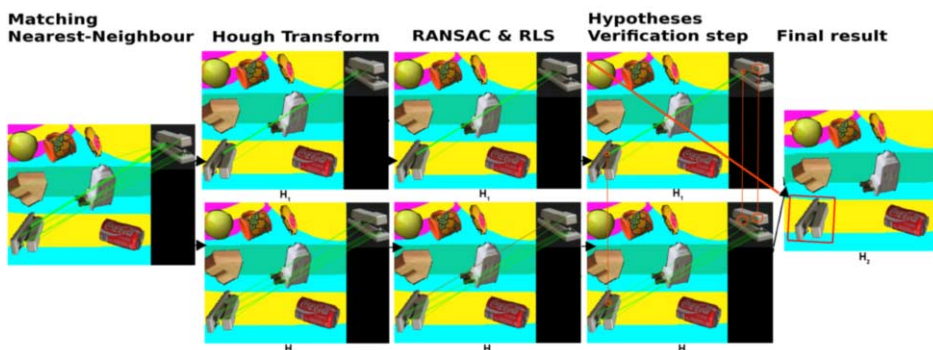


Figure 2. Example of execution where the final hypotheses verification step detects two hypotheses that refers to the same object instance

will be used in the last verification hypothesis step to detect hypothesis that refer to the same object instance and keep only the one which has higher robustness and support.

Next, for all clusters with three or more correspondences, the RANSAC algorithm is used to obtain an estimation of the object pose and identify the remaining outlier if any (see Fig.2 for an example of outliers, displayed as red lines, detected by RANSAC). Although typically the model parameters estimated by RANSAC are not very precise, it is used due to its high tolerance to outliers (it has a breakdown of 50%). Finally, RANSAC best hypotheses inliers are used in the reweighted least squares method (IRLS) to recompute the estimated model parameters accurately.

2.3.1. RANSAC with Bayesian Model

In this section we propose a modification over RANSAC to improve pose estimation results. In the pose estimation process sometimes the correct hypothesis is discarded in favour of a more supported, yet improbable, hypothesis. We define an improbable hypothesis as one that proposes a transformation where detectors are known to have very low repeatability rates. However we observe that given a number of matches between an object and an instance not all pose estimation hypotheses are feasible or equiprobable. Typically RANSAC returns as best hypothesis the one that maximizes the number of inliers or the hypothesis with the least median residual. In our approach we propose to modify these functions to consider not only that the hypothesis gets support from the input data set but also the hypothesis probability given that data set (Eq. 2).

$$V_H^* = V_H \cdot (1 + P(\bar{H} \mid |D|)) \quad (2)$$

where V_H is the typical cost function of RANSAC that calculates how good is one hypothesis, H is the transformation estimation hypothesis and $|D|$ is the cardinality of the set of matches that support it.

We propose a bayesian model to calculate the probability of an hypothesis given a set of matches which uses as prior probabilities the expected detector repeatability rates under different transformations,

$$P(H \mid |D|) = \frac{P(H) \cdot P(|D| \mid H)}{P(|D|)} \quad (3)$$

where H is the pose estimation hypothesis and $|D|$ is the cardinality of the set of matches that support H . We consider $P(|D|)$ equiprobable given a model and we set its value to $\frac{1}{|D^m|}$ where $|D^m|$ is the number of descriptors contained in the model. We also define all the hypotheses space as equiprobable ($P(H)$).

As the object recognition system can use more than one region detector with different robustness and capabilities, we define $P(|D| \mid H)$ in a more general form where the probabilities are calculated for each detector and weighted by its presence in the descriptor matches set:

$$P(|D| \mid H) = \sum_{i \in \text{detectors}} p_i \cdot P(|D_i| \mid H), \quad (4)$$

where p_i is the percentage of matches with regions type i (notice that $\sum_{i \in \text{detectors}} p_i = 1$), $|D_i|$ is the cardinality of the set of matches using the region detector i and detectors is the set of all detectors used in the extraction of image characteristic regions.

Given an hypothesis of the transformation occurred, the probability that the system retrieves a number of matches depends on the robustness of the detectors to that transformation. Hence we propose to define $P(|D| | H)$ in function of the results of the experiments described in detail in Section 3 (see Fig.4 and Fig. 5 for experiment results). The repeatability rate expected for each detector is obtained interpolating the result value of the two closer sampled points of the transformation space in our experiments. The hypothesis probability distribution is modeled using a normal distribution with a mean equal to the number of matches we expect to have (the product between the percentage expected and the total number of regions from the model image) and a variance equal to a half of the mean. The final hypothesis probability is obtained by adding the hypothesis probability calculated for each detector separately weighted by the percentage of the regions extracted with that detector in the input data.

2.4. Final hypotheses verification step

In our experiments we observe that because of in the Hough transform matches can be duplicated in different clusters, final hypotheses can present a non-disjoint set of support data (some repeated matches). To solve this, it is not acceptable to keep just one hypothesis and discard the rest, because we would not consider that an object can have more than one instance in the image. However, since a descriptor match can belong to only one object instance, we can assume that if the inlier data sets of different hypotheses are not disjoint then they must refer to the same object or only one of the hypotheses can be the correct. In that case we propose to keep the hypothesis with the highest number of inliers or, if several hypotheses have an equal number of inliers, the one with less transformation error. To illustrate this process, see Fig. 2 where the Hough Transform ends with two clusters of valid matches from the initial set. These both hypotheses reach the final verification step with different pose estimations but since they have matches in common (displayed as lines between the two images) the scheme detects that they refer to the same object instance and discard the hypothesis with less number of matches.

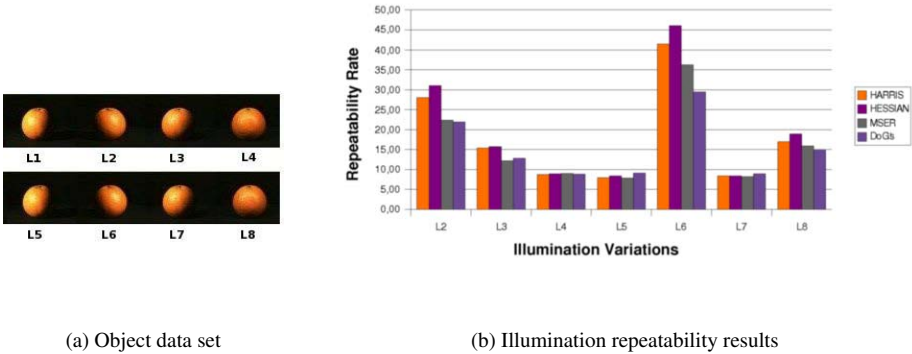
3. Experimental Results

First we explain the experiments designed to assess the robustness and capabilities of the different region detectors and the descriptor used. The empirical results obtained in this test are used as prior probabilities in the Bayesian Model. Secondly we present the experimental results for our object recognition and pose estimation scheme by evaluating its performance with public image databases.

3.1. Region Repeatability Results

As explained in [10] one of the characteristics to measure the performance of a good region detector is repeatability. We evaluate the repeatability rates of each detector under three different transformations: illumination variation, scale change and image rotation. The measure of repeatability takes into account the uncertainty of detection. A point x_i detected in image I_i is repeated in image I_j if the corresponding point x_j is detected in image I_j where x_j is defined as:

$$\{x_j\} = \{x_i \mid T_i \cdot x_i \in I_j\} \quad (5)$$

**Figure 3.** Illumination test

A repeated point is in general not detected exactly at position x_j , but rather in some neighbourhood of x_j . The size of this neighbourhood is denoted by e and repeatability within this neighbourhood is called e -repeatability. The set of points pairs (x_i, x_j) which correspond within an e -neighbourhood is defined by :

$$Rj(e) = \{(x_i, x_j) \mid dist(T_i \cdot x_i, x_j) < e\} \quad (6)$$

We set parameter $e = 1.5$, as is proposed in [10] for all experiments.

3.1.1. Illumination Variation

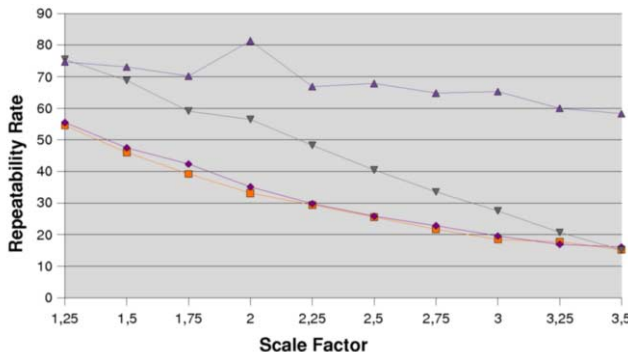
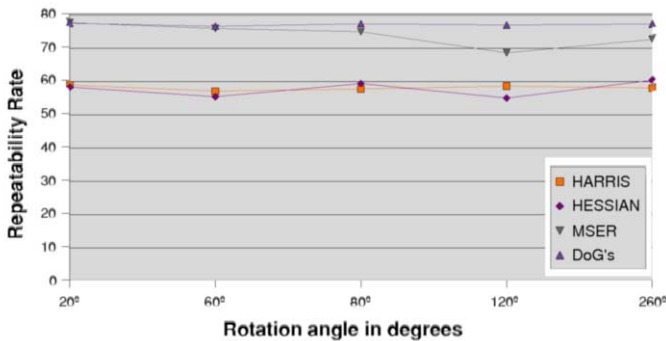
In this experiment we evaluate the repeatability rate of each region detector for a set of scenes where an object is presented under different illumination conditions. We use the ALOI (Amsterdam Library of Object Images) image dataset which provide one-thousand small objects recorded under 24 different illumination conditions (Figure 3(a)).

Fig. 3(b) depicts the means over the tests done with 100 different objects and their respective 24 images grouped by illumination variation. The repeatability rate varies considerably among different illumination changes. Observe that although different detectors generally present similar results, significant differences appear in tests with soft illumination changes (L2,L6). In these cases Hessian and Harris detectors produce considerably better results than MSER and DOG's.

3.1.2. Scale Changes

In this experiment we assess the repeatability rate of the detectors under 10 different scales (1.25, 1.5, 1.75, 2.0, 2.25, 2.5, 2.75, 3.0, 3.25 and 3.5).

Fig. 4 depicts means over the 50 tests run using objects from the ALOI image database. Observe that significant differences appear among different detectors. DoG's detector produces better results than all other detectors keeping their repeatability rate less affected among the scale variations applied. MSER detector achieves higher rates than Hessian and Harris, these last two reporting nearly identical results.

**Figure 4.** Scale repeatability results**Figure 5.** Rotation repeatability results

3.1.3. Image Rotation

In this experiment we evaluate the repeatability rate of the detectors under different rotation angles. We report means over 50 tests run using images of objects from the ALOI image database. Images are rotated at 6 different angles: 0°, 20°, 60°, 80°, 120° and 260°. As you can see in Fig. 5 the detector repeatability rates are independent of the rotation angle applied producing similar results among all rotation angles. However rates obtained when some rotation is applied to the image varies among detectors. While DoG's and MSER produce results close to 80%, Harris and Hessian present a repeatability rate of only 60%.

3.2. Number of regions extracted by detector

In this experiment we aim to compare the number of regions extracted by each detector in 10 different image resolutions. Usually objects represent small regions in images, therefore detectors that retrieve few regions can have problems in order to describe an

object present in a frame. The results reported in Fig. 6 are the means over 50 tests run over different images. Observe that we have a linear relationship between the number of regions extracted by each detector and the image resolution. Furthermore significant differences appear among the number of regions extracted by each detector: DoG's always find the highest number of regions, followed by Hessian, Harris and MSER.

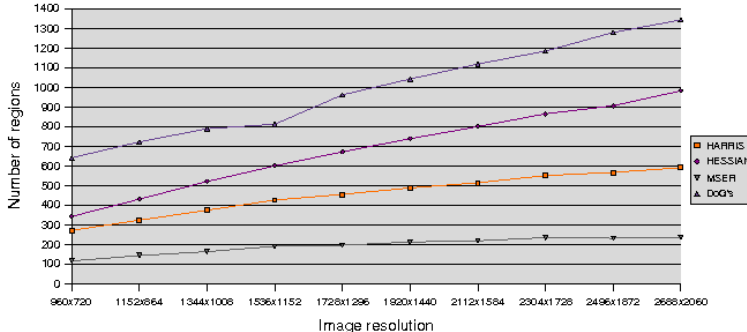


Figure 6. Number of regions extracted per image resolution

3.3. Object recognition and pose estimation experiments

In this experiment we aim to assess the performance of the scheme described in section 2 in the identification of which objects are present in an image scene (object recognition) and which is its transformation with respect to the model (pose estimation). We use the GroundTruth100-for-COIL image database which is composed of 100 images each one with different objects instances from the COIL-100 object image database. Additionally, this database includes information about which objects appear in each image and the scale change and rotation angle applied in each case.

Fig. 7 (left) depicts the percentage of objects correctly detected using each single detector and all detectors combined. Furthermore the figure reports the percentage of correct identified objects for which the object recognition scheme has been capable of generating an estimation of the geometric transformation occurred (a minimum of matches are required in each step of the scheme to calculate the pose estimation).

As you can see in Fig. 7 (right) DoG's produces the highest rate of correct identified objects (93%) , followed by Harris and Hessian detectors (38% and 43% respectively). MSER detector reports the worst results with a very poor percentage of correct matches (13%). It also shows that when all detectors are used to detect object regions the final number of matches increases (99%). These results are correlated with the number of regions found by each detector rather than the repeatability rates reported in our experiments (see section 3.1). Since the image resolution used is quite low, and consequently regions corresponding to objects have small sizes, detectors that extract fewer numbers of regions are likely to have low performances since they detect very few regions or none for each object. Although we could have used images with higher resolutions usually object recognition applications (robot navigation, video surveillance ...) require to work

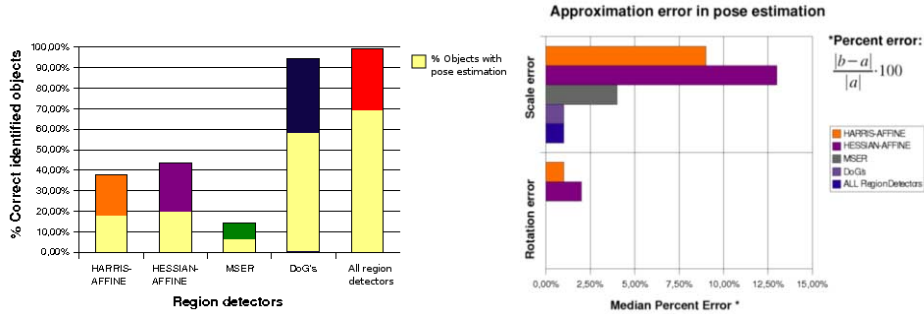


Figure 7. Object recognition results grouped by region detectors.

with limited image sizes. Hence, a suitable detector for object recognition is usually required to achieve good results in poor quality images. Consequently DoG detector is more suitable to be used in that conditions than other detectors like MSER which also present good repeatability rates. We can conclude that when using a recognition object scheme with high tolerance to outliers best performances are achieved by detectors that find higher number of regions (although they have more false matches) than very reliable detectors that give fewer matches.

In that experiment we also measure the accuracy of the pose estimation provided by the object recognition scheme. The results (see Fig. 7) show the median percent error produced in the estimation of the scale change and rotation occurred between the model and the instance. These results match with the scale and rotation repeatability rates reported in our experiments (see Section 3.2) since matches over DoG's and MSER regions allow more accurate scale and rotation approximation than the ones obtained with Harris and Hessian regions. Finally we also observe that when we use all detectors the results are quite similar to the ones produced using only DoG's regions due to the higher number of DoG's regions compared to other detectors.

4. Conclusions

In this work we have evaluated the performance of various state-of-the-art region detectors in the Lowe objection recognition scheme. According to our experiments, region detectors that find a higher number of regions obtain better results in object recognition tasks. From these results we also observe that detectors achieve different performances under different kind of transformations. We also conclude that in order to choose a descriptor is not only important its repeatability also the number of regions that it extracts from the image. Very reliable detectors with high levels of repeatability are not suitable for object description because they extract very few regions per image. Finally we observe that the combination of different region detectors improves object recognition results. Furthermore, we propose two modifications to the original scheme: a bayesian model that uses region detector robustness as prior knowledge to reject improbable transformations and a process to verify final hypothesis. Our work argues in favour of researching how to combine region detectors taking into account the information about its

robustness under different transformations. Finally, as future work, a formal comparison of this new approach with respect to the original object recognition scheme should be provided.

Acknowledgements

This work has been partially funded by the European Social Fund, the MID-CBR project grant TIN2006-15140- C03-01, TIN 2006-15308-C02-02 and FEDER funds. The work of Meritxell Vinyals is supported by the Ministry of Education of Spain (FPU grant AP2006-04636) whereas the work of Arnau Ramisa is supported by the FI grant from the Generalitat de Catalunya.

References

- [1] D. Lowe, "Distinctive image features from scale-invariant keypoints," *International Journal of Computer Vision*, vol. 60, no. 2, pp. 91–110, 2004.
- [2] K. Mikolajczyk and C. Schmid, "Scale & affine invariant interest point detectors," *Int. J. Comput. Vision*, vol. 60, no. 1, pp. 63–86, 2004.
- [3] J. Matas, O. Chum, M. Urban, and T. Pajdla, "Robust wide baseline stereo from maximally stable extremal regions." in *Proceedings of the British Machine Vision Conference 2002, BMVC 2002, Cardiff, UK, 2-5 September 2002*. British Machine Vision Association, 2002.
- [4] T. Kadir, A. Zisserman, and M. Brady, "An affine invariant salient region detector." in *Computer Vision - ECCV 2004, 8th European Conference on Computer Vision, Prague, Czech Republic, May 11-14, 2004. Proceedings, Part I*, ser. Lecture Notes in Computer Science, vol. 3021. Springer, 2004, pp. 228–241.
- [5] K. Mikolajczyk, et al., "A comparison of affine region detectors," *International Journal of Computer Vision*, vol. 65, no. 2, pp. 43–72, 2005.
- [6] D. G. Lowe, "Object recognition from local scale-invariant features," in *ICCV '99: Proceedings of the International Conference on Computer Vision-Volume 2*. Washington, DC, USA: IEEE Computer Society, 1999, p. 1150.
- [7] I. S. I. Systems, "Alois amsterdam library of object images."
- [8] S. K. N. Sameer A. Nene and H. Murase, "Coil-100 columbia object image library." [Online]. Available: http://www1.cs.columbia.edu/CAVE/publications/pdfs/Nene_TR96_2.pdf
- [9] T. of Vision (ITC-irst), "Groundtruth100-for-coil object image database." [Online]. Available: <http://tev.itc.it/DATABASES/objects.html>
- [10] C. Schmid, R. Mohr, and C. Bauckhage, "Evaluation of Interest Point Detectors," *International Journal of Computer Vision*, vol. 37, no. 2, pp. 151–172, 2000.

An input panel and recognition engine for on-line handwritten text recognition¹

Rafael RAMOS-GARIJO, Sergio MARTÍN, Andrés MARZAL², Federico PRAT,
Juan Miguel VILAR, and David LLORENS

Departament de Llenguatges i Sistemes Informàtics, Universitat Jaume I de Castelló

Abstract. A portable input panel and a real-time recognition engine for isolated, handwritten characters are presented. The input panel mimics the one found in standard pen-centered interfaces and the recognition engine is based on approximate Dynamic Time Warping comparisons with prototypes selected by two different fast classification procedures. The error rate obtained on the standard Pendigits task, 0.83%, is significantly lower than the error rate of other recently published techniques.

Keywords. On-line handwritten text recognition, Dynamic Time Warping

1. Introduction

Pen-based input is experiencing great demand since the advent of pen-based computers and devices, such as Tablet PCs, Personal Digital Assistants, digitizing tablets, pressure sensitive screens... State-of-the-art techniques allow the use of on-line character recognition in practical applications, but they are not perfect and usability issues must be taken into account to properly deal with recognition mistakes; otherwise, the user experience can be defeating.

Recent operating systems integrate input controls and text recognition engines to ease programming applications that offer pen-based interaction. For instance, Microsoft Vista and Microsoft XP Tablet PC Edition contain powerful recognition engines which can be accessed by the user via a consistent interface: an input panel such as the one shown in Figure 1 (a). This widget is accesible from .NET which, in principle, should make it available wherever the .NET platform runs (currently Microsoft operating systems and Linux, among others, via Mono). However, the .NET recognition engine is proprietary and can only be accessed from specific operating systems. We have designed and built an open source recognition engine for isolated characters and we have integrated it into our own implementation of the input panel (see Figure 1 (b)). The only requirement of the input panel is the availability of the WindowsForms 2.0 library, which is currently being ported to Mono and, thus, will be soon available in all existing .NET implemen-

¹Work partially supported by the Ministerio de Educación y Ciencia (TIN2006-12767), the Generalitat Valenciana (GV06/302) and Bancaixa (P1 1B2006-31).

²Corresponding Author: Andrés Marzal, Departament de Llenguatges i Sistemes Informàtics, Universitat Jaume I de Castelló. E-mail: amarzal@lsi.uji.es.

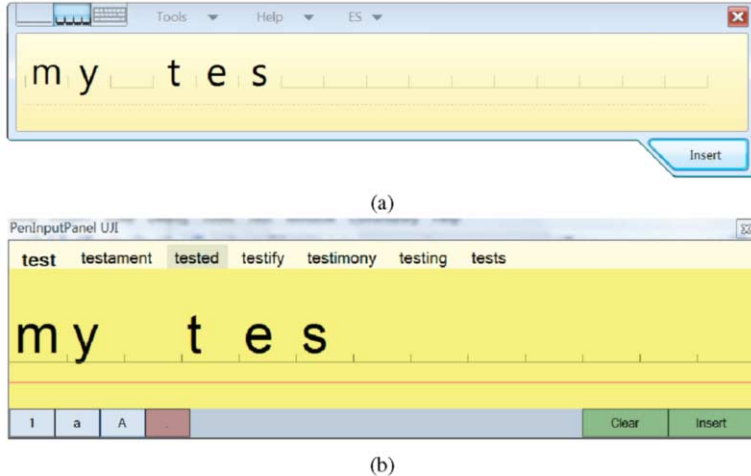


Figure 1. (a) Microsoft Vista standard widget for handwritten text input. (b) Our portable input panel.

tations. Interaction with our widget is similar to the one offered by the Microsoft's widget (ink can be deleted, the output can be edited, mistakes can be corrected by selecting candidates among those offered in a list, etc.) and includes some improvements, such as word completion.

Our recognition engine offers state-of-the-art performance for isolated character recognition and works in real time. In this paper we introduce the recognition engine and tune its parameters from experimental results on our own alphanumeric corpus [1]. The engine uses a k -Nearest-Neighbours (k -NN) classifier with an approximate Dynamic Time Warping similarity measure. In order to accelerate the process, two different fast filtering procedures are applied to the prototypes and only a subset of them is considered by the classifier. The resulting system presents excellent performance on the writer-independent Pendigits [2] standard recognition task (0.83% error rate). On our alphanumeric corpus it obtains an 11.58% error rate on a writer-independent test, which compares favorably with Microsoft's recognition engine on this task: 14.66% error rate. The system runs in real time: around 53 characters per second on a conventional laptop.

2. Basic concepts and preprocessing

Digital ink is a time-ordered sequence of strokes and each stroke is a time-ordered sequence of “packets”. Each packet contains information about the pen at a given instant: (x, y) coordinates, velocity, pressure... We only use (x, y) coordinates, the simplest kind of packets, since we seek portability and coordinates are the least common denominator that pen devices offer. We use the term *glyph* to name ink representing a symbol.

Each glyph is preprocessed to correct slant and to normalize its dimensions. In order to estimate the slant, every pair of consecutive points in a stroke is converted to a vector and all vectors whose angle difference with respect to the vertical axis is equal or less than 50 degrees are selected. Then, vectors pointing downwards are forced to point upwards by changing the sign of both coordinates. The summation of all these upwards vectors is the vector representing the slant, which is corrected by a shear transform of all the

points according to the angle of this vector. Then, each glyph is boxed in a rectangle whose longest side measures one and all the coordinates in the glyph are made relative to the center of mass of the points. When a glyph contains two or more strokes, they are concatenated. There are other preprocessing steps, but they are dependent on the comparison methods employed and we will present them where appropriate.

3. The recognition engine

We follow a template-based approach to recognition. We need to assign a category label to each glyph, but we are also interested in getting a ranked list of good alternatives with two purposes: (a) to offer the user good alternative choices when there is a mistake, and (b) to ease the implementation of word completion. Classification must be performed in real time, i.e. it should take much less than one tenth of a second to provide a responsive interaction experience.

Dynamic Time Warping (DTW) is a well-known technique to compare sequences suffering elastic deformations. It was introduced by Vintsyuk [3] as a comparison method for speech, but it is also appropriate for comparing digital ink. DTW is computationally intensive and does not fulfill our real-time response requirement on currently conventional hardware. There are techniques that speed-up DTW by sacrificing correctness [4,5] but, as we will see, they are still not fast enough to provide real-time interaction. We looked for faster comparison techniques, but they provide too high error rates. Finally, we found a proper trade-off by using the fast techniques to pre-select a few candidates among which the (suboptimal) DTW could find the category in which the glyph is finally classified. As will be shown in the experiments, this two-stage procedure (fast filtering and accurate selection of the best category) achieves a low error rate and fast response while providing a proper list of alternatives.

In the next subsections we will present each step in the procedure and will guide decisions by the experimental results. All the experiments have been performed on a corpus consisting of the 10 digits, the 26 lowercase letters and the 26 uppercase letters from 11 writers. Each person wrote two instances of each symbol on a Tablet PC. Since there are some indistinguishable handwritten characters, such as lower and upper “o” and zero, lower and upper “s”, etc., we consider only 35 categories: 9 for the “1” to “9” digits and 26 for the lower and uppercase version of each letter (where zero is included in the “o” class). With this criterion, the 1.7 version of the Microsoft Tablet PC SDK recognition engine obtained a 14.66% error rate on our corpus data.

All the experiments on our corpus reported below are writer-independent: all the error rates were obtained by cross-validation. The tests were repeated eleven times, each time leaving one writer out. The experiments were run on a laptop PC with an Intel Core 2 CPU at 2 GHz with 2 Gb of RAM on the .NET platform under the Microsoft Vista Business Edition operating system. The programs were coded in C# without unsafe code.

3.1. Nearest-neighbour classification with DTW-based comparisons

Given two sequences, $A = a_1a_2 \dots a_m$ and $B = b_1b_2 \dots b_n$, where a_i and b_j belong to some set Σ for $1 \leq i \leq m$ and $1 \leq j \leq n$, an alignment between them is defined as a sequence of pairs $\langle (i_1, j_1), (i_2, j_2), \dots, (i_p, j_p) \rangle$ such that (1) $0 \leq i_{k+1} - i_k \leq 1$,

$0 \leq j_{k+1} - j_k \leq 1$, and $(i_k, j_k) \neq (i_{k+1}, j_{k+1})$ for $1 \leq k < p$; (2) $(i_1, j_1) = (1, 1)$; (3) $(i_p, j_p) = (m, n)$. Given a dissimilarity measure between elements in Σ , $\delta : \Sigma \times \Sigma \rightarrow \mathbb{R}$, the cost of an alignment $((i_1, j_1), (i_2, j_2), \dots, (i_p, j_p))$ is defined as $\sum_{1 \leq k \leq p} \delta(a_{i_k}, b_{j_k})$. The optimal alignment is the one with minimum cost and the DTW dissimilarity measure is the cost of the optimal alignment. The DTW dissimilarity between A and B can be computed by solving the following recurrence at $\text{DTW}(m, n)$:

$$\text{DTW}(i, j) = \begin{cases} \delta(a_1, b_1), & \text{if } i = 1 \text{ and } j = 1; \\ \text{DTW}(i - 1, 1) + \delta(a_i, b_1), & \text{if } i > 1 \text{ and } j = 1; \\ \text{DTW}(1, j - 1) + \delta(a_1, b_j), & \text{if } i = 1 \text{ and } j > 1; \\ \min \left\{ \begin{array}{l} \text{DTW}(i, j - 1) + \delta(a_i, b_j), \\ \text{DTW}(i - 1, j) + \delta(a_i, b_j), \\ \text{DTW}(i - 1, j - 1) + \delta(a_i, b_j) \end{array} \right\}, & \text{in other case.} \end{cases}$$

The DTW dissimilarity tends to yield smaller values for shorter sequences, since there usually are less terms in the summation of local dissimilarities for the optimal alignment. Some kind of normalization by the sequences length is needed in order to correct this bias and several different variations of the DTW dissimilarity measure have been proposed to cope with the problem. We will redefine the normalized dissimilarity between two sequences, A and B , as $D(A, B) = \text{DTW}'(m, n)/(m + n)$, where

$$\text{DTW}'(i, j) = \begin{cases} 2\delta(a_1, b_1), & \text{if } i = 1 \text{ and } j = 1; \\ \text{DTW}'(i - 1, 1) + \delta(a_i, b_1), & \text{if } i > 1 \text{ and } j = 1; \\ \text{DTW}'(1, j - 1) + \delta(a_1, b_j), & \text{if } i = 1 \text{ and } j > 1; \\ \min \left\{ \begin{array}{l} \text{DTW}'(i, j - 1) + \delta(a_i, b_j), \\ \text{DTW}'(i - 1, j) + \delta(a_i, b_j), \\ \text{DTW}'(i - 1, j - 1) + 2\delta(a_i, b_j) \end{array} \right\}, & \text{in other case.} \end{cases}$$

This recursive equation can be efficiently solved in $O(mn)$ time and $O(\min(m, n))$ space by means of Dynamic Programming. The algorithm computes the shortest path from the bottom-left corner node to the top-right corner node in the acyclic graph of Figure 2 (a). The weight associated to vertical and horizontal arcs ending at node (a_i, b_j) is $\delta(a_i, b_j)$, the weight associated to its incoming diagonal arc is $2\delta(a_i, b_j)$, and the lower-left node is initialized with $2\delta(a_1, b_1)$.

To completely specify the DTW measure, the local dissimilarity measure $\delta : \Sigma \times \Sigma \rightarrow \mathbb{R}$ must be defined. We have studied both the squared euclidean distance between aligned points and a linear combination of the squared euclidean distance and the angular difference of aligned segments.

We preprocessed our data in order to avoid end-point problems in the definition of the local distance: each segment determined by a pair of consecutive points in a stroke, p_i and p_{i+1} , was represented by its middle point and the angle of $\overrightarrow{p_i p_{i+1}}$. The local distance was defined as the squared euclidean distance between the respective segment middle points and α times the angular difference of their respective vectors. Figure 2 (a) shows the error rate as a function of α , the angular difference weight in the local distance. The minimum error rate, 12.10%, is obtained at $\alpha = 0.075$. This error rate is lower than the

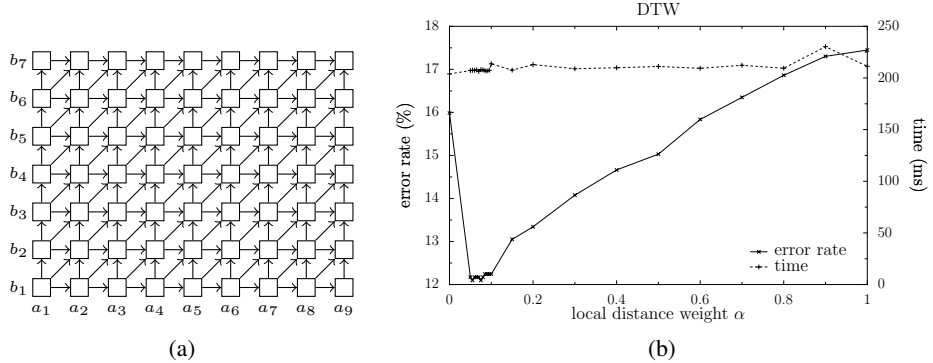


Figure 2. (a) Acyclic graph for DTW computation. (b) Error rate and classification time (per glyph) as a function of α , the angular difference weight in the local distance.

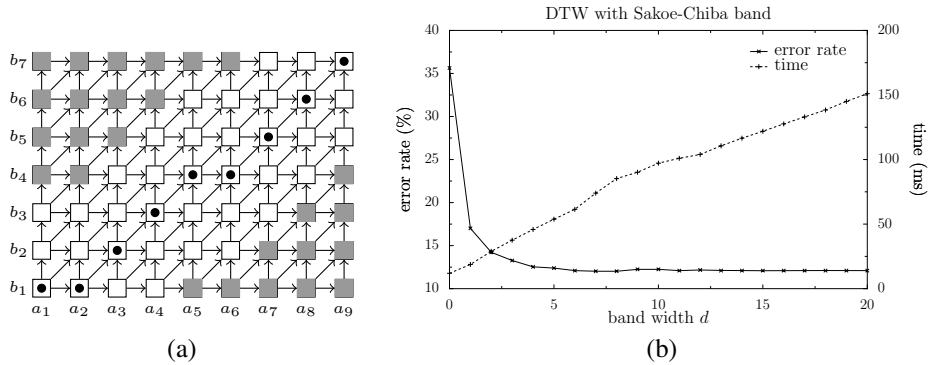


Figure 3. (a) Gray nodes, which are farther than d nodes from the diagonal (marked with dots), are not visited when approximating the DTW with Sakoe and Chiba's technique. (b) Error rate and classification time (per glyph) as a function of d , the maximum distance from the diagonal of visited nodes.

one obtained with Microsoft's recognition engine, but the running time, 208 milliseconds per glyph, makes this approach unsuitable for real time recognition.

3.2. Speeding-up the DTW computation by means of the Sakoe-Chiba band

Sakoe and Chiba proposed a technique to speed-up DTW computation by sacrificing correctness: the shortest-path computation in the DTW acyclic graph is limited to nodes at a given distance d from the bottom-left to top-right diagonal (see Figure 3 (a)) [4]. Since we place the longest sequence on the horizontal axis, the running time of this algorithm is $O(\max(m, n)d)$. Smaller values of d result in faster but less accurate DTW estimations. We have studied the dependence of the error rate and the running time on this parameter. Figure 3 (b) shows that the error rate equals the exact DTW error rate for $d \geq 13$ (12.10%). But there is a better option: at $d = 7$ we obtain a 12.02% error rate and each glyph is classified in 74 milliseconds. This is still too slow to be used in a real-time system.

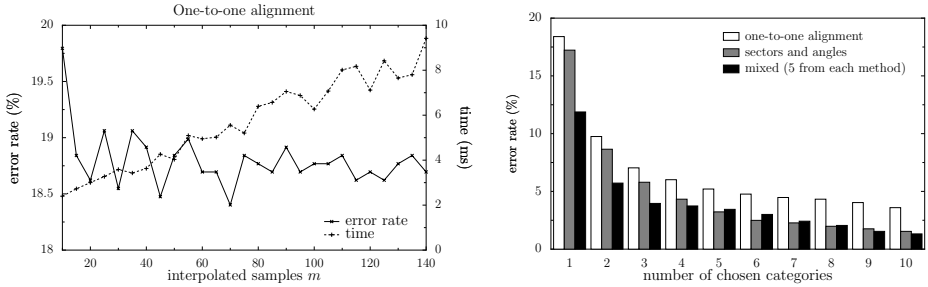


Figure 4. (a) Error rate and classification time (per glyph) as a function of m , the number of segments, when using a dissimilarity measure based on the one-to-one alignment. (b) Percentage of times that the correct category is not found among the (up to) 10 best categories with different methods.

3.3. Faster classification techniques

Two different methods were explored: a one-to-one alignment technique on resampled glyphs and a comparison of vectorial descriptions of glyphs. Both of them provide worse error rates by themselves, but are much faster and can be useful to focus the k -NN search with the approximate DTW method on a reduced set of prototypes.

3.3.1. One-to-one alignment

When sequences have the same length, m , we can compare them by means of a one-to-one alignment: $D(A, B) = \sum_{1 \leq i \leq m} \delta(a_i, b_i)$. This value can be computed in $O(m)$ time, which is significantly faster than the exact and suboptimal DTW techniques. In order to use this measure, glyphs must be resampled to contain exactly m samples: we have first taken $m + 1$ equally spaced points along the original pen trajectory and the resulting m segments have been represented by their middle points and angles. The value of m should be carefully chosen, since the error rate and the running time depend on it. Figure 4 (a) shows the error rate and the time needed to classify a glyph as a function of m , the number of segments. The best error rate, 18.40%, is obtained when $m = 70$, but it is significantly worse than the error rate obtained by means of approximated DTW for $d = 7$. This is a really fast technique: it spends only 6 milliseconds per glyph. It might not be useful as a nearest-neighbour classification method, but it can be used to preselect some candidates to feed the slower, approximate DTW based classification procedure.

The white bars in Figure 4 (b) show the percentage of times that the correct character category was not found among the k different-category nearest-neighbours, for k between 1 and 10. The correct category is not among the 10 selected only 3.59% of times. When we restrict the approximate DTW search to these categories, the error rate is 12.10% and the total running time needed to classify each glyph is 31 milliseconds.

3.3.2. Sectors and angles distribution comparison

We have also followed a second approach to select candidate categories. Each glyph was resampled as before to a given number of segments and the glyph bounding box was partitioned into 9 sectors with a 3×3 grid. Each segment was assigned to its sector in the grid and the segment angles distribution was modelled. In order to properly represent the angles distribution with an histogram, angles were discretized with a 4 or 8 directions

code. The discretization is dependent on a parameter β , the angular width of the regions assigned to diagonal directions. When $\beta = 0$, we get a 4 directions code; and when $\beta = \pi/4$, we obtain the conventional 8 directions code. With this coding technique, each glyph is represented with an histogram consisting of 72 values (9 sectors and 8 directions per sector). Given a glyph A , let us denote with a_i the value at the i -th histogram cell, for $1 \leq i \leq 72$. Given two glyphs, how do we compare their 72 cell histograms? We have considered 3 different distance functions:

- the Euclidean distance,

$$D_E(A, B) = \sqrt{\sum_{1 \leq i \leq 72} (a_i - b_i)^2};$$

- the Manhattan distance,

$$D_M(A, B) = \sum_{1 \leq i \leq 72} |a_i - b_i|$$

- a χ^2 -like distance,

$$D_{\chi^2}(A, B) = \sum_{\substack{1 \leq i \leq 72: \\ a_i + b_i > 0}} \frac{(a_i/n_A - b_i/n_B)^2}{(a_i + b_i)/(n_A + n_B)},$$

where $n_A = \sum_{1 \leq i \leq 72} a_i$ and $n_B = \sum_{1 \leq i \leq 72} b_i$.

Experimental results are shown in Figure 5. Subfigure (a) reveals that the χ^2 distance is consistently better than the other two distances and the minimum error rate, 17.23%, is obtained for this distance when glyphs are represented with 100 segments and $\beta = \pi/4$. Subfigure (b) shows that the running time is nearly constant for different number of samples and that the χ^2 distance is computationally more expensive than the other two. However, it is still a fast technique: it requires 6 milliseconds per glyph.

The gray bars in Figure 4 (b) show the percentage of times that the correct category was not found among the up to 10 categories selected with this method. The correct category is not among the 10 selected only 1.54% of times. When we restrict the approximate DTW nearest-neighbours search to the prototypes in the 10 categories selected with this approach, the error rate drops to 11.51% and the total running time required to classify each glyph is 29 milliseconds.

3.4. The recognition procedure

It should be noted that the two fast candidates selection procedures provide different sets of character categories. The black bars in Figure 4 (b) show the percentage of times that the correct category was not found among the (up to) 10 candidates (5 provided by one fast method and 5 by the other). When 5 candidates from each method are chosen, the correct solution is not found among them 1.32% times.

White bars in Figure 6 show the error rate when the approximate DTW based distance to the reference glyph is used to score the training glyphs in the chosen categories

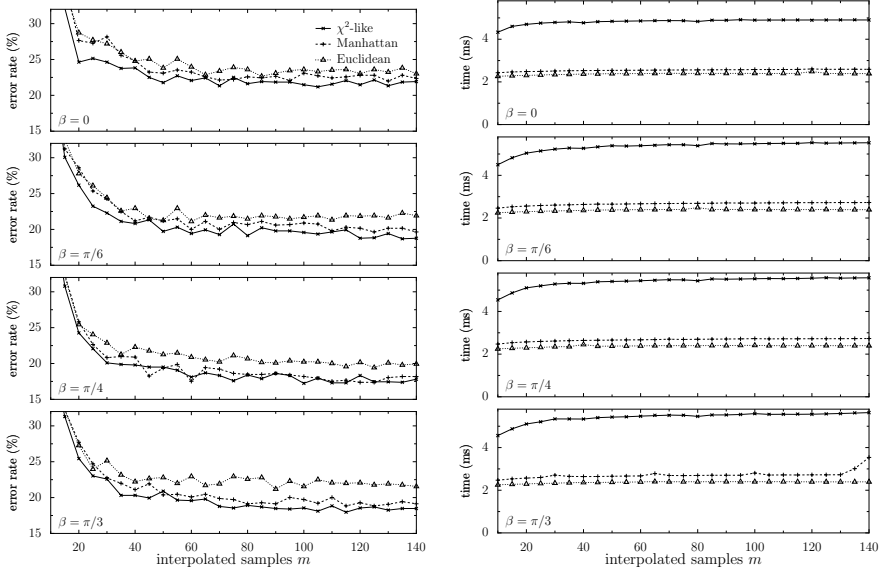


Figure 5. Error rate (left) and classification time per glyph (right) as a function of m (the number of samples), β (the angular width of diagonal directions), and the distance function for the sectors and angles representation.

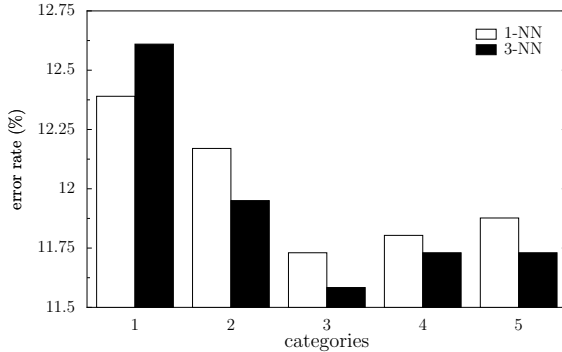


Figure 6. Error rate for the 1-NN and 3-NN classification rules and different number of categories provided by each fast method (from 1 to 5).

(from 1 up to 5 per method) and the 1-NN rule is used in order to classify. When each fast method provides 3 categories, the error rate is 11.58%. Black bars in Figure 6 show that the 3-NN classification rule further decreases the error rate: for 3 candidates from each fast method, the error rate drops to 11.58% and the total time required to classify each glyph was 19 milliseconds. (This error rate is slightly worse than the 11.51% obtained before —due to one additional misclassified glyph,— but the previous method was 50% slower.) The full recognition engine is depicted in Figure 7.

In order to compare the engine performance with that of other recognitions engines, we run a standard experiment on the Pendigits database [2], available at the UCI Machine Learning Repository [6]. This corpus contains handwritten instances of the 10 digits from several writers: 7,494 glyphs from 30 writers are used for training and 3,498 test glyphs

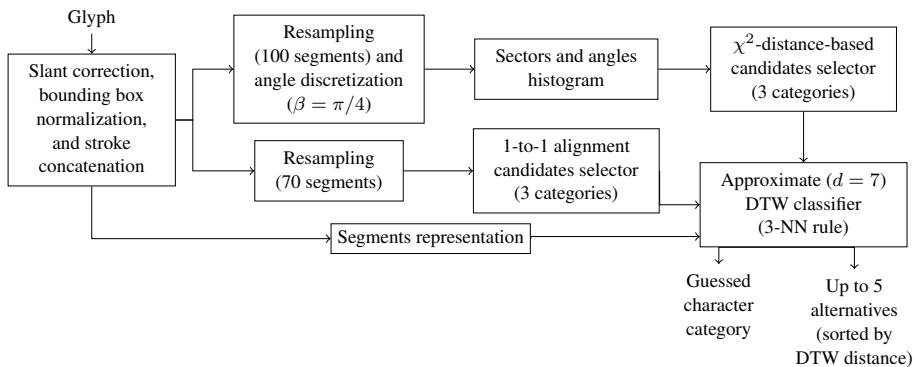


Figure 7. Recognition engine.

from 14 different writers are used as test data. We measured the error rate obtained when classifying all the test digits using all the training glyphs as prototypes. The resulting 0.83% error rate is significantly better than recent results published in the literature for the same experiment: 1.66% in [7] and 2.26% in [8].

4. Conclusions

We have designed, built, and tuned a recognition engine for isolated, handwritten characters recognition and implemented an input panel to guarantee portability of pen-based applications on the .NET platform. The error rate obtained on our alphanumeric corpus (11.58%) is lower than that of Microsoft's recognition engine on the same task (14.66%). The corpus has been made publicly available at the UCI Machine Learning Repository [1]. The engine can process around 53 glyphs per second on a conventional laptop, which makes it amenable for real-time interaction. The error rate achieved on a standard experiment with the Pendigits database outperforms recently published results.

References

- [1] D. Llorens, F. Prat, A. Marzal, J. M. Vilar, UJIpenchars: A Pen-Based Classification Task for Isolated Handwritten Characters, [<http://www.ics.uci.edu/databases/uji-penchars>].
- [2] E. Alpaydin, F. Alimoğlu, Pen-Based Recognition of Handwritten Digits, [<http://www.ics.uci.edu/databases/pendifigits>].
- [3] T. Vintsyuk, Speech Discrimination by Dynamic Programming, *Cybernetics*, **4**(1) (1968), 52–57.
- [4] H. Sakoe, S. Chiba, A Dynamic Programming Algorithm Optimization for Spoken Word Recognition, *IEEE Transactions on Acoustics, Speech, and Signal Processing*, **26** (1978), 43–49.
- [5] P. Capitani, P. Ciaccia, Warping the Time on Data Streams, *Data & Knowledge Engineering*, **62** (2007), 438–458.
- [6] A. Asuncion, D. J. Newman, UCI Machine Learning Repository [<http://www.ics.uci.edu/~mlearn/MLRepository.html>]. Irvine, CA: University of California, Department of Information and Computer Science.
- [7] B. Spillmann, M. Neuhaus, H. Bunke, E. Pękalska, R. P. W. Duin, Transforming Strings to Vector Spaces Using Prototype Selection, *Lecture Notes in Computer Science (SSPR&SPR 2006)*, **4109** (2006), 287–296.

- [8] J. Zhang, S. Z. Li, Adaptive Nonlinear Auto-Associative Modeling Through Manifold Learning, *Lecture Notes in Computer Science (PAKDD 2005)*, **3518** (2005), 599–604.

Georeferencing image points using visual pose estimation and DEM

Xavier Mateo and Xavier Binefa

Universitat Autònoma de Barcelona,

Computer Science Department,

08193 Bellaterra, Barcelona, Spain

{javier.mateo, xavier.binefa}@uab.es

Abstract. In this paper a new method for the georeferencing of low-oblique images is presented. Our georeferencing approach is based on the estimation of the camera pose and the subsequent use of geographical data in order to find global coordinates for every pixel in the image. For this purpose, concepts like Ground Control Point (GCP) or Digital Elevation Model (DEM) are explained and applied, achieving good results in real situations.

Keywords. Image Georeferencing, Ground Control Point, Camera Pose, DEM

1. Introduction

Image georeferencing refers to the assignment of geographical coordinates to the elements present in an image. In most typical situations only the position of the photographer is associated with a whole picture, without taking into account the different localizations for all the elements represented in the image. Obviously, it is much easier to obtain this single information (could be directly obtained from a GPS device) than finding out the georeferencing for every part of the image (and, consequently, for every pixel in the image). The possibility of automatically find out this pixel coordinates could have a wide range of applications, from the use in emergency rescues in vast land environments to the obvious military applications. A relative newcomer application that nowadays is also becoming quite important is the Augmented Reality, whose positioning algorithms depend on image georeferencing [1]. Also important software companies (like Microsoft, Hewlett Packard or Google) are developing different tools heavily depending on the concept of georeferencing, as can be seen in [2], [3] and [4].

In order to achieve this image georeferencing not only the current position of the camera is necessary, but also its orientation (in other words, where is the camera looking at). The combination of both position and orientation is known as camera pose, and the process to find it out is known as pose estimation. Similarly as mentioned previously, if someone could obtain camera position with a GPS device it would also be possible to obtain its orientation with the use of an Inertial Measurement Unit (IMU) [5,6]. Anyway, this combined method can have a high error due to the nature of both devices: on one side, GPS devices can carry an error up to 100 meters and, more worrying, small inexactitudes

in the IMU angle measurement can result in high displacement errors if we are looking at distant points.

In this paper we present a semi-automatic method for the georeferencing of aerial images. Our approach can be divided in two well-separated steps: first of all, we must estimate the camera pose and, in a second step, we find out the georeferencing of image pixels by combining the information from camera pose and the geographical data.

For the pose estimation process we will make use of the concept of Ground Control Points (GCPs). A GCP can be defined as a point on the earth surface which has been accurately geolocalized (i.e. its earth coordinates have been measured with a high exactitude). Use of Ground Control Points is quite usual in closed environments, for example in laboratories (especially for the navigation of autonomous robots), but its utilization in open environments has not been so fully investigated. With some correspondences between image pixels and coordinates of GCPs we will be able, using different algorithms, to obtain the camera pose. It must be considered that the higher the distance covered by the GCPs, the better estimation results we will achieve. For this reason our approach will be mostly centered in low-oblique images [7], where a larger piece of terrain can be observed (Figure 1). This kind of images can be taken from elevated ground positions (mountains, roofs of buildings), or also from airplanes flying at a low altitude.

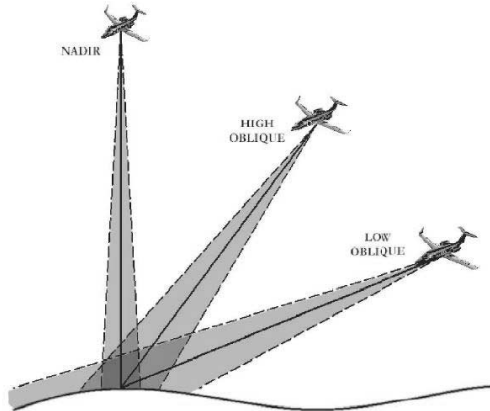


Figure 1. Types of aerial images. Image obtained from [7].

For the second approach step we will make use of a Digital Elevation Model (DEM). A DEM can be seen as a digital representation of a surface relief, giving the elevation for different ground positions at regularly spaced intervals. In other words, given a raster of values indicating latitude and longitude, the DEM give us the corresponding altitude for each one of these coordinates.

This paper is organized as follows: in Section 2 our proposed approach will be explained in detail. Results obtained from our implementation will be presented in Section 3 and, finally, future work and conclusions are explained in Section 4 and Section 5.

2. Proposed approach

As previously mentioned we must divide our approach in two different steps: the pose estimation process and the computation of pixel georeferencing by making use of the DEM. In the following two subsections both steps will be described in detail.

2.1. First step: Pose estimation

Any camera can be completely described by two sets of parameters: the intrinsic parameters (focal distance, principal point, etc.) and the extrinsic parameters (position and orientation of the camera). Determination of both intrinsic and extrinsic parameters is a key element for every mapping application.

Intrinsic parameters can be easily estimated from well-known calibration methods, like the one developed from Zhang [8]. On the other side, extrinsic parameters (i.e. camera pose) can be computed through the correspondence of GCPs and its positioning in the image plane. Given N correspondences between image points (x_i, y_i) and geographical coordinates (X_i, Y_i, Z_i) , position and orientation can be mathematically modeled as a 3×1 vector t and a 3×3 matrix R , fulfilling the following equation

$$l_i \begin{bmatrix} x_i \\ y_i \\ 1 \end{bmatrix} = K \left(R \begin{bmatrix} X_i \\ Y_i \\ Z_i \end{bmatrix} + t \right) \quad i = 1, \dots, N \quad (1)$$

, where l_i represents the projective depths and K is the intrinsic parameters matrix from the camera [8].

Pose estimation is a long time studied subject in computer vision. Traditionally, the problem was solved by using the photogrammetric method known as Direct Linear Transformation (DLT) [9]. DLT method generates two linearly independent equations for every point correspondence, giving rise to an equation system that can be solved by Singular Value Decomposition (SVD). Its main disadvantage is the non-existence of orthonormality in the resultant rotation matrix.

DeMenthon developed during the 90th decade his POSIT (Pose from Orthography and Scaling with Iterations) algorithm [10], which first computes an approximation of the pose by assuming that image was obtained by a scaled orthographic projection instead of a perspective projection. In a second phase, the algorithm repeats iteratively the same process, with the only difference that image points are recalculated assuming that image was taken from the camera pose found in previous iteration and using a scale orthographic projection. POSIT algorithm is fast and easy to implement (in the source paper is implemented with just 25 lines of code), but is quite sensitive to noise and, besides, cannot be used when GCPs are coplanar.

A more recent approach is the one presented from Lu et al. [11], an iterative algorithm which successively improves the rotation matrix estimation and then computes the associated translation vector. Every iteration tries to minimize the sum of the squared error between original image points and reconstructed image points (image points that would be seen, in case image was taken from the pose estimated in current iteration). Results obtained from Lu et al. are expected to be really accurate, but its condition as an iterative algorithm causes that this method could be quite slow in response time.

Also an interesting approach is Fiore's algorithm [12]. Its strategy is first to form a set of linear combinations from the equations resultants from (1), in such a way that rotation matrix and translation vector can be eliminated. This fact makes then possible the estimation of the isolated depth values l_i . Once this information has been achieved, rotation and translation can be estimated by solving the problem known as Orthogonal Procrustes Problem, whose solution can be found through SVD.

Fiore's algorithm can be summarized as follows [13]:

1. Express equation (1) in the following way:

$$K^{-1}l_ip_i = [R|t]P_i \quad i = 1, \dots, N \quad (2)$$

or analogously

$$K^{-1}[l_1p_1, l_2p_2, \dots, l_Np_N] = [R|t][P_1, P_2, \dots, P_N] \quad (3)$$

$$\text{, where } p_i = \begin{bmatrix} x_i \\ y_i \\ 1 \end{bmatrix} \text{ and } P_i = \begin{bmatrix} X_i \\ Y_i \\ Z_i \\ 1 \end{bmatrix}$$

2. Let $S = [P_1, P_2, \dots, P_N]$ and $r = \text{rank } S$. Decompose matrix S by its SVD, $S = UDV^T$ and let V_2 be a matrix composed by the last $n - r$ columns of V , which spans the null-space of S . Then $SV_2 = 0_{3 \times (n-r)}$, so

$$K^{-1}[l_1p_1, l_2p_2, \dots, l_Np_N]V_2 = 0_{3 \times (n-r)} \quad (4)$$

3. This equation can be rewritten as

$$\left(\begin{bmatrix} K^{-1}p_1 & 0 & \dots & 0 \\ 0 & K^{-1}p_2 & \dots & 0 \\ \vdots & \vdots & \ddots & \vdots \\ 0 & 0 & \dots & K^{-1}p_N \end{bmatrix} \begin{bmatrix} l_1 \\ l_2 \\ \vdots \\ l_N \end{bmatrix} \right)^{(3)} V_2 = 0_{3 \times (n-r)} \quad (5)$$

or expressing the matrices in a more compact way

$$(DL)^{(3)}V_2 = 0_{3 \times (n-r)} \quad (6)$$

where symbol "(3)" indicates vector transposition [14]

4. By taking vector transposition on both sides we get:

$$\left((DL)^{(3)}V_2 \right)^{(3)} = 0_{3 \times (n-r)}^{(3)} \iff ((V_2^T \otimes I_{3 \times 3})D)L = 0 \quad (7)$$

where symbol " \otimes " indicates Kronecker product [14]

5. From equation (7) the depth matrix L (containing all depth values l_i) can be recovered, up to an scale factor, by solving a null-space problem
6. Now that the left side of equation (2) is known, we are left with an Absolute Orientation problem [15], whose solution can be given using different well-known methods (like [15] or [16])

Main advantages of Fiore's algorithm are its lower computational cost and its fast response, making possible the use of this algorithm not only for static images but also for video sequences. Since one of the future objectives from this project is the possibility of detecting a higher number of GCPs by using mosaic images extracted from video sequences, and also because of its lower computational cost, we decided to use Fiore's algorithm in our approach.

2.2. Second step: Intersection with DEM

In order to obtain the coordinates of each point represented in the image pixels, we must extent a virtual ray that crosses the optical center we obtained in the pose estimation and the pixel represented in the image plane (accordingly placed in the focal distance with respect to the Z axis) as represented in Figure 2.

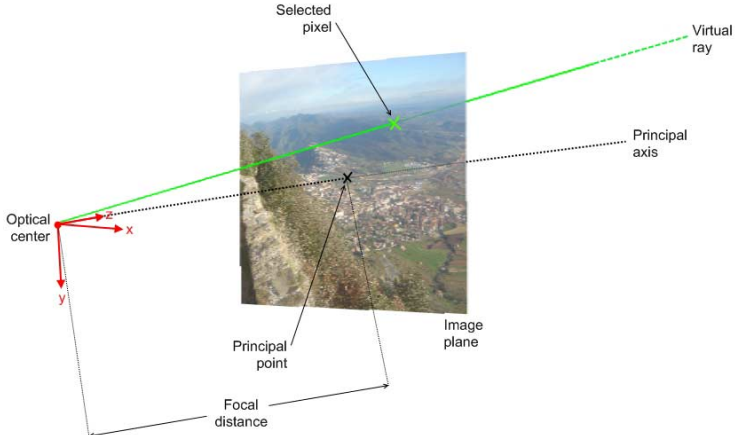


Figure 2. Camera intrinsic parameters and virtual ray

Once we computed this virtual ray, we must extent it until it intersects with the values expressed in the DEM. For this purpose some methods can be applied. A possible approximation could be the assumption of the ground surface as a plane, approximating it by using Least Mean Squares (LMS) Method from the GCPs coordinates. With the creation of this plane is possible to find an approximated intersection of the virtual ray without the necessity of looking values from the DEM. Once this approximation has been carried out, a more precise intersection is found by an iterative inspection of DEM values across the virtual ray.

3. Implementation and experimental results

In order to obtain an evaluation of the proposed approach some tests were performed. The main motivation was to analyze the behaviour of Fiore's pose estimation in case of

inaccurate selection from image points and geographical coordinates. Also a real case of image georeferencing was studied.

A Matlab program was created for the pose estimation simulations. Six random 3D points are created in every simulation, within a confined space of size 10x10x1 kilometers. These points will act as GCPs. Also another 3D point, in this case acting as the camera optical center, is randomly situated at a distance of 8 kilometers from the mean value of the previous six GCPs. Line between optical center and this mean value is considered as the principal axis of the camera (so, defining the camera orientation). In that moment, assuming a focal distance of 6 millimeters, a resolution of 2048x1536 pixels and a CCD size of 5.27x3.96 millimeters, a virtual view of the 6 GCPs in the image plane is computed, giving rise to the six 2D image pixels that will be used for the simulation.

For the simulation performance, we add a variable gaussian noise both to 3D points and 2D points (in order to simulate the possible inaccuracy in the selection of both set of points), and Fiore's algorithm is applied. The metrics that are measured are the relative error of the translation vector t , and the Frobenius norm between the real and the estimated rotation matrix R . Results are displayed in figures 3 and 4.

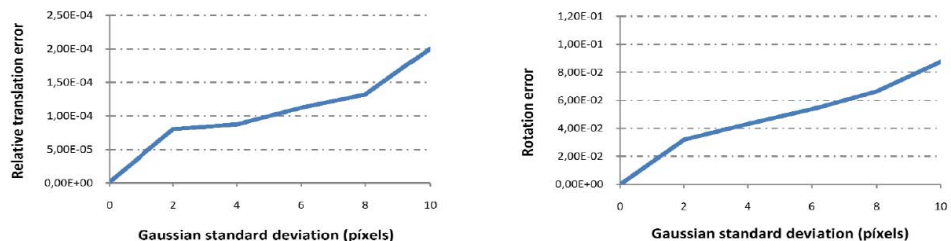


Figure 3. Adding gaussian noise to 2D points

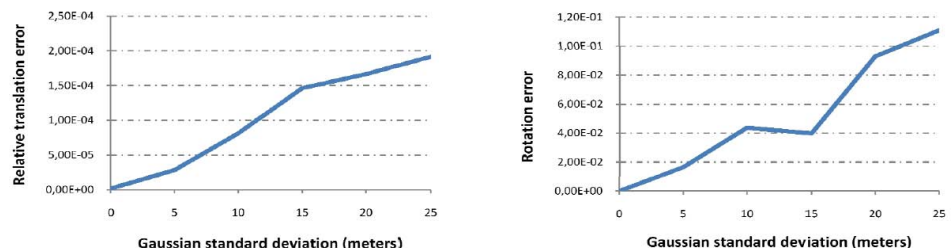


Figure 4. Adding gaussian noise to 3D points

For the real case, we use an image taken from a camera that was previously calibrated through Zhang calibration's method. Image was taken from the central part of Catalonia, zone from where we already had a 30x30 meters DEM. New software was developed, integrating the Google Earth COM API [17] inside our application. Google Earth COM API is a relative new tool that allows developers to embed Google Earth front-end in their applications and interact directly with it. Its possibilities are quite extensive, but in our case we are just interested in embedding the Google Earth front-end in our software,

allow the free navigation through it, and automatically extract the coordinates of the GCPs we selected. As an additional feature, we wish also to automatically store the image containing all the GCPs, which later will be used to texturize the DEM.

A pair of screenshots of the created software and the image can be seen in Figure 5. First step for the user is to select the situation of the Ground Control Points, both in the image and in the Google Earth front-end. Next, the picture pixels situation and the Google Earth coordinates are taken as inputs for the pose estimation algorithm, which will compute the camera pose.

Results from the simulations can be seen in Figure 6, where the estimated position and camera axes are represented in green color. As previously mentioned, exists also the possibility of texturize the 3D surface using the image obtained from Google Earth, achieving a more realistic representation.

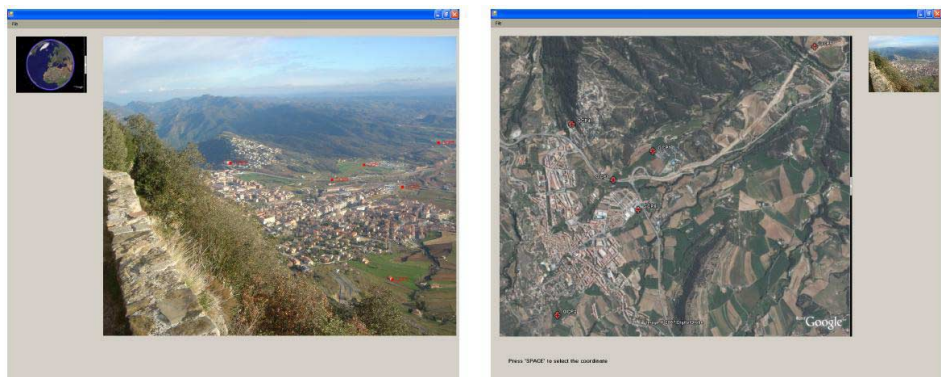


Figure 5. Selection of correspondences between image pixels (red dots in left image) and geographical coordinates (red crosses in right image)

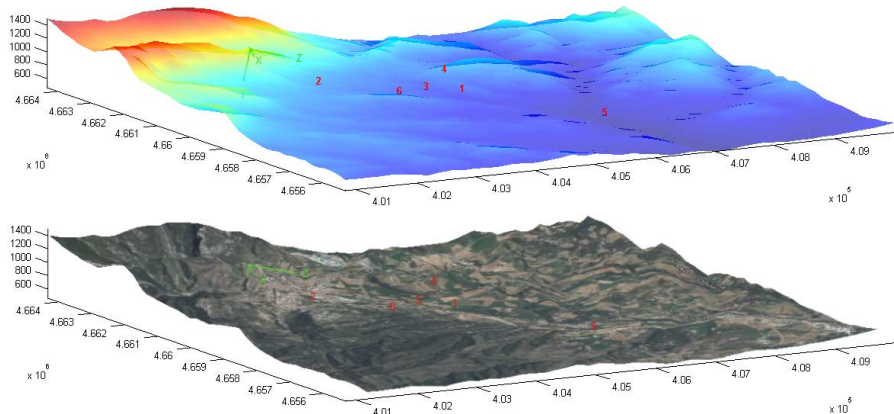


Figure 6. Results from simulation with and without texturization

As a second step, user can afterwards select additional points in the 2D image, provoking the appearance of new virtual rays in the 3D surface. The intersection of these rays with DEM gives us the global coordinates, as displayed in Figure 7.

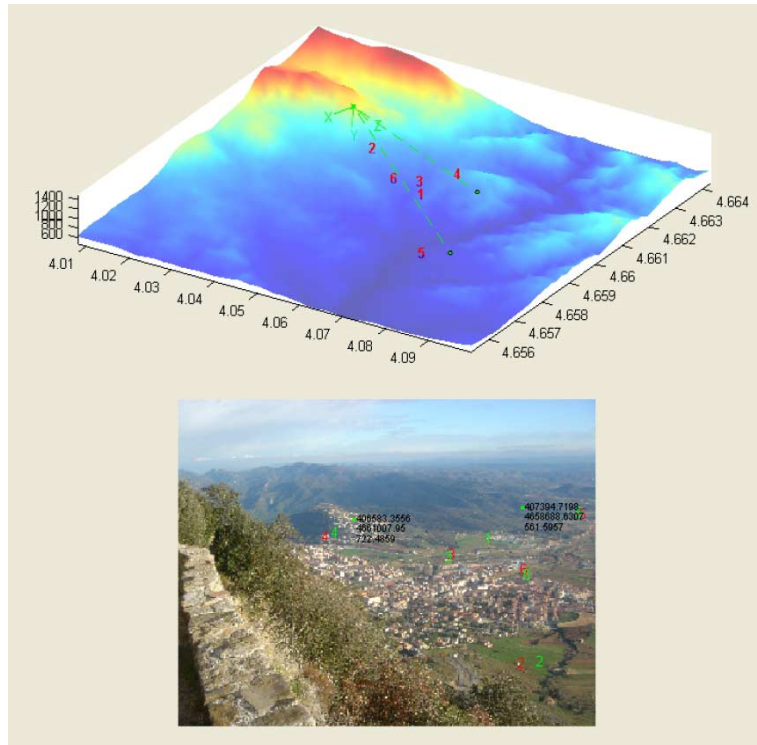


Figure 7. Georeferencing of points selected by the user

4. Future work

Future developments of the proposed approach can be taken in different directions. One of our first intentions is the use of mosaic images created from low-oblique aerial video sequences. Mosaic images will allow a more extensive sight of the terrain, making possible an easier selection of well-defined GCPs. The main problem of this proposal is that, obviously, mosaics consist of images that are taken from different camera poses (either position or orientation, or possibly both of them), so pose estimation method would not be useful for this situation. Anyway, our wish is to find some kind of "virtual pose" that could be valid for the combined image represented in the mosaic, as long as at least focal distance from all the participating images are the same.

Also an important improvement could be the inclusion of image registration [18] in our approach, in order to improve the results of the georeferencing. Only by using the pose estimation obtained from Fiore's algorithm we could have an idea of which part of terrain we are looking for, even if we do not have access to a DEM. With an orthographic

view from this part of terrain (it can be easily obtained, for example from Google Earth) and applying an homography to the 2D image, we can achieve really good results using image registration.

Finally, it is expected in the future to include also LADAR images [19] taken at same time and in the same place as the photographs. With this possibility, some new research routes appear in front of us. One possible application could be a 3D registration between the LADAR image and the DEM [20], or also the possibility of detecting objects that are not necessarily moving on the ground.

5. Conclusions

In this paper we have presented a new approach for georeferencing points from low-altitude aerial images, by using Ground Control Points (GCPs) and a Digital Elevation Model (DEM). The proposed method consists in a first estimation of the camera pose and, in a second step, the determination of the georeferencing for image pixels by using the DEM.

Different results from the pose estimation are presented, and also a real case including the use of a DEM was studied.

In future, some improvements are expected to be included, like the use of mosaicing for a better positioning of GCPs or also the inclusion of registration for more accurate results.

Acknowledgements

This work was supported in part by CIDA (Centro de Investigaciones y Desarrollo de la Armada)

References

- [1] A. Ansar and K. Daniilidis: Linear Pose Estimation from Points or Lines. *IEEE Pattern Analysis and Machine Intelligence*, vol. 25, no. 4, April 2003
- [2] Microsoft Photosynth, <http://labs.live.com/photosynth>
- [3] HP mscape, <http://www.msappers.com>
- [4] Chen, Di Fabbrizio, Gibbon, Jana, Jora, Renger and Wei: GeoTracker – Geospatial and Temporal RSS Navigation. Proceedings of the 16th international conference on World Wide Web, 2007
- [5] N. Yastikli and K. Jacobsen: Direct Sensor Orientation for Large Scale Mapping – Potential, Problems, Solutions. *The Photogrammetric Record*, vol. 20, pp. 274-284, September 2005
- [6] M. Cramer and D. Stallman: On the use of GPS/Inertial Exterior Orientation Parameters in Airborne Photogrammetry. Institute for Photogrammetry, 2002
- [7] Y. Sheikh, S. Khan, M. Shah and R. Cannata: Geodetic Alignment of Aerial Video Frames. 2003
- [8] Z. Zhang: A Flexible New Technique for Camera Calibration. *IEEE Pattern Analysis and Machine Intelligence*, vol. 22, no. 11, pp. 1330-1334, November 2000
- [9] Y. I. Abdel-Aziz and H. M. Karara: Direct linear transformation from comparator coordinates into object space coordinates in close-range Photogrammetry. *Proc. ASP/UI Symp. Close-Range Photogrammetry*, pages 1-18, Urbana, IL, January 1971

- [10] L.S. Davis and D.F. DeMenthon: Model-based object pose in 25 lines of code. International Journal of Computer Vision, 15(2):123–141, 1995
- [11] C. Lu, G.D. Hager, E. Mjolsness: Fast and Globally Convergent Pose Estimation from Video Images. IEEE Pattern Analysis and Machine Intelligence, vol. 22, no. 6, pp. 610-622, June 2000
- [12] P.D. Fiore: Efficient Linear Solution of Exterior Orientation. IEEE Pattern Analysis and Machine Intelligence, vol. 23, no. 2, pp. 140-148, February 2001
- [13] A. Fusiello: Elements of Geometric Computer Vision. March 2006
- [14] T. Minka: Old and new matrix algebra useful for statistics. MIT Media Lab note
- [15] Z. Wang and A. Jepson: A New Closed-Form Solution for Absolute Orientation. IEEE Conf. Computer Vision and Pattern Recognition, pp. 129-134, 1994
- [16] B. Horn: Closed-Form Solution of Absolute Orientation Using Unit Quaternions. J. Optical Soc., vol. 4, pp. 629-642, April 1987
- [17] Google Earth Com API, <http://earth.google.com/comapi/>
- [18] M. Shah and R. Kumar: Video Registration. Kluwer Academic Publishers, 2003
- [19] R.L. Felip, X. Binefa, J. Diaz-Caro: Discerning Objects from Ground and Target Pose Estimation in lidar Data using Robust Statistics. IEEE International Conference on Image Processing, 2006
- [20] P.J. Besl and N.D. McKay: A Method for Registration of 3-D Shapes. IEEE Pattern Analysis and Machine Intelligence, vol. 14, no. 2, pp. 239-256, February 1992

Natural Language Processing

This page intentionally left blank

Semantic disambiguation of taxonomies

David SÁNCHEZ and Antonio MORENO

*Intelligent Technologies for Advanced Knowledge Acquisition (ITAKA)
Research Group*

Department of Computer Science and Mathematics

*Universitat Rovira i Virgili (URV). Avda. Països Catalans, 26. 43007 Tarragona
{david.sanchez, antonio.moreno}@urv.cat}*

Abstract. Polysemy is one of the most difficult problems when dealing with natural language resources. Consequently, automated ontology learning from textual sources (such as web resources) is hampered by the inherent ambiguity of human language. In order to tackle this problem, this paper presents an automatic and unsupervised method for disambiguating taxonomies (the key component of a final ontology). It takes into consideration the amount of resources available in the Web as the base for inferring information distribution and semantics. It uses co-occurrence analysis and clustering techniques in order to group those taxonomical concepts that belong to the same “sense”. The final results are automatically evaluated against WordNet *synsets*.

Keywords. Polysemy disambiguation, ontologies, Web mining.

1. Introduction

In the last years, the success of the Information Society has motivated researchers to develop automated knowledge acquisition methods. Nowadays, there exist many electronic repositories (digital libraries, news repositories and even the Web) that can be a valid source for learning knowledge. Those resources are typically written in natural language. In consequence, due to the inherent ambiguity that characterizes human languages, the learning performance may be seriously hampered. Concretely, *Polysemy* is one of the most difficult problems to tackle when dealing with Natural Language resources [7].

In previous research, we developed knowledge acquisition methodologies for ontology learning [11]. We designed and implemented methods to deal with the main steps of the ontology construction process (i.e. terms discovery, taxonomy construction, non-taxonomic learning and ontology population). The system is able to learn domain ontologies in an automated, unsupervised and domain independent way, using the Web as the source of information. However, until now, problems regarding polysemic concepts and their collateral effects over the final semantic structure were not considered.

As a consequence, if a specific concept has more than one sense (e.g. *organ*), the resulting taxonomy of specialisations may contain concepts from different domains (e.g. “*pipe organ*”, “*lung*” as subclasses of “*organ*”). Although these concepts have been selected correctly, it could be interesting that the branches of the resulting taxonomic tree were somehow grouped if they belong to the same sense of the immediate “father” concept.

So, this paper presents a novel *web based method for polysemy disambiguation of the taxonomical aspect of domain ontologies*. Following the same philosophy as the introduced ontology learning procedure, it works in a completely automatic, unsupervised and domain independent way. It uses Web information distribution in order to infer which domain terms should be grouped (clustered) in the same “sense”. This process is performed by means of co-occurrence measures compiled from the web count returned by Web search engines for specifically constructed queries. Final results are also automatically checked against WordNet *synsets* (concept’s senses) using an especially designed evaluation procedure.

The rest of the paper is organized as follows. Section 2 presents a brief state of the art in this area. Section 3 describes the novel approach for semantic disambiguation of taxonomies. Section 4 describes the designed evaluation procedure. The final section contains the conclusions and proposes lines of future work.

2. Related work

The problem of solving the lexical ambiguity that appears when a given word has several different meanings is commonly called *Word Sense Disambiguation* (WSD). As shown in [7], the *supervised* paradigm is the most efficient. However, due to the lack of big sense tagged corpora (and the difficulty of manually creating them), the *unsupervised* paradigm tries to avoid, or at least to reduce, the knowledge acquisition problem inherent to supervised methods. In fact, unsupervised methods do not need any learning process and they use only a lexical resource (e.g. WordNet) to carry out the word sense disambiguation task [1][9].

In [6] different approaches to unsupervised word sense disambiguation are described. On the one hand there are global, *context-independent* approaches, which assign meanings retrieved from an external dictionary by applying special heuristics. For example, a frequency based approach where always the most frequently applied sense is used. On the other hand there are *context-sensitive* approaches. This kind of methods use the context of a word to disambiguate it. Recently, some authors [10] have been using the Web to disambiguate, analyzing text contexts in comparison to WordNet definitions or hyponym sets. However, in any case, attempting a general solution for complete disambiguation is a very hard task. This is reflected in the less than impressive precision (around 60-70%) presented by the current state of the art approaches [13].

Considering that our goal is to disambiguate taxonomical terms and not to offer a general purpose solution, our approach is a little less ambitious. However, it shares some characteristics of general unsupervised methods such as context assumptions and the use of Web based similarity metrics [3].

3. Semantic disambiguation

As mentioned in the introduction, the problem of polysemy can arise in taxonomy learning when a certain concept has more than one sense or it is used in different contexts (e.g. *organ*). The direct consequence is that the immediate subclasses (e.g. *liver*, *heart*, *pipe_organ*, *symphonic_organ*, *internal_organ*) will cover different domains corresponding to their specific sense (e.g. *specialized structural animal unit* or

musical instrument). A proper solution would be to group those classes according to the specific sense to which they belong (e.g. *liver*, *heart* and *internal_organ*; *pipe_organ* and *symphonic_organ*) or to select only a specific subset.

Attempting to minimize that problem, we have considered the possibility of performing *automatic polysemy disambiguation* of taxonomical entities. In a nut shell, it consists on clusterizing subclasses, using as a similarity measure the amount of co-occurrences of discovered terms within the available web resources.

Our approach is based on the *context* where each concept has been extracted, concretely, the web resources that contain it. It can be assumed that each web document is using the concept in a specific sense, so all candidate concepts that typically co-occur should belong to the same keyword's sense. The observation that words tend to exhibit only one sense in a given discourse or document was tested by Yarowsky [15] on a large corpus (37.232 examples). The accuracy of the claim was very high (around 99% for each tested word), which shows that it can be exploited. Applying this idea over a representative set of documents (as the whole Web) it is possible to find some consistent relations and construct clusters of terms associated to concept's senses. In fact, it has been argued that the number of resources available in the Web is so vast and the amount of people generating web pages is so enormous, that the Web information distribution approximates the actual real distribution as used in society [3]. Following this assumption, it is possible to compute the degree of semantic similarity according to *term co-occurrence*. Co-occurrence measures ("web scale statistics" [4]) can be obtained in a very immediate way from hit counts of web search engines if the appropriate queries are performed [14].

The disambiguation process starts from a previously obtained taxonomy [11]. For a given concept of the taxonomy (for example the root: *organ*) and a concrete level of depth (for example the first one), a classification process is performed by joining the subclasses (e.g. *liver*, *kidney*, *pipe organ*, etc.) which belong to each superclass sense. This process is performed by a *clustering algorithm* that joins the most similar concepts using, as a similarity measure, the degree of co-occurrence between pairs of concepts:

- For each possible pair of concepts of the same taxonomic level (see Figures 1 and 2), a query to the search engine is constructed. Using "web scale statistics" based on estimated hit counts of web search engines, the following score is computed (1).

$$\text{Similarity}(\text{Concept_A}, \text{Concept_B}) = \frac{\text{hits}(\text{"Concept_A"} \text{ AND } \text{"Concept_B"})}{\text{Max}(\text{hits}(\text{"Concept_A"}), \text{hits}(\text{"Concept_B"}))} \quad (1)$$

The system computes the relative degree of co-occurrence between a pair of terms in relation to the most general one (that covers a wider spectrum of web resources). So, the higher it is, the more similar the concepts are.

- With these measures, a similarity matrix between all concepts is constructed. The most similar concepts (in the example shown in Figure 1, *liver* and *kidney* have the highest co-occurrence degree, 0.793) are selected and joined indicating that they belong to the same keyword's sense. The joining process is performed by creating a new class with those concepts and removing them individually from the initial taxonomy.
- For this new class, the similarity measure to the remaining concepts is computed, considering the most distant one (2) (furthest neighbour: *complete linkage*). In consequence, no more Web search engine queries are required. Other measures like considering the nearest neighbour (*single linkage*) or the arithmetic average

have also been tested, obtaining worse results. As they are less restrictive measures, they tend to join all the classes, making it difficult to differentiate final senses.

$$\text{Similarity}(\text{Class}(A, B), C) = \text{Min}(\text{Similarity}(A, C), \text{Similarity}(B, C)) \quad (2)$$

- The similarity matrix is updated with these values and the new most similar concepts/classes are joined (building a dendrogram as shown in Figures 1 and 2).

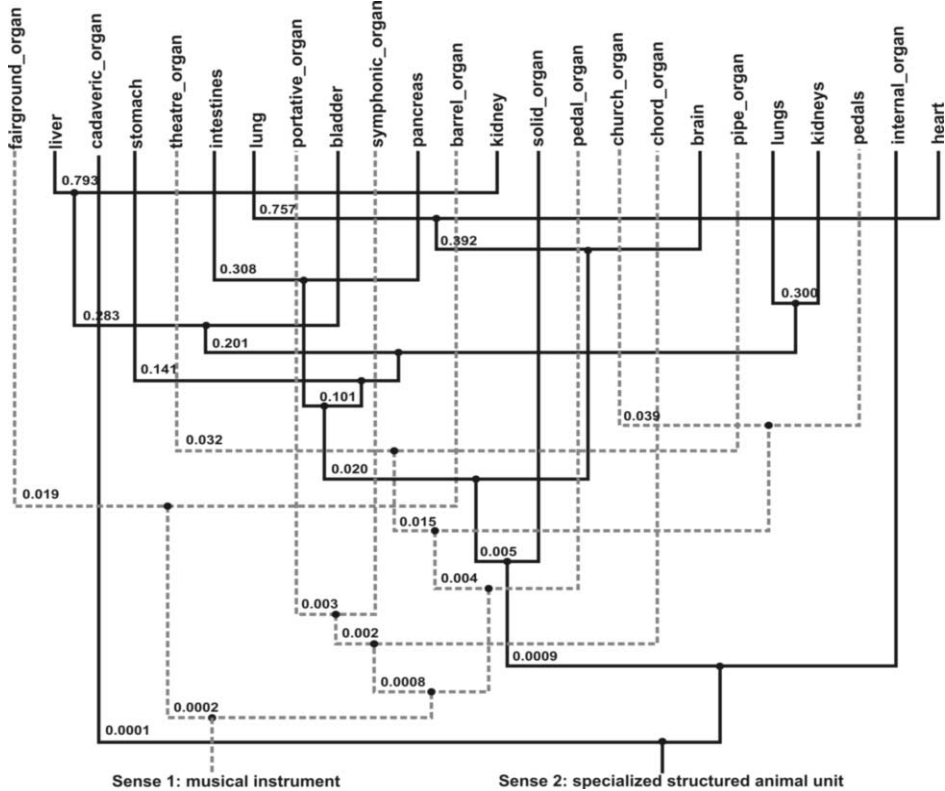


Figure 1. Dendrogram representing semantic associations between classes found for the *organ* domain. Two final clusters are automatically discovered when similarity equals zero.

- The process is repeated until no more elements remain disjoint or the similarity is below a minimum threshold. For domains with well differentiated senses, no threshold is needed in order to detect final clusters: they are automatically defined when the similarity equals zero (no co-occurrence between any of the concepts). This is caused by the use of the restrictive *complete linkage* as the joining criteria

The result is a partition (with 2 elements for the *organ* and *virus* examples) of the classes that groups the concepts that belong to a specific meaning. The number of final classes is, in most cases, automatically discovered by the clustering algorithm. Note that this methodology can be applied to a set of terms at any level of the taxonomy.

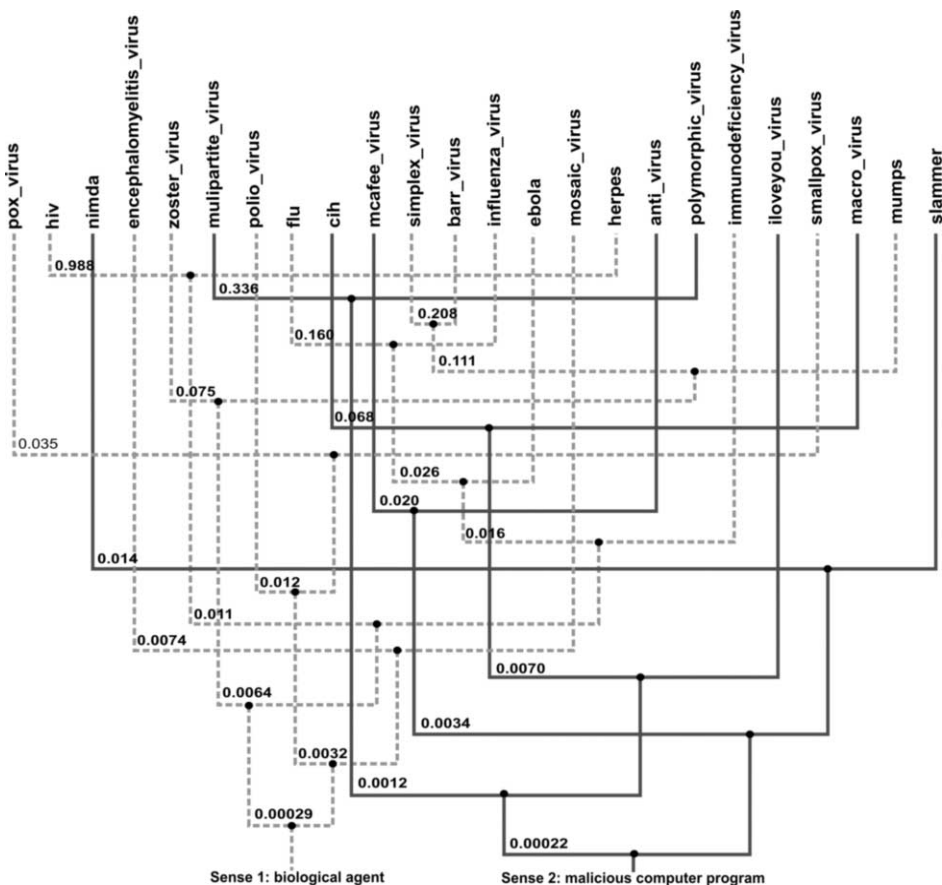


Figure 2. Dendrogram representing semantic associations between classes found for the *virus* domain. Two final clusters are automatically discovered when similarity equals zero. Note that *nimda*, *cih*, *iloveyou* and *slammer* are computer virus names.

4. Evaluation

The purpose of the evaluation procedure is to check the results from two points of view:

- To evaluate if each cluster of concepts is properly associated to one of the senses of the corresponding superclass.
- To check if each concept belongs to the appropriate cluster.

In order to perform an automatic and domain-independent evaluation, we have used the WordNet electronic repository as a gold standard.

4.1 WordNet overview

WordNet [5] offers a lexicon, thesaurus and semantic linkage between the major part of English terms. It is organised in synonym sets (*synsets*): a set of words that are interchangeable in some context, because they share a commonly-agreed upon meaning with little or no variation. They have an associated gloss.

At the next level there exist semantic pointers. They are directed edges in the graph whose nodes are *synsets*. Some interesting semantic pointers are: *hyponym*, *meronym*, *attribute* and *similar to*.

All this information summarizes the meaning of a specific concept and models the knowledge available for a particular domain. Using it, one can compute the similarity and relatedness between concepts. There have been some initiatives for implementing these measures, such as the software *WordNet:Similarity* [8]. More concretely, *similarity measures* use information found in an *is-a* hierarchy of concepts and quantify how much a concept *A* is like another concept *B*. WordNet is particularly well suited for similarity measures, since it organizes nouns and verbs into *is-a* hierarchies and, therefore, it can be adequate to evaluate taxonomical relationships.

4.2 Evaluation procedure

Considering the evaluation goals and the way in which WordNet organizes each concept in function of its corresponding senses (*synsets*), we have designed an especially adapted WordNet based evaluation of the results.

To deal with the first objective of the evaluation, we try to find which of the *synsets* (and their associated glosses) of the superclass (e.g. *organ*) is the most appropriate for the set of concepts contained in each cluster (e.g. cluster1: *brain*, *lung*, *liver*; cluster2: *pipe*, *church*, *symphonic*). In other words, we have to measure which superclass *synset* is the most *similar* to the highest amount of cluster components. As we are working with subclass concepts that are taxonomically related with the superclass, as mentioned in the previous section, WordNet based similarity measures [8] can be computed. For this purpose we have opted for the *path length* similarity measure. It computes the number of semantic pointers that link taxonomically a pair of concepts' *synsets*.

Once the path length measure for each subclass belonging to each cluster against each superclass *synset* has been computed, it can be obtained which of the superclass senses is the most similar to the particular subclass (e.g. the *liver* subclass is most similar to the *organ's synset* defined as “*animal unit specialized in a particular function*”). As a result, the system selects as the sense (*synset+gloss*) of each cluster the one that appears more frequently as the most similar sense to all its subclasses. Evaluating this assignment, one can have an idea of the quality of the clusterization in relation to the number and adequacy of obtained clusters. For example, it is possible to check if the number of clusters with different senses corresponds to the total number of senses of the superclass. In a similar manner, one can check if several clusters should be joined as they share the same particular sense.

On the other hand, to deal with the second objective we can evaluate each individual concept by checking if its associated cluster is the most suitable one. Concretely, once a sense has been assigned to each cluster, for each term of that cluster, it checks if its corresponding selected gloss is really the most similar one (computed in the previous step). In this manner it is possible to verify if the most similar *synset* for

each concept is really the same that the one corresponding to its cluster. This can give us an idea on how correctly was each term classified in the concrete cluster (sense).

4.3 Evaluation examples

First, we offer the evaluation results for the *organ* domain. For that noun, the following synsets are available in WordNet:

- 1) *A fully differentiated structural and functional unit in an animal that is specialized for some particular function.*
- 2) *A government agency or instrument devoted to the performance of some specific function.*
- 3) *An electronic simulation of a pipe organ.*
- 4) *A periodical that is published by a special interest group.*
- 5) *Wind instrument whose sound is produced by means of pipes arranged in sets supplied with air from a bellows and controlled from a large complex musical keyboard.*
- 6) *A free-reed instrument in which air is forced through the reeds by bellows.*

Considering the concepts found for that domain and the clustered sets obtained after the disambiguation process, the similarity between each concept and each of the 6 senses has been measured. As a result, the apparently most suitable superclass sense for each concept of each cluster is obtained.

Observing the results presented in Table 1, for the first cluster of concepts, it is clear that the most suitable superclass sense is number 1. One can see that this is the most adequate sense for the defined cluster and it indicates that is has been correctly defined. In addition, almost all of the concepts belonging to the cluster have the highest similarity against that cluster. This indicates that the classes composing the cluster are correctly classified. For the first two we have not been able to obtain any measure, as they are not linked taxonomically with the corresponding superclass in WordNet.

Table 1. Evaluation of the semantic clusters for the *organ* domain.

Cluster1	Superclass sense	Cluster2	Superclass sense
Cadaveric_organ	Not found	Barrel_organ	3
Internal_organ	Not found	Fairground_organ	1
Brain	1	Chord_organ	Not found
Lung(s)	1	Portative_organ	Not found
Heart	1	Symphonic_organ	Not found
Liver	1	Church_organ	2
Kidney(s)	1	Pedals	3
Bladder	1	Theatre_organ	1
Stomach	1	Pipe_organ	5
Pancreas	1	Pedal_organ	3
Intestines	1		
Solid_organ	1		

For the second cluster, the most common superclass sense is number 3. Even though this can be a suitable sense for the cluster, one may also consider sense number 5 and even number 6 as correct. Analyzing each concept independently, one can see that there is much more variability, including incorrectly obtained senses such as number 1 and 2. This may indicate that some concepts (those with sense #1) should be included in the other cluster or even in new ones. However, one can easily see that the most adequate senses are among 3, 5 and 6. This indicates the poor semantic pointer coverage for many domains in WordNet [14] and the proliferation of barely differentiated word senses [2].

We have also applied the same procedure over the other polysemic domain: *virus*. For that noun, the following synsets are available in WordNet:

- 1) *Infectious agent that replicates itself only within cells of living hosts; many are pathogenic; a piece of nucleic acid (DNA or RNA) wrapped in a thin coat of protein.*
- 2) *A harmful or corrupting agency.*
- 3) *A software program capable of reproducing itself and usually capable of causing great harm to files or other programs on the same computer.*

Evaluation results following the same process over this domain are presented in Table 2. In this case, the classification seems much worse even though one can easily observe that our results are, in general, quite correct. On the one hand, the most common sense for the first cluster appears to be number 2 (*A harmful or corrupting agency*), and not the correct one (*Infectious agent that replicates itself only within cells of living hosts*). In this case, due to the particular semantic organization of WordNet's *is-a* hierarchies, the WordNet-based similarity measure behaves in an incorrect way. On the other hand, for the second cluster, much of the cluster terms are referred to computer names of virus, a very dynamic domain that can be hardly covered in a general purpose repository.

Table 2. Evaluation of the semantic clusters for the *virus* domain

Cluster1	Supercl. sense	Cluster2	Superclass sense
Herpes	1	Multipartite_virus	Not found
Hiv	1	Polymorphic_virus	Not found
Immunodeficiency_virus	2	Iloveyou_virus	Not found
Ebola	2	Cih	Not found
Flu	2	Macro_virus	3
Influenza_virus	2	Mcafee_virus	Not found
Zoster_virus	2	Anti_virus	Not found
Mumps	2	Slammer	1
Simplex_virus	Not found	Nimda	Not found
Barr_virus	Not found		
Smallpox_virus	2		
Pox_virus	2		
Polio_virus	2		
Encephalomyelitis_virus	Not found		
Mosaic_virus	3		

5. Conclusions and future work

The proposed polysemy disambiguation algorithm has been designed as a complement for our ontology learning methodology, and not as a general purpose approach. In order to ensure a feasible integration in the learning process, the disambiguation method has been designed to work in an automatic, domain independent and unsupervised way. Moreover, both methods use Web scale statistics to check the candidates relevance results in a highly efficient, scalable and robust way.

Regarding the evaluation procedure, as any automatic approach, extracted conclusions should be taken with care. Our disambiguation method is designed to distinguish well differentiated senses that really can influence on the quality and structure of the final results. This characteristic does not fit very well with the proliferation of word sense distinctions in WordNet, which is difficult to justify and use in practical terms, since many of the distinctions are unclear [2]. In addition, the employed WordNet based similarity measure heavily depends on WordNet's semantic pointer coverage for the particular domain. In contrast, the Web based semantic distance hardly presents this handicap thanks to the high coverage offered by the Web for almost every possible domain of knowledge.

As a future line of research, we plan to integrate the semantic disambiguation process in conjunction with a previously developed method for *synonym discovery* [12] in the full ontology learning process. On the one hand, synonym sets can be used to expand the search to other web resources that were not potentially retrieved by the keyword-based search engine. This could improve the *recall* of the final results when dealing with narrow domains where a limited amount of resources is retrieved. On the other hand, polysemy disambiguation may aid to improve the *precision* of the final taxonomy in polysemic domains by presenting a more structured hierarchy with clustered classes according to superclass senses.

Acknowledgements

This work has been supported by the "Departament d'Innovació, Universitats i Empresa de la Generalitat de Catalunya i del Fons Social Europeu".

References

- [1] E. Agirre and G. Rigau: A Proposal for Word Sense Disambiguation using Conceptual Distance, in Proceedings of the *International Conference on Recent Advances in NLP (RANLP'95)*, 1995, pp. 16-22.
- [2] E. Agirre, O. Ansa, E. Hovy and D. Martinez: Enriching very large ontologies using the WWW, in Proceedings of the *Workshop on Ontology Construction of the European Conference of AI (ECAI-00)*, Berlin, Germany, 2000.
- [3] R. Cilibrasi and P.M.B. Vitanyi: The Google Similarity Distance, *IEEE Transactions on Knowledge and Data Engineering* **19** (3) (2006), 370-383.
- [4] O. Etzioni, M. Cafarella, D. Downey, A.M. Popescu, T. Shaked, S. Soderland, D.S. Weld and A. Yates: Unsupervised named-entity extraction from the Web: An experimental study, *Artificial Intelligence* **165** (2005), 91-134.
- [5] C. Fellbaum: WordNet: An Electronic Lexical Database, MIT Press, Cambridge, Massachusetts. More information: <http://www.cogsci.princeton.edu/~wn/> 1998.
- [6] N. Ide and J. Veronis, J: Introduction to the Special Issue on Word Sense Disambiguation: The State of the Art, *Computational Linguistics* **24** (1) (1998), 1-40.

- [7] R., Mihalcea and P. Edmonds: Proceedings of Senseval-3, *3rd International Workshop on the Evaluation of Systems for the Semantic Analysis of Text*, Barcelona, Spain, 2004.
- [8] T. Pedersen, S. Patwardhan and J. Michelizzi: WordNet:Similarity – Measuring the Relatedness of Concepts, American Association for Artificial Intelligence, 2004.
- [9] P. Rosso, F. Masulli, D. Buscaldi, F. Pla and A. Molina, A: Automatic Noun Disambiguation, in Proceedings in *Computational Linguistics and Intelligent Text Processing*, LNCS 2588, Springer-Verlag, 2003, pp. 273–276.
- [10] P. Rosso, M. Montes-y-Gomez, D. Buscaldi, A. Pancardo-Rodríguez and L. Villaseñor: Two Web-Based Approaches for Noun Sense Disambiguation, in *Proceedings of CICLing 2005*, LNCS 3406, Springer-Verlag, 2005, pp. 267–279.
- [11] D. Sánchez and A. Moreno: A methodology for knowledge acquisition from the web, *International Journal of Knowledge-Based and Intelligent Engineering Systems* **10** (6) (2006) 453-475.
- [12] D. Sánchez and A. Moreno: Automatic discovery of synonyms and lexicalizations from the Web, in Proceedings of *Vuitè Congrés Català d'Intel·ligència Artificial (CCIA'05)*, Artificial Intelligence Research and Development, Vol. 131, Italy, 2005, pp. 205-212.
- [13] Sens Eval: Evaluation Exercises for the Semantic Analysis of Text. Available at: <http://www.senseval.org/publications/senseval.pdf>. 2004.
- [14] P.D. Turney: Mining the Web for synonyms: PMI-IR versus LSA on TOEFL, in Proceedings of the *Twelfth European Conference on Machine Learning*, Freiburg, Germany, 2001, pp. 491-499.
- [15] D. Yarowsky: Unsupervised Word-Sense Disambiguation Rivalling Supervised Methods, in Proceedings of the *33rd Annual Meeting of the Association for Computational Linguistics*, Cambridge, MA, 1995, pp. 189-196.

POP2.0: A search engine for public information services in local government

Antonio Manuel López Arjona, Miquel Montaner Rigall,
Josep Lluís de la Rosa i Esteva, and Maria Mercè Rovira i Regàs

*Agents Research Laboratory
EASY Centre, CIDEM Technological Innovations Network*

Abstract. Tools such as web search engines are currently focused on the exhaustive recovery of information. These tools, although very useful in certain contexts, do not respond to the needs of public information services, which aim to be precise, dealing with requests from the public without overloading them with irrelevant information. Just as when a member of the public telephones his city's helpline he wants a single response to his question, a web tool which tries to emulate this service also needs to be precise, ideally providing only one response. To achieve this objective, in this paper we present a search engine which offers precise information to the public, allowing them to ask questions in the language with which they are most comfortable, without this affecting the quality of the service provided.

Keywords. Search engine, natural language, text mining, information retrieval.

Introduction

All local government public information systems¹ suffer from a permanent lack of resources, a fact which hinders the proper development of the tasks for which they were conceived. The reason for this lack of resources is growing public demand [1] to use the services offered.

Public information services currently have two channels of response: one face to face and the other over the telephone. This conditions the use which can be made of the service according to the hours when the relevant staff are available and the human resources dedicated to the service. Various options have been proposed to solve this problem.

One option is the use of pre-programmed telephone switchboards. This solution has its drawbacks: the high volume of information that information service databases may contain (in the case of Terrassa² there are more than 18,000 possible responses) makes their installation and maintenance difficult.

Another option is to offer a web-based service which uses a standard search engine. This solution presents problems such as the exhaustive nature of search engines, which conflicts with the aim of these services to provide precise information, as well as legal problems related to access to the information, taking into account data

¹ <http://www.terrassa.cat/ajuntament/010/>

² <http://www.terrassa.cat>

protection legislation [2], problems concerning the impartiality which a public organisation must ensure, trying not to favour any one business over another and, finally, limitations related to the recognition of the natural language used by the public.

The last option is a combination of the previous two: an FAQ-based web system. These systems are built from a limited set of responses which need to be provided. The system is configured so as to relate the possible questions with the pre-established set of responses. As in the first case, this presents problems with regard to maintenance, since adding a new response involves studying all the cases to which it applies. It also presents problems of scalability, making it non-viable to introduce this type of tool into systems with a large set of responses. However, it does solve other problems, such as those of natural language, impartiality and compliance with data protection legislation.

Having looked at the various options, our proposal is to create a web tool which solves the problems of standard search engines. To be specific, we want a search engine which offers precise answers, taking into account that the optimal system would find only one response to each question, one which improves natural language-related aspects, functions better in cases affected by matters such as data protection legislation and impartiality, offers a system which is very simple to use, easily scalable and automatically maintained, with the result that data remain up to date.

We present below the previous work which has been carried out in this field. In section 2 we set out a detailed description of the proposed solution. Section 3 shows the various functionality tests and the ideas that we drew from them. Finally, we present our conclusion and discuss possible future work.

1. Previous research

We have recently witnessed enormous growth in the web[3] and this has led to the appearance of new tools to deal with a need that was previously irrelevant or non-existent[4]. Thanks to this new need, information recovery techniques have received much more attention.

When talking about search engines or information recovery, it is almost inevitable to think of Google. This search engine uses techniques based on the democracy of the web[5]. To do this, it gives a value to all pages based on the other pages which make reference to it and thus calculates what it calls a *PageRank*, based on both the number of pages which refer to it and those pages' own *PageRank*. The use of this tool is simple and transparent for the user. However, it presents problems if one takes into account the stated objectives for the precise nature of the response, natural language processing and impartiality when returning information.

Another type of web search engine, such as Clusty³ and Vivisimo⁴[6], both of which, like Lycos, came out of Carnegie Mellon University, try to solve the problems of the excessive return of information by applying clustering techniques[7]. But they do not succeed in solving the problem of exhaustivity, they merely provide the user with a tool to select from among the results. They also still suffer from Google's other problems with respect to data protection law and impartiality.

Other systems[8] use semantic analysis and these systems generally improve the treatment of natural language, even offering the possibility of improving searches by

³ <http://clusty.com/>

⁴ <http://vivisimo.com/html/velocity>

refining the concepts to search. However, they still have the other problems, including that of complexity of use.

Finally, tools directed at FAQ-based systems, such as Q-GO⁵ and Artificial Solutions⁶, present advantages with respect to ease of use, the precise nature of responses and even compliance with data protection laws and the degree of impartiality required. On the other hand, one can see a clear problem in terms of their scalability. When working with a large set of responses, these systems are non-viable because of the amount of time required to adjust and maintain them. The consequence of this is a high operational cost when adding a response, as well as the problem related to keeping information up to date, bearing in mind that one is working with a high volume of information.

2. Proposed search engine

The search engine proposed presents three distinct phases. The first phase deals with natural language. The system then calculates the degree of match between the question and the possible responses, and finally selects the response or responses which will be shown to the member of the public.

2.1. Treatment of natural language

During the phase dealing with natural language, the search engine eliminates *stopwords*, corrects spelling and makes a morphological analysis. Up to this point, the steps taken are basically the same as those in any text mining or information retrieval process[8] [9] [10]. It then identifies language patterns, applies the semantic network which has been developed, finds expressions with multiple words and identifies frequently used data.

The semantic network represents all the known semantic relationships between the words, thus relating two apparently different words and providing better quality in the analysis and treatment of natural language. This network is based on a prior analysis of the language and improvements made while the system is in use.

The stage related to *stopwords* is based on the identification and subsequent elimination of all words which do not carry useful meaning (such as articles, prepositions, etc.). Then, using free open-source tools such as the OpenOffice⁷ dictionary or the JMySpell⁸ spell-checker, the spelling is corrected, analysing the text and suggesting the correction which best fits the language used by the public. The next step is morphological analysis, which extracts the lemmas of the search words using the Freeling⁹ [11] dictionaries tool.

The most distinctive part of our search engine begins with the treatment of the language patterns used by the public when asking a question. By patterns, we mean the word structures commonly used in a question which make it specific and focus on the

⁵ <http://www.q-go.nl/5300/default.aspx>

⁶ <http://www.artificial-solutions.com/>

⁷ <http://lingucomponent.openoffice.org/>

⁸ <http://jmymspell.jawahispano.net/es/index.html>

⁹ <http://garraf.epsevg.upc.es/freeling/>

aim of the question. After identifying all the existing patterns in the question asked, each case is treated appropriately.

We then apply the semantic network which has been constructed, locating non-standard words, regionalisms (dialect words used in the region where the system is being used), synonyms, hyponyms, hyperonyms or mistakes (words commonly misspelled) and relate these with the root noun of the dictionary, thus building what we call the semantic block. This represents a single semantic value with different representations of itself: the original word, its lexeme or the relationships found through the semantic network.

Finally we identify multiple-word expressions (such as *town hall*), placing great emphasis on those which are specific to the world of officialdom and less used by the public (for example *cohabitation* is popularly known as *common law marriage*), and commonly used time expressions or dates (such as *yesterday*, *weekend* or *Good Friday*), adding these to the search and thus providing more useful information for the system.

2.2. Calculating the degree of match

Before we explain the next phase it should be noted that the set of possible responses available (not forgetting that this tool is to be applied to a public information service) may obviously be classified within a variety of different contexts, just as the questions posed by the public may be classified within the same contexts. For example, common contexts in public information services are the directory of organisations and the agenda of events taking place in the city.

Unlike other search engines, which search websites in order to extract information, the search engine we propose makes direct use of the information service's databases. This enables more precise classification of all the information, building a set of related information for each question based on higher quality descriptors (keywords) than those which other systems can produce. In this way it is better able to adjust the relevance of each piece of information within the response, given that, for example, the working hours of an organisation give us less information than details of what services it provides.

The degree of match between a question and a possible response i ($tLevel_i$), is obtained from the relationship between the semantic blocks built in the question with the descriptors of the response i , from whether it has accessed the relevant information of the response i , from the correlation between the context of the question and that of the response i , and from the popularity of the answer i [12] among the public.

$$\text{Eq. (1)} \quad tLevel_i = \frac{\sum_{k=1}^n sTruth_{k,i} + \sum_{k=1}^m eTruth_{k,i}}{n+m} * q1 + iC_i * q2 + cC_i * q3 + rPopularity_i * q4$$

Where $sTruth_{k,i}$, obtained from Eq.(2), is a value which indicates the correlation between each semantic block k of the question and the descriptors of the response i ; n indicates the number of semantic blocks identified in the question; $eTruth_{k,i}$ indicates the correlation between each expression k in the question and the descriptors of the response i ; m indicates the number of expressions identified in the question; iC_i indicates how many of the semantic blocks and expressions were in relevant positions

in the response i ; cC_i indicates the correlation of the search with respect to the context of the response i ; $rPopularity_{i,j}$, obtained from Eq.(3), is the factor which indicates the popularity of the response i . The values $q1, q2, q3, q4$ are weightings which give greater or lesser importance to the factors involved in the formula. These weightings are adjusted during the implementation of the system. It should be noted that $q4$ is the weighting which allows us to ensure the impartiality of the system, when this is necessary.

$$\begin{aligned} sTruth_{i,j} &= (lEntropy_i * q6 + q7) * \text{Max}(wW_{i,j}, lW_{i,j} * IP, sW_{i,j} * sP, bW_{i,j} * bP, \\ \text{Eq. (2)} \quad pW_{i,j} * pP, hW_{i,j} * hP, mW_{i,j} * mP, iW_{i,j} * iP) \end{aligned}$$

Where $lEntropy_i$, which is calculated from Eq.(4), indicates the lowest entropy (the quantity of information an element may provide, which is inversely related to the number of times it is repeated) among all the elements which make up the semantic block; wW_i indicates the correlation between the word searched for and what has been built by the semantic block i and the descriptors of the response j ; $lW_i, sW_i, bW_i, pW_i, hW_i, mW_i$ and iW_i are the values which indicate the degree of correlation between the lemmas, synonyms, non-standard words, regionalisms, hyponyms, hyperonyms and spelling mistakes belonging to the semantic block i and the descriptors of the response j ; IP, sP, bP, pP, hP, mP and iP are weightings which affect the degree of correlation according to the semantic relationship; $q6$ and $q7$ are adjustable values.

$$\text{Eq. (3)} \quad rPopularity_i = 1 - q5^{\left(\frac{clicks_i + throwings_i}{avgRconsults} \right)}$$

Where $clicks_i$ is the number of times a member of the public voluntarily views a response i and $throwings_i$ is the number of automatic views of response i (see 2.3). $avgRconsults$ indicates the average number of times each response has been consulted, taking into account $clicks$ and $throwings$; $q5$ is a parameter which is also adjusted during the implementation of the system.

$$\text{Eq. (4)} \quad \text{entropy}_i = \left| \log_2 \left(\frac{freq_i}{\max Freq} \right) / \log_2 \left(\frac{\min Freq}{\max Freq} \right) \right|$$

Where $freq_i$ indicates the number of repetitions of word i ; $\max Freq$ indicates the frequency of the word with the highest number of repetitions; $\min Freq$ indicates the frequency of the word with the lowest number of repetitions.

2.3. Selection of the response

The final phase of the search relates to the selection of the response or responses which will be shown to the member of the public. First the responses are ordered, based on the degree of match. The system evaluates whether the first response is sufficiently precise and, if so, the remainder can be ignored. If not then it will reduce the number of responses.

Once the responses are ordered by degree of match, the most relevant response is compared with the others. If the first response meets a specified minimum quality, and

also greatly exceeds the quality of the others, this response will be automatically launched so that the public sees only one response.

If no automatic response is launched, the degree of match of the most relevant response is taken and a selection is made from the other responses based on this, obtaining a smaller set of responses but one of higher quality.

3. Experiments and results

The aim of the experiments we carried out was to demonstrate that our search engine produces more specific answers for the public than the others and is therefore more appropriate for a virtual public information service. The tests were carried out using the various tools which can be found on the website of Terrassa town hall¹⁰, which is where the system described in this paper was installed (iSAC¹¹).

Comparisons were carried out using the Google search engine applied to the Terrassa town hall's website¹², the Metacercador developed by the Administració Oberta de Catalunya¹³, and a search engine developed by Terrassa town hall itself which it used until the implementation of the tools mentioned above¹⁴.

The experiment was carried out using 1,200 real questions posed to the Terrassa public information service between 1st and 10th April 2007, out of a total of more than 35,000 questions asked during the first six months of 2007.

This set of questions was presented to the various tools and the results were compared according to the following scores: the average number of responses returned by the system (# responses) and a value indicated by how precise the responses were and percentage of match (% match), where we consider a match to be when the correct response is found among the first five results displayed by the tool.

Table 1. Table of results:

	iSAC	Google	AOC Search Engine	Terrassa Search Engine
% match	87%	58%	60%	38%
# results	23	547	455	18

Table 1 shows that Terrassa's own search engine produced very few results from the searches carried out, but on the other hand the percentage of matches was very low. This is because the system has no procedures to handle natural language and this greatly limits the search area.

The results of Google and the Metacercador are similar, slightly better in the case of the Metacercador, as this tool was developed specifically for application in local government offices such as town or district councils. In both cases the percentage of

¹⁰ <http://www.terrassa.cat/>

¹¹ <http://isac.terrassa.org/isac/>

¹² <http://www.google.com/custom?hl=es&domains=terrassa.net&btnG=Buscar&sitesearch=terrassa.net>

¹³ <http://cercador.aocat.net/cercador.asp?Origen=20&tipus2=C&OrigenCerca=08279&organisme=08279>

¹⁴ <http://www.terrassa.cat/cercador/>

matches is considerably higher. However, the philosophy behind their development, the search for exhaustive results, means that the number of responses shown is very high, in both cases around 500. This does not provide the functionality we wish to provide in a public information service. Another problem we found was that of impartiality, since these systems are based on rankings by votes without taking this issue into account.

Finally, the search engine proposed here found the correct response in 87% of cases, which is a very good indicator of how it deals with the information. In addition, the average number of results shown was only 23. Although this is a much lower number than either the Metacercador or Google, we think it is still too high since an optimal tool, one which more literally emulates a typical telephone conversation with a public helpline, would return only one single result and that would be the correct one.

It is worth mentioning that response times of the various tools are similar in all cases and within what usability experts have estimated as average user waiting time [13].

4. Conclusions and future lines of research

The project was carried out in three phases: treatment of natural language, classification of possible responses and selection of the correct response/s. Finally the search engine developed was compared with other tools already in use on the Terrassa town hall website, all of which were working and which therefore allowed a valid comparison. The results observed were that although other tools achieved a high percentage of match, they were found lacking with respect to needs for precise responses, data protection or impartiality noted at the beginning of the project. The search engine proposed in this paper presents a high degree of match and sufficiently precise responses to be considered a good tool for a public information service.

When considering related lines of work for the future, it is important to emphasise that people very often ask local government offices questions which are not that particular office's responsibility. When they do not get a response, they are unhappy with the service they have received. In order to deal with this problem we need to develop a system of communication between the search engines installed in the various administrative offices (town halls, district councils, etc.) providing access to any information which may be of interest to the public, transparently and regardless of whose responsibility it is.

We also need to consider content management based on the WIKI philosophy[14], leaving the workings of the system in the hands of the users themselves so as to better adapt and improve it to meet the needs of the public.

Acknowledgements

This work was carried out with the support of a grant from the Catalan government “AOC 2007 “iSAC: el 010 a la web” and European project “No. 34744 ONE: Open Negotiation Environment, FP6-2005-IST-5, ICT-for networked Businesses”.

Bibliography

- [1] *Atenció ciutadana, Dossier de premsa.* (2006)
http://www10.gencat.net/dursi/generados/catala/societat_informacio/recurs/doc/dossier012.pdf
- [2] *LEY ORGÁNICA 15/1999, de 13 de diciembre, de Protección de Datos de Carácter Personal.* (1999)
<http://www.msc.es/organizacion/sns/planCalidadSNS/pdf/transparencia/LOPD19992.pdf>
- [3] M. Castells, Universitat Oberta de Catalunya; *Internet y la Sociedad Red*; Lliçó inaugural del programa de doctorat sobre la societat de la informació i el coneixement. (2001)
- [4] J. Grau, J. Guayar; *El negocio de buscar en Internet. Análisis de mercado de los buscadores 2003*; El profesional de la información, ISSN 1386-6710, vol. 13, Nº 4, pp. 292-300. (2004)
- [5] S. Brin, L. Page; *The Anatomy of a Large-Scale Hypertextual Web Search Engine*; WWW7 / Computer Networks 30(1-7), pp. 107-117 (1998)
- [6] S. Koshman, A. Spink, B. Cansen; *Web searching on the Vivisimo search engine*; Journal of the American Society for Information Science and Technology, Volume 57 , pp. 1875 – 1887, ISSN:1532-2882. (2006)
- [7] Steinbach, M., Karypis, G., & Kumar, V; *A comparison of document clustering techniques*; KDD Workshop on Text Mining. (2000)
- [8] F. Verdejo, J. Gonzalo, D. Fernández, A. Peñas, F. López; *ITEM: un motor de búsqueda multilingüe basado en indexación semántica*; Proceedings JBIDI. (2000)
- [9] F. López-Ostenero, J. Gonzalo, F. Verdejo; *Búsqueda de información multilingüe: estado del arte*; Inteligencia Artificial, Revista Iberoamericana de Inteligencia Artificial, vol. 22 , pp. 11 – 35. (2003)
- [10] A. Broder; *A taxonomy of web search*; SIGIR Forum, Vol. 36, No. 2, pp. 3-10. (2002)
- [11] A. Gelbukh, G. Sidorov; *Analizador Morfológico Disponible: un recurso importante para PLN en español*; Taller de Herramientas y Recursos Lingüísticos para el Español y el Portugués. (2004)
- [12] S. Mizarro; *Quality control in scholarly publishing: A new proposal*; Journal of the American Society for Information Science and Technology (J. Am. Soc. Inf. Sci. Technol.) ISSN 1532-2882, vol. 54, pp. 989-1005. (2003)
- [13] Jakob Nielsen; *Response Times: The Three Important Limits*; ISSN 1548-5552. (1994)
<http://www.useit.com/papers/responsetime.html>
- [14] A. Moreno, J. de la Rosa, C. Carrillo; *WIKIFAQ: Obtaining complete FAQs*; Frontiers in Artificial Intelligence and Applications – AI Research & Development ISSN 0922-6389, vol. 146, pp. 283-290, IOS Press. (2006)

Automatic Reading of Aeronautical Meteorological Messages

Luis DELGADO ⁽¹⁾, Núria CASTELL
Universitat Politècnica de Catalunya, Barcelona, Spain

Abstract. This paper describes the architecture developed to produce an automatic reader of aeronautical meteorological messages. An interlingua has been used and a whole process of natural language generation has been implemented. The system Festival has been used with a modified voice to read the messages generated. The presented system is able to translate the meteorological messages into a natural language text and read it.

Keywords. Aeronautical meteorological messages, interlingua, data flow diagrams, natural language generation, voice generation.

Introduction

This paper describes the general lines of a system developed for the automatic reading of aeronautical meteorological METAR and SPECI [1] [2] messages. The main purpose of this paper is to mark the different techniques we have used to treat the raw message and transform it into a natural language text that can be read using a modified voice of Festival [3].

The METAR (METeorological Airport Report) and SPECI (Special Meteorological Aeronautical Report) messages code the information about the metrological situation at the airports [1] [4]. This information has to be understood by the pilot and has to be read in a decoded way at the ATIS (Automatic Terminal Information Service) [5] frequency of the airport. So, a system as described here can be useful to help the pilot to understand the messages and can be implemented as a part of an automatic ATIS generation.

Nowadays we can find some systems that help us to decode the METAR messages like the one we find in meteofrance.fr [6]. These systems decode for us, in a very simple way, the information coded in the METAR message but it does not produce any kind of text generation. Other systems, like the developed by Computer Network Design [7], can be used to do an automatic ATIS. This system can analyse the meteorological information from the automatic weather observing system (AWOS) [8], but it does not analyse the METAR messages. Moreover, it allows the user to generate speech from text using the speech application programming interface of Microsoft (SAPI) [9], but when we want to do a fully automatic ATIS this kind of systems use a pre-recorded library of words and phrases. Even if these systems can be useful they are too rigid and all the phrases will be generated in the same way. The system we propose here allows us to generate text in a natural way from the METAR messages and later read the text generated using the Festival system.

This paper is divided in 8 sections: First of all, the reader can see the problematic about the meteorological messages for aeronautics and the interest in their automation. Sections 2 and 3 offer an overview of the specification of the system and its architecture. The translation of a message into a natural language text and the connexion with Festival is described in section 4. The work done in Festival to produce speech generation adapted to meteorological messages is described in section 5. Some examples of use are shown in section 6. Further work and conclusions close this paper.

1. Meteorological messages

The METAR, SPECI and TAF [1] [2] (Terminal Aerodrome Forecast) messages are generated by the meteorological observatories located at the airports. The METAR messages are created regularly each fixed interval of time. If the situation changes between two METAR messages then a SPECI message would be generated. The TAF messages give to the pilot the information about how the weather will evolve in the following hours. The METAR, SPECI and TAF messages code the information in a very

¹ Corresponding author: TALP Research Center, UPC, e5785856@est.fib.upc.edu. Second contact: castell@talp.upc.edu

specific way. So using a specific code all the meteorological information is represented. [10][11][12] All the messages have a group of information where is coded the identification of the airport, the date and the hour of the message, the information about the wind in the surface, the visibility, the clouds and the atmospheric pressure. The message will code also if any situation like rain, storms, fog, etc. is produced. The METAR message can have information about how the situation will evolve in the following hours (this is the TREND part of the message). Sometimes if the runway change its characteristics due to the meteorological situation this information is coded also in the METAR message, for example if due to the rain the coefficient of friction of the runway change it can be also coded in the message.

Once these messages are created they are diffused with the NOTAM (Notice To Airmen) information, which inform about the situation of the airport: runway used, if a taxiway is closed, etc. The meteorological information is crucial for the coordination and the development of the operations of approach and landing.

Nowadays the ATIS give this information. The radio transmitter is used to broadcast the information that could be important for the airplanes that operate close to the airport. The ATIS information is changed each time the meteorological information or the airport information is changed. In order to minimize the errors due to the few quality of the radio transmission, many research groups are working on the possibility of transfer all the information relevant to the flight (messages and orders given by controllers) by data-link between the ground and the plane [13]. Thus, the information will arrive coded to the plane and a system on board would show/read it to the pilot. In the same way as the METAR, SPECI and TAF information, the SIGMET [1] (Significant Meteorological Forecast) is sent to the plane to help them to navigate avoiding adverse meteorological phenomenon. In the Figure 1 we can see the flow of information.

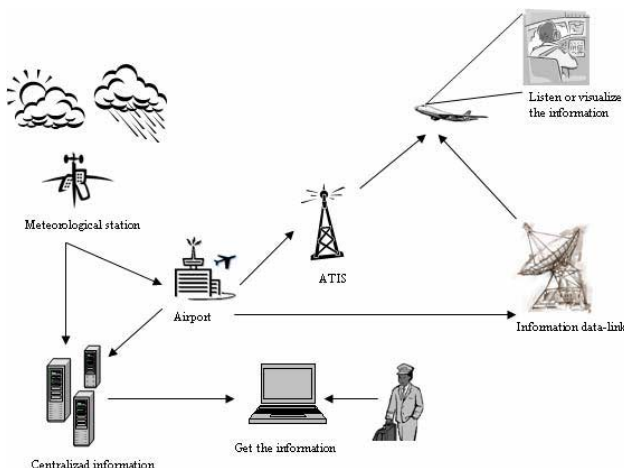


Figure 1. Flow of information

2. System specification

The system we have developed does the translation to natural language of the messages METAR and SPECI. This text generation is followed by a reading of it (speech synthesis). The translation and reading has been done in Spanish. However, the system has been developed in a way that allows the addition of a new language in a very simple way.

For the lecture of the message, our system is connected to Festival [3]. Festival is a framework that allows us to develop our speech synthesizer. Festival has been created by the University of Edinburgh and uses the library Speech Tools Library. The Festival Spanish voice has been modified in order to adapt it to the domain of aeronautical meteorological messages.

3. System architecture

From a functional point of view, the system is divided in three parts (Figure 2.)

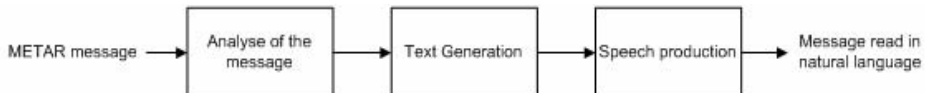


Figure 2. Functional view of the system

1. Analyse of the message to extract the information.
2. Generation of the text in natural language.
3. Synthesization of the voice to read the generated message.

To maximize the characteristics of modularity, reusability, maintainability, just as the easiness of expansion, the system has been developed in three layers and each one has different packages. (Figure 3.)

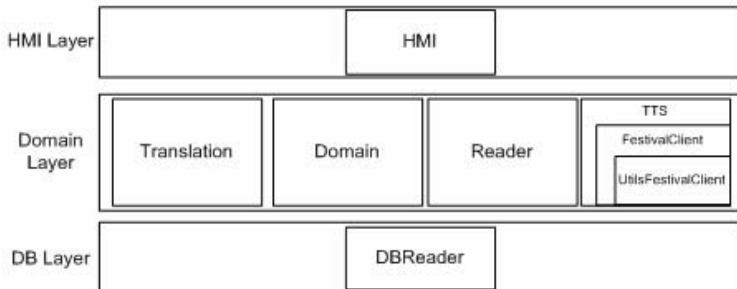


Figure 3. Architecture of the system

- The HMI (Human Machine Interaction) package ensures the interaction with the user.
- The package of Translation analyzes the METAR and SPECI messages.
- The Domain package has the information that is used to represent the information contained in the meteorological message.
- The Reader will generate the text.
- TTS (Text To Speech) and its subs-packages connect our system with Festival to produce the read of the message.
- The DBReader package will connect the Domain Layer with the database that contains the information about the name of the airports.

The Figure 4 shows how the information is sent to Festival to produce the read message.

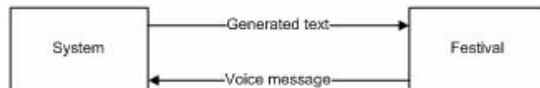


Figure 4. Interaction of the system with Festival

3.1. Analyse of the METAR and SPECI message

As we have said the METAR and the SPECI messages are coded in a very specific way. So, a very simple first version of a system could be as direct as a transducer. (Figure 5.)

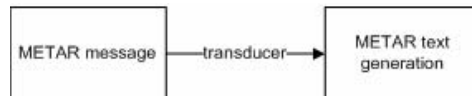


Figure 5. Simple version of the system

However, with this approach we would obtain a solution too much rigid. Our idea is to have a system the most adaptable to changes, so if we change the language we don't want to redo the analysis. For this, we have chosen to pass through an interlingua. The analysis of the message will be an automat that will parse the message and will construct an intermediate structure with all the information contained in the

message. Later, the text generator will use these structures to generate the text in the most natural way as possible. This data flow is shown in the Figure 6.

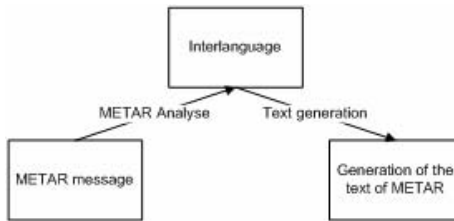


Figure 6. System with an interlanguage

The interlingua is defined as a group of classes with relations between them. These classes represent the information that the meteorological messages could have. Using an interlingua has many benefits: it will allow us to rewrite the message without redoing the analysis. It is useful if we want to obtain different texts generated for the same message. It is also useful because we can use this intermediate structure to other purposes than the transduction to natural language. Once we have decoded the message, this information could be used to do other tasks than give the plain meteorological information to the pilot. So, for example, it could be used to help in the computation of routes on ground or, to decide which airport with an adequate meteorological situation is the closest if the meteorological situation is degraded very fast in a VFR (Visual Flight Rules) flight. This information could be used also to detect, in an automatic way, risky situations (storms, low visibility, strong winds perpendicularly to the axis of the runway, etc), this kind of information would be very useful to the light aviation where the planes are not so equipped as the commercials ones.

The interlingua has an additional interest in the fact that we have separated the analysis of the message from the text generation. This allows us to change the generated text language without changing the analysis.

3.2. Text Generation

Once the message has been analyzed and translated into the interlingua, the text is generated by the Reader package. This package would have one implementation of the reader for each language. It will use the information contained in the interlingua to produce a text the most natural as possible.

3.3. Voice Synthesis

As we have already said, the voice synthesis will be done with Festival. For this purpose the package TTS will connect with Festival that will be executed as a server.

4. System design

4.1. HMI layer

The interaction with the user is done by the package HMI. Its responsibility is to generate the interface and communicate the instructions to the domain layer. With this interface, the use of our system is very simple: the user introduces the METAR or SPECI message and asks the system to translate it or to translate and read it. The system will call to the analyzer who will translate the message to the interlingua. Later, the reader will generate the text in natural language and the TTS package will connect to Festival to produce the voice synthesis.

4.2. Domain layer

This layer is the most important and has four components: translation, domain, reader and TTS.

In this layer we will find the code that implements the automat that analyse the message and generates the message information in the interlingua.

As we have said, the interlingua is defined as a group of classes with relations between them. The number of classes and relations could be very important but the benefit we obtain is worth.

We have tried to generate the text the most natural as possible. If we ask to different people to decode and read a message we will check that everyone will read it in a different way. So if we want a system that produces fully natural language we have to introduce some randomness. However the kind of messages we have to generate are reduced to a very specific domain, so we don't need a very complicated system like the one we could find in a text generator for automatic summary [14][15]. An easy but effective way we have found to model this is the use of data flow diagrams. There's a data flow diagram for each fragment of the message. This allows us to have a system that generates, for a same interlingua, different messages but reduce the points of connexion between the different parts generates. So, it simplifies the modelling of the text generation. We can have a data flow diagram at a level of paragraphs and decompose it in many small diagrams to produce the phrases.

The Figure 7 shows a part of the grammar that we have used to generate a part of the message. This grammar could be shown as a data-flow diagram. To work with these diagrams is also useful from a point of view of software engineering because it is helpful to control the different kinds of messages that can be generated and it is very easy to split the problem of generation of big messages in small parts.

```

ReadWind → SignificantWind | NotSignificantWind
SignificantWind → StrongerThan40kts | NotStrongerThan40kts
StrongerThan40kts → "hay un día ventoso con vientos" WindModificador
WindModificador → "superior a" QuantityAndUnit GustTreatment |
                    "inferior a" QuantityAndUnit GustTreatment |
                    "de" QuantityAndUnit GustTreatment
GustTreatment → Gust | VariableDirectionTreatment
Gust → "con ráfagas de" QuantityAndUnit VariableDirectionTreatment
VariableDirectionTreatment → ". El viento tiene dirección variable" |
                           NotDirectionVariable
NotDirectionVariable → "del" CardinalPoint "( Degrees "grados)" |
                           "de" Degrees "grados"
NotSignificantWind → "el viento está calmado." |
                     "no hay viento significativo."

```

Figure 7. Part of the grammar used to generate the messages

With the grammar shown in Figure 7, we can generate different natural language texts for the part of the message that indicate when the wind is strong. For example the part of the METAR message: 12012G43K has the information that the wind comes from 120 degrees with strength of 12 Kt and with gusts of 43 Kt.

To use the grammar we choose the text generated in function of the values of the message coded in the interlingua and in a random way when many alternatives are possible. So we could generate a message like "hay un día ventoso con vientos de 120 nudos con ráfagas de 43 nudos que proviene de 120 grados" "there is a windy day with wind strength of 120 knots with gusts of 43 knots that comes from 120 degrees" or "hay un día ventoso con vientos de 120 nudos con ráfagas de 43 nudos que proviene del sureste (120 grados)" "there is a windy day with winds of 120 knots with gusts of 43 knots that comes from the southeast (120 degrees)".

Once the text is generated we can connect our system with Festival. So, the steps, the system will do if we ask him to read the text, would be:

1. Creation of the session.
2. Initialization of the system Festival.
3. Ask Festival to use the voice_em_diphone.
4. Give to Festival the text to read.
5. End the session.

The voice_em_diphone is a modified version of the Spanish voice that we can find in Festival. As we will see this voice has been adapted in order to treat the meteorological messages.

4.3. Database layer

The database has the information of the ICAO (International Civil Aviation Organisation) code, name, city and country of all the airports [16][17]. So if the text generator wishes, it can ask the database any information about the airport to add it to the generated text.

5. Speech synthesis with Festival

Festival is a system to convert text to speech developed at University of Edinburgh. It has many voices by default. We have chosen to modify the voice_el_diphone to create the voice_em_diphone.

The voice voice_em_diphone works as the diagram Figure 8 shows:

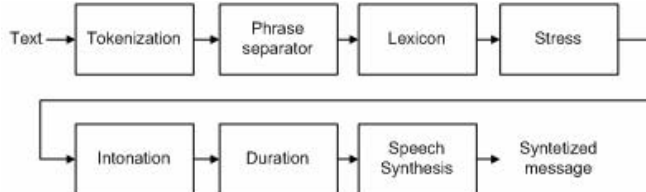


Figure 8. Use of the voices of Festival

So, one voice is composed of:

- Phoneset: basic bloc of construction of a voice.
- Lexicon: set of words associated with their phonetic pronunciation, or letters associated with their phonological symbol.
- Phrase separator: It is used to determine when a phrase starts and ends.
- Duration: The duration of each phoneme will be decided here.
- Signal synthesizer: We can use a system like MBROLA [18] or one phoneme database pre-recorded.

To adapt the Festival voice by default (voice_el_diphone) we have work on the tokenization stage. Here tokens like <"21"> are modified to their pronunciation <"veintiuno">. We have had some functions that allow to:

- Change a group of four capital letters to their international radio language to read the ICAO codes of the airports. So <"AHOD"> will be changed to <"Alfa" "Hotel" "Oscar" "Delta">.
- Read the units and speed: <"kt"> to <"nudos">, <"mph"> to <"millas" "por" "hora">, etc.
- The hours are changed by their numbers: <"21:11"> will be <"22" "11">.

We have had some words to the lexicon to try to improve the pronunciation. But due to the fact that the actual implementation of our system is in Spanish it is not very useful. We don't see a great improvement because the translation done by Festival of the words in Spanish to their phonemes is good enough.

6. Examples of use

Here we can see many messages and how the text is generated in different ways, in Spanish we can see the text generated by the system, in English its translation to a better understanding.

LEBL 172000Z 26005KT 210V010 9999 FEW025 SCT080 BKN170 26/17 Q1019 NOSIG

"Mensaje Metar del día 17. En el aeropuerto LEBL, a las 20:00 hora zulú, el viento viene del oeste (260 grados), con dirección variable entre 210 y 10 grados. El viento tiene una fuerza de 5 Kt.

La visibilidad es superior o igual a 10 kilómetros.

Hay escasas nubes a 2500 pies, nubes dispersas a 8000 pies y nubes fragmentadas a 17000 pies.

La temperatura es de 26 grados, la temperatura de punto de rocío es de 17 grados. La presión es de 1019 hectopascales."

"Metar message of the 17th. At the airport of LEBL, at 20:00 hours zulu, the wind comes from the west (260 degrees), with variable direction from 210 to 10 degrees. The wind has strength of 5 knots.

The visibility is bigger or equal to 10 kilometres.

There are few clouds at 2500 feet, scattered clouds at 8000 feet, broken clouds at 17000 feet.

The temperature is 26 degrees; the dew point is 17 degrees. The pressure is 1019 hectopascals."

"Mensaje Metar del día 17 del mes actual. En LEBL, a las 20:00 horas zulú, hay un viento de 5 Kt, la dirección del viento es de 260 grados, con dirección variable entre 210 y 10 grados.

La visibilidad es superior o igual a 10 kilómetros.

Hay escasas nubes a 2500 pies, nubes dispersas a 8000 pies y nubes fragmentadas a 17000 pies.

La temperatura es de 26 grados y la temperatura de punto de rocío es de 17 grados. La presión ambiente es de 1019 hectopascals."

"Metar message of the 17th of the present month. At LEBL, at 20:00 hours zulu, there is a wind of 5 knots, which directions is 260 degrees, the direction is variable between 210 and 10 degrees.

The visibility is bigger or equal to 10 kilometres.

There are few clouds at 2500 feet, scattered clouds at 8000 feet, broken clouds at 17000 feet.

The temperature is 26 degrees and the temperature of the dew point is 17 degrees. The environment pressure is 1019 hectopascals."

METAR LFPO 101300Z 270P10G25KT 9999SW 6000NE R29/0500N TS SN +TSRAGR vv345 OVC120TCU 18/12 Q2003

"Mensaje Metar del aeropuerto LFPO. El día 10 del mes actual, a las 13:00, el viento viene del oeste (270 grados) con una fuerza superior a 10Kt con ráfagas de 25Kt.

La visibilidad es superior o igual a 10 kilómetros dirección suroeste, con visibilidad máxima de 6 kilómetros dirección noreste. La visibilidad en la pista 29 es de 500 metros, no se esperan cambios.

Hay tormenta, nieve y fuerte lluvia con granizo.

El cielo está oscurecido a 34500 pies y cúmulos de desarrollo vertical cubren todo el cielo a 12000 pies.

La temperatura es de 18 grados, la temperatura de punto de rocío es de 12 grados. La presión ambiente es de 2003 hectopascals."

"Metar message of the airport LFPO. The 10th of the present month, at 13:00, the wind comes from the west (270 degrees) with strength bigger than 10 knots with gusts of 25 knots.

The visibility is bigger or equal to 10 kilometres direction southwest, with maximal visibility of 6 kilometres direction northeast. The visibility of the runway 29 is of 500 meters, no changes are expected.

Overcast at 34500 feet and cumulus of vertical development overcast the sky at 12000 feet.

The temperature is 18 degrees, the the temperature of the dew point is 12 degrees. The environment pressure is 2003 hectopascals."

"Mensaje Metar del día 10 a las 13:00. En el aeropuerto LPO, el viento viene del oeste (270 grados) con una fuerza superior a 10Kt con ráfagas de 25Kt.

La visibilidad es superior o igual a 10 kilómetros dirección suroeste, con visibilidad máxima de 6 kilómetros dirección noreste. La visibilidad en la pista 29 es de 500 metros, no se esperan cambios.

Las condiciones meteorológicas actuales son tormenta, nieve y fuerte lluvia con granizo.

El cielo esta oscurecido a 34500 pies y cumulocongestus que cubren todo el cielo a 12000 pies.

La temperatura es de 18 grados, la temperatura de punto de rocío es de 12 grados. La presión ambiente es de 2003 hectopascals."

"Metar message of the 10th at 13:00. At the airport LFPO, the wind comes from the west (270 degrees) with strength bigger than 10 knots with gusts of 25 knots.

The visibility is bigger or equal to 10 kilometres direction southwest, with maximal visibility of 6 kilometres direction northeast. The visibility of the runway 29 is of 500 meters, no changes are expected.

Overcast at 34500 feet and there are cumulocongestus that cover the sky at 12000 feet.

The temperature is 18 degrees, the the temperature of the dew point is 12 degrees. The environment pressure is 2003 hectopascals."

7. Further work

Many modifications and extensions can be done to our system. Thanks to the use of the interlingua it is very easy to add news languages.

Nowadays there are many internet sites that offer the meteorological information in real time [19][20][21]. So it would be interesting connect our system to one of this sites. If we do it, only with the ICAO code of the airport we could get the meteorological message and obtain a translation to natural language.

The actual system analyse and generate the text for the METAR and SPECI messages, but it already detect if the messages are METAR, SPECI, TAF or SIGMET. So it would be interesting to extend the system to treat the kind of messages that are not already fully analyzed. A huge part of the interlingua could be reused and the Festival voice will be also useful.

As we have emphasized in this paper, our system could be use as a part of a bigger system that does the ATIS in an automatic way or it could be used as a part of a system that would read the information to the pilot when it arrives to the plane with the data-link.

A system that translates the aeronautical meteorological messages to natural language would be also useful to train the pilots to analyze this kind of messages.

Finally, the information decoded that we store in the interlingua could be used to other purposes like the compute of routes to avoid to pass through adverse areas, alarm systems that could alert when the weather situation is dangerous (storms, strong wind,...), etc.

8. Conclusion

In this paper we have described the main ideas of the software we have developed to do the translation and lecture of aeronautical meteorological messages. We have pointed out the advantages of using an interlingua. This will allow to use the decoded information of the message to other purposes than the text generation and will help to add new languages in a very easy way.

We also consider that the use of data flow diagrams to model the text generation is a very good methodology. It has made possible to have a view of the whole text generator system and to add new phrases in a very easy way. It is useful to decompose the generation of the text in the generation of paragraphs that could be decomposed in the generation of phrases.

Our system differs from the existing ones that it can generate fully natural text to express the meaning of the aeronautical messages and the use of a system like Festival to generate the speech synthesis allows us to have a more natural speech generation.

References

- [1] Météorologie, Assistance météorologique à l'aéronautique, Subdivision météorologique de l'ENAC, 4ème édition 2003
- [2] Messages d'observation et de prévisions d'aérodromes. Guide d'utilisation des codes. Édition Juillet 2005. Ref. D21/MO/CODESAERO version 2. Meteo France
- [3] <http://www.cstr.ed.ac.uk/projects/festival/>
- [4] <http://www.ofcm.gov/fmh-1/fmh1.htm>
- [5] http://www.cocesna.org/atis_intro.htm
- [6] <http://www.meteofrance.fr>
- [7] <http://www.cnd.co.nz/>
- [8] <http://www.faa.gov/asos/>
- [9] Hao Shi and Alexander Maier, "Speech-enabled Windows application using Microsoft SAPI", Victoria University, Melbourne, Australia. IJCSNS International Journal of Computer Science and Network Security, VOL.6 No.9.A, September 2006
- [10] "Guía Met, Información meteorológica aeronáutica", Instituto Nacional de Meteorología, 4^a edición, Febrero 2006
- [11] "Guía de servicios MET par a la navegación aérea", Instituto Nacional de Meteorología
- [12] Unidad de Meteorología Aeronáutica, Unidad de Estudios Técnicos y Control, "Tablas de cifrado claves METAR, SPECI y TAF", Instituto Nacional de Meteorología.
- [13] Jennifer King and Mohamed Mahmoud, "Voice over internet protocol communication system for use in air traffic control", Embry-Riddle Aeronautical University Air Traffic Management Research Laboratory, Daytona Beach, Florida
- [14] D.H. Lie, "Sumatra: A system for Automatic Summary Generation", Carp Technologies
- [15] Jiri Hynek and Karel Jezek, "Practical approach to automatic text summarization", Department of computer science and engineering, University of West Bohemia, Czech Republic.
- [16] <http://www.aircraft-charter-world.com/airports/europe/index.htm>
- [17] <http://www.airlinecodes.co.uk/aptcodeseach.asp>
- [18] <http://tcts.fpms.ac.be/synthesis/mbrola.html>
- [19] <http://www.flyingineurope.be/metar.taf.sigmet.htm>
- [20] <http://weather.noaa.gov/weather/metar.shtml>
- [21] <http://ogimet.com>

Uncertainty and Fuzziness

This page intentionally left blank

Maximum and Minimum of Discrete Fuzzy Numbers

Jaume Casasnovas^{a,1}, and J.Vicente Riera^a

^a *Dept. Mathematics and Computer Science
Univ. of the Balearic Islands*

Abstract. In this paper we propose a method to obtain the maximum and the minimum of discrete fuzzy numbers, when the extension principle does not yield a fuzzy subset such that it satisfies the conditions of discrete fuzzy number. Moreover, in the case of discrete fuzzy numbers whose support is a subset of consecutive natural numbers, our method and the extension principle obtain the same discrete fuzzy number.

Keywords. Fuzzy number, Discrete Fuzzy number, Multiset, Operations between discrete fuzzy numbers,

Introduction

Many authors have studied fuzzy numbers and their operations from several viewpoints: theoretical [8,9,10,13], geometric [1,2], applications in engineering [13], social science [12], etc. In 2001, Voxman [19] introduced the concept of the discrete fuzzy number as a fuzzy subset of real numbers with discrete support and analogous properties to a fuzzy number (convexity, normality). Also, like fuzzy numbers, it is possible to consider discrete fuzzy numbers from different points of view: theoretical [19], applications in engineering [11,20], social sciences [18], etc.

In general, arithmetic and lattice operations such as maximum and minimum on fuzzy numbers can be approached either by the direct use of the membership function (by the Zadeh's extension principle) or by the equivalent use of the *r-cuts* representation. For example, Mayor [14] proposes the problem of obtaining a procedure to aggregate fuzzy numbers using the Extension principle obtaining multi-dimensional aggregation functions on the lattice of fuzzy numbers.

Nevertheless, in the discrete case, this process can yield a fuzzy subset that does not satisfy the conditions to be a discrete fuzzy number [3,20]. In a previous work [3] we have presented an approach to a closed addition of discrete fuzzy numbers after associating suitable non-discrete fuzzy numbers, which can be used like a carrier to obtain the desired addition. In a recent paper [4] we prove that a suitable carrier can be a discrete fuzzy number whose support is an arithmetic sequence and even a subset of consecutive natural numbers.

¹Correspondence to: Jaume Casasnovas, Cra. Valldemossa km.7.5, 07122 Palma de Mallorca (Spain). Tel.: +34 971 172980; Fax: +34 971 173003; E-mail:dmijcc0@uib.es

The discrete fuzzy numbers whose support is a subset of natural numbers arise mainly when a fuzzy cardinality of a fuzzy set [6,7] or a fuzzy multiset [5,16,17] is considered. However, we can consider a wider kind of discrete fuzzy numbers in order to implement generalizations of the multiset concept [15]. Thus, given a possible lack of exact knowledge of the cardinal of the set of exact copies of a type, it is possible to consider other possible ways of associating a fuzzy set with finite support to each element of the set of types. So, the idea of discrete fuzzy numbers-valued multisets can be considered. In this framework we point out that, with the proposed method, it is possible to define the union and the intersection of discrete fuzzy numbers-valued multisets.

In this paper, we define a method to obtain the maximum and the minimum of discrete fuzzy numbers when the Zadeh's extension principle does not yield a discrete fuzzy number. Besides, we show that in the case of the discrete fuzzy numbers whose support is a set of terms of an arithmetic sequence with "1" as common difference we can calculate the maximum and the minimum with the Zadeh's extension principle.

1. Preliminaries

Definition 1 [13] A fuzzy subset u of \mathbb{R} with membership mapping

$u : \mathbb{R} \rightarrow [0, 1]$ is called fuzzy number if its support is an interval $[a, b]$ and there exist real numbers s, t with $a \leq s \leq t \leq b$ and such that:

1. $u(x)=1$ with $s \leq x \leq t$
2. $u(x) \leq u(y)$ with $a \leq x \leq y \leq s$
3. $u(x) \geq u(y)$ with $t \leq x \leq y \leq b$
4. $u(x)$ is upper semi-continuous.

We will denote the set of fuzzy numbers by FN .

Definition 2 [19] A fuzzy subset u of \mathbb{R} with membership mapping

$u : \mathbb{R} \rightarrow [0, 1]$ is called discrete fuzzy number if its support is finite, i.e., there are $x_1, \dots, x_n \in \mathbb{R}$ with $x_1 < x_2 < \dots < x_n$ such that $\text{supp}(u) = \{x_1, \dots, x_n\}$, and there are natural numbers s, t with $1 \leq s \leq t \leq n$ such that:

1. $u(x_i)=1$ for any natural number and i with $s \leq i \leq t$ (core)
2. $u(x_i) \leq u(x_j)$ for each natural number i, j with $1 \leq i \leq j \leq s$
3. $u(x_i) \geq u(x_j)$ for each natural number i, j with $t \leq i \leq j \leq n$

From now on, we will denote the set of discrete fuzzy numbers by DFN and $DFN(\mathbb{N})$ will stand for the set of discrete fuzzy numbers whose support is a subset of the set of Natural Numbers. Finally, a discrete fuzzy number will be denoted by dfn .

In general, the operations on fuzzy numbers f, g can be approached either by the direct use of their membership function, $\mu_f(x), \mu_g(x)$, as fuzzy subsets of \mathbb{R} and the Zadeh's extension principle:

$$O(f, g)(z) = \sup\{\mu_f(x) \wedge \mu_g(y) | O(x, y) = z\}$$

or by the equivalent use of the α -cuts representation[13]:

$$O(f, g)^\alpha = O(f^\alpha, g^\alpha) = \{O(x, y) | x \in f^\alpha, y \in g^\alpha\}$$

and

$$O(f, g)(z) = \sup\{\alpha \in [0, 1] | z \in O(f, g)^\alpha\}$$

Nevertheless, in the discrete case, this process can yield a fuzzy subset that does not satisfy the conditions to be a discrete fuzzy number [3,20]. In a previous work [3,4] we have presented an approach to a closed extended addition (\oplus) of discrete fuzzy numbers after associating suitable non-discrete fuzzy numbers, which can be used like a carrier to obtain the desired addition.

In a recent paper [4] we prove that a suitable carrier can be a discrete fuzzy number whose support is an arithmetic sequence and even a subset of consecutive natural numbers. Thus, we obtained the following results:

Proposition 1 [4]

Let \mathcal{A}_r be the set $\{f \in DFN(\mathbb{N}) \text{ such that } \text{supp}(f) \text{ is the set of terms of an arithmetic sequence with } r \text{ as common difference}\}. If $f, g \in \mathcal{A}_r$. The following facts:$

1. $f \oplus g \in DFN(\mathbb{N})$
2. $f \oplus g \in \mathcal{A}_r$

hold.

Remark 1 [4] Note that the set \mathcal{A}_1 is the set of discrete fuzzy numbers whose support is a set of consecutive natural numbers.

Finally, we will use a kind of representation (see section 2) in the study of discrete fuzzy numbers:

Theorem 1 [20] Let u be a dfn and let u^r be the r -cut $= \{x \in \mathbb{R} | u(x) \geq r\}$. Then the following statements (1)-(4) hold:

1. u^r is a nonempty finite subset of \mathbb{R} , for any $r \in [0, 1]$
2. $u^{r_2} \subset u^{r_1}$ for any $r_1, r_2 \in [0, 1]$ with $0 \leq r_1 \leq r_2 \leq 1$
3. For any $r_1, r_2 \in [0, 1]$ with $0 \leq r_1 \leq r_2 \leq 1$, if $x \in u^{r_1} - u^{r_2}$ we have $x < y$ for all $y \in u^{r_2}$, or $x > y$ for all $y \in u^{r_2}$
4. For any $r_0 \in [0, 1]$, there exist some real number r'_0 with $0 < r'_0 < r_0$ such that $u^{r'_0} = u^{r_0}$ (i.e. $u^r = u^{r_0}$ for any $r \in [r'_0, r_0]$).

And conversely, if for any $r \in [0, 1]$, there exist $A^r \subset \mathbb{R}$ satisfying the following conditions (1)-(4):

1. A^r is a nonempty finite for any $r \in [0, 1]$
2. $A^{r_2} \subset A^{r_1}$, for any $r \in [0, 1]$ with $0 \leq r_1 \leq r_2 \leq 1$
3. For any $r_1, r_2 \in [0, 1]$ with $0 \leq r_1 \leq r_2 \leq 1$, if $x \in A^{r_1} - A^{r_2}$ we have $x < y$ for all $y \in A^{r_2}$, or $x > y$ for all $y \in A^{r_2}$
4. For any $r_0 \in [0, 1]$, there exist a real number r'_0 with $0 < r'_0 < r_0$ such that $A^{r'_0} = A^{r_0}$ (i.e. $A^r = A^{r_0}$, for any $r \in [r'_0, r_0]$)

then there exist a unique $u \in DFN$ such that $u^r = A^r$ for any $r \in [0, 1]$.

2. Extended Maximum and Minimum

The following examples show that the maximum and the minimum, defined through the extension principle, do not satisfy in general the conditions to be a discrete fuzzy number.

Example 1 Let $u = \{0.3/1, 0.6/3, 1/4, 0.5/7, 0.4/9\}$, $v = \{0.5/2, 1/5, 0.6/10\}$ be two dfn, then:

$$\text{MAX}(u, v)(z) = \sup_{z=\max(x,y)} \min(u(x), v(y)), \forall z \in \mathbb{R}$$

and $\text{MAX}(u, v) \notin DFN$, because $\text{MAX}(u, v)(7) = 0.5$ and $\text{MAX}(u, v)(9) = 0.4$, but $\text{MAX}(u, v)(10) = 0.6$ and then the property 3 of the definition for dfn fails.

Example 2 Let $u = \{0.3/1, 0.4/3, 1/4\}$, $v = \{0.5/2, 1/5, 1/6\}$ two dfn, then:

$$\text{MIN}(u, v)(z) = \sup_{z=\min(x,y)} \min(u(x), v(y)), \forall z \in \mathbb{R}$$

is not a dfn.

Note that, the support of both MAX and MIN are finite sets.

Definition 3 Let u, v be two dfn. For each $\alpha \in [0, 1]$, let's consider the α -cut sets: $u^\alpha = \{x_1^\alpha, \dots, x_p^\alpha\}, v^\alpha = \{y_1^\alpha, \dots, y_k^\alpha\}$ for u and v respectively and the set $\text{supp}(u) \vee \text{supp}(v) = \{x \vee y | x \in \text{supp}(u), y \in \text{supp}(v)\}$. Let's define the set:

$$A^\alpha = \{z \in \text{supp}(u) \vee \text{supp}(v) | (\min u^\alpha \vee \min v^\alpha) \leq z \leq (\max u^\alpha \vee \max v^\alpha)\}$$

i.e.:

$$A^\alpha = \{z \in \text{supp}(u) \vee \text{supp}(v) | (x_1^\alpha \vee y_1^\alpha) \leq z \leq (x_p^\alpha \vee y_k^\alpha)\}$$

Proposition 2 For each $\alpha \in [0, 1]$ the following properties hold:

1. A^α is a nonempty finite set, because u^α and v^α are both nonempty finite sets (the discrete fuzzy numbers are normal fuzzy subsets) and $\text{supp}(u) \vee \text{supp}(v)$ is a finite set.
2. $A^\beta \subseteq A^\alpha$ for any $\alpha, \beta \in [0, 1]$ with $0 \leq \alpha \leq \beta \leq 1$.
Because if $u, v \in DFN$ and:

$$u^\alpha = \{x_1^\alpha, \dots, x_p^\alpha\}, u^\beta = \{x_1^\beta, \dots, x_r^\beta\}, v^\alpha = \{y_1^\alpha, \dots, y_k^\alpha\}, v^\beta = \{y_1^\beta, \dots, y_l^\beta\}, \quad (1)$$

then:

$$u^\beta \subseteq u^\alpha \text{ implies } x_1^\alpha \leq x_1^\beta \text{ and } x_r^\beta \leq x_p^\alpha \quad (2)$$

$$v^\beta \subseteq v^\alpha \text{ implies } y_1^\alpha \leq y_1^\beta \text{ and } y_l^\beta \leq y_k^\alpha \quad (3)$$

So, the relations 2,3 and 1 yield:

$$\max(x_1^\alpha, y_1^\alpha) \leq \max(x_1^\beta, y_1^\beta)$$

$$\max(x_r^\beta, y_l^\beta) \leq \max(x_p^\alpha, y_k^\alpha)$$

$$\max(x_1^\beta, y_1^\beta) \leq \max(x_r^\beta, y_l^\beta)$$

3. For any $\alpha, \beta \in [0, 1]$ with $0 \leq \alpha \leq \beta \leq 1$, if $x \in A^\alpha - A^\beta$, then $x < y$ for all $y \in A^\beta$, or $x > y$ for all $y \in A^\beta$.

Because, $x \in A^\alpha$, hence $x \in \text{supp}(u) \vee \text{supp}(v)$ and x does not belong to A^β , then either $x < x_1^\beta \vee y_1^\beta$, which is the minimum of A^β , or $x > (x_r^\beta \vee y_l^\beta)$, which is the maximum of A^β .

4. For any $\alpha \in (0, 1]$, there exists a real number α' with $0 < \alpha' < \alpha$ such that $A^{\alpha'} = A^\alpha$ (i.e. $A^r = A^\alpha$, for any $r \in [\alpha', \alpha]$).

Because $u, v \in DFN$ and theorem of representation of the discrete fuzzy numbers [20], for each $\alpha \in (0, 1]$ there exist real numbers α'_1 and α'_2 with $0 < \alpha'_1 < \alpha$ and $0 < \alpha'_2 < \alpha$ such that for each $r \in [\alpha'_1, \alpha]$, we can assure $u^\alpha = u^r$ and $v^\alpha = v^r$, for each $r \in [\alpha'_2, \alpha]$. Thus, if $\alpha' = \alpha'_1 \vee \alpha'_2$, we can obtain:

$$\min(u^r) = \min(u^\alpha) \text{ and } \max(u^r) = \max(u^\alpha)$$

$$\min(v^r) = \min(v^\alpha) \text{ and } \max(v^r) = \max(v^\alpha)$$

for each $r \in [\alpha', \alpha]$ therefore

$$\max(\min(u^r), \min(v^r)) = \max(\min(u^\alpha), \min(v^\alpha))$$

$$\max(\max(u^r), \max(v^r)) = \max(\max(u^\alpha), \max(v^\alpha))$$

Hence,

$$A^\alpha = \{z \in \text{supp}(u) \vee \text{supp}(v) : \min(u^\alpha) \vee \min(v^\alpha) \leq z \leq \max(u^\alpha) \vee \max(v^\alpha)\} =$$

$$\{z \in \text{supp}(u) \vee \text{supp}(v) : \max(\min(u^r), \min(v^r)) \leq z \leq \max(\max(u^r), \max(v^r))\} = A^r$$

Then, by Wang's theorem of representation of discrete fuzzy numbers (see theorem 1), there exists a unique discrete fuzzy number $m \in DFN$ such that

$$m^r = A^r \text{ for any } r \in [0, 1]$$

and

$$m(z) = \sup\{\alpha \in [0, 1] : z \in A^\alpha\}$$

We will denote this discrete fuzzy number m by $MAX_w(u, v)$

Proposition 3 If $u, v \in \mathcal{A}_1$, then $\text{MAX}(u, v)$, defined through the extension principle, coincides with $\text{MAX}_w(u, v)$. So, if $u, v \in \mathcal{A}_1$, $\text{MAX}(u, v)$ is a discrete fuzzy number. Moreover, $\text{MAX}(u, v) \in \mathcal{A}_1$.

Proof. If $u, v \in \mathcal{A}_1$, u, v are fuzzy subsets of \mathbb{R} and the mapping:

$$\text{MAX}(u, v)(z) = \sup\{u(x) \wedge v(y) | x \vee y = z\}$$

is the membership function of a fuzzy subset of \mathbb{R}

The α -cuts of this fuzzy set $\text{MAX}(u, v)$ are $\text{MAX}(u, v)^\alpha = u^\alpha \vee v^\alpha = \{x \vee y | x \in u^\alpha, y \in v^\alpha\}$ [13].

We are going to prove that $u^\alpha \vee v^\alpha = \text{MAX}_w(u, v)^\alpha$ and so we will have:

$$\text{MAX}(u, v)^\alpha = u^\alpha \vee v^\alpha = \{x \vee y | x \in u^\alpha, y \in v^\alpha\} = \text{MAX}_w(u, v)^\alpha, \forall \alpha \in [0, 1],$$

therefore $\text{MAX}(u, v) = \text{MAX}_w(u, v)$ and, in this case, $\text{MAX}(u, v)$ is a discrete fuzzy number.

- $u^\alpha \vee v^\alpha \subset \text{MAX}_w(u, v)^\alpha = A^\alpha$, because if $z \in u^\alpha \vee v^\alpha$, then $z = x \vee y; x \in u^\alpha, y \in v^\alpha$. So, $z \in \text{supp}(u) \vee \text{supp}(v)$ and:

$$\min(u^\alpha) \vee \min(v^\alpha) \leq z \leq \max(u^\alpha) \vee \max(v^\alpha)$$

and $z \in A^\alpha = \text{MAX}_w(u, v)^\alpha$

- $\text{MAX}_w(u, v)^\alpha = A^\alpha \subset u^\alpha \vee v^\alpha$

Because if $z \in A^\alpha = \text{MAX}_w(u, v)^\alpha$, then $z \in \text{supp}(u) \vee \text{supp}(v)$ and:

$$(x_1^\alpha \vee y_1^\alpha) \leq z \leq (x_p^\alpha \vee y_k^\alpha)$$

- * If $x_1^\alpha \vee y_1^\alpha = x_1^\alpha$ and $x_p^\alpha \vee y_k^\alpha = x_p^\alpha$, then $z \in u^\alpha$ and $z = z \vee y_1^\alpha \in u^\alpha \vee v^\alpha$
- * If $x_1^\alpha \vee y_1^\alpha = x_1^\alpha$ and $x_p^\alpha \vee y_k^\alpha = y_k^\alpha$, then $z \in v^\alpha$ and $z = z \vee x_1^\alpha \in u^\alpha \vee v^\alpha$
- * If $x_1^\alpha \vee y_1^\alpha = y_1^\alpha$ and $x_p^\alpha \vee y_k^\alpha = x_p^\alpha$, then $z \in u^\alpha$ and $z = z \vee y_1^\alpha \in u^\alpha \vee v^\alpha$
- * If $x_1^\alpha \vee y_1^\alpha = y_1^\alpha$ and $x_p^\alpha \vee y_k^\alpha = y_k^\alpha$, then $z \in v^\alpha$ and $z = z \vee x_1^\alpha \in u^\alpha \vee v^\alpha$

Besides, if $u, v \in \mathcal{A}_1$, then $u^\alpha = \{z \in \mathbb{N}, \text{ such that } u_1^\alpha \leq z \leq u_p^\alpha\}$ and $v^\alpha = \{z \in \mathbb{N}, \text{ such that } v_1^\alpha \leq z \leq v_k^\alpha\}; \forall \alpha \in [0, 1]$. Therefore $u^\alpha \vee v^\alpha = \{z \in \mathbb{N}, \text{ such that } u_1^\alpha \vee v_1^\alpha \leq z \leq u_p^\alpha \vee v_k^\alpha\}$ and we can assume that $\text{MAX}(u, v)^\alpha = u^\alpha \vee v^\alpha = \text{MAX}_w(u, v)^\alpha$ is a subset of \mathbb{N} of consecutive numbers, for all $\alpha \in [0, 1]$. So, $\text{MAX}(u, v) \in \mathcal{A}_1$.

Analogously,

Definition 4 Let u, v be two dfn. For each $\alpha \in [0, 1]$, let's consider the α -cut sets: $u^\alpha = \{x_1^\alpha, \dots, x_p^\alpha\}, v^\alpha = \{y_1^\alpha, \dots, y_k^\alpha\}$ for u and v respectively and the set $\text{supp}(u) \wedge \text{supp}(v) = \{x \wedge y | x \in \text{supp}(u), y \in \text{supp}(v)\}$. Let's define the set:

$$B^\alpha = \{z \in \text{supp}(u) \wedge \text{supp}(v) | (\min u^\alpha \wedge \min v^\alpha) \leq z \leq (\max u^\alpha \wedge \max v^\alpha)\}$$

i.e.:

$$B^\alpha = \{z \in \text{supp}(u) \wedge \text{supp}(v) | (x_1^\alpha \wedge y_1^\alpha) \leq z \leq (x_p^\alpha \wedge y_k^\alpha)\}$$

Proposition 4 *The finite set B^α , above defined, satisfies the properties 1,2,3 and 4 of Proposition 2 and a discrete fuzzy number, $\text{MIN}_w(u, v)$, whose α -cuts are the finite set B^α exists. Moreover, if $u, v \in \mathcal{A}_1$, then $\text{MIN}(u, v)$, defined through the extension principle, coincides with $\text{MIN}_w(u, v)$. So, if $u, v \in \mathcal{A}_1$, $\text{MIN}(u, v)$ is a discrete fuzzy number and $\text{MIN}(u, v) \in \mathcal{A}_1$.*

Example 3 *Let*

$$u = \{0.4/1, 1/2, 0.8/3, 0.6/4, 0.5/5, 0.4/6, 0.3/7\}$$

and

$$v = \{0.3/4, 0.6/5, 0.7/6, 0.8/7, 1/8, 0.8/9\}$$

be two discrete fuzzy numbers whose supports are a subsets of the set of consecutive natural numbers. Then

$$\text{MAX}(u, v) = \{0.3/4, 0.6/5, 0.7/6, 0.8/7, 1/8, 0.8/9\}$$

and

$$\text{MIN}(u, v) = \{0.4/1, 1/2, 0.8/3, 0.6/4, 0.5/5, 0.4/6, 0.3/7\}$$

3. Conclusions and future work

The operations with discrete fuzzy numbers such as addition, maximum or minimum using the Zadeh's extension principle or equivalently r-cuts, in general, don't obtain a fuzzy subset fulfilling the condition to be a dfn. In this way, we have seen a method to get the maximum and the minimum of discrete fuzzy numbers when the extension principle does not yield a discrete fuzzy number. Moreover, in the case of discrete fuzzy numbers whose support is a subset of consecutive natural numbers, both, our method and the extension principle obtain the same discrete fuzzy number.

Analogously to the structure of distributive lattice of fuzzy numbers [13,14], as future work we will study whether the set DFN has a structure of distributive lattice. We can use a partial order obtained from the operations maximum and minimum defined in this paper. Finally, it is possible to extend the concept of fuzzy numbers valued-multiset [15,16] to the concept of discrete fuzzy numbers valued-multiset using the results for the addition of discrete fuzzy numbers [4] and the results obtained in this article.

Acknowledgements

We would like to express our thanks to anonymous reviewers who have contributed to improve this article.

References

- [1] J.J. Buckley and Y. Qu, Solving systems of linear fuzzy equations, *Fuzzy Sets and Systems*, **43**(2) (1991), 33–43.
- [2] J.J. Buckley and E.Eslami, Fuzzy plane geometry I: Points and lines, *Fuzzy Sets and Systems*, **86**(2) (1997), 179–188.
- [3] J. Casasnovas and J. Vicente Riera, On the addition of discrete fuzzy numbers, *Wseas Transactions on Mathematics* **5**(5) (2006), 549–554.
- [4] J. Casasnovas and J. Vicente Riera, Discrete fuzzy numbers defined on a subset of natural numbers, *Theoretical Advances and Applications of Fuzzy Logic and Soft Computing, Advances in Soft Computing*, Springer, **42**(2007), 573–582.
- [5] J. Casasnovas and F. Rosselló, Scalar and fuzzy cardinalities of crisp and fuzzy multisets, *accepted for the special issue of International Journal of Intelligent Systems*, <http://citeseer.ist.psu.edu/672384.html>
- [6] J. Casasnovas and J.Torrens, An Axiomatic Approach to the fuzzy cardinality of finite fuzzy sets, *Fuzzy Sets and Systems* **133** (2003), 193–209.
- [7] J. Casasnovas and J.Torrens, Scalar cardinalities of finite fuzzy sets for t-norms and t-conorms, *International Journal of Uncertainty, Fuzziness and Knowledge-Based Systems* **11** (2003), 599–615.
- [8] D. Dubois, A new definition of the fuzzy cardinality of finite sets preserving the classical additivity property, *Bull. Stud. Ecch. Fuzziness Appl.(BUSEFAL)* **5** (1981), 11–12.
- [9] D.Dubois and H.Prade, *Fuzzy Sets and Systems:Theory and Applications*, Academic Press, New York, 1980.
- [10] D.Dubois and H.Prade (Eds.),Fundamentals of Fuzzy Sets. The handbooks of Fuzzy Sets Series, Kluwer, Boston,2000.
- [11] M.Hanns, On the implementation of fuzzy arithmetical operations for engineering problems,*Fuzzy Information Processing Society(NAFIPS)*(1999),462–466.
- [12] Wen-Ling Hung and Miin-Shen Yang, Fuzzy clustering on LR-type fuzzy numbers with an application in Taiwanese tea evaluation, *Fuzzy Sets and Systems* **textbf{150}**(2005),561–577.
- [13] George J. Klir and Yuan Bo ,*Fuzzy sets and fuzzy logic (Theory and applications)*, Prentice Hall, 1995.
- [14] G. Mayor et al.,Multi-dimensional Aggregation of Fuzzy Numbers Through the Extension Principle, *Data Mining, Rought sets and Granular Computing*, Eds Lin, Yao, Zadeh, Physica-Verlag, 2002, 350-363.
- [15] S.Miyamoto, Fuzzy Multisets and Their Generalizations, *Multisets Processing, LNCS* ,**2235** (2001),225–235.
- [16] S.Miyamoto, Multisets and Fuzzy Multisets as a Framework of Information Systems, *Lectures in computer science*(2004), 27–40.
- [17] D. Rocacher, On fuzzy bags and their application to flexible querying, *Fuzzy Sets and Systems* **140**(2003) , 93–110.
- [18] D. Tadic, Fuzzy Multi-criteria approach to ordering policy ranking in a supply chain,*Yugoslav Journal of Operations Research*,**2** (2005),243–258.
- [19] W. Voxman, Canonical representations of discrete fuzzy numbers, *Fuzzy Sets and Systems* **54** (2001), 457–466.
- [20] Guixiang Wang,Cong Wu, Chunhui Zhao, Representation and Operations of discrete fuzzy numbers, *Southeast Asian Bulletin of Mathematics* **28**(2005),1003–1010.

A fuzzy rule-based modeling of the Sociology of Organized Action

Sandra Sandri^{a,*} and Christophe Sibertin-Blanc^b

^a IIIA-CSIC, Spain

^b IRIT, France

Abstract. In this work, we address the modeling of the *Sociology of Organized Action* in a fuzzy rule-based environment. We also discuss some game concepts such as Pareto optima in such a framework. We illustrate our approach with an example from the sociology literature.

Keywords. Sociology of Organized Action, fuzzy rule-based systems, social games, Pareto optimum

1. Introduction

The *Sociology of Organized Action* (SOA) was initiated by M. Crozier in the 60s and notably further developed by E. Friedberg (see e. g. [3]). It deals with social organisations or, more generally, with *Systems of Concrete Actions*, that interact with an environment, pursue some goals, and manage means and resources that are used by the members of the organisation according to some rules. According to SOA, the behaviour of a member of an organisation is fully explained neither by the formal and informal rules, norms, etc. of the organisation, nor by individual particularities resulting from his history, nature, etc.

Social actors have a strategic behaviour, i.e., they perform actions with the intention to achieve some goals, and each actor aims, as a meta-objective, at having enough power to preserve or increase his autonomy and capacity of action to achieve his concrete objectives. This power results from, and is exerted through, the mastering of resources that are needed by other actors for their actions, known as uncertainty zones (UZ) in SOA literature. The actor (or group of actors) that masters/controls a UZ sets its exchange rules, i.e., how well other actors can access and use this particular resource. UZs are the means of the power relationships between social actors, and a balance results from the fact that each actor both controls some UZs and depends on some others. Moreover, SOA assumes that each actor behaves strategically although he has only bounded rationality capabilities [12].

The use of fuzzy systems in this framework is very attractive, since the attitudes of players to resources, such as "fully cooperate" or "somewhat defect", can be modeled in a natural way, and it is also promising, considering the tools available to develop them.

* Correspondence to: Sandra Sandri, IIIA, Artificial Intelligence Research Institute CSIC, Spanish National Research Council Campus UAB, 08193 Bellaterra, Spain. Tel.: +34 93 580 9570; Fax: +34 93 580 9661; E-mail: sandri@iiia.csic.es.

A fragment of SOA has been formalized in [11], and is employed in the interactive social game environment SocLab (available at www.sourceforge.net), which allows the user to edit the structure of a SAC and to simulate the behaviour of the social actors [8]. In [10], we addressed the transposition of this formalization to a fuzzy setting, using two approaches to obtain the payoffs; one making use of the extension principle and the other employing fuzzy rule-based systems. The present work focus on the fuzzy rule-based approach, and discusses the means of defining important concepts in game theory such as Pareto optima and Nash equilibria [2] in such a framework.

This work is organized as follows. In Section 2, we briefly present an example of SOA and an extract of the formalization of SOA proposed in [11]. Section 3 brings part of the fuzzy formalism for SOA as proposed in [10] and presents a simple fuzzy formulation for the example. In Section 4, we discuss some game theory concepts in our framework and Section 5 finally brings the conclusion.

2. Formalizing SOA

2.1. Description of an example of SOA

In the following we describe a short version of the SOA example presented in [13]. Travel-Tours is a tour operator with two agencies, TRO1 and TRO2, situated both in Trouville. In the last months, the results of TRO1 have increased, whereas the ones of TRO2 remained stable, or even decreased. The regional director decides to reward TRO1 for its merits. He proposes to give a permanent job to Agn  s, a temporary secretary, and assign her to work exclusively for TRO1. Even though Agn  s is formally attached to TRO1, she has been working half time in each one of the agencies and this obliges her to switch between jobs. The regional director expected both Agn  s and TRO1's director, Paul, to be glad with his proposal. Agn  s would have a permanent job contract and would no longer need to split her work in two parts, while Paul would have a full-time secretary at his disposal in TRO1. However, both of them vigorously refuse the proposal. A more attentive analysis of the case reveals why.

The TRO2 agency is more creative than TRO1 in designing travel packages, while the TRO1 has a very efficient commercial staff; being aware of the TRO2 agency's activity, the secretary provides the director of TRO1 with information from TRO2, which is fully used by TRO1 to design attractive packages. On the other hand, a steady job is not one of Agn  s short-time objectives. Moreover, she greatly appreciates the fact that neither TRO1 nor TRO2 directors can exert a strict control over her work. Thus the situation shift proposed by the regional director would increase the control of TRO1 director on the secretary's activities (something she does not want), and the director would miss the information on TRO2 given by the secretary (something he does not want).

2.2. A formalism for a SOA fragment

The basic social game formalization, as given in [11], can be described by the 5-tuple $G = \langle A, R, effect, m, payoff f \rangle$, where:

- $A = \{a_1, \dots, a_N\}$ is a set of social actors.

- $R = \{r_1, \dots, r_M\}$ is a set of resources, each of which needed by one or more actors in A and controlled by one actor in A . The state of a resource r_i at a given moment, denoted by s_i , is modeled by a value in the interval $[-1, 1]$. The overall state of the game is defined by the state of all the resources, described by a vector $s = (s_1, s_2, \dots, s_M) \in [-1, 1]^M$.
- $control : R \rightarrow A$ indicates which actor controls which resource; it is always assumed that each actor controls at least one resource, and thus $M \geq N$. The access to each resource r_i is bounded by its minimum and maximum values $[b_{min_i}, b_{max_i}] \subseteq [-1, 1]$. In the present implementation, a resource is controlled by a single actor and the resource access boundaries are constant values.
- $effect_i : A \times [-1, 1] \rightarrow [-10, 10]$ is a function that models how well each actor in A can access resource r_i in its current state $s_i \in [-1, 1]$. The worst and best possible accesses are respectively modeled by -10 and +10.
- $stake : A \times R \rightarrow [0, 10]$ is a function that expresses how much the access to a resource is important for an actor. Each actor distributes the same total number of stake points to the resources: $\forall a \in A, \sum_{r_i \in R} stake(a, r_i) = 10$. For a resource $r \in R$, $stake(a, r) = 0$ means that a has no need for r , whereas $stake(a, r) = 10$ means that r is the unique resource needed by a .
- $payoff : A \times [-1, 1]^M \rightarrow \mathbb{R}$ is a function that expresses how much an actor is comfortable with a state s of the game. A high payoff corresponds to a state where the actor has a good quality of access to the resources that are important for him. It can be defined, for example, by a combination of effect functions and stakes.

Some of the noteworthy concepts modeled in this framework depend on the distribution of the stakes, such as the *autonomy* and the *subordination* of an actor. Others, such as the *relevance* of a resource, the *force* of a relation upon an actor, the *power relation* between actors, the consequent *dependencies* of an actor upon another, etc, depend the *effect* values, yet others, such as the *controllability* of each resource r_i on the other hand depends on the size of the interval $[b_{min_i}, b_{max_i}]$. See [11] for details.

The actor who controls a resource is the one deciding the state of this resource. An action of actor a is a vector of the form $(m_i)_{r_i \in control^{-1}(a)}$, where m_i is the move to be applied to the current state of r_i , and that move is feasible if $s_i + m_i \in [b_{min_i}, b_{max_i}]$. A step of the game occurs when each actor has chosen a feasible move m_i for a resource r_i that he/she controls, and the game goes from state (s_1, s_2, \dots, s_M) to state $(s_1', s_2', \dots, s_M')$, where $s_i' = s_i + m_i$.

The game is repeated until it becomes stabilized, or stationary: each actor plays the null action and no longer changes the state of the resources he controls. Such a state of the game is considered a social equilibrium, a balanced situation that is satisfying and accepted by all the actors of the game. In most human organisations, social games are positive sum games: each actor gets some profit from being cooperative, because the other actors will also be cooperative in return. Thus, typical *social equilibria* are Pareto maxima: each actor has a high satisfaction, and any increase of it would entail a decrease of the satisfaction of another actor, which in turn would not accept this disadvantageous situation.

3. A fuzzy rule-based formalism for SOA

The interest to allow fuzziness in SOA is due in part to the fact that humans furnish information, and perceive the information presented to them, imperfectly. In the stage that SOA is insofar mathematically modeled [11], fuzzy formalisms can be used to model vagueness in the definition of values of stakes, states and moves and of functions such as *effect* and *payoff*, among others, and can also be used to set the boundaries of the resources controllability. In [10] we propose two approaches to model this fragment of SOA in a fuzzy framework, one based on the extension principle, when the effect and payoff functions can be modeled simple mathematical expressions, and one using fuzzy rule bases, useful when these functions are not easily defined, specially in problems that involve a large set of resources. When that is the case, a fuzzy rule base approach is particularly useful.

Our fuzzy rule-based approach is grounded on the fact that the knowledge involved in SOA problems are usually of the kind "*the more x is A, the more y is B*", which corresponds to the semantics of what is known as *gradual fuzzy rules* in the literature [5]. For this kind of rules, one can use the the multivariate decision making framework presented in [9], that employs Goguen residuated operator to model the rule implication, and similarity relations to guarantee consistency, i.e. results that are normalized fuzzy sets. An advantage of using this method is that the results are interpretable what is not the case when the implication is modeled by conjunction operators such as the minimum and the product, like in the so-called Mamdani systems [9].

3.1. Gradual fuzzy rule-based formalism equipped with similarity relations

In the rest of the paper, unless stated otherwise, we shall work with fuzzy subsets of the real line, so domain U below is assumed to be \mathbb{R} . The core (respec. support) of a fuzzy set $A : U \rightarrow [0, 1]$ is defined as $\text{core}(A) = \{x \mid A(x) = 1\}$ (respec. $\text{supp}(A) = \{x \mid A(x) > 0\}$). For any $\alpha \in [0, 1]$, the α -cut of A is defined as $A_\alpha = \{x \in U \mid A(x) \geq \alpha\}$. A is said to be *normalized* when there exists x such that $A(x) = 1$, and *convex* when for all x, y, z , if $x \leq y \leq z$, $A(y) \geq \min(A(x), A(z))$. A triangular fuzzy set A (normalized and convex), is denoted as $\langle a, b, c \rangle$, where $\text{supp}(A) = (a, c)$ and $\text{core}(A) = [b, b]$.

In this work, a given knowledge base K consists of a set of gradual rules of the form $\mathbf{R}_i : \text{If } x_1 = A_{i_1} \text{ and } \dots \text{ and } x_k = A_{i_k} \text{ then } y = B_i$. Each rule \mathbf{R}_i induces a fuzzy relation between input and output values which is defined as $R_i(x, y) = (A_i \rightarrow_T B_i)(x, y) = A_i(x) \rightarrow_T B_i(y)$, where \rightarrow_T is a residuated implication operator. The output of a set of gradual rules K in the case of precise (possibly multidimensional) input value x^* , such as the case here, is given by $\text{output}(K, x^*) = R_K(x^*, y) = \min_{i \in I} B'_i(y)$, with $B'_i(y) = \alpha_i \rightarrow_T B_i(y)$, where $\alpha_i = A_i(x^*) = \min_j A_{i_j}(x_j^*)$ stands for the compatibility between the rule and the input. Here Goguen residuated implication operator is used, defined as $a \rightarrow_T b = 1$ if $a \leq b$, and $a \rightarrow_T b = b/a$ otherwise.

The use of gradual rules have the inconvenient of very often issuing inconsistent results, i.e. there exists x^* such that $\text{output}(K, x^*)$ is not normalized. A solution to that problem is to apply a fuzzy similarity relation S , i.e. reflexive ($S(x, x) = 1, \forall x$) and symmetric ($S(x, y) = S(y, x), \forall x, y$), to output fuzzy sets B_i , creating "larger" terms *approximately*- B_i in the rules, in such a way that the output resulting from the modified rules is consistent [6]. The application of a similarity relation S on a fuzzy term B , denoted by $S \circ B$, is formally defined as

$$(S \circ B)(x) = \sup_{y \in U} \min(S(x, y), B(y)).$$

The largest similarity relation is $S^\top(x, y) = 1, \forall x, y$, and is such that $(S \circ B) = U$ and the smallest is $S^\perp(x, y) = 1$ iff $x = y$, which is such that $(S \circ B) = B$.

Given a parameterized family of similarity relations and the input, we first of all find which is the smallest similarity relation from that family that allows the set of rules fired with that input to become consistent. We then apply that similarity relation to the output terms in the rules and finally apply the inference mechanism described above to the transformed rules and the input. In this work we use similarity relations family given by $S_\lambda(x, y) = \max(0, 1 - \lambda^{-1} \cdot |x - y|)$, for $\lambda > 0$, and $S_0 = S^\perp$. We denote by K^λ the rule base obtained after the application of similarity relation S_λ on a rule base K ; note that $K^0 = K$. This formalism needs the following restriction to be useful: if there exists an input value x^* such that two rules R_1 and R_2 are fired with $\alpha_1 = \alpha_2 = 1$, then there must exist a value y^* such that $B_1(y^*) = B_2(y^*) = 1$ ¹. We suppose that all the input domain is covered in all rule bases, i.e. each input is addressed by at least one rule. This restriction can be dealt with nevertheless [7].

3.2. Modeling SOA using gradual fuzzy rules

In [10] we used fuzzy rule bases to model *effect* functions; the resulting fuzzy sets were then aggregated with a fuzzy arithmetic operator to derive the *payoff* functions. Here we present a simpler approach in which we associate a single rule base to each actor: the input variables correspond to the state of the resources involved in the game and the output variable stands for the *payoff* itself (i.e. the overall effect that the states of the resources can have upon the actor). Therefore, for an actor a here we have $\text{payoff}(a, s) = \text{effect}(a, s) = \text{output}(K_a^\lambda, s)$.

Let us examine the Travel-Tours example. We assume there exists only two resources in the problem: r_{Dr} , standing for the overall control the director has on the secretary's job, and r_{Sc} , standing for the amount of information from TRO2 that she furnishes TRO1 with. The states of these resources (i.e. the attitudes the actors may assume), are denoted by s_{Dr} and s_{Sc} respectively.

The rule bases for this problem are presented in Table 1 and the input and output terms are depicted in Figure 1. Input terms C , N and D correspond respectively to cooperative, neutral and opposing (defection) attitudes. The output terms, here defined in $[0, 10]$, correspond to extremely bad (EB), very bad (VB), bad (B), null (N), good (G), very good (VG) or extremely good (EG) payoffs. A rule **If** $s_{Dr} = A_{Dr}$ **and** $s_{Sc} = A_{Sc}$ **then** $\text{payoff} = B$ is denoted as $((A_{Dr}, A_{Sc}), B)$.

For example, rule $((C, C), G)$ in the secretary's rule base K_{Sc} states that her payoff can be considered good (output term G) if the director and herself cooperate (input terms vector (C, C)). She obtains an even better payoff if she is only neutral, through rule $((C, N), VG)$.

Let us suppose that both of them decide to cooperate, placing value 1 for their respective resources, i.e. $(s_{Dr}^*, s_{Sc}^*) = (1, 1)$. In this case, in relation to in K_{Sc} , we obtain $\alpha = 1$ for rule $((C, C), G)$ and $\alpha = 0$ for all the other rules. The output is straightforwardly the output term associated with the rule, i.e. $\text{output}(K_{Sc}^0, (1, 1)) =$

¹If $\alpha_1 = \alpha_2 = 1$ and $\forall y, \max(B_1(y) = B_2(y)) < 1$, we would need $\lambda = \infty$ to obtain a consistent result. But this result would be completely imprecise ($\forall y, \text{output}(K^\infty, x^*)(y) = 1$), and thus useless.

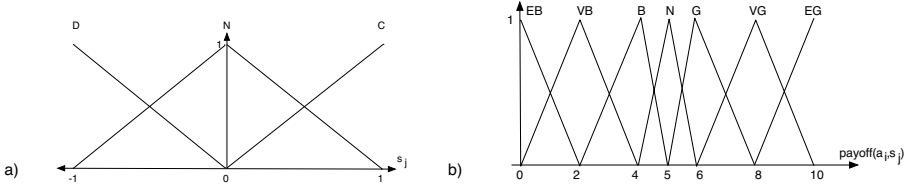


Figure 1. Fuzzy terms: a) input and b) output variables.

Table 1. Director and secretary payoffs.

K_{Dr}

$s_{Sc} s_{Dr}$	D	N	C
C	EG	EG	EG
N	B	N	B
D	VB	VB	EB

K_{Sc}

$s_{Sc} s_{Dr}$	D	N	C
C	EB	B	G
N	VB	N	VG
D	EB	B	G

$G = \langle 5, 6, 8 \rangle$. Similarly, for input $(0, 1)$ rule $((C, N), VG)$ is fired and we obtain $output(K_{Sc}^0, (1, 0)) = VG = \langle 6, 8, 10 \rangle$. For these input values, the corresponding payoffs are original output terms since only a single rule applies in each case. For the intermediary input value $(1, .5)$, both of these rules apply, $((C, C), G)$ with $\alpha = 1$ and $((C, N), VG)$ with $\alpha = .5$, yielding an already consistent result ($output(K_{Sc}^0, (1, .5)) = \langle 6, 7, 8 \rangle$), thus again without the need of applying a similarity relation ($\lambda = 0$).

In relation to K_{Dr} , we have $output(K_{Dr}^0, (1, 1)) = EG = \langle 8, 10, 10 \rangle$ and $output(K_{Dr}^0, (1, 0)) = B = \langle 2, 4, 5 \rangle$. For input $(1, .5)$ we have to use $\lambda = 4.5$ to make the result consistent and, after applying the procedure shown in 3.1, we obtain $output(K_{Dr}^{4.5}, (1, .5)) = \langle 3.5, 6.75, 9.5 \rangle$.

4. Equilibria and optima in the fuzzy framework

Nash equilibria and Pareto optima are fundamental concepts in game theory [2]. A strategy is the set of choices available to a player in a game and a state of a game consists of the strategies chosen by each of the various players at a given moment. A state is said to be a *Nash equilibrium* if no player is tempted to deviate from his/her choice supposing the other players maintain theirs. A state is *Pareto efficient*, or a *Pareto optimum* if, once the game attains that state, a player cannot improve his/her position without making some of the other players worse off. A *Pareto frontier* is the set of Pareto optima payoff vectors. Note that Pareto optimality does not mean fairness: a state that yields a Pareto optimum may be disastrous for all players except for one of them.

Let G be a SOA game as defined in 2.1, with N actors and M resources and let $SS = [-1, 1]^M$ be the set of all possible states of the game. Let $p(s) = (p_1(s), \dots, p_N(s))$ be the payoff vector associated with a state $s \in SS$, i.e. $\forall s \in SS, p_i(s) = payoff(a_i, s)$ and $PP = \{p(s) \mid s \in SS\}$ be the set of all possible payoff vectors in the game. Let us define a preference relation between two vectors $p = (p_1, \dots, p_N)$ and $p' = (p'_1, \dots, p'_N)$

as $p' \succ p$ iff $\forall p'_i \geq p_i$ and $\exists i, p'_i > p_i$. Using our notation, we can formally model the concepts above as follows.

- Pareto frontier: $PP_{Pareto} = \{p \in PP \mid \nexists p' \in PP, p' \succ p\}$
- Pareto optima: $SS_{Pareto} = \{s \in SS \mid p(s) \in PP_{Pareto}\}$
- Nash equilibria: $SS_{Nash} = \{s \in SS \mid \forall a_i \nexists s' \in SS, p_i(s') > p_i(s)\}$

Let us suppose that our example, described by Table 1 and Figure 1 is in fact a discrete non fuzzy game. The states in $\{C, N, D\}$ are just labels for the actors moves and $\{EB, VB, B, N, G, VG, EG\}$ stand for values in \mathbb{R} such that $EB < VB < B < N < G < VG < EG$. In this simple framework, it is easy to verify that the maximal payoffs are respectively (C, N) for the secretary and $\{(C, C), (N, C), (D, C)\}$ for the director, i.e. she has maximal payoff when she is neutral and he cooperates and he has maximal payoff whenever she cooperates. The single Nash equilibria is (N, N) , i.e. when both are neutral, and $\{(C, N), (C, C)\}$ are the only Pareto optima in the game, corresponding to her maximal payoff and to the best payoff she can obtain in case she cooperates.

All these concepts involve the comparison between the payoffs of possible states of the game. Thus, to deal with these concepts in our framework, we need to be able to rank fuzzy payoffs. To do that, we can use any of the methods found in the abundant fuzzy sets theory literature on the ranking of fuzzy sets (see e.g. [14]); alternatively, comparison could be performed over defuzzified results. Also, we could make such concepts gradual, e.g. each estate would have a membership degree to the (fuzzy) Pareto frontier. Here we shall keep a crisp concept of Pareto optima and will not deal with defuzzification.

Before we turn again to the fuzzy framework, let us discuss some issues related to the formalization of SOA as described in Section 2.1. That formalization is very general; it can be applied to any game in which the players choose moves from continuous bounded scales and where the payoffs are taken from continuous domains. A classical game such as the prisoners dilemma can also be modeled in that context, if the players, each of which controlling a single resource, - the player's own testimonial -, are allowed to set a value in the interval $[-1, 1]$ as their resource state, and if the payoffs vary between the four values used in discrete versions of the game, corresponding to the payoffs of the four possible state vectors.

Let $PP_{max}(a_i)$ be the subset of payoff vectors that are maximal in relation to an actor a_i , i.e., $PP_{max}(a_i) = \{p(s) \in PP \mid p_i(s) = max_{s' \in SS} p_i(s')\}$ and let $SS_{max}(a_i) = \{s \in SS \mid p(s) \in PP_{max}(a_i)\}$ be the set of states that generate these payoffs. Let $PP_{max} = \bigcup_i PP_{max}(a_i)$ and $SS_{max}(a_i) = \bigcup_i SS_{max}(a_i)$.

Obviously, at least one of the states that yield maximal benefit for an actor is also a Pareto optimum. Therefore we have $PP_{Pareto \& max} = PP_{max} \cap PP_{Pareto} \neq \emptyset$ and $SS_{Pareto \& max} = SS_{max} \cap SS_{Pareto} \neq \emptyset$. Moreover, any payoff vector in PP_{Pareto} can be placed between payoffs in $SS_{Pareto \& max}$. What is more difficult to state is how can we obtain these sets without comparing every state with each other, something that is impossible to do inside a continuous framework.

We believe that one can efficiently determine those sets in continuous SOA games (fuzzy or not) by defining regions in which it can be proved that the payoff functions for each actor are monotonic. In particular, we believe that in the fuzzy case it suffices to use the cores of the terms in the fuzzy input partitions in order to divide the M -dimensional state space. Moreover, we believe that, due to the interpolative nature of the inference scheme proposed here, we can prove the following postulates.

Postulate 1:

Let $\text{output}(K, x^*)$ denote the output obtained by applying input vector x^* on fuzzy rule-base K , using the procedure sketched in Section 3. Let $A \tilde{\leq} B$ stand for $\forall \alpha \in (0, 1], A_\alpha \leq B_\alpha$ and $\tilde{\min}$ and $\tilde{\max}$ stand for the fuzzy min and max operators, respectively (see e.g. [4]). Let x' and x'' be such that x' , x'' and x^* all belong to the same same monotonic region in the input space. If $\forall k, \min(x'_k, x''_k) \leq x_k^* \leq \max(x'_k, x''_k)$, then $\tilde{\min}(\text{output}(K, x'), \text{output}(K, x'')) \leq \text{output}(K, x^*) \leq \tilde{\max}(\text{output}(K, x'), \text{output}(K, x'')).$

Postulate 2:

If $s^* \in SS_{\text{Pareto}}$ then $\exists s', s'' \in SS_{\text{Pareto}\&\max}$, such that s^* , s' and s'' are all in the same monotonic region in the state space and $\forall k, \min(s'_k, s''_k) \leq s_k^* \leq \max(s'_k, s''_k)$.

Postulate 1 states that ordered input vectors in the same region generate ordered outputs. Postulate 2 states that all Pareto optima lie between the actors optima. So we only need to find the actors optima to determine the regions in which all optima lie. These postulates allow us thus to establish which attitudes from the players lead to optimal states directly from the fuzzy states.

The maximal payoff for the secretary is reached when the director fully cooperates but she is neutral, i.e. $SS_{\max}(Sc) = \{(1, 0)\}$, whereas his maximal payoffs are obtained when she fully cooperates, no matter which strategy he adopts, i.e. in states $SS_{\max}(Dr) = \{(x, 1), x \in [-1, 1]\}$. The set of Pareto optima which also yield maximal payoffs is $SS_{\text{Pareto}\&\max} = \{(1, 0), (1, 1)\}$; $(1, 1)$ can be interpreted as “full cooperation from both”. Another Pareto optimum is e.g. $(1, .5)$ (see Figure 2). Note that these three states belong to the same monotonic region. The only Nash equilibrium is $(0, 0)$ and corresponds to a completely neutral position from both actors. The postulates would allow us to affirm also that all the Pareto optima are between fuzzy states (C, N) and (C, C) , and that the Nash equilibrium is found in fuzzy state (N, N) .

5. Conclusion

We presented a fuzzy rule-based extension for the modeling of a fragment of the Sociology of Organized Action, which is particularly useful when assessments about a SOA case can only be given in qualitative means.

Although some literature exists involving fuzzy sets theory and games theory, few of them address the specificities of our problem: i) we do not deal with *mixed strategies*, that are used in repetitive games in which to each player is associated a probability distribution on his/her possible moves and ii) the states of the game and the payoffs are values taken in continuous domains instead of discrete ones (see [1] for a list of relevant literature), and, particularly, none seems to address SOA.

In the ongoing work we are exploring the modeling of these important concepts also in fuzzy rule based systems that involves modeling payoffs that are functions of fuzzy effects. In [10], for instance, the payoffs are computed as the average of effects on the resources an actor controls and of those that the actor only depends on, correspondingly weighted by the actor’s autonomy and subordination. In what regards fuzzy sets theory specifically, we are studying which restrictions really need to be adopted in the model

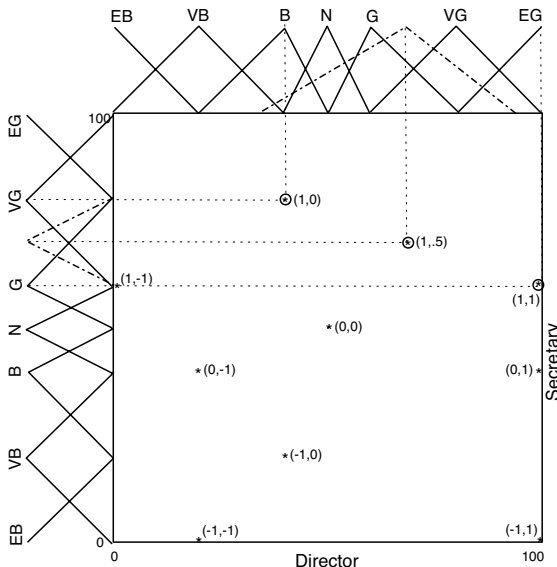


Figure 2. Payoffs for some states of the game; the encircled ones correspond to Pareto optima.

(e.g. Ruspini partitions) and how useful generalizations can be easily incorporated in it (e.g. LR fuzzy sets). As future work, we intend to extend the model to address the cases in which i) a resource can be controlled by more than one actor and ii) an actor can be responsible for the limits on a resource controlled by someone else.

References

- [1] B. Arfi, Linguistic fuzzy-logic social game, *Rationality and Society*, 18:4 (2006), 471-537.
- [2] K. Binmore, *Fun and games: a text on game theory*, D.C. Heath and Company, 1992.
- [3] M. Crozier, E. Friedberg, Organizations and collective action: our contribution to organizational analysis, in: S.B. Bacharrach, P. Gagliardi and B. Mundel (Eds), *Studies of Organizations in the European Tradition*, Series "Research in the Sociology of Organizations", Greenwich Corn. Jay-Press, 13 (1995), 71-93.
- [4] D. Dubois, H. Prade, *Possibility Theory*, Plenum Press, 1988.
- [5] D. Dubois, H. Prade, L. Ughetto, Checking the coherence and redundancy of fuzzy knowledge bases, *IEEE Trans. on Fuzzy Systems*, 5:3 (1997), 398-417.
- [6] L. Godo, S. Sandri, A similarity based approach to deal with inconsistency in systems of fuzzy gradual rules, Proc. IPMU'2002, Annecy (Fr), 2002, 1655-1662.
- [7] L. Godo, S. Sandri, Dealing with covering problems in fuzzy rule systems by similarity-based extrapolation, Proc. FuzzIEEE'02, Honolulu (USA), 2002.
- [8] M. Mailliard, S. Audras, C. Marina, Multi-agents Systems based on classifiers for the simulation of concrete action systems, Proc. EUMAS'03, Oxford University (UK), 2003.
- [9] S. Sandri, C. Sibertin-Blanc, V. Torra, A multicriteria fuzzy system using residuated implication operators and fuzzy arithmetic, Proc. MDAI'07, Kitakyushu (Jp), 2007.
- [10] S. Sandri, C. Sibertin-Blanc, Transposing the Sociology of Organized Action into a fuzzy environment, Proc. ECSQARU'07, Hammamet (Tn).
- [11] C. Sibertin-Blanc, F. Amblard, M. Mailliard, A coordination framework based on the Sociology of Organized Action, in: *Coordination, Organizations, Institutions and Norms in Multi-*

- Agent Systems, Olivier Boissier, J. Padget, V. Dignum, G. Lindemann (Eds.), Springer, LNCS 3913 (2006), 3-17.
- [12] H. Simon, The sciences of the artificial, MIT Press, 1996.
- [13] P. Smets, L'agence Travel-Tours. <http://homepages.ulb.ac.be/~psmets1/travel.pdf>.
- [14] Wang X., Kerre, E.E. Reasonable properties for the ordering of fuzzy quantities. FSS, 118 (2001), 375-385 (I) 387-405 (II).

Multidimensional OWA Operators in Group Decision Making¹

Isabel AGUILÓ^{a,2}, Miguel A. BALLESTER^b, Tomasa CALVO^c,
José Luis GARCÍA-LAPRESTA^d, Gaspar MAYOR^a and Jaume SUÑER^a

^a *Universitat de les Illes Balears, Spain*

^b *Universitat Autònoma de Barcelona, Spain*

^c *Universidad de Alcalá, Spain*

^d *Universidad de Valladolid, Spain*

Abstract. In this paper we consider multi-dimensional OWA operators to be used in the aggregation phase of a sequential group decision making procedure. We analyze when these operators are multi-dimensional aggregation functions and provide a convergent procedure for different ways of defining the weighting triangles.

Keywords. Group decision making, Multi-dimensional OWA, Weighting triangle, Regularity, Max-biasing

1. Introduction

In some cases a society has to decide which members of the group are appropriate for doing a task or regarding an attribute. From a democratic point of view, it seems reasonable to take into account the opinion of each member of the society about all the individuals of the group. In this paper we put in practice this idea by allowing individuals to show their assessments in a gradual way, within the unit interval. By means of an aggregation operator, we obtain a collective assessment for each member of the society. Given a threshold, we select those individuals whose collective assessments reach the fixed threshold. As the opinions of the members of this obtained elite are surely more important for the society than those of the non qualified individuals, we introduce a sequential decision procedure, where only the opinions of the elite are taken into account for obtaining a further elite. This iteration can be repeated until we obtain a final set of qualified individuals, in the sense that subsequent iterations do not change this set. In this case, we say that the procedure is convergent.

¹This work is partially financed by the Spanish Ministerio de Educación y Ciencia (projects MTM2006-08322, SEJ2006-04267/ECON and SEJ2005-01481/ECON), ERDF, CREA, Junta de Castilla y León (project VA040A05), Generalitat de Catalunya (grant 2005SJR00454), Barcelona Economics-XREA and Govern de les Illes Balears (grant PCTIB 2005-GCI-07).

²Corresponding Author: Isabel Aguiló, Departament de Ciències Matemàtiques i Informàtica, Edifici Anselm Turmeda, Cra. de Valldemossa Km. 7.5, 07122 Palma de Mallorca, Spain. Tel.: +34 971 172 900; Fax: +34 971 173 003; E-mail: isabel.aguilo@uib.es.

It is important to emphasize that the analyzed group decision procedure consists of selecting a subset of qualified members of the society, and once this group has been determined, the whole society delegates in that group the task it has been chosen for.

Since in each step of the iteration the number of individuals whose opinions are taken into account is different, this process is intrinsically multi-dimensional; thus aggregation operators satisfying a type of multi-dimensional monotonicity condition must be considered. Among the large variety of aggregation operators, the so-called OWA ("Ordered Weighted Averaging") operators have proved to be very useful for aggregation purposes. This class of operators was introduced by Yager in [8] and they have been widely studied by different authors (see, for instance, [3], [6], [9]). In 1997, Mayor and Calvo ([7]) introduced the concept of multi-dimensional aggregation function and multi-dimensional OWA operators (also called Extended OWA Operators, EOWA for short), and studied the conditions under which an EOWA operator is a multi-dimensional aggregation function. Other interesting papers on the topic can be found in [2], [4] and [5].

Also, Ballester and García-Lapresta study in [1] the sequential group decision making procedure considered in this paper, and they give a sufficient condition, named max-biasing, which guarantees the convergence of the mentioned sequential procedure for the case of EOWA operators.

In this paper we deal with EOWA operators generated by sequences and some classes of fractals and analyze when this class of operators is useful for the aggregation phase of the sequential group decision making procedure mentioned above, in the sense that they should be multi-dimensional aggregation functions and provide a convergent procedure. We begin with Section 2 where some preliminaries on multi-dimensional aggregation operators are given to be used along the paper. In Section 3 we state the sequential group decision making procedure considered and give conditions for the convergence of the procedure. In the case of EOWA operators, we give the so-called max-biasing condition. Finally, Section 4 is devoted to study when different classes of multi-dimensional OWA operators, specially those generated by sequences and fractals, are both multi-dimensional aggregation functions and max-biased EOWA operators.

2. Preliminaries

A *weighting vector* is a list $(w_1^p, \dots, w_p^p) \in [0, 1]^p$ such that $w_1^p + \dots + w_p^p = 1$.

Definition 2.1 *The OWA operator (of dimension p) associated with a weighting vector (w_1^p, \dots, w_p^p) is the function $w^p : [0, 1]^p \rightarrow [0, 1]$ defined by*

$$w^p(a_1, \dots, a_p) = w_1^p \cdot b_1 + \dots + w_p^p \cdot b_p,$$

with b_i the i -th largest of the a_1, \dots, a_p .

The notion of multi-dimensional aggregation functions and EOWA operators (see [7] and [4]) becomes useful for our purposes.

Definition 2.2 *An Extended OWA (EOWA) operator is a family of OWA operators $\{w^p\}$ where w^p is an OWA of dimension p with associated weighting vector (w_1^p, \dots, w_p^p) .*

Thus, given an EOWA operator, we have a collection of weighting vectors, one for each dimension, which can be arranged as a triangle. Then we can give the following definition.

Definition 2.3 A weighting triangle is a set of numbers $w_i^p \in [0, 1]$, with $i = 1, \dots, p$ and $p \in \mathbb{N}$, such that $w_1^p + \dots + w_p^p = 1$ for every $p \in \mathbb{N}$.

$$\begin{array}{ccccccc} & & & & 1 \\ & & & & w_1^2 & w_2^2 \\ & & & & w_1^3 & w_2^3 & w_3^3 \\ & & & & w_1^4 & w_2^4 & w_3^4 & w_4^4 \\ & & & & \dots & & \end{array}$$

Definition 2.4 Let $\mathbf{x} = (x_1, \dots, x_r) \in [0, 1]^r$ and $\mathbf{y} = (y_1, \dots, y_s) \in [0, 1]^s$. The following orderings on $\bigcup_{p \in \mathbb{N}} [0, 1]^p$ can be considered:

- $\mathbf{x} \leq_\pi \mathbf{y}$ if $r = s$ and $x_1 \leq y_1, \dots, x_r \leq y_r$.

- $\mathbf{x} \leq_\wedge \mathbf{y}$ if $r \geq s$ and $(x_1, \dots, x_r) \leq_\pi (y_1, \dots, y_s, \bigwedge_1^s y_i, \dots, \bigwedge_1^s y_i)$.

- $\mathbf{x} \leq_\vee \mathbf{y}$ if $r \leq s$ and $(x_1, \dots, x_r, \bigvee_1^{s-r} x_i, \dots, \bigvee_1^{s-r} x_i) \leq_\pi (y_1, \dots, y_s)$.

Definition 2.5 A mapping $A : \bigcup_{p \in \mathbb{N}} [0, 1]^p \longrightarrow [0, 1]$ is a Multi-dimensional Aggregation Function (MAF) if it satisfies the following two conditions:

1. A is monotonic with respect to \leq_\wedge and \leq_\vee .
2. A is idempotent, i.e., $A(\overbrace{x, \dots, x}^{p\text{-times}}) = x$ for every $x \in [0, 1]$ and any $p \in \mathbb{N}$.

The next result, presented in [7], gives a characterization of EOWA operators that are MAF.

Proposition 2.6 An EOWA operator $\{w^p\}$ is a MAF if and only if the following inequalities hold for each $p \in \mathbb{N}$ and every $m \in \{1, \dots, p\}$

$$\sum_{i=1}^m w_i^{p+1} \leq \sum_{i=1}^m w_i^p \leq \sum_{i=1}^{m+1} w_i^{p+1}. \quad (1)$$

Triangles satisfying (1) are called *regular*.

3. The sequential decision making procedure

We now introduce the sequential decision making procedure appearing in [1].

Consider a finite set of individuals $N = \{1, 2, \dots, n\}$ with $n \geq 2$. We use 2^N to denote the power set of N , i.e., the set of all the subsets of N , and $|S|$ is the cardinal of S . A *profile* is an $n \times n$ matrix

$$P = \begin{pmatrix} p_{11} & \cdots & p_{1j} & \cdots & p_{1n} \\ \cdots & \cdots & \cdots & \cdots & \cdots \\ p_{i1} & \cdots & p_{ij} & \cdots & p_{in} \\ \cdots & \cdots & \cdots & \cdots & \cdots \\ p_{n1} & \cdots & p_{nj} & \cdots & p_{nn} \end{pmatrix}$$

with values in the unit interval, where p_{ij} is the assessment with which the individual i evaluates individual j as being qualified to belong to the committee in question. The set of profiles is denoted by \mathcal{P} . Given a subset of individuals $S \subseteq N$, P_S denotes the $|S| \times n$ submatrix of P composed by those i -rows with $i \in S$. Given $j \in N$, we denote by P_S^j the j -th column vector of P_S . Finally, we denote by $\sigma(P_S^j)$ a permutation of vector P_S^j such that opinions are ordered from best to worst; and $[\sigma(P_S^j)]_i$ denotes the i -th component of $\sigma(P_S^j)$.

Definition 3.1 A Committees' Evaluation Mechanism (CEM) is a family of functions $\{v_S\}$, with $\emptyset \neq S \subseteq N$, where $v_S : \mathcal{P} \times N \rightarrow [0, 1]$ is a function that, given $P \in \mathcal{P}$, assigns a collective assessment $v_S(P, j) \in [0, 1]$ to each individual $j \in N$ in such a way that $v_S(P, j) = v_S(Q, j)$ for all $P, Q \in \mathcal{P}$ satisfying $P_S^j = Q_S^j$.

According to the previous definition, the collective assessment that the subgroup S provides to individual j , $v_S(P, j)$, depends only on the individual assessments of S on the individual j .

A CEM determines individual qualification only in gradual terms. A very natural way to convert a gradual opinion into a dichotomic assessment is by means of thresholds or quotas. An individual is qualified if the collective assessment is above a fixed quota.

Definition 3.2 A family of values $\{\alpha_S\}$, $\emptyset \neq S \subseteq N$, and $\alpha_S \in (0, 1]$ for every S , is called a Threshold Mechanism (TM).

Given a CEM $\{v_S\}$ and a TM $\{\alpha_S\}$, we consider a family of functions $\{V_S\}$, with $S \subseteq N$, where $V_S : \mathcal{P} \rightarrow 2^N$ is the function that, given $P \in \mathcal{P}$, qualifies a new subgroup $V_S(P)$ as follows:

$$V_S(P) = \begin{cases} \{j \in N \mid v_S(P, j) \geq \alpha_S\}, & \text{if } S \neq \emptyset, \\ \emptyset, & \text{otherwise.} \end{cases}$$

The family of functions $\{V_S\}$ is called the Committees' Qualification Mechanism (CQM) associated with $\{\alpha_S\}$ and $\{v_S\}$.

Definition 3.3 Given a CQM $\{V_S\}$, the sequence $\{S_t\}$, where $S_1 = N$ and $S_{t+1} = V_{S_t}(P)$, is called committees' sequence. A committees' sequence is said to be convergent if $\{S_t\}$ has a limit $\lim S_t$ (and it is also said that the sequence converges to $\lim S_t$). The CQM is said to be convergent if for any $P \in \mathcal{P}$ the generated committees' sequence is convergent.

Notice that, since society is a finite set, chain convergence can also be expressed as: the committees' sequence is convergent if there exists a positive integer q such that $S_t = S_q$ for every $t \geq q$.

In some occasions, aggregation operators are defined for a given number of individual opinions. Notice however that for our model to apply, we have to consider collections of operators, one for each possible subgroup of individuals in society. There are multiple options to consider here, and it is our purpose to analyze general classes of operators. For the sake of a more intuitive analysis, we adopt here the following two assumptions about CEMs to be used:

SE *Self-Exclusion*: When an individual has to decide on herself, she will exclude her opinion when possible (i.e., she is not the only reviewer).

CS *Cardinality-Symmetry*: When the same number of opinions have to be aggregated, the same operator will be applied (independently of the names of the reviewers).

We now formally explicit how an EOWA operator can be considered a CEM following the assumptions **SE** and **CS**. This can be done by considering, for every $\emptyset \neq S \subseteq N$:

1. The OWA of dimension $|S|$, $w^{|S|}$, applied to P_S^j , if $j \notin S$.
2. The OWA of dimension $|S| - 1$, $w^{|S|-1}$, applied to $P_{S \setminus \{j\}}^j$, if $j \in S \neq \{j\}$.
3. The OWA of dimension 1, i.e., the identity, applied to $P_{\{j\}}^j = p_{jj}$, if $S = \{j\}$.

Example 3.4 Let us suppose that there is a group $N = \{1, 2, 3, 4, 5\}$ of members and we have the following profile of individual opinions:

$$P = \begin{pmatrix} 1 & 1 & .7 & .6 & .3 \\ 1 & 1 & .8 & .5 & .2 \\ .9 & .8 & .8 & .7 & .4 \\ 1 & 1 & .9 & .8 & .5 \\ .8 & .7 & .9 & .6 & .6 \end{pmatrix}.$$

If we apply the sequential procedure for the specific OWAs maximum, minimum, average and median, with constant thresholds $\alpha = 0.5, 0.6, 0.7, 0.8, 0.9$, we obtain the limit sets included in Table 1.

Table 1. Limit sets for *maximum, minimum, average* and *median* CQMs

α	Best	Worst	Average	Median
0.5	N	$\{1, 2, 3, 4\}$	$\{1, 2, 3, 4\}$	$\{1, 2, 3, 4\}$
0.6	$\{1, 2, 3, 4\}$	$\{1, 2, 3\}$	$\{1, 2, 3, 4\}$	$\{1, 2, 3, 4\}$
0.7	$\{1, 2, 3, 4\}$	$\{1, 2, 3\}$	$\{1, 2, 3\}$	$\{1, 2, 3\}$
0.8	$\{1, 2, 3\}$	$\{1, 2\}$	$\{1, 2\}$	$\{1, 2\}$
0.9	$\{1, 2\}$	$\{1, 2\}$	$\{1, 2\}$	$\{1, 2\}$

As proposition 3.8. below shows, the next property becomes relevant for convergence. In few words, it states that the larger a committee is, the more benevolently judges an individual. Consider two committees, one of dimension p and the other of dimension $p + 1$. Benevolence materializes in the fact that the sum of weights assigned to the m largest opinions (for any m) in the greater committee has to be larger than the sum of weights assigned to the m largest opinions in the smaller committee. Obviously, in the case of larger committees, there are more members to receive a weight, and therefore, the previous idea applies only relatively (using the fraction $\frac{p}{p+1}$) as a corrector. Technically:

Definition 3.5 An EOWA operator $\{w^p\}$ is max-biased if for every dimension p and $m \leq p$:

$$\sum_{i=1}^m w_i^{p+1} \geq \frac{p}{p+1} \sum_{i=1}^m w_i^p.$$

Remark 3.6 An EOWA operator $\{w^p\}$ is max-biased if and only if for all positive integers m, u, v such that $m \leq u \leq v$ it holds

$$\sum_{i=1}^m w_i^v \geq \frac{u}{v} \sum_{i=1}^m w_i^u.$$

Remark 3.7 Observe that, if $\{w^p\}$ is max-biased, then if we take $m = p$,

$$\sum_{i=1}^p w_i^{p+1} \geq \frac{p}{p+1} \sum_{i=1}^p w_i^p \implies 1 - w_{p+1}^{p+1} \geq \frac{p}{p+1} \sum_{i=1}^p w_i^p = \frac{p}{p+1}$$

and thus $w_{p+1}^{p+1} \leq \frac{1}{p+1}$ for every $p \in \mathbb{N}$.

The following result can be found in [1].

Proposition 3.8 Let $\{V_S\}$ be a CQM associated with an EOWA $\{w^p\}$ and a TM $\{\alpha_S\}$. Then $\{V_S\}$ is convergent if the following two conditions are satisfied:

1. $\{w^p\}$ is max-biased,
2. For all $U, V \subseteq N$ such that $\emptyset \neq U \subseteq V$, it holds $|U| \alpha_U \geq (|V| - 1) \alpha_V$,

4. The results

Now we consider different ways of generating weighting triangles for EOWA operators and for each one of them, we analyze when this class of operators is useful for the aggregation phase of the sequential group decision making procedure mentioned above, in the sense that they should be MAFs and satisfy the max-biasing condition.

4.1. EOWAs generated by sequences

Calvo *et al.* introduce in [5] a way of generating triangles by means of sequences.

Definition 4.1 Let $\{\lambda_p\}$ be a sequence of non negative real numbers such that $\lambda_1 > 0$. The triangle generated by $\{\lambda_p\}$ is given by:

$$w_i^p = \frac{\lambda_i}{\lambda_1 + \dots + \lambda_p}, \text{ for } p \in \mathbb{N} \text{ and } i \in \{1, \dots, p\}.$$

It is proved in [5] the following necessary and sufficient condition for a triangle generated by a sequence to be regular.

Proposition 4.2 A triangle generated by $\{\lambda_p\}$ is regular if and only if the sequence $\left\{ \frac{S_{p+1}}{S_p} \right\}$ is decreasing, where $S_p = \lambda_1 + \dots + \lambda_p$.

The next proposition gives a necessary and sufficient condition for this class of triangles to produce a max-biased EOWA operator.

Proposition 4.3 Let $\{w^p\}$ be a triangle generated by a sequence $\{\lambda_p\}$. Then $\{w^p\}$ is max-biased if and only if

$$\frac{\sum_{i=1}^p \lambda_i}{p} \geq \frac{\sum_{i=1}^{p+1} \lambda_i}{p+1}.$$

Finally, we have the following result.

Proposition 4.4 Let $\{w^p\}$ be a triangle generated by a sequence $\{\lambda_p\}$. Then $\{w^p\}$ is regular and max-biased if and only if $\frac{\lambda_{p+2}}{S_{p+1}} \leq \frac{\lambda_{p+1}}{S_p} \leq \frac{1}{p}$ for every $p \in \mathbb{N}$.

Remark 4.5 Observe that, if the sequence $\{\lambda_p\}$ is decreasing, then the above proposition holds.

4.2. EOWAs generated by fractals

Some ways of generating weighting triangles from fractals are given in [5]. For example, the Sierpinski triangle gives the following weighting triangle

$$\begin{array}{ccccccc} & & & 1 & & & \\ & & & 1 \cdot \frac{1}{4} & 3 \cdot \frac{1}{4} & & \\ & & & 1 \cdot \frac{1}{4} & 3 \cdot \frac{1}{4^2} & 3^2 \cdot \frac{1}{4^2} & \\ & & & 1 \cdot \frac{1}{4} & 3 \cdot \frac{1}{4^2} & 3^2 \cdot \frac{1}{4^3} & 3^3 \cdot \frac{1}{4^3} \\ & & & \dots & & & \end{array}$$

whereas the Sierpinski carpet generates the triangle

$$\begin{array}{cccc}
 & & 1 & \\
 & & 1 \cdot \frac{1}{9} & 8 \cdot \frac{1}{9} \\
 & & 1 \cdot \frac{1}{9} & 8 \cdot \frac{1}{9^2} & 8^2 \cdot \frac{1}{9^2} \\
 & & 1 \cdot \frac{1}{9} & 8 \cdot \frac{1}{9^2} & 8^2 \cdot \frac{1}{9^3} & 8^3 \cdot \frac{1}{9^3} \\
 & \dots & \dots & \dots & \dots
 \end{array}$$

A generalization of these two types of fractals is the Sierpinski family. To see how we obtain the corresponding weighting triangle, let us consider an unitary surface and divide it into two parts, one part with an area equal to $\frac{a}{b} < 1$ and the second one with an area equal to $1 - \frac{a}{b} = \frac{b-a}{b}$. After that, we take the surface with area $\frac{b-a}{b}$ and we divide it again into two parts: the first one with area $\frac{a}{b} \cdot \left(\frac{b-a}{b}\right)$ and the other one with area $\left(\frac{b-a}{b}\right)^2$. In order to build the third row of the weighting triangle we need to take into account the surface with area $\frac{a}{b}$; so we obtain

$$\frac{a}{b}, \quad \frac{a}{b} \cdot \left(\frac{b-a}{b}\right), \quad \left(\frac{b-a}{b}\right)^2$$

Therefore, according to this idea we obtain the following weighting triangle

$$\begin{array}{cccc}
 & & 1 & \\
 & & \frac{a}{b} & \frac{b-a}{b} \\
 & & \frac{a}{b} & \frac{a}{b} \cdot \left(\frac{b-a}{b}\right) & \left(\frac{b-a}{b}\right)^2 \\
 & & \frac{a}{b} & \frac{a}{b} \cdot \left(\frac{b-a}{b}\right) & \frac{a}{b} \cdot \left(\frac{b-a}{b}\right)^2 & \left(\frac{b-a}{b}\right)^3 \\
 & \dots & \dots & \dots & \dots
 \end{array}$$

The weights of this triangle are

$$w_i^p = \frac{a}{b} \cdot \left(\frac{b-a}{b}\right)^{i-1}, \quad i = 1, \dots, p-1, \text{ and } w_p^p = \left(\frac{b-a}{b}\right)^{p-1}.$$

Notice that, if we want to obtain a fractal structure at the end of this process we need to assume $\frac{a}{b} \neq \frac{b-a}{b}$, $\frac{a}{b} < 1$ and also that the surface with area $\frac{a}{b}$ should have the same shape as the original surface.

If we take $\frac{a}{b} = \frac{1}{4}$ and $\frac{a}{b} = \frac{1}{9}$ we obtain the weighting triangles generated respectively by the *Sierpinski triangle* and the *Sierpinski carpet*.

Proposition 4.6 Let $\{w^p\}$ be an EOWA operator generated by the Sierpinski family. Then $\{w^p\}$ is max-biased if and only if $\frac{a}{b} \geq \frac{1}{2}$.

Remark 4.7 Observe that neither the weighting triangle obtained from the Sierpinski triangle nor the one obtained from the Sierpinski carpet satisfy the condition above. Nevertheless, the corresponding reversed triangles (that is, the triangles with weights given by

$u_j^p = w_{p-j+1}^p$, for $p > 1$ and all $j \in \{1, \dots, p\}$) produce max-biased EOWAs. On the other hand, both the triangles generated by the Sierpinski family and their reversed are regular, as shown in [5].

5. Conclusions

In this paper we have considered multi-dimensional OWA operators to be used in the aggregation phase of a sequential group decision making procedure. For this class of operators to be suitable for the decision process, two conditions have to be satisfied, namely the max-biasing condition which ensures the convergence of the procedure, and the regularity of the weighting triangle associated to the operator, which ensures that the EOWA operator is a multi-dimensional aggregation function (MAF). The main results of this paper are necessary and sufficient conditions for obtaining max-biased EOWA operators with regular weighting triangles generated by sequences and some classes of fractals. Consequently, we have found the set of this EOWA operators which are MAFs and guarantee the convergence of the mentioned sequential decision procedure. This study will be continued by considering more classes of EOWA operators, and a very interesting future work is to make a compared description of the benefits of every approach.

References

- [1] M.A. Ballester, J.L. García-Lapresta, A recursive group decision procedure based on EOWA operators. *Proc. FUZZ-IEEE 2007*, London, 2007.
- [2] T. Calvo, Two ways of generating Extended Aggregation Functions. *Proc. IPMU'98*, Paris, 1998.
- [3] T. Calvo, A. Kolesárová, M. Komorníková, R. Mesiar, Aggregation operators: Properties, classes and constructions models. In T. Calvo, G. Mayor, R. Mesiar, editors. *Aggregation Operators: New Trends and Applications*. Physica-Verlag, Heidelberg, 2002, pp. 3–104.
- [4] T. Calvo, G. Mayor, Remarks on two types of extended aggregation functions. *Tatra Mountains Mathematical Publications* **16** 1999, pp. 235–253.
- [5] T. Calvo, G. Mayor, J. Torrens, J. Suñer, M. Mas, M. Carbonell, Generation of weighting triangles associated with aggregation functions. *International Journal of Uncertainty, Fuzziness and Knowledge-Based Systems* **8** 2000, pp. 417–451.
- [6] J. Fodor, M. Roubens, *Fuzzy Preference Modelling and Multicriteria Decision Support*. Kluwer Academic Publishers, Dordrecht, 1994.
- [7] G. Mayor, T. Calvo, On extended aggregation functions. *Proceedings of IFSA 97*, vol. I, Prague, 1997, pp. 281–285.
- [8] R.R. Yager, Ordered weighted averaging operators in multicriteria decision making. *IEEE Transactions on Systems, Man and Cybernetics* **8** 1988, pp. 183–190.
- [9] R.R. Yager, J. Kacprzyk, *The Ordered Weighted Averaging Operators: Theory and Applications*. Kluwer Academic Publishers, Norwell, 1997.

Reasoning about actions under uncertainty: A possibilistic approach

Juan Carlos Nieves ^{a,*}, Mauricio Osorio ^b, Ulises Cortés ^a,
 Francisco Caballero ^c and Antonio López-Navidad ^c

^a Software Department (LSI), Universitat Politècnica de Catalunya, Spain

^b Fundación Universidad de las Américas - Puebla, México

^c Hospital de la Santa Creu y Sant Pau, Spain

Abstract. In this paper, we present an action language which is called \mathcal{A}^{Poss} in order to perform reasoning about actions under uncertainty. This language is based on a possibilistic logic programming semantics which is able to deal with reasoning under uncertain information. In order to illustrate the language, we use a medical scenario.

Keywords. Decision making, Uncertainty, Planning, Non-Monotonic Reasoning

1. Introduction

It is well-known that decision making is the physician's major activity. Many researches about how doctors make decisions have been growing steadily during at least the last 60 years. The psychologist Paul Meehl pointed out that the use of mathematical methods could make better clinical decisions than unaided judgment [1]. Meehl's argument for adoption of mathematical methods in decision making was enormously controversial and still is, despite of its considerable influence. But his claim that people frequently make systematic errors in their decision making is no longer questioned [1]. Now the question is, which mathematical methods are suitable for coping medical decision making?

Let us introduce a medical scenario in the human organ transplanting context. In this scenario, there is a donor D which is infected by the hepatitis B virus (HBV+) and there is a recipient R which needs a heart transplantation and is not infected by HBV (HBV-) but his clinical situation is 0-urgency. This means that he needs a heart transplantation in the next 24 hours, otherwise he could die.

According to [2], the common criterion for transplanting an organ from a donor HBV+ suggests that any organ from a donor HBV+ *could be* considered for transplanting if and only if the recipient is HBV+. However, it is known that organs from donors HBV+ *do not always* transmit HBV infection to recipients HBV- [2]. Moreover, *some times* when the HBV infection occurs, the recipient can spontaneously clear the virus and turn

*Correspondence to: Software Department (LSI), Universitat Politècnica de Catalunya. C/Jordi Girona 1-3, E08034, Barcelona, Spain. E-mail: (J.C. Nieves: jcnieves@lsi.upc.edu), (M. Osorio: osoriomauri@googlemail.com), (U. Cortés: ia@lsi.upc.edu)

to HBV-. Hence, the medical question about the scenario is: is the donor's heart viable to be transplanted onto the recipient R ? It is quite obvious that this crucial decision is vital for the recipient's survival. The main complexity of the question is that the decision is taken under uncertainty. This means that the environment in which the decision takes place is *incomplete, imprecise or uncertain*.

One of the first problems we must confront in order to develop a decision support system that could perform reasoning under uncertainty is to identify a specification language able to handle uncertain information. Moreover, it is important that our specification language must be able to capture *actions* in order to overcome a problem which is involved with uncertain information. For instance, in human organ transplanting all the recipients need a post-transplant treatment, then it is important to consider a plan of actions which will be considered after the allocation of an organ to a recipient. It is worth mentioning that each plan of actions is particular to each medical situation.

It is well-known that the most common methods for uncertain reasoning are based on probabilities. However, since medical decision making is susceptible to the evidence of the information, it is not always natural to quantify the medical knowledge in a numerical way. For instance in [3], it is pointed out that the chief disadvantages of the decision theory approach are the difficulties of obtaining reasonable estimates of probabilities and utilities for a particular analysis.

Tversky and Kahneman observed in [4] that many decisions which are made in our common life are based on beliefs concerning the likelihood of uncertain events. For instance, it was pointed out that it is common to use statements such as "I think that . . .", "chances are . . .", "it is *probable* that . . .", "it is *plausible* that . . .", etc., for supporting our decisions. Usually, in this kind of statements we are appealing to our experience or commonsense for solving a problem. In the medical domain, it is not rare that a doctor supports his decisions based on his commonsense when he has uncertain information.

In [5], it was presented a specification language which is able to cope with uncertain reasoning based on a possibilistic approach. This approach permits to explicitly use labels like *possible*, *probable*, *plausible*, etc., for capturing the incomplete state of a belief. However, this specification language does not provide a syntax for dealing with actions.

Since we are interested on modeling medical decision making where not only we want to capture uncertain information but also to generate plans of actions in order to support medical decision making. In this paper, we extend the specification language presented in [5] into an action language which is called \mathcal{A}^{Poss} . Moreover, we present a mapping from \mathcal{A}^{Poss} 's syntax into possibilistic programs in order to formulate planning using possibilistic answer sets.

The rest of the papers is divided as follows: In §2, it is defined the \mathcal{A} 's syntax. In §3, it is presented a mapping from \mathcal{A}^{Poss} 's syntax into possibilistic programs. In the last section, our conclusions are presented and the future work is outlined.

2. The language \mathcal{A}^{Poss}

Our language is based on the syntax of the language \mathcal{A} , proposed by Gelfond and Lifschits in [6]. This language has a simple English-like syntax to express the effects of actions on a world. As Baral pointed out in [7], \mathcal{A} is remarkable for its simplicity and has been extended in several directions to incorporate additional features of dynamic worlds

and to facilitate elaboration tolerance. We now present an extension of \mathcal{A} , which we call \mathcal{A}^{Poss} , in order to capture incomplete states of a belief/fluent.

As in \mathcal{A} 's alphabet, \mathcal{A}^{Poss} 's alphabet consists of two nonempty disjoint sets of symbols **F** and **A**, where **F** is a set of *possibilistic fluents* and **A** is a set of actions. A possibilistic fluent $(f \alpha)$ is a possibilistic literal¹ where intuitively f expresses a property of an item in a world and α expresses f is certain at least to the level α . A state σ is a collection of possibilistic fluents. We say that a fluent $(f \alpha)$ holds in a state σ if $(f \alpha) \in \sigma$ and a fluent literal $(\neg f \alpha)$ holds if $(\neg f \alpha) \notin \sigma$.

For example, let us go back to the medical scenario described in the introduction. In this example, let us assume that any belief about the medical situation could be quantified by *certain*, *likely*, *maybe*, *unlikely* and *false* (see Figure 1). For simplicity, we will only consider the following fluents: Clinical situation (CS), organ function (O), and infection (Inf). Then some possibilistic fluents are: $(CS(stable) certain)$, meaning that it is *certain* that the clinical situation of the recipient is stable, $(inf(positive) maybe)$, meaning that it is *probable* that the recipient could have a positive infection, $(O(delayed_graft_function) certain)$, meaning that the organ has a delay in its functions after it has been transplanted. Some actions about the medical scenario are: *transplant*, meaning that a transplantation is done, *wait*, meaning that nothing is done w.r.t. the clinical situation of the recipient, and *post-transplant treatment*, meaning that a post-transplant treatment is applied to the recipient. Notice that there is not a quantification of the certainty of the actions. This is because the actions are only conditioned by the status of the possibilistic fluents.

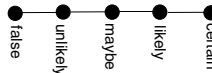


Figure 1. A single lattice where the following relations hold: $false \prec unlikely$, $unlikely \prec maybe$, $maybe \prec likely$, $likely \prec certain$.

Situations are representations of the history of action execution. The initial situation will be the situation where no action has been executed. It is represented by $[]$. The situation $[a_n, \dots, a_1]$ corresponds to the history where action a_1 is executed in the initial situation, followed by a_2 and so on until a_n .

Now we will describe the three sub-languages of \mathcal{A}^{Poss} .

Domain description language Similar to \mathcal{A} , the domain description language is used to succinctly express the transition between states due to actions. This language consists of possibilistic effect propositions of the following form:

$$a \text{ cause } (f \alpha) \text{ if } p_1, \dots, p_n, \neg q_{n+1}, \dots, \neg q_r \quad (1)$$

where a is an action, $(f \alpha)$ is a possibilistic fluent, and $p_1, \dots, p_n, q_{n+1}, \dots, q_r$ are atoms such that there exist the possibilistic fluents $(p_1 \alpha_1), \dots, (p_n \alpha_n)$, $(\neg q_1 \alpha_{n+1}), \dots, (\neg q_r \alpha_r)$. If r is equal to 0 then the possibilistic effect proposition is written as follows :

¹A possibilistic literal is a pair $l = (a, q) \in L \times Q$, where L is a finite set of literals and (Q, \leq) is a finite lattice. We apply the projection $*$ over l as follows: $l^* = a$.

$$a \text{ cause } (f \alpha) \quad (2)$$

Also, if there is a set of possibilistic effect propositions of the form $\{a \text{ cause } (f_1 \alpha_1), \dots, a \text{ cause } (f_m \alpha_m)\}$, then this set could be written as follows:

$$a \text{ cause } (f_1 \alpha_1), \dots, (f_m \alpha_m) \quad (3)$$

In order to illustrate the possibilistic effect propositions, let us consider again our medical scenario. Then a possible possibilistic effect proposition is :

$$\text{wait cause CS(unstable) maybe if CS(stable), } \\ O(\text{terminal_insufficient_function}). \quad (4)$$

The intended meaning is that if the recipient has a stable clinical condition, but he has an organ whose functions are terminal insufficient² and the doctor's action is *wait*, then it is *probable* that the clinical condition of the recipient could be *unstable*. The Figure 2 presents a diagram which expresses the transitions between different states where each arrow could be expressed by a possibilistic effect proposition.

Observation language A set of observations *Obs* consists of possibilistic value propositions which are of the form:

$$(f \alpha) \text{ after } a_1, \dots, a_m \quad (5)$$

where $(f \alpha)$ is a possibilistic fluent and a_1, \dots, a_m are actions. The intuitive reading is that if a_1, \dots, a_m would be executed in the initial situation then in the state corresponding to the situation $[a_1, \dots, a_m]$, $(f \alpha)$ would hold. When m is equal to 0, the possibilistic value propositions are written as follows:

$$\text{initially } (f \alpha) \quad (6)$$

In this case the intuitive meaning is that $(f \alpha)$ holds in the state corresponding to the initial situation. For instance, let us go back again to our medical scenario. We already know that the recipient's clinical situation is 0-urgency. Then this initial value is represented as follows:

$$\text{initially } (CS(0_urgency) certain) \quad (7)$$

Moreover he is not infected by HBV

$$\text{initially } (inf(negative) certain) \quad (8)$$

He has an organ whose functions are terminal insufficient.

$$\text{initially } (O(\text{terminal_insufficient_function}) certain) \quad (9)$$

²We say that an organ has *terminal insufficient* functions when there exists no clinical treatment for improving the organ's functions.

Since the donor was infected by the hepatitis B virus, then it is probable that the recipient could be infected by HBV in case the heart transplantation is done. This information is represented by the following possibilistic value proposition:

$$(inf(positive) \text{ maybe}) \text{ after transplant} \quad (10)$$

Also we know that if the heart transplantation is not done, then the recipient could die.

$$(CS(dead) \text{ maybe}) \text{ after wait} \quad (11)$$

Query Language Queries consist of possibilistic value propositions of the form (5).

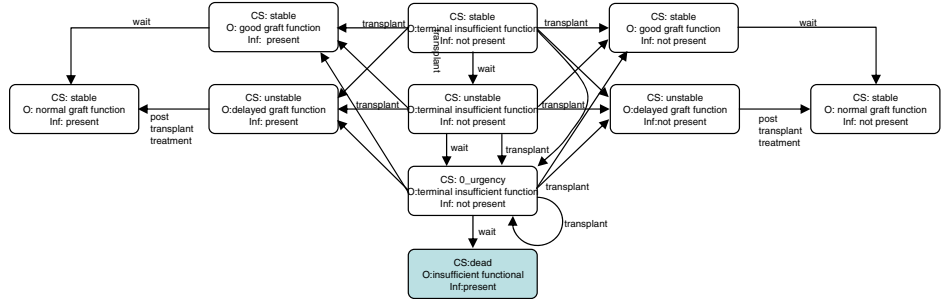


Figure 2. An automata of states and actions for considering infections in organ transplanting.

Executability conditions are not part of the standard \mathcal{A} 's syntax; however they are useful in real applications as is discussed in [7]. Then we will also introduce possibilistic executability conditions which are of the following form:

$$\text{executable } a \text{ if } p_1, \dots, p_n, \neg q_{n+1}, \dots, \neg q_r \quad (12)$$

where a is an action and $p_1, \dots, p_n, q_{n+1}, \dots, q_r$ are atoms such that there exist the possibilistic fluents $(p_1 \alpha_1), \dots, (p_n \alpha_n), (\neg q_1 \alpha_{n+1})$. In order to illustrate the possibilistic executability conditions, let us consider the following possibilistic executability condition which is in the context of our medical scenario:

$$\text{executable } transplant \text{ if } \neg CS(\text{dead}) \quad (13)$$

This executability conditions suggests an obvious condition which is that an organ transplant is not possible if the recipient is dead.

3. Reasoning about actions

In this section, we present a mapping from \mathcal{A}^{Poss} 's syntax into possibilistic programs in order to formulate planning using possibilistic answer sets [5]. Like in Answer Set Planning [7], we divide our encoding into two parts: the domain dependent part and the domain independent part.

We point out that we use the predicate *neg* for denoting the negation of the fluents and we use *not* for denoting the common negation by failure used in logic programming.

3.1. Encoding the domain dependent part

The domain dependent part consists of five parts, defining the domain, the executability conditions, the dynamic causal laws, the initial state, and the goal conditions.

1. The domain part defines the objects in the world, the fluents and the actions. For instance, by considering our medical scenario, a small part of the domain is:

```

certain : patient_states(stable).
certain : patient_states(unstable).
certain : patient_states(zero_urgency).
certain : patient_states(dead).
certain : organ_status(terminal_insufficient_function).
certain : organ_status(delayed_graft_function).
certain : organ_status(good_graft_function), ...
certain : infection_status(present).
certain : infection_status(not_present).
certain : fluent(CS(X))  $\leftarrow$  patient_states(X).
likely : fluent(CS(X))  $\leftarrow$  patient_states(X).
maybe : fluent(CS(X))  $\leftarrow$  patient_states(X).
unlikely : fluent(CS(X))  $\leftarrow$  patient_states(X).
false : fluent(CS(X))  $\leftarrow$  patient_states(X).
certain : fluent(O(X), Y)  $\leftarrow$  organ_status(X), ...
certain : action(transplant).
certain : action(wait).
...

```

2. The executability conditions state the executability conditions of each action. For instance, the possibilistic executability condition (13) is encoded as follows:

```
certain : exec(transplant, neg(CS(dead))).
```

Notice that we are using the predicate *neg* for denoting the negation of the fluents.

3. The dynamic causal laws state the effects of the actions. For instance, the possibilistic effect proposition (4) is mapped to:

```

maybe : cause(wait, CS(unstable), TT)  $\leftarrow$  holds(CS(stable), T),
holds(O(terminal_insufficient_function), T),
time(T), time(TT), TT = T + 1.

```

4. The initial state defines the initial state by explicitly listing which fluents are true in the initial state. In our medical scenario some declaration w.r.t. the initial state are:

```

certain : initially(CS(0_urgency)).
certain : initially(inf(not_present)).
certain : initially(O(terminal_insufficient_function)).

```

It is assumed that the fluents not explicitly listed to be true are false in all the states. This means that the knowledge about all the states are assumed to be com-

plete. Therefore, in order to have our knowledge base complete in our medical scenario, we add the following possibilistic clauses:

```

certain : holds(neg(CS(Y)), T) ← holds(CS(X), T), patient_states(X),
          patient_states(Y), time(T), not eq(X, Y).
ceratin : holds(neg(O(Y)), T) ← holds(o(X), T), organ_status(X),
          organ_status(Y), time(T), not eq(X, Y).
ceratin : holds(neg(inf(Y)), T) ← holds(inf(X), T), infection_status(X),
          infection_status(Y), time(T), not eq(X, Y).

```

5. The goal conditions list the fluents literals that must hold in a goal state. For instance:

```

certain : finally(CS(stable)).
certain : finally(O(normal_graft_function)).

```

This goal suggests that we are expecting that the recipient's clinical situation must be stable and his organ graft must have normal functions.

3.2. Encoding the domain independent part

This part is independent of the instance of a particular domain. Since this part defines the general rules for generating plans of actions, all of the clauses are quantified by the top of the lattice that was considered in the domain dependent part. In our medical example, it will be *certain*.

First, it is defined an exact bound or at least an upper bound of the plan lengths that we want to consider. This length makes that each possibilistic answer set will be finite. Using this length, it is defined the predicate *time* which specifies the time points of our interest:

```
certain : time(1...length).
```

The following possibilistic clauses define when all the goal conditions are satisfied

```

certain : not_goal(T) ← finally(X), not holds(X, T), time(T).
certain : goal(T) ← not not_goal(T), time(T).

```

The following constraint eliminates possible possibilistic answer sets where the goal is not satisfied in the last time point of interest.

```
certain : ← not goal(length).
```

The following possibilistic facts define when a possibilistic fluent literal is the negation of the other.

```

certain : contrary(F, neg(F)).
certain : contrary(neg(F), F).

```

The following two possibilistic clauses use the executability conditions to define when an action *A* is executed in a time *T*.

```

certain : not_executable(A, T) ← exec(A, F), not holds(F, T).
certain : executable(A, T) ← T < length, not not_executable(A, T).

```

The following possibilistic clause states the fluents that are held at time point 1.

```
certain : holds(F, 1) ← initially(T).
```

The following possibilistic clause describes the change in fluent values due to the execution of an action.

```

certain : holds(F, TT) ← T < length, executable(A, T), occurs(A, T), causes(A, F, TT),
          TT = T + 1, time(T), time(TT).

```

The following possibilistic clause describes the fluents which do not change their values after an action is executed (frame action).

certain : $\text{holds}(F, TT) \leftarrow \text{contrary}(F, G), T < \text{length}, \text{holds}(F, T), \text{not holds}(G, TT), TT = T + 1, \text{time}(T), \text{time}(TT).$

The following possibilistic clauses enumerate the action occurrences. They encode that in each possibilistic answer set at each time point only one of the executable actions occurred. Also, for each action that is executed in a possibilistic answer set at a time point, there is a possibilistic answer set where this action occurs at that time point.

certain : $\text{occurs}(A, T) \leftarrow \text{action}(A), \text{not goal}(T), \text{not not_occurs}(A, T), \text{time}(T).$
certain : $\text{not_occurs}(A, T) \leftarrow \text{action}(AA), \text{action}(AA), \text{time}(T), \text{occurs}(AA, T), A \neq AA.$
certain : $\leftarrow \text{action}(A), \text{time}(T), \text{occurs}(A, T), \text{not executable}(A, T).$

3.3. Possibilistic answer set semantics

In the previous subsections, we have presented a mapping from $\mathcal{A}^{\text{Poss}}$'s syntax into possibilistic programs. The possibilistic programs' semantics which permits to explicitly use labels like *possible*, *probable*, *plausible*, etc., was defined in [5]. This semantics is based on the operator T which is inspired in partial evaluation [8] and an inference rule of possibilistic logic [9]. Due to lack of space, we do not present a formal presentation of this semantics, however we will present the general steps in order to decide if a set of possibilistic literals is a possibilistic answer set. Let M be a set of possibilistic literals and P be a possibilistic logic program³.

1. The first step is to verify that M must satisfy that M^* is an answer set of P^* . $*$ is a projection which removes all the possibilistic quantifications of any set of possibilistic literals and possibilistic clauses. For instance, $\{(a, \text{certain}), (b, \text{maybe})\}^* = \{a, b\}$ and $\{(\text{certain} : \text{contrary}(F, \text{neg}(F))), (\text{certain} : \text{contrary}(\text{neg}(F), F))\}^* = \{\text{contrary}(F, \text{neg}(F)), \text{contrary}(\text{neg}(F), F)\}$. Hence, if M is a set of possibilistic literals and P a possibilistic programs, then M^* is a standard set of literals and P^* is a standard logic program.
2. The second step is to reduce the program P by M . The reduced program P^M will be a possibilistic positive logic program, this means that P^M does not have possibilistic clauses which have negative literals in their bodies⁴.
3. The third and last step is to apply the operator T to P^M in order to compute the fix point $\Pi(P^M)$. $\Pi(P^M)$ will suggest a set of possibilistic literals M' . If M' is equal to M , we will say that M is a possibilistic answer set of P .

As we can see the possibilistic answer sets have a strong relation with the common answer sets. In fact, we can observe in the point one, that M^* is an answer set of P^* . By the moment, we do not have a possibilistic answer set solver. However, we have used common answer set solvers for our experiments. For instance, the reader can find a small implementation of our medical scenario in (<http://www.lsi.upc.edu/~jcnieves/>). This implementation is based on the answer set solver SMODELS[10]. In this implementation, we have a concrete implementation of the domain independent part of our mapping and present some mappings from effect propositions to logic program.

Due to lack of space, we can not discuss extensively the generation of plans of actions from our possibilistic action language. However let us consider again our medical scenario in order to illustrate a single plan of action.

³For more details of the possibilistic answer set semantics' definition see [5].

⁴Let l be a literal. *not l* is called negative literal.

First let Φ be a specification in \mathcal{A}^{Poss} which describes our medical scenario. Therefore let Π be the possibilistic logic program which we get from Φ by mapping it to possibilistic logic programs. Hence, in order to infer a possible plan of actions for our medical scenario we have to compute the answer sets of Π^* .

In order to get a plant of actions in two steps, we fix the constant *length* to 2. Remember that *length* is a constant in the encoding of the domain independent part. For the conditions that were described in this paper, the program Π^* will have just one answer set which is:

$$\text{ASP}(\Pi^*) = \{ \text{holds}(\text{cs(zero_urgency)}, 1), \text{holds}(\text{inf(not_present)}, 1), \\ \text{holds}(\text{o(terminal_insufficient_function)}, 1), \text{holds}(\text{cs(stable)}, 2), \\ \text{holds}(\text{o(good_graft_function)}, 2), \text{holds}(\text{inf(present)}, 2), \\ \text{cause}(\text{transplant}, \text{o(good_graft_function)}, 2), \text{occurs}(\text{transplant}, 1) \}^5$$

First of all, we have to remember that our initial states of our fluents are:

$$\begin{aligned} \text{certain : } & \text{initially}(\text{CS}(0_urgency)). \\ \text{certain : } & \text{initially}(\text{inf(not_present)}). \\ \text{certain : } & \text{initially}(\text{O(terminal_insufficient_function)}). \end{aligned}$$

This situation is reflected in $\text{ASP}(\Pi^*)$ by the atoms: $\text{holds}(\text{cs(zero_urgency)}, 1)$, $\text{holds}(\text{inf(not_present)}, 1)$, $\text{holds}(\text{o(terminal_insufficient_function)}, 1)$.

Now our goal conditions are:

$$\begin{aligned} \text{certain : } & \text{finally}(\text{CS(stable)}). \\ \text{certain : } & \text{finally}(\text{O(normal_graft_function)}). \end{aligned}$$

These conditions are reflected in $\text{ASP}(\Pi^*)$ by the atoms: $\text{holds}(\text{o(good_graft_function)}, 2)$, $\text{cause}(\text{wait}, \text{cs(dead)}, 2)$. It is clear that the goal conditions are satisfied, but which actions are applied for satisfying the goal conditions? These actions are suggested by the predicate *occurs*. Notice that $\text{occurs}(\text{transplant}, 1)$ belongs to $\text{ASP}(\Pi^*)$. Therefore the action *organ transplantation* is applied for satisfying the goal conditions.

We accept that this example is really simple, however it is enough for illustrating that the plans of actions are inferred directly by the the possibilistic answer sets of the program Π .

4. Conclusions

We are interested in developing a decision support system in the medical domain. We have observed that one of the main challenges is to identify a specification language in order to capture uncertain and incomplete information. The literature suggests that probability theory is not always a good option for supporting medical decision making [3].

In this paper, we introduce a possibilistic action language \mathcal{A}^{Poss} in order to capture natural specifications from medical specialists. In order to be friendly with medical experts, \mathcal{A}^{Poss} has a simple English-like syntax to express the effects of actions on a world. Moreover, we present a mapping from \mathcal{A}^{Poss} 's syntax into possibilistic programs in order to formulate planning using possibilistic answer sets.

⁵We are listing the atoms which are relevant for our example.

Acknowledgements

We are grateful to anonymous referees for their useful comments. J.C. Nieves wants to thank CONACyT for his PhD Grant. J.C. Nieves and U. Cortés were partially supported by the grant FP6-IST-002307 (ASPIC). The views expressed in this paper are not necessarily those of ASPIC consortium.

References

- [1] John Fox and Subrata Das. *Safe and Sound: Artificial Intelligence in Hazardous Applications*. AAAI Press/ The MIT Press, 2000.
- [2] Antonio López-Navidad and Francisco Caballero. Extended criteria for organ acceptance: Strategies for achieving organ safety and for increasing organ pool. *Clinical Transplantation, Blackwell Munksgaard*, 17:308–324, 2003.
- [3] Peter Szolovits. *Artificial Intelligence and Medicine*. Westview Press, Boulder, Colorado, 1982.
- [4] Amos Tversky and Daniel Kahneman. *Judgment under uncertainty:Heuristics and biases*, chapter Judgment under uncertainty:Heuristics and biases, pages 3–20. Cambridge Univertisy Press, 1982.
- [5] Juan Carlos Nieves, Mauricio Osorio, and Ulises Cortés. Semantics for possibilistic disjunctive programs. In Gerhard Brewka Chitta Baral and John Schlipf, editors, *Ninth International Conference on Logic Programming and Nonmonotonic Reasoning (LPNMR-07)*, number 4483 in LNAI, pages 315–320. Springer-Verlag, 2007.
- [6] Michael Gelfond and Vladimir Lifschitz. Representing Action and Change by logic programs. *Journal of Logic Programming*, 17(2,3,4):301, 323 1993.
- [7] Chitta Baral. *Knowledge Representation, Reasoning and Declarative Problem Solving*. Cambridge University Press, Cambridge, 2003.
- [8] Stefan Brass and Jürgen Dix. Semantics of (Disjunctive) Logic Programs Based on Partial Evaluation. *Journal of Logic Programming*, 38(3):167–213, 1999.
- [9] Didier Dubois, Jérôme Lang, and Henri Prade. Possibilistic logic. In Dov Gabbay, Christopher J. Hogger, and J. A. Robinson, editors, *Handbook of Logic in Artificial Intelligence and Logic Programming, Volume 3: Nonmonotonic Reasoning and Uncertain Reasoning*, pages 439–513. Oxford University Press, Oxford, 1994.
- [10] System SMODELS. Helsinki University of Technology. <http://www.tcs.hut.fi/Software/smodels/>, 1995.

Ranking Features by means of a Qualitative Optimisation Process

Mónica SÁNCHEZ,^{a,1} Yu-Chiang HU^b Francesc PRATS^a Xari ROVIRA,^c
Josep M. SAYERAS,^c and John DAWSON^{c,d}

^a*Universitat Politècnica de Catalunya, Barcelona, Spain*

^b*University of Monaco, Monaco*

^c*ESADE, Universitat Ramon Llull, Barcelona, Spain*

^d*University of Edinburgh, United Kingdom*

Abstract. A set of qualitative measures describing a retail firm is considered. A qualitative ranking process of these features based on the managers' evaluations is presented. In a decision making context, this paper proposes a methodology to synthesise information given by ordinal data. Features are evaluated by each manager on an ordinal scale with different levels of precision and from two points of view: importance of the measure and performance on the measure. A representation for the different evaluations by means of k -dimensional qualitative orders of magnitude labels is proposed. The presented methodology deals with these evaluations to obtain two rankings based on comparing distances against a reference k -dimensional label. The final ranking of features with respect to their importance will help the managers to make decisions to improve the performance.

Keywords. Qualitative reasoning, Group decision-making, Goal programming

1. Introduction

How do people decide? The decision making process has an enormous importance in today's world. This paper contributes to this field with a new approach consisting of an optimization process for ranking a set of evaluated features. How can the information coming from people thoughts be processed in order to make decisions? How can data be treated in order to be useful? The objective of this paper is to prioritize a set of features that have been evaluated by different people. In the real case presented, features are expressed as measures to describe the performance of the firm. The optimization method presented is particularly suitable when aiming at a ranking from qualitative ordinal descriptions.

The starting point is the representation of the initial evaluations of each feature via a k -dimensional qualitative label, consisting, in our example, of the k expert managers evaluations, which can be seen as a hyper-rectangle, being k the number of evaluators. Evaluations are synthesized by means of the distance to a reference k -dimensional label. This is the hyper-rectangle given by the supreme of the sets of evaluations of each feature.

¹MA2, Edifici Omega, Campus Nord, UPC, Jordi Girona 1,3. 08034 Barcelona, Spain. Tel.: +34 934 137 680; Fax: +34 934 137 701; E-mail: monica.sanchez@upc.edu.

The distances between evaluations and their supreme give the ranking of features directly. This method is a qualitative generalization of a type of goal programming method known as the reference point method for vectorial optimization and decision-making support [Gonza, 2001, Kallio, 1980].

The application in this paper starts with the information provided by 84 expert managers about 44 features describing a retailer firm. This information has to be synthesized to make it useful in a decision-making process. Managers evaluate each feature, on the one hand, with respect to its importance for the success of the firm, and, on the other hand, with respect to current performance.

In the evaluation of the measure, a four-point Likert scale is used [Likert, 1932]. A Likert scale is the most widely type of response scale used in survey research. The respondent is asked to indicate his subjective evaluation of the statement. Scales for both importance and performance are described as follows: Codes for importance go from 1=Absolutely Important to 4=Not Very Important, and codes for performance go from 1=Extremely Good to 4=Not Very Good. In this paper, a process of qualitative optimization leads to two different rankings of the features using this information as the starting point. Both importance and performance rankings are carried out by using the same methodology. The two obtained rankings will allow measuring the difference between the importance of features and their current performance. This, in turn, gives an idea of the direction and the order of magnitude of the necessary economic efforts to improve the performance.

Section 2 presents the qualitative models of absolute orders of magnitude, and Section 3 provides a qualitative representation of features in a partially-ordered set. Section 4 introduces the ranking process by defining a total order in the set of features in such a way that the set of labels corresponding to the features becomes a chain (ranking). After the theoretic development of the methodology presented, in Section 5, the application to a real case corresponding to a retail firm is given. Lastly, conclusions and open problems are presented.

2. The Orders of Magnitude Space OM(n)

The one-dimensional absolute orders of magnitude model [Trave, 2003] works with a finite number of qualitative labels corresponding to an ordinal scale of measurement. The number of labels chosen to describe a real problem is not fixed, but depends on the characteristics of each represented variable.

Let's consider an ordered finite set of *basic* labels $S_* = \{B_1, \dots, B_n\}$, each one of them corresponding to a linguistic term, in such a way that $B_1 < \dots < B_n$, as, for instance, "very bad" < "bad" < "acceptable" < "good" < "very good". The complete universe of description for the Orders of Magnitude Space OM(n) is the set $S = S_* \cup \{[B_i, B_j] \mid B_i, B_j \in S_*, i < j\}$, where the label $[B_i, B_j]$ with $i < j$ is defined as the set $\{B_i, B_{i+1}, \dots, B_j\}$.

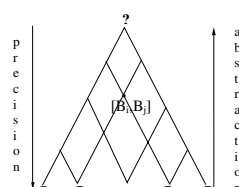


Figure 1: The complete universe of description

The order in the set of basic labels \mathbb{S}_* induces a partial order \leq in \mathbb{S} defined as: $[B_i, B_j] \leq [B_r, B_s] \iff B_i \leq B_r$ and $B_j \leq B_s$, with the convention $[B_i, B_i] = \{B_i\} = B_i$. This relation is trivially an order relation in \mathbb{S} , but a partial order, since there are pairs of non-comparable labels.

Moreover, there is another partial order relation \leq_P in \mathbb{S} “to be more precise than”, given $(X \leq_P Y)$ if $X \subset Y$. The less precise label is $? = [B_1, B_n]$.

3. k -Dimensional Labels

In the proposed ranking problem, each feature is characterized by the judgments of k evaluators, and these evaluations are given by means of qualitative labels belonging to an orders of magnitude space. So, each feature is represented by a k -dimensional label, that is to say, a k -tuple of labels.

Let \mathbb{S} be the orders of magnitude space with the set of basic labels \mathbb{S}_* .

The set of k -dimensional labels or features’ representations \mathbb{E} is defined as:

$$\mathbb{E} = \mathbb{S} \times \dots \times \mathbb{S} == \{(E_1, \dots, E_k) \mid E_i \in \mathbb{S} \forall i = 1, \dots, k\}. \quad (1)$$

Each k -dimensional label $\mathbf{E} = (E_1, \dots, E_k)$ is a set of k qualitative labels (each one associated to an employee evaluation) that define a feature in such a way that, on every component, the relation $E_r \leq E_s$ means that E_s represents better results than E_r .

This order in \mathbb{S} is extended to the Cartesian product \mathbb{E} :

$$\mathbf{E} = (E_1, \dots, E_k) \leq \mathbf{E}' = (E'_1, \dots, E'_k) \iff E_i \leq E'_i, \forall i = 1, \dots, k. \quad (2)$$

$\mathbf{E} < \mathbf{E}'$, that is to say, $\mathbf{E} \leq \mathbf{E}'$ and $\mathbf{E} \neq \mathbf{E}'$, means that feature \mathbf{E}' is better than feature \mathbf{E} .

This order relation in \mathbb{E} is partial, since there are pairs of non-comparable k -dimensional labels (see figure 2).

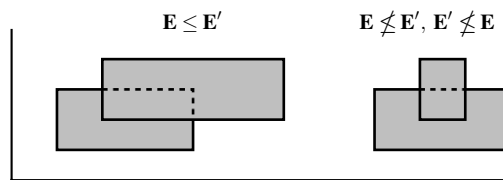


Figure 2: The partial order \leq in \mathbb{E}

4. The Ranking Process

The proposed method for ranking the existing features consists in:

1. Fixing a distance d in \mathbb{E} .
2. Building a reference label $\tilde{\mathbf{E}}$; a proposition of consistency determines that it has to be the supreme, with respect to the order \leq , of the set of features which are to be ranked.

3. Assigning to each k -dimensional label \mathbf{E} the value $d(\mathbf{E}, \tilde{\mathbf{E}})$; so, the features will be totally ordered as a chain.
4. This chain giving the ranking of the features directly.
5. After this process, if a subset of the features is at the same distance to $\tilde{\mathbf{E}}$, the same algorithm being applied to this set, just beginning at the second point.

These steps are developed below.

4.1. A Distance between k -Dimensional Labels

A method for computing distances between k -dimensional labels is presented.

The first step involves codifying the labels in \mathbb{S} by a location function [Agell et al, 2006]. Through this function, each element $E_h = [B_i, B_j]$ in \mathbb{S} is codified by a pair $(l_1(E_h), l_2(E_h))$ of integers: $l_1(E_h)$ is the opposite of the number of basic elements in \mathbb{S}_* that are “between” B_1 and B_i , that is to say, $l_1(E_h) = -(i-1)$, and $l_2(E_h)$ is the number of basic elements in \mathbb{S}_* that are “between” B_j and B_n , i.e., $l_2(E_h) = n - j$. This pair of numbers permits each element in \mathbb{S} , where all different levels of precision are considered, to be “located”.

This “location” can be extended to any feature defined by k orders of magnitude labels; the extension to the set of k -dimensional labels \mathbb{E} is:

$$L(E_1, \dots, E_k) = (l_1(E_1), l_2(E_1), \dots, l_1(E_k), l_2(E_k)) \quad (3)$$

which provides the relative position of a k -tuple of qualitative labels with respect to the basis of \mathbb{E} .

Then, a distance d between labels \mathbf{E}, \mathbf{E}' in \mathbb{S} is defined via any metric R in \mathbb{R}^{2k} and their codifications:

$$d(\mathbf{E}, \mathbf{E}') = d((E_1, \dots, E_k), (E'_1, \dots, E'_k)) = \sqrt{(L(\mathbf{E}) - L(\mathbf{E}'))^t R (L(\mathbf{E}) - L(\mathbf{E}'))} \quad (4)$$

This function inherits all properties of the distance in \mathbb{R}^{2k} . In section 5, in the application of the presented methodology to a retail firm, the metric R considered is the Euclidean distance.

4.2. Ranking the Set of Features

Starting from the distance d in \mathbb{E} and a reference k -dimensional label $\tilde{\mathbf{E}}$, a total order \trianglelefteq will be defined in \mathbb{E} , in such a way that the set of labels $\mathbf{E}^1, \dots, \mathbf{E}'$ corresponding to the available features becomes a chain $\mathbf{E}^{i_1} \trianglelefteq \dots \trianglelefteq \mathbf{E}^{i_l}$, and so a ranking of the features is established.

4.2.1. A Total Order in \mathbb{E}

Let $\tilde{\mathbf{E}} \in \mathbb{E}$ be a k -dimensional label and let us call it the reference label. Let d be the distance defined in \mathbb{E} in Section 4.1. Then the following binary relation in \mathbb{E} :

$$\mathbf{E} \trianglelefteq \mathbf{E}' \iff d(\mathbf{E}', \tilde{\mathbf{E}}) \leq d(\mathbf{E}, \tilde{\mathbf{E}}) \quad (5)$$

is a pre-order, i.e., it is reflexive and transitive.

This pre-order relation induces an equivalence relation \equiv in \mathbb{E} by means of:

$$\mathbf{E} \equiv \mathbf{E}' \iff [\mathbf{E} \preceq \mathbf{E}', \mathbf{E}' \preceq \mathbf{E}] \iff d(\mathbf{E}', \tilde{\mathbf{E}}) = d(\mathbf{E}, \tilde{\mathbf{E}}). \quad (6)$$

Then, in the quotient set \mathbb{E}/\equiv the following relation between equivalence classes:

$$\text{class}(\mathbf{E}) \trianglelefteq \text{class}(\mathbf{E}') \iff \mathbf{E} \preceq \mathbf{E}' \iff d(\mathbf{E}', \tilde{\mathbf{E}}) \leq d(\mathbf{E}, \tilde{\mathbf{E}}) \quad (7)$$

is an order relation. It is trivially a total order.

In this way, given a set of features $\mathbf{E}^1, \dots, \mathbf{E}^l$, these can be ordered as a chain with respect to their proximity to the reference label: $\text{class}(\mathbf{E}^{i_1}) \trianglelefteq \dots \trianglelefteq \text{class}(\mathbf{E}^{i_l})$.

If each class $(\mathbf{E}^{i_j}), j = 1, \dots, l$, contains only the label \mathbf{E}^{i_j} , the process is finished and we obtain the ranking $\mathbf{E}^{i_1} \trianglelefteq \dots \trianglelefteq \mathbf{E}^{i_l}$. If there is some class (\mathbf{E}^{i_j}) with more than one label, then the same process is applied to the set of the labels belonging to class (\mathbf{E}^{i_j}) , and continued until the final ranking $\mathbf{E}^{m_1} \trianglelefteq \dots \trianglelefteq \mathbf{E}^{m_l}$ is obtained.

4.2.2. Consistency of the Ranking Method

The method of ranking via a distance to a reference label previously selected is really necessary when the order relation \leq does not provide a total order in the set of available features.

When the set $\{\mathbf{E}^1, \dots, \mathbf{E}^l\}$ is totally ordered with respect to \leq , that is to say, when a priori the features are already ranked $\mathbf{E}^{i_1} \leq \dots \leq \mathbf{E}^{i_l}$, then the proposed method (via choosing of a suitable reference label) has to reproduce the same ranking. This means that the method has to be *consistent*.

Formally, the method will be consistent if the reference label $\tilde{\mathbf{E}}$ is selected in such a way that:

$$(\forall \mathbf{E}^1, \dots, \mathbf{E}^l \in \mathbb{E}) (\mathbf{E}^1 \leq \dots \leq \mathbf{E}^l \implies \mathbf{E}^1 \trianglelefteq \dots \trianglelefteq \mathbf{E}^l) \quad (8)$$

This requirement is equivalent to the following:

$$(\forall \mathbf{E}, \mathbf{E}' \in \mathbb{E}) (\mathbf{E} \leq \mathbf{E}' \implies \mathbf{E} \trianglelefteq \mathbf{E}') \quad (9)$$

In effect, $(8) \implies (9)$ is obvious. Reciprocally, if (9) is satisfied, then when $\mathbf{E}^1 \leq \dots \leq \mathbf{E}^l$ it suffices to apply (9) to each pair $\mathbf{E}^i \leq \mathbf{E}^{i+1}$.

Before establishing the way of choosing the reference label $\tilde{\mathbf{E}}$, in order for property of consistency to be accomplished, let us compute the supreme of a set of hyperrectangles with respect to the partial order \leq introduced in Section 3.

Given any $\mathbf{E}^1, \dots, \mathbf{E}^l$, let \mathbf{E}^{sup} be the supreme of the set $\{\mathbf{E}^1, \dots, \mathbf{E}^l\}$, i.e., the minimum label in \mathbb{E} which satisfies $\mathbf{E}^i \leq \mathbf{E}^{\text{sup}}, i = 1, \dots, l$.

Its computation is as follows:

Let $\mathbf{E}^r = (E_1^r, \dots, E_k^r)$, with $E_h^r = [B_{i_h}^r, B_{j_h}^r]$ for all $h = 1, \dots, k$, and for all $r = 1, \dots, l$. Then

$$\mathbf{E}^{\text{sup}} = \sup\{\mathbf{E}^1, \dots, \mathbf{E}^l\} = (\tilde{E}_1, \dots, \tilde{E}_k),$$

where

$$\tilde{E}_h = [\max\{B_{i_h}^1, \dots, B_{i_h}^l\}, \max\{B_{j_h}^1, \dots, B_{j_h}^l\}], \quad (10)$$

(see Figure 3).

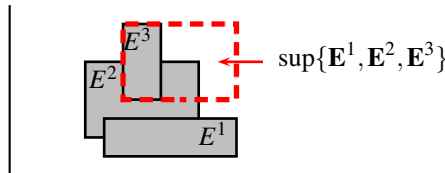


Figure 3: The supreme of a set $\{E^1, \dots, E^l\}$

Proposition 3 (of consistency) The ranking method is consistent in the above sense if and only if, for any set of features E^1, \dots, E^l , the reference label \tilde{E} is chosen as the supreme of the set $\{E^1, \dots, E^l\}$.

Proof. If the label associated to any set of labels is its supreme, statement (10) is trivial, because if $E \leq E'$ then $E' = \sup\{E, E'\} = \tilde{E}$ and $d(E', \tilde{E}) = 0 \leq d(E, \tilde{E})$, that is to say, $E \trianglelefteq E'$.

To prove that it is necessary to choose the supreme to assure the consistency, it suffices to present as a counterexample of (10) the case in which \tilde{E} is not the supreme. The easiest of these consists of the pair E, E' , with $E \leq E'$ and $\tilde{E} = E$. It is clear that $E \not\trianglelefteq E'$.

5. An Application to Improving Performance of a Retailer Firm

The previous methodology is applied to the set of 44 features of a retailer firm. These features will be prioritized taking into account two different criteria included in the information provided. The perceived performance of the firm in relation with each feature, and the perceived importance of the features have been given by 84 managers. The methodology has been applied to the two sets of data, and therefore two rankings are obtained.

The two obtained rankings can be compared to help managers to make decisions to improve the performance of the firm. Measuring the difference between the importance of features and their current performance gives an idea of the direction and the order of magnitude of the necessary economic efforts to improve the performance. Moreover, the analysis of the rankings can help managers to decide about the direction of these efforts.

5.1. Description of Data

Using literature sources and 25 in-depth interviews with retail stakeholders, 170 performance related variables were identified.

Resource area	Resource concept	Measure evaluated
Physical Resource	Reach Ability	1. Number of customer visits 2. Store location
Legal Resource	Brand Strength Strength	3. The sales of private brand products 4. Social responsibility
Human Resource	Human Management	5. Turnover 6. Staff training
Organizational Resources	Expansion Ability Productivity	7. Franchise system 8. Store opening strategy 9. Sales per store 10. Spend-per-visit rate
	General Management	11. Internal procedures
	Technology Management	12. Achievement of year-end goals
	Management	13. Investments in technology development
	Organizational Management	14. Quality of data collection and process system
	Management	15. Empowerment
	Inventory Management	16. The listening ability of management
	Marketing Management	17. Loss control
	Financial Management	18. Inventory service level
	Product Innovation	19. Market positioning
	Innovation	20. Store renovation/redecoracion
	Loan Repay Ability	21. Cost control ability
	Diversification	22. Percentage of part-time staff 23. Shelf-life of new products 24. The speed of new products development 25. Past credit history 26. Stockholder's background 27. Capital expenditures in internet channel 28. Maintaining target customer in market diversification
	Market Segment	29. Following fashion trends
	Risk	30. Facing seasonal demands
	Strategic Vision	31. Openness to criticism 32. Willingness to innovate
Relational Resources	Stakeholder Relations	33. Customer complaints management 34. Cost sharing with suppliers on promotions 35. Joint venture opportunity
External Factors	The Actions from Outside Stakeholders	36. Changes in customer's preferences 37. Changes in supplier's contract content 38. The innovation and imitation from competitors
	Political Environmental	39. Change in government laws 40. Stability of government
	Technological Environmental	41. Innovation of new technology equipment 42. New management system software development
	Socio-culture Environmental	43. Change of population structure 44. Change of lifestyle

Table 1. The 44 features considered

This extensive list was further reviewed in terms of the nature of the resource (legal, organizational, informational, human, etc) to which the variable referred and 44 were identified as main performance variables. Details of the process of defining these variables are provided in [Hu et al, 2007] and measures evaluated are listed in table 1. A two

part questionnaire was designed incorporating the 44 variables. The first part of the survey instrument sought from respondents an evaluation of the importance of each measure to the performance of the firm. The second part of the instrument sought an evaluation of the level of performance of the firm in respect of each measure. The perceptions of managers, thus, were collected on the relative importance of the various items and the performance on these items. The managers, all in executive positions, were considered as having expert knowledge. The survey was implemented in a major retail firm in Taiwan and data from 84 expert managers were collected.

The 44 features considered in this study are in Table 1 as they relate to the resource bases of the firm.

Evaluations in both cases are given in Likert scales of four points. Codes for importance and codes for performance go from:

Code	Importance	Performance
1	Absolutely Important	Extremely Good (or Extremely Strong)
2	Very important	Very Good (or Very Strong)
3	Moderately Important	Moderately Good (or Moderately Strong)
4	Not Very Important	Not Very Good (or Not Very Strong)
5	Don't Know (identified as missing value)	Don't Know (identified as missing)

Table 2. Codes for importance and performance

Representing data in a one-dimensional absolute orders of magnitude model of granularity 4: OM(4), the code 5 would be interpreted as "the less precise label" that is ?.

5.2. Experiment and Results

The two sets of data have been ranked using the described optimization process and results are compared. Ranking for importance allows the n features to be codified from 1 to n from the most important to the least (note that this is the inverse of the order considered in section 3). Ranking for performance contains the code-numbers of features from the one with a best performance to the one with the worst. Duple are represented by a scatter diagram. It is a graph depicting how measures are related to each other (see Figure 4). Points in the diagonal are features with the same perceived importance and perceived performance; those far above from the diagonal are features ranked with high importance and a low performance. And so, they are the ones that have to be taken into account to improve the performance of the firm.

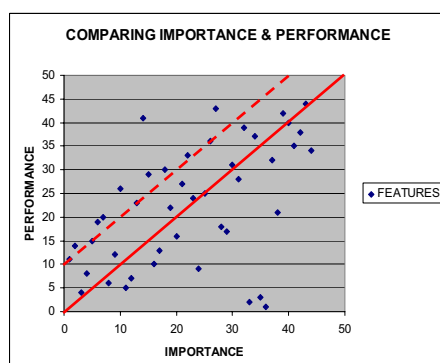


Figure 4: Comparing Importance and Performance.

Observing the position of each feature in the graph, those located far above the diagonal corresponds to features that have a mismatch between importance and performance in a negative sense because they are perceived as important but with a low performance. Nine of these features have been selected and listed in the following table:

Resource area	Features	Ranking of importance	Ranking of performance
Physical	Number of customer visits	2	14
Organizational	Sales per store	6	19
	Store opening strategy	7	20
	Franchise system	10	26
Human	Staff training	14	41
Organizational	Quality of data collection and process system	15	29
External Factors	Innovation of new technology equipment	18	30
	Change in government laws	22	33
Organizational	The listening ability of management	27	43

Table 3. Selected Features

These are the features where the perceived importance is high while the perceived performance of the firm is notably lower. These therefore can be considered as key areas for managerial action to address the perceived underperformance of the firm. Given this information policies can be implemented to address these deficiencies and the data collected again after a period to evaluate the extent to which policies have been effective and how performance on perceived important measures has changed.

The dots line can be seen as a soft margin that can be considered near or far away from the diagonal depending on the specific situation of the treated problem. Moreover, in that case, the investment capacity and the general strategy of the firm would have to be also taken into account.

It is also possible to consider items where performance is high but importance is low. It is these areas where the resource input could be considered and a view taken on whether too much resource is being applied to these areas of lesser importance. Therefore, a new dots line would have to be placed as far as necessary under the diagonal in the scatter plot. Points out of the band between dots lines are suitable to be considered to balance managerial policies.

6. Conclusion and Future Research

This paper proposes a methodology that synthesizes evaluations given by an experts' committee. Evaluations are considered in an ordinal scale, for this reason a set of labels describing orders of magnitude is considered. A group decision method is given in order to rank the features based on comparing distances to a reference k-dimensional label. The methodology presented allows, on the one hand, the ordinal information given by experts on the specific application to be handled without previous normalisation, and, on the other, the methods of "goal programming" to be generalised without the need for previous knowledge of the ideal goal.

The results applied to a real case show the applicability of the methodology. In the application a group of managers evaluating a set of features with respect to the perceived importance they have for the firm and, at the same time, with respect to the perceived per-

formance. It is important to point out that the methodology presented allows imprecision in the evaluations given by the managers to be considered.

The optimization process gives two rankings, for both importance and performance, of the features, and then they can be compared to help the manager to improve the firm.

As a future work the design of an automatic system to perform the decision process described will be implemented. The data from the survey of expert managers will be analysed in more detail by considering the specific managerial expertise of the managers in the survey. The expert managers work in different departments of the firm (accounting and finance, marketing, operations and store development, R&D, etc). As such they have different knowledge bases. It is proposed to employ the technique described in this paper to compare the perceptions of managers from the different departments to gain a better understanding of how the overall performance of the firm is evaluated.

Acknowledgements

This research has been partially supported by the AURA research project (TIN2005-08873-C02-01 and TIN2005-08873-C02-02), funded by the Spanish Ministry of Science and Information Technology.

References

- [Agell et al, 2006] Agell, N., Sánchez, M., Prats, F. & Rovira, X., 2006. Using Orders of Magnitude in Multi-attribute Decision-making. In *Proc. of the 20th International Workshop on Qualitative Reasoning . Hanover; New Hampshire, 15-19.*
- [Gonza, 2001] González Pachón, J. & Romero López, C., 2001. "Aggregation of Partial Ordinal Rankings. An Interval Goal Programming Approach". *Computers and Operations Research*. 28, 827-834.
- [Hu et al, 2007] Hu,Y.C., Dawson, J. & Ansell, J., 2007. "A framework for retail performance measurement: an application of resource advantage theory of competition". *Working paper series, School of Management and Economics, the University of Edimburgh.*
- [Likert, 1932] Likert, Rensis, 1932, "A Technique for the Measurement of Attitudes". *Archives of Psychology*. 140: pp. 1-55.
- [Kallio, 1980] Kallio, M., Lewandowski, A. & Orchard-Hays, W., 1980. An Implementation of the Reference Point Approach for Multi-Objective Optimization. In *WP-80-35, IIASA, Luxemburg.*
- [Keeney, 1993] Keeney, R.L. & Raiffa, H., 1993. *Decisions with multiple objectives preferences and value trade-offs*. Cambridge University Press.
- [Romero, 2001] Romero López, C., 2001. Extended Lexicographic Goal Programming: A Unifying Approach. *The International Journal of Management Science*, 29, 63-71.
- [Romero et al, 2001] Romero López, C., Tamiz, M. & Jones, D., 2001. Comments on Goal Programming, Pompromise Programming and Reference Point Method Formulations: Linkages and Utility Interpretations-A Reply. *Journal of the Operational Research Society*, 52, 962-965.
- [Trave, 2003] Travé-Massuyès, L. & Dague, P., 2003. *Modèles et raisonnements qualitatifs*. Ed. Lavoisier, Hermes Science, Paris, France.
- [Wier, 1980] Wierzbicki, A.P., 1980. The Use of Reference Objectives in Multiobjective Optimization. In *G. Fandel, T. Gal (eds.): Multiple Criteria Decision Making, Theory and Applications, Lecture Notes in Economic and Mathematical Systems. 177 Springer-Verlag, Berlin- Heidelberg*, 468-486.

This page intentionally left blank

Robotics

This page intentionally left blank

Tactical Modularity in Cognitive Systems

Cecilio Angulo^{a,1}, Ricardo A. Téllez^b and Diego E. Pardo^a

^aGREC - Knowledge Engineering Research Group

UPC - Technical University of Catalonia

^bPAL Technology Robotics

Abstract. Novel theories have recently been proposed to try to explain higher cognitive functions as internal representations of action and perception of an embodied autonomous agent in a situated environment. A new paradigm based on tactical modularity have been developed using neural evolutionary robotics in the form of modules, called intelligent hardware units (IHUs). The new concept of a collaborative control architecture allows the construction of a behavior-based system as a result of interactions between the control system and both the external and internal environments generated by the modules. The full separation achieved between the inner world of the autonomous agent and the real external world gives some insight into how the mind–body problem can be solved. An experiment on a two-sensor, two-motor simulated robot orbiting around an object illustrates the performance of the proposed paradigm and lead to discussion of concepts in the robot’s inner world.

Keywords. Embodied intelligence, Internal representations, Dynamical hypothesis, Collaborative control architecture, Robotics

1. Introduction

The study of cognitive systems for engineering purposes involves the creation of artificial systems that reliably exhibit some desired level of cognitive performance or behavior [4]. Traditional approaches during the 60-70s to modeling cognitive systems were computational [5], based on concepts of the theory of computation. Cybernetics preceded and has much in common with cognitive science, but it has not had much impact on it. Recently, the dynamical systems theory have been proposed as an alternative for handling cognition [15]. Opposed to the dominant *computational hypothesis* claiming that cognitive agents are digital computers, the *dynamical hypothesis* considers cognitive agents as dynamical systems that can be understood dynamically. Hence, much of the current work in embodied cognitive science is in a sense returning to its cybernetic roots [17], focusing on agent–environment interaction and bodily and sensorimotor mechanisms [3].

Novel theories have recently been proposed that try to explain higher cognitive functions as *internal simulations* of action and perception of an embodied autonomous agent in a situated environment, leading to a different vision from the former contrasting frameworks. Modularization is accepted as the most naturally occurring structure able to exhibit complex behaviors from a network of individually simple components, which

¹Correspondence to: Cecilio Angulo, Rambla de l’Exposició s/n., E-08800 Vilanova i la Geltrú, Spain. Tel.: +34 938967798; Fax: +34 938967700; E-mail: cecilio.angulo@upc.edu.

interact with each other in relatively simple ways. Collaborative elements are usually information-processing *software* units, such as neurons, or dynamically *simulated* entities, such as bees with swarm intelligence, so that the coordinated behavior of the group *emerges* from the interaction of these simple agent behaviors. The approach proposed is also based on simple collaborative information-processing components, albeit as close as possible to the *hardware* devices (sensors and actuators), called *intelligent hardware units* (IHUs), embodying a physical autonomous agent to design a new control architecture concept.

Robot control architectures are usually decomposed into a number of layers, each with access to sensors and motors, and each responsible for generating different levels of behavior, such as ‘collision avoidance’ or ‘map-making’, the so-called *subsumption architecture* (strategic concept). However, retaining some of the ideas of von Foerster’s work [16], by separating these functions from the totality of cognitive processes, the original problem is abandoned and transformed to a search for mechanisms that implement entirely different functions.

We demonstrate in this article that a modular architecture based on IHUs (tactical concept) allows us the emergence of behaviors as a result of the interactions of a collaborative control system with both the external and internal environments in that it implements the von Foerster concept of *double closure*: an embodied agent can be *autonomous* and *organizationally closed*, but at the same time *structurally coupled* to the environment it is situated in, which in the constructivist sense is its own *invented reality*. Hence, the architecture obtained is not based on internal models trying to exactly model the environment, but the internal model that emerges invents a reality based on interaction with the environment that is useful for reaching the proposed goals.

In the next section, tactical and strategic modular concepts are introduced for autonomous agent control, with IHUs proposed as possible modules for implementation of tactical modularity. Section 3 discusses the new paradigm and shows, using a control engineering discourse, how this tactical approach allows us the generation of a truly inner world with internal representations of perception. The full separation achieved between the inner world of the autonomous agent and its external real world provides some insight into how the mind–body problem can be solved. A simple experiment on a two-input, two-output simulated robot and experiments for the generation of walking gaits on the Aibo robot, a complex task in a complex environment, illustrate the performance of the proposed paradigm. Finally, some conclusions and proposals for further research conclude the article.

2. Collaborative Control Architecture: A Tactical Modular Concept

For the control of an artificial autonomous physical agent, sensory information must be obtained through sensors. This information must then be processed and used to guide the actions of the agent so that it can perform the task in question. When the number of sensors is large and the task at hand is complex, difficulties arise on how to integrate all the sensory information in order to guide the action [1]. We propose modularization at the level of sensors and actuators to solve this problem.

In the design of modular neural controllers, most tasks have been influenced by the mixture of experts of Jacobs et al. [7]. Their basic idea was to design a system composed

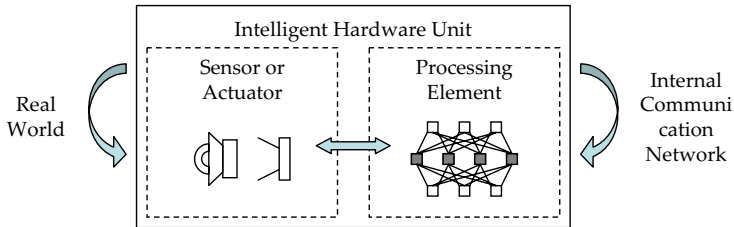


Figure 1. Schematic diagram of an IHU.

of several networks, each of which handles a subset of the complete set of cases required to solve the problem. Their system has been widely used and improved upon by several authors in different classification problems [12,10]. Even though all the studies were successful, it has been not reported how this type of neural controller could control more complex robots with a greater number of sensors and actuators [13].

We will define *strategic modularity* as the modular approach that identifies which sub-tasks are required for an autonomous agent in order to perform the global task. In contrast, we define *tactical modularity* as the approach that creates the sub-modules required to implement a given sub-task. In contrast to strategic modularity, tactical modularity must be implemented for each sub-task using the actual devices that make the robot act and sense, i.e., its sensors and actuators. In tactical modularity, subdivision is performed at the level of the physical elements actually involved in accomplishment of the sub-task. We are mainly interested in the reactive interpretation of the mind, and thus are concerned with behavior emergence rather than deliberative behavior. However, the use of one type of modularity is not in opposition to the use of the other type.

Once a sub-task has been determined for the robot, the tactical modularity concept is applied to implement the sub-task using the sensors and actuators at hand. Tactical modularity is implemented by designing a decentralized controller composed of small processing modules around each of the robot devices, called IHUs (Figure 1). Every IHU comprises a sensor or an actuator and an artificial neural network (ANN) that processes the information arising from the associated device: it receives sensor information, or it sends commands to the actuator. All the IHUs are interconnected to each other to be aware of what the other IHUs are doing. Each particular neural processor translates information received from the sensor (or from the network) to the network (or to the actuator).

Putting computational power at each sensor is not a new idea [1]. The novel approach presented here is the simultaneous introduction of computational power into each actuator that generates internal representations of the external world, and the design of a complete information-sharing network between all devices. The approach involves building simple but complete systems, rather than dealing with the complexity problem by dividing cognition in sub-domains.

Using a neuro-evolutionary algorithm, neural nets learn how to collaborate with each other and how to control associated elements, allowing the whole robot to perform the required sub-task [13].

3. Internal Representation of Perception: The Mind–Body Separation Problem

In this section, the proposed IHU-based tactical modular architecture is justified as a dynamical system approach to cognitive robotics using a control engineering perspective. Our aim is to demonstrate that the proposed network structure of IHUs provides the autonomous agent with an ‘inner world’ based on internal representations of perception rather than an explicit representational model, following the ideas of the double closure scheme of von Foerster. Hence, we are interested in building a simple but complete system rather than in dealing with the complexity problem by dividing cognition into sub-domains.

3.1. Control engineering perspective

Feedback is a simple control structure that considers the relationship between outputs and inputs in a plant. In a typical feedback control system, the *inner world* can be defined as the part of the control system corresponding to controller-based units. Similarly, the *outer world* would be defined as the part of the control system corresponding to process-based units, i.e., the physical world in which the autonomous agent is situated. From a basic control engineering perspective, so that the whole system reaches the set point (SP), the control elements (inner world) must be designed using a model as close as possible to the outer world, the so-called *process model*.

A particular element helping in understanding the concept is the role of the set point. The external SP must be translated to an internal SP based on the same units for the controller as for the inner world. For example, a thermostat translates external SPs from temperature units to voltage units in a range similar to that for the conditioner. It is usually assumed that this conditioning is known to the control engineer designing the control system, so sensors and actuators are considered as part of the process. However, when this knowledge is not available, unlike in traditional approaches, a learning procedure or adapting module must exist for designing or modifying the agent’s internal representations and intentionality. As observed in Figure 2, the internal translation of the external SP, which is selected according to the task, affects both control elements (conditioner and controller) in an unknown manner. The autonomous agent can be defined as the embodiment of *Me*, whereas the part of the autonomous agent that processes information is defined as the *Mind*: control is performed for three elements, the *conditioner*, the *controller* and the *translator*, all of which are directly affected by or affect the internal SP, i.e., the internal translation of the SP and not the real world SP. These elements comprising the mind of the autonomous agent are responsible for adapting the relationship between the autonomous agent (embodiment) and the environment (situation).

Broadly speaking, *Me* depends on the goal (goal-directed training) interpreted by the translator, on the environment (outer world) interpreted by the conditioner, and on the body (mind, sensor and actuator) acting through the controller. Hence, *Me* is based on the *Mind* (translator–conditioner–controller). Information from the environment is *mentally presented*, instead of *mentally represented*: there is no need, as in the traditional approach, to consider any accurate correspondence between the internal model and the real world via a process model. The internal model is built from interaction of the body with the environment; however, in contrast to Parisi [11], it does not try to exactly imitate the world, but is an interpretation of it [8]. The important point is that the agent’s view of

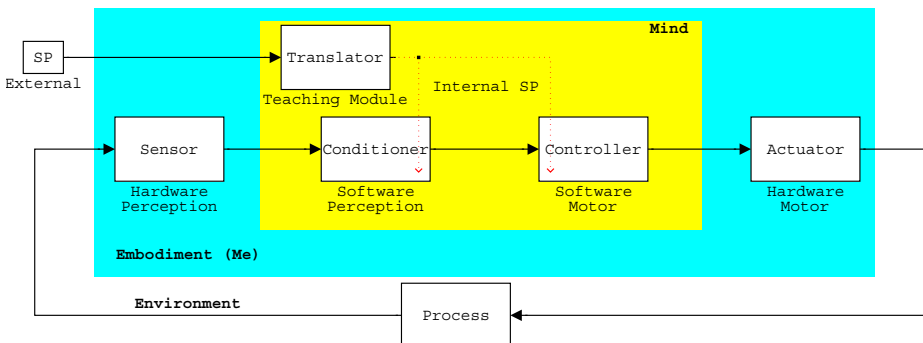


Figure 2. Mind is embodied in Me (the autonomous agent) and is situated in an environment (the process).

the outer world makes sense to the agent himself. Experience and information obtained from the world are therefore highly subjective.

3.2. Internal model: solving the ‘mind–body’ problem

From Figure 2 it is evident that sensor processes (hardware–software perception) and motor processes (software–hardware motion) are separated in Me. However, feedback from the outer world is not enough to achieve the von Foerster concept of *double closure*; perception and motion must be connected to each other in such a form that information has its origin in this creative circle. Motor stimuli must also be sent to the sensor elements to ‘predict’ what to sense upon real sensation in the outer world.

In terms of control engineering, an internal model control (IMC) structure [6] can be chosen to introduce the concept that an information flow exists from the actuator control signals to the conditioner. These signals model the environment, and hence a *modeler* is defined for modeling the environment and conditioning the outer world to the inner world units. The inner signals sent by the controller are fed back to the modeler, instead of real world signals from the actuator, since this structure does not pretend to exactly model the world, or to obtain a subjective internal representation of the outer world. Our answer to the ‘mind–body’ separation problem in a typical multi-input, multi-output (MIMO) system is shown in Figure 3 using the IHU control concept.

As argued by Cañamero [2], current embodied approaches are not well enough developed to be able to model ‘higher-level’ aspects of behaviors. In this sense, our tactical modular concept represents a new reactive interpretation of the mind based on internal representations of the real world for its design, i.e., the control elements, to successfully carry out a task.

Although our proposed architecture is focused on the emergence of behavior and not on deliberative interpretation of the mind, it can facilitate the integration of both reactive and deliberative controls in two forms. First, use of our tactical modularity is not in opposition to use of the strategic approach. Use of both types of modularity in the same controller could be the required solution for complex behaviors in complex robots. Secondly, autonomous agents (robots) beyond those completely reactive to the

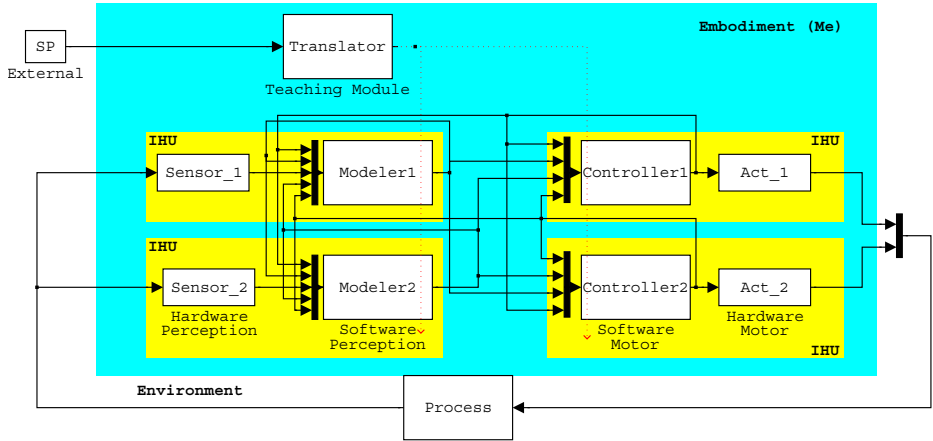


Figure 3. Mind designed on collaborative IHUs in the form of a MIMO and decentralized control architecture.

environment can be obtained using recurrent neural networks, so that they can initiate action independent of the immediate situation and organize behavior in anticipation of future events.

4. Experiment and Discussion

The goal in the experiment is to obtain an autonomous robot able to find a square object in the middle of the Webots' simulated environment [14], starting from a randomly selected point and then orbiting around the object in an endless loop at a close distance. This behavior emerges from the cooperation of four IHUs associated with two infrared sensors placed at the upper-left corner of the robot, one pointing to the front (Front IR) and another pointing to the left (Left IR), and two motors driving two wheels placed at the bottom of a square platform. Sensors were modeled that can detect objects within a limited range, such that they are not detected when they are not close enough. Each IHU is implemented by a static feed-forward ANN with a sigmoidal activation function.

Signals obtained from a complete experiment involving 200 steps taken by a trained robot are depicted in Figure 4. The top plot shows actual IR sensor readings, the middle plot shows IHU sensor translation for the signals, and the bottom plot shows the IHU actuator control commands sent to the motors. It is evident that the IHU sensors have learnt to translate sensor readings in a nearly exact scaled form, except for the instant at which the robot finds the object (first red line from the left in Figure 4). In such a situation, both IR signals are magnified and are even proportionally inverted. The experiment starts with null signals being sent from the IR sensors to the associated IHUs because no object is detected. These signals are translated to noisy signals for the IHU sensors because signals received from the IHU actuators are noisy. However, the robot has learnt

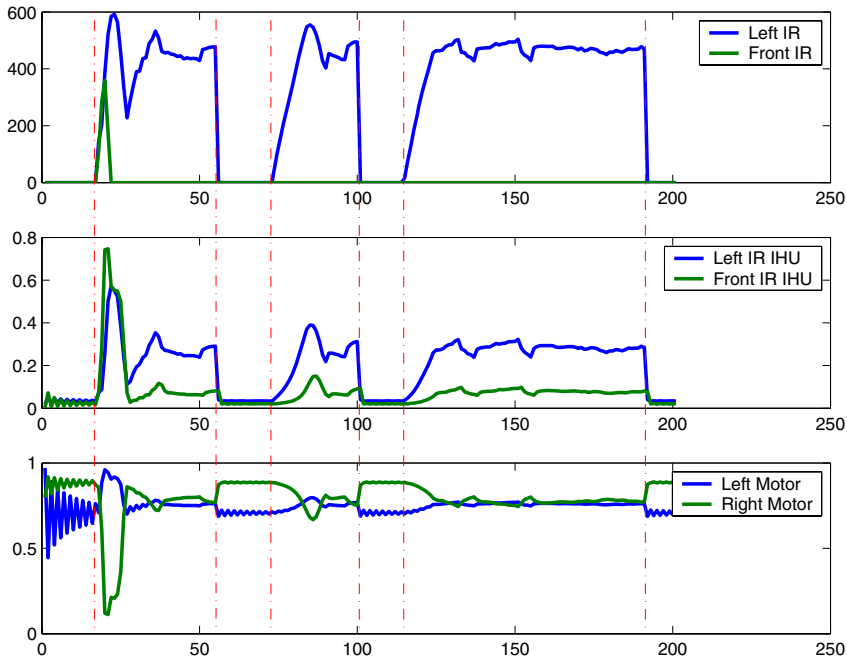


Figure 4. Signals from sensors, IHU sensor translation and IHU motor actuation for the orbiting simulated robot experiment.

to send a higher driving control to the right motor than to the left one, obligating the robot to turn around. At a certain moment, the robot finds the object and turns until it can orbit around the object. Owing to the sharpness of the central object to be detected and orbited, and the use of static feed-forward networks, the robot loses contact with the object when orbiting. During this time, the robot has learnt that, as previously, it is better to always turn to the left by increasing power on the right motor and decreasing it on the left motor.

5. Conclusions

A new paradigm is presented based on tactical modularity that explains higher cognitive functions as internal representations of action and perception of an embodied autonomous agent in a situated environment. In tactical modularity, subdivision into modules is performed at the level of the physical elements of the autonomous agent (sensors and actuators) involved in accomplishment of a task, the so-called *intelligent hardware units* (IHUs). The IHU-based tactical modular architecture proposed has been justified as a dynamical systems approach to cognitive robotics using a control engineering perspective. It has been demonstrated that a network structure of IHUs provides an autonomous agent with an ‘inner world’ based on internal simulations of perception rather than an explicit representational model. Thus, the full separation achieved between the inner world of the autonomous agent and its external real world gives an insight into how

the mind–body problem can be resolved. The architecture proposed was experimentally processed.

Our tactical modular architecture is focused on the emergence of behavior and not on deliberative interpretation of the mind; however, it can facilitate the integration of both reactive and deliberative controls. Further studies should be developed to analyze in detail the functionality of the translator module and its ability to integrate both types of control.

Acknowledgements

This work was partly supported by an ADA grant (DPI2006-15630-C02-01) from the Spanish Ministry of Education and Science and Network Action of the EU-funded IST CogSys Coordinated Action, euCognition.

References

- [1] R. Brooks, S. Iyengar, *Multi-sensor fusion: fundamentals and applications with software*, Prentice-Hall, Inc., 1998.
- [2] L. Cañamero, Emotion understanding from the perspective of autonomous robots research, *Neural Networks* 18 (4) (2005) 445–455.
- [3] S. Cheng, P. N. Sabes, Modeling sensorimotor learning with linear dynamical systems, *Neural Computation* 18 (4) (2006) 760–793.
- [4] D. Cliff, Biologically-inspired computing approaches to cognitive systems: A partial tour of the literature, Technical Report HPL-2003-011, HP Labs (2003).
- [5] J. Fodor, *The Language of Thought*, Cambridge, MA: MIT Press, 1975.
- [6] A. Isidori, L. Marconi, A. Serrani, *Robust autonomous guidance*, Springer, 2003.
- [7] R. Jacobs, M. Jordan, S. Nowlan, G. E. Hinton, Adaptative mixture of local experts, *Neural Computation* 1 (3) (1991) 79–87.
- [8] K. Kalveram, T. Schinrauer, S. Beirle, P. Jansen-Osmann, Threading neural feedforward into a mechanical spring: How biology exploits physics in limb control, *Biological Cybernetics* 92 (4) (2005) 229–240.
- [9] R. McCain, *Game Theory : A Non-Technical Introduction to the Analysis of Strategy*, South-Western College Pub, 2003.
- [10] R. W. Paine, J. Tani, How hierarchical control self-organizes in artificial adaptive systems, *Adaptive Behavior* 13 (3) (2005) 211–225.
- [11] D. Parisi, Internal robotics, *Connection Science* 16 (4) (2004) 325–338.
- [12] J. Tani, S. Nolfi, Learning to perceive the world as articulated: an approach for hierarchical learning in sensory-motor systems, *Neural Networks* 12 (1999) 1131–1141.
- [13] R. A. Téllez, C. Angulo, D. E. Pardo, Evolving the walking behaviour of a 12 dof quadruped using a distributed neural architecture, Proc. BioADIT 2006, Osaka, Japan, vol. 3853 of Lecture Notes in Computer Science, Springer, 2006.
- [14] R. A. Téllez, C. Angulo, Webots Simulator 5.1.7, developed and supported by Cyberbotics Ltd., *Artifcial Life* 13 (3) (2007).
- [15] T. van Gelder, *The MIT Encyclopedia of Cognitive Sciences*, chap. Dynamic approaches to cognition, MIT Press, Cambridge, MA, 1999, pp. 244–246.
- [16] H. von Foerster, *Cognition: A multiple view*, chap. Thoughts and Notes on Cognition, Spartan Books, New York, 1970, pp. 25–48.
- [17] T. Ziemke, Cybernetics and embodied cognition: on the construction of realities in organisms and robots, *Kybernetes* 34 (1/2) (2005) 118–128.

Using the Average Landmark Vector Method for Robot Homing

Alex GOLDHOORN^{a,b} Arnau RAMISA^{a,1} Ramón López DE MÁNTARAS^a
Ricardo TOLEDO^c

^a IIIA (*Artificial Intelligence Research Institute*) of the CSIC

^b University of Groningen, The Netherlands

^c CVC (*Computer Vision Center*), Spain

Abstract. Several methods can be used for a robot to return to a previously visited position. In our approach we use the average landmark vector method to calculate a homing vector which should point the robot to the destination. This approach was tested in a simulated environment, where panoramic projections of features were used. To evaluate the robustness of the method, several parameters of the simulation were changed such as the length of the walls and the number of features, and also several disturbance factors were added to the simulation such as noise and occlusion. The simulated robot performed really well. Randomly removing 50% of the features resulted in a mean of 85% successful runs. Even adding more than 100% fake features did not have any significant result on the performance.

Keywords. Mobile Robot Homing, Average Landmark Vector, Invariant features

1. Introduction

The objective of this work consists in evaluating the suitability of a biologically inspired visual homing method, the ALV (Average Landmark Vector), for a mobile robot navigating in an indoor environment. For these first experiments, we have developed and used a simulated environment to assess the robustness of the algorithm to different levels of noise and changes in the scene.

Based on the work of Wehner [9], Lambrinos et al. studied in [4] the navigation strategies of an ant species which lives in the Sahara, the Cataglyphis. This ant cannot use pheromones (hormones which are dropped by the ants in order to 'define' a path, these hormones can be detected by other ants) to find their way back, because the pheromones evaporate in the desert. Three main strategies were found to be used by the Cataglyphis: path integration, visual piloting and systematic search. Path integration with the help of a biological compass is the main ant navigation technique, but either visual piloting or systematic search, depending on the availability of landmarks, are also used to finally find the nest.

¹Correspondence to: Arnau Ramisa, Campus Universitat Autònoma de Barcelona, 08193 Bellaterra, Catalonia, Spain Tel.: +34 93 5809570; Fax: +34 93 5809661; E-mail: aramisa@iiia.csic.es.

The snapshot model has been used to explain the insect visual piloting techniques for about two decades [1]. This model assumes that a panoramic image of the target location is created and stored by the animal. When an insect wants to go back to the stored position it uses a matching mechanism to compare the current retinal image to the stored panorama. The authors of [4] suggest the Average Landmark Vector model as a better way to explain the comparison. This model assumes that the animal stores an average landmark vector instead of a snapshot. Landmarks can be (simple) features like edges. The direction to the destination is the difference of the ALV at the destination and the ALV at the current location. A significant advantage of the ALV is that it does not use any matching technique, thus being a much less computationally expensive method that can be used in real time. Posterior to this first simulated evaluation we plan to test this method on a real robot and, if the results are satisfactory, we will use it to complement the topological navigation system we are developing.

In [6] the authors successfully tested the ALV method on a small real robot under complete analog control, however this was in an $1\text{ m} \times 1\text{ m}$ environment with walls of 30 cm height and black pieces of paper on the wall which served as landmark.

In [7], Smith et al. propose some improvements for the ALV to use it in large scale environments, and test it in a computer simulation. In their simulation a unidimensional sensor for the robot is used, and the landmarks are cylinders of different sizes spread across the environment. Their experiment is designed to simulate the biological model of an ant colony where ants have to reach some food in the environment and then return to the nest.

Another difference between our work and that of Smith et al. is that we designed our simulation to use automatically extract features from panoramic images. In a real robot, these features can be extracted from the images using, for example, a Harris corner detector or DoG extrema, and we do not need to manually set up special landmarks within the environment.

The rest of the paper is divided as follows: In Section 2 the ALV visual homing method is explained. In Section 3, the computer simulation environment is explained as well as the experiments designed to test the performance of the ALV method. Section 4 discusses the results, and finally, in Section 5 we present the main conclusions extracted from the results and we mention some future work.

2. Method

The Average Landmark Vector is the average of the feature vectors:

$$ALV(F, \vec{x}) = \frac{1}{n} \sum_{i=0}^{i=n} \vec{F}_i - \vec{x} \quad (1)$$

Where F is a n by 3 matrix containing the positions of the n features. \vec{F}_i is the i th feature position vector and \vec{x} is the current position of the robot. Eqn. 1 shows the ALV in a world centered system, therefore the current position of the robot (\vec{x}) is subtracted.

The next step is to calculate the direction to the destination (or home) this is called the homing vector. It can be calculated by subtracting the ALV at the destination location (i.e. home: \vec{d}) from the ALV at the current location (\vec{x}):

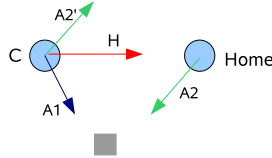


Figure 1. The calculation of the homing vector. Both ALV's (A_1 and A_2) point to the average feature position, which is drawn as a gray block. The homing vector (H) is calculated by subtracting the ALV at the destination location (A_2) from the ALV at the current location (A_1). This subtraction is shown, by the addition of the inverse vector, A'_2 , to A_1 . The robots are aligned in this example.

$$\text{homing}(F, \vec{x}, \vec{d}) = \text{ALV}(F, \vec{x}) - \text{ALV}(F, \vec{d}) \quad (2)$$

In this work we will use automatically extracted features from panorama images. One of the most relevant problems for using this method in the real world is that the panoramas have to be aligned before the homing vector can be calculated, this is not taken into account in the simulation. However we have done tests with random rotation of the panoramas to perceive the effect of non-aligned panoramas.

Figure 1 shows an example of the calculation of the homing vector. To simplify the image we only show the average feature position (the gray square). The ALV is calculated from two positions: c_1 and c_2 where the panoramas were taken. The ALV's from both panoramas are shown: A_1 and A_2 . The homing vector is calculated (with c_1 as current position and c_2 as home; figure 1) by subtracting the ALV at the destination position (A_2) from the ALV at the current position (A_1). This can be done by adding the opposite vector of A_2 (shown as A'_2) to A_1 . This results in the homing vector, H_1 , which points to the destination location. It can be easily proven that the destination will be reached when there is no noise present [4, 3].

In the previously discussed example the depth was known and therefore the destination was found in one step. However in our examples the depth is not known, because we only use one panorama image, therefore the process of calculating the homing vector has to be repeated several times.

A constraint of the homing method discussed here is that it assumes an isotropic feature distribution [2]. This means that the frequency and distance of the features are independent of the location where the panoramas were taken. A last constraint is that the features are static, that is they do not change over time.

3. Simulation and experiments

The simulation environment contains one or more walls which make up a room. These walls are defined by feature points (the dots in figure 2). In the simulation the robot only moves in a plane (xz-plane), so the robot will not change its height (y-direction). The camera is set 1 m from the ground (at $y = 1.0$ m).

Four slightly different worlds have been created where the center of the room is set to $(0, 0)$ on the xz-plane. Figure 2 shows the first world (world 1) and it shows the letters for each wall. The figure also shows the start and end location of the robot. The other worlds are similar to the first world, but not all the walls are present. Table 1 shows in which world which walls are present. The walls have a height of 2 m and a roughness of

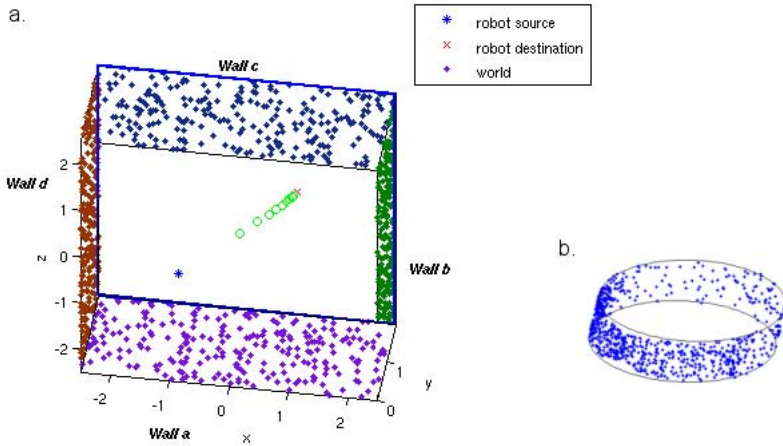


Figure 2. a. World 1 of the simulation. In this case the world consists of four walls (world 1). The dots represent the features by which the robot recognizes the wall. The robot origin (source) and destination are also shown and the path which the robot took (green circles). b. A panorama projection image at the destination location.

Table 1. The different worlds used in experiment 1 and per world which walls were present.

World	Description	Wall a	Wall b	Wall c	Wall d
1	All walls	x	x	x	x
2	2 sided, I	-	-	x	x
3	2 sided, II	x	-	x	-
4	1 sided	-	-	x	-

1 mm (i.e. the deviation from the 'straight' line). The locations of the features on each wall have been randomized (uniformly) before each test-run of the virtual robot.

The default amount of features for each world is 1000. These features are uniformly distributed in all the present walls (for example, in a world with four walls, each wall will have 250 features).

The virtual robot acquires information about the environment using a simulated omnidirectional camera, which captures a cylindrical projection of the features of the world at its current location. The images of the feature points in the panoramic image are used to calculate the ALV as in Eq. 1. The next step is to compute the homing vector (Eq. 2).

Which features are visible to the robot depends on their closeness and their y-position (height). The image plane has a limited vertical field of view, but it has a 360° view in the xz-plane. To test the performance of the ALV, we added Gaussian noise to the positions of the features before projecting them. We also added the possibility of features to disappear or new features to appear during a test-run.

3.1. Experiments

The influence of the variables listed in table 2 are investigated by the experiments which will be discussed in this section. The table shows the default values as bold. The noise parameter is the standard deviation of the Gaussian noise which is added to the position

Table 2. The tested parameter values. The values in bold are the default values. The values in italic are the values which have been tested in a second experiment.

Parameter	Tested values
wall length (<i>m</i>)	3, 5 , 10, 15, 20, 30, 50
standard deviation of the Gaussian noise added to the feature position	0 , 0.001, 0.01, 0.05, 0.1, 0.5, 1
number of features per world	20, 40, 100, 500, 1000 , 5000, 10000
number of added fake features	0 , 1, 5, 10, 20, 50, 500, 700, 900, 950, 980, 990, 995
number of removed features	0 , 1, 5, 10, 20, 50, 500, 700, 900, 950, 980, 990, 995
maximum random rotation angle of the projected panorama (<i>rad</i>)	0 , $\frac{1}{10}\pi$, $\frac{2}{10}\pi$, $\frac{3}{10}\pi$, ..., π

of the not yet projected features. Random features are added or removed to simulate occlusions. If no features are projected in the current panorama, because they are not visible to the robot for example, the robot tries to use the previous homing vector as it should point to the destination. If the previous vector is not available (i.e. has a zero length), a random vector is used. If no vector can be computed more than five times in a row, the test-run counts as a failure.

To prevent the simulation from running endlessly, a limit on the number of steps (iterations) was added. We experimentally found that 2000 was an appropriate limit. As a last constraint, the robot is allowed to travel at a maximum distance of ten times the ideal distance. We expect the robot to perform worse when the amount of disturbance is higher.

4. Analysis of the results

The experiments discussed in this work were done in a simulated environment in worlds with four, two or only one wall present. For each parameter, each of its values listed in table 2 were tested twenty times for all four worlds thereby using default values for the other parameters. The default value of each parameter is shown in table 2 as bold.

A run is marked as successful if it does not violate one of the previously mentioned three requirements: stay within the limits of 2000 iterations, do not drive a longer distance than ten times the ideal distance and do not use the previous or a random homing vector more than five times in a row. From the successful runs the difference between the driven distance and the ideal distance will be compared. At last we compare the number of iterations which the simulated robot used to reach its goal.

Since almost none of the results were normally distributed, we use the Wilcoxon Rank Sum test (also called the Mann-Whitney U test; [10]). In the discussion of the results, $\alpha = 0.05$ will be used. A more extended discussion of the results can be found in [3].

4.1. Noise in the feature position

Adding Gaussian noise to the positions of the features before each projection showed that the robot was able to reach its goal in almost all test-runs within our set limitations, when the noise had a standard deviation of 0.001 or less. Except for 40% of the runs in world 4 in which the test failed. All test-runs failed for a standard deviation of 0.5 and more.

As expected a higher noise rate increased the number of iterations which were used and also the difference with the ideal distance. It is difficult to compare the amount of noise to a situation in the real world. In the simulation we used Gaussian noise, because noise in nature generally is normal. We have found the level at which noise is tolerated by the model.

4.2. Occlusions

Occlusions were simulated by removing randomly chosen features before every projection. Removing until 500 of the 1000 features per world did not have any significant effect on the performance. In world 4 however, the result dropped to a success rate of 50%. When 95% of the features were removed, the success rate for worlds 1 to 4 was respectively : 60%, 35%, 40% and 15%. For 99.0% removed features 15% of runs in world 2 succeeded, 10% in world 3 and none in worlds 1 and 4. For 99.5% removed features none of the runs succeeded. The ALV method assumes an isotropic feature distribution [2]. This assumption can explain why the results in world 4 were worse than in the other worlds. The robot used more iterations when more features were removed, which was not significant for all number of removed features but was to be expected since the ALV every time has a different error. Also the difference with the ideal distance increased with the amount of removed features.

Adding fake features, which can be thought of previously occluded objects which become visible, resulted in no performance drop at all. Even when 100,000 fake features were added, within the bounds set by the world (width \times length \times height). This might also be explained by the uniform distribution of the fake features. The mean of the uniformly distributed fake features is the center of the room, therefore it should not have any influence in or near the center of the room. To confirm this, experiments can be done in which the fake features are not uniformly distributed.

4.3. Number of features

Having more (reliable) features present in the world increases the performance of the robot (higher success rate, less iterations and a smaller difference with the ideal distance). The success rate was 100% for 100 and more features for world 1, for 500 and more features for worlds 2 and 3 and 1000 and more features for world 4. The success rate for 20 features per world varies from 80% for world 1 to 50% for world 4. Having more features available increases the amount of information, and therefore it should improve the performance of the robot when it uses the features to navigate.

4.4. Wall length

When we look at the size of the room than we see that almost all runs were successful in square rooms. However in rectangular rooms in which the wall in the x direction was much longer than the wall in the z direction, the robot was less successful. All 20 runs succeeded for all worlds for a wall length of 5 and 10 m. For a wall length of 30 m in the x direction about 60% of the runs succeeded.

The robot performed worse in rooms in which one wall was much larger than the other, this can be explained by the way the features are projected. Feature pairs which are at the same distance on the wall, will be projected closer to each other on the panorama when they are further away than when they are closer to the robot. In [8] the same prob-

lem is mentioned: the vergence angle α is small near the antipodal direction and therefore the uncertainty of the depth is high. The result of a small vergence angle is that the projections of the features on both panoramas are very close to each other, therefore the difference between the vectors pointing to the projected features on both panoramas is very small. In our experiments there were about 1000 features equally divided over each present wall. To calculate the homing vector, the AL vectors are subtracted, but in the case of the features on the walls in the x-direction, this results in very short vectors. We have measured the length of the homing vectors to verify this. The mean length of the homing vector in a room of $5\text{ m} \times 5\text{ m}$ was 0.025 m (and a standard deviation of 0.007 m). However when one wall of the room was 50 m and the other 5 m , it resulted in very small homing vectors of 10^{-6} m . For this reason a lot of runs failed because the maximum number of iterations (2000) had been exceeded.

The number of iterations increases with increasing wall length, but the difference with the ideal distance is not significant in all worlds.

4.5. Rotation of the panorama projection

As expected the method did not work when the panorama was rotated randomly, therefore the panoramas (or at least the ALV's) should be aligned before calculating the homing vector. This can be accomplished by using a compass for example.

4.6. Results per world

The results of the different worlds show that the distribution of the features makes a difference. The robot performs best in world 1, in which the features are spread equally over all four walls and worst in world 4 where only one wall is present. The results of worlds 2 and 3, which both have two walls present, are between world 1 and 4 in performance. However we cannot conclude any significant difference between the first three worlds from our results. This can be explained by the isotropic feature distribution assumption for the same reason we expect that the system works worse in worlds 2 and 3 than in world 1.

From these experiments can be concluded that using the ALV for visual homing is a robust method. The next step is to try this method on a real robot. In the real world there can be problems with the 'noisiness' of the features, but this depends on which sensor is used and which feature detector.

5. Conclusions and Future work

In this work we evaluated the robustness of a homing method which uses the average feature vector which is calculated from data of a panorama. A big advantage of the ALV is its simplicity: the only requirement is that it needs features extracted from the environment. In the simulation the method was always successful in worlds with 1000 features and more.

Observations in the real world however, are almost never the same, therefore we have tested how robust the method is to noise and occlusions. Removing up to 50% of the features present in the world resulted in a mean success rate of 85%. Adding fake features had unexpectedly no significant negative effect on the results. A maximum

tolerated noise level has been found but tests have to be done with sensors in the real world to find out the degree of noise tolerance in the real world.

As expected the robot performed best in world 1 which has four walls and therefore satisfies to the isotropic distribution which is one assumption of the method. In the simulation the panoramas were always aligned, but in the real world an alignment method should be used, for example a compass could be used.

In the future simulated tests can be done in a world in which the features are not uniformly distributed over the walls, and where the worlds contain some objects. We will continue doing experiments with this homing method on a real robot. For this experiment we will use a panorama image and extract SIFT features [5].

Acknowledgements

The authors want to thank David Aldavert for the base code for the simulation environment. This work has been partially supported by the FI grant from the Generalitat de Catalunya and the European Social Fund, the MID-CBR project grant TIN2006-15140-C03-01 and FEDER funds and the Marco Polo Fund of the University of Groningen.

References

- [1] B. A. Carwright and T. S. Collet. Landmark learning in bees: Experiments and models. *Journal of Comparative Physiology*, 151:521–543, 1983.
- [2] M. O. Franz, B. Schölkopf, H. A. Mallot, , and H. H. Bülthoff. Where did i take the snapshot? scene-based homing by image matching. *Biological Cybernetics*, (79):191–202, 1998.
- [3] A. Goldhoorn, A. Ramisa, R. L. de Mántaras, and R. Toledo. Robot homing simulations using the average landmark vector method. Technical Report RR-III-2007-03, IIIA-CSIC, Bellaterra, 2007.
- [4] D. Lambrinos, R. Möller, T. Labhart, R. Pfeifer, and R. Wehner. A mobile robot employing insect strategies for navigation. *Robotics and Autonomous Systems*, 30(1-2):39–64, 2000.
- [5] D. G. Lowe. Distinctive Image Features from Scale-Invariant Keypoints. *International Journal of Computer Vision*, 60(2):91–110, 2004.
- [6] R. Möller. Visual homing in analog hardware. *International Journal of Neural Systems*, 1999.
- [7] L. Smith, A. Philippides, and P. Husbands. Navigation in large-scale environments using an augmented model of visual homing. In S. Nolfi, G. Baldassarre, R. Calabretta, J. C. T. Hallam, D. Marocco, J.-A. Meyer, O. Miglino, and D. Parisi, editors, *SAB*, volume 4095 of *Lecture Notes in Computer Science*, pages 251–262, 2006.
- [8] A. S. K. Wan, A. M. K. Siu, R. W. H. Lau, and C.-W. Ngo. A robust method for recovering geometric proxy from multiple panoramic images. In *ICIP*, pages 1369–1372, 2004.
- [9] R. Wehner. Spatial organization of foraging behavior in individually searching desert ants, *Cataglyphis*(Sahara Desert) and *Ocymyrmex*(Namib Desert). *Experientia. Supplementum*, (54):15–42, 1987.
- [10] F. Wilcoxon. Individual comparisons by ranking methods. *Biometrics Bulletin*, 1:80–83, 1945.

Distance Sensor Data Integration and Prediction

Zoe Falomir¹, M. Teresa Escrig¹, Juan Carlos Peris², Vicente Castelló¹

Universitat Jaume I

¹*Engineering and Computer Science Department*

²*Languages and Computer Science Systems Department*

Campus Riu Sec, Castellón, E-12071 (Spain)

zfalomir@icc.uji.es, escrigm@icc.uji.es, jperis@lsi.uji.es, castellv@guest.uji.es

Abstract. In this paper we describe an approach to sensor data integration in order to obtain a qualitative and robust interpretation of the robot environment, which could be used as input in the qualitative robot navigation algorithms developed by our group. This approach consists of: obtaining patterns of distance zones from the sensor readings; comparing statically these patterns in order to detect non-working sensors; integrating the patterns obtained by each kind of sensor in order to obtain a final pattern which detects obstacles of any sort; predicting how the distance pattern will be influenced by robot motion and comparing this prediction with reality in order to detect incoherent sensorimotor situations. This approach has been applied to a real Pioneer 2 robot and promising results are obtained.

Keywords: Sensor integration, reasoning under uncertainty, qualitative reasoning.

1. Introduction

Human beings use many kinds of sensory information in order to obtain a complete and reliable representation of their surroundings. In the same way, robots can incorporate different kinds of sensors –each one sensitive to a different property of the environment– whose data can be integrated to make the perception of the robot more robust and to obtain new information, otherwise unavailable.

Although, both sonar and laser sensors measure the same physical magnitude (length), these sensors are sensitive to different properties of the environment: noise and light, respectively. Therefore, data coming from these kinds of sensors can be integrated in order to overcome each disadvantage. The main problems of sonar sensors are: multiple reflections in corners; uncertainty in locating the target due to its cone-shaped beam; and external ultrasound sources or crosstalk. Although laser sensors usually provide accurate readings, they may also present some drawbacks dealing with the nature of the target surfaces. Poor reflectance surfaces, like dark colours or soft materials, absorb the laser beam and return it with a feeble intensity; while high reflectance surfaces present more serious problems: mirrors reflect the laser beam in any direction, while glasses can react to the laser beam as transparent, partial mirrors or perfect mirrors, depending on the glass type, thickness and angle of incidence. In literature, sonar and laser data fusion for mobile robot navigation has been characterized by the use of

probabilistic techniques: Kalman filters [1][2], Gauss approximation methods and vector maps [3], grid maps [4], grid maps and Bayes' theorem [5], etc. These quantitative methods can manage incomplete and inaccurate information, but at a high computational cost, and they usually obtain a description of the world which is more accurate for the task to be performed than the one is actually needed. Moreover, simulated robots that use qualitative navigation methods [6] do not require explicit geometric representations of the environment. However, a model that provides a reliable qualitative sensor output that could be used as input in such qualitative navigation algorithms has not yet been devised.

Moreover, human beings are efficient exploring their environment since they can relate its sensory information to its motor actions and they can also predict how their motor actions will influence the sensory information which they will perceive in the future. If predictions made do not take place, human beings are alerted that something unexpected happens [7]. In the same way, if robots could relate the information obtained by their sensors to its motor actions, they would detect sensorimotor incoherences and would be able to react to unexpected situations.

This paper presents an approach to obtain a qualitative and robust interpretation of the robot environment, which consists of (1) obtaining a reliable distance pattern by integrating distances coming from the sonar and laser sensors of a Pioneer 2 robot, and (2) checking if the predicted evolution of distance patterns is coherent with robot motion.

The remainder of this paper is organized as follows. Section 2 details what our approach consists of. Section 3 explains distance sensor data processing. In section 4, sonar and laser data integration is explained. Section 5 describes how we compare distance patterns with robot motion and how we predict the new situation of the robot environment. Section 6 describes the application of our approach to a real Pioneer 2 robot and the results obtained. Finally, in section 7, our conclusions and future work are explained.

2. Qualitative Robot Environment Description and Sensorimotor Coherence Detection

As it is shown in Figure 1, our approach to obtain a qualitative and robust interpretation of the robot environment at a high level of abstraction consists of processing the distance sensor readings coming from each kind of sensor in order to obtain patterns of fuzzy distance zones, which represent the robot environment in a simplified and more intuitive way. After comparing these patterns statically, sensors which are not working properly are detected and a final distance pattern is obtained for each kind of sensor. Then, patterns provided by each kind of sensor are integrated in order to overcome each sensor disadvantages and to obtain a final pattern which can detect any sort of obstacle. Moreover, as sensory information is influenced by robot motion, we can predict how the distance patterns obtained will evolve and by comparing its evolution with the reality we can determine if the situation detected by the robot is sensorimotor coherent or not. Our approach will produce outputs such as: the distribution of qualitative distances in the robot area, what sort of obstacles are included in the area (simple obstacle, glass window, mirror, etc.), if any of the sensors has technical problems and its location, the robot situation with respect to a frontal obstacle (approaching or moving away) and if the distance pattern evolution is coherent with the robot motion or not.

Our approach can be extended and generalized for any kind of sensor. If the sensor to be introduced into the system is a distance sensor, we can apply the *Qualitative Distance Sensor Processing (QDSP)* to it, while other kinds of sensors (such as a camera) could be treated similarly in order to obtain features which could be integrated with those obtained by distance sensors.

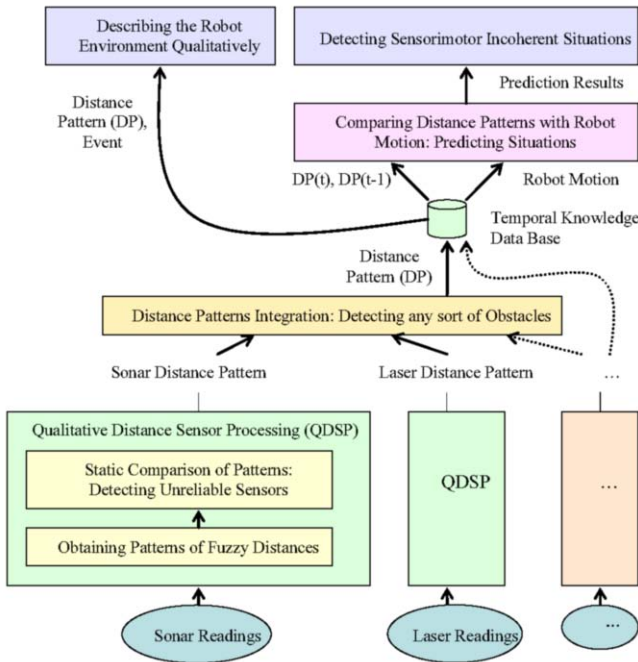


Figure 1. Distance sensor data integration and prediction approach.

3. Qualitative Distance Sensor Processing (QDSP)

Our *Qualitative Distance Sensor Processing (QDSP)* approach consists of: obtaining patterns of fuzzy distance zones, as it is described in section 3.1; and comparing the patterns obtained in order to detect sensors with technical problems, as it is described in section 3.3. In order to compare fuzzy distance zones with each other, we have developed a *Dissimilarity Factor (DF)* and a *Dissimilarity Factor between Fragments of Patterns (DFbFP)*, which are explained in section 3.2.

3.1. Obtaining Patterns of Fuzzy Distances from Sensor Numerical Readings

In order to interpret distance sensor data qualitatively, our approach uses the fuzzy sets described in Figure 2 (a). For each numerical sensor reading, we calculate its certainty of belonging to each distance fuzzy set and we select those fuzzy distances that obtain a certainty which is different to zero. Each fuzzy distance is composed of a qualitative distance name and a certainty. Numerical readings which are negative or exceed its sensor range are classified as *out_of_range* distances with the maximum certainty.

In Figure 2 (a), each fuzzy set limit depends on the diameter of the robot (d), as the application on which we want to apply our approach consists of sweeping an indoor surface with a vacuum cleaner robot, which will follow the wall in spiral or zigzag situating itself from the wall at a further qualitative distance any time.

After transforming all sensor readings into fuzzy distances and grouping those with the same qualitative distance names, patterns of fuzzy distance zones are obtained (Figure 2 (b)). Each *zone* includes its starting and ending angular position, the event corresponding to the zone and a list of fuzzy distances related to it. The certainty of these fuzzy distances is obtained as the mean of all the certainties originally included in the zone. A collection of zones related to the same sensor scan defines a *distance pattern* ($P(t)$), as it is described:

$$\text{Distance Pattern } (DP_t) = \text{Type_of_sensor}([\text{Zone}_0, \dots, \text{Zone}_N]).$$

$$\text{Type_of_sensor} = \{\text{sonar, laser, infrared, etc.}\}$$

$$\text{Zone} = [\text{Start}, \text{End}, \text{Fuzzy_distance_Set}, \text{Event}]$$

$$\text{Fuzzy_distance_Set } (\text{FdSet}) = [\text{Fuzzy_distance}_0, \dots, \text{Fuzzy_distance}_N]$$

$$\text{Fuzzy_distance } (\text{Fd}) = [\text{Qualitative_name}, \text{Certainty}]$$

$$\text{Qualitative_name_Set } (\text{QnSet}) = \{\text{none, at, very_close, close, quite_near, near, medium, quite_far, far, very_far, too_far, extremely_far, out_of_range}\}$$

$$\text{Certainty} = [0.0, 1.0]$$

$$\text{Event} = \{\text{simple_obstacle, glass_or_mirror, sound_reflection_in_corner, sonar_error, laser_error, sonar_and_laser_error, sonar_out_of_range, laser_out_of_range, sonar_and_laser_out_of_range, non_defined}\}$$

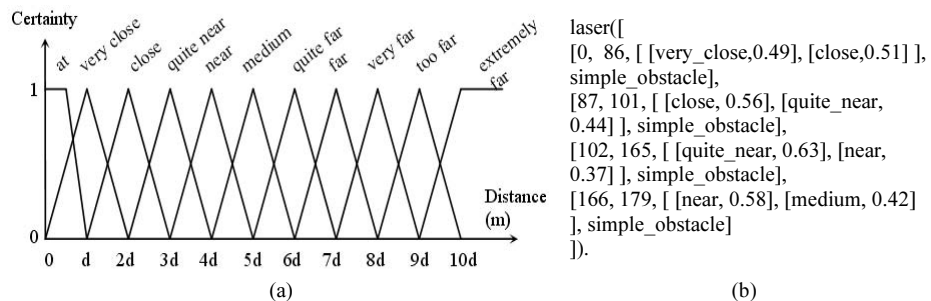


Figure 2. (a) Definition of distance fuzzy sets, where d is the diameter of the robot. (b) An example of a pattern obtained by a laser sensor.

3.2. Comparing Fuzzy Distances and Fuzzy Distance Zones

In order to know if two fuzzy values are similar or not in meaning, we calculate the dissimilarity between them. The *dissimilarity value* between two fuzzy values with the same qualitative name is zero and between two different but consecutive fuzzy values is one unit: positive, if the first name is placed more to the right (in the qualitative name set or QnSet) than the second one, and negative, otherwise:

$$\text{QnSet} = \{ \text{none} \xrightarrow{-1} \text{at} \xrightarrow{+1} \text{very_close} \dots \text{near} \xrightarrow{+1} \text{medium} \dots \text{extremely_far} \xrightarrow{+1} \text{out_of_range} \} \quad (1)$$

As a consequence, we calculate the *Dissimilarity Factor* (DF) between two sets of fuzzy values (FdSet_A and FdSet_B) by accumulating the *dissimilarity value* between each

pair of elements which composes each relation obtained by the Cartesian product of the two sets involved. Then we weight the result obtained by the cardinality of the Cartesian product, that is, the number of the relations obtained and, as the sets involved are finite, it coincides with the product of both set cardinalities.

$$DF(FdSet_A, FdSet_B) = \frac{\sum_{i=1}^{card(FdSet_A)} \sum_{j=1}^{card(FdSet_B)} dissimilarity(FdSet_A[i], FdSet_B[j])}{card(FdSet_A) \cdot card(FdSet_B)}; \quad DF = R \in [-card(QnSe), card(QnSe)] \quad (2)$$

The DF can take values between the cardinality of the qualitative name set used in the fuzzy set definition with negative sign and the same cardinality with positive sign. Besides, DF calculus is only based on the order of qualitative name set used in the fuzzy set definition and it does not depend on the certainty of each value.

Moreover, in order to compare two fragments of different distance patterns (fDP_0 , fDP_1) which refer to the same angular positions related to an area of interest in the robot environment, such as front, left or right, we define the *Dissimilarity Factor between Fragments of Patterns (DFbFP)*. The fragments of distance patterns compared can be composed by different number of distance zones. Two distance zones will *overlap* if the starting position of one of them is smaller than the ending position of the other one. Therefore, for each overlapping zone in both distance patterns, we calculate the *Dissimilarity Factor* between them and we weight it by the fraction of amplitude corresponding to the overlapping zone with respect to the total angular amplitude of the fragment.

$$overlap(Zone_i, Zone_j) \Leftrightarrow \{end_i < start_j \vee end_j < start_i\} \quad \text{where } Zone_i \in fDP_0 \wedge Zone_j \in fDP_1$$

$$DFbFP(fDP_0, fDP_1) = \sum_{i=1}^{card(fDP_0)} \sum_{j=1}^{card(fDP_1)} DF(overlap(FdSet_{Zone_i}, FdSet_{Zone_j})) \cdot \frac{Overlap_Amplitude}{Fragment_Amplitude} \quad (3)$$

A $DFbFP$ calculus is shown as an example:

$$fDP_0 = \text{sonar}([[80, 99, [[near, 0.23], [medium, 0.77]]]]).$$

$$fDP_1 = \text{sonar}([[80, 95, [[near, 0.32], [medium, 0.68]]], [96, 99, [[medium, 0.74], [quite_far, 0.26]]]]).$$

$$DFbFP = \frac{DF([near, medium] \times [near, medium]) \cdot 16/20 + DF([near, medium] \times [medium, quite_far]) \cdot 4/20}{(card([near, medium]) \cdot card([near, medium])) \cdot 16/20 + ((dissimilarity(near, near) + dissimilarity(near, medium) + dissimilarity(medium, near) + dissimilarity(medium, medium)) / (card([near, medium]) \cdot card([near, medium]))) \cdot 16/20 + ((dissimilarity(near, medium) + dissimilarity(near, quite_far) + dissimilarity(medium, medium) + dissimilarity(medium, quite_far)) / (card([near, medium]) \cdot card([medium, quite_far]))) \cdot 4/20} = ((0+1-1+0) / (2 \cdot 2)) \cdot 16/20 + ((1+2+0+1) / (2 \cdot 2)) \cdot 4/20 = 0.2$$

As it can be observed, the $DFbFP$ in the example proposed is very small because the biggest part of both fragments of patterns coincides; and it is positive, because there is an increase in distance between the previous pattern (fDP_0) and the actual one (fDP_1).

3.3. Static Comparison of Patterns: Detecting unreliable sensors

In order to detect sensor malfunctions, we scan statically the robot environment three times and we compare qualitatively the three distance patterns obtained (DP_t , DP_{t-1} , DP_{t-2}). Assuming that all the objects in the robot environment are static, if we find that

a sensor obtains different readings depending on time and not on the situation, we can think that this sensor has a possible technical problem.

The static comparison of patterns consists of comparing the actual pattern (DP_t) to the two previous ones (DP_{t-1} , DP_{t-2}) and finding those patterns which are *qualitatively similar* (*Qsimilar*) to each other. Two distance patterns are *Qsimilar* if they are composed by the same number of zones with the same qualitative distance tags. If the actual pattern is qualitatively similar to at least one of the two previous ones, we select the actual pattern (DP_t) as the final pattern. Otherwise, we compare the two previous patterns and if they are *Qsimilar*, we select the most actual pattern (DP_{t-1}) as the final one.

However, if none of the patterns are completely *Qsimilar*, we build a new pattern with the *zones* which are *Qsimilar* or *Close in Meaning* (the *DF* between each zone is lower than a threshold) in at least two of the three original patterns. Finally, if there is any angular position where all the fuzzy distances are very different from each other, we cannot know anything about the real distance and, therefore, we categorize this reading with *none* distance name with the maximum certainty. *None* will suggest technical problems with the sensor located in the angular position where the reading was taken.

4. Integrating Sonar and Laser Distance Patterns: Detecting Special Obstacles

As sonar and laser sensors have problems in different situations of the robot environment, we can integrate their readings to overcome these problems also to identify the specific situation the robot is facing.

After obtaining sonar and laser final patterns, first we check if any of the sensors has technical problems (distances defined as *none* or *out of range*). If both kinds of sensors show technical problems in the same angular positions, the final distance pattern will indicate *laser and sonar error* as the event. If, for the same angular position, one sensor has technical problems while another one works well, we include the distance obtained by the second one in the final distance pattern and the kind of sensor which is having technical problems (*sonar error* or *laser error*) as the event for that angular position. If none of the sensors have technical problems for the same angular position, then we compare the distances obtained by them by calculating the *Dissimilarity Factor* (*DF*) of the fuzzy distances located at that angular position in both patterns. If there is a *Large Dissimilarity Factor* (*LDF*) between each sensor reading (which consists of obtaining a *DF* upper than a threshold in absolute value), we can determine that:

- If $LDF > 0$, the distance obtained by the laser sensor is much larger than the sonar one. Therefore the robot could be facing *a glass window or a mirror* which reflects the laser beam in any direction and this will be the event determined.
- If $LDF < 0$, the distance obtained by the sonar sensor is much larger than the laser one. Therefore, the robot could be facing a corner, which could have made the sound waves rebound and not return to the receiver. Therefore, the event determined will be *sound reflection in corner*.

If there is not a *LDF* between the distances obtained by each kind of sensor, then we determine that the final distance for that angular position is that obtained by the laser

sensor, as it is the most accurate sensor, and the event determined will be *simple obstacle*.

As an example of integration, we can observe the distance patterns obtained when the robot is located inside a small room and in front of a mirror (Figure 3). If we observe sonar and laser distance patterns, we can realize that sonar distance pattern has obtained a larger distance than laser distance pattern for 50 to 69 angular positions. Therefore, if we compare the final pattern and the situation scheme in Figure 3, we can realize that both point out that there is a sound reflection in a corner there. Moreover, we can realize that laser distances for 79 to 86 angular positions are more larger than sonar ones, that is because the final pattern include the sonar zone as the right one and points out that there is a mirror in that angular position.

```
sonar([
[0, 29, [[ very_close, 0.29 ], [ close, 0.71 ]], non_defined],
[30, 49, [[ at, 0.21 ], [ very_close, 0.8 ]], non_defined],
[50, 69, [[ very_far, 0.97 ], [ too_far, 0.03 ]], non_defined],
[70, 109, [[ at, 0.73 ], [ very_close, 0.3 ]], non_defined],
[110, 129, [[medium, 0.12], [ quite_far, 0.88 ]], non_defined],
[130, 149, [[ close, 0.6], [ quite_near, 0.4 ]], non_defined],
[150, 179, [[very_close, 0.91], [close, 0.09]], non_defined]
]).
```

```
laser([
[0, 31, [[ very_close, 0.54 ], [ close, 0.46 ]], non_defined],
[32, 68, [[ at, 0.52 ], [ very_close, 0.51 ]], non_defined],
[69, 78, [[ near, 0.55 ], [ medium, 0.45 ]], non_defined],
[79, 86, [[ quite_far, 0.9 ], [ far, 0.09 ]], non_defined],
[87, 107, [[ at, 0.54 ], [ very_close, 0.48 ]], non_defined],
[108, 124, [[ quite_far, 0.76 ], [ far, 0.23 ]], non_defined],
[125, 134, [[ medium, 0.37 ], [quite_far, 0.62 ]], non_defined],
[135, 142, [[ quite_far, 0.76 ], [far, 0.24 ]], non_defined],
[143, 149, [[ extremely_far, 1.0]], non_defined],
[150, 159, [[ close, 0.63 ], [quite_near, 0.37]], non_defined],
[160, 179, [[ very_close, 0.76 ], [ close, 0.24 ]], non_defined]
]).
```

```
final_pattern([
[0, 31, [[very_close,0.54], [close, 0.46]], simple_obstacle],
[32, 68, [[at, 0.5],[very_close, 0.5]],sound_reflection_in_corner],
[69, 78, [[near, 0.55], [medium, 0.47]], simple_obstacle],
[79, 109, [[at, 0.73], [very_close, 0.3]], glass_or_mirror],
[110, 124, [[quite_far, 0.76], [far, 0.23]], simple_obstacle],
[125, 134, [[medium, 0.37], [quite_far, 0.63]], simple_obstacle],
[135, 142, [[quite_far, 0.76], [far, 0.24]], simple_obstacle],
[143, 159, [[close, 0.63], [quite_near, 0.37]], simple_obstacle],
[160, 179, [[very_close, 0.77], [close, 0.23]], simple_obstacle]
]).
```

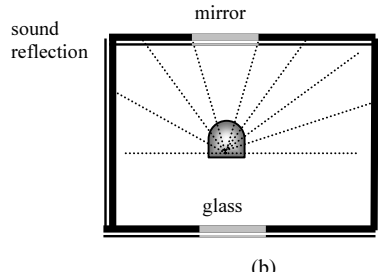


Figure 3. Example of a Pioneer 2 robot situation.

5. Comparing Distance Patterns with Robot Motion and Predicting Situations

If we try to find a relation between simple robot motion (moving forwards/backwards or turning around itself) and the distance patterns obtained by its sensors, we can determine if a situation is sensorimotor coherent or not and we can also predict how the zones in the distance patterns will evolve in the future in order to detect unexpected situations.

If the robot is *moving forwards or backwards*, we expect that the distances in the frontal zone of the distance pattern will become shorter or larger, respectively, as the robot could be approaching/moving away to/from an obstacle located in front of it. In order to compare the frontal zones of the actual and previous sensor patterns the *DFbFP* is used. If the *DFbFP* is positive/negative, it means that the distance between the previous pattern and the actual one have increased/decreased, respectively. Finally, by comparing the prediction made with the tendency in the frontal zone of the distance pattern (distances increasing or decreasing), we can check if the sensors are coherent with the robot motion or not.

If the robot is *turning to the right around itself*, we can predict that new distance zones will appear at the end of the next distance pattern, while distance zones located at the beginning of the actual pattern will disappear. In the other way round, if the robot is *turning to the left around itself*, new distance zones will appear at the beginning of the next distance pattern, while distance zones located at the end of the actual pattern will disappear. By comparing these predictions with the evolution of the actual and the next distance pattern, we can check if the perception of the robot environment is coherent with robot motion.

6. Implementation and Results

We have implemented our approach in a C++ controller for a real Pioneer 2¹ robot and we have tested it in a static and simple environment (a rectangular small room without obstacles with a mirror and a glass included as walls).

In order to generalize our approach, sensor characteristics and distance fuzzy sets used are defined as Prolog facts in Prolog modules (Figure 4). ECLiPSe² libraries have been used to obtain backtracking results back in the robot controller. Moreover, as it can be observed in Figure 3(b), distance patterns obtained by our approach are also expressed as Prolog facts, so that they could be processed later in a more abstract level.

<pre>fuzzy_set(Kind_of_set, Name, Type_of_set, P1, P2, P3, P4). Type_of_set = linear decreasing (ld) or increasing (li), triangular or trapezoidal (tp). P1, P2, P3, P4 = points which define the Type_of_set</pre>	<pre>type_of_sensor(Name, Max_reading_range, Readings_number, Angular_range, Senors_location_List).</pre>
<pre>fuzzy_set(distance, at, ld, 0.03,1D,0,0). (...)</pre>	<pre>distance_sensor(sonar, 3.00, 8, 20, [0, 40, 60, 80, 100, 120, 140, 179]. distance_sensor(laser, 10.00, 180, 1, [0, 180]).</pre>
(a)	(b)

Figure 4. (a) Fuzzy sets and (b) robot sensor characteristics defined as Prolog facts.

In order to test our approach in the Pioneer 2 robot, we have designed a controller that make the robot turn around itself and move forwards or backwards from one wall of its world to the other one located in front or back, respectively. We have observed that all percentages of coherence obtained are high as nothing unexpected occurred during the testing (Figure 5). In average, final distance patterns were coherent with robot motion 100% of times moving forwards, 95% of times moving backwards and 94% of times while the robot was turning around itself.

Dealing with the *static comparison* of distance patterns, we have obtained that, in average, the 89% and 98% of patterns obtained by the sonar and laser sensors, respectively, are qualitatively similar (*Qsimilar*), which means that, both kind of sensors in our Pioneer 2 robot are quite reliable, although laser measures are usually more accurate than sonar ones (Figure 5).

¹ <http://www.activrobots.com>

² <http://eclipse.crosscoreop.com>

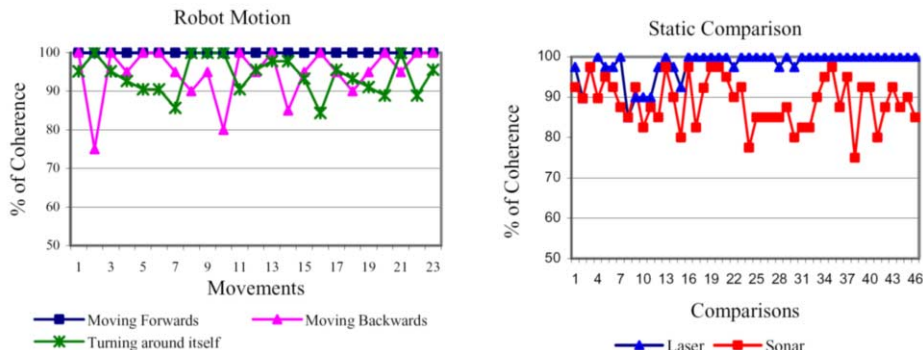


Figure 5. Percentages of coherence resulting from comparing distance patterns statically and after robot motion.

Dealing with *sensor data integration*, we have observed that (1) Pioneer sonar sensors usually obtain a larger distance than the real one in the angular position where a corner is placed, due to sound rebound, and (2) Pioneer SICK laser scanner fail to detect mirrors and some kind of glasses, since laser beam reflection. Our approach has made the robot succeed in (1) detecting mirrors and glasses which stands vertically included as walls in the robot world, (2) obtaining the real distance to corners, since the sound rebounds are detected; and (3) detecting non-working sensors, such as laser sensor disconnection, and navigating properly without the information provided by them. However, it has failed in detecting mirrors and glasses which has about 45 degrees of incline with respect to vertical walls. In this situation, both sensors obtain a larger distance than the real one: sonar sound waves rebound to the ceiling and the laser beam is reflected in any direction.

7. Conclusions and Future Work

In this paper, we have presented an approach to obtain a qualitative and robust interpretation of the robot environment, which consists of obtaining patterns of distance zones from the sensor readings; comparing statically these patterns in order to detect non-working sensors; integrating the patterns obtained by each kind of sensor in order to obtain a final pattern which detects obstacles of any sort; predicting how the distance pattern will be influenced by robot motion and comparing this prediction with reality in order to detect incoherent sensorimotor situations.

Our approach has been implemented and tested by using a C++ controller for a real Pioneer 2. After our testing we have proved that in a high percentage of situations we could establish a coherent relation between sensory information and motor actions by predicting situations and checking them in the moment of happening. Moreover, by means of sensor data integration, our approach has made the robot succeed in detecting mirrors and glasses, obtaining real distance to corners and detecting non-working sensors and navigating properly without the information provided by them. However, we have found some problems in detecting mirrors and glasses with about 45 degrees of incline.

As for future work, we intend (1) to improve our sensor data integration approach in order to overcome special situations and so that dynamic obstacles could be included

in the robot environment, (2) to test our approach in a more complex environment which will include obstacles, (2) to define strategies to react when the robot detect an incoherent sensorimotor situation, and (3) to apply distance patterns obtained to robot navigation, in order to make a vacuum cleaner robot sweep room surfaces by following the wall in spiral or zigzag situating itself from the wall at a further qualitative distance any time.

Acknowledgments

This work has been partially supported by CICYT and Generalitat Valenciana under grant numbers TIN2006-14939 and BFI06/219, respectively.

References

- [1] Díosí, A. & Kleeman, L. 2004, "Advanced sonar and laser range finder fusion for simultaneous localization and mapping", *Intelligent Robots and Systems, 2004.(IROS 2004).Proceedings.2004 IEEE/RSJ International Conference on*, vol. 2, pp. 1854-1859 vol.2.
- [2] Díosí, A., Taylor, G. & Kleeman, L. 2005, "Interactive SLAM using Laser and Advanced Sonar", *Robotics and Automation. ICRA 2005. Proceedings of the 2005 IEEE International Conference on*, pp. 1103-1108.
- [3] Vamossy, Z., Kladek, D. & Fazekas, L. 2004, "Environment mapping with laser-based and other sensors", *Robot Sensing, 2004. ROSE 2004.International Workshop on*, pp. 74-78.
- [4] Klaus-Werner Jörg. "World modelling for an autonomous mobile robot using heterogeneous sensor information". *Robotics and Autonomous Systems*, 14:159-170, 1995.
- [5] Xue-Cheng Lai, Cheong-Yeen Kong, Shuzhi Sam Ge & Al Mamun, A. 2005, "Online map building for autonomous mobile robots by fusing laser and sonar data", *Mechatronics and Automation, 2005 IEEE International Conference*, vol. 2, pp. 993-998 Vol. 2.
- [6] Escrig, M. T. & Toledo, F. "Qualitative Spatial Reasoning: theory and practice. Application to Robot Navigation". *IOS Press, Frontiers in Artificial Intelligence and Applications*, ISBN 90 5199 4125. 1998.
- [7] J. Hawkins, S. Blakeslee, "Sobre la Inteligencia", Ed. Espasa-Calpe. ISBN. 8467017376, 2005.

Applications

This page intentionally left blank

Neural Network Modeling of a Magnetorheological Damper

Mauricio Zapateiro ^{a,1}, Ningsu Luo ^a

^a *Institute of Informatics and Applications. University of Girona, Spain*

Abstract. This paper presents the results of modeling a magnetorheological (MR) damper by means of a neural network. The MR damper is a device extensively used to mitigate hazardous vibrations in systems such as vehicles, bridges and buildings. The advantages of these dampers over other devices of their class rely on the cost, size, simplicity and performance. However, these devices are highly nonlinear; their dynamics is characterized by friction and hysteresis, phenomena that has been difficult to model following physical laws. In this paper, a recurrent neural network is trained to reproduce the behavior of the damper and it will be shown that the results are better than those obtained by approximate physical models.

Keywords. recurrent neural network, hysteresis, friction, magnetorheological damper

1. Introduction

Magnetorheological (MR) dampers are devices that have been widely studied during the last fifteen years. Their characteristics make them attractive for implementation in systems such as vehicles and civil engineering structures to protect them from hazardous vibrations and to improve the human comfort. MR dampers can generate a high force with low energy requirements and a simple mechanical design at low production costs. Their main component, the MR fluid, is a substance that can change the rheological behavior in the presence of a magnetic field, allowing for controllability.

It is well known that, for successful control, the system components (sensors, actuators and others) should be accurately modeled. MR dampers are highly nonlinear devices with hysteresis that may cause serious problems to stability and robustness [1]. The force response to the velocity input describes a hysteretic loop which makes it a challenging task to find a model that can reproduce their behavior. Several models have been proposed for MR dampers: the Bingham model [2], the Bi-viscous model, the polynomial model, the Bouc-Wen model [3], Neural network models [4], ANFIS based models [5] and others derived from the previously mentioned ones are some examples.

Neural networks have extensively been used in many fields of research due to their ability to model nonlinear systems. Neural networks can be trained to learn complicated

¹Correspondence to: Mauricio Zapateiro, Universitat de Girona. Edifici P4. 17071, Girona, SPAIN. Tel.: +34-972-418487; Fax: +34-972-418976; E-mail: mauricio.zapateiro@udg.edu.

relationships between sets of inputs and outputs. They can be thought of parallel processors that have retained information from previous experiences and use it to predict the response of a system. Neural networks are trained with experimental data that describes all, or at least the most relevant scenarios that the system can face. Their ability to learn complicated nonlinear systems has been exploited to describe the behavior of MR dampers. See for example, the works by Du et al. [6], Wang and Liao [7], Zapateiro et al. [8,9] and Zhang and Roschke [4].

The neural network model of an MR damper prototype will be presented in this paper. The prototype is to be used in experimental vibration control of structures, hence the importance of an accurate model. This paper is organized as follows. Section 2 gives a brief description of the recurrent neural networks and the training algorithm to be used throughout this paper. Section 3 describes the experiment setup and how the training data was collected. Section 4 shows the results of the experiments and some comparisons are also offered. Finally, conclusions and future work are discussed in Section 5.

2. Recurrent neural networks

Neural networks can be classified as static or dynamic. Static networks do not have memory so the response to specific inputs will be the same no matter the order in which they are presented. On the other hand, dynamic or recurrent networks make use of memory and feedback trajectories to compute responses to an input. Because the hysteresis phenomenon depends on the time history of the variables, a recurrent network will be used to model the MR damper.

Multilayer networks are usually trained using a backpropagation algorithm. In this algorithm, the weights are updated based on the error between the outputs and the targets. The algorithm computes the gradient vector of the error surface; it indicates where to move on the error surface so that it can reach the minimum point on this surface. One concern is the size of the step since large steps may make the algorithm go in the wrong direction though converge quickly, but small steps may make it take much longer to find a solution.

There are several backpropagation algorithms that try to improve the speed of convergence while maintaining a good performance. One example is the resilient backpropagation algorithm. What it does is to eliminate the harmful influence of the size of the partial derivative on the weight step ($\partial E / \partial w$). It only uses the sign of this derivative to determine which direction to move on so its magnitude does not have any effect on it. The size of the weight update is increased if the sign of the derivative of the performance function in the previous iterations is the same, otherwise it is decreased. If the derivative is zero, then the update value remains the same. In case of oscillations, the weight change is reduced and if it remains following the same direction, then the weight change is decreased [10].

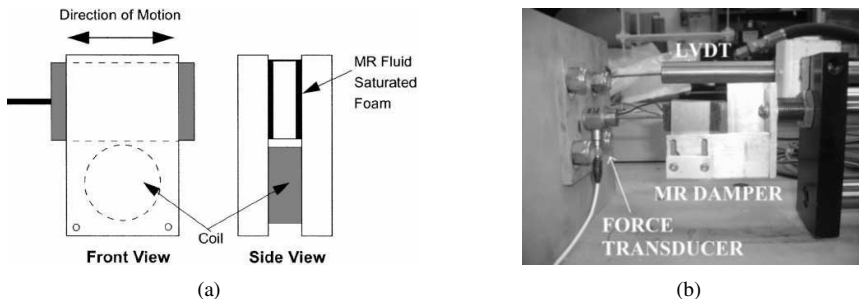


Figure 1. (a) Schematic of the prototype MR damper. (b) Experiment setup.

3. Experiment setup

The experiments to model the MR damper were performed at the Structural Control and Earthquake Engineering Laboratory (Washington University in St. Louis). The MR damper used is a prototype obtained from the Lord Corporation (Cary, N.C.). A schematic of the MR damper is shown in Figure 1(a). It consists of two steel parallel plates, separated by 0.635 cm. A paddle coated with a foam saturated with an MR fluid is placed between the steel plates. The thickness of the paddle used is 0.315 cm. A coil placed in the bottom of the device generates the magnetic field. The dimensions of the device are $4.45 \times 1.9 \times 2.5$ cm. The configuration of the damper allows it to produce forces up to 20 N.

The magnetic field is generated by the current supplied by a pulse width modulator (PWM) circuit whose maximum output is 2 A. This device is voltage-controlled and its input-output relationship is linear.

As shown in Figure 1(b), the MR damper is placed on the piston of a hydraulic actuator. This actuator, 2000 lbf rated, is used to apply forces to the MR damper. A force transducer is placed in series with the damper and a linear variable differential transformer (LVDT) is used to measure the displacement. The velocity is then calculated using a central differences algorithm.

The experiments are carried out as follows: the MR damper is excited with sinusoidal displacements at frequencies between 0.5 and 5 Hz; currents between 0 and 1.6 A ($\sim 0.6 - 4V$); and amplitude displacements between 0.20 and 0.80 cm. Data are sampled at a rate of 256 samples/sec, with null means and the noise is removed with a low pass filter at 80 Hz. Control voltage will be used for describing the models due to its linear relationship with the output current of the PWM circuit.

4. Numerical results

The hysteresis behavior of the damper is readily observed in Figure 2. The force-displacement and force-velocity loops correspond to the response of the damper to a sinusoidal displacement input at 4 Hz and various control voltages. The amplitude of the

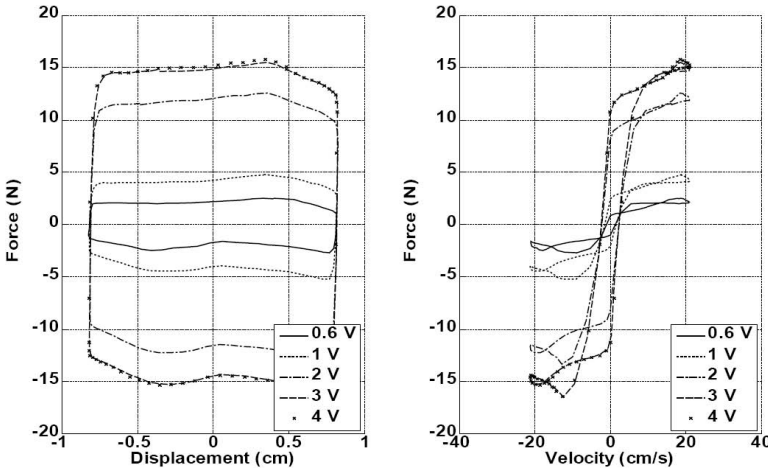


Figure 2. Hysteresis response of the MR damper.

sinusoidal wave is 0.80 cm. The force generated by the damper increases as long as the current through the coil increases until the fluid reaches the magnetic saturation and no higher forces are possible. This occurs when the control voltage is 3 V and higher. The force fluctuations observed in the force-displacement loops as displacement goes from the maximum to the minimum values and vice versa are due to friction in the hydraulic actuator.

In order to evaluate the feasibility of modeling the MR damper with a neural network, it was trained using data representing different frequencies and voltages. The network takes four inputs: displacement, velocity, voltage and force. The forth input (force) is fed back from the output. Additionally, the inputs are stored in memory for a period of time and are updated after each output computation. The structure of the network during the training session is shown in Figure 3(a). This structures allows for fast and more reliable training. Basically, given four inputs, the network must reproduce only the fourth one. The final model is shown in Figure 3(b).

After a trial and error process, it was found that a 3-layer network with 10, 4 and 1 neuron in each layer respectively was able to reproduce a set of experimental data. The transfer function of the neurons of the first and the second layers is a sigmoid tangent and that of the output layer is a purely linear transfer function. The inputs are passed through a 4-units-of-time memory register. The network was trained with a resilient backpropagation algorithm available in MATLAB. As a comparison, the network response to a sinusoidal input at 4 Hz, 0.40 cm amplitude and 3 V is shown in Figure 4(a).

In order to compare these results to those of other models, a parametric approach, the so-called Bouc-Wen model, will be used as a reference. A Bouc-Wen model for this same device has been obtained and its results already reported in [8,9,11,12]. The Bouc-Wen model is based on the physical behavior of the device, including terms that try to approximate the viscosity, friction and hysteresis of the damper. Figure 4(b) shows the response of the MR damper using the Bouc-Wen model, for the same case of a 4 Hz,

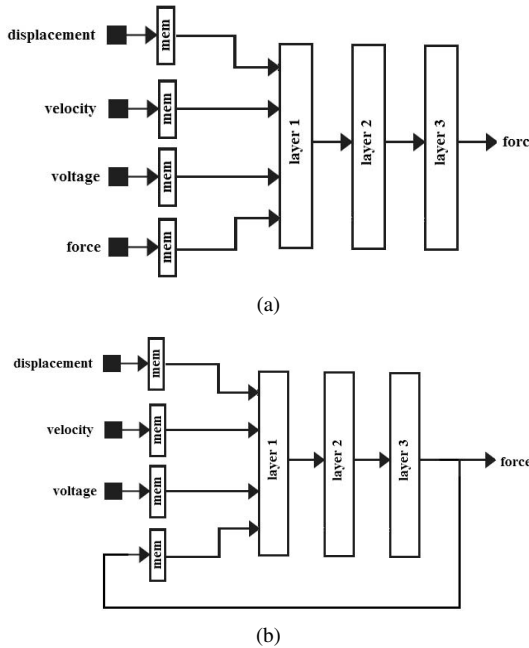


Figure 3. Neural networks: (a) Training structure. (b) Test structure.

0.40 cm amplitude and 3 V sine wave.

The experimental observations show that the response loops are smooth near the zero-velocity region, where the velocity and the acceleration have different signs. The response predicted by the Bouc-Wen model seems no to capture the smoothness, exhibiting some discontinuity in slope at this point. It could be due to mistuning of the parameters or dynamics not considered by the model. The neural network model does capture the smoothness. A numerical comparison is made by means of the error norms between the predicted force and the measured force as a function of time, displacement and velocity as a function of time. Such error norms are given by:

$$E_t = \frac{\varepsilon_t}{\sigma_F} \quad E_x = \frac{\varepsilon_x}{\sigma_F} \quad E_{\dot{x}} = \frac{\varepsilon_{\dot{x}}}{\sigma_F} \quad (1)$$

$$\sigma_F^2 = \frac{1}{F} \int_0^T (F_{exp} - \mu_F)^2 dt \quad (2)$$

$$\varepsilon_t^2 = \frac{1}{T} \int_0^T (F_{exp} - F_{pre})^2 dt \quad (3)$$

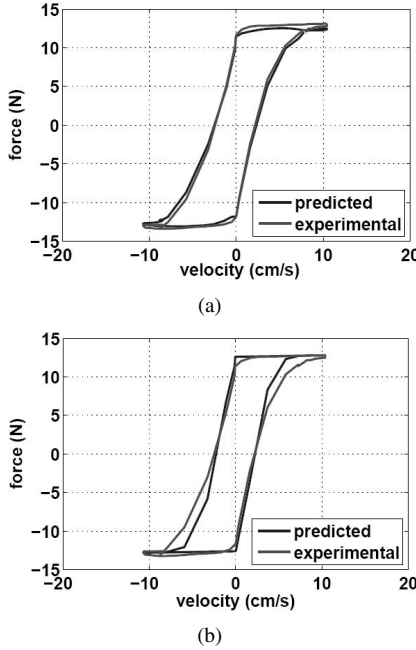


Figure 4. Model response comparison: (a)Neural network. (b) Bouc-Wen model.

Table 1. Error norms of the models studied.

Model	E_t	E_x	$E_{\dot{x}}$
Bouc-Wen	0.0586	0.1205	1.1656
Neural network	0.0301	0.0747	0.3793

$$\varepsilon_x^2 = \frac{1}{T} \int_0^T (F_{exp} - F_{pre})^2 \left| \frac{dx}{dt} \right| dt \quad (4)$$

$$\varepsilon_{\dot{x}}^2 = \frac{1}{T} \int_0^T (F_{exp} - F_{pre})^2 \left| \frac{d\dot{x}}{dt} \right| dt \quad (5)$$

where E_t , E_x and $E_{\dot{x}}$ are the time, displacement and velocity error norms respectively; F_{exp} is the experimental force, F_{pre} is the predicted force and μ_F is the mean of the experimental force. The resulting error norms, shown in Table 1, confirm the visual observations discussed previously. The error norms were calculated using values from a sinusoidal cycle at 4 Hz, 0.40 cm amplitude and 3 V.

5. Conclusions

A neural network model for a magnetorheological damper was obtained based on the experimental information. A 3-layer recurrent network was able to reproduce the hysteretic force-velocity behavior characteristic of these devices. The results were compared to a model based on the physical dynamics of the device which is extensively used in the literature. The superiority of the neural network approach was numerically confirmed. Future work should include the improvement of the network and take into account other kinds of inputs such as random displacements and voltages and the reduction of the complexity of the neural network model.

Acknowledgments

This work has been partially funded by the European Union (European Regional Development Fund) and the Commission of Science and Technology of Spain (CICYT) through the coordinated research projects DPI-2005-08668-C03 and by the Government of Catalonia through SGR00296. The first author acknowledges the FI Grant of the Department for Innovation, University and Enterprise of the Government of Catalonia (Spain). The authors are also grateful to Shirley J. Dyke and Ellen Taylor from the Washington University Structural Control and Earthquake Engineering Laboratory (St. Louis, U.S.A.) for their valuable support during the execution of the experiments.

References

- [1] P.M. Sain, M.K. Sain, and B.F. Spencer. Models for hysteresis and applications to structural control. In *Proceedings of the American Control Conference*, June 1997.
- [2] R. Stanway, J.L. Sproston, and N.G. Stevens. Non-linear modeling of an electrorheological damper. *Electrostatics*, 20:167–184, 1987.
- [3] B.F. Spencer, S.J. Dyke, M.K. Sain, and J.D. Carlson. Phenomenological model of a magnetorheological damper. *ASCE Journal of Engineering Mechanics*, 123:230–238, 1997.
- [4] J. Zhang and P.N. Roschke. Neural network simulation of magnetorheological damper behavior. In *Proceedings of the International Conference on Vibration Engineering*, Dalian, China, August 6-9 1998.
- [5] K.C. Schurter and P.N. Roschke. Fuzzy modeling of a magnetorheological damper using ANFIS. In *The Ninth IEEE International Conference on Fuzzy Systems*, San Antonio, Texas, U.S.A., June 2000.
- [6] H. Du, J. Lam, and N. Zhang. Modelling of a magneto-rheological damper by evolving radial basis function networks. *Engineering Applications of Artificial Intelligence*, 19:869–881, 2006.
- [7] D.H. Wang and W.H. Liao. Neural network modeling and controllers for magnetorheological fluid dampers. In *2001 IEEE International Fuzzy Systems Conference*, 2001.
- [8] M. Zapateiro and N. Luo. Parametric and non-parametric characterization of a shear mode magnetorheological damper. In *3rd International Conference on Mechatronic Systems and Materials 2007*, Kaunas, Lithuania, September 27-29 2007.
- [9] M. Zapateiro, N. Luo, E. Taylor, and S.J. Dyke. Modeling and identification of a class of MR fluid foam damper. In *III ECCOMAS Thematic Conference, Smart Structures and Materials.*, Gdansk, Poland, July 9-11 2007.

- [10] H. Demouth, M. Beale, and M. Hagan. *Neural Network Toolbox for use with Matlab*. Mathworks, 2006.
- [11] M. Zapateiro, N. Luo, E. Taylor, and S.J. Dyke. Experimental identification of a shear-mode MR damper and numerical evaluation of hysteretic models. In *ASME 2007 International Design Engineering Technical Conferences & Computers and Information in Engineering Conference*, Las Vegas U.S.A., September 4-7 2007.
- [12] M. Zapateiro, E. Taylor, S.J. Dyke, and N. Luo. Modeling and identification of the hysteretic dynamics of an MR actuator for its application to semiactive control of flexible structures. In *Proceedings of the SPIE Symposium on Smart Structures and Materials & Nondestructive Evaluation and Health Monitoring*, San Diego, California, U.S.A., March 2007.

Knowledge Discovery in a Wastewater Treatment Plant with Clustering Based on Rules by States

Karina Gibert ¹, Gustavo Rodríguez Silva

Universitat Politècnica de Catalunya

Abstract. In this work we present the advances in the design of an hybrid methodology that combines tools of Artificial Intelligence and Statistics to extract a model of explicit knowledge in regards to the dynamics of a Wastewater Treatment Plant (*WWTP*). Our line of work is based in the development of methodologies of AI & Stats to solve problems of Knowledge Discovery of Data (*KDD*) where an integral vision of the pre-process, the automatic interpretation of results and the explicit production of knowledge play a role as important as the analysis itself. In our current work we approach the knowledge discovery with a focus that we named Clustering Based on Rules by States (*CIBRxE*), which consists in the analysis of the stages that the water treatment moves through, to integrate the knowledge discovered from each subprocess into a unique model of global operation of the phenomenon.

Keywords. clustering, rules, dynamics, states, wastewater

1. Data Presentation

To correctly treat wastewater different operations and unique processes are required. A mixture of physics, chemical and biological agents is needed to form the diagram of the process of each wastewater station. The global process always follows a logical sequence of treatment divided in different stages that can varied according to the structure and objectives of the plant [1]. In this work a sample of 396 observations taken from September the first of 1995 to September the 30th of 1996 from a Catalan *WWTP* are used, corresponding to 40 variables for each daily observation with missing values in some of them [2], table 1. The plant is described daily with measures taken in the following stages of the depuration process: Input(E), Settler(D), Biologic Treatment (B) and Output (S).

According to this, in the database we identified 4 different stages of the depuration process. Table 1 represents a selection of 25 variables considered the most relevant by the opinion of an expert and indicated which variables correspond to each stage of the depuration process. To interpret and conceptualize we considered all variables.

¹Universitat Politècnica de Catalunya, Campus Nord Edif. C5, Jordi Girona 1-3, 08034 Barcelona. Tel.: +34 93 401 73 23; Fax: +34 93 401 58 55; E-mail: karina.gibert@upc.edu

Table 1. Variables used in the Clustering

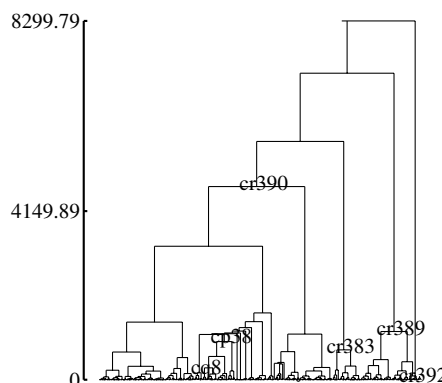
INPUT (E)	SETTLER (D)	BIOREACTOR (B)	OUTPUT (S)
1.Inflow (Q-E)	1.Hydrogen Potential (pH-D)	1.Inflow (QB-B)	1.Hydrogen Potential (pH-S)
2.Iron pre-treatment (FE-E)	2.Suspended Solids (SS-D)	2.Recirculated Inflow (QR-G)	2.Suspended Solids (SS-S)
3.Hydrogen Potential (pH-E)	3.Volatile Suspended Solids (SSV-D)	3.Purge Inflow (QP-G)	3.Volatile Suspended Solids (SSV-S)
4.Suspended Solids (SS-E)	4.Chemical Organic Matter (DQO-D)	4.Aireation (QA-G)	4.Chemical Organic Matter (DQO-S)
5.Volatile Suspended Solids (SSV-E)	5.Biodegradable Organic Matter (DBO-D)	5.Index 30 at the Biological Reactor (V30-B)	5.Biodegradable Organic Matter (DBO-S)
6.Chemical Organic Matter (DQO-E)		6.Mixed Liquor Suspended Solids (MLSS-B)	
7.Biodegradable Organic Matter (DBO-E)		7.Mixed Liquor Volatile Suspended Solids (MLVSS-B)	
		8.Mean Cell Residence Time (MCRT-B)	

2. Previous Work

This data has been previously clustered using Clustering Based on Rules (*CIBR*) with a knowledge base that collects the legal limits of certain physics and biological parameters that classify the quality of wastewater at the plant's exit, see [3] for details on this technique and for comparison with other clustering techniques. *CIBR* is implemented on *KLASS* software [2], this can take advantage of a prior knowledge base to bias classes construction to improve interpretability [3]. The rules base \mathcal{R} is as follows:

- r_1 : If $(SS-S) > 20 \ \& \ (DBO-S) > 35 \longrightarrow S$ (abnormal operation in general)
- r_2 : If $(SS-S) > 20 \ \& \ (DBO-S) < 35 \longrightarrow P$ (failure in suspended solids treatment)
- r_3 : If $(SS-S) < 20 \ \& \ (DBO-S) > 35 \longrightarrow Q$ (failure in organic matter treatment)

Because all variables are numeric, squared euclidean distance and Ward criterion were used and dendrogram of Figure 1 was produced. As usual in hierarchical clustering, the final partition is the horizontal cut of the tree that maximizes the ratio between *heterogeneity* between classes with respect to *homogeneity* within classes, what guarantees the *distinguishability* between classes. Following this classical criterion and validated by the experts, a partition in four clusters was performed $P_4 = \{c383, c389, c390, c392\}$.

**Figure 1.** General tree of the Clustering Based on Rules. $[\tau_{Gi2,R1}^{En,G}]$

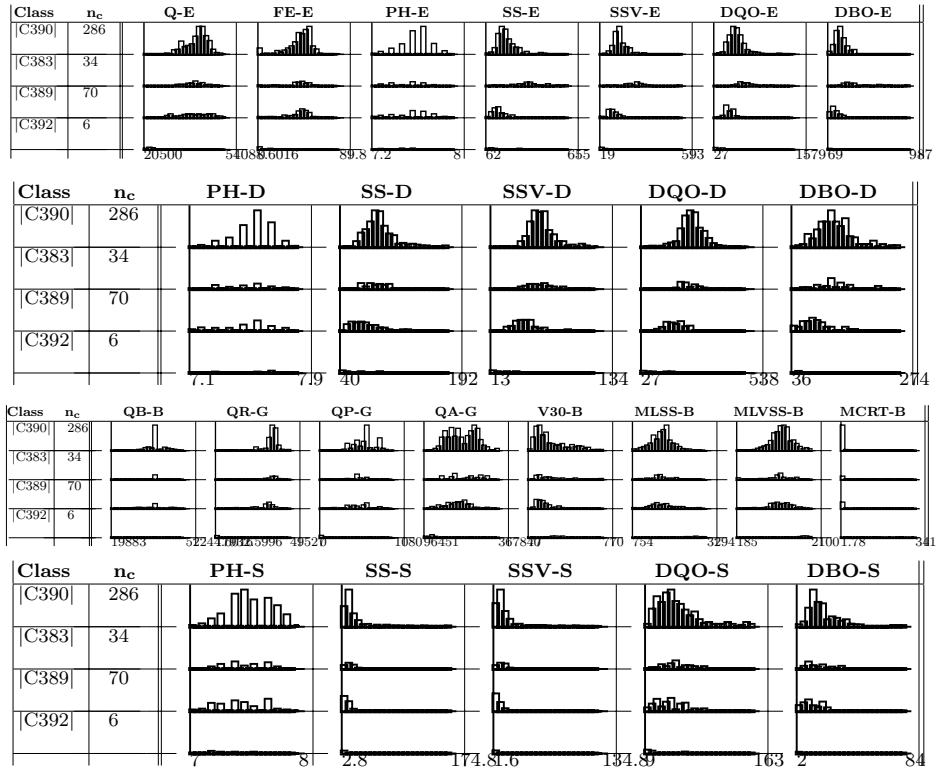


Figure 2. Class Panel Graph of all variables versus Global Clustering in 4 classes $[\tau_{Gi2,R1}^{En,G}]$

It was seen that classes identified different typical situations in the plant [2], where statistics from each class and Class Panel Graph, figure 2 helped us in the interpretation [4]. This interpretation was also supported by the rules-induced with CCCE methodology, that allows to automatically identify one class from the others.

Class C₃₉₂: This class contains many variables with specific values of this class, most of them at low values. Verifying the corresponding dates assigned to C₃₉₂, allowed the experts identify this class as the storm days. To face the storm, the decision is to protect the system minimizing inflow (Q-E), closing input valves and maintaining bioreactor microorganism's trough minimizing purged flow (QP-G). This produces an increment of biomass in the reactor and justifies the high values of (MCRT-B).

Class C₃₈₉: This class has input inflow, recirculated inflow and purge inflow at non-low values, cellular age is not high, on the contrary of C₃₉₂. These days the plant works very well even reduces ammonium (NH4-D y NKT-D lows) in spite of not being a plant specifically designed for this. In addition, the reactor is working a full yield (QB-B high) and the degradation is good (MCRT-B low), as a result the water is so clean. The experts identify this class with a profile of excellent working of the plant.

Class C₃₈₃: In this class, the input inflow, bioreactor inflow, recirculated inflow and purge inflow are lows, cellular age is non-high, ammonium reduction is lower, output flow is no so clean (DBO-S non-low). Contains days where water is very dirty (SS-E, SSV-E, DQO-E and DBO-E highs) as in organic material as in suspended solids. According to the experts exists a shock of load (organic material) of solids in the input of the process, as indicates the volatile suspended solids inside bioreactor are very lows (MLVSS-B).

Class C₃₉₀: The assigned days in this class present some punctual problem, the inflow is not so dirty (as indicated by the low or medium values of SS-E, SSV-E, DQO-E and DBO-E), but suspended solids in biological reactor are higher than expected (MLVSS-B), indicating a non-optimal depuration.

In this work the same data base is analyzed with the hybrid methodology *CLBRxE* which use prior knowledge to bias classes construction by states.

3. Clustering Based on Rules by States (CLBRxE)

Given an environmental domain in which a process is taking place in such a way that it can be divided in $\mathcal{S} = \{e_1 \dots e_E\}$ states or subprocesses, with $\mathcal{I} = \{i_1 \dots i_n\}$ observations described by $X_1 \dots X_K$ variables and given an apriori knowledge base \mathcal{R} , which can be partial, containing logic rules as described in [3], our proposal is:

1. Calculate a rules-induced partition on \mathcal{I} by evaluating \mathcal{R} over $X_1 \dots X_K$ ($\mathcal{P}_{\mathcal{R}}$).
2. Divide the variables based on the subprocess to which they refer (let $X_1^e, \dots, X_{K_e}^e$ be the set of variables referring to the subprocess e).
3. For each subprocess $\mathcal{S} = \{e_1 \dots e_E\}$:
 - a Do $\mathcal{IDe} = \{i \in \mathcal{I} : x_{i1}^e = x_{i2}^e = \dots = x_{iK_e}^e = *\}$
 - b Do a *CLBR* [3] over $\mathcal{I} \setminus \mathcal{IDe}$ with variables referring to state e $X_1^e, \dots, X_{K_e}^e$ but using $\mathcal{P}_{\mathcal{R}}$ as a rules-induced partition for all the states of the process. Elements of \mathcal{IDe} can not be used in state e since they miss useful information.
 - c Analyze the resulting dendrogram τ^e , perform an horizontal cut to obtain \mathcal{P}_e^* and associate concepts to each resulting class $\mathcal{C} \in \mathcal{P}_e^*$.
 - d Construct $\mathcal{P}_e = \mathcal{P}_e^* \cup \{\mathcal{IDe}\}$
4. Construct cross tables $\mathcal{P}^e \times \mathcal{P}^{e+1}$ applying required delay if any between observations and analyze most probable trajectories of water through classes of sequential states. Crossing can be done at different stages of the process by considering that the wastewater that is in Bioreactor delay some time till the exit. Thus, cell C, C' of the cross table contains the number of elements that $x_{(i-d)K_e} = C$ and $x_{iK_{e+1}} = C'$ instead of $x_{iK_e} = C \wedge x_{iK_{e+1}} = C'$ where d is the delay of the water from state e to $e + 1$. Delays between steps are to be provided by experts. This information allows wider analysis of the dynamics of the process and we are studying if this approach can give richer models than the instantaneous conjoint global analysis of all phases performed previously.
5. Identify trajectories related to information's flow between the $\mathcal{S} = \{e_1 \dots e_E\}$ subprocess and interpret trajectories.

4. Knowledge discovery in Wastewater Treatment Plant with CIBRxE

In our methodology \mathcal{R} is evaluated on \mathcal{I} and a partition is induced $\mathcal{P}_{\mathcal{R}} = \{S, P, Q, Residual\}$. S contains 11 elements of \mathcal{I} that satisfy r_1 , P contains 40 elements of \mathcal{I} that satisfy r_2 , Q contains 10 elements of \mathcal{I} that satisfy r_3 and Residual contains 335 elements of \mathcal{I} that do not satisfy any rule or many at the same time which are contradictory. Each stage is treated separately then the relationship between subprocesses is analyzed. It is important here to remark that the number of classes is identified a posteriori for each subprocess upon the resulting dendrogram.

Input Subprocess. 7 variables are available: Q-E, FE-E, PH-E, SS-E, SSV-E, DQO-E, DBO-E. All prototypes will be calculated for each rules-induced partition in the previous step. We will manually construct an extended residual class that includes those prototypes in addition to residual objects. Finally, we perform a clustering without rules of the extended residual class with the following criteria: Normalized euclidean quadratic metric, since all the variables are numerical in this application. Wards linkage criteria, which is equivalent to perform a *CIBR* of the Input variables using a knowledge base that includes variables from another state. This is a technical solution to be used in the meanwhile, statistical software *KLASS* is modified to include this case. The tree τ_E of clustering process is shown in Figure 3. Analyzing this tree a partition of 5 classes was performed and the corresponding Class Panel Graph is shown in figure 4. With these elements some concepts can be related to each class. \mathcal{P}^E :

C331 wastewater at normal level [(Q-E)High], [(FE-E)(SS-E)(SSV-E)(DQO-E)(DBO-E)Medium]

C330 a lot of dirty wastewater [(PH-E)Low]

C328 a lot of wastewater with low pollution [(Q-E)High], [(FE-E)Medium], [(SS-E)(SSV-E)(DQO-E)(DBO-E)Low]

C318 a few inflow [(Q-E)Medium], [(DQO-E)Low]

C329 low degree of FE [(FE-E)(DQO-E)Low]

Settler Subprocess. 5 variables are available: PH-D, SS-D, SSV-D, DQO-D, DBO-D. We proceed on the same way as in the Input stage. The tree τ_D of clustering process is shown in figure 3. Analyzing this tree a partition of 5 classes was made and figure 4 shows the corresponding class panel graph. Some concepts could be related to each class. \mathcal{P}^D :

C328 medium levels of SS, SSV [(SS-D)Medium, (SSV-D)Medium, (DQO-D)Medium, (DBO-D)Medium]

C312 low level of pH [(SS-D)Low, (DQO-D)Low]

C327 low level of SS [(pH-D)High, (SS-D)Low, (DQO-D)Low]

C323 high levels of SSV, DBO [(SS-D)High, (SSV-D)High, (DQO-D)High, (DBO-D)High]

C322 high levels of SS, DQO [(pH-D)High, (SS-D)High, (DQO-D)High]

Bioreactor Subprocess. 8 variables are available: QB-B, QR-G, QP-G, QA-G, V30-B, MLSS-B, MLVSS-B, MCRT-B. We proceed on the same way as in the Input stage. The tree τ_B of clustering process is shown in figure 3. Analyzing this tree a partition of 5 classes was made and figure 4 shows the corresponding class panel graph. With these elements some concepts could relate to each class. \mathcal{P}^B :

C326 clean wastewater with high aeration [(QP-G)High, (QA-G)High, (V30-B)Low, (MLSS-B)Low]

C332 clean wastewater with low aeration [(QA-G)Medium, (V30-B)High, (MLSS-B)Low]

C324 clean wastewater with medium purge [(QP-G)Medium, (QA-G)High, (V30-B)Low, (MLSS-B)Low]

C325 dirty wastewater with high of aeration [(QA-G)High, (V30-B)High, (MLSS-B)High]

C333 protected bioreactor [(QB-B)Low, (QR-G)Low, (QP-G)Low, (QA-G)Low, (MLSS-B)High, (MLVSS-B)High, (MCRT-B)High]

Output Subprocess. 5 variables are available: PH-S, SS-S, SSV-S, DQO-S, DBO-S. The rules provided by the expert affected the variables that are used in this stage, therefore we directly realized *CIBR* with the following criteria: Normalized euclidean Squared Metric, Linkage Wards Criteria. The tree τ_S of clustering process is shown in figure 3. Analyzing this tree a partition of 5 classes was made and figure 4 shows the corresponding class panel graph. Some concepts could relate to each class. \mathcal{P}^S :

C373 very clean water [(pH-S)Low, (DQO-S)Low, (DBO-S)Low]

C374 clean water with high pH [(pH-S)High, (DQO-S)Low]

C375 water medium quality [(pH-S)Low, (DQO-S)Medium, (DBO-S)Medium]

C376 dirty water with high DQO [(pH-S)High, (DQO-S)High]

C370 dirtier water [(DQO-S)High, (DBO-S)High]

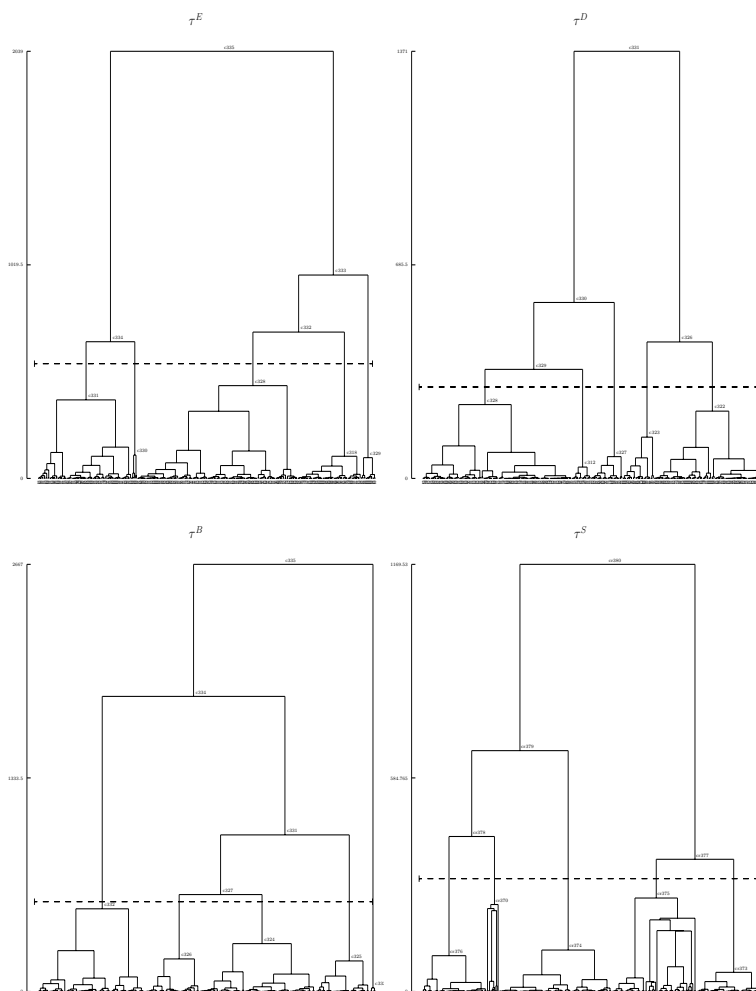


Figure 3. (τ^E) , (τ^D) , (τ^B) and (τ^S) partition in 5 Classes

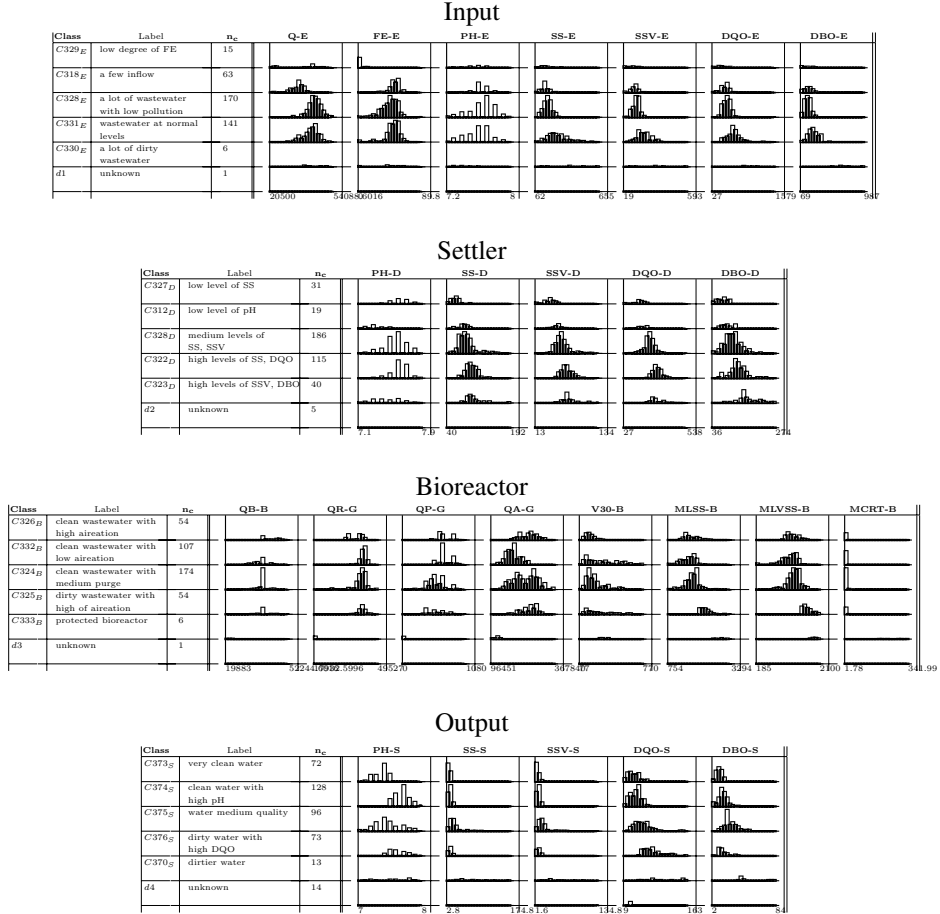


Figure 4. Class Panel Graph of (\mathcal{P}^E) , (\mathcal{P}^D) , (\mathcal{P}^B) and (\mathcal{P}^S)

5. Integration

Once the typical situations in each stage of the process are identified, we proceed to study the transit of the wastewater from one stage to the next. The starting point will be the crossing between the partition of two consecutive stages. On this specific application we worked with daily averages and wastewater keeps only few hours at each stage. According to this we did not need to apply a delay between stages before we perform the crossing. In other applications were we worked with hourly data we used this possibility. Table 2 shows the frequencies of the Settler stage conditioned by the Input stage, for example shows that dirty water hardly ever comes out of the plant when the Bioreactor is functioning correctly ($f_{C324_B, C370_S} = 0.0632$) or that the tendency to exit water with higher concentration of DQO increases when the Bioreactor has sedimentation problems.

Table 2. Frequencies of state conditioned by $(\mathcal{P}^D \mid \mathcal{P}^E)$, $(\mathcal{P}^B \mid \mathcal{P}^D)$ and $(\mathcal{P}^S \mid \mathcal{P}^B)$

$E \setminus D$	C327	C312	C328	C322	C323	d2	tot.	useful	$D \setminus B$	C326	C332	C324	C325	C333	d3	tot.	useful
C329	0.2667	0.0667	0.2	0.2667	0.1333	0.0667	1	15	C327	0.1613	0.3226	0.2903	0.0968	0.129	0	1	31
C318	0.1429	0.0635	0.4762	0.2698	0.0317	0.0159	1	63	C312	0.1579	0.1053	0.5263	0.1579	0.0526	0	1	19
C328	0.0941	0.0706	0.4588	0.3059	0.0588	0.0118	1	170	C328	0.1882	0.1882	0.4946	0.1237	0.0054	0	1	186
C331	0.0142	0.0142	0.5319	0.2768	0.1631	0	1	141	C322	0.087	0.4174	0.3564	0.1391	0	0	1	115
C330	0	0	0	0.5	0.5	0	1	6	C323	0.025	0.225	0.525	0.225	0	0	1	40
d1	0	0	0	0	0	1	1	1	d2	0	0.6	0.2	0	0	0.2	1	5
margin	0.0783	0.048	0.4697	0.2904	0.101	0.0126	1	396	margin	0.1364	0.2702	0.4394	0.1364	0.0152	0.0025	1	
useful	31	19	186	115	40	5			useful	54	107	174	54	6	1		396

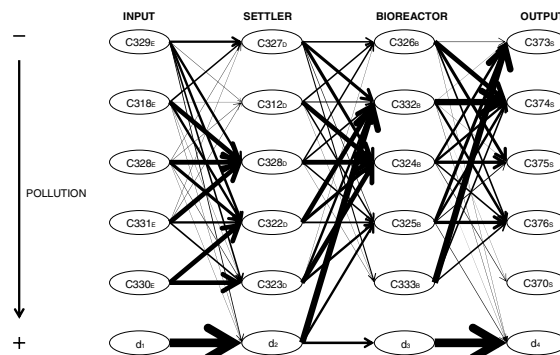
$B \setminus S$	C373	C374	C375	C376	C370	d4	tot.	useful
C326	0.1111	0.4074	0.3148	0.1296	0	0.037	1	54
C332	0.0654	0.5701	0.0654	0.243	0.0187	0.0374	1	107
C324	0.2126	0.1839	0.3851	0.1322	0.0632	0.023	1	174
C325	0.3333	0.2222	0.0926	0.2963	0	0.0556	1	54
C333	0.6667	0.1667	0	0.1667	0	0	1	6
d3	0	0	0	0	0	1	1	1
margin	0.1818	0.3232	0.2424	0.1843	0.0328	0.0354	1	
useful	72	128	96	73	13	14		396

We are analyzing this tables with experts to obtain as much information as possible when classes of each subprocess has been previously interpreted, as it is the case, the tables can be the input for:

- a A probability knowledge base.
- b A transition graph.
- c A Bayesian network.

In figure 5 the transition graph derived from table 2 is shown, classes identified for each subprocess are aligned from cleaner water at the top to more polluted water at the bottom. Transition probability is visualized with the thickness of arrows. Currently, we are studying which of the mentioned possibilities contributes to a better support for building an IEDSS model for the plant. Figure 5 shows the most probable transitions of wastewater along the water treatment process. For example, when the water is really dirty in the Input ($C330_E$) it never moves into a protected Bioreactor ($C333_B$), etc.

In addition, we are studying most probable trajectories of wastewater, being a trajectory the sequence of classes of wastewater through the steps of the process. For example, wastewater flows from $C331_E$ to $C328_D$ to $C324_B$ and $C375_S$ on 12-IX-1995, where $C331_E \in \mathcal{P}_E$, $C328_D \in \mathcal{P}_D$, $C324_B \in \mathcal{P}_B$ y $C375_S \in \mathcal{P}_S$. What means that water has normal levels of pollutants at the entry, still keeps medium levels of solids in the settler, water is clean with medium purge in the bioreactor and exits with medium quality.

**Figure 5.** Transition Diagram between states

This information, regarding the dynamics of the process, is richer than static information originally obtained from a global *CIBR* without considering the structure in subprocesses of the target phenomena. In the cases where the delay of the observations is important this approach could be more adequate because global *CIBR* just permits to identify situations in which the plant may be at moment but does not permit to study the evolution of the wastewater treatment process itself.

6. Conclusions

Automatization and semi-automatization of the knowledge extraction can improve the decision-making process in an *IEDSS* reducing the decision time and assisting decision makers in the evaluation of alternatives. In this work, we applied an hybrid tool of AI and Stats as an alternative for knowledge discovery of a *WWTP*. The automatic interpretation of results and the explicit production of knowledge play a role as important as the analysis itself [5]. *CIBRx E* is designed in such a way that prior knowledge of the experts is integrated into the analysis to improve the quality of the clustering processes. Analysis is performed step by step and final integration permits construction of models for dynamics behavior of the plant in qualitative terms. Dynamics of Wastewater treatment is very difficult to model by classical methods and here combination of statistics and knowledge bases and transition graphs provides a nice frame to face modelling. The design of a methodology for dynamic analysis by subprocesses to obtain knowledge about the process is complementary to the identification of characteristic situations in a *WWTP* which was done by global cluster with all variables in previous works. *CIBRx E* allows to analyze trajectories of wastewater along the treatment process as well as to predict the plant's evolution, in the short or mid-term, identifying the most typical trajectories to be observed. Linking this to the characteristic situations previously identified provides a knowledge that improves the decision-making support. We are formalizing this methodology and we are developing a technique focused on most significative trajectories of the transition graph to the automatic generation of the correspondent characterization.

7. Acknowledgments

This research has been partially financed by TIN 2004-01368

References

- [1] Metcalf and Eddy, Inc., *Wastewater engineering treatament. Disposal and reuse*,4th Ed. revised by George Tchobanoglou McGraw Hill, 2003.
- [2] Gibert, K., Roda, I., *Identifying characteristic situations in wastewater treatment plants*, In Workshop in Binding Environmental Sciences And Artificial Intelligence ECAI vol. 1, 2000.
- [3] Gibert, K. *The use of symbolic information in automation of statistical treatment for ill-structured domains*. *AI Communications*, 9(1):36–37, 1996.
- [4] Gibert, K., Nonell, R., Velarde, J. M., Colillas, M. M., *Knowledge Discovery with clustering: Impact of metrics and reporting phase by using KLASS*, Neural Network World, 2005.
- [5] Fayyad, U., Piatetsky-Shapiro, G., Smyth, P., Uthurusamy, R., *Advances in Knowledge Discovery and Data Mining*, AAAI Press, 1996.

Forecasting New Customers' Behaviour by Means of a Fuzzy Unsupervised Method¹

Germán SÁNCHEZ^{a,b,2}, Juan Carlos AGUADO^c and Núria AGELL^a

^a *ESADE-URL. Avda. Pedralbes, 60-62. 08034 Barcelona*

e-mail: {german.sanchez,nuria.agell}@esade.edu

^b *ESAIU-UPC. Avda. Diagonal, 647. 08028 Barcelona*

^c *ESAIU-UPC. Avda. del Canal Olímpic, s/n. 08860 Castelldefels*

e-mail: juan.carlos.aguado@upc.edu

Abstract. The use of unsupervised fuzzy learning classifications techniques allows defining innovative classifications to be applied on marketing customer's segmentation. Segmenting the clients' portfolio in this way is important for decision-making in marketing because it allows the discovery of hidden profiles which would not be detected with other methods. Different strategies can be established for each defined segment. In this paper a case study is conducted to show the value of unsupervised fuzzy learning methods in marketing segmentation, obtaining fuzzy segmentations via the LAMDA algorithm. The use of an external decision variable related to the loyalty of the current customers will provide useful criteria to forecast potentially valuable new customers. The use of the introduced methodology should provide firms with a significant competitive edge, enabling them to design and adapt their strategies to customers' behaviour.

Keywords. Fuzzy connectives, unsupervised learning, marketing applications, loyalty forecast

1. Introduction

The objective of Relationship Marketing is to build and develop long-term relationships between a company and each of its customers. In order to shape loyal customers, marketers must ensure that the company is increasingly responsive to customer's demands and is able not only to meet customer expectations but also to anticipate customer needs.

Customers are more demanding every day, and if companies are to compete successfully in the marketplace, they need to design and introduce new ways to offer customer value. However, the process is not complete until they: design control systems; provide a support decision tool able to identify and distinguish customer behaviour profiles ac-

¹This work has been partially supported by the MEC (Spanish Ministry of Education and Science), AURA Projects (TIN2005-08873-C02-01) and (TIN2005-08873-C02-02).

²Correspondence to: Germán Sánchez, Avda. Pedralbes, 60-62. 08034 Barcelona, Spain.
Tel.: +34 93 280 61 62; Fax: +34 93 204 81 05; E-mail: german.sanchez@esade.edu.

cording to their loyalty; and help marketers readapt Relationship Marketing Strategies in order to increase efficiency.

Firms that commercialize their products via other firms ("sell to other firms") are known as B2Bs (or business-to-business companies). One of the main challenges for these firms is knowing and understanding the behaviour of the businesses that later sell their products. The distribution of these products is directly affected by the interest and the performance of the points of sale or specialized shops.

For this reason, knowing and understanding how each point of sale behaves is crucial to designing marketing strategies. In this sense, the use of segmentation techniques in the B2B market allows us to determine groups to which the mentioned strategies can be directed. Segmentation in the B2B environment is complex due to the need to consider not only the characteristics of the points of sale but also their relationship with the buyer, the one who ultimately opts for the product.

The objective of this paper is to show the utility of the unsupervised learning techniques applied in marketing segmentation. In particular, the LAMDA algorithm (Learning Algorithm for Multivariate Data Analysis) [1,2] is used. Also, an index to determine the optimal classification according to an external variable is defined and applied in the case study. This article examines the ability of the LAMDA classifier in predicting new customers' behaviour.

The study carried out in this project is based on data gathered from a Spanish firm, Textil Seu, S.A. (with Grifone as trademark), specialized in outdoor sporting equipment and clothing that operates in a B2B environment.

The paper is structured as follows: Section 2 is a brief introduction to the theoretical framework. Section 3 states the experimental case, interpreting the results obtained and drawing conclusions. The paper concludes with Section 4, which makes proposals for future research.

2. Theoretical Framework

In classical segmentations, the concept of similarity between individuals has usually been considered as the main reason for their allocation to a given segment. However, this paper introduces the concept of *adequacy*, a term used to describe how well a customer fits in a given segment.

2.1. Adequacy Degree

This concept of adequacy can be used to associate to each one of the patterns a vector of values between 0 and 1. Each one of its components can be considered a degree of membership to each one of the considered segments (classes). This characteristic is very helpful in Marketing strategies, because analysts would know not only the customers belonging to a chosen segment, but also all the customers with an adequacy degree over a prefixed landmark (alfa-cuts in fuzzy terminology).

2.2. The LAMDA Algorithm

LAMDA is a hybrid connectives-based classification method that combines some of the most interesting capabilities of both purely numeric and purely symbolic algorithms. In

order to do so, both employ the interpolation capabilities of logic operators over fuzzy environments [6].

A linearly compensated hybrid connective is an interpolation between a t-norm and its dual t-conorm ($H = \beta T + (1 - \beta)T^*$). It can be noted that for $\beta = 1$, the t-norm is obtained and, for $\beta = 0$, the t-conorm is the result. Taking into account that the t-norms are fuzzy operators associated to an intersection or conjunction and the t-conorms are associated to a union or disjunction, the parameter β determines the exigency level of the classification. Obviously, we can define $\lambda = 1 - \beta$ as the tolerance level of a given classification.

In this work, the LAMDA algorithm is employed as a classifier. It was developed by Josep Aguilar in collaboration with a series of authors [1,2,3] as an original technique in which the input data are the values that a set of observations exhibit for a number of descriptors. Each of these descriptors within the database can be either qualitative (a linguistic label) or quantitative (numerical). The basic LAMDA learning operation is depicted in Figure 1:

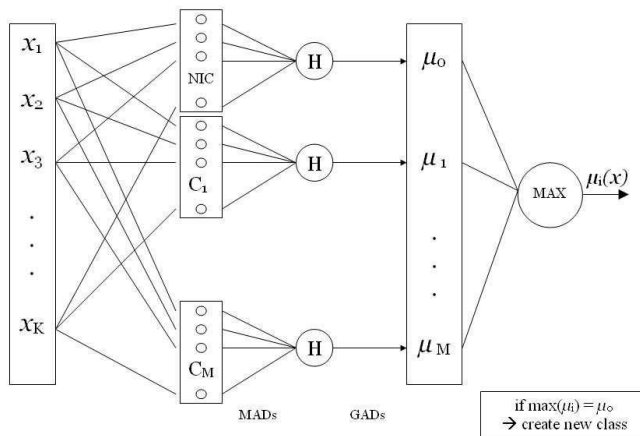


Figure 1. Hybrid Connectives-based Classification

MAD and GAD stand for the Marginal Adequacy Degree and Global Adequacy Degree, respectively, of each individual to a given class. MAD is computed for each descriptor, class and individual, and these partial results are aggregated by means of the hybrid connectives H to supply the GAD of an individual to a class. LAMDA exhibits greater flexibility than neural networks, for example, in its ability to perform either a supervised or an unsupervised learning process indistinctly and its capability to combine pattern recognition with a simple, non-iterative class upgrading.

Whenever the unsupervised learning LAMDA capabilities are employed, the first individual is always placed in a class by itself. Subsequent individuals can then be assigned to the already existing class(es) or a new one is created. In order to determine when this occurs, the algorithm generates, first of all, a special class called NIC (Non-Informative Class) which represents maximum entropy, with the characteristic of returning the same

(low) GAD for every possible individual. As such, the decision-making process consists of comparing the GAD of the individual to the NIC class with the GADs to every other existing class. If one of the real classes returns the maximum GAD, the new individual will be assigned to it and the class will be modified accordingly. But if the NIC is the one with the highest GAD, this means that none of the existing classes are close enough to the individual and so a new class has to be created by the LAMDA algorithm.

The generated classification by unsupervised learning depends, on the one hand, on the hybrid connective employed and, on the other hand, on the selected exigency or tolerance level (also on the assumed distribution for numerical descriptors). Maximum exigency means that an individual will be assigned to a class only if every descriptor points to this, whereas a minimum exigency implies that the individual will be assigned to the class if this is indicated by at least one of the descriptors. Any in-between exigency degree is possible, and our algorithm is able to automatically explore these and generate every possible partition.

Additionally, the obtained results are not only a classical partition. The algorithm returns the Global Adequacy Degree for every individual to each class, that is, a fuzzy partition. These results enable marketing experts to further explore a whole set of possible solutions.

2.3. Selecting a classification

The use of unsupervised learning algorithms allows suggesting segmentations that, in principle, are not trivial. In this sense, behavioural patterns or “interesting” profiles can be established by using this type of algorithm and they may reveal new profiles not known by the experts. In an area of application such as marketing, finding new and creative solutions is worthwhile because these allow for the definition of new marketing strategies. However, when a large amount of different segmentations are obtained, how do we choose the one that really adjusts to the proposed objective?

The use of an external variable, called *decision variable* and chosen by some experts, is considered in this paper to select a classification. A high dependency on the decision variable will mean that the classification discriminates the feature described by the decision variable.

The dependency degree of a classification on a decision variable is defined by means of the value of the statistic χ^2 computed via the contingency table (Table 1), where $C_1 \dots C_i \dots C_M$ represent the classes of the considered segmentation, $D_1 \dots D_s \dots D_S$ the values of the external variable and q_{is} the number of observations that take the D_s value in C_i class.

If we take, for example, e_{is} as the expected frequency obtained when the variable is independent of the classification, i.e.:

$$e_{is} = \frac{M_{i+} \cdot M_{+s}}{N} \quad (1)$$

the statistic χ^2 is determined through the expression:

$$\chi^2 = \sum_{i=1}^N \sum_{s=1}^S \frac{(q_{is} - e_{is})^2}{e_{is}}. \quad (2)$$

Class	Descriptors or intervals				Total classes
	D_1	D_2	\dots	D_S	
C_1	q_{11}	q_{12}	\dots	q_{1S}	M_{1+}
\dots	\dots	\dots	\dots	\dots	\dots
C_i	q_{i1}	q_{i2}	\dots	q_{iS}	M_{i+}
\dots	\dots	\dots	\dots	\dots	\dots
C_M	q_{M1}	q_{M2}	\dots	q_{MS}	M_{M+}
Total descriptors	M_{+1}	M_{+2}	\dots	M_{+S}	N

Table 1. Contingency Table

For each classification, the dependency of the decision variable is studied, and those classifications that have a high dependency on this external variable will be chosen. For this reason the statistic χ^2 has to exhibit a high value.

It is important to note that this criterion can be used directly when the decision variables are qualitative. In the case of quantitative decision variables, it is advisable to previously discretize them into intervals (D_s). For each problem, the discretization criterion will be specifically chosen [5,7].

Because the range of values of χ^2 can change according to the number of classes of the segmentation, a modification of Tschuprow's coefficient [9] is used to calculate the *Indicator of Relation with the Decision Variable*:

$$I_R = \frac{\chi^2}{\sqrt{M - 1}} \quad (3)$$

where M is the number of classes of this segmentation.

3. An application to forecast customers' behaviour

3.1. Problem presentation

The problem addressed in this paper is framed within to a broader project in which Artificial Learning techniques are applied to a field where there has been few contributions to date: market segmentation [4]. In particular, this paper presents a preliminary study evaluating the efficiency of the LAMDA classifier in designing segmentations for B2B environments. The global objective is to create an application capable of identifying and classifying points of sale which will enable appropriate marketing strategies to be defined. To this end a survey to 650 outdoor sporting equipment stores distributed all over Spain was conducted.

The LAMDA algorithm has been used to detect a segmentation reflecting the potentiality of new points of sale as Grifone customers. Among the 650 stores to whom the survey was administered, there were 157 that were already customers of Grifone and the rest where the potential ones.

The number of current customers, i.e. those whose behaviour was known, was too small to consider a supervised learning. For this reason, an unsupervised learning process was performed and the chosen segmentation was the one grouping together a higher number of current loyal customers.

3.2. Data set construction

From the responses obtained by means of the telephonic survey, a database containing information about a group of 217 shops was obtained. Each of the points of sale was considered as an individual pattern and it was described by means of the variables defined in Table 2.

Scale	Feature	Description	Range
Nominal	Physical desc.	Shop size vs. display window size	AA/BB, AB, BA
		Shop size vs. n. of sales assistants	AA/BB, AB, BA
		Point of sale display	No, Yes-little, Yes-much
	Promot. activities	Promotional events	No, Yes
		ISPO: Int. trade Show for Sports Equipment and Fashion	No, Yes
	Sales impact	Best product line	coats, skins, trousers, underwear
Ordinal	Clients sensitivity	Fashion sensitivity	Low, Medium, High
		Technology sensitivity	Low, Medium, High
		Price sensitivity	Low, Medium, High
	Loyalty	Sales increase	A, B, C

Table 2. Description of Variables

All the variables considered were qualitative. The first group, measured on a nominal scale, contained variables describing physical features of the point of sale, the interest of the responsible in attending promotional activities of the sector and the type of product with higher sales impact. The second group, measured on an ordinal scale, included variables describing the clients sensitivity in terms of fashion, technology and price. Finally, the variable *Sales increase* obtained by a discretization of the increment of sales volume over a 12-month period was included for current customers. According to the company marketing experts the landmarks considered to discretize the variable were -15% and 30%.

Thanks to the unsupervised learning capabilities of the LAMDA algorithm, a variety of segmentations were obtained but it was not trivial how to assess those segmentations.

It should be noticed that the variable *Sales increase* was not used in the automatic learning process. From the results obtained by the LAMDA algorithm in its version of unsupervised learning, the criterion defined in the previous section 2.3 was applied to choose the points of sale's optimal classification using the variable *Sales increase* as a decision variable.

3.3. Experimental results

Taking advantage of LAMDA's unsupervised learning capability, 57 classifications were obtained, 50 of which reached stability before the fixed maximum number of iterations. The parameters used in this process were the following:

Fuzzy Hybrid Connectives: only connectives with $T = \min$ have been considered [8].

Tolerance: an automatic tolerance level was fixed by employing the unsupervised learning capability of LAMDA.

Maximum Variability: a 0 percent variability (the number of individuals that change assignation classes between iterations) was chosen to ensure the stability of the obtained segmentations.

Maximum Number of Iterations: 10 iterations were chosen to ensure a maximum number of stable segmentations.

Obtained segmentations with more than 5 classes were discarded due to their unmanageability, thus reducing the set of classifications to 6. Table 3 shows the composition of each one of the classifications including the number of pattern in each class.

Classif.	Class 1	Class 2	Class 3	Class 4	Class 5	I_R
# 27	75	55	83	3	1	10.03
# 28	76	55	83	3		8.61
# 29	77	121	19			2.95
# 30	77	127	13			1.84
# 31	61	156				2.09
# 32	153	64				2.10

Table 3. Final Classifications considered

Computing the value of indicator I_R defined in (3), section 2.3, permits to select classification #27 as the one that better discriminates the decision variable. In our case, this means that this segmentation groups in a single segment a large number of clients of Type A.

Class	Type "A"	Type "B"	Type "C"
1	24	7	7
2	6	7	8
3	10	6	11
4	1	0	0
5	0	0	0

Table 4. Distribution of the current customers in segmentation #27

Segmentation #27 has 5 classes and class 1 contains most of the Type A current customers previously selected.

As a result, marketing strategies will be focused on all the shops belonging to the segment 1. A descriptive analysis of this segment 1 would previously be done to define specific marketing actions. In addition, the fuzzy nature of the LAMDA algorithm will allow to know for each one of the potential customers the degree of adequacy to segment 1. Thanks to that, a specific marketing strategy could be addressed to all customers that exhibit a degree of adequacy to segment 1 higher than a fixed value.

4. Conclusions and Future Work

In conclusion, the use of the unsupervised capability of the LAMDA algorithm has released potential applications in the Marketing field. One of the firms' main goal is to find new loyal customers. One way of doing this is by using knowledge of their customers' behaviour to be closer to them. The adaptability and dynamic adjustment capability of the LAMDA algorithm will allow dealing in an effective way with the ever-changing customer behaviour.

As future work, it is planned to use expert knowledge to enlarge the description of each customer. The information about customers provided by sales representatives, considered as experts on customers' behaviour, will be very valuable and will surely improve the significance and validity of the results obtained.

It is important to highlight that the information obtained in this study will help the company decide the commercial policy, avoiding usual segmentation based on demographic or geographic criteria. In fact, the empirical results obtained in this research were presented to the company and real commercial actions are being developed and applied.

Additionally, to improve marketing and sales management, two new actuation lines should be developed. On the one hand, a systematization of the segmentation process presented above in order to periodically adapt the marketing strategies. On the other hand, taking further advantage from the fuzzy segmentation and description provided by the LAMDA algorithm, when analyzing the customers' dynamic behaviour.

Acknowledgments

The support from Textil Seu, S.A. (Grifone, <http://www.grifone.com>), is gratefully acknowledged.

References

- [1] J. C. Aguado. *A Mixed Qualitative-Quantitative Self-Learning Classification Technique Applied to Situation assessment in Industrial Process Control*. PhD thesis, Universitat Politècnica de Catalunya, 1998.
- [2] J. C. Aguado, A. Català, and X. Parra. Comparison of structure and capabilities between a non-standard classification technique and the radial basis function neural networks. In *Proceedings of the 13th European Simulation Multiconference (ICQFN 99)*, volume II, pages 442–448, Warsaw, Poland, 1999.
- [3] J. Aguilar and R. López de Mántaras. The process of classification and learning the meaning of linguistic descriptors of concepts. *Approximate Reasoning in Decision Analysis*, pages 165–175, 1982.
- [4] I. Alon, M. Qi, and R.J. Sadowski. Forecasting aggregate retail sales: a comparison of artificial networks and traditional methods. *Journal of Retailing and Consumer Services*, 8(3):147–156, 2001.
- [5] J. Dougherty, R. Kohavi, and M. Sahami. Supervised and Unsupervised Discretization of Continuous Features. In *Machine Learning: Proceedings of the 12th International Conference*, San Francisco, CA., 1994.
- [6] J.G. Klir and B. Yuan. *Fuzzy sets and fuzzy logic, Theory and Apps*. Pr. Hall, 1995.
- [7] L. A. Kurgan, and K. J. Cios. CAIM discretization algorithm. In *Knowledge and Data Engineering, IEEE Transactions on*, volume 16, issue 2, pages 145–153, 2004.
- [8] C. Olmo, G. Sánchez, F. Prats, and N. Agell. Linearly Compensated Hybrid Connectives for Customers Patterns Segmentation. In *Actas del Taller “Inteligencia Computacional: aplicaciones en marketing y finanzas”, Caepia 2005*, pages 19–24, Nov. 2005.
- [9] A. A. TSchuprow, and M. Kantorowitsch. Principles of the mathematical theory of correlation. In *Journal of the American Statistical Association*, volume 34, number 208, page 755, December 1939.

Integrating a Feature Selection Algorithm for Classification of Voltage Sags Originated in Transmission and Distribution Networks

Abbas Khosravi ^{a,1}, Toni Martinez ^a, Joaquim Melendez ^a, Joan Colomer ^a and
Jorge Sanchez ^b

^a *eXiT Group, Dept. of Electronics, Informatics and Automatics, University of Girona*

^b *ENDESA Distribucion, Barcelona, Spain*

Abstract. As a global problem in the power quality area, voltage sags are matter of high interest for both utilities and customers. With a view to resolving the problem of sag source location in the power network, this paper introduces a new method based on dimension reduction capability of Multiway Principal Component Analysis (MPCA). MPCA models are developed using three dimensional databases of voltage and current Root Mean Square (RMS) values. Computed scores are then used for training commonly used classifiers for putting sags in two classes. A feature selection algorithm is successfully applied for determining the optimal subsets of scores for training classifiers and also the number of principal components in the MPCA models. The proposed method is tested with success using some real voltage sags recorded in some substations. Also, through some experiments we demonstrate that satisfactorily high classification rates must be attributed to the applied feature selection algorithm.

Keywords. voltage sag, MPCA, direction, hybrid method

1. Introduction

Defined in terms of magnitude (amplitude) and duration (length), voltage events appear in the form of sags, swells, impulses, and total harmonic distortion. Among them voltage sags are the most troublesome one in term of occurrence frequency per year. According to IEEE standards a voltage sag is a momentary decrease in voltage magnitude for a few cycles. Typically, voltage sags are unbalanced and last for 0.5 cycle to 1 minute with a magnitude of 0.1-0.9 pu. (per unit) on the RMS basis [1]. Voltage sag events can be caused by bad weather, utility power distribution equipment failures, or other anomalies in transmission and distribution networks. Sags can affect equipment performance in different ways. Usually, the ultimate impact of such events is determined by the sensitivity of the equipment on the branch circuit. As more electronic control devices in industry

¹Correspondence to: Abbas Khosravi, Edifici P-II, Av. Lluis Santaló, s/n, 17071-Girona Tel.: +34 972 41 8391; Fax: +34 972 41 8098; E-mail: khosravi@eia.udg.es.

have been developed to be more complex and smaller, they have become less tolerant of voltage disturbance. Voltage sags, for instance, in semiconductor manufacturing processes can cost as much as \$2 million dollars in revenue per day. In the ceramic, steel, and pharmaceutical industries those losses are economically quite huge as well. An EPRI study in 2005 suggests that the cost to North American industry of production stoppages caused by voltage sags exceeds US\$250 billion per annum. When it comes to the domestic loads, the proliferation of sensitive power electronics-based appliances has provoked the concerns of customers about bad power quality. Voltage sags can easily trip off or shutdown equipment, cause memory and data loss, lead to disc drive crashes, etc. Owing to those economical losses, identifying who is to blame for originating sags and then imposing penalties to the responsible party are matter of high interests for both utilities and industrial facilities. From the other side, direction discrimination of detected sags is quite necessary for improvement of mitigation algorithms as well as accurate diagnosis of faults. Taking into account all these explanations, automatic analysis and source location of voltage sags have become an essential requirement for power quality monitoring.

So far a couple of interesting methods have been introduced for sag source location in the transmission and distribution networks. Authors in [3] review and compare different methods introduced in [2], [8], [9], and [10] for locating sag sources. In the simulations they have generated symmetrical and asymmetrical faults to examine and evaluate powerfulness of the considered methods. This exploratory work clearly shows that suggested methods fail to identify different sag sources in the networks particularly for meshed systems. Also it's interesting to mention that those methods all poorly perform when dealing with asymmetrical voltage sags.

Beholding those demands and weakness of common methods, this paper aims at developing a data-driven reliable approach for putting sags in two categories: whether they have originated in the transmission system or in the distribution network. Those categories will hereafter be cited within the text as High Voltage (HV) and Medium Voltage (MV) classes. The developed method is a hybrid MPCA-based one which first uses MPCA for compressing data and extracting some features from them and then hires four well known classifiers for identifying sag type, i.e. it's HV or MV. To determine the number of scores which should be retained in the MPCA models and to decrease the time and space demanding for classifier training, we develop a methodology for selecting the most useful features for each classifier.

We have organized the rest of this paper in the following way. Theoretical background needed for this research has been presented in the next section. Section 3 outlines the proposed method in details. Section 4 discusses the results obtained using real data. Finally, we finish paper with some conclusions and remarks for future work.

2. Theoretical Background

2.1. Multiway Principal Component Analysis (MPCA)

Principal Components Analysis (PCA) is a method that reduces data dimensionality by performing a covariance analysis between observations. As such, it is suitable for data sets in multiple dimensions, such as a large experiment in gene expression. PCA projects the data along the directions (principal components) where the data varies the most.

These directions are determined by the eigenvectors of the covariance matrix corresponding to the largest eigenvalues.

In a PCA model, a decision is made on the number of components to be retained as significant contributors to the model. The remaining components are considered to be due to noise and errors and are grouped as an error term, E . The reduced form of a PCA model containing k retained principal components can be expressed as:

$$X = \sum_{i=1}^k t_i p_i^T + E \quad (1)$$

Here t_i are known as score vectors and p_i are the loading vectors/principal components (i.e. eigenvectors of covariance matrix of X). The scores describe where the data points are projected in the PCA subspace, while the loading vectors describe the linear combination of the original variables that constitute each principal component. The lack of model fit can be measured using two statistical criteria named Q-residual (measure of the non-deterministic variation) and T^2 (measure of the distance from the multivariate mean).

There is no general convention for determining the number of principal components to retain in a PCA model. Common methods for determining k in Eq. (1) are based on magnitude of eigenvalues, sharp drops in the tabulated eigenvalues, cross validation techniques, and predetermining captured variance.

PCA has been extended to Multiway PCA to account for the three way data array decomposition of databases. The relation between MPCA and PCA is that MPCA is equivalent to performing ordinary PCA on a large two dimensional matrix formed by unfolding the three way array of data. Batch-wise, variable-wise, and time-wise are possible ways for unfolding those matrices that first two ones are more common than the last one. Three dimensional databases could be variable time histories for different runs of a batch process, or databases recorded in meteorology, biology, semiconductor industry, etc. Further information about PCA and MPCA could be found in reputable work and references such as [6] [11] [12].

2.2. Feature Selection

When training a classifier with a great deal of irrelevant or redundant inputs, there are always several annoying problems: need for more computational resources and memory, threat of curse of dimensionality, convergence difficulties of training algorithms, and poor generalization of the developed classifier [4]. Feature selection algorithms usually evaluate fitness of the features first, then search different combinations of features in the whole feature space with the goal of obtaining maximum fitness value. Many advanced methods have been developed to analyze how features cope with a certain classification task.

Best Individual Feature (BIF) algorithm is a filter approach to get an insight into the relevance of individual features. Each feature in the original set is being evaluated in respect to some criterion function. It is assumed that the features with the highest score are the best candidates for an optimal subset. The main advantage of this method is its linear scalability. The computation can be easily performed on collections containing thousands of features. Because each feature is evaluated separately there is no problem

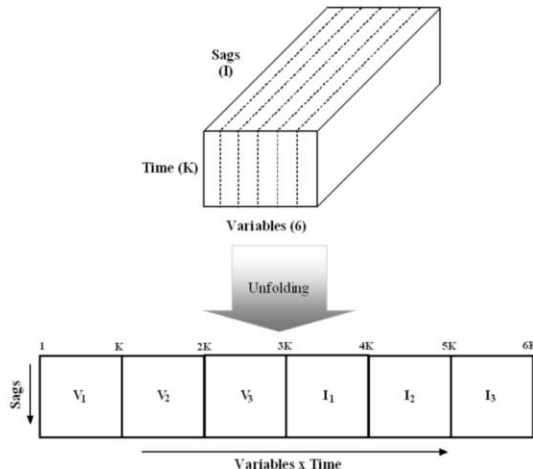


Figure 1. Database construction and batch-wise unfolding.

with the peaking phenomenon [13]. BIF algorithm is quite common and widely used in text categorization due to the mentioned properties especially being fast and efficient [7] [5].

3. Proposed Method

In this section we provide details of the proposed method for sag source location and selection.

The key idea in developing our method is database construction in a way which is suitable for MPCA. Definitely we should prepare a three dimensional matrix using available measurements (voltages and currents). Before every thing, we compute RMS values of voltages and currents for each occurred sag and then organize them in the format shown in Figure 1. The dimension of this matrix which contains time histories of measurements for all sags is $Time \times 6 \times number\ of\ sags$. Such a matrix is built and labeled for both HV and MV voltage sags. These matrices can be interpreted as databases gathered from a batch process or a semiconductor manufacturing process. Therefore, the same well-known and widely used methodologies and techniques that have been developed so far for analyzing those databases can be easily employed and applied to these databases.

After databases construction using RMS values, we apply MPCA algorithm to decrease their dimension and also extract some features from them. The batch-wise unfolding used in MPCA has been shown in Figure 1 for changing databases to two dimensional matrices. To give voltages and currents equal chance to be described by the MPCA model, we perform autoscaling on the unfolded matrices. With autoscaling the averages of each variable is removed, and all variables are scaled by their standard deviation. In this way HV and MV MPCA models are developed and projection of each sag (scores) upon them are computed. The obtained scores are representative for different sags. In fact, we have transformed each sag from $6 \times Time$ dimensions to k dimensions, where k is the number of principal components retained in the MPCA models.

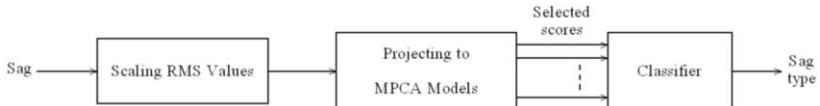


Figure 2. Online application of the proposed method.

To separate sags in HV and MV categories, we hire some classifiers fed by the computed scores. How many scores we must retain in the MPCA models and then put them into the considered classifiers is matter of importance and needs to be dealt well. To address those issues, we first rank all of the computed scores based on the BIF algorithm explained before. The criterion used for ranking is the classifier performance when it is trained by an individual score. After determining the best individual features for each classifier, we put them in some subsets and train the corresponding classifier with them. We expect that as we increase the number of used scores for training based on their ranks, the classification rates will plateau or even decline. In this way, we choose an optimal subset of features (scores) which using it not only decreases the dimension of trained classifiers, but also leads to satisfactory high rates, even better than the case of using all features.

Online application of the proposed method is quick and straightforward. Figure 2 simply displays three stages of sag source locating procedure. Whenever a new sag happens, RMS values of its voltages and currents are scaled and then projected to MPCA models. Classifier afterwards determines the type of sags based on some specific computed scores.

4. Application and Experimental Results

Table 1 represents dimensions of databases used in the upcoming experiments. All sags are real and have been registered in some substations in Catalonia, Spain in the course of one year. Asymmetrical type accounts for the vast majority of sags in the databases particularly in the MV database aggravating the task of sag source location. Through applying Fast Fourier Transform (FFT) in the fundamental frequency of the network to waveforms in a sliding window, we obtain a continuous estimation of the RMS values of voltages and currents (39 periods for each measure).

We employ four widely used classifiers: k-Nearest-Neighbor (kNN), Multilayer Perceptron (MLP), Radial Basic Functions (RBF), and Support Vector Machines (SVM), and compare their performance based on the mean accuracy of a stratified four fold cross validation run. For the first classifier, k has been set to three in all experiments.

Since trained classifiers using the computed scores from MV MPCA models poorly perform classification of sags, here we just provide results from HV MPCA models. This implicitly means that always HV MPCA models are developed using HV database and MV sags after being projected to these models are used for training the considered classifiers.

We start experiments with retaining twenty principal components in MPCA models. Figure 3 shows the average classification errors for different classifiers after applying a stratified four fold cross validation. The horizontal axis indicates the number of features (scores) hired for training each classifier. In this experiment we just apply the same pri-

Table 1. Dimensions of HV and MV databases

Substation	HV	MV
Three substations	$4993 \times 6 \times 141$	$4993 \times 6 \times 81$

ority determined by MPCA for putting scores into classifiers. For example, when we are using three features for training, those are scores obtained from projection of sags upon the first, second, and third principal components.

In the second experiment, we first apply BIF algorithm. So, those that individually better does classification task of sags are ranked above others. Then we increase the number of features for training classifiers based on this ranking. The average classification error rates for the four considered classifiers are in Figure 4.

We can discuss the obtained results from different points of view. In top of every thing, we should mention that the obtained correct classification rates for classifiers in the second experiments are satisfactory high, in particular for SVM. Training this classifier using only three up to six scores results in around 90% overall average classification rate. After this classifier and in the second place, kNN when the number of used scores is a few (2-3) functions quite well in separating sags in two classes. These rates mean that the proposed method is quite reliable for sag source location in the power network.

The proposed method also skillfully solves the problem of determining number of principal components which must be retained in the developed MPCA models. Without loss of generality, consider that we just use the best three scores for training SVM classifier. Among those, score that has the lowest rank in the MPCA ranking list determines the number of principal component that we must retain in the MPCA models. For instance if the best three scores from BIF algorithm are score 5, 10, and 3, we just need to retain only 10 principal components in the MPCA models and compute these specific scores for classifying a sag.

Besides, there are some conceptual points that mentioning and discussing them is interesting. First if we compare these two recent figures, we see that applying score rank determined by MPCA for training classifiers not only doesn't guarantee good classification rates, but also leads to some strange fluctuations in the classification rates. With those oscillations, it's approximately impossible to determine the optimal subset of scores for training classifiers.

The classification errors when using a few scores from the list of MPCA leads the worst results. This implicitly means that variations captured in the first principal components of HV MPCA models are the same for both HV and MV sags. Therefore, the MPCA ranking list is not much reliable for training classifiers.

Also obtained results clearly back this claim that when using MPCA for feature extraction and then classification, applying a feature selection technique is vital. Evolutions of average classification rates in Figure 3 demonstrate that hiring more scores, if is not harmful in term of classification rates, generally doesn't lead to better results. According to these evidences, applying a feature selection algorithm for optimizing the training procedure and enhancing results is to some extent necessary.

The last but not the least, although SVM classifier in both experiments roughly performs well, but the number of required scores for showing those performances in the first experiment is five times bigger than that number in the second experiment. This point more and better reveals usefulness of the applied feature selection algorithm for decreas-

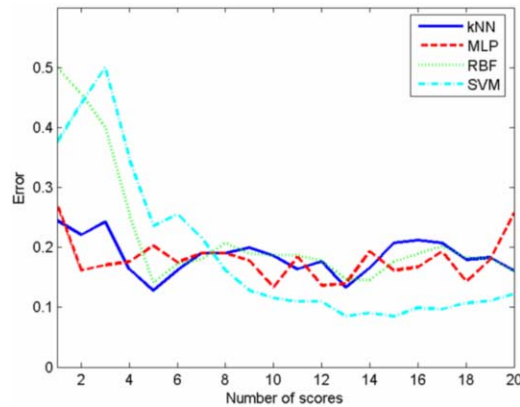


Figure 3. Classification errors when using scores ranked by MPCA for training classifiers.

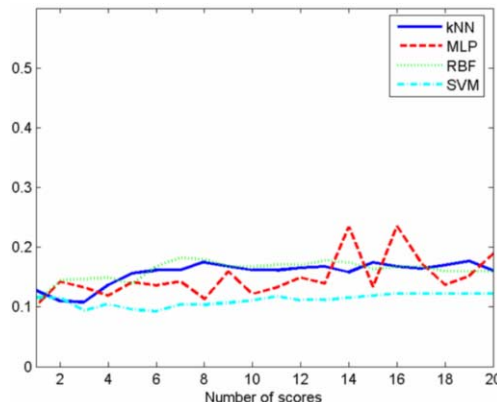


Figure 4. Classification errors when using ranked scores by BIF algorithm for training classifiers.

ing the dimension of training subsets which will address our concerns about classifier size.

5. Conclusion

In this exploratory work we developed a new hybrid method for sag source location in the power network. Through a skilful rearrangement of RMS values of currents and voltages, we developed MPCA models well representing HV and MV sag behavior. Then optimal subsets of scores determined by BIF algorithm were applied for training four widely used classifiers. Average classification rates from a four fold cross validation test proved the powerfulness of the proposed hybrid method for solving the problem of sag source location. Also we showed that no matter which ranking system (MPCA or BIF) we use, hiring more scores for training classifiers leads to poorer results.

Using linear supervised dimension reduction techniques which are algorithmically similar to PCA or equipping the developed method with nonlinear dimension reduction techniques can enhance the obtained results. More will be done and revealed latter.

Acknowledgements

The authors gratefully acknowledge the helpful contribution of Mr Esteban Gelso for database construction and Ms R. Naghavizadeh for preparing this paper. The exploratory work has been developed on the basis of the research project Diagnóstico de Redes de Distribución Eléctrica Basado en Casos y Modelos -DPI2006-09370- and PTR1995-1020-0P from the research and transfer programs, respectively, of the Spanish Government. Also it has been supported by the project of Development of an intelligent control system applied to a Sequencing Batch Reactor (SBR) for the elimination of organic matter, nitrogen and phosphorus DPI2005-08922-C02-02 supported by the Spanish Government.

References

- [1] IEEE Std. 1159-1995. *IEEE Recommended Practice for Monitoring Power Quality*.
- [2] N. Hamzah, A. Mohamed, and A. Hussain. A new approach to locate the voltage sag source using real current component. *Electric Power Systems Research*, 72:113–123, 2004.
- [3] R.C. Leborgne, D. Karlsson, and J. Daalder. Voltage sag source location methods performance under symmetrical and asymmetrical fault conditions. In *IEEE PES Transmission and Distribution Conference and Exposition Latin America, Venezuela*, 2006.
- [4] J. Li, J. Yao, R.M. Summers, and A.Hara. An efficient feature selection algorithm for computer-aided polyp detection. In *Proceedings of 18th International Florida Artificial Intelligence Research Society Conference (FLAIR)*, 2005.
- [5] D. Mladenic. *Machine Learning on non-homogeneous, distributed text data*. PhD thesis, Faculty of Computer and Information Science, University of Ljubljana, 1998.
- [6] P. Nomikos and J.F. MacGregor. Monitoring batch processes using multi-way principal component analysis. *AIChE*, 40(8):1361–1375, 1994.
- [7] J. Novovicova, P. Somol, and P. Pudil P. Oscillating feature subset search algorithm for text categorization. In *Progress in Pattern Recognition, Image Analysis and Applications Iberoamerican Congress on Pattern Recognition (CIARP)*, 2006.
- [8] A.C. Parsons, W.M. Grady, E.J. Powers, and J.C. Soward. A direction finder for power quality disturbances based upon disturbance power and energy. *IEEE Transactions on Power Delivery*, 15(3):1081–1086, 2000.
- [9] A.K. Pradhan and A. Routray. Applying distance relay for voltage sag-source detection. *IEEE Transactions on Power Delivery*, 20(1):529–531, 2005.
- [10] T. Tayjasanant, C. Li, and W. Xu. A resistance sign-based method for voltage sag source detection. *IEEE Transactions on Power Delivery*, 20(4):2544–2551, 2005.
- [11] B.M. Wise, N.B. Gallgher, S.W. Butler, D.D. Jr white, and G.G. Barna. A comparison of principal component analysis, multiway principal component analysis, trilinear decomposition and parallel factor analysis for fault detection in a semiconductor etch process. *Chemometrics*, 13:379–396, 1999.
- [12] S. Wold, P. Geladi, K. Esbensen, and J. Ohman. Multi-way principal component and pls analysis. *Journal of Chemometrics*, 1:41–56, 1987.
- [13] M. Zarzycki, T. Schneider, D. Meyer-Ebrecht, and 2005. A. Bocking in *Bildverarbeitung fur die Medizin. BVM 2005 pp. 410–414*. Classification of cell types in feulgen stained cytologic specimens using morphologic features. In *Bildverarbeitung fur die Medizin BVM*, 2005.

Multiobjective Evolutionary Algorithm for DS-CDMA Pseudonoise Sequence Design in a Multiresolutive Acquisition

Rosa Maria ALSINA PAGÈS^{a,1}, Lluís FORMIGA FANALS^a
 Joan Claudi SOCORÓ CARRIÉ^a and Ester BERNADÓ MANSILLA^b

^a *Grup de Recerca en Processament Multimodal (GPMM)*

^b *Grup de Recerca en Sistemes Intel.ligents (GRSI)*

Enginyeria i Arquitectura La Salle - Universitat Ramon Llull

Abstract. In DS-CDMA communications, pseudonoise sequence sets must fulfil crosscorrelation and autocorrelation minimization properties in order to minimize multiuser interference and improve the probability of acquisition. When a multiresolutive acquisition scheme is to be used [3] the pseudonoise sequences (PN) have to satisfy more strict constraints for achieving proper acquisition performance. In this paper we present a multiobjective evolutionary algorithm to design a set of pseudonoise sequences meeting all the constraints that the receiver of DS-CDMA communication system demands. The new pseudonoise sequence set accomplishes not only the basic pseudorandom waveform properties but also the new crosscorrelation and autocorrelation features required by the multiresolutive structure, obtaining better results in terms of crosscorrelation and stability. This way a better trade off between mean acquisition time and computational requirements can be achieved regarding traditional adquisition schemes.

Keywords. Pseudonoise sequence design, evolutionary algorithm, multiobjective, decimation, crosscorrelation, autocorrelation, CDMA.

1. Introduction

In Direct Sequence Spread Spectrum (DS-SS) communication systems, the transmitted signal is spread over a wide frequency band much wider than the minimum bandwidth required to transmit information [1,2]. This feature allows to work in a multiuser environment (Code Domain Multiple Access or CDMA) where all users share the same bandwidth, but each of them is assigned a distinct spreading code (pseudonoise or PN sequence) which appears random to anyone but the intended user. The main advantages of this system are its high spectrum efficiency, its multipath diversity combination capacity and also its high interference rejection.

In a DS-CDMA system a robust acquisition of the PN sequence is crucial to demodulate the transmitted information properly. Several algorithms have been designed for

¹Correspondence to: Rosa Maria Alsina Pagès, Carrer Quatre Camins, 2, 08022 Barcelona (Spain). Tel.: +34 93 290 24 53; Fax: +34 93 290 24 70; E-mail: ralsina@salle. URL.edu.

acquiring the PN sequence, such as serial search algorithms [4] and parallel search schemes [1]. In our system, the acquisition scheme is based on the multiresolutive structure introduced in [3]. In order to improve acquisition in the multiresolutive receiver, a set of PN sequences with specific properties is needed [5]. The existing PN sequence sets are generated using mathematical algorithms, i.e. linear feedback functions in shift registers. However, none of the current PN sequence sets, such as Gold or Hadamard family sets, satisfy the properties that the multiresolutive structure requires. Thus, a mathematical algorithm has been defined yielding PN sequences satisfying the desired features. So as to tackle this issue, this work introduces a step further in our current work [5] to obtain PN sequences not only fulfilling the basic properties but also all other multiresolutive constraints. Specifically, a multiobjective evolutionary algorithm [13] is used to design this new PN sequence set.

This paper is organized as follows. An overview of spread spectrum synchronization and PN sequences is given in section 2. Next, we describe the multiobjective evolutionary algorithm used to design the multiresolutive PN sequence set. Results are reported in section 4, and some conclusions and future work are summarized in section 5.

2. Spread Spectrum Systems and PN Sequence Design

2.1. PN Sequence Characteristics

The spreading PN sequences are bivaluated $\{1, -1\}$ pseudorandom waveforms. Although they are generated by mathematically precise rules, they do not fully satisfy statistically the requirements of a real random sequence. They have to accomplish the following properties:

- **Balance property:** in each period of the sequence the number of binary $1s$ and $-1s$ must differ by at most one digit.
- **Run-length distribution:** it would be desirable that about half of the runs² would be of length one, about one-fourth of length two, about one-eighth of length three, and so on.
- **Autocorrelation:** the autocorrelation function for a periodic sequence is defined as the number of agreements minus the number of disagreements in a term by term comparison of one full period of the sequence [6]. For our purpose, the focus is on its average value excluding the maximum value, and the goal is to minimize this value:

$$Rac_i = \frac{1}{K} \sum_{\tau=1}^{K-1} \sum_{n=0}^{K-1} C_i[n] \cdot C_i[n + \tau] \quad (1)$$

- **Crosscorrelation:** the crosscorrelation defines the interference between two PN codes $C_i[n]$ and $C_j[n]$ (for $i \neq j$):

$$Rcc_{ij} = \frac{1}{K} \sum_{\tau=0}^{K-1} \sum_{n=0}^{K-1} C_i[n] \cdot C_j[n + \tau] \quad (2)$$

²A run is a sequence of a single type of binary digits.

The ideal case occurs when $R_{cc_{ij}}$ is zero, i.e. the codes are orthogonal, thus there is no interference between users in the same channel. However, the codes are usually not perfectly orthogonal, hence the crosscorrelation between the different users' codes introduces a performance degradation that limits the capacity of the channel. This distortion is called multiuser interference (MAI). Also in the ideal case R_{ac} should be zero, but in practice the autocorrelation can increase false alarm tax due to high peak values. According to [8], it is impossible to minimize the autocorrelation and the crosscorrelation simultaneously. Thus, we seek for a trade-off between the autocorrelation and crosscorrelation values.

2.2. Multiresolutive Acquisition Structure for a DS-CDMA Receiver and its Requirements

The aim of the multiresolutive scheme is to improve the acquisition performance in terms of a good balance between speed and complexity [3]. For this purpose, the input space is divided into H disjoint subspaces by means of a decimation structure. In our case, $H = 4$ (C_A, C_B, C_C and C_D), and the length of the PN sequence is $K = 128$. Therefore, four new PN sequences have been generated due to decimation (i.e. their length will be $\frac{K}{H}$), distributing the information of the original PN sequence. The more uncorrelated the decimated sequences C_i are from the decimated sequences of other users, the faster the receiver will converge to the correct acquisition.

The structure of the multiresolutive receiver adds some extra constraints to the PN sequence design, because it works with the decimated signal in the receiver. This means that the features described in section 2.1 are still well-founded, but the decimated sequences (C_A, C_B, C_C and C_D) will have to accomplish also the following constraints. The mean crosscorrelation between the different decimated sequences must be minimized. The mean crosscorrelation for the decimated sequences (corresponding $R_{cc_{Aij}}$ to the first branch and for users i and j) is computed according to equation 2, considering the fact that these sequences are of length $\frac{K}{H}$, so the summation must be modified according to this number. The decimated sequences must minimize also the autocorrelation for each branch (corresponding $R_{ac_{Ai}}$ to the first branch for the user i), adapting equation 1 for a sequence length $\frac{K}{H}$.

2.3. Properties of Existing PN Sequence Sets

In order to evaluate our approach, we compare the PN sequences obtained by our design with Gold Sequences and Walsh Hadamard Sequences. These are two sets commonly used to work with spread spectrum communications.

Gold codes [7] are generated as a product code achieved by a modulo-2 adding of two maximum-length sequences with the same length (*m-sequences*). Following this approach, a large number of codes with the same length can be obtained, controlling their crosscorrelation. A pair of *m-sequences* is required to obtain a new Gold sequence. If the *m-sequences* are chosen from a pair of preferred sequences, the generated Gold codes have a controlled three valued crosscorrelation.

Walsh Hadamard codes are generated in a very simple way through an iterative algorithm [1]. When the sequences are perfectly synchronized, their crosscorrelation is zero. They are periodic PN codes, consequently problems come out if the synchronization is based on autocorrelation.

3. Design of the Evolutionary Algorithm

3.1. Problem Description

The new PN sequence set should satisfy several requirements, which can be classified into: *strong constraints* and *minimization constraints*. *Strong constraints* are the balance property and the run-length distribution. Each sequence of the set must accomplish these properties, because they are fundamental to improve the minimization constraints.

Minimization constraints are about minimizing correlation features. First of all, there is the autocorrelation (Rac) between the entire sequences (C_i), as defined in equation 1, and then the crosscorrelation (Rcc) between all the sequences in the set, defined in equation 2. These two parameters are usually taken into account by the existing PN sequence sets like Gold sequences [7]. Additionally, the crosscorrelation (Rcc) between the decimated sequences (C_{Ai} , C_{Bi} , C_{Ci} and C_{Di}) and their autocorrelation (Rac) should also be minimized in order to improve the multiresolutive structure performance.

3.2. Multiobjective Evolutionary Algorithms

An algorithm inspired by a multiobjective evolution strategy (MOEAs) of type $(\mu + \lambda)$ was used for the design of the PN sequences set. Evolutionary algorithms, and more specifically, evolution strategies were initially proposed in [9,10] for numerical optimization applications. The notation $(\mu + \lambda)$ -ES stands for an evolution strategy with μ individuals in the population, and λ offspring, where the offspring replace the worst solutions of the population. The best and the worst individuals within the population are ranked by a fitness function which measures their specific quality. In each iteration, parents are selected randomly. These solutions suffer mutation and/or crossover, and λ children are obtained. Replacement is deterministic, since the offspring replace the worst parents.

We use the scheme of an evolutionary algorithm $((\mu + \lambda)\text{-EA})$ for the design of PN sequences in the following way. μ is set to be the number of needed PN sequences, while λ is set to 1. Each solution represents a PN sequence, which is coded by a vector of K binary digits (in the alphabet $\{-1, 1\}$). In each iteration, one individual is obtained by mutating a random parent. Only one offspring is generated in order to evaluate the global performance of the specifications taking into account this new individual. This individual replaces the worst solution of the population if it improves the global fitness. In this case, crossover between individuals is not applied to avoid similarities between sequences and minimize interferences among all solutions. The solution of the algorithm is the set of μ sequences obtained when the stop criterion is met.

A particularity of the current application is that fitness measures not only autocorrelation, but also crosscorrelation of each sequence against the rest of sequences. Thus, fitness is relative to the population, which means that each time a solution is introduced into the population, the fitness of all individuals must be computed again. We also consider a global fitness, which is the quality of the overall solution. Next section describes these two measures in detail.

3.3. Fitness Functions

The optimum solution should minimize the five crosscorrelation parameters (Rcc_i , Rcc_{Ai} , Rcc_{Bi} , Rcc_{Ci} and Rcc_{Di}) and the five autocorrelation parameters (Rac_i , Rac_{Ai} ,

Rac_{Bi} , Rac_{Ci} and Rac_{Di}) at the same time. For this reason, we use of a multiresolutional algorithm [12,13]. As detailed in [13], some multiobjective optimization problems are usually considered under the paradigm of single objective optimization because their objectives are grouped in a weighted lineal fitness function. Thus, the first fitness function we considered was a weighted compound crosscorrelation and autocorrelation taking into account not only both measures for the entire sequences, but also for the four decimated sequences. But we realized that there was a strong dependency on the weight configuration used, and avoiding it could lead us to reach a more homogenous optimization.

Pure multiobjective methods base its efficiency on Pareto dominance [11]. In the context of multiobjective optimization, it is often difficult to find a global optimum that maximizes all objectives simultaneously. According to Pareto, a dominant solution is a solution whose objective function is not improved simultaneously by any other solution. That is, there is not any other solution with better values in all their objectives. Multiobjective evolutionary algorithms based on Pareto dominance evolve a set of non-dominated solutions, where each solution represents a compromise in their objectives. There is not any solution globally better than the rest of solutions. This set of solutions is called the Pareto optimal set. The algorithm guides the search towards the Pareto optimal set. This is done by classifying the solutions into categories. The first category, which is assigned rank 1, is formed by the solutions which are non-dominated by any other solution of the current population. The second category, rank 2, is formed by all non-dominated solutions after removing the solutions of the first rank and so on³. Thus, once the solutions are classified into ranks, the genetic pressure tends to lead the population towards the Pareto optimal set.

To understand the kind of data we were dealing with, we conducted some preliminary tests where we applied multiobjective algorithms based on Pareto dominance. The (unreported) results showed that the algorithm could not guide the search towards the Pareto front, because it was difficult (in most part of the studied cases) to find dominant solutions. There was not any solution in the population that could dominate another solution. Thus, all solutions were considered with the same rank and no effective search could be applied. In fact, this problem is usual in multiobjective optimization when the number of objectives to optimize is very high (in our case we worked with ten objectives). For this reason, a new fitness function was designed considering partial dominance between the solutions as follows. For each individual (sequence) we computed the *feature dominance value* of the individual with respect to each of the sequences of the population. The *feature dominance value* of the individual i compared to individual j is the number of objectives whose values in i are better than in j . Then, the fitness of the individual corresponded to the average of all feature dominance values. Later, the individuals are ranked due to this averaged feature dominance value.

3.4. Algorithm Description

The algorithm details are the following:

³A non-dominated solution is a solution not improved simultaneously by any other solution of the search space. During the run, the algorithm may find non-dominated solutions in the population; that is, solutions that are not dominated by any other solution of the current population. The aim is to guide these solutions to the *real* non-dominated solutions.

Algorithm 1 Pseudocode of the Evolutionary Algorithm Proposed to Design New PN Sequence Sets

```

procedure designSeq()
1:  $P := \{PNseq_1 \dots PNseq_\mu \mid \forall PNseq_i \in P : \text{constrained}(PNseq_i)\}$ 
2: while  $\neg \text{stopCriteria}(P)$  do
3:    $F := \{\forall F_i \in F \Rightarrow F_i = \text{avgFeatDom}(PNseq_i, P)\}$ 
4:    $P_{eager} := P - \text{last}(F, P)$ 
5:    $PNseq_{new} := \text{mutateConstrained}(\text{rand}(P_{eager}))$ 
6:   while  $worst(F) \leq \text{rank}(PNseq_{new}, P_{eager})$  do
7:      $PNseq_{new} := \text{mutateConstrained}(\text{rand}(P_{eager}))$ 
8:   end while
9:    $P := \{P_{eager}, PNseq_{new}\}$ 
10: end while
11: return  $P$ 
  
```

1. Initially, a random population of μ individuals is generated. Each individual is defined as a PN sequence. Each sequence must accomplish the *strong constraints*. If there are any sequences that do not fit the constraints they are rejected and created again randomly.
2. Once the population of μ valid individuals is generated, the averaged feature dominance value F_i is computed for all the members of the population.
3. The members of the population are sorted by decreasing averaged feature dominance value.
4. The last member in the list, which is the worst ranked, will be selected for deletion.
5. Another new individual will be created using mutation of one of the $\mu - 1$ parents. If the new individual does not fit the constraints, it will be rejected and a new individual must be created until it accomplishes the *strong constraints*.
6. The averaged feature dominance value is computed again for all μ individuals, considering the new member. The degree of improvement is evaluated before the new individual is accepted or rejected. It will be accepted if it achieves a better ranking than the deleted one. If $rank_{new}$ is smaller than that the deleted PN sequence, we accept the new candidate and the algorithm goes back to step 3. Otherwise, we reject the new member and go back to step 5.

The criteria to stop the algorithm can be both computation time and stability of the results. In this case, the number of trials has been used as a limit.

4. Results

In this section we analyze the results of the Multiobjective EA Sequences. Their performance is compared with Gold Sequences and Walsh Hadamard Sequences. $\mu = 40$ is the number of sequences created to fulfill our system requirements and $K = 127$ for Gold sequences and $K = 128$ for Walsh Hadamard sequences. Thus, the comparison is made with $\mu = 40$ of the number of sequences that each set contains, using the $\mu = 40$ codes that perform best for our specifications for Gold and Hadamard codes according

to equations 2 and 1. The first comparisons are made using the average crosscorrelation and the average autocorrelation for the entire sequences as a reference (see equations 1 and 2). These results can be observed in figure 1. The average autocorrelation values remain similar to Gold ones. And the average crosscorrelation shows a trade-off with some higher values for crosscorrelation than the reference Gold sequences.

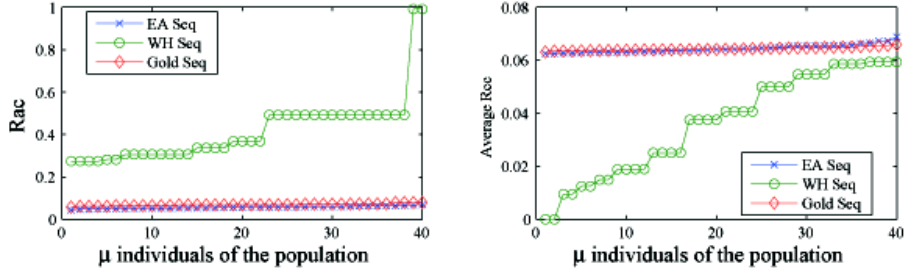


Figure 1. Average Autocorrelation and Crosscorrelation for the entire sequences C_i

The second comparison criterion is the average autocorrelation (Rac) obtained for the decimated sequences (C_A , C_B , C_C and C_D). The best results are obtained by the EA Sequences, despite being similar to Gold sequences ones (see four upper plots of figure 2). Finally, the third comparison is the average crosscorrelation (Rcc) between the decimated sequences. The best results for the first sequences of the family are given by Walsh Hadamard sequences (see figure 2, four lower plots), but when reaching the last sequences of the set, the EA Sequences show better results. It is also remarkable the stability of the EA Sequences results for all the sequences in the family.

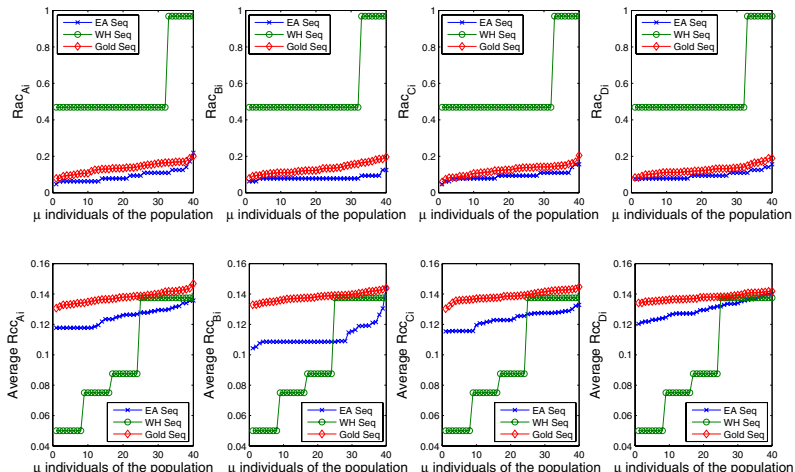


Figure 2. Autocorrelation (Rac) and Average Crosscorrelation (Rcc) for the decimated sequences

5. Conclusions and Future Work

The Multiobjective EA Sequence set improves the performance of the existing PN sequences sets in terms of the constraints introduced by the multiresolutive acquisition scheme. With this new set of sequences, the both the autocorrelation and the crosscorrelation are minimized not only for the complete sequences, but also for the decimated sequences, besides obtaining very stable values for all the EA Sequences in the set, specially if compared with Walsh Hadamard set. Thus, no user's transmission is improved only because its sequence is privileged.

This encourages us to test this new set of sequences in our multiresolutive system in near future work. Bit Error Rate is expected to be minimized in the receiver using this new family of PN sequences. The EA Sequences will probably increase the capacity of the channel reducing multiuser interference. In addition, we are planning to conduct and exhaustive analysis of the crosscorrelation and autocorrelation minimization values so as to know the multiobjective evolutionary algorithm limits in terms of results improvement.

References

- [1] J.G. Proakis: Digital Communications, McGraw-Hill, Singapore, 1995.
- [2] R.L. Peterson, R.E. Ziemer and D.E. Borth: Introduction to Spread Spectrum Communications, Prentice Hall, New Jersey, 1995.
- [3] J.A. Morán, J.C. Socorro, X. Jové, J.L.I. Pijoan and F. Tarrés: Multiresolution Adaptive Structure for acquisition in DS-SS receivers, proceedings of the ICASSP 2001, Salt Lake City, USA.
- [4] S.G. Glisic et al: Instantaneous CFAR Algorithm, Proceedings of IEEE Conference on Global Communications, San Diego, California, December 2-5, 1990.
- [5] R.M. Alsina, E. Bernadó, J.A. Morán: Evolution Strategies for DS-CDMA Pseudonoise Sequence Design, IOS Press Frontiers in Artificial Intelligence and Applications, Proceedings of CCIA 2005, Alghero (Italy).
- [6] A. Leon-Garcia: Probability and Random Processes for Electrical Engineering, Addison-Wesley, 1994.
- [7] D.V. Sarwate, M.B. Pursley: Crosscorrelation Properties of Pseudorandom and Related Sequences, Proceedings of the IEEE, Volume 68, Number 5, Pages 593-619, 1980.
- [8] B. Natarajan, S. Das and D. Stevens: An Evolutionary Approach to Designing Complex Spreading Codes for DS-CDMA, IEEE Transactions on Wireless Communications, Vol.4, no.5, September 2005.
- [9] I. Rechenberg: Evolutionsstrategie: Optimierung technischer Systeme nach Prinzipien der biologischen Evolution, Stuttgart: Frommann-Holzboog, 1973.
- [10] H.P. Schwefel: Evolutionsstrategie und numerische Optimierung, Ph.D. Thesis, 1975, Technische Universität Berlin.
- [11] V. Pareto: Cours d'Economie Politique, volume I and II, F. Rouge, Lausanne, 1896.
- [12] J. Horn, N. Nafpliotis and D.E. Goldberg: A Niched Pareto Genetic Algorithm for Multiobjective Optimization, Proc. of the First IEEE Conference on Evolutionary Computation, IEEE World Congress on Computational Intelligence, vol.1, Piscataway, New Jersey, 1994.
- [13] N. Srinivas and K. Deb: Multiobjective Optimization Using Nondominated Sorting in Genetic Algorithms, Journal on Evolutionary Computation, vol. 2, num. 3, 1994.

Renewable energy for domestic electricity production and prediction of short-time electric consumption

Stéphane Grieu¹, Frédéric Thiery, Adama Traoré and Monique Polit
Laboratoire ELIAUS, Université de Perpignan Via Domitia, France

Abstract. Modern interest in renewable energy development is linked to concerns about exhaustion of fossil fuels and environmental, social and political risks of extensive use of fossil fuels and nuclear energy. It is a form of energy development with a focus on renewable energy. In this sense, the present work takes part in a global study of solar energy and wind power for generating electricity. This paper is focused, by means of time series analysis and Kohonen self organizing maps, on predicting short-time electric consumption for a family of four people living in the south of France (Perpignan city). A cost study for the installation at the family's house of photovoltaic solar cells and/or windmills for generating electricity was also carried out. Lastly, the produced electricity cost was compared with the price of electricity sold by the French national company Electricité de France (EDF).

Keywords. Short-time electric consumption, Kohonen self-organizing maps, time series, photovoltaic solar cells, windmills.

1. Introduction

Renewable Energy is energy derived from resources that are regenerative or for, all practical purposes, that cannot be depleted. For this reason, renewable energy sources are fundamentally different from fossil fuels and do not produce as many greenhouse gases and other pollutants as fossil fuel combustion. Mankind's traditional uses of wind, water, and solar energy are widespread in developed and developing countries, but the mass production of electricity using renewable energy sources has become more commonplace recently, reflecting the major threats of climate change, exhaustion of fossil fuels, and the environmental, social and political risks of fossil fuels. Consequently, many countries promote renewable energies through tax incentives and subsidies [1].

France has few indigenous sources, only of small amounts of coal, oil and gas. The exploitation of these resources has steadily decreased over the last two decades and nuclear power has dominated the energy supply market. Nuclear energy supplied over 77 % of France's electricity and 40 % of its primary energy needs in 2003. France also exports electric power to most European countries. France had a national target of

¹ Correspondence to: Stéphane Grieu, Laboratoire ELIAUS, Université de Perpignan Via Domitia, 52 Avenue Paul Alduy, 66860 Perpignan, France. Tel.: +33 4 68 66 22 40; Fax: + 33 4 68 66 22 87; E-mail: grieu@univ-perp.fr.

reducing carbon dioxide emissions by 20 per cent by 2005, compared with their 1988 levels. In the context of the EU's Burden-Sharing Agreement, France is committed to have its annual average greenhouse gas emissions at 1990 levels for 2008-2012 [2].

Renewable energy contributed 7 % of France's total energy supply and 15 % of total electricity supply in 2001 compared to EU averages of 5.8 % and 15.5 % respectively [3]. The majority of non-hydro renewable energy use was solid biomass (particularly wood), almost all of which is used for residential heating. Municipal and industrial wastes are also being used to generate increasing quantities of electricity and heat. Small amounts of geothermal heat, solar energy and, increasingly, wind is also used [4, 5].

This paper is focused on predicting, by means of time series analysis and Kohonen self organizing maps, short-time electric consumption for a family of four people living in the south of France (Perpignan city). A cost study, for the installation at the family's house of photovoltaic solar cells and/or windmills for generating electricity, was also carried out. Lastly, the produced electricity cost was compared with the price of electricity sold by the French national company Electricité de France (EDF) [4].

2. Study area

2.1. The Perpignan city

The used family for our study is composed of four members (two adults and two children) and lives in the south of France, in Perpignan city. Perpignan is the administrative capital city of the Pyrénées-Orientales department in southern France. Its population is about 120 000 in the city proper and 250 000 in the metropolitan area. Perpignan was the capital of the former county of Roussillon.

A Mediterranean type of climate is found in Perpignan: high temperature in summer and mild climate for the rest of the year. The weather is globally hot, with dry summers, mild and humid winters and just a few rainy days during the year. Perpignan is a very sunny and windy city and is a good place to develop the electricity production by means of photovoltaic solar cells and/or windmills.

2.2. The family's house

The livable space of the family's house located in Perpignan is about 100 m². It is composed of a kitchen, a living room, three rooms, an office, a bathroom, toilets, a corridor and a storeroom. Table 1 presents the surfaces of each part of the house:

Table 1. Surfaces of each part of the house.

<i>Part</i>	<i>Surface (m²)</i>	<i>Part</i>	<i>Surface (m²)</i>
Kitchen & living room	24.13	Office	10.34
Room 1	13.26	Bathroom & toilets	15.5
Room 2	13.14	Corridor	4.32
Room 3	12.79	Storeroom	6.22
<i>Total surface (m²)</i>	<i>99.7</i>		

This house is equipped with many modern amenities: lamps, refrigerating freezer, lava linen, domestic iron, furnace, coffee machine, lava crockery, vacuum cleaner,

television, cordless phone, hi-fi systems, central heating and water-heater. The following table (Table 2) presents their annual electric consumptions (in kWh) for our four-member family:

Table 2. House's equipments and annual electric consumptions.

Equipment	Annual electric consumption (kWh)	Equipment	Annual electric consumption (kWh)
Lamps	450	Lava crockery	230
Refrigerating freezer	600	Vacuum cleaner	15
Lava linen	250	Television	150
Domestic iron	40	Cordless phone	20
Furnace	200	Hi-fi system	30
Coffee machine	30	Central heating & water-heater	500
Total annual electric consumption (kWh)			2515

3. Materials and methods

3.1. Electric consumption database

Family's daily electric consumptions for year 2002 have been used to carry out the short-time predictions by means of both time series study and Kohonen self organizing maps. They were also used for the cost study of the implementation in the family's house of photovoltaic solar cells and/or windmills in order to generate electricity.

The available database was thus composed of 365 daily electric consumptions expressed in kWh (52 weeks). This database characterizes the considered family, its house and its life practices.

3.2. Time series analysis

In statistics, signal processing, and econometrics, a time series is a sequence of data points, measured typically at successive times, spaced at (often uniform) time intervals. Time series analysis comprises methods that attempt to understand such time series, often either to understand the underlying theory of the data points (where did they come from? what generated them?), or to make forecasts (predictions). Time series prediction is the use of a model to predict future events based on known past events: to predict future data points before they are measured. The standard example is the opening price of a stock share based on its past performance [6, 7].

Each week of the electric consumption database is considered as a time series: each daily electric consumption belongs to a whole of seven elements. Twenty weeks, uniformly distributed over the year 2002, were selected to carry out the prediction of short-time electric consumption. For each one of these time series, a prediction of consumption for one of the days of each week was carried out (the value was considered as missing or non measured), after calculating the Euclidian distances between the twenty selected weeks and the thirty two remaining weeks. For each one of these twenty selected weeks, the nearest remaining time series were thus determined and the "missing" value replaced by the equivalent value of the nearest time series. That is the methodology used to carry out the short-time prediction using time series analysis.

3.3. The Kohonen self-organizing map (KSOM)

3.3.1. Network structure

The Kohonen self-organizing map consists of a regular, usually two-dimensional, grid of neurons (output neurons). Each neuron i is represented by a weight, or model vector, $m_i = [m_{i1}, \dots, m_{in}]^T$ where n is equal to the dimension of the input vectors. The set of weight vectors is called a codebook [8].

The neurons of the map are connected to adjacent neurons by a neighborhood relation, which dictates the topology of the map. Usually rectangular or hexagonal topology is used. Immediate neighbors belong to the neighborhood N_i of the neuron i . The topological relations and the number of neurons are fixed before the training phase allowing the map configuration. The number of neurons may vary from a few dozens up to several thousands. It determines the granularity of the mapping, which affects the accuracy and generalization capability of the KSOM.

3.3.2. Training algorithm

The Kohonen feature map creates a topological mapping by adjusting not only the winners' weights, but also adjusting the weights of the adjacent output units in close proximity or in the neighborhood of the winner (Figure 1). So not only does the winner get adjusted, but the whole neighborhood of output units gets moved closer to the input pattern. Starting from randomized weight values, the output units slowly align themselves such that when an input pattern is presented, a neighborhood of units responds to the input pattern. As training progresses, the size of the neighborhood radiating out from the winning unit is decreased. Initially large numbers of output units will be updated, and later on smaller and smaller numbers are updated until at the end of training only the winning unit is adjusted. Similarly, the learning rate will decrease as training progresses, and in some implementations, the learn rate decays with the distance from the winning output unit [8].

3.3.3. Prediction of short-time electric consumption with KSOM

A prediction of short-time electric consumption can be done using Kohonen self organizing maps in the same way that this kind of neural networks can be used to estimate missing (unknown) values in a database. The KSOM, after a training phase carried out using available complete input vectors, can be used to estimate missing values in new input vectors, by means of BMU (Best Matching Unit) weight vectors.

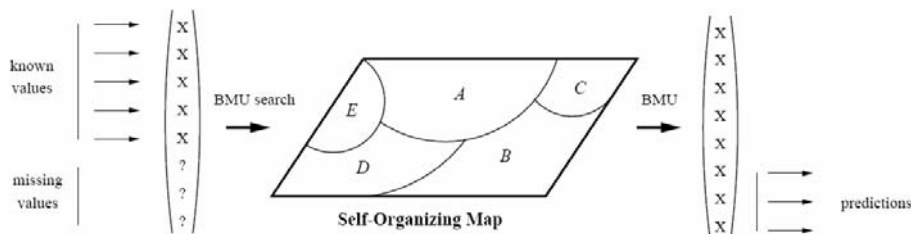


Figure 1. Prediction of missing components of an input vector using a KSOM.

General regression of s on e is usually defined by $\hat{s} = f(s|e)$. That is the expectation of the output s given the input vector e . To motive the use of the KSOM for regression, it is worth noting that the codebook vectors represent local averages of the training data. Regression is accomplished by searching for the best matching unit using the known vector component of e . As an output, an approximation of the unknown components of the codebook vector is given (Figure 1) [8]. That is the methodology used to carry out the short-time prediction using Kohonen self organizing maps [9].

4. Results of the short-time electric consumption prediction

All the results of the short-time electric consumption prediction are presented in this paragraph, using time series analysis and KSOM (Tables 3, 4 and 5).

4.1. Results of the short-time electric consumption prediction using time series analysis

Table 3. Short-time electric consumption prediction using time series analysis.

Day	Electric consumption (kWh)	Predicted electric cons. (kWh)	Relative error (%)
March, 31	8.03	8.96	11.54
April, 8	6.32	7.36	16.51
April, 26	6.98	6.74	3.44
May, 16	5.74	7.31	27.28
June, 6	6.47	6.36	1.70
June, 21	6.26	5.31	15.14
July, 9	5.84	5.32	8.92
July, 27	4.91	4.55	7.34
August, 16	5.35	5.79	8.30
Sept., 6	6.56	6.93	5.55
Sept., 21	5.71	4.98	12.74
October, 9	7.54	6.07	19.60
October, 27	5.10	5.53	8.55
Nov., 12	8.74	8.78	0.39
Nov., 27	8.84	8.28	6.33
Dec., 21	7.92	8.17	3.18
January, 8	9.81	9.53	2.85
January, 20	7.05	6.96	1.26
February, 1	8.50	7.40	12.92
February, 13	7.76	8.80	13.38
March, 6	8.06	7.95	1.34
Mean relative error (%)			8.97

4.2. KSOM optimization

Table 4. KSOM grid size and epochs number optimization.

Grid size	Epochs number: short / Neighborhood function: Gaussian		
	Quantization error	Topographic error	Prediction mean relative error (%)
10x1	0.847	0	12.70
10x2	0.797	0.032	12.78
11x1	0.839	0	12.93
11x2	0.776	0	12.86
12x1	0.821	0	13.20
12x2	0.760	0	13.16

Epochs number: medium / Neighborhood function: Gaussian			
Grid size	Quantization error	Topographic error	Prediction mean relative error (%)
10x1	0.845	0	12.72
10x2	0.795	0	12.75
11x1	0.839	0	12.93
11x2	0.776	0	12.86
12x1	0.821	0	13.20
12x2	0.760	0.032	13.10
Epochs number: long / Neighborhood function: Gaussian			
Grid size	Quantization error	Topographic error	Prediction mean relative error (%)
10x1	0.845	0	12.72
10x2	0.800	0	11.77
11x1	0.845	0	12.72
11x2	0.773	0	11.16
12x1	0.824	0	13.08
12x2	0.760	0.032	13.10

4.3. Results of the short-time electric consumption prediction using KSOM

Table 5. Short-time electric consumption prediction using KSOM.

Day	Electric consumption (kWh)	Predicted electric cons. (kWh)	Relative error (%)
March, 31	8.03	8.03	0.07
April, 8	6.32	6.86	8.53
April, 26	6.98	7.42	6.27
May, 16	5.74	6.71	16.93
June, 6	6.47	6.77	4.68
June, 21	6.26	6.34	1.26
July, 9	5.84	6.35	8.74
July, 27	4.91	5.23	6.65
August, 16	5.35	6.18	15.53
Sept., 6	6.56	6.94	5.82
Sept., 21	5.71	6.20	8.63
October, 9	7.54	8.73	15.71
October, 27	5.10	5.64	10.68
Nov., 12	8.74	10.73	22.74
Nov., 27	8.84	10.13	14.66
Dec., 21	7.92	9.75	23.21
January, 8	9.81	12.06	22.99
January, 20	7.05	7.14	1.29
February, 1	8.50	9.33	9.84
February, 13	7.76	8.80	13.38
March, 6	8.06	9.40	16.65
Mean relative error (%)			11.16

5. Cost study for installing photovoltaic solar cells and/or windmills

5.1. Generating electricity with windmills

According to their characteristics, their production capabilities and the family's electricity consumption, two types of domestic windmills were selected in order to be installed at family's house. Table 6 presents for the two selected windmills (500 W and 1 kW), their monthly and annual electricity productions according to wind average speeds in Perpignan (year 2002).

Table 6. 500 W and 1 kW windmills electricity production.

<i>Month (year 2002)</i>	<i>Wind average speed (m/s)</i>	<i>500 W windmill production (kWh)</i>	<i>1 kW windmill production (kWh)</i>
<i>January</i>	4.44	63.3	85.1
<i>February</i>	6.54	137.7	207.1
<i>March</i>	5.64	107.1	145.9
<i>April</i>	6.57	128.9	176.1
<i>May</i>	5.88	109.2	147.3
<i>June</i>	5.26	97.7	125.2
<i>July</i>	6.50	142.2	204.1
<i>August</i>	5.63	99.8	138.9
<i>September</i>	5.04	79.5	107.5
<i>October</i>	4.75	73.5	102.2
<i>November</i>	5.73	111.5	159.8
<i>December</i>	5.19	103.4	149.4
<i>Annual windmill production (kWh)</i>		1247.9	1478.2

5.2. Generating electricity with photovoltaic solar cells

According to their characteristics, their production capabilities and the family's electricity consumption, solar panels were dimensioned in order to be installed at family's house. Table 7 presents for various panel surfaces, their annual electricity productions according to daily average solar irradiation in Perpignan (year 2002).

Table 7. Solar panels electricity production.

<i>Perpignan (Latitude: 43.73°N; Longitude: 2.90°E; Altitude: 43 m)</i>			
<i>Daily average horizontal solar irradiation (Wh/m²)</i>	<i>Daily average 60°S solar irradiation (Wh/m²)</i>	<i>Panels surfaces (m²)</i>	<i>Annual electricity production (kWh)</i>
		<i>21.16</i>	<i>2500</i>
		14.42	1703.7
		13	1536
		11.88	1403.6
3992	4313	11	1299.7
		10.6	1252.1
		10	1181.5
		8.65	1021.8

5.3. Cost of produced electricity

The cost of produced electricity was calculated according to the prices of the two domestic windmills, the price of the solar panels m², the installation cost, the maintenance cost and the storage cost. This cost takes into account various subsidies and taxes deductions offered by the French government in order to promote renewable energy [1, 4]. Table 8 presents the cost of produced electricity for three kinds of systems: only windmill, only photovoltaic solar panels and hybrid systems. This table highlights the systems allowing producing the annual 2500 kWh consumed by our family of four people (a 21.16 m² solar panel and an hybrid system 8.65 m² solar panel + 1 kW windmill) and the system allowing producing the less expensive electricity (14.42 m² solar panel + 1 kW windmill). For all the considered systems, produced electricity is more expensive than electricity sold by EDF (average cost: 0.092 €/kWh).

Table 8. Cost of produced electricity.

<i>Production system</i>	<i>Installation cost (€)</i>	<i>Total cost (€)</i>	<i>Annual production (kWh)</i>	<i>Cost of electricity (€/kWh)</i>
21.16 m²	9881.72	15193.72	2500	0.304
500 W	795	6107	1247.9	0.245
1 kW	1445	6757	1478.2	0.229
10 m ² + 500 W	5465	10777	2429.4	0.222
10.6 m ² + 500 W	5745.2	11057.2	2500	0.221
11 m ² + 500 W	5932	11244	2547.6	0.2206
11.88 m ² + 500 W	6342.96	11654.96	2651.5	0.220
13 m ² + 500 W	6866	12178	2783.9	0.219
14.42 m ² + 500 W	7526.14	12841.14	2951.6	0.218
8.65 m² + 1 kW	5484.55	10796.55	2500	0.216
10 m ² + 1 kW	6115	11427	2659.7	0.215
10.6 m ² + 1 kW	6395.2	11707.2	2730.3	0.2144
11 m ² + 1 kW	6582	11894	2779.9	0.214
11.88 m ² + 1 kW	6992.96	12304.96	2881.8	0.2135
13 m ² + 1 kW	7516	12828	3014.2	0.213
14.42 m ² + 1 kW	8179.14	13491.14	3181.9	0.212

6. Conclusions

This paper is focused on predicting, by means of time series analysis and Kohonen self organizing maps, short-time electric consumption for a four-member family living in the south of France. A cost study for the installation at the family's house of photovoltaic solar cells and/or windmills for generating electricity was also carried out.

Methodology and used tools for the prediction of short-time electric consumption proved to be efficient. The obtained results are satisfactory. The information provided by both time series analysis and Kohonen self organizing map neural network is sufficiently reliable and precise to be exploitable in order to anticipate electricity requirements. The cost study for installing at the family's house photovoltaic solar cells and/or windmills for generating electricity proved that such installation is able to respond (partially or entirely) to the family's electricity requirements but with a produced electricity more expensive than electricity sold by EDF, for any of the possible systems (only photovoltaic solar panels, only windmill or hybrid system).

References

- [1] European Renewable Energy Council, Renewable Energy Policy Review - France, Brussels, 2004.
- [2] Oberthur S. and Ott H., The Kyoto protocol, international climate policy for the 21st century, Springer, 1999.
- [3] International Energy Agency, Renewables Information, 2006.
- [4] Groupe Electricité de France (EDF), <http://www.edf.fr>.
- [5] ADEME - French state agency for the environment and energy conservation, <http://www.ademe.fr>.
- [6] Brockwell P. J. and Davis R. A., Introduction to Time Series and Forecasting, Springer, 1997.
- [7] Brockwell P. J. and Davis R. A., Time Series: Theory and Methods, 2nd edition, Springer 1991.
- [8] Alhoniemi E., Simula O. and Vesanto J., Analysis of complex systems using the self organising map, Laboratory of computer and information science, Helsinki University of Technology, Finland, 1997.
- [9] Simula O., Vesanto J., Alhoniemi E. and Hollmen J., Analysis and modelling of complex systems using the self-organizing map, Laboratory of computer and information science, Helsinki University of Technology, Finland, 1999.

An Argument-Based Approach to Deal with Wastewater Discharges

Montse AULINAS^{a,c,1}, Pancho TOLCHINSKY^a, Clàudia TURON^b,
Manel POCH^c and Ulises CORTÉS^a

^a*Knowledge Engineering & Machine Learning Group, Technical University of Catalonia, Barcelona, Spain*

^b*Consorci per a la Defensa de la Conca del Riu Besòs, Barcelona, Spain*

^c*Laboratory of Chemical and Environmental Engineering, University of Girona, Spain*

Abstract: In this paper we propose the use of an argument-based model – *ProCLAIM* – that has the potential to minimize ecological impact of industrial wastewater discharges into water bodies. On the one hand, the diversity and unpredictability of many of industrial wastewater discharges and on the other, the complexity of ecological systems that finally receive the discharge (i.e. fluvial ecosystems) illustrates the difficulty to attain a good ecological status of water bodies as required by one of the main priorities of the European Water Framework Directive (2000/60/EC). *ProCLAIM* enables *agents* involved in the wastewater management process deliberate over whether proposed actions (e.g. industrial spills) are environmentally safe, thus, making each undertaken action a more informed decision.

Keywords: agents, argumentation, integrated management, wastewater.

Introduction

Daily basis experiences show frequent uncontrolled discharges into the sewer system that sometimes are very difficult to treat and may even cause Wastewater Treatment Plant's (WWTP) operational problems. Consequently, wastewater without a proper treatment is discharged to water bodies, causing the deterioration of aquatic ecosystems.

Furthermore, these wastewater discharges do not account for the fact that 1) environmental technicians (as well as ecologists and other stakeholders involved) may disagree as to whether a toxic or a wastewater substance is or is not safe for the final receiving media (e.g. the river); 2) different policies in different regions exist (even local regions such as municipalities from the same river basin); 3) safety of substances in wastewater is not an intrinsic property of that substance, but rather an integral concept that also involves the industry, the receiving media (e.g. the river) and all the course of action to be undertaken in the discharge and wastewater treatment process.

¹ Corresponding Author: Montse Aulinás Masó, Knowledge Engineering and Machine Learning Group, Technical University of Catalonia, Campus Nord – Edifici C5, Jordi Girona 1-3, 08034, Barcelona, Spain; E-mail: montseaulinas@gmail.com; Laboratory of Chemical and Environmental Engineering, University of Girona, 17071, Girona, Spain; E-mail: aulinás@lequia.udg.cat

The emergency of these situations due to an increase and diversity of industrial activity makes necessary to provide a tool for a better integrated management and control of the industrial spills in a fluvial basin, taking into account all the agents involved (*e.g.* industries, sanitation infrastructures and water bodies). Among the Artificial Intelligence (AI) technologies available, *software agents* are considered best suited for applications that are *modular, decentralized, changeable, ill-structured* and *complex* [1]. The intended holistic approach of wastewater management bears similar characteristics: multiple users and service levels are involved; it is necessary to integrate data and information from heterogeneous sources as well as to deal with data with spatial and temporal reference and to adapt to changing conditions. Moreover, according to [2], environmental applications inherit both the uncertainty and the complexity involved in the natural environment. On the other hand, argumentation (broadly, the process of creating arguments for and against competing claims) have in recent years emerged as one of the most promising paradigms for formalizing reasoning in the above mentioned contexts [3, 4, 5].

In this paper we propose the use of the agent's argument-based model *ProCLAIM* (see [6]) to support multi-agent deliberation over action proposal. And thus, provide a mechanism to make more informed and safe decisions in the wastewater domain. Accordingly, in section 1 we introduce the *ProCLAIM* model. In section 2 we describe the model's protocol-based exchange of arguments that defines all the legal moves at each stage of the dialog, and more importantly, facilitates the exploration of all possible lines of reasoning that should be pursued *w.r.t.* a given issue. In section 3 we illustrate the model's application in dealing with the industrial wastewater discharge, as part of the whole management of wastewater in a river basin. Finally, in section 4 we present our conclusions and plan for future work.

1. The *ProCLAIM* Model

Broadly construed, the *ProCLAIM* model consists of a Mediator Agent (*MA*) directing *proponent agents* in an argument based collaborative decision making dialog, in which the final decision (a proposed action) should comply with certain domain dependent guidelines. However, the arguments submitted by the proponent agents may persuade the *MA* to accept decisions that deviate from the guidelines.

Three tasks are defined for the *MA*: 1) The *MA* guides proponent agents as to what their legal dialectical moves are at each stage in a dialogue; 2) the *MA* also decides whether submitted arguments are valid (in the sense that instantiations of schemes are relevant *w.r.t.* the domain of discourse); 3) the *MA* evaluates the submitted valid arguments in order to provide an assessment of the appropriateness of the proposed action.

In order to undertake these tasks, *MA* makes use of four knowledge resources, as shown diagrammatically in Figure 1 and described below:

Argument Scheme Repository (ASR): In order to direct the proponent agents in the submission and exchange of arguments, the *MA* makes use of a repository of Argument Schemes (AS) and their associated Critical Questions (CQs). The AS and CQs are instantiated by agents in order to construct arguments, and effectively encode the full *space of argumentation*, *i.e.*, all possible lines of reasoning that should be pursued *w.r.t* a given issue.

Guideline Knowledge (GK): This component enables the *MA* to check whether the arguments comply with the established knowledge, by checking what the valid instantiations of the schemes in ASR are (the ASR can be regarded as an abstraction of the GK). This is of particular importance in safety critical domains where one is under extra obligation to ensure that spurious instantiations of argument schemes should not bear on the outcome of any deliberation.

Case-Based Reasoning Engine (CBRe): This component enables the *MA* to assign strengths to the submitted arguments on the basis of their associated evidence gathered from past deliberations, as well as provide additional arguments deemed relevant in previous similar situations (see [7]).

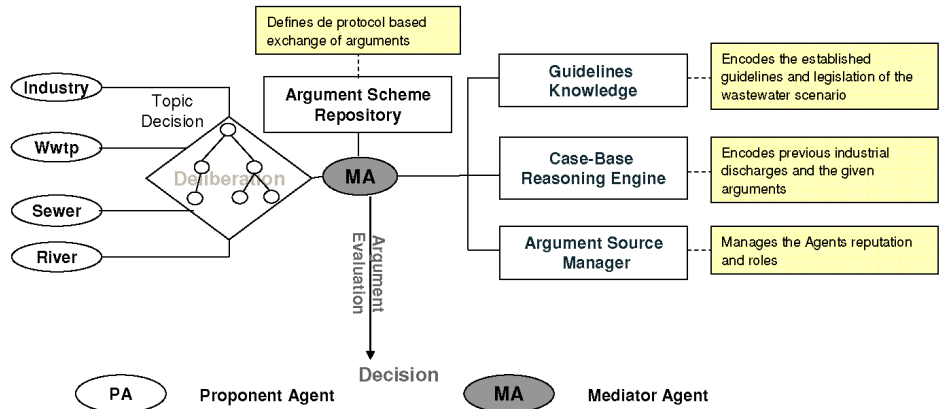


Figure 1. *ProCLAIM*'s Architecture. Shaded boxes identify the model's constituent parts specialised for the wastewater scenario introduced in section 3.

Argument Source Manager (ASM): Depending on the source from whom, or where, the arguments are submitted, the strengths of these arguments may be readjusted by the *MA*. Thus, this component manages the knowledge related to, for example, the agents' roles and/or reputations.

The deliberation begins with one of the agents submitting an argument proposing an action. The *MA* will then guide the proponent agents in the submission of further arguments that will attack or defend the justification given for the proposed action.

Each submitted argument instantiates a scheme of the ASR. The *MA* references the ASR in order to direct the proponent agents as to what their legal argument moves are at each stage of the deliberation. The validity and strength of each submitted argument is determined by the *MA* in referencing the other three knowledge resources, *viz.* GK, CBRe and ASM. Given all the accepted arguments, their strength and their interactions (based on the attack relation, see Figure 4) the *MA* then applies Dung's seminal *calculus of opposition* [8] to determine the justified or winning arguments. Hence, if the initial argument is a winning argument, the proposed action is deemed appropriate, otherwise, it is rejected.

2. Argument Schemes as a Protocol for Argumentation

The ASR is based on one AS for action proposal from which the protocol for the exchange of arguments is defined:

Definition 1: An argument is represented as a 5-tuple²:

$\langle \text{Context}, \text{Fact}, \text{Prop_Action}, \text{Effect}, \text{Neg_Goal} \rangle$

Where **Context** is a set of facts that are not under dispute, that is, assumed to be true. **Fact** is a set of facts such that given the context *Context*, then the proposed action (or set of actions) **Prop_Action** result in a set of states **Effect** that realises some undesirable goal **Neg_Goal**. *Fact* and *Effect* may be empty sets and *Neg_Goal* may be equal to nil, representing that no undesirable goal is realised. So, arguments in favour of a proposed action are of the form: $\langle \text{Context}, \text{Fact}, \text{Prop_Action}, \text{Effect}, \text{nil} \rangle$ whereas arguments against a proposed action, for instance against an industrial spill, highlight some negative goal that will be realised e.g.:

$\langle \text{Context}, \text{Fact}, \text{Prop_Action}, \text{Effect}, \text{fauna_death} \rangle$

Hence, the arguments used in the dialogue take into account: 1) the current state of affairs referenced by the facts deemed relevant by the proponent agents; 2) the proposed actions; 3) the new state achieved if a proposed action is undertaken and; 4) the undesirable goals which the new state realises.

In *ProCLAIM*, a proposed action (e.g. spill an industrial waste) is deemed to be appropriate if there are no expected undesirable side effects. Thus, a proposed action is by default assumed appropriate. Nonetheless, there must be some minimum set of conditions for proposing such an action (e.g. an industry with wastewater, and a receiving media). Thus, the dialogue starts by submitting an argument that claims the appropriateness of an action and the subsequent dialogue moves will attack or defend the presumptions present in that argument by claiming there is (*resp.* there is not) an undesirable side effect.

The six schemes we now introduce are partial instantiation of the more general scheme introduced in definition 1. These more specific schemes are intended to identify the legal instantiation of the more general scheme at each stage of the dialogue.

Let us consider R and S to be finite sets of facts in the current state and the resultant state respectively. Let A be a finite set of actions and G^- a finite set of undesirable, or negative, goals ($\text{nil} \in G^-$).

Thus, a dialogue starts with the submission of the argument:

AS1: $\langle m_c, \{\}, p_a, \{\}, \text{nil} \rangle$

Where $m_c \subseteq R$ is a minimum set of facts that an agent requires for proposing a nonempty set of actions $p_a \subseteq A$.

An argument proposing an action (via AS1) can be attacked via the argument scheme AS2 (see Figure 2). An argument instantiating AS2 introduces a new set of facts, fact, deemed to be a contraindication (e.g. a certain toxic in the spill), and thus, attacks the proposed action appropriateness, *proposed_actions*. To defend the initial proposed action, an argument instantiating AS2 can in turn be attacked by either AS3, AS4 or AS5. These schemes respectively stand for: AS3) Current circumstances are such that the introduced set of facts fact, via scheme AS2, will not result in the stated set of effects effect that realise the undesirable goal neg_goal. AS4) Current circumstances are such that the stated set of effects effect does not realise the stated undesirable goal neg_goal. And, AS5) a complementary set of actions can be undertaken in order to prevent the stated undesirable set of effects effect. Figure 2 illustrates the schemes' structure and interaction. Figure 3 illustrates examples of their use in the wastewater scenario.

² This basic argument scheme is in turn based on Atkinson's *et al.* schemes for action proposal [9].

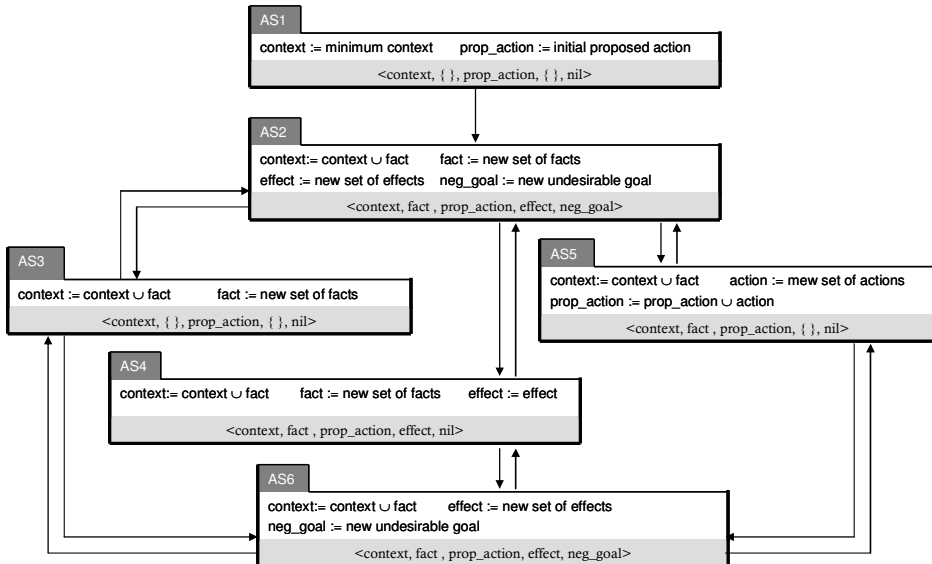


Figure 2. Schematic representation of the dialogue game (adapted from [6])

Arguments instantiating schemes AS3, AS4, AS5, are of the form $\langle \text{Context}, \text{Fact}, \text{Prop_Action}, \text{Effect}, \text{nil} \rangle$, with fact and effect possibly empty. These arguments introduce either a new fact or new complementary actions that may in turn warrant, respectively cause, some undesirable secondary effect. Hence, arguments instantiating these schemes may be attacked instantiating AS6.

An argument instantiating AS6 can in turn be attacked by arguments instantiating AS3, AS4 or AS5. Also, an argument instantiating AS3, AS4 or AS5, alter either the context or proposed action set. Hence, as depicted in Figure 2 this argument can be attacked by an argument instantiating AS2.

3. Deliberating in the Wastewater Scenario

Decision making in the wastewater domain requires participation of all the actors that affect or may be affected by a wastewater discharge. We now present a simplified example that illustrates the use of the *ProCLAIM* model in supporting deliberation among multiple agents on whether an industrial wastewater discharge is environmentally safe. This deliberation accounts for the fact that agents have different interests and knowledge. Although not covered here, *ProCLAIM* also accounts for the fact that decisions should comply with the domain's guidelines and that previous similar experiences help identify the appropriateness of a decision (see [7]).

Let us suppose an industry (*ind*) represented by the Industry Agent (*Ind_Ag*) arrives to an urgency situation in which it has to deal with a substantial amount of wastewater with high concentration of nitrogen (high_N_load). Now, as stated above, it is not only to *Ind_Ag* to decide what to do with this wastewater. We illustrate this deliberation with the following agents:

- Sewer Agent (*S_Ag*) representing the sewer system (SS) that transports wastewater (ww) from industry to the nearest WWTP.
- WWTP1 Agent (*WWTP1_Ag*) representing the nearest WWTP to industry. This facility cannot nitrify/denitrify properly. Its goal is to spill treated ww below legal limits.
- River Agent (*R_Ag*) representing the final receiving media of treated ww and the river's interest which is to reduce the damage of the arriving discharges.

	ID	Type	Argument
Example 1	A1	AS1	<{ww, sewer, wwtp1}, {}, {}, {α₀}, {}, nil>
	B1	AS2	<{ww, sewer, wwtp1}, {high_N_load}, {α₀}, {N_shock}, bad_qual_eff>
Example 2	C1	AS3	<{ww, sewer, wwtp1, high_N_load}, {rain}, {α₀}, {}, nil>
	D1	AS6	<{ww, sewer, wwtp1, high_N_load, rain}, {}, {α₀}, {hydraulic_shock}, bad_qual_eff>
	C2	AS5	<{ww, sewer, wwtp1} ∪ {high_N_load}, {}, {α₀, primary_treatment}, {}, nil>
	D2	AS6	<{ww, sewer, wwtp1, high_N_load}, {}, {α₀, primary_treatment}, {toxicity}, fish_poison>
	E1	AS3	<{ww, sewer, wwtp1, high_N_load}, {river (pH, T, F)}, {α₀, primary_treatment}, {}, nil>

Figure 3. Two example dialogues resulting from the submission of an argument *A1* proposing an emergent industrial discharge to sewer system (sewer).

Commonly, an industry discharges its ww to the sewer system that transports it to the WWTP, which after the proper treatment, discharges the ww to the final receiving media (e.g. the river). Let us call this course of action $α_0$. *Ind_Ag* may thus, propose undertaking to discharge its ww with *high_N_load* following $α_0$. This is done submitting argument *A1* = <{ind, ww, sewer, wwtp1}, {}, { $α_0$ }, {}, nil> instantiating scheme AS1. However, the high concentration of nitrogen can cause a nitrogen shock to the WWTP1. Consequently, it is of *WWTP1_Ag*'s interest to attack argument *A1*.

Let the sets R, A, S, G^- as introduced in section 2 be $R=\{\text{ind, ww, ss, wwtp1, rain, high_N_load}\}$, $A=\{\alpha_0, \text{primary_treatment}\}$, $S=\{\text{N_shock, hydraulic_shock, toxicity}\}$, and $G^- = \{\text{bad_qual_eff, fish_poison}\}$. Where *N_shock* stands for a nitrogen shock at WWTP that receives ww, and *bad_qual_eff* stands for the fact that a bad quality effluent will result if $α_0$ is done. Figure 3 illustrates the instantiations of the argument schemes, and Figure 4 their interaction. Succinctly, argument *B1* attacks *A1* identifying a contraindication (*high_N_load*) in ww causing N-shock at wwtpl that realises the negative goal of having a *bad_qual_eff*. However, argument *C1* attacks *B1* claiming that this consequence will not be achieved thanks to the dilution effect caused by *rain*. But depending on rain intensity another argument, *D1*, can be submitted attacking *C1* arguing that the rain will cause a *hydraulic-shock* that can produce lost of microorganisms (washout of microorganisms) and so an inappropriate biological treatment at wwtpl. In the second example argument *C2* identifies a new set of actions such as perform only a primary-treatment in order to prevent further problems to WWTP and then discharge the effluent to the river. Of course this new set of actions can cause toxicity problems to the receiving water body, argued by *D2*, but if the river situation (pH, temperature and flow) are appropriate to attenuate the effect caused by the

discharge, the proposed action will be deemed adequate (argument *E1* depicts this possibility).

In general a submitted argument attacks the argument it replies to. However, the attack can be asymmetrically (\rightarrow) or symmetrically (\leftrightarrow) depending on the argument schemes they instantiate. In the symmetric cases there is a disagreement in which the new introduced factor (new set of facts or new prop_action) is or is not a contraindication for the proposed action.

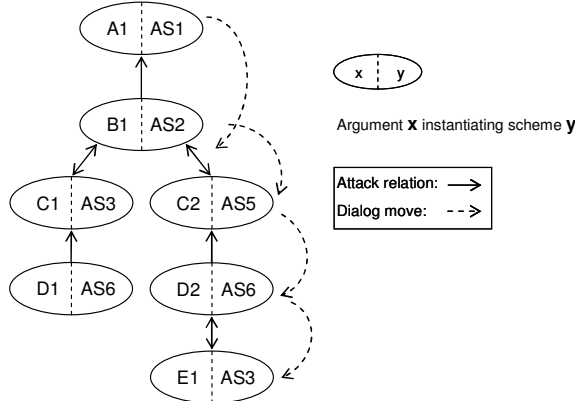


Figure 4. Dialogue graph showing the interaction between the arguments used in the two examples given in Figure 3.

In order to decide whether the agents' proposed action is appropriate, the *MA* has to determine if argument *A1* is a winning argument. In example 1 if *B1*, *C1* and *D1* are accepted as valid arguments, the proposed discharge will be rejected, as *A1* would be defeated by *B1*, and *B1* is defended from *C1* by *D1*. However in example 2 if all arguments are accepted as valid, the discharge will be deemed environmentally safe if and only if, both *E1* is preferred to *D2* (*i.e.* in effect, the river situation attenuates the effect caused by the discharge) and *C1* is preferred to *B1* (a primary-treatment prevents WWTP1's nitrogen shock). *MA*'s evaluation process is described in more detail in [7].

4. Conclusions and Future Work

In this paper we propose the use of a novel argument-based model, *ProCLAIM*, to support decision making in a wastewater scenario. *ProCLAIM* provides an environment for agents to deliberate over the appropriateness of proposed actions, accounting for the domain's guidelines, the agents' role and or reputation and the resolution of previous deliberations.

This paper extends our work presented in [10] where we focused on motivating the need for an integrated management of wastewater in a river basin. Focus here is in the deliberation process that allows agents to argue on whether a proposed action *is or is not appropriate*. That is, whether it will affect negatively any of the actors involved in managing and/or receiving wastewater. This deliberation accounts for the facts that 1) agents may disagree on the appropriateness of an action or plan of actions; 2) decisions should comply with the domain guidelines 3) but there may be exceptional circumstances where deviating from such guidelines may be justified.

One problem in the wastewater scenario is that in many emergency situations (e.g. shutdown of an industry implying a punctual overload of some pollutants due to the cleaning process; or a problem during production that result in an emergent undesirable discharge), no course of action exist that can avoid undesirable effects (including doing nothing at all) nonetheless, an action must be taken. In this special circumstances, what accounts as an appropriate course of action is that which has the least undesirable effects (rather than none). Thus, changes need to be made in the *ProCLAIM* model to accommodate this wastewater scenario requirement.

ProCLAIM defines the basic protocol for the exchange of arguments, where a new introduced argument must attack an earlier one. However, this scenario requires that agents exchange messages that may not be *attacking arguments*. For example, an industry agent (*Ind_ag*) may ask the *wwtp_agent* for the most appropriate moment for a punctual discharge, before actually proposing the spill. Namely initiating an information seeking dialog (see [11]). Thus, another task for the future is to define the dialog protocol for the participant agents.

Acknowledgments

This paper was supported in part by the Grant FP6-IST-002307 (ASPIC).

References

- [1] H. v. D. Parunak, 2000. Agents in overalls: Experiences and Issues in the Development and Deployment of Industrial Agent-Based Systems, *International Journal of Cooperative Information Systems* 9 (3), pp. 209-227.
- [2] I. N. Athanasiadis, 2005. A review of agent-based systems applied in environmental informatics. In *MODSIM 2005 Int'l Congress on Modelling and Simulation*, Melbourne, Australia, pp. 1574-1580.
- [3] ASPIC. Deliverable D2.1: Theoretical frameworks for argumentation. <http://www.argumentation.org/Public Deliverables.htm>, June 2004.
- [4] H. Prakken and G. Vreeswijk, 2002. Logical Systems for Defeasible Argumentation. In *Handbook of Philosophical Logic*, volume 4 of D. Gabbay and F. Guenther (eds.), second edition, pp. 218-319. Kluwer Academic Publishers, Dordrecht.
- [5] C. Chesñevar, A. Maguitman and R. Loui, 2000. Logical Models of Argument, *ACM Computing Surveys* 32 (4), pp. 337-383.
- [6] P. Tolchinsky, K. Atkinson, P. Mc. Burney, S. Modgil, U. Cortés, 2007. Agents deliberating over action proposals using *ProClaim* Model. Submitted to CEEMAS 2007 (Available at: <http://www.lsi.upc.edu/~tolchinsky/publications/ceemas07.pdf>)
- [7] P. Tolchinsky, S. Modgil, U. Cortés and M. Sánchez-Marré, 2006. CBR and Argument Schemes for collaborative Decision Making. In *Conference on Computational Models of Argument (COMMA 06)*, volume 144 of *Frontiers in Artificial Intelligence and Applications*, P.E. Dunne and T.J. M. Bench-Capon (eds.), pp. 71-92. IOS Press
- [8] P. M. Dung, 1995. On the acceptability of arguments and its fundamental role in nonmonotonic reasoning, logic programming and *n*-person games. *Artificial Intelligence*, 77:321-357.
- [9] Atkinson K., 2005. What should we do? Computational Representation of Persuasive Argument in Practical Reasoning. PhD thesis, Department of Computer Science, University of Liverpool, UK.
- [10] M. Aulinás, P. Tolchinsky, C. Turon, M. Poch, U. Cortés, 2007. Is my spill environmentally safe? Towards an integrated management of wastewater in a river basin using agents that can argue. *7th International IWA Symposium on Systems Analysis and Integrated Assessment in Water Management (WATERMATEX 2007)*, Washington DC, USA.
- [11] D.N. Walton & E.C.W. Krabbe, 1995. Commitment in Dialogue: Basic Concepts of Interpersonal Reasoning, J. T. Kearns (ed.), State University of New York Press, New York.

Analysis of Common Cause Failure in Redundant Control Systems Using Fault Trees

David BAYONA I BRU¹, and Joaquim MELÉNDEZ^a and Gabriel OLGUIN^b

^a *Grup eXiT, Universitat de Girona*

^b *ABB AB, Corporate Research*

Abstract: This paper highlights the importance of reliability studies for systems where high reliability is a must. The common cause failure concept is introduced and studied due to its relevancy. A simple hypothetical control system is used to illustrate the methodology. Fault tree is used to assess the reliability of the workbench system. The comparison between different tests shows the importance of common cause failure.

Keywords. Common cause failure, reliability, fault tree, redundant control

1. Introduction

Redundancy in control systems (sensors, control units, input/output cards, communication system and actuators) is usually applied to those processes which operation is critical. The redundant control systems in nuclear power plants and pharmacy industry to fulfil international safety standards is a good example of such systems. The actual implementation of redundancy can follow different strategies. Control system components have different failure probability and different sensitivity to external common disturbances. Redundancy implies an extra cost and therefore an accurate reliability analysis to discover critical components is needed in order to assist the design of such facilities.

In this paper fault tree modelling is used to analyse control reliability. Fault trees allow a hierarchical and visual representation of the system under analysis. A modular decomposition of the system at different levels and the identification of interactions among them is used to build the tree. The failure rate associated to each module or component is used in the reliability analysis of the whole system. Reliability is hardly affected by common cause failures (CCF), i.e. events that affect more than one component at the same time. CCF are in general unpredictable. They might be the result of an event that affects a common area where several components are located. Floods, fire, ambient conditions... are possible situations that affect a large numbers of devices reducing drastically reliabil-

¹Correspondence to: ; E-mail: dbayona at gmail dot com

bility. Therefore the analysis of CCF is an important task in order to ensure the continuous operation of critical processes.

The paper is organised as follows. Section 2 introduces the basis of the theoretical background of reliability and fault trees. Section 3 presents a simple work-bench control system which is then used in Section 4, Test and Results, to illustrate the fault tree and CCF analysis. Finally, Section 5 discusses the results and presents the main conclusions.

2. Fundamentals on Reliability Analysis

Reliability has become more important with the increasing complexity and risk of modern industrial processes. Reliability assessment has economical benefits,[1], due to reduction of production loses, maintenance cost and accidents. From the various techniques to quantify reliability, fault tree analysis (FTA) is one of the most commonly used. Other techniques as Failure Mode and Effect Analysis, Markov analysis, Monte Carlo between others can be combined with FTA to empower the outcome.

Reliability is a complex theory. Different concepts exist applicable to different systems; depending on its features, e.g. repairable or not. Next lines define some of the most important and basic concepts, where no higher knowledge on mathematics is required; but the reader must remember that the theory bases on statistics.

Reliability r , is the probability that an item will perform its intended function for a specified time interval under stated conditions, [2].

Availability A , is the probability that a given system is performing successfully at time t independently of its previous states. Average availability measures the uptime as a proportion of a given working cycle, Eq. 1.

$$A_{average} = \frac{uptime}{total\ time} \quad (1)$$

Failure rate(λ), It is widely used as measure of reliability, it gives the number of failures per unit time from a number of components exposed to failure, [3]. It is frequently measured in failures per billion² hours and these units are denoted as FIT.

Availability reaches a steady state condition when time tends to infinity, which is affected only by failure and repair rates. Moreover, one must suppose that the probability distribution function (PDF) of failure is exponential, [4], and it is a frequently supposition for electronic devices, [3]. Under such consideration Eq. 1 can be reformulated as Eq. 4, where MTBF stands for Mean Time Between Failures, MTTR stands for Mean Time To Repair, and ∞ means steady state.

$$\lambda(\infty) = \frac{1}{MTBF}. \quad (2)$$

²Billion in American notation equals to 10^9

$$\mu(\infty) = \frac{1}{MTTR}. \quad (3)$$

$$A(\infty) = \frac{\mu}{\mu + \lambda}. \quad (4)$$

λ in Eq. 2 stands for the failure rate introduced above. In Eq. 3, μ stands for the repair rate. Both are the basic formula that relate the output with the data from the devices.

2.1. Fault tree approach

Fault tree analysis (FTA) was developed by H.A. Watson [5]. FTA has been used to model nuclear power plants and aerospace industry between others, [6]. Fault tree provides a concise and visual representation of combinations of possible events affecting a system in a set of odd behaviours previously defined. The basis of FTA lies in Boolean algebra for simple analysis and it is extended to probability and statistics analysis allowing more complex models. FTA is an “up-bottom” technique oriented to represent failure modes of the systems. The basic rules to build a fault tree are: [7].

- Describe the top event accurately and the boundaries of the system behaviour.
- Divide the problem into scenarios as technical failures, human errors or software, and develop them as deep as necessary³
- Use consistent nomenclature for all devices and events, otherwise the analysis can be incorrect.

FTA construction ends with a system failure probability model where the combination of elements that lead the system to failure are explicitly represented. A basic model consists in connecting logical gates (ANDs and ORs are the basic ones) that describe elements and dependencies among subsystems. AND is a logical operator used to represent that all the inputs must occur simultaneously to cause the output, (See Eq.5). On the other hand, the OR gate is fired only when one input occurs, (See Eq. 6). Eq. 5 and 6 represents the probability at the output of the gate and $P(a_i)$ is the probability of the elements involved (input). There are different ways to assess the failure probability of the basic events. When there is no database available the data can be found in manufactures datasheets of the components, but if such information is not provided there are standards for different nature of components.

$$P_{and} = P(a_1 \cap \dots \cap a_n) = \prod_{i=1}^n P(a_i). \quad (5)$$

³The depth of the study depends on the available information, knowledge and experience about the system

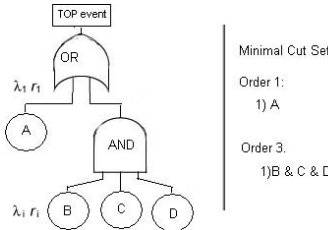


Figure 1. Fault tree and Cut sets

$$P_{or} = P(a_1 \cup \dots \cup a_n) = \sum_{i=1}^n P(a_i) - \prod_{i=1}^n P(a_i). \quad (6)$$

In the construction of the fault tree the top node represent the failure mode and collects the influence of all the components and subsystems through branches composed by logical gates. When branches cannot be further developed those elements placed at the bottom are called basic events. They must be sufficiently detailed to relate them to those devices which failure and repair rates are available or can be calculated. Previous formula are then used to derive the final availability of the whole system and analyse the influence of each component and event.

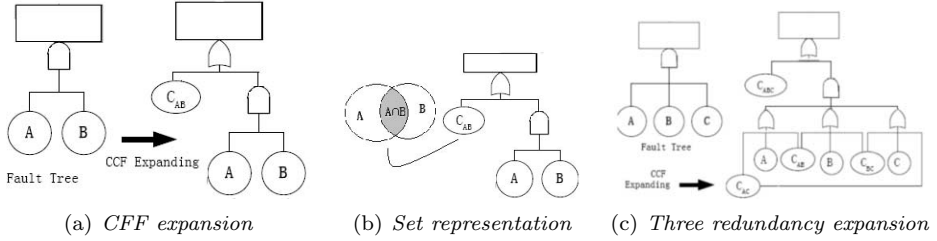
Cut sets is a group of basic events whose simultaneous occurrence leads the system to fail. Its influence is propagated to the top event through the logical gates. A cut set is said to be minimal when it cannot be reduced without loosing its status. So, cut sets permit to study relation between events from different parts of the system [8]. Figure 1 illustrates the concept of cut sets. The order of the cut set is understood as the number of basic events in the cut set. However, technical software can differ from this definition and their specifications must be carefully read.

2.1.1. Common cause failure

Those elements affected by the same adverse influences (stressors), typically those that are placed together or submitted to the same ambient conditions, are candidates to be affected by common cause failures (CCF). Typical CCF are environment, temperature, electromagnetic fields or floods. In redundant systems studies the consideration of CCF are very important because the total reliability without considering them can be too optimistic [9]. β -model and Multiple Error Shock Model (MESH) are two different approaches to deal with the analysis of CCF in fault trees. In this paper the β -model has been used because its use is widely extended. It consists in splitting the total failure rate (λ_t) in two parts. One becomes the new failure rate of the individual component (λ_n) and the second part is the failure rate associated to the CCF. Eq. 7 summarises this simple decomposition.

$$\lambda_{CCF} = \sum_{i=1}^2 (1 - \beta \lambda_{ti}). \quad (7)$$

The β -model is easily understood when explained through the set theory. Figure

Figure 2. β -model representation

2(a) illustrates the expansion of the new fault tree when the CCF are assessed. The shadow region represents the events for λ_{CCF} . Applying β -model one assume that the events become dependent instead of independent, which is the first assumption when designing fault trees in redundant systems and it modifies the results of the reliability analysis. It does not exist any methodology to assess β , in spite of this [3] describes a method briefly. Figure 2(c) shows the fault tree expansion for systems with three redundant elements that fails when two elements fail in their function.

3. Workbench description

A simple system has been used to analyse the effect of redundancies in presence of common cause failures. Figure 3(a) depicts this system. It is a controlled tank, where the control unit regulates the level. Flow and level sensors are used to monitor the system behaviour. Actuators are manual and automatic valves operated by the controller. In the reliability analysis faults in the transmitters are not considered and in the first analysis only those the elements listed in Table 1 have been considered for building the fault tree. The failure rates in the table have been obtained from standard manuals [10] containing information about common failure rates of generic devices. The values on the second column are typical times to repair for those systems and they are rated in hours. In the last column, q is the unavailability of the system, which equals to one minus the availability (defined above).

	λ (failures / hour)	MTTR	q
pump (p)	1,50E-05	15,00	2,25E-04
controlled valves (cv x)	4,61E-07	4,00	1,84E-06
valves (v x)	2,40E-07	3,50	8,40E-07
Check valves (ck x)	1,00E+00	4,50	8,18E-01
flow sensors (s xx)	1,67E-06	2,00	3,34E-06
level sensor (level)	9,76E-05	2,00	1,95E-04
cell sensor (cell)	9,76E-05	2,00	1,95E-04
Controller unit (cpu)	3,39E-06	10,00	3,39E-05

Table 1. Elements' data

When building the fault tree, a failure mode is defined by those conditions that cause to empty the tank. Different casuistic can be given according to how

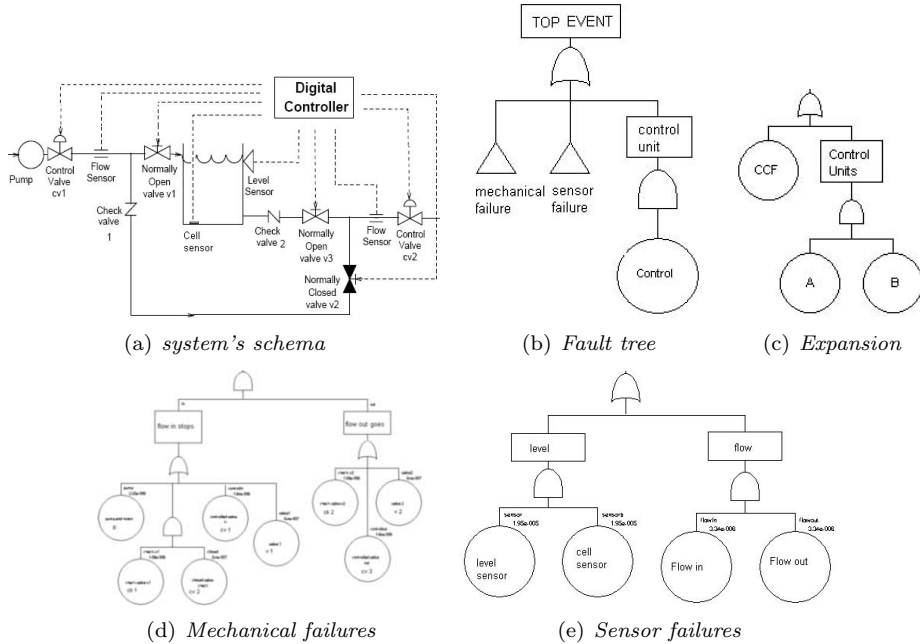


Figure 3. System

components interact. From this analysis the fault tree in Figure 3(b) is obtained, where the round event represents the control unit that later will be expanded to consider redundancy. Mechanical failures and sensor failures have been separated in two different scenarios represented by triangles. Each triangle represents an entire fault tree expanded in Figure 3(d) and 3(e).

4. Tests and results

The workbench has been tested with OpenFTA, a software package covered by *GPL* license, [11]. The tests are divided in three different scenarios. The first one is the analysis of the system as presented above where redundancy does not exist in any element. The results obtained permits us to define the two other scenarios because redundancy must be applied to those elements with higher importance if one wants to be consistent with the theory. The first column of Table 2 and 3 points out the weakest element: the control unit. The following tests study the redundancy of the control unit. The first test lacks of common cause failure influences. The next three tests are computed when common cause failure arise and the control unit in Figure 3(b) is expanded as Figure 3(c) shows. The three tests differ between them from the β values. The results of all this test are presented in Table 2 and 3 under the name single for the first test, redun. for the second scenario and CCF for the last three test explained.

Typical β values for systems placed together, fed by same power supplies without isolation starts from 0.02 and above as [3] stats. The higher β used here is 0.01,

what would mean that CCF's effects are few in our system, therefore it represents the most realistic case of the three β values.

	Single	Redun.	CCF		
			$\beta=0,0001$	$\beta=0,001$	$\beta=0,01$
ck 1 (valve)	0,00	0,00	0,00	0,00	0,00
cl 2 (valve)	0,00	0,33	0,10	0,01	0,00
v 2 (valve)	0,00	0,00	0,00	0,00	0,00
cv 1 (valve)	0,00	0,37	0,12	0,02	0,00
cv 2 (valve)	0,00	0,50	0,16	0,02	0,00
s in (sensor)	0,00	0,72	0,23	0,03	0,00
s out (sensor)	0,00	0,72	0,23	0,03	0,00
p (pump)	0,00	0,51	0,16	0,02	0,00
level (sensor)	0,00	24,38	7,68	1,07	0,11
cell (sensor)	0,00	24,38	7,68	1,07	0,11
v 1 (valve)	0,00	0,19	0,06	0,01	0,00
v 3 (valve)	0,00	0,25	0,08	0,01	0,00

Table 2. Less important events

control	100	73,82	23,26	3,25	0,34
control2	no	73,82	23,26	3,25	0,34
common	no	no	68,49	95,60	99,54
q	3,39E-05	1,56E-09	4,95E-09	3,54E-08	3,40E-07

Table 3. Major contribution events and un-availability

The rows in Table 2 and rows above q in Table 3 represent the contribution of the element to the failure of the system using *P-models* and it is presented in %. The contribution is important when comparing elements in the same test, but it cannot be compared among different tests. The last row, q is the unavailability in failures/hour. It permits to compare the results of the different tests because it measures the same parameter.

The reader will see that the unavailability is highly increased when the weakest parts are redundant, comparison between first and second column. Being realistic and considering β the increase starts to decrease and as higher the β is lower the improvement. The total improvement coming from this test tumbles 2 orders of magnitude between the most realistic case and when redundancy without CCF are compared.

5. Conclusions

This paper portraits the importance of common cause failure consequences and therefore the importance of CCF analysis. The analysis of a non-redundant system gives an important relation of the weakest parts of the system. These parts will be prone to be reinforced through redundancy or better quality components. After seeing the results we can conclude that CCF must be taken into account in any analyses in order to not jeopardise the reliability of the system. The results of such studies, like the ones presented here, can drive designers to redesign the

implementation of the project if they are performed during design stage, which intends to provide higher reliability and reduce the costs.

When the systems become larger and more complex reliability studies become more complicated and hundred if not thousands basic events exist. Some typical disciplines inside artificial intelligence (AI) can help to find elements affected by the same CCF in a basic events database e.g. data mining.

Acknowledgements

This work has been partially supported by ABB Corporate Research, Västerås, Sweden and the research project DPI2006-09370 funded by the Spanish Government and developed in the eXiT research group of the University of Girona, which is part of AEDS - Automation Engineering and Distributed Systems -, awarded with a consolidated distinction (SGR-00296) for the 2005-2008 period in the Consolidated Research Group (SGR) project of the Generalitat de Catalunya.

References

- [1] D. J. Smith, *Reliability Maintainability and Risk*. Burlington, MA: Butterworth Heineann Ltd., 2003.
- [2] *Definitions of Effectiveness Terms for Reliability, Maintainability, Human Factors and Safety*, U.S. Department of Defense Std. MIL-STD-721B, 1981.
- [3] W. M. Goble, *Control systems safety evaluation & reliablility*. Research triangle park, NC: ISA, 1998.
- [4] C. Bono, R. Alexander, et al., "Analyzing reliability- a simple yet rigorous approach," in *IEEE Trans. Applicat. Ind.*, vol. 40, no. 4, 2004, pp. 950-957.
- [5] H. Watson, *Launch control safety study*. Bell Labs.: Murray Hill, NJ, 1961, vol. 1.
- [6] C. Ericson, "Fault tree analysis- a history," in *Proc. of the 17/th International System safety Conference*, Seattle, Washington, 1999.
- [7] W. Vesely, F. Goldberg, et al., *Fault Tree Handbook*. Wasington, D.C.: U.S. nuclear regulatory comission, 1981.
- [8] R. A. Long, "Beauty and the beast- use and abuse of the fault tree as a tool," *Hernandez engineering, Inc*, USA,AL.
- [9] A. Mosleh et al., "Procedure for treating common cause failure in safety and reliability studies," in *U.S. Nuclear regulatory commission*, Washington, DC, 1988.
- [10] *Reliability Prediction of Electronic Equipment*, U.S. Department of Defense Std. MIL-HDBK-217.
- [11] Formal Software Construction Ltd. (1991) The openfta website. [Online]. Available: <http://www.openfta.com/>

Kalman Filters to Generate Customer Behavior Alarms

Josep Lluis de la Rosa¹, Ricardo Mollet², Miquel Montaner³, Daniel Ruiz⁴, Víctor Muñoz⁵

Abstract Aggressive marketing campaigns to attract new customers only covers customer churn, resulting in neither growth nor profitability. Retaining current customers, increasing their lifetime value, and reducing customer churn rates, thereby allowing greater efforts and resources to be dedicated to capturing new customers are the goals of a commercial director. But how can that loss be detected in time and avoided—or at least reduced? There is the 3A program to keep customers loyal, based on analyzed information from our customers, to construct an expert alarm agent and one-to-one retention actions. In this paper we show how to apply the Kalman filter and study how to configure it to predict the normal behavior of customers by projecting their consumption patterns into the future. Abnormal behavior detected by the Kalman filter triggers alarms that lead to commercial actions to avoid customer churn.

Keywords: relational marketing, customer retention and loyalty, one-to-one actions, Kalman filter, intelligent agents

1. Motivation: Why Retain Customers?

1.1 The 3A Loyalty Program

It is a marketing service that consists of the purchasing behavior of customer (by means of an engine called 2A) to retain the most valuable customers. The fact is that if a company has a relatively small number of customers, commercial technicians or agents can closely monitor each one of them. However, when the company has a large number—thousands or even hundreds of thousands—of customers, the sales network will be unable to fully and dynamically control the behavior of many of them, focusing efforts on capturing new customers and monitoring current, generally heavy use customers. Even though that information exists and can be obtained through well-organized database enquiries or found in company reports, it is usually unfeasible for a sales network to analyze the data for each client. In addition to the effort made by the

^{1,3,5} Josep Lluis de la Rosa, Miquel Montaner, Victor Muñoz : EASY Center of the Xarxa IT CIDEM, University of Girona. Campus Montilivi (Edif. PIV) 17071. Girona, Catalonia. Tel. + 34 972418854, E-mail: {peplluis, mmontane, vmunoz}@eia.udg.es

^{2,4} Ricardo Mollet, Daniel Ruiz, PSM-Carlson Marketing Group, Barcelona-Madrid, Spain, {ricardo, daniel_ruiz}@psm.es

sales network, a large part of company resources are aimed at capturing new customers: brand advertising, product advertising, promotions, discounts, direct marketing, etc. One example is the use of bold campaigns by cell phone companies in Spain in recent years to capture new customers. Unfortunately, in many of these situations limited resources and other strategic focuses mean that customer loss is only detected when it is already too late and recapturing them would be too difficult or too expensive. Retaining customers is profitable: published studies have indicated this; despite the difficulties studying the effects of an increase in customer loyalty on a company (it must be done using comparable test areas, under *the same* conditions, with reliable information about the competition and general market trends, etc.).

1.2 How do Customer Acquisition and Loyalty Programs Work?

First of all, customers are reached by exposing them to “the product or service” (advertising, sales networks, recommendations from other customers) and obtain “product or service proof”. However, to attain loyalty from customers—and to retain them—we must be able to strengthen the *head share* to ensure their purchasing actions are repeated (the purchases repetition is the differential factor to know whether the customer values the product) [7]. Product and/or service quality, adequate prices and customer service are obviously essential, but not sufficient, conditions for their loyalty. Customers “become accustomed” to those aspects and are no longer surprised: they “forget” the company. Satisfying customer expectations is an unending task: establishing mechanisms of continued communication with customers, using special promotions, reinforcing brand image and the image of products and services, etc. are also necessary to maintain and increase the *head share* of the product or service in the minds of customers as well as the emotional links with them—special treatment, privileges and deals only for customers.

Loyalty programs are meant to achieve this objective: in each transaction customers accumulate points they can exchange for products, gifts, etc. or, after a certain volume of transactions, they can take advantage of discounts they would not have had otherwise. For example, airline company loyalty cards let us accumulate points for each flight and then use them to obtain free flights, and let the company gather knowledge about the customer behavior. Likewise, accumulating transactions (flights) can lead to special treatment, privileges and exclusive deals that create particular bonds among customers and companies. In addition, reminding customers of the points they have obtained establishes periodic contact with them in a natural way. And, it should not be forgotten that a record of customer transactions means that an otherwise anonymous service becomes a valuable source of information.

2. What does the 3A Customer Retention Consist Of?

3A is supported by an integrated management system consisting of various marketing, statistical, computer, communication and promotional techniques with the same objectives: generating trust, retaining customers and increasing their *life time value*.

2.1 General Description of the 3A Program

Briefly, the 3A program can be implemented in three separate phases:

1. **Datamining the database** through *statistical* techniques, to segment customers and detect their behavior [4] based on a small group of basic values (for example, in a transportation company, total shipments made, kilos sent, revenue per kilo sent). Subsequently, the behavior analysis of each customer can be made more sophisticated using multiple variables (for example, use of each of the products or services; time/urgency, documents, geographic areas...).
2. Establishing an **expert alarm agent** to personalize actions for individual customers and detect both positive and negative changes in their behavior. In other words, an agile and adaptable alarm system to ensure we act in time. Here, the agent needs the application of a filter, the Kalman filter, as we will show in the following sections.
3. Developing a different **action plan** according to customer type, behavior and profitability. The actions will have been pre-established according to anticipated changes in behavior, although the results of the alarm system will undoubtedly make us reconsider some of the actions or indicate new ones. The actions will be *one-to-one* intended only for those customers who have triggered a specific type of alarm.

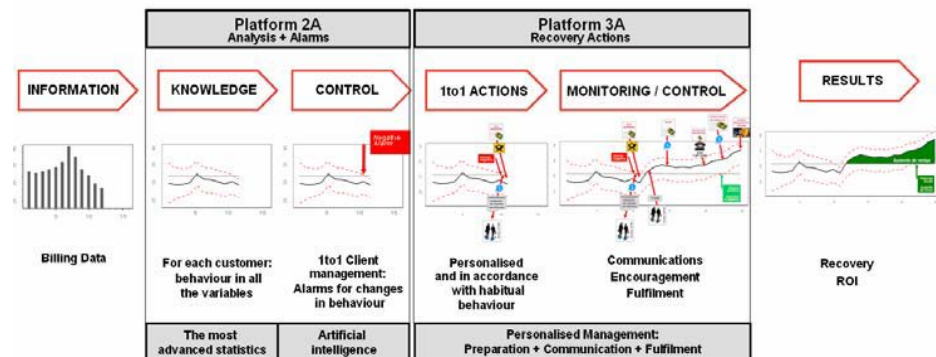


Fig. 1. The 3A program of loyalty actions of the PSM Company

2.2 Expert Alarms Agent and the Need of Kalman Filters

The objective, as we have explained in the description of the 3A program, is to develop an agile alarm system in an agent platform [3] which detects changes in customer activity. Based on what was explained in the previous section, it might seem natural for a good alarm system to detect changes in customer categories. However, this approach (creating alarms by clustering) has three serious disadvantages:

- Customers who are about to change categories can trigger an alarm even though the change in activity is very small. However, customers at the upper end of the interval can substantially reduce their activity before a category change occurs.
- Inclusion in a category of activity is usually based on interannual data (12th order moving average, if we use monthly accumulations) so that the category change can occur with unacceptable delay relative the change in activity.

- We do not take into account the ‘history’ of customers in terms of their variability and seasonality of their behavior. We should not consider decreases in consumption—for example, over two consecutive months—of customers with stable trajectories in terms of the use of a product or service to be the same as decreases in consumption of customers with much more erratic behavior, or seasonal behavior (ice creams in summer, Christmas sweets in winter, etc).

Here follows the need to filter the individual behavior of every customer instead of by clustering them. However, the *agent* must come across yet another problem: the lack of precision in alarms caused by data noise or by **the lack of exact activity bounds algorithms in the state of the art** [1]. In that respect, approaches used in many companies, such as percentage change (increases or decreases) based on annual, semiannual or quarterly accumulations, are not very reliable in terms of alarm sensitivity and specificity. And using Markov chains to predict the risk of collective customer loss is interesting as a *macro* analysis, but it has obvious disadvantages when we need a system to act in a personalized way. What therefore is the alternative? Our proposal is related to dynamic prediction models, especially the state space model, namely the Kalman filter. We have used Bayesian prediction techniques and dynamic models in monitoring and prediction processes in short-term time series in industrial, economic and commercial spheres of activity.

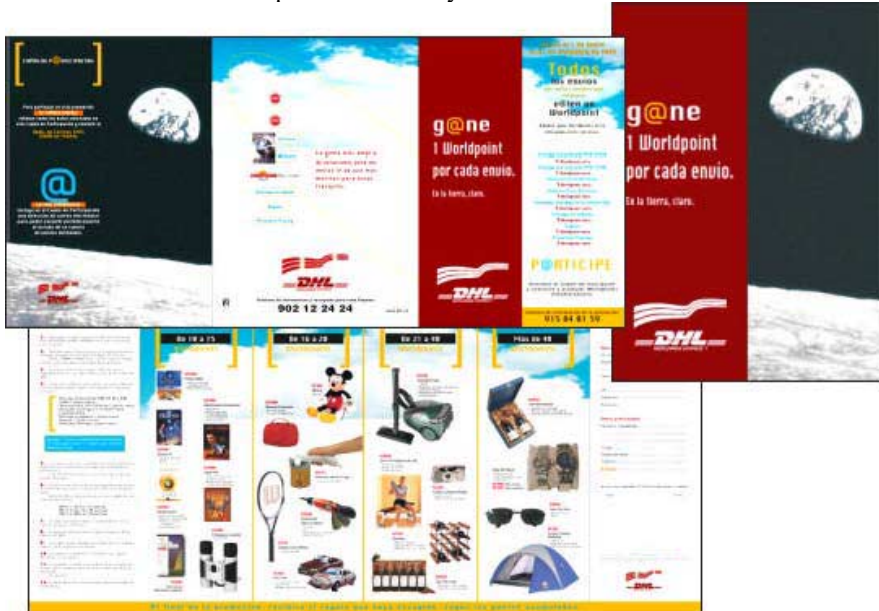


Fig. 2 Examples of generic actions based on models of customer activity with the 3A retention program

3. Applying the Kalman Filter to Predict Customer Purchasing Patterns

Kalman filter provides an estimation of model parameters, detailed predictions and the uncertainty measures associated with these predictions. The great flexibility of the Kalman filter model formulation makes it possible to deal with situations in which, during the process, structural changes may need to be monitored. Likewise, it is

possible to introduce control components (interventions) and predict in advance or evaluate afterwards their impact on the system. The incorporation of sequential information allows adaptive estimation and automatic filtering based on Bayesian methods to update and extend the knowledge of the system. The linear dynamic systems formulated in state space constitute an extension of inference and prediction techniques associated with classic methods (exponential smoothing, EWMA [8] [9]). Tools developed for these models, like the Kalman filter equations [5] [6], make it possible to predict, filter, and smooth the trajectory corresponding to the state of the system, based on observations made of it. If the distribution of the activity indicators approaches normal distribution, the model used corresponds to a DLM (dynamic linear model). If customer behavior is stable, the values of the indicators will be constant (constant prediction function), while erratic behaviors will vary the indicators.

The activity observed in a customer during a certain period can be modeled as a ‘real’ level of underlying activity plus a perturbation originating in ‘external factors’. The aim of the monitoring process is to estimate and predict that level of underlying activity to detect structural changes (tendencies, and significant, transitory or level changes).

The objective of the Kalman filter [5] is to estimate and predict customers’ levels of underlying activity for each indicator detect structural changes in their behavior and generate an alarm. The Kalman filter is a set of mathematical equations that predicts an efficient recursive solution of the method of squared minimums. This solution lets us calculate a linear, unbiased and optimal estimator of the state of a process at any moment of time using the information available at moment $t-1$, and update those estimations with the additional information available at moment t .

In this representation the customer is described with a set of variables, called state variables, containing all the information relative to the customer at a certain moment of time. This information should allow customer behavior to be inferred and future behavior to be predicted. Based on the information obtained about past and predicted customer behavior, we will decide to set off an alarm when an important structural change is detected. First we will define the model used in the Kalman filter and then we will specify the criteria used to set off alarms according to the results of the filter.

3.1 Definition of a User Model by means of Kalman Filter

The state of the filter is characterized by two variables:

- $\hat{x}_{k|k}$, the estimator of the state in time k . (i.e. the number of transactions)
- $P_{k|k}$, the error covariance matrix (precision of the estimation of the state)

Prediction

- $\hat{x}_{k|k-1} = F_k \hat{x}_{k-1|k-1} + B_k u_k$ (prediction of the state)
- $P_{k|k-1} = F_k P_{k-1|k-1} F_k^T + Q_k$ (prediction of the estimated covariance)

Update

- $\hat{y}_k = z_k - H_k \hat{x}_{k|k-1}$; $S_k = H_k P_{k|k-1} H_k^T + R_k$
- $K_k = P_{k|k-1} H_k^T S_k^{-1}$ (Kalman gain)
- $\hat{x}_{k|k} = \hat{x}_{k|k-1} + K_k \hat{y}_k$ (Updated estimation of the state)
- $P_{k|k} = (I - K_k H_k) P_{k|k-1}$ (Estimation of the updated covariance)

where z_k is the real value of the state at time k .

The prediction phase uses the estimation from the previous step to estimate the current state. In the update phase, the information about current step measurements is used to refine the prediction and obtain a new, more precise estimator.

3.2 Simplification of the Model

To create the customer activity model with the Kalman filter, we formulate the following hypotheses to simplify the model:

- The customer activity for period t **will be the same** as in period $t-1$. Therefore, the transition matrix F is the identity matrix.
- We do not know which external factors can modify customer behavior. Therefore, the vector u_k is void.
- The measurement of the variable is correct; therefore the matrix H is the identity matrix.

With these assumptions our simplified user model is as follows:

Prediction

- $\hat{x}_{k|k-1} = \hat{x}_{k-1|k-1}$ (prediction of the state)
- $P_{k|k-1} = P_{k-1|k-1} + Q_k$ (estimated prediction of the covariance)

Update

- $\hat{y}_k = z_k - \hat{x}_{k|k-1}$; $S_k = P_{k|k-1} + R_k$
- $K_k = P_{k|k-1} S_k^{-1}$ (Kalman gain)
- $\hat{x}_{k|k} = \hat{x}_{k|k-1} + K_k \hat{y}_k$ (updated estimation of the state)
- $P_{k|k} = (I - K_k) P_{k|k-1}$ (updated estimation of the covariance)

3.3 Filtering Process

According to the previous simplified user model, the filtering process will consist of:

Initialization

- Establish initial state values: x ($x_{0|0}$) and P ($P_{0|0}$)

Iterations (beginning with $k=1$)

- Prediction calculation:

$$\hat{x}_{k|k-1} = \hat{x}_{k-1|k-1} ; P_{k|k-1} = P_{k-1|k-1} + Q_k$$
- Update: the update is done with the known value of the analyzed variable at moment k (“Input Value” column of the table of significant data, which is the real value of the variable or the seasonally adjusted value when the series is seasonally adjusted previously) and the values calculated in the prediction.

$$\begin{aligned} \hat{y}_k &= z_k - \hat{x}_{k|k-1} & S_k &= P_{k|k-1} + R_k & K_k &= P_{k|k-1} S_k^{-1} \\ \hat{x}_{k|k} &= \hat{x}_{k|k-1} + K_k \hat{y}_k & P_{k|k} &= (I - K_k) P_{k|k-1} \end{aligned}$$

As we can see, these equations use the variables Q_k and R_k , which are the errors at moment k . We propose calculating them in the following way:

$$R_k = Q_k = \bar{x}_k$$

where \bar{x}_k is the median in the last k periods.

Example:

In Table 1 we can see an example of the Kalman filter calculation for a DHL customer and a specific indicator. Initial values have been set at $x_{0|0} = 10$ and $P_{0|0} = 5$.

Table 1. Results of experiment 1

k	z_t	$\hat{x}_{k k-1}$	$P_{k k-1}$	S_k	K_k	$\hat{x}_{k k}$	$P_{k k}$	10	5
0									
1	11	10	5.1	5.85	0.8718	108.718	0.6538		
2	11	108.718	0.7538	15.038	0.5013	109.361	0.376		
3	9	109.361	0.476	1.226	0.3882	101.844	0.2912		
4	12	101.844	0.3912	11.412	0.3428	108.068	0.2571		
5	7.5	108.068	0.3571	11.071	0.3225	97.402	0.2419		
6	8	97.402	0.3419	10.919	0.3131	91.953	0.2348		
7	10	91.953	0.3348	10.848	0.3087	94.437	0.2315		
8	6.5	94.437	0.3315	10.815	0.3065	85.414	0.2299		
9	9.5	85.414	0.3299	10.799	0.3055	88.342	0.2291		
10	6.5	88.342	0.3291	10.791	0.305	81.223	0.2287		
11	7	81.223	0.3287	10.787	0.3047	77.803	0.2286		
12	5	77.803	0.3286	10.786	0.3046	69.333	0.2285		
13	5	69.333	0.3285	10.785	0.3046	63.445	0.2284		
14	5	63.445	0.3284	10.784	0.3045	5.935	0.2284		
15	6	5.935	0.3284	10.784	0.3045	59.548	0.2284		
16	4	59.548	0.3284	10.784	0.3045	53.595	0.2284		
17	6	53.595	0.3284	10.784	0.3045	55.546	0.2284		
18	7.5	55.546	0.3284	10.784	0.3045	6.147	0.2284		
19	5	6.147	0.3284	10.784	0.3045	57.977	0.2284		
20	5	57.977	0.3284	10.784	0.3045	55.548	0.2284		
21	4	55.548	0.3284	10.784	0.3045	50.813	0.2284		
22	6	50.813	0.3284	10.784	0.3045	53.611	0.2284		
23	8	53.611	0.3284	10.784	0.3045	61.647	0.2284		
24	10	61.647	0.3284	10.784	0.3045	73.326	0.2284		
25	11	73.326	0.3284	10.784	0.3045	84.494	0.2284		
26	10	84.494	0.3284	10.784	0.3045	89.216	0.2284		
27		89.216	0.3284						

Table 2. Results of experiment 2

k	z_t	Baseline	$\hat{x}_{k k-1}$	$P_{k k-1}$	$\hat{x}b^+_{k k-1}$	$\hat{x}b^-_{k k-1}$	1	11	11	10	5.1	14.263	55.737
1	11						2	11	11	108.718	0.7538	125.736	9.17
2	9						3	9	9	109.361	0.476	122.883	95.839
3	12						4	12	1033.333	101844	0.3912	114.103	89.586
4	7.5						5	7.5	10.75	108.068	0.3571	119.78	96.355
5	8						6	8	10.1	97.402	0.3449	108.863	85.941
6	6.5						7	10	9.75	91.953	0.3348	103.295	80.611
7	6.5						8	6.5	9.785.714	94.437	0.3315	105.721	83.152
8	9.5						9	9.5	9.375	85.414	0.3299	96.671	74.156
9	6.5						10	6.5	9.388.889	88.342	0.3291	99.586	77.098
10	7						11	7	9.1	81.223	0.3287	92.461	69.985
11	5						12	5	8.909.091	77.803	0.3286	89.038	66.568
12	5						13	5	8.583.333	69.333	0.3285	80.567	5.81
13	5						14	5	8.083.333	63.445	0.3284	74.678	52.213
14	6						15	6	7.583.333	5.935	0.3284	70.583	48.118
15	4						16	4	7.333.333	59.548	0.3284	7.078	48.316
16	6						17	6	6.666.667	53.595	0.3284	64.827	42.363
17	6						18	7.5	6.541667	55.546	0.3284	66.778	44.314
18	5						19	5	6.5	6.147	0.3284	72.702	50.238
19	5						20	5	6.083.333	57.977	0.3284	69.209	46.745
20	4						21	4	5.958.333	55.548	0.3284	6.678	44.316
21	6						22	6	5.5	50.813	0.3284	62.045	39.581
22	8						23	8	5.458.333	53.611	0.3284	64.843	42.379
23	10						24	10	5.541667	61.647	0.3284	72.879	50.415
24	11						25	11	5.958.333	73.326	0.3284	84.558	62.094
25	10						26	10	6.458.333	84.494	0.3284	95.726	73.262
26	27							27	6.875	89.216	0.3284	100.448	77.984

4. Alarm Activation

Alarms are activated according to a baseline. The baseline tells us the normal level of activity of the customer. When real activity is “considerably” far from the baseline, an alarm goes off.

To determine this “considerable” distance, we define activity bounds, which establish a confidence interval around the activity of the customer. The alarm will sound when the activity bounds do not include the baseline of the customer.

Three activity bounds will be defined: the most restrictive (closest to the activity of the customer) will generate low-level alarms; the middle one will generate mid-level alarms; and the least restrictive (most removed from the activity) will generate the alarms at the highest level.

4.1 Activity Bounds

The activity bounds are calculated with the following formula:

$$xb_i = x_i \pm r \cdot \sqrt{P}$$

where x_i is the value of the activity, P is the variance of this value (so \sqrt{P} is the typical deviation), and r is the tolerance index which, in a Gauss distribution, must be 1.96 to include 95% of the values, or 2.58 to include 99% of them.

4.2 Customer baseline

The customer baseline is calculated using the moving average method, which incorporates seasonal variation. This method contains five parts. The first four are optional and make up part of the process of seasonal adjustment of the series.

1. Calculation of the seasonally adjusted baseline.
2. Median of “Time Window” periods.

Calculation of the seasonally adjusted baseline

$$D_t = \frac{Y_t}{IVE_t}$$

where

$$IBVE_t = \frac{Y_t}{MM_t}, \quad \text{and} \quad IVE_h = IVE *_h \frac{L}{\sum_{j=1}^L IVE *_j} \quad \text{and} \quad IVE *_h = \frac{\sum_{t \in h} IBVE_t}{T-1}$$

and the calculation of the moving averages is as follows: Given a time window L , the moving averages for each period t are calculated, for odd L

$$MM(L)_t = \frac{1}{L} \sum_{i=t-\frac{L-1}{2}}^{t+\frac{L-1}{2}} y_i$$

where y_i is the value of the variable in the period i . Meanwhile, for even L (in this case the moving average with $L = 2$ is done again):

$$MM(L)_{t+0.5} = \frac{1}{L} \sum_{i=t-\left(\frac{L}{2}-1\right)}^{t+\frac{L}{2}} y_i$$

Calculation of the final baseline

A median is used for the baseline using the “Time window” parameter (N):

$$Baseline_t = \frac{\sum_{i=t}^{t+N} D_i}{N}$$

Example:

In Table 2 we can observe the calculation of the baseline and of the activity bounds of a customer; in this case only activity bounds of a single level have been created. In the example the values $r=1.96$ and $n=12$ have been chosen.

4.3 Example

In this plot we can see the activity of the customer from Table 1:

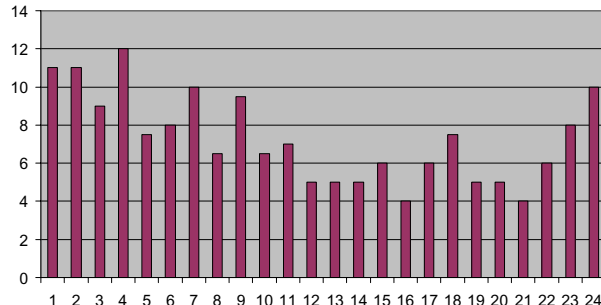


Fig. 3. Consumption of a DHL customer during 24 months

The result of the Kalman filter on said customer, adding the calculation of the activity bands and baseline is the following:

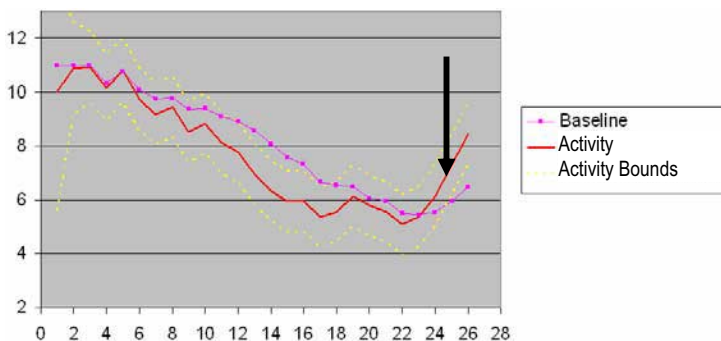


Fig. 4. Activity baseline and higher and lower bounds

We see how at the indicated point an alarm would sound, given that the trust interval of the prediction does not include the baseline of the customer. Each warning (alarm) will have an associated impact. The impact will be calculated with the formula given in the table of significant variables.

Adjusting the Parameters

As we have seen, there is a series of parameters that must be calibrated in the system:

- $x_{0|0}$: Value of the initial state.
- $P_{0|0}$: Value of the covariance of the initial state.
- r : Tolerance index used in the delimitation of the activity bounds.
- n : Number of periods used in the time window where the customer baseline

The values of r and n can be global for all the customers and indicators, but the parameters $x_{0|0}$ and $P_{0|0}$ must be adjusted individually.

- r is the tolerance index, used to calculate the activity bounds. In a Gauss distribution it is 1.96 to include 95% of the values, or 2.58 to include 99% of them. We propose **1.96** for the 1st bound, **2.58** for the 2nd and **3.5** for the 3rd.
- n , is used to calculate the baseline of the customer and represents the number of previous periods that are taken into account. Depending on the seasonal variation of the activity of customers, values of 12, 18 or 24 (months) can be chosen. In the DHL example we propose **12** months.

5. Future Work

The Kalman filter is applicable to predict the behavior of customers from a dynamic point of view. However, the individual values belong to customers and are calculated according to their activity. In conclusion, we propose the individual values as:

$$x_{0|0} = x_{1|1} \quad \text{and} \quad P_{0|0} = \left(\frac{x_{0|0}}{2r} \right)^2 - Q_{1|1}$$

In the future, we will compare this Kalman method of prediction with the interval uncertainty model [1] to create autotuning methods for this filter to avoid overbounding, and regarding the particular type of customers of every company. We expect the number of false behavior warnings will be less than it is with other methods.

Acknowledgements

The PSM company, the Spanish Ministry of Science and Technology (project TIN2006-15111/Estudio sobre Arquitecturas de Cooperación) and the EU (project No. 34744 ONE: Open Negotiation Environment, FP6-2005-IST-5, ICT-for Networked Businesses).

References

- [1] Armengol J., Travé-Massuyès L., Vehí J., and de la Rosa J. Ll., A survey on interval model simulators and their properties related to fault detection ISSN: 1367-5788, Annual Reviews in Control, Vol. 24, No. 1. pp. 31-39, Springer-Verlag, Oxford, UK, 2002.
- [2] Berry M., Linoff G. (1997). Data Mining Techniques: For Marketing, Sales, and Customer Support. Wiley, New York.
- [3] Acebo, E., Muntaner, E., *Una plataforma para la Simulación de Sistemas Multiagente Programados en Agent-0*. Workshop de Docencia en Inteligencia Artificial, Congreso de la Asociación Española para la Inteligencia Artificial CAEPIA-TTIA, Gijón (2001). Utrecht University (2003).
- [4] Bezdek J. C. (1981). Pattern recognition with fuzzy objective functions. Plenum Press. New York.
- Gan, F. (1995). Joint monitoring of process mean and variance using exponentially weighted moving average control charts. *Technometrics*, 37: 446-453.
- [5] Kalman, Rudolph E., A New Approach to Linear Filtering and Prediction Problems, *Transactions of the ASME-Journal of Basic Engineering*, Vol. 82, Series Dm pp. 35-45, 1960.
- [6] Oliva, F., De Caceres, M., Font, X., and Cuadras, C. M. (2001). Contribuciones desde una perspectiva basada en distancias al fuzzy C-means clustering. XXV Congreso Nacional de Estadística e Investigación Operativa. Úbeda, 2001.
- [7] J.Ll. de la Rosa, La Lucha por la fidelidad del Consumidor, Internet Global Conference IGC 2002, Internet Global Conference 4^a Edición, Barcelona, April 27-30, 2002
- [8] Shumway, R. and Stoffer, D. (2000). Time series analysis and its applications. Springer-Verlag.
- [9] West, M. and Harrison, J. (1999). Bayesian Forecasting and Dynamic Models. Springer-Verlag.

A Knowledge Discovery Methodology for Identifying Vulnerability Factors of Mental Disorder in an Intellectually Disabled Population

Xavier LLUIS MARTORELL^a, Raimon MASSANET VILA^a, Karina GIBERT^{b,c}, Miquel SÀNCHEZ-MARRÈ^{b,d}, Juan Carlos MARTÍN^c, Almudena MARTORELL^e

^aFacultat d'Informàtica de Barcelona, Barcelona

^bKnowledge Engineering and Machine Learning Group, UPC, Barcelona

^cEstadística i Investigació Operativa, Universitat Politècnica de Catalunya, Barcelona

^dLlenguatges i Sistemes Informàtics, Universitat Politècnica de Catalunya, Barcelona

^eCarmen Pardo-Valcarce Foundation, Madrid

Abstract. This paper proposes a knowledge discovery methodology for generating new hypothesis to a particular knowledge theory. A combination of AI and Statistical techniques is proposed to increase the corpus of current knowledge of the target domain. In this paper a particular application to analyze comorbid mental disorders with intellectual disability is presented as an example.

Keywords. Knowledge Discovery, Data Mining, Mental disorder, WAIS, WHO-DAS, ECFOS.

Introduction

A number of studies have shown higher rates of mental health disorders in people with Intellectual Disability (ID), compared to those without ID [1] suggesting an increased bio-psychosocial vulnerability [2, 3]. Greater vulnerability in people with ID is probably the result of both external and internal factors, including increased dependency on others, and reduced cognitive mechanisms to cope with stressful events. Models which could explain these outcomes of increased psychopathology among people with intellectual disability would be really useful in order to shed some light to this phenomenon as well as for designing preventive interventions.

This paper is an example of how a knowledge discovery and data mining approach can turn data into useful knowledge. Although the methodological approach presented here is generic and can be applied to any data source, in this paper a real application to increase the corpus of current knowledge in Intellectual Disability is presented as an example.

Throughout the study two objectives were kept in mind:

- To give information on vulnerability factors that concern the development of mental disorders in intellectually disabled people, using knowledge discovery tools that allow working with numerical and qualitative variables, which is not a common practice in the mental health scope.
- To study different realizations of the proposed working methodology by combining different methods and algorithms at each point, and making a comparative analysis to determine the best way of capturing unknown information from the database.

This paper is mainly split in three sections. Section one describes a general methodology to extract new non-obvious knowledge from a data set. Section two describes a particular realization of the methodology for a given problem: the study of the vulnerability factors for developing a mental disorder in an intellectually disabled population. Finally, conclusions and future work are discussed in section three.

1. Methodology

Most common used methodologies in business for knowledge discovery practice are the SEMMA (Sample, Explore, Modify, Model, Assess) methodology [4] and the CRISP-DM (Cross-Industry Standard Process for Data Mining) methodology [5]. Both methodologies share a splitting of the process in iterative and interactive tasks. SEMMA is more oriented to the technical aspects of the process development and it is strongly related to the SAS products. On the other hand, CRISP-DM was designed in late 1996 by a very important consortium of companies in Europe: NCR, Daimler-Benz (AG), ISL (SPSS) and OHRA, as a neutral methodology regarding the software tool used in the process, more focused on the real business problem, and being a free and open distribution methodology.

Both methodologies are specializations of the general framework of knowledge discovery procedure proposed by Fayyad [6]. Our proposed methodology is also a particular concretion of the general framework proposed by Fayyad. Main feature of our methodology is that is specially oriented to discovering new non-obvious knowledge patterns hidden in a concrete domain. Our methodology can be applied to whatever domain.

The proposed knowledge discovery procedure is performed according to the following steps:

1. Data preprocessing. This step includes data cleaning, meta-information validation with experts, and the generation of a graphical summary for each variable.
2. Preliminary hierarchical clustering with all numerical variables¹ to determine the proper number of classes to be build. The level indexes of the resulting dendrogram were plotted and used to determine the number of different classes in the population.

¹ If the software permits a hierarchical clustering with both numerical and categorical variables, this step can be skipped and hierarchical clustering used in step 4.

3. Identification of the most informative variables using an unsupervised feature weighting method. Some unsupervised methods are very good at detecting redundancies among variables, which might not have been previously detected by the expert.
4. Clustering using variable weights obtained in step 3, with all variables, both numerical and qualitative. An algorithm taking feature weights into account was used. This kind of algorithms usually work better as they prioritize important attributes when determining classes. This will identify typical patterns of individuals to be treated homogeneously.
5. Interpretation of the classes. In this paper two approaches are compared:
 - 5.1. Using an additional supervised feature weighting.
 - 5.1.1. Computation of each attribute's relevance with regard to the response variable using a supervised feature weighting algorithm.
 - 5.1.2. Selection of variables that have a weight over some threshold, in order to build explicative models taking only really significant variables into account. To do this, variable weights were plotted in order to find an important discontinuity, then a threshold value was chosen at that discontinuity.
 - 5.2. Not using any additional feature weighting. Selection of all variables.
6. Interpretation of profiles obtained in step 4 using supervised learning methods with variables selected in step 5.1.2. Decision trees were used to try to explain the class assigned to each individual in step 4 as a combination of the significant variables selected in step 5.1.2. These trees give a very graphical and expressive description of the classes and are very useful in determining the clustering quality.
7. Definition and calculation of leaf contamination index for the class variable (see below for details).
8. Response variable projection on each leaf of the decision tree.
9. Labeling of the tree leaves with the dominant value of the response variable.
10. Calculation of the leaf contamination index (CI) regarding the response variable (see below for details).
11. Identification of the relevant patterns as those extracted from leaves with $CI > 0.9$
12. Interpretation and validation of the results.

A *leaf contamination index* is specifically defined here to evaluate the quality of the results. This index is defined in the following way: *Given a leaf L of a decision tree and a qualitative variable X with values v_1, v_2, \dots, v_s ; let v_d be the dominant value of X in L , and let C_i be the sets of individuals in L whose value for X is v_i . Then the leaf*

$$\text{contamination index } CI = \frac{\sum_{i \neq d} \|C_i\|}{\sum_i \|C_i\|}$$

This rate gives an idea of how pure a leaf is.

This is a generic methodology and there are plenty of algorithms that can be used at each step. In our experimentation the following were used:

- Ward method and Euclidean distance for hierarchical clustering in step 2.
- UEB1 (Unsupervised Entropy Based-1) method for unsupervised feature weighting in step 3 [7].
- K-means using $L'Eixample$ distance measure for clustering in step 4. [8]
- CVD (Class Value Distribution) method for supervised feature weighting in step 5. [9]
- CART (Classification and Regression Tree) as a supervised classification technique [10] in step 7.

2. Application

2.1. Data

The database contains 34 variables, which are the result of a previous feature selection process performed together with the experts from a larger set of 279 variables. Some of these attributes are scores obtained by individuals in several clinical scales that measure different aspects of the state of the patient as functional disability (WHO-DAS), intellectual disability (ICAP, WAISS), or amount of attention required from the family (ECFOS). There are some other attributes collecting some socio-economical information like age, gender, type of residence and number of people living in residence. Finally, other attributes were generated specifically by the expert, like age difference between the individual and his or her mother, or age difference between the individual's parents. The response variable (PRESENCE) was a binary variable indicating whether the individual has or has had any mental disorder.

2.2. Results

First of all, it is interesting to remark that the direct induction of a decision tree performed with the variable PRESENCE as the target has been done, and it produces obvious patterns according to the experts point of view, so that very low scores in the ICAP.TC (which measures conduct disorders) are predictors of mental disorder, which do not significantly improve the know-how on the problem. This is the reason why the proposed methodology is used instead.

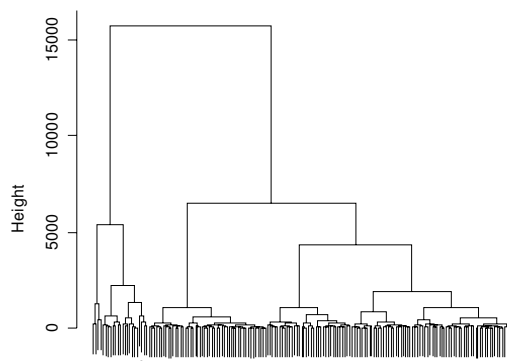


Figure 1. Cluster dendrogram

The first step after the exploratory statistical analysis of data is to build a hierarchical clustering using numerical variables. Figure 1 shows the resulting dendrogram. A 4-cluster partition is performed according to the classical criteria of maximizing the ratio of inertia between and within classes. The dendrogram indicates a good partition although we are not considering qualitative attributes, that accounts for the 37% (13 of 35) of attributes.

Then two experiments were performed:

- a) K-means with four classes using Euclidean distance without weighting the variables followed by the induction of the decision tree to explain the classes.
- b) K-means with four classes using *L'Eixample* distance with the variables weight calculated by UEB1 algorithm, taking into account that previous research has shown that this configuration used to produce better results [4]. In this case, CVD algorithm is used to assess the relevance of the variables regarding the target PRESENCE, and the induction of the final decision tree is performed only using the variables with a weight higher than a certain threshold. Figure 2 shows the CVD results of each attribute. It can be seen that there is a discontinuity around the value of 5. This gap indicates that 5 is a good threshold to discard attributes below. Doing so, only 22 out of 35 variables were kept. The resulting models will be validated and evaluated by a mental health expert. Below, the two induced decision trees are shown. For each node the distribution of the instances among the target clusters is shown together with the label of the dominant cluster, in order to allow manual post pruning.

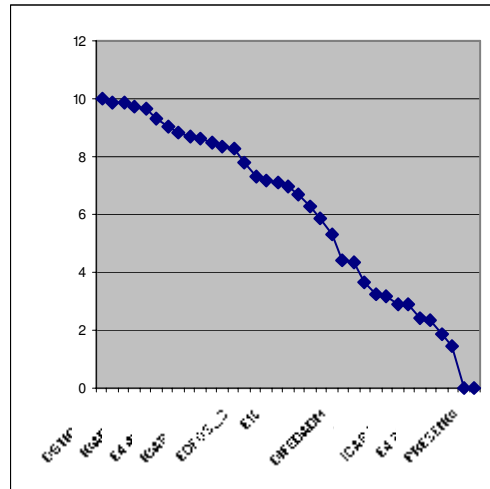


Figure 2. Plot of each attribute's score using CVD

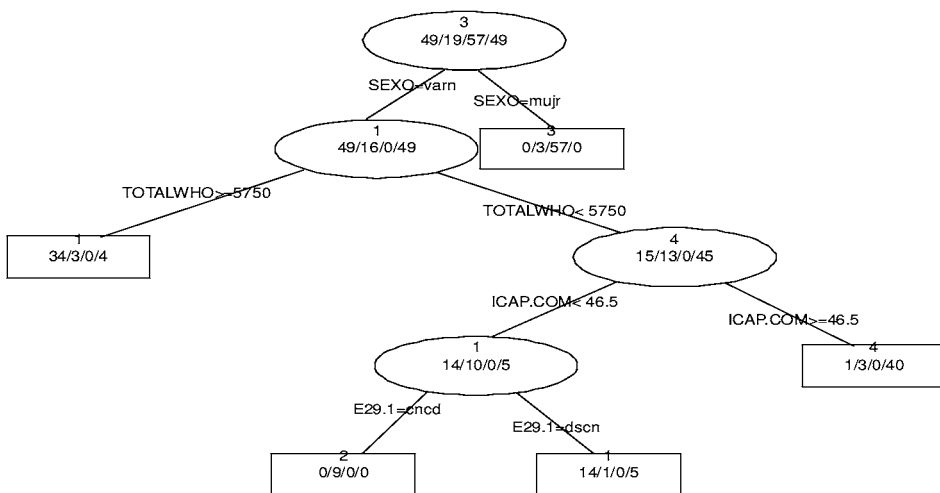


Figure 3. Induced decision tree corresponding to experiment a).

Next step is to analyze for every tree which is the relationship with the target PRESENCE. Table 1 shows the distribution of the values of PRESENCE in the different leaves of the decision tree in the experiment a), which is depicted in figure 3. Those leaves with contamination lower than 10% will be pure enough, on the expert's opinion, to be labeled as those patterns with comorbid intellectual disability and mental disorders. For this particular experiment a) no pure-enough patterns were discovered.

Table 1. Contamination table for experiment a)

		Leaf				
		1	2	3	4	5
PRESENCE	Yes	75,61%	44,44%	30,00%	20,45%	26,67%
	No	24,39%	55,56%	70,00%	79,55%	73,33%
CI		24,39%	44,44%	30,00%	20,45%	26,67%
Average CI		29,19%			Max CI	44,44%

cluster tree - eixample clustering

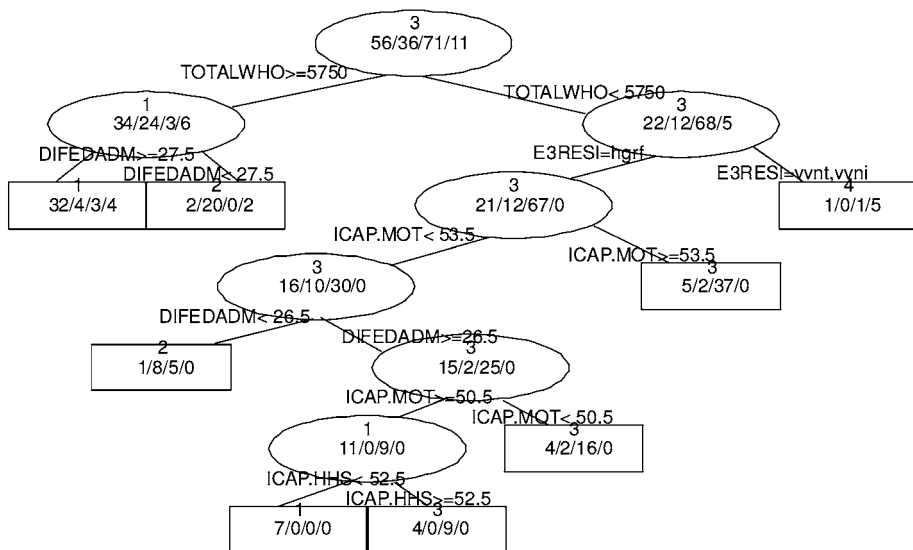


Figure 4. Induced decision tree corresponding to experiment b).

For experiment b), results are significantly better. Figure 4 shows the decision tree induced with the 25 selected variables. Table 2 shows the distribution of the PRESENCE values along the final leaves of the tree.

Table 2. Contamination table for experiment b)

	Leaf							
	1	2	3	4	5	6	7	8
PRESENCE Yes	74,14%	75,00%	82,35%	87,50%	92,86%	81,48%	83,02%	70,00%
PRESENCE No	25,86%	25,00%	17,65%	12,50%	7,14%	18,52%	16,98%	30,00%
CI	34,88%	33,33%	21,43%	14,29%	7,69%	22,73%	20,45%	42,86%
Av. CI	24,71%				Max CI	42,86%		

A similar analysis was performed by the expert with experiment b). In this case, experts found results meaningful. The characterization of clusters according to experiment b) would be:

Cluster 1:

- TOTALWHO >= 5750 & DIFEDADM >= 27.5 (43)
- TOTALWHO < 5750 & DIFEDADM >= 26.5 & E3RESI = family home & 50.5 <= ICAP.MOT < 53.5 & ICAP.HHS < 52.5 (7)

Cluster 2:

- TOTALWHO >= 5750 & DIFEDADM < 27.5 (24)
- TOTALWHO < 5750 & E3RESI = family home & ICAP.MOT < 53.5 & DIFEDADM < 26.5 (14)

Cluster 3:

- TOTALWHO < 5750 & E3RESI = family home & ICAP.MOT >= 53.5 (44)
- TOTALWHO < 5750 & E3RESI = family home & DIFEDADM >= 26.5 & ICAP.MOT < 50.5 (22)
- TOTALWHO < 5750 & E3RESI = family home & DIFEDADM >= 26.5 & 50.5 <= ICAP.MOT < 53.5 & ICAP.HHS >= 52.5 (13)

Cluster 4:

- TOTALWHO < 5750 & E3RESI = independent or tutelary home (7)

In this case, there is one pattern associated with a very low contamination, the one corresponding to leaf 5 (5^{th} leaf visited in pre-order traversal), which permits identification of a new and relevant knowledge pattern which medical experts didn't have in mind, although they found very interesting. This leaf can be labelled as people with comorbid intellectual disability and mental disorders, and it identifies a specific pattern related with this comorbidity. People in this leaf responds to the following characterization: Individuals with TOTALWHO less than 5750 (low degree of functioning), who live with family, with relatively big age difference with their mother (DIFEDADM), with motorial problems (ICAP.MOT between 50.5 and 53.5) and high social abilities (ICAP.HHS >= 52.5). These are individuals living in a social structure, with social abilities but their motorial and functioning problems for sure generate some disequilibrium than could be the origin of a mental disorder.

These results identify a very specific pattern associated with comorbid intellectual disability and mental disorder and constitute a new hypothesis on the knowledge corpus of the target domain and can increase the know-how on the problem if they can be confirmed by the corresponding later experiments specifically designed for this purpose.

So, the proposed methodology is useful to identify new knowledge-hypothesis about the patterns associated to a certain medical situation, which may contribute to increase the know-how on the problem.

Most of preliminary data preparation computations, data relevance analysis, data mining algorithms and model result visualizations were done using the GESCONDA knowledge discovery tool [11].

3. Conclusions

In this work a specific combination of AI and Statistical techniques is designed as a new methodology for discovering new knowledge regarding the interaction of a response variable and a set of patterns. Projecting a response variable on a decision tree induced from the classes discovered in a domain is a good possibility for discovering non trivial relationships between the response variable and some specific pattern discovered in an unsupervised way. This is an interesting alternative to be taken into account in these applications where the direct use of supervised methods on the response variable does not provide results other than obvious or trivial. It was found that the use of both AI and statistical methods together improved the quality of the knowledge extracted.

Clustering is used to discover a first structure in the domain. Also, the use of unsupervised feature weighting methods can improve the quality of the results of clustering algorithms, as weighting improves the measure of the similarity/distance function [6]. The use of decision trees when applied to clustering results helps inducing knowledge patterns directly understandable by domain experts. The co-joint use of decision trees, clusters and projection of response variable give more detailed insight about the structure of the clusters, and are a good complement to a clustering study.

Here a real application of the proposed methodology to the discovery of the vulnerability factors for comorbid mental disorders and intellectual disability is presented. A new pattern associated to the development of mental disorder in intellectual disabled person is discovered. Experts found interesting this results and will develop further medical research to verify that intellectually disabled persons leaving in the family with old-aged mothers, high social abilities and motorial and functioning problems are very likely to develop a comorbid mental disorder.

This experience shows the potential capacity of the proposed methodology to generate scientific hypothesis in the target domain which are appealing to the expert's point of view and which can contribute to the improvement of the domain know-how.

Acknowledgements

This research has been partially funded by project TIN2004-1368.

References

- [1] M. Campbell and R.P. Malone. Mental retardation and psychiatric disorders. *Hospital and Community Psychiatry* **42** (1991), 374–379.
- [2] World Health Organization. Clasificación Internacional del Funcionamiento, de la Discapacidad y de la Salud: CIF. Ed. IMSERSO, 2001.
- [3] J.L. Matson and J.A. Sevin (1994). Theories of dual diagnosis in mental retardation. *Journal of Consulting and Clinical Psychology* **62** (1994), 6-16.
- [4] G. Held. The process of data mining, in: *Proceedings of the Eighth International Symposium on Applied Stochastic Model and Data Analysis*, 1997, pp. 155–164.
- [5] C. Shearer. The CRISP-DM model: the new blueprint for data mining. *Journal of Data Warehousing* **5** (2000), 13-22.

- [6] U.M. Fayyad, G. Piatetsky-Shapiro, and P. Smyth: From Data Mining to Knowledge Discovery: An Overview. In *Advances in Knowledge Discovery and Data Mining*, MIT Press, 1996, 1-34.
- [7] H. Núñez and M. Sànchez-Marrè. Instance-Based Learning Techniques of Unsupervised Feature Weighting do not perform so badly! In *Proceedings of ECAI'2004*, IOS Press, 2004, pp. 102-106.
- [8] R. Dubes and A.K. Jain. Clustering Methodologies in Exploratory Data Analysis, volume 19, *Advances in Computers* **19** (1980).
- [9] H. Núñez, M. Sànchez-Marrè and U. Cortés. Improving Similarity Assessment with Entropy-Based Local Weighting. In ICCBR'2003 Proceedings. LNAI-2689, 2003, pp.377-391.
- [10] L. Breiman, J.H. Friedman, R.A. Olshen and C.J. Stone, *Classification and Regression Trees*, Wadsworth, Belmont, 1984.
- [11] K. Gibert, M. Sànchez-Marrè and I. Rodríguez-Roda. GESCONDA: An Intelligent Data Analysis System for Knowledge Discovery and Management in Environmental Data Bases. *Environmental Modelling & Software* **21**(1) (2006), 116-121.

This page intentionally left blank

Author Index

Agell, N.	368	Golobardes, E.	153
Aguado, J.C.	368	González, J.	161
Aguiló, I.	291	Grieu, S.	392
Albós, A.	87	Hormazábal, N.	77, 104
Alsina Pagès, R.M.	384	Hu, Y.-C.	310
Angulo, C.	v, 323	Isern, D.	67
Ansótegui, C.	19	Khosravi, A.	376
Armengol, E.	153	Kovac, N.	112
Aulinas, M.	400	Larriba-Pey, J.L.	141
Ballester, M.A.	291	Levy, J.	19
Baró, X.	189	Llorens, D.	223
Bauk, S.	112	Lluís Martorell, X.	426
Bayona i Bru, D.	408	Lopardo, G.A.	77
Bernadó Mansilla, E.	133, 384	López Arjona, A.M.	255
Binefa, X.	181, 233	López de Mántaras, R.	331
Bonet, M.L.	19	Lopez, B.	11
Brito, I.	38	López-Navidad, A.	300
Caballero, F.	300	López-Sánchez, M.	95, 112
Calvo, T.	291	Lugosi, G.	3
Casasnovas, J.	273	Luo, N.	351
Castell, N.	263	Macià-Antolínez, N.	133
Castelló, V.	339	Manyà, F.	19
Cerquides, J.	95	Martín, J.C.	426
Colomer, J.	376	Martín, S.	223
Cortés, U.	300, 400	Martinez, B.	181
Dawson, J.	310	Martinez, T.	376
de Givry, S.	29	Martínez-Bazan, N.	141
de la Rosa i Esteva, J.L.	77, 104, 120, 255, 416	Martorell, A.	426
de los Llanos Tena, M.	120	Marzal, A.	223
del Acebo, E.	104	Massanet Vila, R.	426
Delgado, L.	263	Mateo, X.	233
Dellunde, P.	57	Mauri, J.	197
Escríg, M.T.	339	Mayor, G.	291
Falomir, Z.	339	Meléndez, J.	376, 408
Fernández-Nofrerías, E.	197	Merida-Campos, C.	49
Formiga Fanals, L.	384	Meseguer, P.	38
Fornells, A.	153	Mollet, R.	416
García, F.A.	161	Montaner Rigall, M.	255, 416
García-Lapresta, J.L.	291	Moreno, A.	67, 245
Gibert, K.	359, 426	Muñoz, V.	416
Godó, L.	v	Muntés-Mulero, V.	141
Goldhoorn, A.	331	Murillo, J.	11
		Nieves, J.C.	300

Nin, J.	141	Sanchez, J.	376
Olguin, G.	408	Sanchez, Marti	29
Orozco, J.	161	Sánchez, Mónica	310
Osorio, M.	300	Sàncchez-Marrè, M.	426
Pardo, D.E.	323	Sandri, S.	281
Perez-Rovira, A.	181	Sayeras, J.M.	310
Peris, J.C.	339	Schiex, T.	29
Poch, M.	400	Sibertin-Blanc, C.	281
Polit, M.	392	Sierra, C.	95
Prat, F.	223	Socoró Carrié, J.C.	384
Prats, F.	310	Suñer, J.	291
Puig, A.	95	Téllez, R.A.	323
Puig, M.L.	171	Thiery, F.	392
Radeva, P.	197	Tolchinsky, P.	400
Ramisa, A.	213, 331	Toledo, R.	213, 331
Ramos-Garijo, R.	223	Traoré, A.	392
Riera, J.V.	273	Traver, V.J.	171
Rodríguez Silva, G.	359	Turon, C.	400
Rodríguez, I.	95	Vanrell, M.	205
Rodriguez-Aguilar, J.A.	112	Vazquez, E.	205
Rotger, D.	197	Vazquez, J.	205
Rovira i Regàs, M.M.	255	Vilar, J.M.	223
Rovira, X.	310	Vinyals, M.	213
Ruiz, D.	416	Vitrià, J.	6, 189
Salamó, M.	95	Ward, A.	87
Salvatella, A.	205	Willmott, S.	49
Sánchez, D.	67, 245	Zapateiro, M.	351
Sánchez, G.	368		

This page intentionally left blank

This page intentionally left blank